Acta Polytechnica

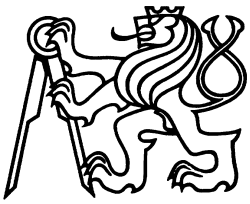

Title of journal: Acta Polytechnica. **Volume:** 62. **Number:** 1.
Periodicity: Bimonthly; 6 issues per year. **Date of issue:** February 28, 2022.
Published by: Czech Technical University in Prague,
Jugoslávských partyzánů 1580/3, 160 00 Praha 6 – Dejvice, Czech Republic.
IČO: 68407700.

Editorial Office: CTU — Central Library,
Technická 6, 160 80 Praha 6, Czech Republic.
acta@cvut.cz

Acta Polytechnica is available at http://ojs.cvut.cz/ojs/index.php/ap
Each article is assigned a digital object identifier https://doi.org/10.14311/AP.2022.62.⟨*4-digit article page number*⟩

ISSN 1805–2363 (online)

Dear Reader

The Acta Polytechnica journal that you have just opened is a scientific journal published by the Czech Technical University in Prague. This journal first appeared in 1961 under the name "Proceedings of the Czech Technical University". The main purpose of the journal was to support publication of the results of scientific and research activities at the Czech technical universities. Five years later, in 1966, the name of the journal was changed to Acta Polytechnica, and it started appearing quarterly. The main title Acta Polytechnica is accompanied by the subtitle Journal of Advanced Engineering, which expresses the scope of the journal more precisely. Acta Polytechnica covers a wide spectrum of engineering topics in civil engineering, mechanical engineering, electrical engineering, nuclear sciences and physical engineering, architecture, transportation science, biomedical engineering and computer science and engineering. The scope of the journal is not limited to the realm of engineering. We also publish articles from the area of natural sciences, in particular physics and mathematics.

Acta Polytechnica is now being published in an enlarged format. Our aim is to be a high-quality multi-disciplinary journal publishing the results of basic research and also applied research. We place emphasis on the quality of all published papers. The journal should also serve as a bridge between basic research in natural sciences and applied research in all technical disciplines.

We invite researchers to submit high-quality original papers. The conditions of the submission process are explained in detail on: `http://ojs.cvut.cz/ojs/index.php/ap`. All papers will be reviewed, and accepted papers are published in English.

We hope that you will find our journal interesting, and that it will serve as a valuable source of scientific information.

Editorial Board

In September 2021, the XVIII$^{\text{th}}$ continuation of the series of the international, mathematically oriented conferences "Analytic and Algebraic Methods in Physics" (AAMP) had to be organized, for well-known reasons, online. Fortunately, every cloud has a silver lining: the related reduction of the capacity of the scientific communication channels led to the willingness of the participants to return to the recently almost abandoned tradition of complementing the Zoom-mediated meeting by a subsequent preparation of an AAMP-oriented Special Issue (SI) of Acta Polytechnica.

The main purpose of this SI is twofold. Firstly, it is intended to offer, in written form, a sufficiently representative sample of what has been presented online. This means that in the form of the standard refereed papers, the readers of this SI will be rewarded by the up-to-the-minute information about the current state of art. Secondly, in an ambition which reaches behind the meeting itself, the contributing authors felt motivated by the idea that a compact and comprehensible presentation of their results might find a broader readership among people who would not normally participate in the conference but who could still find at least some of the presented results potentially relevant for their own field of research.

In comparison with the AAMP meeting itself (where the separate subjects covered by 36 talks have been subdivided into 12 sections), a minor disadvantage of our present SI lies, from the point of view of its readers at least, in the (traditional) alphabetical ordering of the contributions by their first authors. Fortunately, interested readers might get more info about the subdivisions of the subjects via the webpage of the conference [1]. Another weakness of the SI collection could be seen, mainly by the 75 AAMP participants themselves, in an incomplete coverage of the talks. Indeed, roughly one third of them was not eligible for our SI because the material was based on the recently published papers. Again, the related complementary information is available via the AAMP homepage [1].

This being said, the readers of this SI are expected to make their own selection of the consumption out of the menu. All of the papers belong to the AAMP framework, but even such a restriction admitted the inclusion of a broad spectrum of subfields, which are all bridging the gaps between the existing abstract mathematical structures (ranging from our understanding of ordinary differential equations up to the applications of the various forms of symmetries, antilinear symmetries, supersymmetries and nonlinearities) and their possible practical implementations (ranging again from multiple elementary models and methodical considerations up to certain fairly complicated phenomenological questions as encountered, say, in the relativistic quantum field theory).

In the AAMP context, we could speak about the tradition of the search for a deeper understanding of the connection between mathematics and physics. This led, in 2007, to the formulation of the project and to the organization of the series of the dedicated international conferences. At that time, indeed, the analytic and algebraic methods were particularly actively developed by the Founding Fathers from the Nuclear Physics Institute of the CAS in Řež. In this sense, the mathematical side of the bridge to physics has been (and, in fact, it is still being) restricted to the analytic and algebraic methods. In parallel, the physics side of the same bridge proved quickly growing with time. At present, its scope covers so many parts of physics that even the originally tacitly assumed specification "quantum physics" would and could be considered over-restrictive.

One can only conclude that the interaction between mathematics and physics remains enormously productive. We believe that our SI will contribute to this productivity, counteracting the extent of damages caused to the scientific world by the coronavirus. One of its most damaging effects was, indeed, the interruption of many regular series of international conferences, of which the series "Analytic and Algebraic Methods in Physics" (AAMP), regularly taking place in Prague every year, is just one of many examples. In fact, the original hopes that the interruption might only last one year were not fulfilled.

Equally disappointing proved to be our slow but definite empirical discovery that the success and efficiency of the transformation of these conferences into virtual meetings (mediated, say, by Zoom) remains limited. What was saved was only a form, not the full contents; not the essence. We all revealed that there exists no real substitute for the face-to-face meetings, converting the hours of isolated research performed by individuals into an exchange of ideas and providing a platform for their critical re-evaluation. Creating a genuine living science which can acquire its final, collective and truly creative character only after multiple informal debates and only after multiple active personal interactions.

For all of these reasons, the organizers of the AAMP series came to the conclusion that one of the possible reactions to the unpleasant current circumstances would be an enrichment of the internet-mediated standard

form of the meetings (in which one listens to talks for a few days, without having a real opportunity of discussing the subjects in the couloirs) via a return to an apparently obsolete practice of a subsequent preparation and publication of at least some of the talks in their written, more lasting and better accessible form, better suitable for the subsequent critical re-evaluation.

In this special issue of Acta Polytechnica, the readers will have the opportunity of seeing and, perhaps, appreciating the result. Surprisingly, many speakers decided to contribute. For us, this is a proof that the production of special issues characterized by a well-defined and not-too-broad range of subjects still makes sense.

On behalf of organizers, the guest editors of the special issue,

Andrii Khrabustovskii and Miloslav Znojil, University of Hradec Králové

References

[1] http://www.ujf.cas.cz/en/departments/department-of-theoretical-physics/events/conferencies/AAMP/index.html

Contents

CONSERVED QUANTITIES IN NON-HERMITIAN SYSTEMS VIA VECTORIZATION METHOD

KAUSTUBH S. AGARWAL, JACOB MULDOON, YOGESH N. JOGLEKAR*

Indiana University Purdue University Indianapolis (IUPUI), Indianapolis, Indiana 46202 U.S.A.

* corresponding author: yojoglek@iupui.edu

ABSTRACT. Open classical and quantum systems have attracted great interest in the past two decades. These include systems described by non-Hermitian Hamiltonians with parity-time ($\mathcal{PT}$) symmetry that are best understood as systems with balanced, separated gain and loss. Here, we present an alternative way to characterize and derive conserved quantities, or intertwining operators, in such open systems. As a consequence, we also obtain non-Hermitian or Hermitian operators whose expectations values show single exponential time dependence. By using a simple example of a $\mathcal{PT}$-symmetric dimer that arises in two distinct physical realizations, we demonstrate our procedure for static Hamiltonians and generalize it to time-periodic (Floquet) cases where intertwining operators are stroboscopically conserved. Inspired by the Lindblad density matrix equation, our approach provides a useful addition to the well-established methods for characterizing time-invariants in non-Hermitian systems.

KEYWORDS: Parity-time symmetry, pseudo-Hermiticity, conserved quantities.

1. INTRODUCTION

Since the seminal discovery of Bender and coworkers in 1998 [1], non-Hermitian Hamiltonians H with real spectra have become a subject of intense scrutiny [2–4]. The initial work on this subject focused on taking advantage of the reality of the spectrum to define a complex extension of quantum theory [5] where the traditional Dirac inner product is replaced by a Hamiltonian-dependent ($\mathcal{CPT}$) inner product. Soon it became clear that this process can be thought of as identifying positive definite operators $\hat{\eta} \geq 0$ that intertwine with the Hamiltonian [6–8], i.e. $\hat{\eta}H = H^\dagger\hat{\eta}$, and that a non-unique complex extension of standard quantum theory is generated by each positive definite $\hat{\eta}$ [9, 10]. These mathematical developments were instrumental to elucidating the role played by non-Hermitian, self-adjoint operators, biorthogonal bases, and non-unitary similarity transformations that change an orthonormal basis set into a non-orthogonal, but linearly independent basis set in physically realizable classical and quantum models [11].

A decade later, this mathematical approach gave way to experiments with the recognition that non-Hermitian Hamiltonians that are invariant under combined operations of parity and time-reversal ($\mathcal{PT}$) represent open systems with balanced gain and loss [12–15]. The spectrum of a $\mathcal{PT}$-symmetric Hamiltonian $H_{\rm PT}(\gamma)$ is purely real when the non-Hermiticity γ is small. With increasing γ, a level attraction and resulting degeneracy turns the spectrum into complex-conjugate pairs when the non-Hermiticity exceeds a nonzero threshold $\gamma_{\rm PT}$ [16]. This transition is called $\mathcal{PT}$-symmetry breaking transition, and at the threshold $\gamma_{\rm PT}$ the algebraic multiplicity of the degenerate eigenvalue is larger than the geometric multiplicity, i.e. **it is** an exceptional point (EP) [17].

Fueled by this physical insight, the past decade has seen an explosion of experimental platforms, usually in classical wave systems, where effective $\mathcal{PT}$-symmetric Hamiltonians with balanced gain and loss have been realized. They include evanescently coupled waveguides [18], fiber loops [19], microring resonators [20, 21], optical resonators [22], electrical circuits [23–25], and mechanical oscillators [26]. The key characteristics of this transition, driven by the non-orthogonality of eigenstates, are also seen in systems with mode-selective losses [27–29]. In the past two years, these ideas have been further extended to minimal quantum systems, thereby leading to observation of $\mathcal{PT}$-symmetric breaking and attendant phenomena in a single spin [30], a single superconducting transmon [31], ultracold atoms [32], and quantum photonics [33].

We remind the readers the effective Hamiltonian approach requires Dirac inner product, and is valid in both $\mathcal{PT}$-symmetric and $\mathcal{PT}$-broken regions. Apropos, the non-unitary time evolution generated by the effective $H_{\rm PT}$ signals the fact that the system under consideration is open. In this context, every intertwining operator $\hat{\eta}$ – positive definite or not – represents a time-invariant of the system. In other words, although the state norm $\langle\psi(t)|\psi(t)\rangle$ or the energy $\langle\psi(t)|H_{\rm PT}|\psi(t)\rangle$ of a state $|\psi(t)\rangle = \exp(-iH_{\rm PT}t)|\psi(0)\rangle$ of a $\mathcal{PT}$-symmetric system are not conserved [8], the expectation values $\langle\psi(t)|\hat{\eta}|\psi(t)\rangle$ remain constant with time. For a system with N degrees of freedom, a complete characterization of intertwining operators for a given system is carried out by solving the set of N^2 simultaneous, linear equations, i.e.

$$\hat{\eta}H_{\rm PT} = H_{\rm PT}^\dagger\hat{\eta}. \tag{1}$$

In the past, several different avenues have been used to obtain these conserved quantities. They include spectral decomposition methods [8, 34], an explicit recursive construction to generate a tower of intertwining operators [25, 35], sum-rules method [36], and the Stokes parametrization approach for a $\mathcal{PT}$-symmetric dimer [37]. Here, we present yet another approach to the problem, and illustrate it with two simple examples. The plan of the paper is as follows. In Section 2, we present the eigenvalue-equation approach for intertwining operators and the details of the vectorization scheme. This method is valid for any finite dimensional $\mathcal{PT}$-symmetric Hamiltonian. In Section 3, we present results of such analysis for a quantum $\mathcal{PT}$-symmetric dimer with static or time-periodic gain and loss. Corresponding results for a classical $\mathcal{PT}$-symmetric dimer are presented in Section 4. We conclude the paper with a brief discussion in Section 5.

2. Intertwining operators as an eigenvalue problem

For a $\mathcal{PT}$-symmetric system undergoing coherent but non-unitary dynamics with static Hamiltonian $H_{\rm PT}$, the expectation value of an operator $\hat{\eta}$ satisfies the following linear-in-$\hat{\eta}$ first-order differential equation

$$\partial_t \langle\psi(t)|\hat{\eta}|\psi(t)\rangle = -i\langle\psi(t)|\hat{\eta}H_{\rm PT} - H_{\rm PT}^\dagger\hat{\eta}|\psi(t)\rangle. \quad (2)$$

This equation is reminiscent of the Gorini Kossakowski Sudarshan Lindblad (GKSL) equation [38, 39] (henceforth referred to as the Lindblad equation) that describes the dynamics of the reduced density matrix of a quantum system coupled to a much larger environment [40–42]. Interpreting $\hat{\eta}$ as an $N\times N$ matrix, all $\hat{\eta}$s that satisfy Eq. (2) can be obtained from the corresponding eigenvalue problem

$$\mathcal{E}_k\hat{\eta}_k = -i(\hat{\eta}_k H_{\rm PT} - H_{\rm PT}^\dagger\hat{\eta}_k) \equiv \mathcal{L}\hat{\eta}_k, \quad (3)$$

for $1\le k\le N^2$. We vectorize the matrix $\hat{\eta}$ into an N^2-sized column vector $|\eta^v\rangle$ by stacking its columns, i.e. $[\hat{\eta}]_{pq}\to\eta^v_{p+(q-1)N}$ [43]. Under this vectorization, the Hilbert-Schmidt trace inner product carries over to the Dirac inner product, $\mathrm{Tr}(\hat{\eta}_1^\dagger\hat{\eta}_2) = \langle\eta_1^v|\eta_2^v\rangle$ where $\langle\eta_1^v|$ is the Hermitian-conjugate row vector obtained from the column vector $|\eta_1^v\rangle$. Using the identity $A\hat{\eta}B\to(B^T\otimes A)|\eta^v\rangle$, the eigenvalue problem Eq. (3) becomes $\det(\mathcal{L}-\mathcal{E}\mathbb{1}_{N^2})=0$ where the $N^2\times N^2$ "Liouvillian" matrix is given by

$$\mathcal{L} = -i\left[H_{\rm PT}^T\otimes\mathbb{1}_N - \mathbb{1}_N\otimes H_{\rm PT}^\dagger\right], \quad (4)$$

and $\mathbb{1}_m$ is the $m\times m$ identity matrix. Thus, the intertwining operators are distinct eigenvectors $|\eta_m^v\rangle$ with zero eigenvalue in Eq. (3). The N^2 eigenvalues of the Liouvillian $\mathcal{L}$ are simply related to N eigenvalues ϵ_m of the $H_{\rm PT}$ as

$$\mathcal{E}_{pq} = -i(\epsilon_p - \epsilon_q^*). \quad (5)$$

Since the spectrum of $H_{\rm PT}$ is either real ($\epsilon_p=\epsilon_p^*$) or complex conjugates ($\epsilon_p=\epsilon_q^*$ for some pair), there are N zero eigenvalues of $\mathcal{L}$ when $H_{\rm PT}$ has no symmetry-driven degeneracies; the number of zero eigenvalues grows to N^2 if the Hamiltonian is proportional to the identity matrix [34]. This analysis also provides a transparent way to construct corresponding intertwining operators via the spectral decomposition of $H_{\rm PT}$ [8]. Note that when $\mathcal{E}=0$, due to the linearity of the intertwining relation, Eq. (1), without loss of generality, we can choose the N intertwining operators $\hat{\eta}_m$ to be Hermitian.

So what is the advantage of this approach? For one, it gives us $N(N-1)$ other, (generally non-Hermitian) operators whose expectation value *in any arbitrary state evolves simply exponentially in time.* When $\mathcal{E}_{pq}$ is purely imaginary, it leads to the non-Hermitian $\hat{\eta}_{pq}$ whose expectation value in any state remains constant in magnitude; on the other hand, if $\mathcal{E}_{pq}$ is purely real, one can choose a Hermitian $\hat{\eta}_{pq}$ whose expectation value exponentially grows or decays with time.

This analysis of constants of motion is valid for systems with a static, $\mathcal{PT}$-symmetric Hamiltonian. It can be suitably generalized to time-periodic, $\mathcal{PT}$-symmetric Hamiltonians via the Floquet formalism [25, 28, 32, 44, 45]. When $H_{\rm PT}(t)=H_{\rm PT}(t+T)$ is periodic in time, the long-time dynamics of the system is governed by the Floquet time-evolution operator [46]

$$G_F(T) = \mathbb{T}e^{-i\int_0^T H_{\rm PT}(t')dt'}, \quad (6)$$

where $\mathbb{T}$ stands for the time ordered product that takes into account non-commuting nature of the Hamiltonians at different times. The (stroboscopic) dynamics of the system at times $t_m=mT$ is then given by $|\psi(t_m)\rangle = G_F^m|\psi(0)\rangle$, and the corresponding, Hermitian, conserved operators $\hat{\eta}=\hat{\eta}^\dagger$ are determined by [25, 34]

$$G_F^\dagger\hat{\eta}G_F = \hat{\eta}. \quad (7)$$

Vectorization of Eq. (7) implies the conserved quantities are given by eigenvectors of the "Floquet Liouville time-evolution" matrix

$$\mathcal{G} = G_F^T\otimes G_F^\dagger \quad (8)$$

with unit eigenvalue. Since $G_F(T)$ inherits the $\mathcal{PT}$ symmetry of the time-periodic Hamiltonian, the eigenvalues κ_m of $G_F(T)$ either lie on a circle ($|\kappa_p|=$ const.; $\mathcal{PT}$-symmetric phase) or occur along a radial line in pairs with constant geometric mean ($|\kappa_p\kappa_q|=$ const.; $\mathcal{PT}$-broken phase). Therefore, it is straightforward to see that among the N^2 eigenvalues $\lambda_{pq}\equiv\kappa_p\kappa_q^*$ of $\mathcal{G}$, there are N unit eigenvalues, giving rise to N conserved quantities. As in the case with the static Hamiltonian, the remaining $N(N-1)$ eigenvectors give operators that vary exponentially with the stroboscopic time t_m irrespective of the initial state $|\psi(0)\rangle$.

If λ_{pq} is real, we can choose them to be Hermitian, as in the case of a static Hamiltonian.

We now demonstrate these ideas with two concrete examples.

3. Quantum $\mathcal{PT}$-symmetric dimer

We first consider the prototypical $\mathcal{PT}$-symmetric dimer ($N = 2$) with a Hamiltonian given by

$$H_1(t) = J\sigma_x + i\gamma f(t)\sigma_z = H_1^T \neq H_1^\dagger. \tag{9}$$

We call this model "quantum" because it arises naturally in minimal quantum systems undergoing Lindblad evolution when we confine ourselves to trajectories that undergo no quantum jumps [31], as well as in wave systems [18–22]. Here $J > 0$ denotes coupling between the two degrees of freedom and $\gamma > 0$ is the strength of the gain-loss term. H_1 is $\mathcal{PT}$-symmetric with the parity operator $\mathcal{P} = \sigma_x$ and time-reversal operator $\mathcal{T} = *$ (complex conjugation). The eigenvalues $\epsilon_{1,2} = \pm\sqrt{J^2 - \gamma^2} \equiv \pm\Delta(\gamma)$ of the Hamiltonian $H_1(\gamma)$ remain real when $\gamma < \gamma_{\rm PT} = J$ and become purely imaginary when γ exceeds the threshold.

In the static case, $f(t) = 1$, using Eq. 1, it is easy to show that $\hat{\eta}_1 = \mathcal{P} = \sigma_x$ is the first intertwining operator [34, 35], and the recursive construction gives the second intertwining operator as $\hat{\eta}_2 = \hat{\eta}_1 H_1/J = \mathbb{1} + (\gamma/J)\sigma_y$. However, the corresponding 4×4 Liouvillian matrix $\mathcal{L}$, Eq. (4), has two nonzero eigenvalues that are given by $\mathcal{E}_\pm = \pm 2i\Delta$. The corresponding eigen-operators are given by

$$\hat{\eta}_\pm = \frac{1}{J^2}\begin{bmatrix} (\gamma \pm i\Delta)^2 & -i(\gamma \pm i\Delta) \\ +i(\gamma \pm i\Delta) & 1 \end{bmatrix}. \tag{10}$$

Note that the 2×2 matrices $\hat{\eta}_\pm$ have rank 1, and thus are not invertible. In the $\mathcal{PT}$-symmetric region ($\Delta \in \mathbb{R}$), the operators $\hat{\eta}_\pm$ are not Hermitian, whereas in the $\mathcal{PT}$ broken region ($\Delta \in i\mathbb{R}$), they are Hermitian.

Next we consider the time-periodic case, i.e. $f(t) = f(t+T)$ where $f(t) = \mathrm{sgn}(t)$ for $|t| < T/2$ denotes a square wave. This piecewise constant gain and loss means that the Hamiltonian switches from $H_{1+} = J\sigma_x + i\gamma\sigma_z$ for $0 \le t < T/2$ to $H_{1-} = \mathcal{T}H_{1+}\mathcal{T} = J\sigma_x - i\gamma\sigma_z$ for $T/2 \le t < T$. The non-unitary Floquet time-evolution operator can be explicitly evaluated as [47]

$$G_F(T) = e^{-iH_{1-}T/2}e^{-iH_{1+}T/2}, \tag{11}$$

$$= G_0\mathbb{1}_2 + iG_x\sigma_x + G_y\sigma_y, \tag{12}$$

where $G_0 = [J^2\cos(\Delta T) - \gamma^2]/\Delta^2$, $G_x = -J\sin(\Delta T)/\Delta$ and $G_y = -J\gamma[1 - \cos(\Delta T)]/\Delta^2$ are coefficients that remain real irrespective of where $\Delta(\gamma)$ is real or purely imaginary. When $\gamma \to 0$, this reproduces the expected result $G_F(T) = \exp(-iJ\sigma_x T)$ and in the limit $T \to 0$, the time-evolution operator reduces to $\mathbb{1}_2$ as expected. On the other hand, as $\Delta \to 0$, the power series for $G_F(T)$ terminates at *second order in* T in a sharp contrast to the static case, where it terminates at first order in time.

The eigenvalues of G_F, Eq. (12), are

$$\kappa_{1,2} = G_0 \pm i\sqrt{G_x^2 - G_y^2}. \tag{13}$$

Thus the EP contours separating the $\mathcal{PT}$-symmetric phase ($|\kappa_1| = |\kappa_2|$) from the $\mathcal{PT}$-broken phase ($|\kappa_1| \neq |\kappa_2|$) are given by $G_x = \pm G_y$ [47]. It is easy to check that $\hat{\eta}_1 = \sigma_x$ satisfies $G_F^\dagger\hat{\eta}_1 G_F = \hat{\eta}_1$ and is a stroboscopically conserved quantity. The second conserved operator is obtained from the symmetrized or antisymmetrized version of the recursive construction [34], i.e.

$$\hat{\eta}_2 = \begin{cases} (\hat{\eta}_1 G_F + G_F^\dagger\hat{\eta}_1)/2, \\ -i(\hat{\eta}_1 G_F - G_F^\dagger\hat{\eta}_1)/2. \end{cases} \tag{14}$$

In the present case, the symmetrized version returns $\hat{\eta}_1$ while the antisymmetrized version gives the second, linearly independent conserved operator as $\hat{\eta}_2 = G_x\mathbb{1}_2 + G_y\sigma_z$. Following the procedure outlined in Section 2 gives us two unity eigenvalues of $\mathcal{G}$, Eq. (8), with corresponding conserved operators. The remaining two eigenvalues are complex conjugates with unit length in the $\mathcal{PT}$-symmetric region, i.e. $\lambda_3 = \lambda_4^* = e^{i\phi}$ with eigen-operators $\hat{\eta}_+ = \hat{\eta}_-^\dagger$ that are Hermitian conjugates of each other. In the $\mathcal{PT}$-broken region, the two complex eigenvalues with equal phase satisfy $|\lambda_3\lambda_4| = 1$.

Figure 1 shows expectation values normalized to their initial values,

$$\eta_\alpha(t) \equiv \frac{\langle\psi(t)|\hat{\eta}_\alpha|\psi(t)\rangle}{\langle\psi(0)|\hat{\eta}_\alpha|\psi(0)\rangle} \tag{15}$$

calculated with initial state $|\psi(0)\rangle = |+x\rangle$ as a function of dimensionless time t/T. The system parameters are $\gamma = 0.5J$, $JT = 1$, and $|+x\rangle$ is the eigenstate of σ_x with eigenvalue $+1$. Thus, the system is in the $\mathcal{PT}$-symmetric region. Figure 1a shows that $\eta_1(t)$ is conserved in this evolution at all times, not just stroboscopically at $t_m = mT$. On the other hand $\eta_2(t)$, shown in Figure 1b, has a periodic behavior with a period $\sim 30T$ (not shown). Although $\eta_2(t)$ varies with time, it is stroboscopically conserved, $\eta_2(t_m) = 1$. The dotted red line shows $\Re\lambda_2^t = 1$. Figure 1c shows that the real part of $\eta_+(t)$, with eigenvalue $\lambda_3 = -0.44 + 0.9i$, also shows periodic variation. The dotted black line shows $\Re\lambda_3^t$, and the fact that $\Re\eta_+(t_m)$ matches it stroboscopically confirms the simple sinousoidal variation of this eigen-operator. Figure 1d shows corresponding results for the fourth operator $\hat{\eta}_- = \hat{\eta}_+^\dagger$ with eigenvalue $\lambda_4 = -0.44 - 0.9i$.

We conclude this section with transformation properties of $G_F(T)$ and the conserved operators $\hat{\eta}$. When the periodic Hamiltonian is Hermitian, i.e. $H_0(t) = H_0^\dagger(t) = H_0(t+T)$, shifting the zero of time to t_0 leads to a unitary transformation,

$$G_F(T + t_0, t_0) = U(t_0)G_F(T)U^\dagger(t_0), \tag{16}$$

$$U(t_0) = \mathbb{T}e^{-i\int_0^{t_0} H_0(t')dt'}. \tag{17}$$

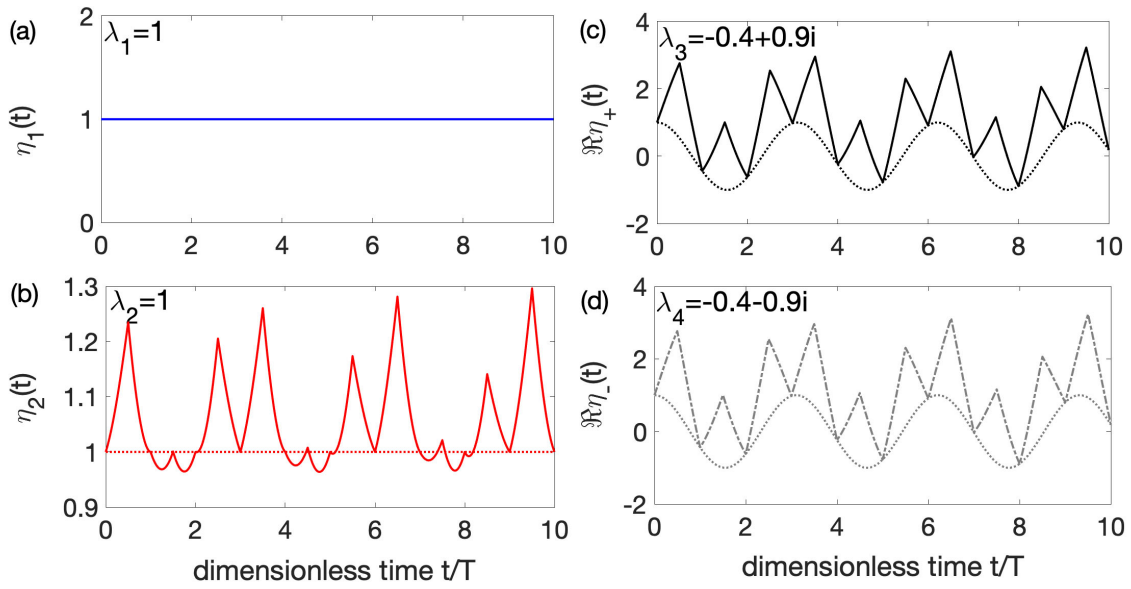

FIGURE 1. Conserved quantities for a Floquet, quantum $\mathcal{PT}$-symmetric dimer. System parameters are $\gamma = 0.5J$, $JT = 1$, $|\psi(0)\rangle = |+x\rangle$, and $\eta_\alpha(t)$ denote normalized expectation values. (a) $\hat{\eta}_1 = \sigma_x$ is an eigen-operator of $\mathcal{G}$ with eigenvalue $\lambda_1 = 1$; $\eta_1(t)$ is constant. (b) $\hat{\eta}_2 = G_x \mathbb{1}_2 + G_y \sigma_z$ is the second eigen-operator of $\mathcal{G}$ with $\lambda_2 = 1$; $\eta_2(t)$ oscillates with time, but is stroboscopically constant at $t/T = n$; the dotted red line shows $\Re\lambda_2^t = 1$. (c) $\hat{\eta}_+$ is a non-Hermitian eigen-operator with unit-length eigenvalue $\lambda_3 = -0.44 + 0.9i$. The real part of its normalized expectation value stroboscopically matches $\Re\lambda_3^t$ shown in dotted black. (d) Corresponding result for $\hat{\eta}_- = \hat{\eta}_+^\dagger$ with eigenvalue $\lambda_4 = \lambda_3^*$.

Therefore the conserved operators are also unitarily transformed. However, in our case, Eq. (16) becomes a *similarity transformation*, $G_F(T + t_0, t_0) = S G_F(T) S^{-1}$ where $S = \mathbb{T}\exp(-i\int_0^{t_0} H_{\rm PT}(t')dt')$ does not satisfy $S^\dagger S = \mathbb{1} = SS^\dagger$. Under this transformation, the conserved operators change as $\hat{\eta} \to S^{-1\dagger}\hat{\eta}S^{-1}$. This non-unitary transformation of the conserved quantities under a shift of zero of time suggests that they are not related to "symmetries" of the open system with balanced gain and loss.

4. CLASSICAL $\mathcal{PT}$-SYMMETRIC DIMER

We now consider a different example characterized by a non-Hermitian Hamiltonian with purely imaginary entries. We call such a system "classical" because having $H_{\rm PT} = -H_{\rm PT}^*$ ensures that the non-unitary time evolution operator $\exp(-iH_{\rm PT}t)$ is purely real, and therefore $|\psi(t)\rangle$ remains real if $|\psi(0)\rangle$ is. Such classical Hamiltonian arises naturally in describing the energy density dynamics in mechanical or electrical circuits [23–26, 28], where $|\psi(t)\rangle$ encodes time-dependent positions, velocities, voltages, currents, etc. and is obviously real. As its simplest model, we consider a dimer governed by the Hamiltonian

$$H_2(t) = J\sigma_y + i\gamma f(t)\sigma_z = -H_2^*. \qquad (18)$$

On one level, the Hamiltonian $H_2(t)$, Eq. (18), is "just a change of basis" from $H_1(t)$, Eq. (9); $H_2(t) = \exp(-i\pi\sigma_z/4)H_1(t)\exp(+i\pi\sigma_z/4)$. However, since $H_2(t)$ models effective, classical systems where the entire complex state space is physically accessible, it is necessary to treat it differently. A physical realization of $H_2(t)$ is found in a single LC circuit whose inductance $L(t)$ and capacitance $C(t)$ are varied such that its characteristic frequency $J = 1/\sqrt{L(t)C(t)}$ remains constant [25].

Hamiltonian $H_2(t)$ is $\mathcal{PT}$-symmetric with $\mathcal{PT} = \sigma_x *$. In the static case ($f(t) = 1$), the two, Hermitian intertwining operators are given by $\hat{\eta}_1 = \sigma_y$ and $\hat{\eta}_2 = \hat{\eta}_1 H_2/J = \mathbb{1}_2 - (\gamma/J)\sigma_x$. In addition, the vectorization approach gives two, rank-1 eigen-operators

$$\hat{\eta}_\pm = \frac{1}{J^2}\begin{bmatrix} (\gamma \pm i\Delta)^2 & -(\gamma \pm i\Delta) \\ -(\gamma \pm i\Delta) & 1 \end{bmatrix}, \qquad (19)$$

with eigenvalues $\mathcal{E}_\pm = \pm 2i\Delta$. As we discussed in Section 3, these operators are not Hermitian in the $\mathcal{PT}$-symmetric phase, and become Hermitian in the $\mathcal{PT}$-broken phase.

For the Floquet case, we choose a gain-loss term that is nonzero only at discrete times. This is accomplished by choosing the dimensionless function $f(t)$ as

$$f(t) = T\left[\delta(t) - \delta(t - T/2)\right] = f(t + T). \qquad (20)$$

The resulting Floquet time-evolution operator $G_F(T)$ can be analytically calculated [25]. Since the Hamiltonian $H_2(t)$ is Hermitian at all times except $t_k = kT/2$, the evolution is mostly unitary, punctuated by non-unitary contributions that occur due to δ-functions at

times t_k. The result is

$$G_F(T) = e^{+\gamma T\sigma_z} e^{-iJT\sigma_y/2} e^{-\gamma T\sigma_z} e^{-iJT\sigma_y/2} = G_0 \mathbb{1}_2 + G_x\sigma_x + iG_y\sigma_y + G_z\sigma_z, \quad (21)$$

where the four real coefficients G_k are given by

$$G_0 = \cos^2(JT/2) - \sin^2(JT/2)\cosh(2\gamma T), \quad (22)$$
$$G_x = -\sin(JT)\sinh(2\gamma T)/2, \quad (23)$$
$$G_y = -\sin(JT)[1+\cosh(2\gamma T)]/2. \quad (24)$$
$$G_z = -\sin^2(JT/2)\sinh(2\gamma T). \quad (25)$$

As is expected, the purely real $G_F(T)$ reduces to $\exp(-iJT\sigma_y)$ in the Hermitian limit $\gamma \to 0$. The EP conoturs, on the other hand, are determined by the constraint $G_x^2 + G_y^2 - G_z^2 = 0$, which reduces to $\cos(JT/2) = \tanh(\gamma T)$ [25].

Two linearly independent Floquet intertwining operators obtained by solving Eq. (7) are given by $\hat{\eta}_1 = \sigma_y$ and $\hat{\eta}_2 = -i(\hat{\eta}_1 G_F - G_F^\dagger \hat{\eta}_1)/2$. The latter simplifies to $\hat{\eta}_2 = G_y\mathbb{1}_2 + G_z\sigma_x - G_x\sigma_z$. We leave it for the reader to check that, as in the case of Floquet quantum $\mathcal{PT}$ dimer problem, the symmetrized version of the recursive procedure, Eq. (14), does not lead to a result that is linearly independent of $\hat{\eta}_1$. Following the recipe in Section 2, we supplement these analytical results with symbolic or numerical results for four eigenvalues λ_k and four eigen-operators $\hat{\eta}_1, \hat{\eta}_2, \hat{\eta}_\pm$ of $\mathcal{G}$, Eq. (8).

Figure 2 shows the behavior of normalized expectation values $\eta_\alpha(t)$ calculated with $|\psi(0)\rangle = |+x\rangle$ as a function of time. The system parameters are $\gamma = 0.5J$ and $JT = 1$, and therefore the system is in the $\mathcal{PT}$-symmetric region. Note that since $|\psi(t)\rangle$ is purely real, $\langle\psi(t)|\hat{\eta}_1|\psi(t)\rangle = 0$ independent of time [25]. On the other hand $\eta_2(t)$, shown in Figure 2a, has a periodic behavior. Although $\eta_2(t)$ varies with time, it is stroboscopically conserved, $\eta_2(t_m) = 1$. Figure 2b shows that the real part of $\eta_+(t)$, with unit-magnitude eigenvalue $\lambda_3 = -0.65 + 0.756i$, also varies periodically. The dotted black line shows $\Re\lambda_3^t$, and the fact that $\Re\eta_+(t_m)$ matches it stroboscopically confirms the simple sinousoidal variation of this eigen-operator. Since the system is in the $\mathcal{PT}$-symmetric phase, $\hat{\eta}_- = \hat{\eta}_+^\dagger$, and therefore $\Re\eta_-(t) = \Re\eta_+(t)$. Figure 2c shows the corresponding imaginary parts $\Im\eta_+(t) = -\Im\eta_-(t)$ for the eigen-operator with the complex conjugate eigenvalue $\lambda_4 = \lambda_3^*$. We note that in the $\mathcal{PT}$-broken regime, the non-unit-modulus eigenvalues are not complex conjugates of each other, and therefore the corresponding eigen-operators will not satisfy the relations shown in Figures 2b-c.

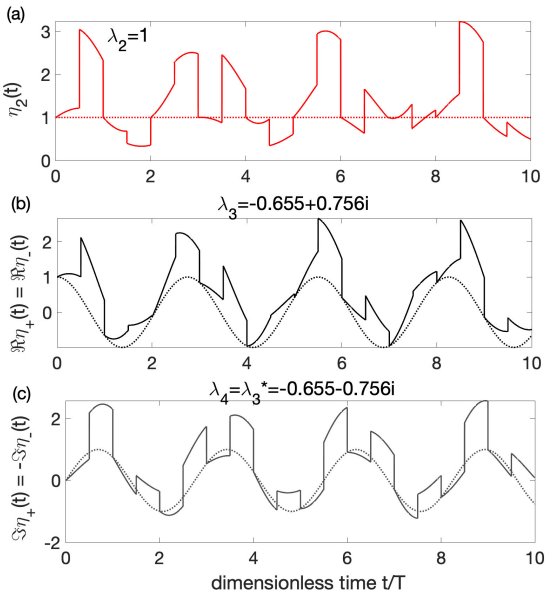

FIGURE 2. Conserved quantities for a classical $\mathcal{PT}$-symmetric dimer with $\gamma = 0.5J$, $JT = 1$, $|\psi(0)\rangle = |+x\rangle$. Since $|\psi(t)\rangle$ is purely real, the expectation value of $\hat{\eta}_1 = \sigma_y$ is always zero. (a) $\hat{\eta}_2 = G_y\mathbb{1}_2 + G_x\sigma_z - G_z\sigma_x$ is the second eigen-operator of $\mathcal{G}$ with $\lambda_2 = 1$. $\eta_2(t)$ oscillates with time, but is stroboscopically constant at $t/T = n$; the dotted red line shows $\Re\lambda_2^t = 1$. (b) Since the system is in the $\mathcal{PT}$-symmetric phase, $\Re\eta_+(t) = \Re\eta_-(t)$ (solid black) shows periodic behavior with values that stroboscopically match $\Re\lambda_3^t$, shown in dotted black. (c) Corresponding imaginary parts, $\Im\eta_-(t) = -\Im\eta_+(t)$ (dot-dashed black) show similar, stroboscopically matching behavior.

5. CONCLUSIONS

In this article, we have presented a new method to obtain intertwining operators or conserved quantities in $\mathcal{PT}$-symmetric systems with static or time-periodic Hamiltonians. In this approach, these operators appear as zero-$\mathcal{E}$ eigenmodes of the static Liouvillian $\mathcal{L}$ or as $\lambda = 1$ eigenmodes of the Floquet $\mathcal{G}$. For an N-dimensional system, in addition to the N constants of motion, this approach also leads to $N(N-1)$ operators whose expectation values *in any arbitrary state* undergo simple exponential-in-time change. We have demonstrated these concepts with two simple, physically motivated examples of a $\mathcal{PT}$-symmetric dimer with different, periodic gain-loss profiles. We have deliberating stayed away from continuum models because extending this approach or the recursive construction [34, 35] to infinite dimensions will probably be plagued by challenges regarding domains of resulting, increasingly higher-order differential operators.

The definition of an intertwining operator via Eq. (1) can be generalized to obtain conserved observables for Hamiltonians that posses other antilinear symmetries, such as anti-$\mathcal{PT}$ symmetry [48–50] or anyonic-$\mathcal{PT}$ symmetry [51, 52]. The recursive procedure to generate a tower of such operators [34], and the vectorization method presented in Section 2 remains valid for arbitrary antilinear symmetry. Thus, this approach can be used to investigate constants of motion in such systems as well.

References

[1] C. M. Bender, S. Boettcher. Real spectra in non-Hermitian Hamiltonians having $\mathcal{PT}$ symmetry. *Physical Review Letters* **80**(24):5243–5246, 1998. https://doi.org/10.1103/PhysRevLett.80.5243.

[2] G. Lévai, M. Znojil. Systematic search for $\mathcal{PT}$-symmetric potentials with real energy spectra. *Journal of Physics A: Mathematical and General* **33**(40):7165–7180, 2000. https://doi.org/10.1088/0305-4470/33/40/313.

[3] C. M. Bender, D. C. Brody, H. F. Jones. Must a Hamiltonian be Hermitian? *American Journal of Physics* **71**(11):1095–1102, 2003. https://doi.org/10.1119/1.1574043.

[4] C. M. Bender. Making sense of non-Hermitian Hamiltonians. *Reports on Progress in Physics* **70**(6):947–1018, 2007. https://doi.org/10.1088/0034-4885/70/6/r03.

[5] C. M. Bender, D. C. Brody, H. F. Jones. Complex extension of quantum mechanics. *Physical Review Letters* **89**(27):270401, 2002. https://doi.org/10.1103/PhysRevLett.89.270401.

[6] A. Mostafazadeh. Pseudo-Hermiticity versus $\mathcal{PT}$ symmetry: The necessary condition for the reality of the spectrum of a non-Hermitian Hamiltonian. *Journal of Mathematical Physics* **43**(1):205–214, 2002. https://doi.org/10.1063/1.1418246.

[7] A. Mostafazadeh. Exact $\mathcal{PT}$-symmetry is equivalent to Hermiticity. *Journal of Physics A: Mathematical and General* **36**(25):7081–7091, 2003. https://doi.org/10.1088/0305-4470/36/25/312.

[8] A. Mostafazadeh. Pseudo-Hermitian representation of quantum mechanics. *International Journal of Geometric Methods in Modern Physics* **07**(07):1191–1306, 2010. https://doi.org/10.1142/s0219887810004816.

[9] M. Znojil, H. B. Geyer. Construction of a unique metric in quasi-Hermitian quantum mechanics: Nonexistence of the charge operator in a 2×2 matrix model. *Physics Letters B* **640**(1-2):52–56, 2006. https://doi.org/10.1016/j.physletb.2006.07.028.

[10] M. Znojil. Complete set of inner products for a discrete $\mathcal{PT}$-symmetric square-well Hamiltonian. *Journal of Mathematical Physics* **50**(12):122105, 2009. https://doi.org/10.1063/1.3272002.

[11] M. Znojil. Special issue "Pseudo-Hermitian Hamiltonians in quantum physics in 2014". *International Journal of Theoretical Physics* **54**(11):3867–3870, 2015. https://doi.org/10.1007/s10773-014-2501-2.

[12] A. Ruschhaupt, F. Delgado, J. G. Muga. Physical realization of $\mathcal{PT}$-symmetric potential scattering in a planar slab waveguide. *Journal of Physics A: Mathematical and General* **38**(9):L171–L176, 2005. https://doi.org/10.1088/0305-4470/38/9/l03.

[13] R. El-Ganainy, K. G. Makris, D. N. Christodoulides, Z. H. Musslimani. Theory of coupled optical PT-symmetric structures. *Optics Letters* **32**(17):2632–2634, 2007. https://doi.org/10.1364/OL.32.002632.

[14] K. G. Makris, R. El-Ganainy, D. N. Christodoulides, Z. H. Musslimani. Beam dynamics in $\mathcal{PT}$ symmetric optical lattices. *Physical Review Letters* **100**:103904, 2008. https://doi.org/10.1103/PhysRevLett.100.103904.

[15] S. Klaiman, U. Günther, N. Moiseyev. Visualization of branch points in $\mathcal{PT}$-symmetric waveguides. *Physical Review Letters* **101**:080402, 2008. https://doi.org/10.1103/PhysRevLett.101.080402.

[16] Y. N. Joglekar, C. Thompson, D. D. Scott, G. Vemuri. Optical waveguide arrays: quantum effects and PT symmetry breaking. *The European Physical Journal Applied Physics* **63**(3):30001, 2013. https://doi.org/10.1051/epjap/2013130240.

[17] T. Kato. *Perturbation Theory for Linear Operators*. Springer, Berlin Heidelberg, 1995. https://doi.org/10.1007/978-3-642-66282-9.

[18] C. E. Rüter, K. G. Makris, R. El-Ganainy, et al. Observation of parity-time symmetry in optics. *Nature Physics* **6**(3):192–195, 2010. https://doi.org/10.1038/nphys1515.

[19] A. Regensburger, C. Bersch, M.-A. Miri, et al. Parity–time synthetic photonic lattices. *Nature* **488**(7410):167–171, 2012. https://doi.org/10.1038/nature11298.

[20] H. Hodaei, M.-A. Miri, M. Heinrich, et al. Parity-time–symmetric microring lasers. *Science* **346**(6212):975–978, 2014. https://doi.org/10.1126/science.1258480.

[21] B. Peng, Ş. K. Özdemir, F. Lei, et al. Parity–time-symmetric whispering-gallery microcavities. *Nature Physics* **10**(5):394–398, 2014. https://doi.org/10.1038/nphys2927.

[22] L. Chang, X. Jiang, S. Hua, et al. Parity–time symmetry and variable optical isolation in active–passive-coupled microresonators. *Nature Photonics* **8**(7):524–529, 2014. https://doi.org/10.1038/nphoton.2014.133.

[23] J. Schindler, A. Li, M. C. Zheng, et al. Experimental study of active LRC circuits with $\mathcal{PT}$ symmetries. *Physical Review A* **84**(4):040101, 2011. https://doi.org/10.1103/PhysRevA.84.040101.

[24] T. Wang, J. Fang, Z. Xie, et al. Observation of two $\mathcal{PT}$ transitions in an electric circuit with balanced gain and loss. *The European Physical Journal D* **74**(8), 2020. https://doi.org/10.1140/epjd/e2020-10131-7.

[25] M. A. Quiroz-Juárez, K. S. Agarwal, Z. A. Cochran, et al. On-demand Parity-Time symmetry in a lone oscillator through complex, synthetic gauge fields, 2021. arXiv:2109.03846.

[26] C. M. Bender, B. K. Berntson, D. Parker, E. Samuel. Observation of $\mathcal{PT}$ phase transition in a simple mechanical system. *American Journal of Physics* **81**(3):173–179, 2013. https://doi.org/10.1119/1.4789549.

[27] D. Duchesne, V. Aimez, R. Morandotti, et al. Observation of $\mathcal{PT}$-symmetry breaking in complex optical potentials. *Physical Review Letters* **103**(9):093902, 2009. https://doi.org/10.1103/physrevlett.103.093902.

[28] R. de J. León-Montiel, M. A. Quiroz-Juárez, J. L. Domínguez-Juárez, et al. Observation of slowly decaying eigenmodes without exceptional points in Floquet dissipative synthetic circuits. *Communications Physics* **1**(1), 2018. https://doi.org/10.1038/s42005-018-0087-3.

[29] Y. N. Joglekar, A. K. Harter. Passive parity-time-symmetry-breaking transitions without exceptional points in dissipative photonic systems [Invited]. *Photonics Research* **6**(8):A51–A57, 2018. https://doi.org/10.1364/prj.6.000a51.

[30] Y. Wu, W. Liu, J. Geng, et al. Observation of parity-time symmetry breaking in a single-spin system. *Science* **364**(6443):878–880, 2019. https://doi.org/10.1126/science.aaw8205.

[31] M. Naghiloo, M. Abbasi, Y. N. Joglekar, K. W. Murch. Quantum state tomography across the exceptional point in a single dissipative qubit. *Nature Physics* **15**(12):1232–1236, 2019. https://doi.org/10.1038/s41567-019-0652-z.

[32] J. Li, A. K. Harter, J. Liu, et al. Observation of parity-time symmetry breaking transitions in a dissipative Floquet system of ultracold atoms. *Nature Communications* **10**(1):855, 2019. https://doi.org/10.1038/s41467-019-08596-1.

[33] F. Klauck, L. Teuber, M. Ornigotti, et al. Observation of $\mathcal{PT}$-symmetric quantum interference. *Nature Photonics* **13**(12):883–887, 2019. https://doi.org/10.1038/s41566-019-0517-0.

[34] F. Ruzicka, K. S. Agarwal, Y. N. Joglekar. Conserved quantities, exceptional points, and antilinear symmetries in non-Hermitian systems. *Journal of Physics: Conference Series* **2038**(1):012021, 2021. https://doi.org/10.1088/1742-6596/2038/1/012021.

[35] Z. Bian, L. Xiao, K. Wang, et al. Conserved quantities in parity-time symmetric systems. *Physical Review Research* **2**(2), 2020. https://doi.org/10.1103/physrevresearch.2.022039.

[36] M. V. Berry. Optical lattices with PT symmetry are not transparent. *Journal of Physics A: Mathematical and Theoretical* **41**(24):244007, 2008. https://doi.org/10.1088/1751-8113/41/24/244007.

[37] M. H. Teimourpour, R. El-Ganainy, A. Eisfeld, et al. Light transport in $\mathcal{PT}$-invariant photonic structures with hidden symmetries. *Physical Review A* **90**:053817, 2014. https://doi.org/10.1103/PhysRevA.90.053817.

[38] V. Gorini, A. Kossakowski, E. C. G. Sudarshan. Completely positive dynamical semigroups of N-level systems. *Journal of Mathematical Physics* **17**(5):821–825, 1976. https://doi.org/10.1063/1.522979.

[39] G. Lindblad. On the generators of quantum dynamical semigroups. *Communications in Mathematical Physics* **48**(2):119–130, 1976. https://doi.org/10.1007/BF01608499.

[40] M. Ban. Lie-algebra methods in quantum optics: The Liouville-space formulation. *Physical Review A* **47**(6):5093–5119, 1993. https://doi.org/10.1103/physreva.47.5093.

[41] V. V. Albert, L. Jiang. Symmetries and conserved quantities in Lindblad master equations. *Physical Review A* **89**:022118, 2014. https://doi.org/10.1103/PhysRevA.89.022118.

[42] D. Manzano. A short introduction to the Lindblad master equation. *AIP Advances* **10**(2):025106, 2020. https://doi.org/10.1063/1.5115323.

[43] J. Gunderson, J. Muldoon, K. W. Murch, Y. N. Joglekar. Floquet exceptional contours in Lindblad dynamics with time-periodic drive and dissipation. *Physical Review A* **103**:023718, 2021. https://doi.org/10.1103/PhysRevA.103.023718.

[44] Y. N. Joglekar, R. Marathe, P. Durganandini, R. K. Pathak. $\mathcal{PT}$ spectroscopy of the Rabi problem. *Physical Review A* **90**(4):040101, 2014. https://doi.org/10.1103/physreva.90.040101.

[45] T. E. Lee, Y. N. Joglekar. $\mathcal{PT}$-symmetric Rabi model: Perturbation theory. *Physical Review A* **92**:042103, 2015. https://doi.org/10.1103/PhysRevA.92.042103.

[46] P. Hänggi. *Driven quantum systems*, 1998. [2020-10-31], https://www.physik.uni-augsburg.de/theo1/hanggi/Chapter_5.pdf.

[47] A. K. Harter, Y. N. Joglekar. Connecting active and passive $\mathcal{PT}$-symmetric Floquet modulation models. *Progress of Theoretical and Experimental Physics* **2020**(12):12A106, 2020. https://doi.org/10.1093/ptep/ptaa181.

[48] P. Peng, W. Cao, C. Shen, et al. Anti-parity–time symmetry with flying atoms. *Nature Physics* **12**(12):1139–1145, 2016. https://doi.org/10.1038/nphys3842.

[49] Y. Choi, C. Hahn, J. W. Yoon, S. H. Song. Observation of an anti-PT-symmetric exceptional point and energy-difference conserving dynamics in electrical circuit resonators. *Nature Communications* **9**(1), 2018. https://doi.org/10.1038/s41467-018-04690-y.

[50] F. Zhang, Y. Feng, X. Chen, et al. Synthetic anti-PT symmetry in a single microcavity. *Physical Review Letters* **124**:053901, 2020. https://doi.org/10.1103/PhysRevLett.124.053901.

[51] S. Longhi, E. Pinotti. Anyonic $\mathcal{PT}$ symmetry, drifting potentials and non-Hermitian delocalization. *EPL (Europhysics Letters)* **125**(1):10006, 2019. https://doi.org/10.1209/0295-5075/125/10006.

[52] G. Arwas, S. Gadasi, I. Gershenzon, et al. Anyonic Parity-Time symmetric laser, 2021. arXiv:2103.15359.

QUANTUM DESCRIPTION OF ANGLES IN THE PLANE

Roberto Beneduci[a], Emmanuel Frion[b], Jean-Pierre Gazeau[c,*]

[a] *Università della Calabria and Istituto Nazionale di Fisica Nucleare, Gruppo c. Cosenza, 87036 Arcavacata di Rende (Cs), Italy*

[b] *University of Helsinki, Helsinki Institute of Physics, P. O. Box 64, FIN-00014 Helsinki, Finland*

[c] *Université de Paris, CNRS, Astroparticule et Cosmologie, 75013 Paris, France*

[*] corresponding author: gazeau@apc.in2p3.fr

Abstract.

The real plane with its set of orientations or angles in $[0, \pi)$ is the simplest non trivial example of a (projective) Hilbert space and provides nice illustrations of quantum formalism. We present some of them, namely covariant integral quantization, linear polarisation of light as a quantum measurement, interpretation of entanglement leading to the violation of Bell inequalities, and spin one-half coherent states viewed as two entangled angles.

Keywords: Integral quantization, real Hilbert spaces, quantum entanglement.

1. Introduction

The formulation of quantum mechanics in a real Hilbert space has been analyzed by Stueckelberg in 1960 [1] in order to show that the need for a complex Hilbert space is connected to the uncertainty principle. Later, Solèr [2] showed that the lattice of elementary propositions is isomorphic to the lattice of closed subspaces of a separable Hilbert space (over the reals, the complex numbers or the quaternions). In other words, the lattice structure of propositions in quantum physics does not suggest the Hilbert space to be complex. More recently, Moretti and Oppio [3] gave stronger motivation for the Hilbert space to be complex which rests on the symmetries of elementary relativistic systems.

In this contribution, we do not address the question of the physical validity of the real Hilbert space formulation of quantum mechanics but limit ourselves to use the real 2-dimensional case, i.e. the Euclidean plane, as a toy model for illustrating some aspects of the quantum formalism, as quantization, entanglement and quantum measurement. The latter is nicely represented by the linear polarization of light. This real 2-dimensional case relies on the manipulation of the two real Pauli matrices

$$\sigma_1 = \begin{pmatrix} 0 & 1 \\ 1 & 0 \end{pmatrix}, \quad \sigma_3 = \begin{pmatrix} 1 & 0 \\ 0 & -1 \end{pmatrix}, \tag{1}$$

and their tensor products, with no mention of the third, complex matrix $\sigma_2 = \begin{pmatrix} 0 & -\mathrm{i} \\ \mathrm{i} & 0 \end{pmatrix}$. As a matter of fact, many examples aimed to illustrate tools and concepts of quantum information, quantum measurement, quantum foundations, ... (e.g., Peres [4]) are illustrated with manipulations of these matrices.

In [5], it was shown that the set of pure states in the plane is represented by half of the unit circle and the set of mixed states by half the unit disk, and also that rotations in the plane rule time evolution through Majorana-like equations, all of this using only real quantities for both closed and open systems.

This paper is a direct extension of our previous paper [6], and for this reason we start the discussion by recalling some key elements of the mathematical formalism.

2. Background

2.1. Definition of POVMs

We start with the definition of a normalized Positive-Operator Valued measure (POVM) [7]. It is defined as a map $F : \mathcal{B}(\Omega) \to \mathcal{L}_s^+(\mathcal{H})$ from the Borel σ-algebra of a topological space Ω to the space of linear positive self-adjoint operators on a Hilbert space $\mathcal{H}$ such that

$$F\left(\bigcup_{n=1}^{\infty} \Delta_n\right) = \sum_{n=1}^{\infty} F(\Delta_n) \quad F(\Omega) = \mathbb{1}\,. \tag{2}$$

In this definition, $\{\Delta_n\}$ is a countable family of disjoint sets in $\mathcal{B}(\Omega)$ and the series converges in the weak operator topology. If $\Omega = \mathbb{R}$, we have a real POVM. If $F(\Delta)$ is a projection operator for every $\Delta \in \mathcal{B}(\Omega)$, we recover the usual projection-valued measure (PVM).

A quantum state is defined as a non-negative, bounded self-adjoint operator with trace 1. The space of states is a convex space and is denoted by $S(\mathcal{H})$. A quantum measurement corresponds to an affine map $S(\mathcal{H}) \mapsto \mathcal{M}_+(\Omega)$ from quantum states to probability measures, $\rho \mapsto \mu_\rho$. There is [8] a one-to-one correspondence between POVMs $F : \mathcal{B}(\Omega) \to \mathcal{L}_s^+(\mathcal{H})$ and affine maps $S(\mathcal{H}) \mapsto \mathcal{M}_+(\Omega)$ given by $\mu_\rho(\Delta) = \mathrm{Tr}(\rho F(\Delta))$, $\Delta \in \mathcal{B}(\Omega)$.

2.2. Integral quantization

Quantum mechanics is usually taught in terms of projection operators and PVM, but measurements usually

give a statistical distribution around a mean value, incompatible with the theory. We recall here a generalization of a quantization procedure, the *integral quantization*, based on POVMs instead of PVM. The basic requirements of this programme are the following: the quantization of a classical function defined on a set X must respect

(1.) *Linearity.* Quantization is a linear map $f \mapsto A_f$:

$$\mathfrak{Q} : \mathcal{C}(X) \mapsto \mathcal{A}(\mathcal{H}) , \qquad \mathfrak{Q}(f) = A_f , \qquad (3)$$

where

- $\mathcal{C}(X)$ is a vector space of complex or real-valued functions $f(x)$ on a set X, i.e. a "classical" mathematical model,
- $\mathcal{A}(\mathcal{H})$ is a vector space of linear operators in some real or complex Hilbert space $\mathcal{H}$, i.e., a "quantum" mathematical model, notwithstanding the question of common domains in the case of unbounded operators.

(2.) *Unity.* The map (3) is such that the function $f = 1$ is mapped to the identity operator $\mathbb{1}$ on $\mathcal{H}$.

(3.) *Reality.* A real function f is mapped to a self-adjoint or normal operator A_f in $\mathcal{H}$ or, at least, a symmetric operator (in the infinite-dimensional case).

(4.) *Covariance.* Defining the action of a symmetry group G on X by $(g, x) \in G \times X$ such as $(g, x) \mapsto g \cdot x \in X$, there is a unitary representation U of G such that $A_{T(g)f} = U(g) A_f U(g^{-1})$, with $(T(g)f)(x) = f\left(g^{-1} \cdot x\right)$.

Performing the integral quantization [9] of a function $f(x)$ on a measure space (X, ν) boils down to the linear map:

$$f \mapsto A_f = \int_X \mathsf{M}(x)\, f(x)\, \mathrm{d}\nu(x) , \qquad (4)$$

where we introduce a family of operators $\mathsf{M}(x)$ solving the identity. More precisely, we have

$$X \ni x \mapsto \mathsf{M}(x) , \quad \int_X \mathsf{M}(x)\, \mathrm{d}\nu(x) = \mathbb{1} . \qquad (5)$$

If the $\mathsf{M}(x)$ are non-negative, they provide a POVM. Indeed, the quantization of the characteristic function on the Borel set Δ, $A(\chi_\Delta)$,

$$F(\Delta) := A(\chi_\Delta) = \int_\Delta \mathsf{M}(x)\, \mathrm{d}\nu(x) . \qquad (6)$$

is a POVM which provides a quantization procedure

$$f \mapsto A_f = \int_X f(x)\, dF(x).$$

3. Euclidean plane as Hilbert space of quantum states

3.1. Mixed states as density matrices

Density matrices act as a family of operators which can be used to perform covariant integral quantization.

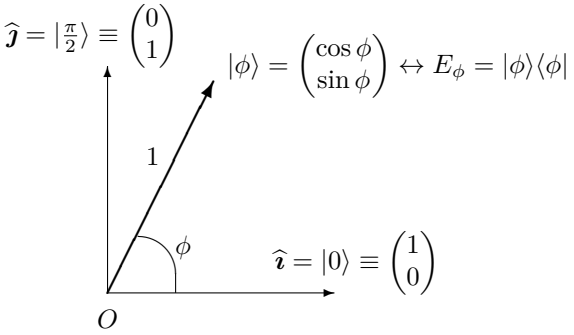

$$\langle 0|0\rangle = 1 = \left\langle \tfrac{\pi}{2} \middle| \tfrac{\pi}{2} \right\rangle , \quad \left\langle 0 \middle| \tfrac{\pi}{2} \right\rangle = 0$$

FIGURE 1. The Euclidean plane and its unit vectors viewed as pure quantum states in Dirac ket notations.

In the context of the Euclidean plane and its rotational symmetry, one associates the polar angle $\phi \in [0, 2\pi)$ with the unit vector $\widehat{\mathbf{u}}_\phi$ to define the pure state $|\phi\rangle := |\widehat{\mathbf{u}}_\phi\rangle$.

As shown in Figure 1, two orthogonal pure states $\widehat{\boldsymbol{\imath}} = |0\rangle$ and $\widehat{\boldsymbol{\jmath}} = \left|\frac{\pi}{2}\right\rangle$ are readily identified with the unit vectors spanning the plane. In this configuration, the pure state $|\phi\rangle$ is defined by an anticlockwise rotation of angle ϕ of the pure state $|0\rangle$. Denoting the orthogonal projectors on $\widehat{\boldsymbol{\imath}}$ and $\widehat{\boldsymbol{\jmath}}$ by $|0\rangle\langle 0|$ and $\left|\frac{\pi}{2}\right\rangle \left\langle \frac{\pi}{2}\right|$ respectively, we visualize the resolution of the identity as follows

$$\begin{gathered} \mathbb{1} = |0\rangle\langle 0| + \left|\frac{\pi}{2}\right\rangle \left\langle \frac{\pi}{2}\right| \\ \Updownarrow \\ \begin{pmatrix} 1 & 0 \\ 0 & 1 \end{pmatrix} = \begin{pmatrix} 1 & 0 \\ 0 & 0 \end{pmatrix} + \begin{pmatrix} 0 & 0 \\ 0 & 1 \end{pmatrix} . \end{gathered} \qquad (7)$$

Recalling that a pure state in the plane, equivalently an orientation, can be decomposed as $|\phi\rangle = \cos\phi\, |0\rangle + \sin\phi\, \left|\frac{\pi}{2}\right\rangle$, with $\langle 0|\phi\rangle = \cos\phi$ and $\left\langle \frac{\pi}{2} \middle| \phi \right\rangle = \sin\phi$, it is straightforward to find the orthogonal projector corresponding to the pure state $|\phi\rangle$,

$$E_\phi = \begin{pmatrix} \cos^2\phi & \cos\phi\sin\phi \\ \cos\phi\sin\phi & \sin^2\phi \end{pmatrix} , \qquad (8)$$

from which we can construct the density matrix corresponding to all the mixed states

$$\rho = \left(\frac{1+r}{2}\right) E_\phi + \left(\frac{1-r}{2}\right) E_{\phi+\pi/2} , \quad 0 \le r \le 1 . \qquad (9)$$

In this expression, the parameter r represents the degree of mixing. Hence the upper half-disk (r, ϕ), $0 \le r \le 1$, $0 \le \phi < \pi$ is in one-to-one correspondence

with the set of density matrices $\rho \equiv \rho_{r,\phi}$ written as

$$\rho_{r,\phi} = \frac{1}{2}\mathbb{1} + \frac{r}{2}\mathcal{R}(\phi)\sigma_3\mathcal{R}(-\phi) = \begin{pmatrix} \frac{1}{2} + \frac{r}{2}\cos 2\phi & \frac{r}{2}\sin 2\phi \\ \frac{r}{2}\sin 2\phi & \frac{1}{2} - \frac{r}{2}\cos 2\phi \end{pmatrix} = \frac{1}{2}\left(\mathbb{1} + r\sigma_{2\phi}\right), \tag{10}$$

where $\mathcal{R}(\phi) = \begin{pmatrix} \cos\phi & -\sin\phi \\ \sin\phi & \cos\phi \end{pmatrix}$ is a rotation matrix in the plane, and

$$\sigma_\phi := \cos\phi\,\sigma_3 + \sin\phi\,\sigma_1 \equiv \overrightarrow{\boldsymbol{\sigma}}\cdot\widehat{\mathbf{u}}_\phi = \begin{pmatrix} \cos\phi & \sin\phi \\ \sin\phi & -\cos\phi \end{pmatrix} = \mathcal{R}(\phi)\,\sigma_3\,. \tag{11}$$

The observable σ_ϕ has eigenvalues $\{\pm 1\}$ and eigenvectors $\left|\frac{\phi}{2}\right\rangle$ and $\left|\frac{\phi+\pi}{2}\right\rangle$ respectively. It plays a crucial rôle since, as we show right after, it is at the core of both the non-commutative character and the entanglement of two quantum states of the real space. It is a typical observable used to illustrate quantum formalism [4].

3.2. Describing non-commutativity and finding Naimark extensions through rotations

Let us apply integral quantization with the real density matrices (10). With $X = \mathbb{S}^1$, the unit circle, equipped with the measure $\mathrm{d}\nu(x) = \frac{\mathrm{d}\phi}{\pi}$, $\phi \in [0, 2\pi)$, we obtain the resolution of the identity for an arbitrary ϕ_0,

$$\int_0^{2\pi} \rho_{r,\phi+\phi_0}\,\frac{\mathrm{d}\phi}{\pi} = \mathbb{1}\,. \tag{12}$$

Hence, quantizing a function (or distribution) $f(\phi)$ on the circle is done through the map

$$f \mapsto A_f = \int_0^{2\pi} f(\phi)\rho_{r,\phi+\phi_0}\,\frac{\mathrm{d}\phi}{\pi} = \begin{pmatrix} \langle f\rangle + \frac{r}{2}C_c\left(R_{\phi_0}f\right) & \frac{r}{2}C_s\left(R_{\phi_0}f\right) \\ \frac{r}{2}C_s\left(R_{\phi_0}f\right) & \langle f\rangle - \frac{r}{2}C_c\left(R_{\phi_0}f\right) \end{pmatrix} = \langle f\rangle\,\mathbb{1} + \frac{r}{2}\left[C_c\left(R_{\phi_0}f\right)\,\sigma_3 + C_s\left(R_{\phi_0}f\right)\,\sigma_1\right], \tag{13}$$

with $\langle f\rangle := \frac{1}{2\pi}\int_0^{2\pi} f(\phi)\,\mathrm{d}\phi$ the average of f on the unit circle and $R_{\phi_0}(f)(\phi) := f(\phi - \phi_0)$. Here we have defined cosine and sine doubled angle Fourier coefficients of f

$$C_{\substack{c\\ s}}(f) = \int_0^{2\pi} f(\phi)\left\{\begin{array}{c}\cos\\ \sin\end{array}\right. 2\phi\,\frac{\mathrm{d}\phi}{\pi}\,. \tag{14}$$

In [6], we drew three consequences from this result. The first consequence is that, upon identification of $\mathbb{R}^3$ with the subspace $V_3 = \mathrm{Span}\Big\{e_0(\phi) := \frac{1}{\sqrt{2}}, e_1(\phi) := \cos 2\phi, e_2(\phi) := \sin 2\phi\Big\}$ in $L^2(\mathbb{S}^1, \mathrm{d}\phi/\pi)$, the integral quantization map with $\rho_{r,\phi+\phi_0}$ yields a non-commutative version of $\mathbb{R}^3$:

$$A_{e_0} = \frac{\mathbb{1}}{\sqrt{2}}\,,$$
$$A_{e_1} = \frac{r}{2}[\cos 2\phi_0\,\sigma_3 + \sin 2\phi_0\,\sigma_1] \equiv \frac{r}{2}\sigma_{2\phi_0}\,,$$
$$A_{e_2} = \frac{r}{2}[-\sin 2\phi_0\,\sigma_3 + \cos 2\phi_0\,\sigma_1] \equiv \frac{r}{2}\sigma_{2\phi_0+\pi/2}\,.$$

Now, the commutation rule reads

$$[A_{e_1}, A_{e_2}] = -\frac{r^2}{2}\tau_2\,, \quad \tau_2 := \begin{pmatrix} 0 & -1 \\ 1 & 0 \end{pmatrix} = -\mathrm{i}\sigma_2\,,$$

which depends on the real version of the last Pauli matrix and on the degree of mixing.

A second consequence, typical of quantum-mechanical ensembles, is that all functions $f(\phi)$ in V_3 yielding density matrices through this map imply that

$$\rho_{s,\theta} = \int_0^{2\pi} \underbrace{\left[\frac{1}{2} + \frac{s}{r}\,\cos 2\phi\right]}_{f(\phi)} \rho_{r,\phi+\theta}\,\frac{\mathrm{d}\phi}{\pi}\,. \tag{15}$$

If $r \geq 2s$, this continuous superposition of mixed states is convex. Therefore, a mixed state is composed of an infinite number of other mixed states. This has consequences in quantum cryptography, for example, since the initial signal cannot be recovered from the output.

The third and last consequence we mention here concerns the Naimark extension of a function defined on the circle. In particular, we focus on the Toeplitz quantization of $f(\phi)$, which is a kind of integral quantization. In [6], we used this framework to show there exist orthogonal projectors from $L^2(\mathbb{S}^1, \mathrm{d}\phi/\pi)$ to $\mathbb{R}^2$ such that for a function $f(\phi)$ the multiplication operator on $L^2(\mathbb{S}^1, \mathrm{d}\phi/\pi)$, defined by

$$v \mapsto M_f v = fv\,, \tag{16}$$

maps M_f to A_f. They are precisely Naimark's extensions of POVMs represented by density matrices (see [6] for details).

3.3. Linear polarization of light as a quantum phenomenon

In this section, we recall that the polarization tensor of light can be expressed as a density matrix, which allows us to relate the polarization of light to quantum phenomena such as the Malus Law and the incompatibility between two sequential measurements [6].

First, remember that a complex-valued electric field for a propagating quasi-monochromatic electromagnetic wave along the z-axis reads as

$$\overrightarrow{\mathcal{E}}(t) = \overrightarrow{\mathcal{E}_0}(t)\,e^{\mathrm{i}\omega t} = \mathcal{E}_x\,\widehat{\boldsymbol{\imath}} + \mathcal{E}_y\,\widehat{\boldsymbol{\jmath}} = (\mathcal{E}_\alpha)\,, \tag{17}$$

in which we have used the previous notations for the unit vectors in the plane. The polarization is determined by $\overrightarrow{\mathcal{E}_0}(t)$. It slowly varies with time, and can be

measured through Nicol prisms, or other devices, by measuring the intensity of the light yielded by mean values $\propto \mathcal{E}_\alpha \mathcal{E}_\beta$, $\mathcal{E}_\alpha \mathcal{E}_\beta^*$ and conjugates. Due to rapidly oscillating factors and a null temporal average $\langle\cdot\rangle_t$, a partially polarized light is described by the 2×2 Hermitian matrix (Stokes parameters) [10–12]

$$\frac{1}{J}\begin{pmatrix} \langle \mathcal{E}_{0x}\mathcal{E}_{0x}^*\rangle_t & \langle \mathcal{E}_{0x}\mathcal{E}_{0y}^*\rangle_t \\ \langle \mathcal{E}_{0y}\mathcal{E}_{0x}^*\rangle_t & \langle \mathcal{E}_{0y}\mathcal{E}_{0y}^*\rangle_t \end{pmatrix} \equiv \rho_{r,\phi} + \frac{A}{2}\sigma_2 = \frac{1+r}{2}E_\phi + \frac{1-r}{2}E_{\phi+\pi/2} + \mathrm{i}\frac{A}{2}\tau_2\,.$$

Here, J describes the intensity of the wave. In the second line, it is clear that the degree of mixing r describes linear polarization, while the parameter A ($-1 \le A \le 1$) is related to circular polarization. In real space, we have $A = 0$, so we effectively describe the linear polarization of light.

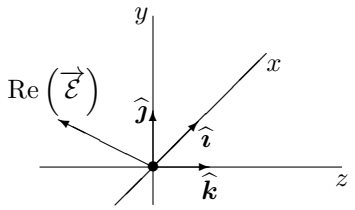

We now wish to describe the interaction between a polarizer and a partially linear polarized light as a quantum measurement. We need to introduce two planes and their tensor product: the first one is the Hilbert space on which act the states $\rho^M_{s,\theta}$ of the polarizer viewed as an orientation *pointer*. Note that the action of the generator of rotations $\tau_2 = -\mathrm{i}\sigma_2$ on these states corresponds to a $\pi/2$ rotation :

$$\tau_2 \rho^M_{s,\theta}\tau_2^{-1} = -\tau_2\rho^M_{s,\theta}\tau_2 = \rho^M_{s,\theta+\pi/2}\,. \tag{18}$$

The second plane is the Hilbert space on which act the partially linearized polarization states $\rho^L_{r,\phi}$ of the plane wave crossing the polarizer. Its spectral decomposition corresponds to the incoherent superposition of two completely linearly polarized waves

$$\rho^L_{r,\phi} = \frac{1+r}{2}\,E_\phi + \frac{1-r}{2}\,E_{\phi+\pi/2}\,. \tag{19}$$

The pointer detects an orientation in the plane determined by the angle ϕ. Through the interaction pointer-system, we generate a measurement whose time duration is the interval $I_M = (t_M - \eta, t_M + \eta)$ centred at t_M. The interaction is described by the (pseudo-) Hamiltonian operator

$$\widetilde{H}_{\mathrm{int}}(t) = g^\eta_M(t)\tau_2 \otimes \rho^L_{r,\phi}\,, \tag{20}$$

where g^η_M is a Dirac sequence with support in I_M, i.e.,

$$\lim_{\eta\to 0}\int_{-\infty}^{+\infty} \mathrm{d}t\, f(t)\, g^\eta_M(t) = f(t_M)\,.$$

The interaction (20) is the tensor product of an antisymmetric operator for the pointer with an operator for the system which is symmetric (i.e., Hamiltonian). The operator defined for $t_0 < t_M - \eta$ as

$$U(t,t_0) = \exp\left[\int_{t_0}^t \mathrm{d}t'\, g^\eta_M(t')\,\tau_2 \otimes \rho^L_{r,\phi}\right] = \exp\left[G^\eta_M(t)\,\tau_2 \otimes \rho^L_{r,\phi}\right]\,, \tag{21}$$

with $G^\eta_M(t) = \int_{t_0}^t \mathrm{d}t'\; g^\eta_M(t')$, is a **unitary evolution operator**. From the formula involving an orthogonal projector P,

$$\exp(\theta\tau_2 \otimes P) = \mathcal{R}(\theta)\otimes P + \mathbb{1}\otimes(\mathbb{1}-P)\,, \tag{22}$$

we obtain

$$U(t,t_0) = \mathcal{R}\left(G^\eta_M(t)\,\frac{1+r}{2}\right)\otimes E_\phi + \mathcal{R}\left(G^\eta_M(t)\,\frac{1-r}{2}\right)\otimes E_{\phi+\pi/2}\,. \tag{23}$$

For $t_0 < t_M - \eta$ and $t > t_M + \eta$, we finally obtain

$$U(t,t_0) = \mathcal{R}\left(\frac{1+r}{2}\right)\otimes E_\phi + \mathcal{R}\left(\frac{1-r}{2}\right)\otimes E_{\phi+\pi/2}\,. \tag{24}$$

Preparing the polarizer in the state $\rho^M_{s_0,\theta_0}$, we obtain the evolution $U(t,t_0)\,\rho^M_{s_0,\theta_0}\otimes\rho^L_{r_0,\phi_0}\,U(t,t_0)^\dagger$ of the initial state for $t > t_M + \eta$

$$\begin{aligned} &\rho^M_{s_0,\theta_0+\frac{1+r}{2}}\otimes\frac{1+r_0\cos 2(\phi-\phi_0)}{2}\,E_\phi \\ &+\rho^M_{s_0,\theta_0+\frac{1-r}{2}}\otimes\frac{1-r_0\cos 2(\phi-\phi_0)}{2}\,E_{\phi+\pi/2} \\ &+\frac{1}{4}\left(\mathcal{R}(r)+s_0\sigma_{2\theta_0+1}\right)\otimes r_0\sin 2(\phi-\phi_0)\,E_\phi\tau_2 \\ &-\frac{1}{4}\left(\mathcal{R}(-r)+s_0\sigma_{2\theta_0+1}\right)\otimes r_0\sin 2(\phi-\phi_0)\,\tau_2 E_\phi\,. \end{aligned} \tag{25}$$

Therefore, the probability for the pointer to rotate by $\frac{1+r}{2}$, corresponding to the polarization along the orientation ϕ is

$$\mathrm{Tr}\left[\left(U(t,t_0)\,\rho^M_{s_0,\theta_0}\otimes\rho^L_{r_0,\phi_0}\,U(t,t_0)^\dagger\right)(\mathbb{1}\otimes E_\phi)\right] = \frac{1+r_0\cos 2(\phi-\phi_0)}{2}\,, \tag{26}$$

that for the completely linear polarization of the light, i.e. $r_0 = 1$, becomes the familiar Malus law, $\cos^2(\phi-\phi_0)$. Similarly, the second term gives the probability for the perpendicular orientation $\phi+\pi/2$ and the pointer rotation by $\frac{1-r}{2}$

$$\mathrm{Tr}\left[\left(U(t,t_0)\,\rho^M_{s_0,\theta_0}\otimes\rho^L_{r_0,\phi_0}\,U(t,t_0)^\dagger\right)\left(\mathbb{1}\otimes E_{\phi+\pi/2}\right)\right] = \frac{1-r_0\cos 2(\phi-\phi_0)}{2}\,, \tag{27}$$

corresponding (in the case $r_0 = 1$) to the Malus law $\sin^2(\phi-\phi_0)$.

4. ENTANGLEMENT AND ISOMORPHISMS

In this section, we develop our previous results further by giving an interpretation in terms of quantum entanglement. Previously, we described the interaction between a polarizer and a light ray as the tensor product (20), which is analogous to the quantum entanglement of states, since it is a logical consequence of the construction of tensor products of Hilbert spaces for describing quantum states of composite system. In the present case, we are in presence of a remarkable sequence of vector space isomorphisms due to the fact that $2 \times 2 = 2 + 2$ [1] :

$$\mathbb{R}^2 \otimes \mathbb{R}^2 \cong \mathbb{R}^2 \times \mathbb{R}^2 \cong \mathbb{R}^2 \oplus \mathbb{R}^2 \cong \mathbb{C}^2 \cong \mathbb{H}\,, \quad (28)$$

where $\mathbb{H}$ is the field of quaternions. Therefore, the description of the entanglement in a real Hilbert space is equivalent to the description of a single system (e.g., a spin 1/2) in the complex Hilbert space $\mathbb{C}^2$, or in $\mathbb{H}$. In Section 4.3 we develop such an observation.

4.1. BELL STATES AND QUANTUM CORRELATIONS

It is straightforward to transpose into the present setting the 1964 analysis and result presented by Bell in his discussion about the EPR paper [13] and about the subsequent Bohm's approaches based on the assumption of hidden variables [14]. We only need to replace the Bell spin one-half particles with the horizontal (i.e., $+1$) and vertical (i.e., -1) quantum orientations in the plane as the only possible issues of the observable σ_ϕ (11), supposing that there exists a pointer device designed for measuring such orientations with outcomes ± 1 only.

In order to define Bell states and their quantum correlations, let us first write the canonical, orthonormal basis of the tensor product $\mathbb{R}^2_A \otimes \mathbb{R}^2_B$, the first factor being for system "A" and the other for system "B", as

$$\begin{aligned} &|0\rangle_A \otimes |0\rangle_B\,, \quad \left|\frac{\pi}{2}\right\rangle_A \otimes \left|\frac{\pi}{2}\right\rangle_B\,, \\ &|0\rangle_A \otimes \left|\frac{\pi}{2}\right\rangle_B\,, \quad \left|\frac{\pi}{2}\right\rangle_A \otimes |0\rangle_B\,. \end{aligned} \quad (29)$$

The states $|0\rangle$ and $\left|\frac{\pi}{2}\right\rangle$ pertain to A or B, and are named "q-bit" or "qubit" in the standard language of quantum information. Since they are pure states, they can be associated to a pointer measuring the horizontal (resp. vertical) direction or polarisation described by the state $|0\rangle$ (resp. $\left|\frac{\pi}{2}\right\rangle$).

There are four Bell pure states in $\mathbb{R}^2_A \otimes \mathbb{R}^2_B$, namely

$$|\Phi^\pm\rangle = \frac{1}{\sqrt{2}}\left(|0\rangle_A \otimes |0\rangle_B \pm \left|\frac{\pi}{2}\right\rangle_A \otimes \left|\frac{\pi}{2}\right\rangle_B\right)\,, \quad (30)$$

$$|\Psi^\pm\rangle = \frac{1}{\sqrt{2}}\left(\pm|0\rangle_A \otimes \left|\frac{\pi}{2}\right\rangle_B + \left|\frac{\pi}{2}\right\rangle_A \otimes |0\rangle_B\right)\,. \quad (31)$$

[1] Remind that $\dim(V \otimes W) = \dim V \dim W$ while $\dim(V \times W) = \dim V + \dim W$ for 2 finite-dimensional vector spaces V and W

We say that they represent *maximally entangled* quantum states of two qubits. Consider for instance the state $|\Phi^+\rangle$. If the pointer associated to A measures its qubit in the standard basis, the outcome would be perfectly random, with either possibility having a probability 1/2. But if the pointer associated to B then measures its qubit instead, the outcome, although random for it alone, is the same as the one A gets. There is *quantum correlation*.

4.2. BELL INEQUALITY AND ITS VIOLATION

Let us consider a bipartite system in the state Ψ^-. In such a state, if a measurement of the component $\sigma^A_{\phi_a} := \overrightarrow{\boldsymbol{\sigma}}^A \cdot \widehat{\mathbf{u}}_{\phi_a}$ ($\widehat{\mathbf{u}}_{\phi_a}$ is an unit vector with polar angle ϕ_a) yields the value $+1$ (polarization along the direction $\phi_a/2$), then a measurement of $\sigma^B_{\phi_b}$ when $\phi_b = \phi_a$ must yield the value -1 (polarization along the direction $\frac{\phi_a+\pi}{2}$), and vice-versa. From a classical perspective, the explanation of such a correlation needs a predetermination by means of the existence of *hidden* parameters λ in some set Λ. Assuming the two measurements to be separated by a space-like interval, the result $\varepsilon^A \in \{-1, +1\}$ (resp. $\varepsilon^B \in \{-1, +1\}$) of measuring $\sigma^A_{\phi_a}$ (resp. $\sigma^B_{\phi_b}$) is then determined by ϕ_a and λ only (locality assumption), not by ϕ_b, i.e. $\varepsilon^A = \varepsilon^A(\phi_a, \lambda)$ (resp. $\varepsilon^B = \varepsilon^B(\phi_b, \lambda)$). Given a probability distribution $\rho(\lambda)$ on Λ, the **classical** expectation value of the product of the two components $\sigma^A_{\phi_a}$ and $\sigma^B_{\phi_b}$ is given by

$$\mathsf{P}(\phi_a, \phi_b) = \int_\Lambda \mathrm{d}\lambda\, \rho(\lambda)\, \varepsilon^A(\phi_a, \lambda)\, \varepsilon^B(\phi_b, \lambda)\,. \quad (32)$$

Since

$$\int_\Lambda \mathrm{d}\lambda\, \rho(\lambda) = 1 \quad \text{and} \quad \varepsilon^{A,B} = \pm 1\,, \quad (33)$$

we have $-1 \leq \mathsf{P}(\phi_a, \phi_b) \leq 1$. Equivalent predictions **within the quantum setting** then imposes the equality between the classical and quantum expectation values:

$$\begin{aligned} \mathsf{P}(\phi_a, \phi_b) &= \left\langle \Psi^- \right| \sigma^A_{\phi_a} \otimes \sigma^B_{\phi_b} \left| \Psi^- \right\rangle \\ &= -\widehat{\mathbf{u}}_{\phi_a} \cdot \widehat{\mathbf{u}}_{\phi_b} = -\cos(\phi_a - \phi_b)\,. \end{aligned} \quad (34)$$

In the above equation, the value -1 is reached at $\phi_a = \phi_b$. This is possible for $\mathsf{P}(\phi_a, \phi_a)$ only if $\varepsilon^A(\phi_a, \lambda) = -\varepsilon^B(\phi_a, \lambda)$. Hence, we can write $\mathsf{P}(\phi_a, \phi_b)$ as

$$\begin{aligned} \mathsf{P}(\phi_a, \phi_b) &= -\int_\Lambda \mathrm{d}\lambda\, \rho(\lambda)\, \varepsilon(\phi_a, \lambda)\, \varepsilon(\phi_b, \lambda)\,, \\ \varepsilon(\phi, \lambda) &\equiv \varepsilon^A(\phi, \lambda) = \pm 1\,. \end{aligned} \quad (35)$$

Let us now introduce a third unit vector $\widehat{\mathbf{u}}_{\phi_c}$. Due to $\varepsilon^2 = 1$, we have

$$\begin{aligned} \mathsf{P}(\phi_a, \phi_b) - \mathsf{P}(\phi_a, \phi_c) = \int_\Lambda \mathrm{d}\lambda\, \rho(\lambda)\, \varepsilon(\phi_a, \lambda)\, \varepsilon(\phi_b, \lambda) \\ \times \left[\varepsilon(\phi_b, \lambda)\, \varepsilon(\phi_c, \lambda) - 1\right]\,. \end{aligned} \quad (36)$$

From this results the (baby) Bell inequality:

$$|\mathsf{P}(\phi_a,\phi_b)-\mathsf{P}(\phi_a,\phi_c)| \leq \int_\Lambda \mathrm{d}\lambda\,\rho(\lambda)\,[1-\varepsilon(\phi_b,\lambda)\,\varepsilon(\phi_c,\lambda)] = 1+\mathsf{P}(\phi_b,\phi_c)\,.$$

Hence, the validity of the existence of hidden variable(s) for justifying the quantum correlation in the singlet state Ψ^-, and which is encapsulated by the above equation, has the following consequence on the arbitrary triple (ϕ_a,ϕ_b,ϕ_c):

$$1-\cos(\phi_b-\phi_c)\geq|\cos(\phi_b-\phi_a)-\cos(\phi_c-\phi_a)|\,.$$

Equivalently, in terms of the two independent angles ζ and η,

$$\zeta=\frac{\phi_a-\phi_b}{2}\,,\quad \eta=\frac{\phi_b-\phi_c}{2}\,,$$

we have

$$\left|\sin^2\zeta-\sin^2(\eta+\zeta)\right|\leq\sin^2\eta\,. \tag{37}$$

It is easy to find pairs (ζ,η) for which the inequality (37) does not hold true. For instance with $\eta=\zeta\neq 0$, i.e.,

$$\phi_b=\frac{\phi_a+\phi_c}{2}\,,$$

we obtain

$$|4\sin^2\eta-3|\leq 1\,, \tag{38}$$

which does not hold true for all $|\eta|<\pi/4$, i.e., for $|\phi_a-\phi_b|=|\phi_b-\phi_c|<\pi/2$. Actually, we did not follow here the proof given by Bell, which is a lot more elaborate. Also, Bell considered unit vectors in 3-space. Restricting his proof to vectors in the plane does not make any difference, as it is actually the case in many works devoted to the foundations of quantum mechanics.

4.3. Entanglement of two angles

Quantum entanglement is usually described by the complex two-dimensional Hilbert space $\mathbb{C}^2$. As a complex vector space, $\mathbb{C}^2$, with canonical basis $(\mathbf{e}_1,\,\mathbf{e}_2)$, has a real structure, i.e., is isomorphic to a real vector space which makes it isomorphic to $\mathbb{R}^4$, itself isomorphic to $\mathbb{R}^2\otimes\mathbb{R}^2$. A **real** structure is obtained by considering the vector expansion

$$\begin{aligned}\mathbb{C}^2\ni\mathbf{v}&=z_1\mathbf{e}_1+z_2\mathbf{e}_2\\&=x_1\mathbf{e}_1+y_1\,(\mathrm{i}\mathbf{e}_1)+x_2\mathbf{e}_2+y_2\,(\mathrm{i}\mathbf{e}_2)\,,\end{aligned} \tag{39}$$

which is equivalent to writing $z_1=x_1+\mathrm{i}y_1$, $z_2=x_2+\mathrm{i}y_2$, and considering the set of vectors

$$\{\mathbf{e}_1,\mathbf{e}_2,(\mathrm{i}\mathbf{e}_1),(\mathrm{i}\mathbf{e}_2)\} \tag{40}$$

as forming a basis of $\mathbb{R}^4$. Forgetting about the subscripts A and B in (29), we can map vectors in the Euclidean plane $\mathbb{R}^2$ to the complex "plane" $\mathbb{C}$ by

$$|0\rangle\mapsto 1\,,\qquad \left|\frac{\pi}{2}\right\rangle\mapsto\mathrm{i}\,, \tag{41}$$

which allows the correspondence between bases as

$$\begin{aligned}&|0\rangle\otimes|0\rangle=\mathbf{e}_1\,,\quad \left|\frac{\pi}{2}\right\rangle\otimes\left|\frac{\pi}{2}\right\rangle=-\mathbf{e}_2\,,\\&|0\rangle\otimes\left|\frac{\pi}{2}\right\rangle=(\mathrm{i}\mathbf{e}_1)\,,\quad \left|\frac{\pi}{2}\right\rangle\otimes|0\rangle=(\mathrm{i}\mathbf{e}_2)\,.\end{aligned} \tag{42}$$

Also, the spin of a particle in a real basis, given by the "up" and "down" states, are defined by

$$\mathbf{e}_1\equiv|\uparrow\rangle\equiv\begin{pmatrix}1\\0\end{pmatrix}\,,\qquad \mathbf{e}_2\equiv|\downarrow\rangle\equiv\begin{pmatrix}0\\1\end{pmatrix}\,. \tag{43}$$

Finally, we obtain an unitary map from the Bell basis to the basis of real structure of $\mathbb{C}^2$

$$\begin{aligned}&\big(|\Phi^+\rangle\quad|\Phi^-\rangle\quad|\Psi^+\rangle\quad|\Psi^-\rangle\big)=\\&\big(\mathbf{e}_1\quad\mathbf{e}_2\quad(\mathrm{i}\mathbf{e}_1)\quad(\mathrm{i}\mathbf{e}_2)\big)\,\frac{1}{\sqrt{2}}\begin{pmatrix}1&1&0&0\\-1&1&0&0\\0&0&1&-1\\0&0&1&1\end{pmatrix}\,.\end{aligned}$$

In terms of respective components of vectors in their respective spaces, we have

$$\begin{pmatrix}x_1\\x_2\\y_1\\y_2\end{pmatrix}=\frac{1}{\sqrt{2}}\begin{pmatrix}1&1&0&0\\-1&1&0&0\\0&0&1&-1\\0&0&1&1\end{pmatrix}\begin{pmatrix}x^+\\x^-\\y^+\\y^-\end{pmatrix}\,. \tag{44}$$

In complex notations, with $z^\pm=x^\pm+\mathrm{i}y^\pm$, this is equivalent to

$$\begin{pmatrix}z^+\\z^-\end{pmatrix}=\frac{1}{\sqrt{2}}\begin{pmatrix}1&-\mathsf{C}\\\mathsf{C}&1\end{pmatrix}\begin{pmatrix}z_1\\z_2\end{pmatrix}\equiv\mathcal{C}_@\begin{pmatrix}z_1\\z_2\end{pmatrix}\,, \tag{45}$$

in which we have introduced the conjugation operator $\mathsf{C}z=\bar{z}$, i.e., the mirror symmetry with respect to the real axis, $-\mathsf{C}$ being the mirror symmetry with respect to the imaginary axis.

Let us now see what is the influence of having real Bell states on Schrödinger cat states. The operator "cat" $\mathcal{C}_@$ can be expressed as

$$\mathcal{C}_@=\frac{1}{\sqrt{2}}\,(\mathbb{1}+\mathsf{F})\,,\quad \mathsf{F}:=\mathsf{C}\tau_2=\begin{pmatrix}0&-\mathsf{C}\\\mathsf{C}&0\end{pmatrix}\,. \tag{46}$$

Therefore, with the above choice of isomorphisms, Bell entanglement in $\mathbb{R}^2\otimes\mathbb{R}^2$ is **not** represented by a simple linear superposition in $\mathbb{C}^2$. It involves also the two mirror symmetries $\pm\mathsf{C}$. The operator F is a kind of "flip" whereas the "cat" or "beam splitter" operator $\mathcal{C}_@$ builds, using the *up* and *down* basic states, the two elementary Schrödinger cats

$$\mathsf{F}\,|\uparrow\rangle=|\downarrow\rangle\,,\quad \mathcal{C}_@\,|\uparrow\rangle=\frac{1}{\sqrt{2}}(|\uparrow\rangle+|\downarrow\rangle)\,, \tag{47}$$

$$\mathsf{F}\,|\downarrow\rangle=-|\uparrow\rangle\,,\quad \mathcal{C}_@\,|\downarrow\rangle=\frac{1}{\sqrt{2}}(-|\uparrow\rangle+|\downarrow\rangle)\,. \tag{48}$$

The flip operator also appears in the construction of the spin one-half coherent states $|\theta,\phi\rangle$, defined in

terms of spherical coordinates (θ, ϕ) as the quantum counterpart of the classical state $\hat{\mathbf{n}}(\theta, \phi)$ in the sphere $\mathbb{S}^2$ by

$$|\theta, \phi\rangle = \left(\cos\frac{\theta}{2}\,|\uparrow\rangle + e^{\mathrm{i}\phi}\sin\frac{\theta}{2}\,|\downarrow\rangle\right) \equiv \begin{pmatrix}\cos\frac{\theta}{2}\\ e^{\mathrm{i}\phi}\sin\frac{\theta}{2}\end{pmatrix} = \begin{pmatrix}\cos\frac{\theta}{2} & -\sin\frac{\theta}{2}e^{-\mathrm{i}\phi}\\ \sin\frac{\theta}{2}e^{\mathrm{i}\phi} & \cos\frac{\theta}{2}\end{pmatrix}\begin{pmatrix}1\\0\end{pmatrix} \equiv D^{\frac{1}{2}}\left(\xi_{\hat{\mathbf{n}}}^{-1}\right)|\uparrow\rangle\,. \tag{49}$$

Here, $\xi_{\hat{\mathbf{n}}}$ corresponds, through the homomorphism $\mathrm{SO}(3) \mapsto \mathrm{SU}(2)$, to the specific rotation $\mathcal{R}_{\hat{\mathbf{n}}}$ mapping the unit vector pointing to the north pole, $\hat{\boldsymbol{k}} = (0, 0, 1)$, to $\hat{\mathbf{n}}$. The operator $D^{\frac{1}{2}}\left(\xi_{\hat{\mathbf{n}}}^{-1}\right)$ represents the element $\xi_{\hat{\mathbf{n}}}^{-1}$ of SU(2) in its complex two-dimensional unitary irreducible representation. As we can see in matrix (49), the second column of $D^{\frac{1}{2}}\left(\xi_{\hat{\mathbf{n}}}^{-1}\right)$ is precisely the flip of the first one,

$$D^{\frac{1}{2}}\left(\xi_{\hat{\mathbf{n}}}^{-1}\right) = \left(|\theta, \phi\rangle \quad \mathsf{F}|\theta, \phi\rangle\right)\,. \tag{50}$$

Actually, we can learn more about the isomorphisms $\mathbb{C}^2 \cong \mathbb{H} \cong \mathbb{R}_+ \times \mathrm{SU}(2)$ through the flip and matrix representations of quaternions. In quaternionic algebra, we have the property $\hat{\boldsymbol{\imath}} = \hat{\boldsymbol{\jmath}}\hat{\boldsymbol{k}}$ + even permutations, and a quaternion q is represented by

$$\begin{aligned}\mathbb{H} \ni q &= q_0 + q_1\hat{\boldsymbol{\imath}} + q_2\hat{\boldsymbol{\jmath}} + q_3\hat{\boldsymbol{k}}\\ &= q_0 + q_3\hat{\boldsymbol{k}} + \hat{\boldsymbol{\jmath}}\left(q_1\hat{\boldsymbol{k}} + q_2\right)\\ &\equiv \begin{pmatrix}q_0 + \mathrm{i}q_3\\ q_2 + \mathrm{i}q_1\end{pmatrix} \equiv Z_q \in \mathbb{C}^2\,,\end{aligned} \tag{51}$$

after identifying $\hat{\boldsymbol{k}} \equiv \mathrm{i}$ as both are roots of -1. Then the flip appears naturally in the final identification $\mathbb{H} \cong \mathbb{R}_+ \times \mathrm{SU}(2)$ as

$$q \equiv \begin{pmatrix}q_0 + \mathrm{i}q_3 & -q_2 + \mathrm{i}q_1\\ q_2 + \mathrm{i}q_1 & q_0 - \mathrm{i}q_3\end{pmatrix} = \begin{pmatrix}Z_q & \mathsf{F}Z_q\end{pmatrix}\,. \tag{52}$$

Let us close this article with a final remark on spin-1/2 coherent states as vectors in $\mathbb{R}^2_A \otimes \mathbb{R}^2_B$. The "cat states" in $\mathbb{C}^2$ given by (49) and equivalently viewed as 4-vectors in $\mathbb{H} \sim \mathbb{R}^4$ as

$$|\theta, \phi\rangle \mapsto \begin{pmatrix}\cos\frac{\theta}{2}\\ -\sin\frac{\theta}{2}\cos\phi\\ \sin\frac{\theta}{2}\sin\phi\\ 0\end{pmatrix}\,, \tag{53}$$

are represented as entangled states in $\mathbb{R}^2_A \otimes \mathbb{R}^2_B$ by

$$\begin{aligned}|\theta, \phi\rangle = &\cos\frac{\theta}{2}|0\rangle_A \otimes |0\rangle_B \; - \sin\frac{\theta}{2}\cos\phi\left|\frac{\pi}{2}\right\rangle_A \otimes \left|\frac{\pi}{2}\right\rangle_B\\ &+ \sin\frac{\theta}{2}\sin\phi|0\rangle_A \otimes \left|\frac{\pi}{2}\right\rangle_B + 0\left|\frac{\pi}{2}\right\rangle_A \otimes |0\rangle_B\,.\end{aligned}$$

Therefore, we can say that two entangled angles in the plane can be viewed as a point in the upper half-sphere $\mathbb{S}^2/\mathbb{Z}_2$ in $\mathbb{R}^3$ shown in Figure 2.

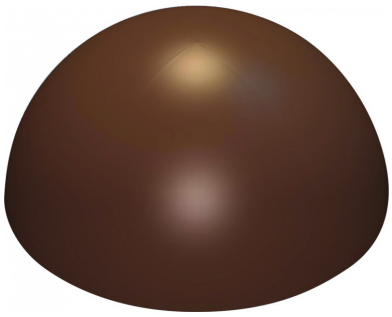

Figure 2. Each point in the upper half-sphere is in one-to-one correspondence with two entangled angles in the plane.

5. Conclusions

Integral quantization is a quantization scheme constructed on Positive Operator-Value Measures. When applied to a two-dimensional real space, it allows for a description of quantum states as pointers in the real unit half-plane. We recalled in this paper that in this case, a family of density matrices is sufficient to perform this kind of quantization as it describes all the mixed states in this space. Furthermore, a density matrix in a two-dimensional real space depends on the usual observable $\sigma_\phi = \begin{pmatrix}\cos\phi & \sin\phi\\ \sin\phi & -\cos\phi\end{pmatrix}$, which captures the essence of non-commutativity in real space. As a consequence, commutation relations are expressed in terms of the real matrix τ_2, which serves as the basis to the description of quantum measurement.

We provide an illustration considering linearly-polarized light passing through a polarizer. The pointer, associated with τ_2, can rotate by an angle $(1 \pm r)/2$ with r the degree of mixing of the density matrix, with a probability given by the usual Malus' laws (26) and (27). We extended the analysis by showing that the interaction between a polarizer and a light ray is equivalent to the quantum entanglement of two Hilbert spaces. Orientations in the plane have only two outcomes (± 1), which are the possible issues of σ_ϕ. We showed that for a general bipartite system, the classical and quantum measurement of σ_ϕ deny the existence of local hidden variables, resulting in the well-known violation of Bell inequalities, here given by (37). Finally, we demonstrated that the isomorphism $\mathbb{C}^2 \simeq \mathbb{R}^4$ allows to write Bell states in real space, with the introduction of the "flip" operator (46). This operator is necessary for constructing spin one-half coherent states, that we can fully describe by a set of orientations in $\mathbb{R}^3$, as shown in (53).

Acknowledgements

R.B. The present work was performed under the auspices of the GNFM (Gruppo Nazionale di Fisica Matematica).

EF thanks the Helsinki Institute of Physics (HIP) for their hospitality.

References

[1] E. C. G. Stueckelberg. Quantum theory in real Hilbert space. *Helvetica Physica Acta* **33**(8):727–752, 1960.

[2] M. P. Solèr. Characterization of Hilbert spaces by orthomodular spaces. *Communications in Algebra* **23**(1):219–243, 1995. https://doi.org/10.1080/00927879508825218.

[3] V. Moretti, M. Oppio. Quantum theory in quaternionic Hilbert space: How Poincaré symmetry reduces the theory to the standard complex one. *Reviews in Mathematical Physics* **31**(04):1950013, 2019. https://doi.org/10.1142/S0129055X19500132.

[4] A. Peres. Neumark's theorem and quantum inseparability. *Foundations of Physics* **20**:1441–1453, 1990. https://doi.org/10.1007/BF01883517.

[5] H. Bergeron, E. M. F. Curado, J.-P. Gazeau, L. M. C. S. Rodrigues. Orientations in the plane as quantum states. *Brazilian Journal of Physics* **49**(3):391–401, 2019. https://doi.org/10.1007/s13538-019-00652-x.

[6] R. Beneduci, E. Frion, J.-P. Gazeau, A. Perri. Real POVMS on the plane: integral quantization, Naimark theorem and linear polarization of the light. *Quantum Physics* 2021. arXiv:2108.04086.

[7] R. Beneduci. Joint measurability through Naimark's dilation theorem. *Reports on Mathematical Physics* **79**(2):197–214, 2017. https://doi.org/10.1016/S0034-4877(17)30035-6.

[8] A. Holevo. *Probabilistic and statistical aspects of quantum theory*. Springer Science & Business Media, 2011. https://doi.org/10.1007/978-88-7642-378-9.

[9] H. Bergeron, J.-P. Gazeau. Integral quantizations with two basic examples. *Annals of Physics* **344**:43–68, 2014. https://doi.org/10.1016/j.aop.2014.02.008.

[10] W. H. McMaster. Polarization and the Stokes parameters. *American Journal of Physics* **22**(6):351–362, 1954. https://doi.org/10.1119/1.1933744.

[11] B. Schaefer, E. Collett, R. Smyth, et al. Measuring the Stokes polarization parameters. *American Journal of Physics* **75**(2):163–168, 2007. https://doi.org/10.1119/1.2386162.

[12] L. D. Landau, E. M. Lifshitz. *The Classical Theory of Fields. Vol. 2.* (4th ed.). Butterworth-Heinemann, 1975. ISBN 978-0-7506-2768-9.

[13] J. S. Bell. On the Einstein-Podolsky-Rosen paradox. *Physics* **1**(3):195–200, 1964. https://doi.org/10.1103/PhysicsPhysiqueFizika.1.195.

[14] D. Bohm. A suggested interpretation of the quantum theory in terms of "hidden" variables. I. *Physical Review* **85**(2):166–179, 1952. https://doi.org/10.1103/PhysRev.85.166.

ON SOME ALGEBRAIC FORMULATIONS WITHIN UNIVERSAL ENVELOPING ALGEBRAS RELATED TO SUPERINTEGRABILITY

Rutwig Campoamor-Stursberg

Universidad Complutense de Madrid, Instituto de Matemática Interdisciplinar–UCM, Plaza de Ciencias 3, E-28040 Madrid, Spain

correspondence: rutwig@ucm.es

Abstract. We report on some recent purely algebraic approaches to superintegrable systems from the perspective of subspaces of commuting polynomials in the enveloping algebras of Lie algebras that generate quadratic (and eventually higher-order) algebras. In this context, two algebraic formulations are possible; a first one strongly dependent on representation theory, as well as a second formal approach that focuses on the explicit construction within commutants of algebraic integrals for appropriate algebraic Hamiltonians defined in terms of suitable subalgebras. The potential use in this context of the notion of virtual copies of Lie algebras is briefly commented.

Keywords: Enveloping algebras, commutants, quadratic algebras, superintegrability.

1. Introduction

Both the study of (quasi-)exactly solvable systems, as well as that of super-integrable systems make an extensive use of the universal enveloping algebras of Lie algebras, either in the context of the so-called hidden algebras or as symmetry algebras of the system. Of particular interest are those systems that, beyond super-integrability properties, also belong to the class of (quasi-)exactly solvable systems [1–5]. In particular, quadratic subalgebras have been shown to be a powerful tool for classifying and comparing super-integrable systems, as shown in [6], where the scheme of superintegrable systems on a two-dimensional conformally flat space has been characterized in terms of contractions. Additional examples in higher dimensions [7] lead us to suspect that n-dimensional super-integrable systems are somehow associated to (higher rank) polynomials in a suitable enveloping algebra [8], further stimulating the search of alternative algebraic approaches based on the structural properties of enveloping algebras. Although the precise fundamental properties of enveloping algebras of generic semidirect sums of simple and solvable Lie algebras are still far from being completely understood, a purely formal ansatz applied to the case of the Schrödinger algebras $\widehat{S}(n)$ has recently been shown to provide some interesting features [9].

In this work we comment on some purely algebraic approaches formulated in the enveloping algebras of Lie algebras for the identification or construction of quadratic algebras that may lead to super-integrable systems, once a suitable realization of the enveloping algebra by first-order differential operators has been chosen. The motivation for this analysis lies primarily on the inspection of super-integrable systems from the point of view of the algebraic properties of first integrals seen as elements of an enveloping algebra, as well as an attempt to determine to which extent these integrals are characterized algebraically by the hidden algebra [10]. This moreover suggests a realization-free description of systems in terms of commutants of algebraic Hamiltonians in enveloping algebras [11], in which elements of the coadjoint representation of Lie algebras may be useful to simplify computations.

2. First algebraic reformulation

In the context of (quasi)-exactly solvable problems, the Hamiltonians are described as differential operators in p variables that admit an expression as elements in the enveloping algebra of a Lie algebra $\mathfrak{g}$, commonly known as the hidden algebra, not necessarily associated to any symmetry algebra of the system. The main requirement is the existence of a representation of $\mathfrak{g}$ that is invariant for the Hamiltonian, a constraint that allows us to determine its spectrum (either partially or completely) using algebraic methods [12]. So, for example, the universal enveloping algebra of the simple Lie algebra $\mathfrak{sl}(2,\mathbb{R})$ and its realization as first-order differential operators on the real line provide a characterization of quasi-exactly solvable one-dimensional systems [13]. A second type of systems that uses the structural properties of enveloping algebras is given by super-integrable systems, where both the Hamiltonian and the constants of the motion are interpreted in the enveloping algebra of some Lie algebra $\mathfrak{g}$. Merely integrable n-dimensional systems can be interpreted as the image, via a realization Φ by first-order differential operators, of an Abelian subalgebra $\mathcal{A}$ of $\mathcal{U}(\mathfrak{g})$, while super-integrable systems would correspond to non-Abelian extensions of $\mathcal{A}$. The problem under what conditions a system both exhibits super-integrability and (quasi-)exact solvability has been analyzed in detail, and large classes of super-integrable systems that are exactly solvable have been found (see [3, 14, 15] and references therein).

A first algebraic formulation, as developed in [10], is motivated by the use of quadratic algebras in the context of super-integrable (and exactly solvable) systems with a given hidden algebra $\mathfrak{g}$ [3]. To this extent, we consider a Hamiltonian $\mathcal{H}$ expressed in terms of a subalgebra $\mathfrak{m} \subset \mathfrak{g}$ via a realization Φ by differential operators of the Lie algebra $\mathfrak{g}$:

$$\mathcal{H} = \sum_{i,j=1}^{\dim \mathfrak{m}} \alpha_{ij} \Phi(X_i)\Phi(X_j) + \sum_{k=1}^{\dim \mathfrak{m}} \beta_k \Phi(X_k) + \gamma_0, \quad (1)$$

where $\alpha_{ij}, \beta_k, \gamma_0$ are constants and $\{X_1, \ldots, X_{\dim \mathfrak{m}}\}$ is a basis of $\mathfrak{m}$. In this context, the Hamiltonian $\mathcal{H}$ is obtained as the image of a quadratic element $\mathcal{H}_a$ in the universal enveloping algebra $\mathcal{U}(\mathfrak{m}) \subset \mathcal{U}(\mathfrak{g})$. Similarly, the (independent) constants of the motion $\varphi_1, \ldots, \varphi_s$ can also be rewritten as the image of elements in the enveloping algebra $\mathcal{U}(\mathfrak{g})$. As differential operators they satisfy the commutators

$$[\mathcal{H}, \varphi_j] = 0, \ 1 \leq j \leq s. \quad (2)$$

The commutators $[\varphi_i, \varphi_j]$ provide additional (dependent) higher-order constants of the motion. A specially interesting case is given whenever the first integrals generate a quadratic algebra.

Abstracting from the specific realization Φ, and focusing merely on the underlying algebraic formulation, the formal polynomial

$$\mathcal{H}_a = \sum_{i,j=1}^{\dim \mathfrak{m}} \alpha_{ij} X_i X_j + \sum_{k=1}^{\dim \mathfrak{m}} \beta_k X_k + \gamma_0$$

in the enveloping algebra $\mathcal{U}(\mathfrak{m})$ of $\mathfrak{m}$ allows us to recover Hamiltonian $\mathcal{H}$ of the system once the generators are realized by the differential operators. In analogous form, we can find elements $J_1, \ldots, J_s$ in $\mathcal{U}(\mathfrak{g})$ that correspond, via the realization Φ, to the first integrals $\varphi_1, \ldots, \varphi_s$ of the system. While for the initial system the relations

$$[\mathcal{H}, \varphi_k] = 0, \quad 1 \leq k \leq s,$$

are ensured, there is no necessity that the polynomials J_k commute with $\mathcal{H}_a$ in $\mathcal{U}(\mathfrak{g})$, although the relation

$$[\mathcal{H}_a, J_k] = 0 \pmod{\Phi} \quad (3)$$

is satisfied. Similarly, for the polynomial relations $[\varphi_i, \varphi_j] = \alpha_{ij}^{k\ell} \varphi_k \varphi_\ell + \beta_{ij}^k \varphi_k$ of the first integrals, the commutators in $\mathcal{U}(\mathfrak{g})$ lead to the relation

$$[J_i, J_j] = \alpha_{ij}^{k\ell} J_k J_\ell + \beta_{ij}^k J_k \pmod{\Phi} \quad (4)$$

If equations (3) and (4) are satisfied for any realization Φ, then the problem is entirely characterized algebraically by the reduction chain $\mathfrak{m} \subset \mathfrak{g}$. It should be observed that this situation is rather exceptional, as the analysis of the exactly solvable systems described in [3] from the point of view of the first algebraic formulation indicates that, in general, the first integrals of the system do not correspond, at the level of the enveloping algebra of the hidden algebra, to polynomials that commute with the algebraic Hamiltonian, showing that the commutativity properties are a consequence of the realization by differential operators.

Using the correspondence existing between the representations of $\mathfrak{g}$ and those of its enveloping algebra $\mathcal{U}(\mathfrak{g})$ (see e.g. [11]) and identifying a Lie algebra $\mathfrak{g}$ with the first-order (left-invariant) differential operators on a Lie group G admitting $\mathfrak{g}$ as its Lie algebra, it follows that the universal enveloping algebra can be seen as the set of (left-invariant) differential operators on G of arbitrary order. Therefore, if $\Phi : \mathfrak{g} \to \mathfrak{X}(\mathbb{R}^n)$ is some realization of the Lie algebra by first-order differential operators, it can be uniquely extended to a realization $\widehat{\Phi} : \mathcal{U}(\mathfrak{g}) \to \mathfrak{X}(\mathbb{R}^n)$.

In this context, this first algebraic reformulation of the system is still strongly related to the representation theory of Lie algebras. More precisely, supposed that $\mathcal{H}_a \in \mathcal{U}(\mathfrak{m})$ is an algebraic Hamiltonian defined in the enveloping of some subalgebra $\mathfrak{m} \subset \mathfrak{g}$ and that the (independent) polynomials $J_1, \ldots, J_s$ generate a quadratic algebra, that is, satisfy the conditions

$$[J_i, J_j] = \alpha_{ij}^{k\ell} J_k J_\ell + \beta_{ij}^k J_k, \quad (5)$$

we consider the (two-sided) ideal $\mathcal{I}$ in $\mathcal{U}(\mathfrak{g})$ generated by the polynomials

$$Q_i := [\mathcal{H}_a, J_i], \quad 1 \leq i \leq s.$$

The problem is now to analyze whether there exists an equivalence class of (faithful) representations $\Phi : \mathfrak{g} \to \mathfrak{X}(\mathbb{R}^n)$ such that for the corresponding extension $\widehat{\Phi} : \mathcal{U}(\mathfrak{g}) \to \mathfrak{X}(\mathbb{R}^n)$, the image of the ideal $\mathcal{I}$ is contained in the kernel $\ker \widehat{\Phi}$, ensuring that the realized polynomials $\widehat{\Phi}(Q_i)$ correspond to first integrals of the Hamiltonian in the given realization. In some sense, this is a special case of an important and still unsolved problem, namely the embedding of a Lie algebra $\mathfrak{g}$ into the enveloping algebra $\mathcal{U}(\mathfrak{k})$ of another Lie algebra $\mathfrak{k}$, for which currently only the case of embeddings $\iota : \mathfrak{g} \to \mathcal{U}(\mathfrak{g})$ for $\mathfrak{g}$ semisimple has been completely solved [16], using techniques of deformation theory [17].

We illustrate the preceding procedure considering the six-dimensional non-solvable Lie algebra $\mathfrak{r} \subset \mathfrak{sl}(3, \mathbb{R})$ with basis $\{X_1, \ldots, X_6\}$ and nonvanishing commutators

$$\begin{array}{lll} [X_1, X_2] = X_1, & [X_1, X_5] = X_4, & [X_2, X_5] = X_5, \\ [X_2, X_6] = -X_6, & [X_3, X_4] = -X_4, & [X_3, X_5] = -X_5, \\ [X_3, X_6] = X_6 & [X_4, X_6] = X_1, & [X_5, X_6] = X_2 - X_3. \end{array}$$

Superintegrable systems based on this hidden algebra $\mathfrak{r}$ and the vector field realization

$$\begin{aligned} X_1 = \partial_t, \ X_2 = t\partial_t - \frac{N}{3}, \ X_3 = su\partial_u - \frac{N}{3}, \\ X_4 = \partial_u, \ X_5 = t\partial_u, \ X_6 = u\partial_t, \end{aligned} \quad (6)$$

have been extensively studied in [4], where in addition their exact solvability was analyzed. We consider a special case of the generic Hamiltonians studied there. Taking the values $s = k = \omega = 1$, $a = b = -\frac{1}{2}$ and $N = 0$, we obtain the Hamiltonian h_1 and two quadratic integrals

$$\begin{aligned} h_1 &= -4t\partial_t^2 - 8u\partial_{tu}^2 - 4u\partial_u^2 + 4t\partial_t + 4u\partial_u, \\ \varphi_1 &= 4u(u-t)\partial_u^2,\ \varphi_2 = 4(t-u)\left(\partial_t^2 - \partial_t\right). \end{aligned} \tag{7}$$

Now $h_1, \varphi_1, \varphi_2$ are the image by the realization of the following polynomials in the enveloping algebra of $\mathfrak{r}$:

$$\begin{aligned} H_1 &= 4X_2(1-X_1) + 8(1-X_3)X_1 + 4(1-X_4)X_3, \\ P_1 &= -4X_3X_5 + 4X_3^2 - 4X_3, \\ Q_1 &= 4(X_2X_1 - X_6X_1 + X_6 - X_2). \end{aligned}$$

At the purely algebraic level we have

$$[H_1, P_1] \neq 0, \quad [H_1, Q_1] \neq 0,$$

showing that the polynomials P_1 and Q_1 do not belong to the commutant of H_1 in $\mathcal{U}(\mathfrak{r})$. Therefore, the origin of the quadratic integrals of system (7) is not algebraic, but a consequence of the specific realization (6).

If we maintain the algebraic Hamiltonian as given above and search for quadratic polynomials in $\mathcal{U}(\mathfrak{r})$ commuting with it, we find that only two such operators exist (see [10] for the general case), given by

$$\begin{aligned} A_1 &= X_4 - X_3 - X_6 + X_1(1 + X_3 + X_6) + (X_3 + X_6)X_4, \\ B_1 &= -4X_1 - X_2 + X_6 + X_1X_2 + X_1X_3 - X_1X_6 - X_6X_4. \end{aligned}$$

These polynomials are not independent, as they satisfy the relation $A_1 + B_1 + \frac{1}{4}H_1 = 0$. Now, if we extend the analysis to cubic polynomials in $\mathcal{U}(\mathfrak{r})$, we find the following operator C_1 that commutes with H_1:

$$\begin{aligned} C_1 = {} & 3X_1 - 2X_3 - X_5 - 4X_6 + 2X_1X_3 + 4X_1X_6 + X_3^2 \\ & + X_2X_4 + X_3^2 - X_3X_5 + X_3X_6 + X_6X_4 - X_6X_5 \\ & - X_1X_3^2 - X_1X_3X_6 + X_2X_3X_4 + X_2X_6X_4. \end{aligned}$$

The operators A_1 and C_1 generate a finite-dimensional polynomial algebra in $\mathcal{U}(\mathfrak{r})$, with explicit nonvanishing commutators

$$\begin{aligned} &[A_1, C_1] = D_1, \quad [A_1, D_1] = D_1, \quad [B_1, C_1] = -D_1, \\ &[C_1, D_1] = \frac{1}{2}\{B_1, D_1\} - \frac{1}{2}\{A_1, D_1\} - 12A_1 \\ &\qquad - 12A_1 + 4B_1 + 4C_1 - 2\{A_1, B_1\}, \end{aligned}$$

where $\{\circ, \circ\}$ is the anticommutator.

Now, as the operators H_1, A_1, C_1 commute at the algebraic level, for any realization of $\mathfrak{r}$ by vector fields they give rise to a Hamiltonian system possessing a quadratic and a cubic integral, respectively.[1] For the particular realization (6), it follows that the resulting system is actually equivalent to the initial one (7), as the image of the ideal $\mathcal{J}$ generated by A_1, B_1, C_1, D_1 is properly contained in the ideal spanned by φ_1 and φ_2, thus being functionally dependent on these integrals.

[1] Provided that the transformed operators are independent.

3. Commutants in enveloping algebras and coadjoint representations

A second algebraic approach, of a more general nature, can be proposed considering chain reductions $\mathfrak{g}' \subset \mathfrak{g}$ of (reductive) Lie algebras, and analyzing the structure of the commutant of $\mathfrak{g}'$ in the enveloping algebra $\mathcal{U}(\mathfrak{g})$, in order to identify polynomial (in particular, quadratic) subalgebras [9]. In the generic analysis of commutants, elements of the theory the coadjoint representation of Lie algebras can be used, in order to simplify some of the computations in enveloping algebras. If $\mathfrak{g}$ is a Lie algebra with generators $\{X_1, \ldots, X_n\}$ and commutators $[X_i, X_j] = C_{ij}^k X_k$, the X_i's are realized in the space $C^\infty(\mathfrak{g}^*)$ by means of the first-order differential operators:

$$\widehat{X}_i = C_{ij}^k x_k \frac{\partial}{\partial x_j}, \tag{8}$$

where $\{x_1, \ldots, x_n\}$ are the coordinates of a covector in a dual basis of $\mathbb{R}\{X_1, \ldots, X_n\}$. The invariants of $\mathfrak{g}$ (in particular, the Casimir operators) correspond to the solutions of the following system of partial differential equations:

$$\widehat{X}_i F = 0, \quad 1 \leq i \leq n. \tag{9}$$

For an embedding of Lie algebras $f : \mathfrak{g}' \to \mathfrak{g}$, a basis $\{X_1, \ldots, X_r\}$ of the subalgebra can be extended to a basis $\{X_1, \ldots, X_n\}$ of $\mathfrak{g}$. Therefore, we can consider the subsystem formed by the first r equations of (9), corresponding to the generators of the subalgebra $\mathfrak{g}'$. The solutions of this subsystem, that in particular encompass the invariants of $\mathfrak{g}'$, are usually called subgroup scalars [18].

By means of the standard symmetrization map

$$\Lambda\left(x_{i_1} \ldots x_{i_p}\right) = \frac{1}{p!} \sum_{\sigma \in S_p} X_{\sigma(i_1)} \ldots X_{\sigma(i_p)} \tag{10}$$

polynomial solutions of the subsystem correspond to elements in the enveloping algebra $\mathcal{U}(\mathfrak{g})$ of $\mathfrak{g}$ that commute with the subalgebra $\mathfrak{g}'$. If we now define an algebraic Hamiltonian

$$\mathcal{H} = \mathcal{H}(X_1, \ldots, X_r) \in \mathcal{U}(\mathfrak{g}'), \tag{11}$$

in terms of the subalgebra generators, the commutant

$$C_{\mathcal{U}(\mathfrak{g})}(\mathcal{H}) = \{U \in \mathcal{U}(\mathfrak{g}) \mid [\mathcal{H}, U] = 0\}$$

certainly includes the solutions of (9) common to the $\mathfrak{g}'$-generators, i.e.

$$C_{\mathcal{U}(\mathfrak{g})}(\mathcal{H}) \supset \left\{\Lambda(\varphi) \mid \widehat{X}_1(\varphi) = \cdots = \widehat{X}_r(\varphi) = 0\right\},$$

where $\varphi(x_1, \ldots, x_n) \in C^\infty(\mathfrak{g}^*)$.

Depending on the structure of $\mathfrak{g}$ and the subalgebra $\mathfrak{g}'$, as well as on the choice of $\mathcal{H}$, two possible cases arise for a polynomial $P \in C_{\mathcal{U}(\mathfrak{g})}(\mathcal{H})$:

(1.) P commutes with all $X_1, \ldots, X_r$.

(2.) There is an index k_0 with $[P, X_{k_0}] \neq 0$.

Polynomials P in the first case actually commute with the Hamiltonian $\mathcal{H}$, and thus belong to the two-sided ideal $\langle \mathcal{I} \rangle$ generated by the set $\mathcal{I} = \{J_1, \ldots, J_s\}$ of elements corresponding to the symmetrization of independent polynomials satisfying the subsystem of (9) corresponding to $\mathfrak{g}'$. For these elements, it follows at once that $[J_k, J_\ell]$ belongs to $\mathcal{I}$. In the general case, the Hamiltonian $\mathcal{H}$ does not commute with all X_j-generators, and in order to find the commutant $C_{\mathcal{U}(\mathfrak{g})}(\mathcal{H})$, we can restrict the analysis to the determination of a basis of the factor module $C_{\mathcal{U}(\mathfrak{g})}(\mathcal{H})/\langle \mathcal{I} \rangle$. Although the problem is computationally cumbersome, certain algorithms in terms of Gröbner bases have been developed that allow its precise determination [19].

A (restricted) systematic procedure that circumvents the above-mentioned obstruction and allows us to analyze polynomial algebras with respect to a reduction chain $\mathfrak{g}' \subset \mathfrak{g}$ can be proposed starting from the polynomials in $\mathcal{U}(\mathfrak{g})$ that commute with all the generators intervening in the expression of the algebraic Hamiltonian $\mathcal{H} \in \mathcal{U}(\mathfrak{g}')$. More precisely, if the Hamiltonian $\mathcal{H}$ is given as a polynomial $P(X_{i_1}, \ldots, X_{i_s})$ in terms of the generators of the subalgebra $\mathfrak{g}'$ with basis $\{X_1, \ldots, X_r\}$, we consider the subsystem of (9) given by

$$\widehat{X}_{i_j} F(x_1, \ldots, x_n) = 0, \quad 1 \leq j \leq s.$$

We then extract a maximal set of independent polynomial solutions $\{Q_1, \ldots, Q_p\}$ of (9), which in the reductive case forms an integrity basis for the solutions. Symmetrizing these functions we obtain elements M_j in the commutant $C_{\mathcal{U}(\mathfrak{g})}(\mathcal{H})$. Starting from the set of polynomials $\mathcal{S} = \{\mathcal{H}, M_1, \ldots, M_p\}$, we inspect their commutators and determine whether, either adjoining new (dependent) elements to $\mathcal{S}$ or discarding some elements of $\mathcal{S}$, a finite-dimensional quadratic algebra $\mathcal{A}$ can be found. Although there is some ambiguity in the construction, as there is no quadratic algebra "canonically" associated to the reduction chain $\mathfrak{g}' \subset \mathfrak{g}$, it provides an alternative method that does not require a specific realization by vector fields, as the integrability condition is guaranteed by the commutant.

This ansatz has been successfully applied in [9] to the enveloping algebra of the Schrödinger algebras $\widehat{S}(n)$ for arbitrary values of $n \geq 1$ and various choices of algebraic Hamiltonian, showing that the construction is formally of use for the analysis of hidden algebras that are not reductive.

4. Virtual copies in enveloping algebras

In the solution of the embedding problem into enveloping algebras for semisimple algebras, the vanishing of the first cohomology group with values in $\mathcal{U}(\mathfrak{g})$ plays an important role, as it allows to provide a general solution for the perturbation problem [16]. For nonsemisimple Lie algebras, the application of the procedure is quite complicated for both computational reasons and the currently incomplete understanding of the precise structure of the corresponding enveloping algebras. However, for certain types of semidirect sums of simple and solvable Lie algebras, some analogous statements may be proposed, providing copies of semisimple Lie algebras in the enveloping algebra of a semidirect sum, up to a polynomial factor.

Supposed that $\mathfrak{s}$ is the Levi subalgebra of a semidirect sum $\mathfrak{g} = \mathfrak{s} \overrightarrow{\oplus}_\Gamma \mathfrak{r}$, we seek for elements of degree $d \geq 2$ in the generators in $\mathcal{U}(\mathfrak{g})$ that transform according to the structure tensor of $\mathfrak{s}$, up to a (polynomial) factor. The procedure can be summarized as follows: Consider a basis $\{X_1, \ldots, X_n\}$ of $\mathfrak{s}$ with commmutators

$$[X_i, X_j] = C_{ij}^k X_k. \tag{12}$$

and extend it to a basis $\{X_1, \ldots, X_n, Y_1, \ldots, Y_m\}$ of of the semidirect sum $\mathfrak{g}$. We now define operators

$$X_i' = X_i \, R\,(Y_1, \ldots, Y_m) + P_i\,(Y_1, \ldots, Y_m) \tag{13}$$

in $\mathcal{U}(\mathfrak{g})$, where P_i and R are still undetermined polynomials. In order to simplify computations, they can be considered as homogeneous polynomials of degrees k and $k-1$ respectively, so that X_i' is homogeneous of degree k. We require that these operators commute with the generators Y_k of the radical $\mathfrak{r}$, so that the identity

$$[X_i', Y_j] = 0, \quad 1 \leq i \leq n,\ 1 \leq j \leq m$$

is satisfied for all indices. Expanding the latter leads to the expression

$$\begin{aligned}[X_i', Y_j] =& [X_i R, Y_j] + [P_i, Y_j] \\ =& X_i\,[R, Y_j] + [X_i, Y_j]\ R + [P_i, Y_j]\,.\end{aligned}$$

Taking into account the homogeneity degree of the terms with respect to the generators of $\mathfrak{s}$ and the representation space, it follows that $X_i\,[R, Y_j]$ can be seen as a polynomial of degree $(k-1)$ in the variables $\{Y_1, \ldots, Y_m\}$. On the other hand the terms of $[X_i, Y_j]\ R + [P_i, Y_j]$ have degree k, allowing us to further separate the commutator as

$$\begin{aligned}[R, Y_j] &= 0, \\ [X_i, Y_j]\ R + [P_i, Y_j] &= 0.\end{aligned} \tag{14}$$

From the first equation we conclude that the factor R commutes with all generators Y_i, thus defines an invariant of the solvable Lie algebra $\mathfrak{r}$. We further require that the operators X_i' transform by the action of $\mathfrak{s}$ as the generators of the latter algebra, i.e.

$$[X_i', X_j] \quad = [X_i, X_j]' := C_{ij}^k\,(X_k R + P_k)\,. \tag{15}$$

As this relation must hold for all the generators of the semidirect sum $\mathfrak{g}$, further structural constraints on the polynomials R and P_i are obtained. Expanding the left-hand term of condition (15) yields

$$[X_i', X_j] = [X_i, X_j]\ R - X_i\,[X_j, R] + [P_i, X_j]\,.$$

As the Y_j are the generators of the representation space Γ, it follows that the term $[X_i, X_j]\ R - X_i\,[X_j, R]$ is linear in the generators of $\mathfrak{s}$ and of degree $(k-1)$ in the Y_j's, while $[P_i, X_j]$ does not involve generators of $\mathfrak{s}$. Comparing now with the right-hand side of (15), the condition again separates into two parts:

$$\begin{aligned}[X_i, X_j]\ R - X_i\,[X_j, R] &= C_{ij}^k X_k R,\\ [P_i, X_j] &= C_{ij}^k P_k.\end{aligned} \tag{16}$$

Simplifying the first equations shows that

$$X_i\,[X_j, R] = 0,$$

hence implying that R also commutes with the generators of the Lie algebra. As R corresponds simultaneously to an invariant polynomial of the radical, it must correspond to an invariant of $\mathfrak{g}$ that depends only on the generators of its maximal solvable ideal.[2] The second equation shows that the polynomials P_i transform according to the adjoint representation of the semisimple Lie algebra $\mathfrak{s}$. Supposed that all the conditions are satisfied, we obtain the commutators of the operators X_i' in the enveloping algebra $\mathcal{U}(\mathfrak{g})$ as

$$\begin{aligned}\left[X_i', X_j'\right] &= [X_i R + P_i, X_j R + P_j]\\ &= [X_i R + P_i, X_j R] + [X_i R + P_i, P_j]\\ &= C_{ij}^k X_k R^2 + C_{ij}^k P_k R + [X_i', P_j]\,.\end{aligned} \tag{17}$$

As the X_i' commute with the Y_j, it follows from equation (17) that $[X_i', P_j] = 0$ and therefore that $\left[X_i', X_j'\right] = [X_i, X_j]'\,R$, showing that the operators reproduce the commutators of $\mathfrak{s}$, up to the invariant factor R. It should be emphasized that R is not necessarily a central element, but an invariant of $\mathfrak{g}$ that solely depends on the generators of the characteristic representation Γ.

It follows in particular from this construction that the operators $\{R, X_1', \ldots, X_n'\}$ generate a finite dimensional quadratic algebra $\mathcal{A}$ in the enveloping algebra $\mathcal{U}(\mathfrak{g})$, with commutators

$$[R, X_i'] = 0,\ \left[X_i', X_j'\right] = C_{ij}^k X_k' R, \quad 1 \leq i, j, k \leq n.$$

Under some specific conditions, these so-called virtual copies of semisimple Lie algebras in enveloping algebras can be used to construct (formal) Hamiltonians with first integrals given by some of the operators X_i'. Let us outline one possibility, based on the branching rules of representations of semisimple Lie algebras. To this extent, we fix a semisimple subalgebra $\mathfrak{s}'$ of the Levi factor $\mathfrak{s}$ of the semidirect sum $\mathfrak{g}$. Further suppose that the adjoint representation $\mathrm{ad}(\mathfrak{s})$ decomposes, as a representation of $\mathfrak{s}'$, as follows

$$\mathrm{ad}(\mathfrak{s}) \downarrow \mathrm{ad}(\mathfrak{s}') + \Gamma_1 + \cdots + \Gamma_s, \tag{18}$$

where $\Gamma = \Gamma_1 + \cdots + \Gamma_s$ is the so-called characteristic representation [20]. Suppose that the trivial representation Γ_0 of $\mathfrak{s}'$ has multiplicity $k > 0$ in the decomposition (18). This means specifically that we can find k generators $\left\{\tilde{X}_1, \ldots, \tilde{X}_k\right\}$ of $\mathfrak{s}$ that commute with the subalgebra $\mathfrak{s}'$. Now, by condition (15), for the corresponding operators $\tilde{X}_s$ $(1 \leq s \leq k)$ we have that

$$\left[\tilde{X}_i', Z\right] = \left[\tilde{X}_i, Z\right]' = 0, \quad Z \in \mathfrak{s}', \tag{19}$$

from which it follows that for any algebraic Hamiltonian $\mathcal{H} \in \mathcal{U}(\mathfrak{s}')$ the integrability condition

$$\left[\tilde{X}_i', \mathcal{H}\right] = [R, \mathcal{H}] = 0,\ 1 \leq i \leq k \tag{20}$$

is satisfied. On the other hand, by condition (17), it is straightforward to verify that

$$\left[\mathcal{H}, \left[\tilde{X}_i', \tilde{X}_j'\right]\right] = 0. \tag{21}$$

This last identity implies that the terms appearing in the commutator $\left[\tilde{X}_i', \tilde{X}_j'\right]$ also transform according to the trivial representation of the subalgebra $\mathfrak{s}'$.

We conclude that the set $\left\{R, \tilde{X}_1', \ldots, \tilde{X}_k'\right\}$ generates a finite-dimensional quadratic algebra in the enveloping algebra $\mathcal{U}(\mathfrak{g})$ that are (formal) first integrals for the Hamiltonian $\mathcal{H}$. Whether or not these integrals are sufficient for guaranteeing (super-)integrability, essentially depends on the subalgebra $\mathfrak{s}'$ and the associated branching rule. In any case, the preceding construction determines the maximal number of operators X_i' that commute with the Hamiltonian $\mathcal{H}$, independently of any realization of the hidden algebra $\mathfrak{g}$ by first-order differential operators. For the case where the characteristic representation Γ does not contain the trivial representation of the subalgebra $\mathfrak{s}'$, i.e., when no generators of $\mathfrak{s}$ simultaneously commute with the elements of $\mathfrak{s}'$, the integrability condition for the operators would not be a consequence of the structure of the enveloping algebra, but the specific consequence of a realization of $\mathfrak{g}$, relating this approach with the first algebraic formulation.

We finally observe that the construction presented here, that depends essentially on the homogeneity of the operators X_i', is specially suitable for semidirect sums admitting a nonvanishing centre and the class of one-dimensional non-central extensions of double inhomogeneous Lie algebras [21, 22], while the argument is not valid whenever the Levi factor $\mathfrak{s}$ and the radical do not have nonconstant invariants in common. Due to this obstruction, it is formally conceivable to propose a generalized construction by skipping the homogeneity assumption. It should however be taken into account that using operators of different degrees in (13) may lead to incompatibilities in the commutators, as equations (14)-(16) cease to hold, and more general constraints depending on the particular degrees of each P_i would be required. If and under what specific assumptions a solution can be found for a generalized inhomogeneous set of generators (13), is still an unanswered question that is currently being studied in detail.

[2] This fact actually provides information concerning the dimension of the characteristic representation Γ in the semidirect sum.

5. Conclusions

Two possible approaches to the problem of determining quadratic algebras as subalgebras of the enveloping algebra of a Lie algebra have been commented. The first approach corresponds to an algebraic abstraction of already known systems, which are analyzed purely from the perspective of the Hamiltonian and the integrals as the image by a realization of differential operators of elements in some enveloping algebra, trying to determine to which extent such integrals are realization-dependent [10]. In a the second algebraic formulation, commutants of subalgebras $\mathfrak{g}' \subset \mathfrak{g}$ in the enveloping algebra of $\mathfrak{g}$ are considered, from which quadratic algebras formed by polynomials that commute with a given algebraic Hamiltonian defined in $\mathcal{U}(\mathfrak{g}')$ are deduced. In order to simplify the computations in the enveloping algebra, distinguished elements in the commutant can be deduced from the coadjoint representation. For the subalgebras found with this method, a realization by vector fields of an appropriate number of variables automatically provides a (super-)integrable system for the given Hamiltonian [9]. The method of virtual copies, initially introduced in the context of invariant theory, provides an additional approach that combines elements of the two algebraic formulations, and refers to a number of still open problems, such as the general solution of the embedding problem of Lie algebras into enveloping algebras [16], as well the classification problem of realizations of Lie algebras in terms of differential operators [23]. Whether these approaches are compatible or can be combined with other procedures like the quadratic deformations of Lie algebras or the formalism of Racah algebras (see e.g. [8, 24, 25] and references therein) is a problem worthy to be inspected. We hope to report on some progress in these directions in a near future.

Acknowledgements

The author is indebted to Alexander V. Turbiner and Ian Marquette for valuable critical comments, to Artur Sergyeyev for providing reference [15], as well as to the referees for several remarks that have greatly improved the presentation. During the preparation of this work, the author was financially supported by the research grant PID2019-106802GB-I00/AEI/10.13039/501100011033 (AEI/ FEDER, UE).

References

[1] A. M. Perelomov. *Integrable Systems of Classical Mechanics and Lie Algebras*. Birkhäuser Verlag, Basel, 1990.

[2] L. Freidel, J. M. Maillet. Quadratic algebras and integrable systems. *Physics Letters B* **262**(2-3):278–284, 1991. https://doi.org/10.1016/0370-2693(91)91566-E.

[3] P. Tempesta, A. V. Turbiner, P. Winternitz. Exact solvability of superintegrable systems. *Journal of Mathematical Physics* **42**(9):4248, 2001. https://doi.org/10.1063/1.1386927.

[4] F. Tremblay, A. Turbiner, P. Winternitz. An infinite family of solvable and integrable quantum systems on a plane. *Journal of Physics A: Mathematical and Theoretical* **42**(24):242001, 2009. https://doi.org/10.1088/1751-8113/42/24/242001.

[5] P. Letourneau, L. Vinet. Superintegrable systems: polynomial algebras and quasi-exactly solvable Hamiltonian. *Annals of Physics* **243**(1):144–168, 1995. https://doi.org/10.1006/aphy.1995.1094.

[6] W. Miller, S. Post, P. Winternitz. Classical and quantum superintegrability with applications. *Journal of Physics A: Mathematical and Theoretical* **46**(42):423001, 2013. https://doi.org/10.1088/1751-8113/46/42/423001.

[7] C. Daskaloyannis, Y. Tanoudis. Quadratic algebras for three-dimensional superintegrable systems. *Physics of Atomic Nuclei* **73**:214–221, 2010. https://doi.org/10.1134/S106377881002002X.

[8] D. Latini, I. Marquette, Y.-Z. Zhang. Embedding of the Racah algebra $R(n)$ and superintegrability. *Annals of Physics* **426**:168397, 2021. https://doi.org/10.1016/j.aop.2021.168397.

[9] R. Campoamor-Stursberg, I. Marquette. Quadratic algebras as commutants of algebraic Hamiltonians in the enveloping algebra of Schrödinger algebras. *Annals of Physics* **437**:168694, 2022. https://doi.org/10.1016/j.aop.2021.168694.

[10] R. Campoamor-Stursberg, I. Marquette. Hidden symmetry algebra and construction of quadratic algebras of superintegrable systems. *Annals of Physics* **424**:168378, 2021. https://doi.org/10.1016/j.aop.2020.168378.

[11] J. Dixmier. *Algèbres enveloppantes*. Hermann, Paris, 1974.

[12] M. A. Shifman, A. V. Turbiner. Quantal problems with partial algebraization of the spectrum. *Communications in Mathematical Physics* **126**:347–365, 1989. https://doi.org/10.1007/BF02125129.

[13] A. V. Turbiner, A. G. Ushveridze. Spectral singularities and quasi-exactly solvable quantal problem. *Physics Letters A* **126**(3):181–183, 1987. https://doi.org/10.1016/0375-9601(87)90456-7.

[14] M. A. Rodríguez, P. Winternitz. Quantum superintegrability and exact solvability in n dimensions. *Journal of Mathematical Physics* **43**:1309–1322, 2002. https://doi.org/10.1063/1.1435077.

[15] A. Sergyeyev. Exact solvability of superintegrable Benenti systems. *Journal of Mathematical Physics* **48**(5):052114, 2007. https://doi.org/10.1063/1.2738829.

[16] V. Ovsienko, A. V. Turbiner. Plongements d'une algèbre de Lie dans son algèbre enveloppante. *Comptes Rendus de l'Académie des Sciences Paris* **314**:13–16, 1992.

[17] A. Verona. *Introducere in coomologia algebrelor Lie*. Editura Academiei Rep. Soc. România, Bucuresti, 1974.

[18] R. T. Sharp, C. S. Lam. Internal-labeling problem. *Journal of Mathematical Physics* **10**(11):2033–2038, 1969. https://doi.org/10.1063/1.1664799.

[19] J. Apel, W. Lassner. An extension of Buchberger's algorithm and calculations in enveloping fields of Lie algebras. *Journal of Symbolic Computation* **6**(2-3):361–370, 1988. https://doi.org/10.1016/S0747-7171(88)80053-1.

[20] W. G. McKay, J. Patera. *Tables of Dimensions, Indices and Branching Rules for Representations of Simple Lie Algebras*. Marcel Dekker, New York, 1981.

[21] R. Campoamor-Stursberg. Intrinsic formulae for the Casimir operators of semidirect products of the exceptional Lie algebra g_2 and a Heisenberg Lie algebra. *Journal of Physics A: Mathematical and General* **37**(40):9451–9466, 2004. https://doi.org/10.1088/0305-4470/37/40/009.

[22] R. Campoamor-Stursberg, I. Marquette. Generalized conformal pseudo-Galilean algebras and their Casimir operators. *Journal of Physics A: Mathematical and Theoretical* **52**(47):475202, 2019. https://doi.org/10.1088/1751-8121/ab4c81.

[23] A. González López, N. Kamran, P. J. Olver. Lie algebras of vector fields in the real plane. *Proceedings of the London Mathematical Society* **64**(2):339–368, 1992. https://doi.org/10.1112/plms/s3-64.2.339.

[24] L. A. Yates, P. D. Jarvis. Hidden supersymmetry and quadratic deformations of the space-time conformal superalgebra. *Journal of Physics A: Mathematical and Theoretical* **51**(14):145203, 2018. https://doi.org/10.1088/1751-8121/aab215.

[25] P. Gaboriaud, L. Vinet, S. Vinet, A. Zhedanov. The generalized Racah algebra as a commutant. *Journal of Physics: Conference Series* **1194**:012034, 2019. https://doi.org/10.1088/1742-6596/1194/1/012034.

PHOTONIC GRAPHENE UNDER STRAIN WITH POSITION-DEPENDENT GAIN AND LOSS

Miguel Castillo-Celeita[a,*], Alonso Contreras-Astorga[b], David J. Fernández C.[a]

[a] *Cinvestav, Physics Department, P.O. Box. 14-740, 07000 Mexico City, Mexico*

[b] *Cinvestav, CONACyT – Physics Department, P.O. Box. 14-740, 07000 Mexico City, Mexico*

[*] corresponding author: mfcastillo@fis.cinvestav.mx

Abstract. We work with photonic graphene lattices under strain with gain and loss, modeled by the Dirac equation with an imaginary mass term. To construct such Hamiltonians and their solutions, we use the free-particle Dirac equation and then a matrix approach of supersymmetric quantum mechanics to generate a new Hamiltonian with a magnetic vector potential and an imaginary position-dependent mass term. Then, we use a gauge transformation that maps our solutions to the final system, photonic graphene under strain with a position-dependent gain/loss term. We give explicit expressions for the guided modes.

Keywords: Graphene, Dirac materials, photonic graphene, matrix supersymmetric, quantum mechanics.

1. Introduction

Graphene is the last known carbon allotrope, it was isolated for the first time by Novoselov, Geim, et al. in 2004 [1]. This material consists of a two-dimensional hexagonal arrangement of carbon atoms. Graphene excels for its interesting properties, such as mechanical resistance, electrical conductivity, and optical opacity [2, 3]. The study of graphene has contributed to the development of different areas in physics, for example, in solid-state, graphene has prompted the discovery of other materials with similar characteristics, such as borophene and phosphorene. At low energy, the charge carriers in graphene behave like Dirac massless particles, and from this approach, graphene has allowed the verification of the Klein tunneling paradox as well as the quantum Hall effect. These phenomena have gained a special interest in particle physics and quantum mechanics [4].

Exploring graphene in an external constant magnetic field has allowed identifying the discrete bound states in the material, the so-called Landau levels. Moreover, theoretical physicist have analyzed the behavior of Dirac electrons in graphene under different magnetic field profiles as well. Supersymmetric quantum mechanics is a useful tool to find solutions of the Dirac equation under external magnetic fields [5–9]. Following this approach, a mechanical deformation in a graphene lattice is equivalent to introducing an external magnetic field [10, 11].

Graphene has its analog in photonics, called *photonic graphene*. It is constructed through a two-dimensional photonic crystal with weakly coupled optical fibers in a three-dimensional setting [12–17]. Photonic graphene under strain is modeled through a deformation in the coupled optical fiber lattice [18–21].

Compared with the conventional graphene Hamiltonian, the photonic graphene Hamiltonian has an extra term that represents the gain/loss in the fibers. The literature on this topic always considers a constant gain/loss in space. With the previous motivation, we will apply supersymmetric quantum mechanics in a matrix approach (matrix SUSY-QM) to obtain solutions of the Dirac equation for strain photonic graphene with a position-dependent gain/loss.

2. Strain in photonic graphene

The graphene structure consists of carbon atoms in a hexagonal arrangement similar to a honeycomb lattice. This structure can be described by two triangular sublattices of atoms, which are denoted as type A and type B. The base vectors to the unitary cell are given by

$$\mathbf{a}_1 = \frac{a}{2}(\sqrt{3}, 3), \quad \mathbf{a}_2 = \frac{a}{2}(-\sqrt{3}, 3), \tag{1}$$

where a is the interatomic distance, for graphene $a = 1.42$ Å (see Figure 1a). The position of the atoms in the whole lattice can be defined by the set of vectors $R_l = l_1\mathbf{a}_1 + l_2\mathbf{a}_2$, with $l_1,\ l_2 \in \mathbb{Z}$. An alternative description of graphene is through the first neighbors, which are connected by the vectors δ_n

$$\delta_1 = \frac{a}{2}(\sqrt{3}, 1), \quad \delta_2 = \frac{a}{2}(-\sqrt{3}, 1), \quad \delta_3 = a(0, -1). \tag{2}$$

A reciprocal lattice can be defined in the momentum space, which is also hexagonal, as shown in Figure 1b. It is rotated 90° with respect to the original carbon network. A hexagon in the reciprocal lattice is recognized as the first Brillouin zone. In this zone, there are only two inequivalent points, $\mathbf{K}_\pm = (\pm\frac{4\pi}{3\sqrt{3}a}, 0)$.

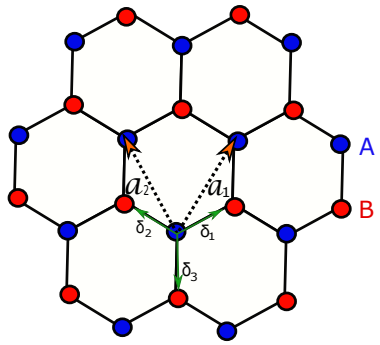

(A).

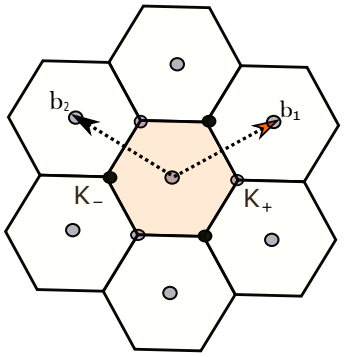

(B).

Figure 1. (A) Hexagonal graphene lattice. The lattice is constructed by type A and type B atoms, in this case, $\mathbf{a}_1$ and $\mathbf{a}_2$ correspond to the lattice unitary vectors, and δ_n are the vectors that connect the atoms A(B) with the nearest neighbors. (B) Reciprocal lattice, which is characterized by the $b_{1,2}$ vectors and $K_\pm$ correspond to the two possible inequivalent points in the lattice.

All subsequent corners are determined from either $\mathbf{K}_+$ or $\mathbf{K}_-$ plus integer multiples of the vectors

$$\mathbf{b}_1 = \frac{2\pi}{3a}(\sqrt{3}, 1), \quad \mathbf{b}_2 = \frac{2\pi}{3a}(-\sqrt{3}, 1). \tag{3}$$

Vectors $\mathbf{a}_i$ and $\mathbf{b}_j$ fulfill the condition $\mathbf{a}_i \cdot \mathbf{b}_j = 2\pi\delta_{ij}$.

2.1. Tight-binding model

The tight-binding Hamiltonian describes the hopping of an electron from an atom A (B) to an atom B (A)

$$H = -t\sum_{R_i}\sum_{n=1}^{3}(|A_{R_i}\rangle\langle B_{R_i+\delta_n}| + |B_{R_i+\delta_n}\rangle\langle A_{R_i}|), \tag{4}$$

where $t \approx$ 3 eV is called the hopping integral, R_i runs over all sites in the sublattice A, thus $|A_{R_i}\rangle$ is a state vector in these sites, the same applies to B and $|B_{R_i+\delta_n}\rangle$, recall that δ_n connects the atoms of the sublattice $A(B)$ with its nearest neighbors in the sublattice $B(A)$. The translational symmetry suggests the use of Bloch states

$$|\Psi_{Bloch}\rangle = \frac{1}{\sqrt{N_c}}\sum_{R_j}(e^{ik\cdot R_j}\psi_A(k)|A_{R_j}\rangle + e^{ik\cdot(R_j+\delta_3)}\psi_B(k)|B_{R_j+\delta_3}\rangle), \tag{5}$$

where N_c is the number of the unitary cell [22]. Then $H|\Psi\rangle = E|\Psi\rangle$ becomes a matrix problem

$$\begin{pmatrix} 0 & -t\sum_{n=1}^{3} e^{-ik\cdot\delta_n} \\ -t\sum_{n=1}^{3} e^{ik\cdot\delta_n} & 0 \end{pmatrix}\begin{pmatrix}\psi_A \\ \psi_B\end{pmatrix} = E\begin{pmatrix}\psi_A \\ \psi_B\end{pmatrix}, \tag{6}$$

with $\psi_A \equiv \psi_A(k)$ and $\psi_B \equiv \psi_B(k)$ and the energy term given by

$$E_\pm = \pm\left|t\sum_{n=1}^{3} e^{-ik\cdot\delta_n}\right| = \pm t\sqrt{3 + 2\cos(\sqrt{3}k_x a) + 4\cos(\sqrt{3}k_x\frac{a}{2})\cos(3k_y\frac{a}{2})}.$$

To obtain an effective Hamiltonian at low energy, we can consider the Taylor series around the Dirac points $H(k = \mathbf{K}_\pm + q) \approx q\cdot\nabla_k H|_{\mathbf{K}_\pm}$. Note that $E(\mathbf{K}_\pm) = 0$, as a consequence, at these points, the valence and conduction bands are connected. The above calculus leads to the analog of the Dirac-Weyl equation

$$H_\varrho\Psi = \hbar v_0(\varrho\sigma_1 q_x + \sigma_2 q_y)\Psi = E\Psi, \tag{7}$$

where $\varrho = \pm 1$ correspond to the $\mathbf{K}_\pm$ valleys, v_0 is called the Fermi velocity, in graphene, $v_0 = 3ta/2\hbar \approx c/300$, with c being the velocity of light, σ_i are the Pauli matrices

$$\sigma_1 = \begin{pmatrix}0 & 1\\ 1 & 0\end{pmatrix},\ \sigma_2 = \begin{pmatrix}0 & -i\\ i & 0\end{pmatrix},\ \sigma_3 = \begin{pmatrix}1 & 0\\ 0 & -1\end{pmatrix}, \tag{8}$$

and Ψ is a bi-spinor. The matrix nature of this equation is related to the sublattices A and B, this degree of freedom is called pseudo-spin. Notice that at low energies, the dispersion relation is linear, given by $E_\pm(q) = \pm\hbar v_0|q|$, then, the Dirac cones are connecting at $E_\pm = 0$, as expected for particles without mass [23].

2.2. Uniform strain

The photonic analog of a graphene lattice is built with weakly coupled optical fibers. This kind of photonic system is described by the same tight-binding Hamiltonian in graphene with an additional term $\gamma_{A/B}$; that represents the gain and loss in the optical fibers in the position A/B, this new term produces an attenuation or amplification in the optical modes.

If we consider uniform strain in the lattices, which is represented by a strain tensor

$$\mathbf{u} = \begin{pmatrix}\mathbf{u}_{11} & 0\\ 0 & \mathbf{u}_{22}\end{pmatrix}, \tag{9}$$

the Fermi velocity is modified in the following form

$$\mathbf{v}_{ij} = v_0(1 + (1-\beta)\mathbf{u}_{ij}). \tag{10}$$

The hopping integrals are modified with a little perturbation $t \to t_n$, that, considering the changes in the orbitals by the modification of the carbon distances

$$t_n \approx t\left(1 - \frac{\beta}{a^2}\delta_n\cdot\mathbf{u}\cdot\delta_n\right), \tag{11}$$

where

$$\beta = -\frac{\partial \ln t}{\partial \ln a} \tag{12}$$

is the Grüneisen parameter that depends on the model; for graphene, β is between 2 and 3 [10] (see also [24, 25]). In photonic graphene, a is the distance between adjacent waveguides. The Hamiltonian of a photonic graphene with a uniform strain reads as

$$H = \gamma_A \sum_{R_i} |A_{R_i}\rangle \langle A_{R_i}| + \gamma_B \sum_{R_i} |B_{R_i+\delta_n}\rangle \langle B_{R_i+\delta_n}| - \sum_{R_i}\sum_{n=1}^{3} t_n (|A_{R_i}\rangle \langle B_{R_i+\delta_n}| + |B_{R_i+\delta_n}\rangle \langle A_{R_i}|). \tag{13}$$

The deformation of the lattice produces a shift of the Dirac points $\mathbf{K}_{\pm}^{D} \approx (\mathbf{1} - \mathbf{u}) \cdot \mathbf{K}_{\pm} \pm \mathbf{A}$, where $\mathbf{A} = (\mathbf{A}_x, \mathbf{A}_y)$

$$\mathbf{A}_x = \frac{\beta}{2a}(\mathbf{u}_{11} - \mathbf{u}_{22}), \quad \mathbf{A}_y = -\frac{\beta}{2a}(2\mathbf{u}_{12}). \tag{14}$$

Using the Bloch solution, the Hamiltonian under strain takes the form:

$$H = \begin{pmatrix} \gamma_A & -\sum_{n=1}^{3} t_n e^{-ik\cdot(\mathbf{1}-\mathbf{u})\cdot\delta_n} \\ -\sum_{n=1}^{3} t_n e^{ik\cdot(\mathbf{1}-\mathbf{u})\cdot\delta_n} & \gamma_B \end{pmatrix}, \tag{15}$$

under the assumption $|\mathbf{u}\cdot\delta_n| \ll a$. In this work, we will assume that $\gamma_A = i\gamma$ and $\gamma_B = \gamma_A^*$, then, for positive γ, the waveguides in the sublattice A (B) present the energy gain (loss), as in the arrangements proposed in [14]. Expanding this Hamiltonian around the Dirac points, through the substitution $k = \mathbf{K}_{\pm}^{D} + q$, one arrives at a Dirac Hamiltonian analog with minimal coupling

$$H = v_0 \sigma \cdot (\mathbf{1} + \mathbf{u} - \beta\mathbf{u})q + i\gamma\sigma_3. \tag{16}$$

Comparing with (7), the effect of strain is equivalent, to consider magnetic-like field modeled through a pseudo-magnetic vector potential $\mathbf{A}$. The last term represents a gain/loss balance in sublattices A/B. In photonic graphene, strain could be generated by deformations in the geometry of the optical-fiber lattice.

2.3. Non-uniform strain

For non-uniform strain, the deformation matrix depends of the position, $\mathbf{u} \to \mathbf{u}(r)$. Thus, the expression for the Hamiltonian becomes

$$H = -i\sigma_i \sqrt{\mathbf{v}_{ij}}\partial_j \sqrt{\mathbf{v}_{ij}} + v_0 \sigma_i \mathbf{A}_i + i\gamma\sigma_3, \tag{17}$$

considering a strain tensor of the form

$$\mathbf{u} = \begin{pmatrix} \mathbf{u}_{11}(x) & 0 \\ 0 & \mathbf{u}_{22}(y) \end{pmatrix}, \tag{18}$$

and equations (10) and (14), still apply. We can also write the strain Hamiltonian as

$$H(x,y) = -i\sigma_1\sqrt{\mathbf{v}_{11}}\partial_x\sqrt{\mathbf{v}_{11}} - i\sigma_2\sqrt{\mathbf{v}_{22}}\partial_y\sqrt{\mathbf{v}_{22}} + \sigma_1\frac{v_0\beta}{2a}(\mathbf{u}_{11}(x) - \mathbf{u}_{22}(y)) + i\gamma\sigma_3, \tag{19}$$

where $\mathbf{v}_{11} = \mathbf{v}_{11}(x)$, $\mathbf{v}_{22} = \mathbf{v}_{22}(y)$.

We can relate the eigenvalue equation of this Hamiltonian, $H\Psi = E\Psi$, with a strain-free one using the following transformation. First, we define the coordinates

$$r = \int \frac{v_0}{\mathbf{v}_{11}(x)}dx, \quad s = \int \frac{v_0}{\mathbf{v}_{22}(y)}dy, \tag{20}$$

and the operator

$$G(x,y) = \frac{\sqrt{\mathbf{v}_{11}\mathbf{v}_{22}}}{v_0} \exp\left(\frac{iv_0\beta}{2a}\int_0^x \frac{\mathbf{u}_{11}(q)}{\mathbf{v}_{11}(q)}dq\right), \tag{21}$$

then, H will be related with a flat Fermi velocity Hamiltonian H_0 as

$$H(x,y) = G^{-1}(x,y)H_0(r(x),s(y))G(x,y), \tag{22}$$

where

$$H_0\Phi = \left(-iv_0\sigma_1\partial_r - iv_0\sigma_2\partial_s - \frac{v_0\beta}{2a}\mathbf{u}_{22} + i\gamma\sigma_3\right)\Phi, \tag{23}$$

and $\mathbf{u}_{22} = \mathbf{u}_{22}(y(r,s))$. The solutions are mapped as

$$\Psi(x,y) = G^{-1}(x,y)\Phi(r(x),s(y)). \tag{24}$$

The energy spectrum is the same for both Hamiltonians [18, 19, 26].

3. Supersymmetric quantum mechanics: matrix approach

Supersymmetric quantum mechanics (SUSY-QM) is a method that relates two Schrödinger Hamiltonians through an intertwining operator [27, 28]. Another approach is the matrix SUSY-QM, which intertwines two Dirac Hamiltonians H_0, H_1 by a matrix operator L. In this work, we use the latter to construct an appropriate Hamiltonian H_1 that will be linked via the operator G introduced in (21) to a photonic graphene system under strain. For the sake of completeness we will give a brief review of matrix SUSY-QM (more details can be found in [29]).

We start by proposing the following intertwining relation:

$$L_1 H_0 = H_1 L_1, \tag{25}$$

where the Dirac Hamiltonians are given by

$$H_0 = -i\sigma_2\partial_s + V_0(s), \quad H_1 = -i\sigma_2\partial_s + V_1(s), \tag{26}$$

and the intertwining operator is

$$L_1 = \partial_s - U_s U^{-1}, \tag{27}$$

with U being a matrix function called *seed* or *transformation matrix*, the subindex in U_s represent the derivative respect to s, and U must satisfy $H_0 U = U\Lambda$. Let us write U in a general form and Λ as a diagonal matrix

$$U = \begin{pmatrix} u_{11} & u_{12} \\ u_{21} & u_{22} \end{pmatrix}, \quad \Lambda = \begin{pmatrix} \lambda_1 & 0 \\ 0 & \lambda_2 \end{pmatrix}. \tag{28}$$

From the intertwining relation and the given definitions, the potential V_1 can be written in terms of the potential V_0 and the transformation matrix as

$$V_1 = V_0 + i[U_s U^{-1}, \sigma_2]. \tag{29}$$

Solutions of the Dirac equation $H_0\xi = E\xi$ can be mapped onto solutions of $H_1\Phi = E\Phi$ using the intertwining operator as $\Phi \propto L_1\xi$. There are some extra solutions, usually referred to *missing states*. They can be obtained from each column of $(U^T)^{-1}$, named Φ_{λ_j}, $j = 1, 2$, which satisfy $H_1\Phi_{\lambda_j} = \lambda_j\Phi_{\lambda_j}$. If the vectors Φ_{λ_j} fulfill the boundary conditions of the problem, λ_j must be included in the spectrum of H_1. As a summary, with this technique, we start from H_0, its eigenspinors and spectrum, then we construct H_1, obtain the solutions of the corresponding Dirac equation and the spectrum. Now, let us mention that it is possible to iterate this technique. The main advantage comes from the modification of the spectrum, since with each iteration, we can add more energy levels. The second-order matrix SUSY-QM can be reached through a second intertwining relation

$$L_2 H_1 = H_2 L_2, \tag{30}$$

which is similar to (25). The intertwining operator now takes the form

$$L_2 = \partial_s - (\mathcal{U}_2)_s \mathcal{U}_2^{-1}. \tag{31}$$

The operator L_1 is used to determine the transformation matrix of the second iteration, $\mathcal{U}_2 = L_1 U_2$, where U_2 fulfills the relation $H_0 U_2 = U_2\Lambda_2$. In this case, Λ_2 is an Hermitian matrix that we choose diagonal once again,

$$\Lambda_2 = \begin{pmatrix} \widetilde{\lambda}_1 & 0 \\ 0 & \widetilde{\lambda}_2 \end{pmatrix}, \quad U_2 = \begin{pmatrix} w_{11} & w_{12} \\ w_{21} & w_{22} \end{pmatrix}. \tag{32}$$

The elements of Λ_2 are such that $(\widetilde{\lambda}_1, \widetilde{\lambda}_2) \neq (\lambda_1, \lambda_2)$. Therefore, the second order potential is given by

$$V_2 = V_1 + i\left[(\mathcal{U}_2)_s \mathcal{U}_2^{-1}, \sigma_2\right]. \tag{33}$$

The solutions of $H_2\chi = E\chi$ are obtained from the eigenspinors of H_1 as $\chi \propto L_2\Phi$. The second-order matrix SUSY-QM generates, in principle, two sets of eigenspinors that correspond to the columns of the matrices $(\mathcal{U}_2^T)^{-1}$ and $L_2(U^T)^{-1}$.

4. Photonic graphene under strain and position-dependent gain and loss

In this section, we start from the auxiliary Dirac equation of a free particle with imaginary mass, and using a matrix SUSY-QM and a gauge transformation G, we obtain a photonic graphene model with strain and position dependent gain/loss. We show that we can iterate the technique to add more propagations modes.

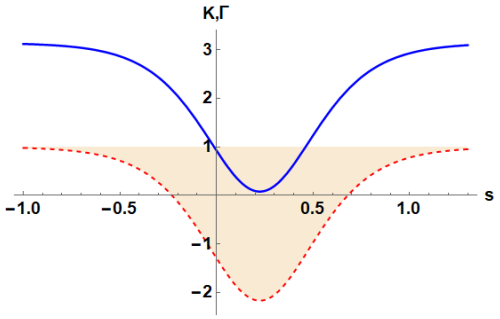

Figure 2. Graph of the functions $v_0k_r + K(s)$ (line blue) and the gain/loss term $\gamma - \Gamma(s)$ (dashed red line) for $\epsilon = 1.5$, $k_r = \pi$, $\gamma = 1$, $v_0 = 1.0$. Notice that $\gamma - \Gamma(s)$ coincides asymptotically with γ.

4.1. Photonic Graphene with a single mode

Let us start from the free particle Dirac equation where we included a purely imaginary mass term:

$$H_0\Phi = (-iv_0\sigma_1\partial_r - iv_0\sigma_2\partial_s + i\gamma\sigma_3)\Phi. \tag{34}$$

Considering $\Phi(r, s) = \exp(ik_r r)(\phi_A(s), \phi_B(s))^T$, the Hamiltonian can be written as

$$H_0(r, s) = -iv_0\sigma_2\partial_s + V_0, \tag{35}$$

where $V_0 = v_0k_r\sigma_1 + i\gamma\sigma_3$. Now, we use the matrix SUSY-QM to construct a new system. A convenient selection of the Λ elements is $\lambda_1 = \epsilon = -\lambda_2$. We build the transformation matrix U with the entries $u_{21} = u_{22}^* = \cosh(\kappa s) + i\sinh(\kappa s)$, the corresponding momentum in s is given by $\kappa = \sqrt{k_r^2 - (\gamma^2 + \epsilon^2)/v_0^2}$. The other two components are found through the equation:

$$u_{1j} = \frac{v_0}{(\lambda_j - i\gamma)}(-u'_{2j} + k_r u_{2j}), \quad j = 1, 2. \tag{36}$$

From (29) we obtain V_1 as

$$V_1 = V_0 + \sigma_1 K(s) - i\sigma_3\Gamma(s), \tag{37}$$

where $\Gamma(s)$, $K(s)$ are given by

$$\Gamma = 2\gamma + \frac{2\epsilon\left(\kappa(\gamma\sinh(2\kappa s) + \epsilon) - \gamma k_r\cosh(2\kappa s)\right)}{\kappa(\gamma - \epsilon\sinh(2\kappa s)) + k_r\epsilon\cosh(2\kappa s)},$$

$$K = \frac{2v_0k_r\epsilon\left(k_r\cosh(2\kappa s) - \kappa\sinh(2\kappa s)\right)}{\kappa(\gamma - \epsilon\sinh(2\kappa s)) + k_r\epsilon\cosh(2\kappa s)} - 2v_0k_r.$$

Figure 2 shows a plot of the functions $v_0k_r + K(s)$ and $\gamma - \Gamma(s)$. The new Hamiltonian takes the form

$$H_1(r, s) = -i\sigma_2v_0\partial_s + \sigma_1(-iv_0\partial_r + K) + i\sigma_3(\gamma - \Gamma). \tag{38}$$

This system supports two single bound states. They are the columns of the matrix $(U^T)^{-1} = (\Phi_\epsilon, \Phi_{-\epsilon})$. The eigenvector associated with ϵ is given by

$$\Phi_\epsilon(r, s) = \frac{e^{ik_r r}}{2}\begin{pmatrix} -\frac{(\gamma^2+\epsilon^2)(\cosh(\kappa s)+i\sinh(\kappa s))}{v_0\kappa(\gamma-\epsilon\sinh(2\kappa s))+v_0k_r\epsilon\cosh(2\kappa s)} \\ \frac{(\gamma-i\epsilon)((\kappa+ik_r)\cosh(\kappa s)-(k_r+i\kappa)\sinh(\kappa s))}{\kappa(\gamma-\epsilon\sinh(2\kappa s))+k_r\epsilon\cosh(2\kappa s)} \end{pmatrix}. \tag{39}$$

Our next step is to apply the gauge transformation defined in (20)-(22). The strain and Fermi velocity tensors that we consider are

$$\mathbf{u} = \begin{pmatrix} 0 & 0 \\ 0 & -\frac{2aK(y))}{\beta} \end{pmatrix},$$
$$\mathbf{v} = v_0 \begin{pmatrix} 1 & 1 \\ 1 & 1-(1-\beta)\frac{2aK(y)}{\beta} \end{pmatrix}, \qquad (40)$$

see (18). The change of variables in (20) becomes

$$r = x, \quad s = \int \frac{1}{1-(1-\beta)\frac{2aK(y)}{\beta}} dy, \qquad (41)$$

and the operator $G(x,y) = \sqrt{1-(1-\beta)\frac{2aK(y)}{\beta}}$. This choice leads to the following Hamiltonian

$$H_1(x,y) = -iv_0\sigma_1\partial_x - i\sigma_2\sqrt{\mathbf{v}_{22}(y)}\partial_y\sqrt{\mathbf{v}_{22}(y)} - \sigma_1\frac{v_0\beta}{2a}\mathbf{u}_{22}(y) + i(\gamma-\Gamma(y))\sigma_3. \qquad (42)$$

Bounded eigenstates of H_1 can be found as $\Psi_\epsilon(x,y) = G^{-1}(x,y)\Phi_\epsilon(r(x),s(y))$. In this system, there is a single mode in the upper Dirac cone and another in the bottom cone.

The strain generates an analog of a magnetic field perpendicular to the graphene layer $\vec{\mathbf{B}}(y) = (\beta/2a)\partial_y\mathbf{u}_{22}\hat{z}$. Since we are working with a photonic graphene, such a pseudo-magnetic field affects light. Moreover, the term $i\Gamma(y)\sigma_3$ indicates a position dependent gain/loss in the optical fibers of the sublattice A/B. Figure 3a shows the square modulus of each component of $\Phi_\epsilon = (\phi_{\epsilon A}, \phi_{\epsilon B})^T$ (shadowed curves) and the intensity $|\phi_{\epsilon A}|^2 + |\phi_{\epsilon B}|^2$ (red curve). Figure 3b shows the same for the mode Ψ_ϵ.

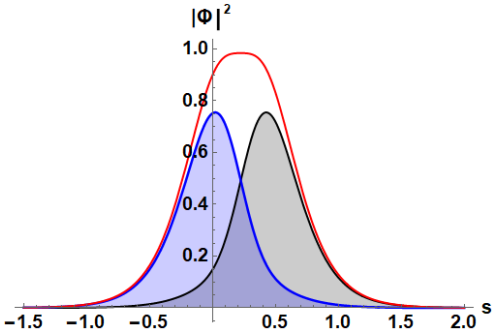

(A).

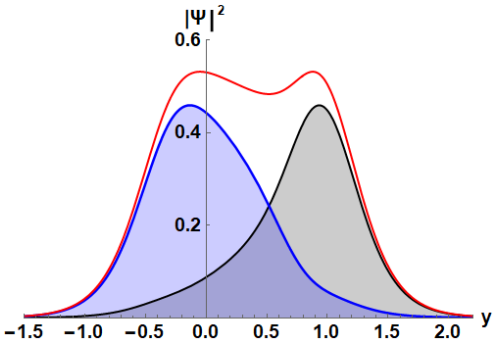

(B).

FIGURE 3. (A) Plot of the individual intensities $|\phi_{\epsilon A}|^2$ (gray curve) and $|\phi_{\epsilon B}|^2$ (blue curve) and the total intensity $|\phi_{\epsilon A}|^2 + |\phi_{\epsilon B}|^2$ (red line). (B) Analog of the (A) plot for the solution Ψ_ϵ of the Hamiltonian under strain. The parameters in this case are: $k_r = \pi$, $\epsilon = 1.5$, $a = 1.0$, $\beta = 0.8$, $\gamma = 1$, $v_0 = 1.0$.

4.2. Photonic Graphene with two modes

In this subsection, we use two iterations of the matrix SUSY-QM, starting again from the free-particle Hamiltonian. Let us choose an initial system with zero gain/loss ($\gamma = 0$), which is a massless fermion in graphene. In the first matrix SUSY-QM step we use the same transformation matrix U as in the example above. The first matrix SUSY-QM partner Hamiltonian has the form

$$H_1 = -i\sigma_2 v_0\partial_s + \sigma_1 K(s) + i\sigma_3\Gamma(s), \qquad (43)$$

where $K(s) = k_r v_0$,

$$\Gamma(s) = \frac{2\epsilon v_0\kappa}{\kappa v_0\sinh(2\kappa s) - k_r v_0\cosh(2\kappa s)}, \qquad (44)$$

with $\kappa = \sqrt{(k_r v_0)^2 - \epsilon^2}/v_0$. As a result of the first matrix SUSY-QM step, it is generated a position dependent gain/loss term $\Gamma(s)$. The iteration of the method requires to define the second diagonal matrix Λ_2, with $\widetilde{\lambda}_1 = -\widetilde{\lambda}_2 = \epsilon_1 \neq \epsilon$, and the second transformation matrix U_2. For this example, we

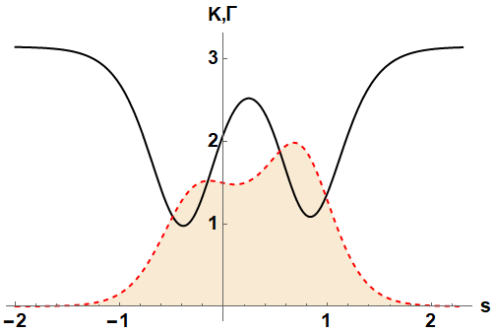

FIGURE 4. Graph of the function $v_0k_r + K_2(s)$ (black line), and the gain/loss function $\Gamma(s) + \Gamma_2(s)$ (red dashed line), for $\epsilon = 1.5$, $\epsilon_1 = 2.0$, $k_r = \pi$, $\gamma = 0$, $v_0 = 1.0$.

choose $w_{21} = \cosh(\kappa_2 s)$ and $w_{22} = \cosh(\kappa_2 s)$, where $\kappa_2 = \sqrt{(k_r v_0)^2 - \epsilon_1^2}/v_0$. The other two components can be found through the equation

$$w_{1j} = \frac{v_0}{\widetilde{\lambda}_j}(-w'_{2j} + k_r w_{2j}), \quad j = 1, 2. \qquad (45)$$

The potential V_2 can be calculated from (33), $V_2 = V_1 + \sigma_1 K_2(s) + i\sigma_3\Gamma_2(s) = V_0 + \sigma_1 K_2 + i\sigma_3(\Gamma + \Gamma_2)$. The functions $v_0k_r + K_2(s)$ and $\Gamma(s) + \Gamma_2(s)$ are shown in Figure 4. It is important to highlight that the gain/loss term remains a pure imaginary quantity.

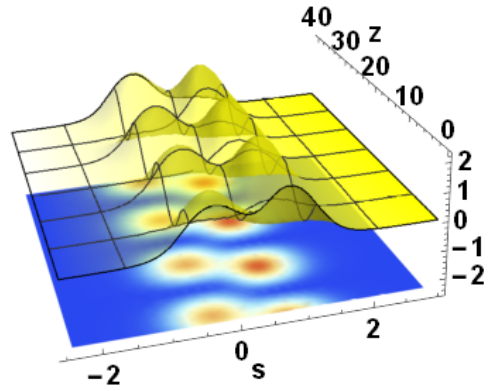

(A).

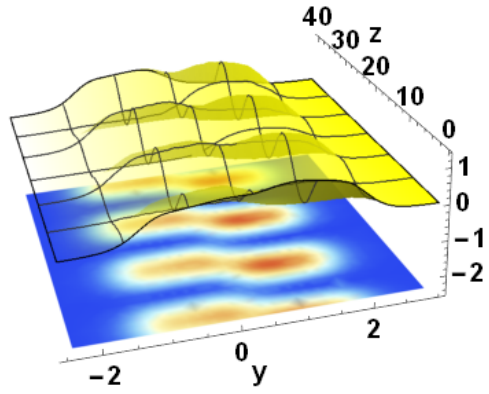

(B).

Figure 5. (A) Intensity of the superposition $|\bar{\Phi}(s,z)|^2$ propagating in the z-axis. (B) Intensity of the superposition $|\bar{\Psi}(y,z)|^2$. The values of the parameters taken are $\epsilon = 1.5$, $\epsilon_1 = 2.0$, $k_r = \pi$, $\gamma = 0$, $\beta = 0.8$, $a = 1.0$, $v_0 = 1.0$.

The second matrix SUSY-QM step introduces two new sets of eigenmodes. They can be extracted from the columns of the matrix $(\mathcal{U}_2^T)^{-1} = (\chi_{\epsilon_1}, \chi_{-\epsilon_1})$. The eigenmodes added in the first step are mapped as $\chi_{\pm\epsilon} = L_2\Phi_{\pm\epsilon}$. Similar to the previous example, it is possible to perform the gauge transformation (20)-(22). Then, in the system under strain, the modes become

$$\Psi_{\pm\epsilon_1}(x,y) = G^{-1}(x,y)\chi_{\pm\epsilon_1}(r(x),s(y)),$$
$$\Psi_{\pm\epsilon}(x,y) = G^{-1}(x,y)\chi_{\pm\epsilon}(r(x),s(y)).$$

Therefore, in this new optical system, two guided modes are created in the upper Dirac cone and two more in the bottom Dirac cone. Finally, let us mention that we can have superpositions of the introduced modes and let them propagate along the z-axis inside the photonic graphene. For example, in the flat Fermi velocity system (before the gauge transformation),

$$\bar{\Phi}(s,z) = A_1 e^{-i\epsilon z}\Phi_\epsilon(s) + A_2 e^{-i\epsilon_1 z}\Phi_{\epsilon_1}(s), \qquad (46)$$

becomes

$$\bar{\Psi}(y,z) = A_1 e^{-i\epsilon z}\Psi_\epsilon(y) + A_2 e^{-i\epsilon_1 z}\Psi_{\epsilon_1}(y), \qquad (47)$$

in the photonic graphene system under strain with the position dependent gain/loss balance. Figure 5a shows the propagation along z-axis of the intensity $|\bar{\Phi}(s,z)|^2$, while Figure 5b shows $|\bar{\Psi}(s,z)|^2$.

5. Summary

This article shows a natural way to construct Hamiltonians associated with a photonic graphene under strain with a position-dependent gain/loss balance. The main tools that we use are a matrix approach to supersymmetric quantum mechanics and a gauge transformation. With a correct choice of a transformation matrix U, it is possible to add a bound state to the free-particle Hamiltonian using the matrix SUSY-QM, but the Dirac equation will have two new terms in the potential, $V_1 = V_0 + \sigma_1 K(s) - i\sigma_3\Gamma(s)$. The function K could be associated with a magnetic vector potential, but the function $i\Gamma$ is related to an imaginary mass term, which is difficult to interpret or realize in a solid-state graphene. The gauge transformation G maps solutions from the flat Fermi velocity system of the previous step to a graphene system under strain. At this point, it becomes relevant to work with the photonic graphene. The magnetic vector potential translates into deformations of the lattice of optical fibers, while the $i\Gamma$ function indicates the gain/loss of the fibers in the sublattice A/B. We end with the Hamiltonian of photonic graphene with a single mode. This mode is confined by the strain and the position-dependent gain/loss balance. Finally, we show that the technique can be iterated, to have two or more modes in the photonic graphene.

Acknowledgements

The authors acknowledge the support of Conacyt, grant FORDECYT-PRONACES/61533/2020. M. C-C. acknowledges as well the Conacyt fellowship 301117.

References

[1] K. S. Novoselov, A. K. Geim, S. V. Morozov, et al. Electric field effect in atomically thin carbon films. *Science* **306**(5696):666–669, 2004. https://doi.org/10.1126/science.1102896.

[2] R. C. Andrew, R. E. Mapasha, A. M. Ukpong, N. Chetty. Mechanical properties of graphene and boronitrene. *Physical Review B* **85**(12):125428, 2012. https://doi.org/10.1103/PhysRevB.85.125428.

[3] S.-E. Zhu, S. Yuan, G. C. A. M. Janssen. Optical transmittance of multilayer graphene. *EPL (Europhysics Letters)* **108**(1):17007, 2014. https://doi.org/10.1209/0295-5075/108/17007.

[4] A. K. Geim, K. S. Novoselov. The rise of graphene. In *Nanoscience and technology: a collection of reviews from nature journals*, pp. 11–19. 2009. https://doi.org/10.1142/9789814287005_0002.

[5] Ş. Kuru, J. Negro, L. M. Nieto. Exact analytic solutions for a Dirac electron moving in graphene under magnetic fields. *Journal of Physics: Condensed Matter* **21**(45):455305, 2009. https://doi.org/10.1088/0953-8984/21/45/455305.

[6] B. Midya, D. J. Fernández C. Dirac electron in graphene under supersymmetry generated magnetic fields. *Journal of Physics A: Mathematical and Theoretical* **47**(28):285302, 2014. https://doi.org/10.1088/1751-8113/47/28/285302.

[7] A. Contreras-Astorga, A. Schulze-Halberg. The confluent supersymmetry algorithm for Dirac equations with pseudoscalar potentials. *Journal of Mathematical Physics* **55**(10):103506, 2014. https://doi.org/10.1063/1.4898184.

[8] M. Castillo-Celeita, D. J. Fernández C. Dirac electron in graphene with magnetic fields arising from first-order intertwining operators. *Journal of Physics A: Mathematical and Theoretical* **53**(3):035302, 2020. https://doi.org/10.1088/1751-8121/ab3f40.

[9] A. Contreras-Astorga, F. Correa, V. Jakubský. Super-Klein tunneling of Dirac fermions through electrostatic gratings in graphene. *Physical Review B* **102**(11):115429, 2020. https://doi.org/10.1103/PhysRevB.102.115429.

[10] G. G. Naumis, S. Barraza-Lopez, M. Oliva-Leyva, H. Terrones. Electronic and optical properties of strained graphene and other strained 2D materials: a review. *Reports on Progress in Physics* **80**(9):096501, 2017. https://doi.org/10.1088/1361-6633/aa74ef.

[11] M. Oliva-Leyva, C. Wang. Theory for strained graphene beyond the Cauchy–Born rule. *Physica Status Solidi (RRL)–Rapid Research Letters* **12**(9):1800237, 2018. https://doi.org/10.1002/pssr.201800237.

[12] M. Polini, F. Guinea, M. Lewenstein, et al. Artificial honeycomb lattices for electrons, atoms and photons. *Nature Nanotechnology* **8**(9):625–633, 2013. https://doi.org/10.1038/nnano.2013.161.

[13] Y. Plotnik, M. C. Rechtsman, D. Song, et al. Observation of unconventional edge states in 'photonic graphene'. *Nature Materials* **13**(1):57–62, 2014. https://doi.org/10.1038/nmat3783.

[14] H. Ramezani, T. Kottos, V. Kovanis, D. N. Christodoulides. Exceptional-point dynamics in photonic honeycomb lattices with $\mathcal{PT}$ symmetry. *Physical Review A* **85**(1):013818, 2012. https://doi.org/10.1103/PhysRevA.85.013818.

[15] G. G. Pyrialakos, N. S. Nye, N. V. Kantartzis, D. N. Christodoulides. Emergence of type-II Dirac points in graphynelike photonic lattices. *Physical Review Letters* **119**(11):113901, 2017. https://doi.org/10.1103/PhysRevLett.119.113901.

[16] S. Grosche, A. Szameit, M. Ornigotti. Spatial Goos-Hänchen shift in photonic graphene. *Physical Review A* **94**(6):063831, 2016. https://doi.org/10.1103/PhysRevA.94.063831.

[17] T. Ozawa, A. Amo, J. Bloch, I. Carusotto. Klein tunneling in driven-dissipative photonic graphene. *Physical Review A* **96**(1):013813, 2017. https://doi.org/10.1103/PhysRevA.96.013813.

[18] A. Szameit, M. C. Rechtsman, O. Bahat-Treidel, M. Segev. $\mathcal{PT}$-symmetry in honeycomb photonic lattices. *Physical Review A* **84**(2):021806, 2011. https://doi.org/10.1103/PhysRevA.84.021806.

[19] H. Schomerus, N. Y. Halpern. Parity anomaly and Landau-level lasing in strained photonic honeycomb lattices. *Physical Review Letters* **110**(1):013903, 2013. https://doi.org/10.1103/PhysRevLett.110.013903.

[20] M. C. Rechtsman, J. M. Zeuner, A. Tünnermann, et al. Strain-induced pseudomagnetic field and photonic Landau levels in dielectric structures. *Nature Photonics* **7**(2):153–158, 2013. https://doi.org/10.1038/nphoton.2012.302.

[21] D. A. Gradinar, M. Mucha-Kruczyński, H. Schomerus, V. I. Fal'ko. Transport signatures of pseudomagnetic Landau levels in strained graphene ribbons. *Physical Review Letters* **110**(26):266801, 2013. https://doi.org/10.1103/PhysRevLett.110.266801.

[22] C. Bena, G. Montambaux. Remarks on the tight-binding model of graphene. *New Journal of Physics* **11**(9):095003, 2009. https://doi.org/10.1088/1367-2630/11/9/095003.

[23] P. Dietl, F. Piéchon, G. Montambaux. New magnetic field dependence of Landau levels in a graphenelike structure. *Physical Review Letters* **100**(23):236405, 2008. https://doi.org/10.1103/PhysRevLett.100.236405.

[24] T. M. G. Mohiuddin, A. Lombardo, R. R. Nair, et al. Uniaxial strain in graphene by Raman spectroscopy: G peak splitting, Grüneisen parameters, and sample orientation. *Physical Review B* **79**(20):205433, 2009. https://doi.org/10.1103/PhysRevB.79.205433.

[25] F. Ding, H. Ji, Y. Chen, et al. Stretchable graphene: a close look at fundamental parameters through biaxial straining. *Nano Letters* **10**(9):3453–3458, 2010. https://doi.org/10.1021/nl101533x.

[26] A. Contreras-Astorga, V. Jakubskỳ, A. Raya. On the propagation of Dirac fermions in graphene with strain-induced inhomogeneous Fermi velocity. *Journal of Physics: Condensed Matter* **32**(29):295301, 2020. https://doi.org/10.1088/1361-648X/ab7e5b.

[27] D. J. Fernández C. SUSY quantum mechanics. *International Journal of Modern Physics A* **12**(01):171–176, 1997. https://doi.org/10.1142/S0217751X97000232.

[28] D. J. Fernández C., N. Fernández-García. Higher-order supersymmetric quantum mechanics. *AIP Conference Proceedings* **744**(1):236–273, 2004. https://doi.org/10.1063/1.1853203.

[29] L. M. Nieto, A. A. Pecheritsin, B. F. Samsonov. Intertwining technique for the one-dimensional stationary Dirac equation. *Annals of Physics* **305**(2):151–189, 2003. https://doi.org/10.1016/S0003-4916(03)00071-X.

LINEARISED COHERENT STATES FOR NON-RATIONAL SUSY EXTENSIONS OF THE HARMONIC OSCILLATOR

Alonso Contreras-Astorga[a], David J. Fernández C.[b], César Muro-Cabral[c, b, *]

[a] *CONACyT-Centro de Investigación y de Estudios Avanzados del I. P. N., Departamento de Física, Av. Instituto Politécnico Nacional No. 2508, Col. San Pedro Zacatenco, C.P. 07360, Ciudad de México, México*

[b] *Centro de Investigación y de Estudios Avanzados del I. P. N., Departamento de Física, Av. Instituto Politécnico Nacional No. 2508, Col. San Pedro Zacatenco, C.P. 07360, Ciudad de México, México*

[c] *Centro de Investigación y de Estudios Avanzados del I. P. N., Unidad Querétaro, Libramiento Norponiente No. 2000, Fracc. Real de Juriquilla, C. P. 76230, Querétaro, Qro., México*

[*] corresponding author: cesar.muro@cinvestav.mx

Abstract. In this work, we derive two equivalent non-rational extensions of the quantum harmonic oscillator using two different supersymmetric transformations. For these extensions, we built ladder operators as the product of the intertwining operators related with these equivalent supersymmetric transformations, which results in two-step ladder operators. We linearised these operators to obtain operators of the same nature that follow a linear commutation relation. After the linearisation, we derive coherent states as eigenstates of the annigilation operator and analyse some relevant mathematical and physical properties, such as the completeness relation, mean-energy values, temporal stability, time evolution of the probability densities, and Wigner distributions. From these properties, we conclude that these coherent states present both classical and quantum behaviour.

Keywords: Supersymmetric quantum mechanics, non-rational extensions, linearised ladder operators, coherent states.

1. Introduction

In quantum physics, supersymmetric quantum mechanics (SUSY) is considered the most efficient technique to generate new quantum potentials from an initial solvable one (see [1–5] for reviews on the topic). This method allows modifying the energy spectrum of an initial Hamiltonian to obtain new Hamiltonians with known eigenstates and eigenvalues. These potentials obtained with SUSY are known as extensions or SUSY partners of the considered initial potential. Moreover, when two different SUSY transformations lead to the same potential (up to an additive constant), it can be said that the extensions are equivalent [6, 7].

Equivalent rational extensions of the quantum harmonic oscillator are very attractive in mathematical physics since its eigenstates are written in terms of exceptional orthogonal polynomials and the results are useful for studying superintegrable systems or generating solutions to the Painlevé equations [8–10]. In a recent work of the authors [11], it was shown that the equivalence between SUSY transformations goes beyond rational extensions and can be extended to non-rational extensions of the harmonic oscillator, i.e. extensions whose potentials cannot be written as the quotient of two polynomials, by considering not only polynomial solutions but also general solutions of the Schrödinger equation.

However, since the birth of quantum theory, it has been relevant to study the quantum states at the border between classical and quantum regimes. In this sense, it is well-known that Schrödinger, in 1926 [12], derived quantum states of the harmonic oscillator that resemble classical behaviour on the phase-space as the classical oscillator does. Later on, in 1962, Glauber rediscovered these states, known as coherent states, and found that they provided the quantum description of coherent light [13]. Since then, there has been a continuous research activity in quantum physics looking for quantum states with a behaviour at the border between classical and quantum regimes by examining semi-classical phase-space properties, in particular, by systems generated by SUSY [4, 14–20].

The coherent states of the harmonic oscillator are Gaussian states, labeled by a complex number z, that minimize the Heisenberg uncertainty relation. They can be constructed either as displaced versions of the ground state or as eigenvectors of the annihilation operator. Moreover, they form an overcomplete set in the sense that

$$\frac{1}{\pi}\int_{\mathbb{C}} |z\rangle\langle z|\, d^2z = \mathbb{1}. \tag{1}$$

These four properties are commonly used as definitions of coherent states when we have a potential different from the harmonic oscillator, see for example [21–25]. Each definition gives, in general, different sets of coherent states. In this work, we obtain coherent states of non-rational extensions of the harmonic oscillator as eigenvectors of the annihilation operator.

For this purpose, we need to find ladder operators of the system.

The outline of the work is the following: In the next section, we present a short summary of SUSY. In Section 3, we generate two equivalent non-rational extensions of the harmonic oscillator. Then, we construct ladder operators as the product of the intertwining operators of the SUSY transformations. In the Section 4, we linearise the ladder operators to obtain a linear commutation relationship, then, we derive coherent states as eigenstates of the annihilation operator and study some of their properties. Our conclusions are presented in the last section.

2. Supersymmetric quantum mechanics

With this technique, we start with two Hamiltonians

$$H = -\frac{1}{2}\frac{d^2}{dx^2} + V(x), \quad \widetilde{H} = -\frac{1}{2}\frac{d^2}{dx^2} + \widetilde{V}(x), \quad (2)$$

where H is the initial Hamiltonian with known eigenfunctions $\psi_n(x)$ and eigenvalues E_n, $n = 0, 1, 2, \ldots$, whereas $\widetilde{H}$ is the Hamiltonian under construction. The potential $\widetilde{V}$ is known as the *extension* or *supersymmetric partner* of V. Now, we propose the existence of k-th order differential operators B, B^+ that intertwine H and $\widetilde{H}$ as

$$\widetilde{H}B^+ = B^+H, \quad B\widetilde{H} = HB. \quad (3)$$

By properly choosing k general solutions u_j $(j = 1, 2, \ldots, k)$ of the stationary Schrödinger equation $Hu_j = \epsilon_j u_j$, with corresponding energies ϵ_j, the SUSY partner potential $\widetilde{V}(x)$ reads

$$\widetilde{V}(x) = V(x) - [\ln W(u_1, u_2, \ldots, u_k)]'', \quad (4)$$

where $W(f_1, f_2, \ldots, f_k)$ denotes the Wronskian of the functions in its argument. The functions u_j are usually referred to as *seed solutions* and the constant ϵ_j as *factorization energies*. Be aware that to have a regular potential, we must choose the seed solutions in such a way the Wronskian has no zeroes.

If $B^+\psi_n \neq 0$, the eigenfunctions $\widetilde{\psi}_n$, $n = 0, 1, \ldots$, of $\widetilde{H}$ can be computed with the relation

$$\widetilde{\psi}_n(x) = \frac{B^+\psi_n(x)}{\sqrt{(E_n - \epsilon_1)\ldots(E_n - \epsilon_k)}} = \frac{1}{\sqrt{(E_n - \epsilon_1)\ldots(E_n - \epsilon_k)}}\frac{W(u_1, u_2, \ldots, u_k, \psi_n)}{W(u_1, u_2, \ldots, u_k)}. \quad (5)$$

The constructed Hamiltonian $\widetilde{H}$ may contain additional eigenfunctions $\widetilde{\psi}_{\epsilon_i}$, known as *missing states*, for some of the factorization energies ϵ_i, given by

$$\widetilde{\psi}_{\epsilon_i} \propto \frac{W(u_1, \ldots, u_{i-1}, u_{i+1}, \ldots, u_k)}{W(u_1, \ldots, u_k)}. \quad (6)$$

If $\widetilde{\psi}_{\epsilon_j}$ fullfills the boundary conditions of the quantum problem, then ϵ_j must be included in the spectrum of $\widetilde{H}$.

In particular, for second-order supersymmetric quantum mechanics, the intertwining operators have the explicit form [26]

$$B = \frac{1}{2}\left[\frac{d^2}{dx^2} + g(x)\frac{d}{dx} + g'(x) + h(x)\right], \quad (7)$$

$$B^+ = \frac{1}{2}\left[\frac{d^2}{dx^2} - g(x)\frac{d}{dx} + h(x)\right]. \quad (8)$$

where the functions $g(x), h(x)$ are found in terms of the only two seed solutions u_1, u_2 with the corresponding factorization energies ϵ_1, ϵ_2, as

$$g = \frac{W'(u_1, u_2)}{W(u_1, u_2)}, \quad h = \frac{g'}{2} + \frac{g^2}{2} - 2V + \frac{\epsilon_1 + \epsilon_2}{2}. \quad (9)$$

Finally, the intertwining operators B and B^+ fulfill the following factorization relations:

$$B^+B = (\widetilde{H} - \epsilon_1)\ldots(\widetilde{H} - \epsilon_k), \quad (10)$$

$$BB^+ = (H - \epsilon_1)\ldots(H - \epsilon_k), \quad (11)$$

i.e., the product of B^+ and B are polynomials of the Hamiltonians H and $\widetilde{H}$.

3. Non-rational extensions of the quantum harmonic oscillator and their ladder operators

Let us consider the harmonic oscillator potential $V = \frac{1}{2}x^2$ and the Hamiltonian H as

$$H = -\frac{1}{2}\frac{d^2}{dx^2} + \frac{1}{2}x^2, \quad (12)$$

whose eigenfunctions and eigenvalues are

$$\psi_n(x) = \sqrt{\frac{1}{2^n\sqrt{\pi}n!}}e^{-\frac{x^2}{2}}H_n(x), \quad E_n = n + \frac{1}{2},$$

where $n = 0,\ 1,\ 2, \ldots$ and $H_n(x)$ are Hermite polynomials [27].

When eigenfunctions of a Hamiltonian are employed as seed functions to generate its SUSY partner, the results are rational extensions and the transformation is called Krein-Adler transformation [6, 7, 28].

Moreover, rational extensions can also be built by employing the polynomial non-normalizable solutions of the Schrödinger equation

$$\varphi_m(x) = e^{\frac{x^2}{2}}\mathcal{H}_m(x), \quad E_{-m-1} = -\left(m + \frac{1}{2}\right),$$

where $m = 0, 1, 2, \ldots$, and $\mathcal{H}_m(x) = (-i)^m H_m(ix)$ are the modified Hermite polynomials [29], which are free of nodes for even m and possess a single node at $x = 0$ for m odd. In the case of m even, the reciprocal of these solutions are square-integrable functions [6].

We can generate non-rational extensions of the harmonic oscillator potential using non-polynomial solutions of the Schrödinger equation as seed functions

in a SUSY transformation. Let us write down the general solution of the stationary Schrödinger equation, with an arbitrary factorization energy denoted by $\mathcal{E} = \lambda + 1/2$, as

$$u(x) = e^{-\frac{x^2}{2}}[H_\lambda(x) + \gamma H_\lambda(-x)], \tag{13}$$

where

$$H_\lambda(x) \equiv \frac{2^\lambda \Gamma\left(\frac{1}{2}\right)}{\Gamma\left(\frac{1-\lambda}{2}\right)} {}_1F_1\left(-\frac{\lambda}{2}; \frac{1}{2}; x^2\right) + \frac{2^\lambda \Gamma\left(-\frac{1}{2}\right)}{\Gamma\left(-\frac{\lambda}{2}\right)} x\, {}_1F_1\left(\frac{1-\lambda}{2}; \frac{3}{2}; x^2\right), \tag{14}$$

are defined as Hermite functions [30, 31],

$${}_1F_1(a; b; z) \equiv \frac{\Gamma(b)}{\Gamma(a)} \sum_{n=0}^{\infty} \frac{\Gamma(a+n)}{\Gamma(b+n)} \frac{z^n}{n!}, \tag{15}$$

is the confluent hypergeometric function, and γ is a real parameter. If $\gamma > 0$, the solution will have an even number of zeroes and for $\gamma < 0$, an odd number of nodes.

3.1. First SUSY transformation

As the first non-rational extension of the harmonic oscillator, we perform a second-order SUSY transformation where we add two new levels with factorization energies $-3/2 < \mathcal{E}_1 < 1/2$ and $\mathcal{E}_2 = E_{-2} = -3/2$, both below the ground state energy. We start by choosing the seed solutions as

$$\begin{aligned} u_1^{(1)}(x) &= e^{-\frac{x^2}{2}}[H_{\lambda_1}(x) + \gamma H_{\lambda_1}(-x)], \\ u_2^{(1)}(x) &= \varphi_1(x), \end{aligned} \tag{16}$$

where $\lambda_1 = \mathcal{E}_1 - 1/2$. To obtain a nodeless Wronskian $W(u_1^{(1)}, u_2^{(1)})$, we take $\gamma > 0$. Notice that $\mathcal{E}_1$ is an arbitrary energy between $E_0 = 1/2$ and $E_{-2} = -3/2$. By following the relation (8), we can define a set of second-order intertwining operators $B^{(1)}, B^{(1)+}$ which satisfy the relations

$$\widetilde{H}^{(1)} B^{(1)+} = B^{(1)+} H, \tag{17}$$

and its adjoint. The SUSY partner potential is

$$\widetilde{V}^{(1)} = \frac{1}{2}x^2 - \left[\ln W(u_1^{(1)}, u_2^{(1)})\right]''. \tag{18}$$

Since $u_1^{(1)}$ is an infinite series, the potential $\widetilde{V}^{(1)}$ is a non-rational extension of V. To find the eigenfunctions of the Hamiltonian $\widetilde{H}^{(1)}$, we use the operator $B^{(1)+}$ as

$$\widetilde{\psi}_n^{(1)} = \frac{B^{(1)+}\psi_n}{\sqrt{(E_n - \mathcal{E}_1)(E_n - \mathcal{E}_2)}}, \quad n = 0, 2, 3, \dots \tag{19}$$

Regarding both missing states of this extension

$$\widetilde{\psi}_{\mathcal{E}_1}^{(1)} \propto \frac{u_2^{(1)}}{W(u_1^{(1)}, u_2^{(1)})}, \quad \widetilde{\psi}_{\mathcal{E}_2}^{(1)} \propto \frac{u_1^{(1)}}{W(u_1^{(1)}, u_2^{(1)})}, \tag{20}$$

due to a stronger divergent behaviour of the Wronskian when $|x| \to \infty$ than the solutions $u_1^{(1)}$,$u_2^{(1)}$, the Hamiltonian $\widetilde{H}^{(1)}$ contains two new bounded states $\widetilde{\psi}_{\mathcal{E}_1}^{(1)}$, and $\widetilde{\psi}_{\mathcal{E}_2}^{(1)}$, so its spectrum is $\mathrm{Sp}\{\widetilde{H}^{(1)}\} = \{E_{-2}, \mathcal{E}_1, E_n,\ n = 0,\ 1,\ 2, \dots\}$.

3.2. Second but equivalent SUSY transformation

We can obtain the same Hamiltonian $\widetilde{H}^{(1)}$, up to an additive constant, with a different second-order SUSY transformation. Let us choose the following seed solutions:

$$\begin{aligned} u_1^{(2)}(x) &= \psi_1(x), \\ u_2^{(2)}(x) &= e^{-\frac{x^2}{2}}[H_{\lambda_2}(x) + \gamma H_{\lambda_2}(-x)], \end{aligned} \tag{21}$$

with the factorization energies $\mathcal{E}_3 = E_1$, and $\mathcal{E}_4 = \mathcal{E}_1 + 2$, respectively. Note that $\lambda_2 = \lambda_1 + 2$. Again, through the relations (7) and (8), we can define second-order differential operators $B^{(2)}$, $B^{(2)+}$, which intertwine a Hamiltonian $\widetilde{H}^{(2)}$ with H as

$$\widetilde{H}^{(2)} B^{(2)+} = B^{(2)+} H. \tag{22}$$

The supersymmetric partner potential is

$$\widetilde{V}^{(2)} = \frac{1}{2}x^2 - \left[\ln W(u_1^{(2)}, u_2^{(2)})\right]''. \tag{23}$$

Since $u_2^{(2)}$ is an infinite series, $\widetilde{V}^{(2)}$ is a non-rational extension of V. The eigenfunctions of its Hamiltonian are

$$\widetilde{\psi}_n^{(2)} = \frac{B^{(2)+}\psi_n}{\sqrt{(E_n - \mathcal{E}_3)(E_n - \mathcal{E}_4)}}, \quad n = 0, 2, 3, \dots, \tag{24}$$

and the missing states

$$\widetilde{\psi}_{\mathcal{E}_3}^{(2)} \propto \frac{u_2^{(2)}}{W(u_1^{(2)}, u_2^{(2)})}, \quad \widetilde{\psi}_{\mathcal{E}_4}^{(2)} \propto \frac{u_1^{(2)}}{W(u_1^{(2)}, u_2^{(2)})}. \tag{25}$$

In this case, owing to the divergent asymptotic behaviour of the solution $u_2^{(2)}$ when $|x| \to \infty$, the missing state $\widetilde{\psi}_{\mathcal{E}_3}^{(2)}$ is not normalizable, and since $u_1^{(2)}$ converges, the state $\widetilde{\psi}_{\mathcal{E}_4}^{(2)}$ is square-integrable. Therefore, the energy spectrum of $\widetilde{H}^{(2)}$ is $\mathrm{Sp}(\widetilde{H}^{(2)}) = \{E_0, \mathcal{E}_3, E_2, \dots\}$.

It is important to notice that the seed functions $u_1^{(1)}$, $u_2^{(1)}$ used to construct $\widetilde{H}^{(1)}$ are related to the seed solutions $u_1^{(2)}$, $u_2^{(2)}$ involved in $\widetilde{H}^{(2)}$. The functions $u_1^{(1)}$ and $u_2^{(2)}$ satisfy $u_2^{(1)} = \sqrt{2\sqrt{\pi}} e^{x^2} u_1^{(2)}$, and $a^- a^- u_2^{(2)} = 2\lambda(\lambda - 1) u_1^{(1)}$, where a^- is the annihilation operator of the harmonic oscillator. Then, by a direct substitution, it can be shown that

$$\widetilde{H}^{(2)} = \widetilde{H}^{(1)} + 2.$$

Thus, $\widetilde{V}^{(1)}$ and $\widetilde{V}^{(2)}$ are equivalent non-rational extensions of the harmonic oscillator. Notice that due to this equivalence, the eigenfunctions obtained by both

transformations are the same but with eigenvalues displaced. In the first extension, the ground state is the missing state $\widetilde{\psi}^{(1)}_{\mathcal{E}_2}$, which is also obtained by $B^{(2)+}\psi_0$. Moreover, the missing state $\widetilde{\psi}^{(1)}_{\mathcal{E}_1}$ corresponds to the missing state $\widetilde{\psi}^{(1)}_{\mathcal{E}_4}$. Finally, relations (19) and (24) are also equivalent as $\widetilde{\psi}^{(2)}_n \propto \widetilde{\psi}^{(1)}_{n-2}$, where $n = 2, 3, 4, \ldots$

3.3. Ladder operators

Since both Hamiltonians $\widetilde{H}^{(1)}$ and $\widetilde{H}^{(2)}$ are equivalent, we can simplify the notation by defining $\widetilde{H}^{(2)}$ as $\widetilde{H}$, its eigenfunctions simply by $\widetilde{\psi}$, the potential $\widetilde{V}^{(2)}$ as $\widetilde{V}$, and $\mathcal{E}_3$ as ϵ. Be aware that $1/2 < \epsilon < 5/2$.

Now, we can define the ladder operators for the SUSY extension $\widetilde{H}$ as the product of the intertwining operators related to the equivalent SUSY transformations as in [32], i.e.

$$\mathcal{L}^+ = B^{(1)+}B^{(2)}, \quad \mathcal{L}^- = B^{(2)+}B^{(1)}. \tag{26}$$

They satisfy the following commutation algebra

$$[\widetilde{H}, \mathcal{L}^\pm] = \pm 2\mathcal{L}^\pm, \tag{27}$$

and

$$\begin{aligned}[\mathcal{L}^-, \mathcal{L}^+] = &(\widetilde{H} + 2 - \mathcal{E}_1)(\widetilde{H} + 2 - \mathcal{E}_2) \\ &(\widetilde{H} + 2 - \mathcal{E}_3)(\widetilde{H} + 2 - \mathcal{E}_4) \\ &- (\widetilde{H} - \mathcal{E}_1)(\widetilde{H} - \mathcal{E}_2)(\widetilde{H} - \mathcal{E}_3)(\widetilde{H} - \mathcal{E}_4).\end{aligned} \tag{28}$$

From the relation (27) and the diagram in Figure 1, we can observe how these operators are two-step ladder operators. Furthermore, the commutation relation (28) indicates that these operators, together with $\widetilde{H}$, realize a polynomial Heisenberg algebra of third-order [33], with a generalized number operator:

$$\begin{aligned}N_4(\widetilde{H}) &= \mathcal{L}^+\mathcal{L}^- \\ &= (\widetilde{H} - \mathcal{E}_1)(\widetilde{H} - \mathcal{E}_2)(\widetilde{H} - \mathcal{E}_3)(\widetilde{H} - \mathcal{E}_4).\end{aligned} \tag{29}$$

The kernel of the annihilation operator $\mathcal{L}^-$ is composed by the functions

$$K_{\mathcal{L}^-} = \{\widetilde{\psi}_{E_0}, \widetilde{\psi}_\epsilon, \widetilde{\psi}_{E_3}, B^{(1)+}u^{(2)}_2\}. \tag{30}$$

The first three elements of the kernel are eigenfunctions of $\widetilde{H}$ and the last one is a non-normalizable solution of the corresponding Schrödinger equation. By applying iteratively the operator $\mathcal{L}^+$ onto these three eigenfunctions, we can construct a basis of three subspaces of the Hilbert space, the direct sum of the three Hilbert-subspaces compose the whole Hilbert space (see Figure 2). Notice that $\widetilde{\psi}_\epsilon$ is annihilated by $\mathcal{L}^+$, then the corresponding subspace will be one-dimensional whereas the other two are infinite-dimensinal subspaces.

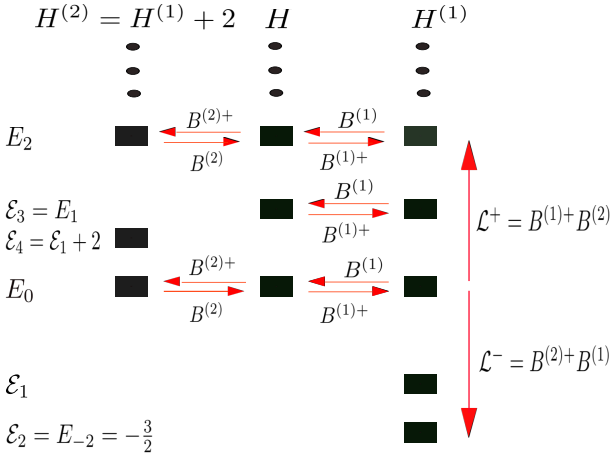

FIGURE 1. Diagram of the mechanism of the two-step ladder operators (26)

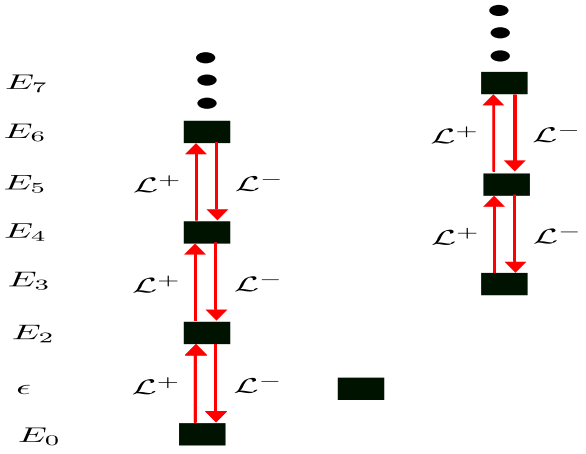

FIGURE 2. Three independent energy ladders that make up the spectrum of $\widetilde{H}$. This spectrum is composed by two infinite energy ladders and a single-element one.

4. Linearised coherent states and their properties

Once we have defined the ladder operators $\mathcal{L}^\pm$ in (26), and clarify how they divide the Hilbert space into two infinite subspaces (or energy ladders) plus a one-dimensional subspace, we proceed to linearise them. We focus on the two infinite subspaces since the construction of the coherent state of the third subspace is trivial. We define new ladder operators for each infinite subspace as

$$l^+_\nu = \sigma_\nu(\widetilde{H})\mathcal{L}^+, \quad l^-_\nu = \sigma_\nu(\widetilde{H} + 2)\mathcal{L}^-, \tag{31}$$

where $\nu = 0,\ 3$ is the index of the subspace. When $\nu = 0$, we refer to the subspace span$\{\widetilde{\psi}_0,\ \widetilde{\psi}_2, \widetilde{\psi}_4,\ \ldots\}$ and, when $\nu = 3$, we refer to the subspace span$\{\widetilde{\psi}_3,\ \widetilde{\psi}_5,\ \widetilde{\psi}_7,\ \ldots\}$. The operators σ_ν are defined as

$$\begin{aligned}\sigma_0(\widetilde{H}) &= [(\widetilde{H} - \mathcal{E}_1)(\widetilde{H} - \mathcal{E}_3)(\widetilde{H} - \mathcal{E}_4)]^{-1/2}, \\ \sigma_3(\widetilde{H}) &= [(\widetilde{H} - \mathcal{E}_1)(\widetilde{H} - \mathcal{E}_2)(\widetilde{H} - \mathcal{E}_3)]^{-1/2}.\end{aligned} \tag{32}$$

From (27), and considering $\sigma_\nu(x)$ a regular function, we obtain the following useful relations.

$$\sigma_\nu(\widetilde{H})\mathcal{L}^+ = \mathcal{L}^+\sigma_\nu(\widetilde{H}+2), \quad \sigma_\nu(\widetilde{H})\mathcal{L}^- = \mathcal{L}^-\sigma_\nu(\widetilde{H}-2);$$
$$\mathcal{L}^+\sigma_\nu(\widetilde{H}) = \sigma(\widetilde{H}-2)\mathcal{L}^+, \quad \mathcal{L}^-\sigma_\nu(\widetilde{H}) = \sigma_\nu(\widetilde{H}+2)\mathcal{L}^-.$$

Using (29), it is direct to show that the operators $l_\nu^\pm$ fulfill the linear commutation relation

$$[l_\nu, l_\nu^+] = 2\mathbb{1}_{\mathbb{H}^\nu}, \tag{33}$$

where $\mathbb{1}_{\mathbb{H}^\nu}$ is the identity in the subspace $\mathbb{H}^\nu$. Therefore, on both Hilbert subspaces, the action of the linearised ladder operators is

$$\begin{aligned} l_\nu^-\widetilde{\psi}_{\nu+2n} &= \sqrt{2n}\widetilde{\psi}_{\nu+2(n-1)}, \\ l_\nu^+\widetilde{\psi}_{\nu+2n} &= \sqrt{2(n+1)}\widetilde{\psi}_{\nu+2(n+1)}, \end{aligned} \tag{34}$$

where $n = 0, 1, 2, \ldots$

At this stage, we can define the linearised coherent states as eigenstates of the linear annihilation operator,

$$l_\nu^- |z^\nu\rangle = z |z^\nu\rangle, \quad \nu = 0,\ 3, \tag{35}$$

where $z \in \mathbb{C}$. We can make the expansion

$$|z^\nu\rangle = \sum_{n=0}^{\infty} c_n |\nu + 2n\rangle, \tag{36}$$

where $\widetilde{\psi}_{\nu+2n}(x) = \langle x|\nu+2n\rangle$ are the eigenfunctions of the SUSY Hamiltonian, and following the definition (35), we find that the explicit form of the normalised coherent states is

$$|z^\nu\rangle = e^{-\frac{|z|^2}{4}} \sum_{n=0}^{\infty} \frac{(z/\sqrt{2})^n}{\sqrt{n!}} |\nu + 2n\rangle. \tag{37}$$

Notice that we obtained a similar expression of the standard coherent states but with the relevant difference that the expansion is in terms of eigenfunctions of the supersymmetric partner Hamiltonian $\widetilde{H}$ in the subspace ν.

4.1. Completeness relation

An important property that the constructed coherent states fulfill is that they form an over-complete set on Hilbert subspaces, i.e., they solve an identity expression [25]

$$\frac{1}{2\pi}\int_{\mathbb{C}} |z^\nu\rangle \langle z^\nu| \, d^2z = \mathbb{1}_{\mathbb{H}^\nu}. \tag{38}$$

4.2. Mean-energy values

The eigenvalue equation of the Hamiltonian $\widetilde{H}$ is given by

$$\widetilde{H} |\nu + 2n\rangle = \left(\nu + \frac{1}{2} + 2n\right) |\nu + 2n\rangle, \tag{39}$$

which leads to the energy expectation

$$\langle z^\nu| \widetilde{H} |z^\nu\rangle = \nu + \frac{1}{2} + |z|^2. \tag{40}$$

We observe that we obtain the well-known quantity of energy-growth corresponding to the oscillator coherent states, this result is another direct consequence of the linear commutation relation between the linearised ladder operators.

4.3. Temporal stability

Another relevant property of the coherent states is that they must remain coherent as they evolve in time. By applying the time evolution operator $U(t)$, we obtain

$$U(t) |z^\nu\rangle = e^{-i\left(\nu+\frac{1}{2}\right)t} |z^\nu(t)\rangle,$$

i.e., our linearised coherent states fulfill this condition. The period of evolution of these states is $\tau = \pi$, the half of the harmonic oscillator coherent states ($T = 2\pi$). This means that in the phase-space, our states need just the half of the time to return to the same point with an acquired phase. This represents a first clear indication of non-classical behaviour.

4.4. Evolution of the probability densities

Let us analyse the time evolution of the probability densities. For the classical coherent states, this quantity is represented by a Gaussian wave packet oscillating around the minimum of the potential. In our case, we have:

$$\begin{aligned} \rho_z(z,x,t) &= |\langle x| U(t) |z^\nu\rangle|^2 \\ &= |\sum_{n=0}^{\infty} e^{-\frac{|z|^2}{4}} \frac{(ze^{-i2t}/\sqrt{2})^n}{\sqrt{n!}} \widetilde{\psi}_{\nu+2n}(x)|^2. \end{aligned} \tag{41}$$

In the Figure 3, we plot this evolution. We observe that each coherent state is composed by two wavepackets with a back-and-forth motion resembling a semi-classical behaviour, since each wavepacket looks like a harmonic-oscillator coherent state. The two wavepackets interfere with each other, and it is more noticeable when they collide around $x = 0$. A parity symmetry $x \to -x$, is only apparent and cannot be guaranteed for the SUSY extensions since the potential $\widetilde{V}$ is only symmetric around $x = 0$ when the parameter $\gamma = 0$ in the seed function $u_2^{(2)}$.

4.5. Wigner distributions

An efficient tool to determine the nature of quantum wave functions is the Wigner quasiprobability distribution in the phase space, defined by

$$W(x,p) \equiv \frac{1}{2\pi}\int_{-\infty}^{\infty} \psi^*\left(x - \frac{y}{2}\right)\psi\left(x + \frac{y}{2}\right) e^{ipy} dy. \tag{42}$$

In Figure 4, we show the corresponding Wigner functions of coherent states for both subspaces. We observe that the distributions possess regions with non-positive values, which is a clear indication of the non-classical behaviour or pure quantum nature of our linearised coherent states.

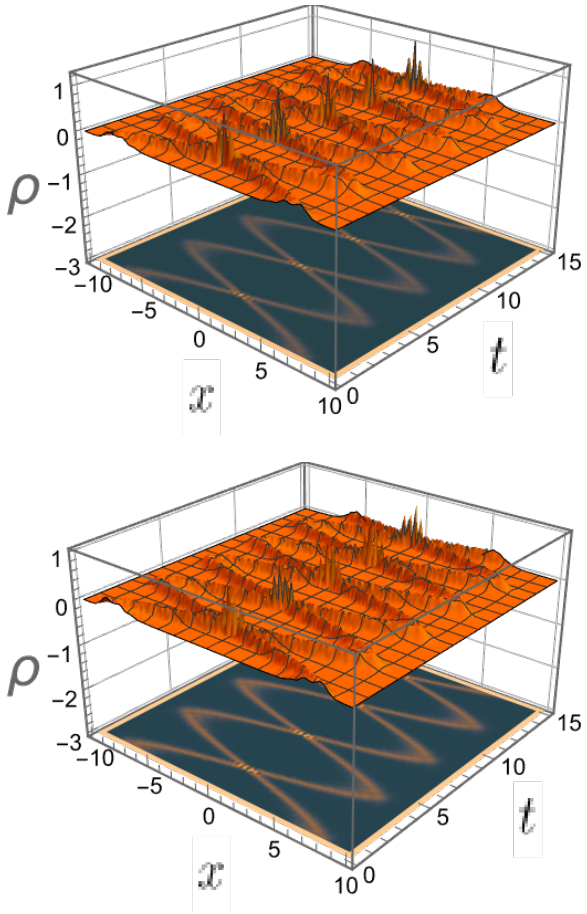

FIGURE 3. Time evolution of the probability densities (41) of the linearised coherent states (37) with $\epsilon = 2$, $\gamma = 2$, **Top:** $\nu = 0$, $z = 5$, and **Bottom:** $\nu = 3$, $z = 5$.

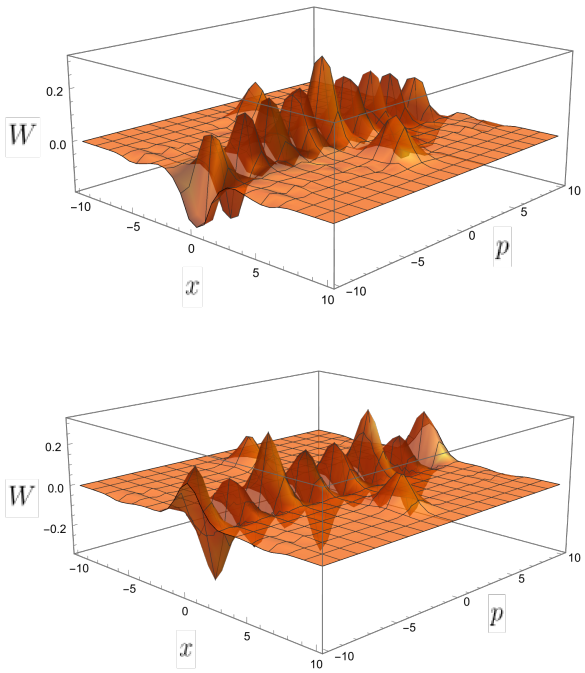

FIGURE 4. Wigner distributions of the linearised coherent states with $\epsilon = 2$, $\gamma = 2$, $z = 5$, **Top:** $\nu = 0$, and **Bottom:** $\nu = 3$.

4.6. HEISENBERG UNCERTAINTY RELATION

First, we introduce two Hermitian quadrature operators

$$X_1 = \frac{l_\nu^+ + l_\nu^-}{2}, \quad X_2 = \frac{l_\nu^- - l_\nu^+}{2i}, \tag{43}$$

and the uncertainties

$$\sigma_{X_i}^2 = \langle X_i^2 \rangle_{z^\nu} - \langle X_i \rangle_{z^\nu}^2, \quad i = 1, 2. \tag{44}$$

Since the coherent states are eigenfunctions of l^-, it is found that these uncertainties follow the product

$$\sigma_{X_1}^2 \sigma_{X_2}^2 = \frac{1}{4}, \tag{45}$$

indicating that they saturate the Heisenberg inequality.

5. CONCLUSIONS

We have found a family of equivalent non-rational extensions of the harmonic oscillator potential generated through two different SUSY transformations involving general solutions of the stationary Schrödinger equation in terms of Hermite functions. These SUSY transformations consisted in moving the first-excited state to an arbitrary level between the ground and the second-excited states, and, on the other hand, adding two new levels below the ground state. We built fourth-order differential ladder operators as the product of the intertwining operators related to the equivalent SUSY transformations. Then, we linearised these ladder operators to have a linear commutation relation. In addition, we realized that these operators divide the entire Hilbert space of eigenfunctions into two infinite energy ladders or Hilbert-subspaces, and one single-element subspace. Then, we derived coherent states of the linearised annihilation operator as eigenstates. We uncovered that they are temporally stable cyclic states with a period $\tau = \pi$, and we showed as well that they form an overcomplete set in each subspace. Moreover, they present the same energy growth as the oscillator coherent states. For the time evolution of the probability densities, we obtained the structure of two oscillating wave-packets, each one with a period 2π, but the collective behaviour with a period τ. For the Wigner functions, we observed that they possess regions with non-positive values, unveiling the quantum nature of these states. Finally, by defining two Hermitian quadrature operators as in the harmonic oscillator, we got the linearised coherent states saturate the Heisenberg inequality. Therefore, as we already mentioned, we conclude that our states present both classical and quantum behaviour.

Acknowledgements

The authors acknowledge Consejo Nacional de Ciencia y Tecnología (CONACyT-México) under grant FORDECYT-PRONACES/61533/2020.

References

[1] C. V. Sukumar. Supersymmetric quantum mechanics of one-dimensional systems. *Journal of Physics A: Mathematical and General* **18**(15):2917, 1985. https://doi.org/10.1088/0305-4470/18/15/020.

[2] V. B. Matveev, M. A. Salle. *Darboux Transformations and Solitons*. Springer Series in Nonlinear Dynamics. Springer Berlin Heidelberg, 1992. ISBN 9783662009246.

[3] F. Cooper, A. Khare, U. Sukhatme. Supersymmetry and quantum mechanics. *Physics Reports* **251**(5-6):267–385, 1995. https://doi.org/10.1016/0370-1573(94)00080-m.

[4] D. J. Fernández C., N. Fernández-García. Higher-order supersymmetric quantum mechanics. *AIP Conference Proceedings* **744**:236–273, 2004. https://doi.org/10.1063/1.1853203.

[5] G. Junker. *Supersymmetric Methods in Quantum, Statistical and Solid State Physics*. IOP Expanding Physics. Institute of Physics Publishing, 2019. ISBN 9780750320245.

[6] S. Odake, R. Sasaki. Krein-Adler transformations for shape-invariant potentials and pseudo virtual states. *Journal of Physics A: Mathematical and Theoretical* **46**(24):245201, 2013. https://doi.org/10.1088/1751-8113/46/24/245201.

[7] D. Gomez-Ullate, Y. Grandati, R. Milson. Extended Krein-Adler theorem for the translationally shape invariant potentials. *Journal of Mathematical Physics* **55**(4):043510, 2014. https://doi.org/10.1063/1.4871443.

[8] D. Bermudez, D. J. Fernández C. Supersymmetric quantum mechanics and Painlevé IV equation. *SIGMA Symmetry, Integrability and Geometry: Methods and Applications* **7**:025, 2011. https://doi.org/10.3842/sigma.2011.025.

[9] D. Bermudez, D. J. Fernández C., J. Negro. Solutions to the Painlevé V equation through supersymmetric quantum mechanics. *Journal of Physics A: Mathematical and Theoretical* **49**(33):335203, 2016. https://doi.org/10.1088/1751-8113/49/33/335203.

[10] P. Clarkson, D. Gómez-Ullate, Y. Grandati, R. Milson. Cyclic Maya diagrams and rational solutions of higher order Painlevé systems. *Studies in Applied Mathematics* **144**(3):357–385, 2020. https://doi.org/10.1111/sapm.12300.

[11] C. Muro-Cabral. *Ladder operators and coherent states for supersymmetric extensions of the harmonic oscillator*. Master's thesis, Physics department, Cinvestav, 2020.

[12] E. Schrödinger. Der stetige Übergang von der Mikro- zur Makromechanik. *Naturwissenschaften* **14**(28):664–666, 1926. https://doi.org/10.1007/bf01507634.

[13] R. J. Glauber. Coherent and incoherent states of the radiation field. *Physical Review* **131**(6):2766, 1963. https://doi.org/10.1103/physrev.131.2766.

[14] H. Bergeron, J. P. Gazeau, P. Siegl, A. Youssef. Semi-classical behavior of Pöschl-Teller coherent states. *EPL (Europhysics Letters)* **92**(6):60003, 2011. https://doi.org/10.1209/0295-5075/92/60003.

[15] D. J. Fernández C., L. M. Nieto, O. Rosas-Ortiz. Distorted Heisenberg algebra and coherent states for isospectral oscillator Hamiltonians. *Journal of Physics A: Mathematical and General* **28**(9):2693, 1995. https://doi.org/10.1088/0305-4470/28/9/026.

[16] D. J. Fernández C., V. Hussin, O. Rosas-Ortiz. Coherent states for Hamiltonians generated by supersymmetry. *Journal of Physics A: Mathematical and Theoretical* **40**(24):6491, 2007. https://doi.org/10.1088/1751-8113/40/24/015.

[17] D. Bermudez, A. Contreras-Astorga, D. J. Fernández C. Painlevé IV coherent states. *Annals of Physics* **350**:615–634, 2014. https://doi.org/10.1016/j.aop.2014.07.025.

[18] S. E. Hoffmann, V. Hussin, I. Marquette, Z. Yao-Zhong. Coherent states for ladder operators of general order related to exceptional orthogonal polynomials. *Journal of Physics A: Mathematical and Theoretical* **51**(31):315203, 2018. https://doi.org/10.1088/1751-8121/aacb3b.

[19] S. E. Hoffmann, V. Hussin, I. Marquette, Z. Yao-Zhong. Ladder operators and coherent states for multi-step supersymmetric rational extensions of the truncated oscillator. *Journal of Mathematical Physics* **60**(5):052105, 2019. https://doi.org/10.1063/1.5091953.

[20] S. Garneau-Desroches, V. Hussin. Ladder operators and coherent states for the Rosen-Morse system and its rational extensions. *Journal of Physics A: Mathematical and Theoretical* **54**(47):475201, 2021. https://doi.org/10.1088/1751-8121/ac2549.

[21] A. O. Barut, L. Girardello. New "coherent" states associated with non-compact groups. *Communications in Mathematical Physics* **21**(1):41–55, 1971. https://doi.org/10.1007/bf01646483.

[22] A. M. Perelomov. Coherent states for arbitrary Lie group. *Communications in Mathematical Physics* **26**(3):222–236, 1972. https://doi.org/10.1007/bf01645091.

[23] M. M. Nieto, L. M. Simmons. Coherent states for general potentials. I. Formalism. *Physical Review D* **20**:1321–1331, 1979. https://doi.org/10.1103/physrevd.20.1321.

[24] V. V. Dodonov, E. V. Kurmyshev, V. I. Manko. Generalized uncertainty relation and correlated coherent states. *Physics Letters A* **79**(2-3):150–152, 1980. https://doi.org/10.1016/0375-9601(80)90231-5.

[25] J. P. Gazeau, J. R. Klauder. Coherent states for systems with discrete and continuous spectrum. *Journal of Physics A: Mathematical and General* **32**(1):123, 1999. https://doi.org/10.1088/0305-4470/32/1/013.

[26] D. J. Fernández C. *Integrability, Supersymmetry and Coherent States: A Volume in Honour of Professor Véronique Hussin*, chap. Trends in Supersymmetric Quantum Mechanics, pp. 37–68. Springer International Publishing, Cham, 2019. https://doi.org/10.1007/978-3-030-20087-9_2.

[27] M. Abramowitz, I. A. Stegun (eds.). *Handbook of mathematical functions, with formulas, graphs, and mathematical tables*. Dover, 1965.

[28] V. E. Adler. A modification of Crum's method. *Theoretical and Mathematical Physics* **101**(3):1381–1386, 1994. https://doi.org/10.1007/bf01035458.

[29] K.-H. Kwon, L. L. Littlejohn. Classification of classical orthogonal polynomials. *Journal of the Korean Mathematical Society* **34**(4):973–1008, 1997.

[30] N. N. Lebedev, R. A. Silverman. Special functions and their applications. *Physics Today* **18**(12):70–72, 1965. https://doi.org/10.1063/1.3047047.

[31] L. Weisner. Generating functions for Hermite functions. *Canadian Journal of Mathematics* **11**:141–147, 1959. https://doi.org/10.4153/cjm-1959-018-4.

[32] I. Marquette, C. Quesne. New ladder operators for a rational extension of the harmonic oscillator and superintegrability of some two-dimensional systems. *Journal of mathematical physics* **54**(10):102102, 2013. https://doi.org/10.1063/1.4823771.

[33] J. M. Carballo, D. J. Fernández C., J. Negro, L. M. Nieto. Polynomial Heisenberg algebras. *Journal of Physics A: Mathematical and General* **37**(43):10349, 2004. https://doi.org/10.1088/0305-4470/37/43/022.

ABOUT THE TIME EVOLUTION OF COHERENT ELECTRON STATES IN MONOLAYERS OF BORON ALLOTROPES

Erik Díaz-Bautista

Instituto Politécnico Nacional, Unidad Profesional Interdisciplinaria de Ingeniería Campus Hidalgo, Departamento de Formación Básica Disciplinaria, Ciudad del Conocimiento y la Cultura, Carretera Pachuca-Actopan km 1+500, San Agustín Tlaxiaca, 42162 Hidalgo, México

correspondence: ediazba@ipn.mx

Abstract. In this paper, we theoretically analyze the massless Dirac fermion dynamics in two-dimensional monolayers of boron allotropes, 8B and 2BH $-$ *pmmn* borophene, interacting with external electric and magnetic fields. We study the effect of the Dirac cone tilt in these materials, which is known as valley index, through the time evolution of probability density of coherent electron states as well as their phase-space representation obtained via the Wigner function. Our results show that the time evolution of the coherent electron states in these materials is valley dependent, which is reinforced in the presence of external electric fields.

Keywords: Tilted Dirac cones, anisotropic Dirac materials, borophene, coherent states, Wigner function.

1. Introduction

Coherent states (CSs) are minimal uncertainty states [1, 2], so that they are considered the most classical states in quantum mechanics. For this reason, they arise in multiple branches of physics, mainly in quantum optics [2] and information processes [3, 4]. Although the wave function provides interesting features about any state, its experimental realization in several quantum systems [3] requires a different approach. In this sense, the Wigner function (WF) constitutes one of the most important theoretical tools for describing quantum systems in the phase-space representation. The WF for a bidimensional system is a quasi-probability distribution defined as [5–7]

$$W(\mathbf{r},\mathbf{p}) = \frac{1}{(2\pi)^2}\int_{-\infty}^{\infty} \mathrm{e}^{i\,\mathbf{p}\cdot\mathbf{q}}\,\Psi\left(\mathbf{r}-\frac{\mathbf{q}}{2}\right)\Psi^{\dagger}\left(\mathbf{r}+\frac{\mathbf{q}}{2}\right)d\mathbf{q}, \tag{1}$$

where $\Psi(\mathbf{r})$ is the wave function, $\mathbf{r} = (x, y)$ and $\mathbf{p} = (p_x, p_y)$ are two-dimensional vectors representing the classical position and momentum values in phase space, respectively; and $\mathbf{q} = (q_1, q_2)$ is a position vector needed in the integration process. In contrast with the probability density of any quantum state, the WF can take negative values, which indicates the nonclassicality of a state and it is a sign of quantumness [3, 8, 9]. Despite this, it has been implemented in quantum optics [3, 4, 9–13], and recently also applied in condensed matter for studying electron dynamics in two-dimensional materials, particularly in graphene under the presence of electromagnetic fields [3, 14–26] as well as in strained honeycomb lattices with dispersive pseudo-Landau-levels [27].

Following this trend, and since the number of two-dimensional materials has been increasing recently, our aim is to provide an adequate description in phase space of the physics of certain quantum macroscopic phenomena, and their semi-classical representation, that occurs in condensed matter systems in the context of valleytronics [28–30]. In this emerging research area, two-dimensional materials such as $8-pmmn$ borophene [31–35], strained graphene [36], Weyl semimetals [37–40], and the organic compound α-(BEDT-TTF)$_2$I$_3$ [41–44], characterize due to the presence of anisotropy and tilted Dirac cones at their low-energy band structure [31, 32, 40, 43, 45–53]. The anisotropy and tilt can be intrinsic, as occurs in borophene [31–34] and phosphorene [54, 55], or induced by strain-engineering and external electric fields, as observed in graphene [20, 36, 56–72].

In this work, we will focus on two-dimensional monolayers of boron allotropes, 8B and 2BH $-$ *pmmn* borophene [73], which have recently attracted attention due to the boron capacity of flexible bonding [47, 74, 75]. The geometry of two-dimensional boron-based Dirac cone materials is much more complicated than that of the pristine honeycomb structure of graphene and, as a consequence, their electronic and transport properties are valley dependent due to the tilting of Dirac cones. These features motivate the research of unusual effects by the intrinsic Dirac cone tilt under the presence of external electric and magnetic fields. For instance, the study of $8-pmmn$ borophene conductivity in the presence of crossed electric and magnetic fields exhibits a clear valley-dependence in magnetotransport properties and polarization currents [33, 34]. It exists the possibility of the realization of coherent electron states in the laboratory and the development of electron quantum optics [15, 76, 77] due to the recent advances in the experimental reconstruction of the WF of electronic systems in quantum tomography experiments.

Thus, this paper is organized as follows. In Section 2, we describe the Dirac Hamiltonian of monolayers of boron allotropes at low-energy regime in the presence of external electric and magnetic fields, and obtain the corresponding Landau states and energy spectra. In Section 3, we discuss the construction of the matrix ladder operators associated to the physical system and also construct the corresponding coherent electron states as eigenstates of the annihilation operator. We also study the time evolution of the probability density and the corresponding phase-space representation. In Section 4, we present our conclusions.

2. Electron dynamics in monolayers of boron allotropes

$8-pmmn$ borophene [31–34] and other two-dimensional monolayers of boron allotropes, such as 8B and 2BH $-pmmn$ borophene [73], present tilted Dirac cones at their low electronic band structure, so that their electronic properties are described by the continuous Dirac Hamiltonian

$$H = \nu\,(v_t\sigma_0 p_y + v_x\sigma_x p_x + v_y\sigma_y p_y), \tag{2}$$

where the matrices $\sigma_{x,y}$ are the Pauli matrices, while σ_0 is the identity matrix. The quantity ν, known as valley index, allows us to transit from valley K ($\nu = 1$) to valley K' ($\nu = -1$). The terms v_x and v_y are the anisotropic Fermi velocities and v_t is the velocity that quantifies the tilting of the Dirac cone. These velocities depend on the material. For instance, the velocity values $\{v_x, v_y, v_t\}$ in multiples of the Fermi velocity $v_\mathrm{F} = 1$ for three different allotropes of boron are shown in Table 1.

Boron allotrope	v_x	v_y	v_t
$8-pmmn$	0.86	0.69	0.32
8B $-pmmn$	0.534	0.785	-0.345
2BH $-pmmn$	0.77	1.348	-0.386

Table 1. The velocities v_x, v_y and v_t in units of the Fermi velocity $v_\mathrm{F} = 10^6$ m/s, for three boron allotropes in the low-energy single-particle effective model.

2.1. Effective Dirac-Weyl Hamiltonian

Now, let us consider massless Dirac fermions in a two-dimensional boron monolayer under the presence of an in-plane electric field $\mathbf{E} = \mathcal{E}\hat{x}$ and a perpendicular magnetic field $\mathbf{B} = B\hat{z}$. These fields are included in the Hamiltonian in Eq. (2) through the scalar and vector potentials

$$U = -x\,\mathcal{E}, \quad \mathbf{A} = x\,B\hat{y}, \tag{3}$$

to obtain the following eigenvalue equation in natural units ($e = -1$ and $\hbar = 1$) [35, 42, 43]:

$$\begin{aligned} &H'\bar{\Psi}(\mathbf{r}) \\ &= (\nu\,[v_x\sigma_x p_x + (v_t\sigma_0 + v_y\sigma_y)(p_y + xB)] + x\mathcal{E}\sigma_0)\,\bar{\Psi}(\mathbf{r}) \\ &= E\bar{\Psi}(\mathbf{r}). \end{aligned} \tag{4}$$

Taking advantage of the translational invariance along the y-axis, so that $\bar{\Psi}(\mathbf{r}) = \exp(ik_y y)\Psi(x)$, the eigenvalue equation in Eq. (4) becomes:

$$\left[\left(\frac{\overline{E} - x_c\,\overline{\mathcal{E}}}{v'_\mathrm{F}}\right)\sigma_0 + i\partial_x\sigma_x - \frac{\left(x_c\,\omega_\mathrm{B} + 2k_y^c\right)}{2}\sigma_y\right]\Psi(x) = 0, \tag{5}$$

where $\overline{E} = E - \nu\,v_t k_y$, $\overline{\mathcal{E}} = (\mathcal{E} + \nu\,v_t B)\sqrt{v_x/v_y}$, $\omega_\mathrm{B} = 2B$, $x_c = x\sqrt{v_y/v_x}$, $k_y^c = k_y\sqrt{v_y/v_x}$, and $v'_\mathrm{F} = \sqrt{v_x v_y}$ is an effective Fermi velocity. By introducing the parameter β_ν and the dimensionless quantity ξ,

$$\beta_\nu = \frac{\overline{\mathcal{E}}}{v'_\mathrm{F}B} = \frac{v_\mathrm{d}}{v_y} + \nu\frac{v_t}{v_y}, \quad \xi = \sqrt{\frac{\omega_\mathrm{B}}{2}}\left(x_c + \frac{2k_y^c}{\omega_\mathrm{B}}\right), \tag{6}$$

with $v_\mathrm{d} = \mathcal{E}/B$ being the drift velocity, Eq. (5) can be rewritten as

$$\left[\left(\epsilon_0 - \sqrt{\frac{\omega_\mathrm{B}}{2}}\beta_\nu\xi\right)\sigma_0 + i\sqrt{\frac{\omega_\mathrm{B}}{2}}\frac{\mathrm{d}}{\mathrm{d}\xi}\sigma_x - \sqrt{\frac{\omega_\mathrm{B}}{2}}\xi\sigma_y\right]\Psi(\xi) = 0, \tag{7}$$

where $\epsilon_0 = \overline{E}/v'_\mathrm{F} + k_y^c\beta_\nu = (E + k_y v_\mathrm{d})/v'_\mathrm{F}$.

2.1.1. Energy spectrum

In order to find the solutions of the initial problem, we proceed as follows [78, 79]. Multiplying by $-i\sigma_x$ to the left of Eq. (7), we get:

$$\begin{aligned}\left[\sqrt{\frac{\omega_\mathrm{B}}{2}}\frac{\mathrm{d}}{\mathrm{d}\xi}\sigma_0 - i\left(\epsilon_0 - \sqrt{\frac{\omega_\mathrm{B}}{2}}\beta_\nu\xi\right)\sigma_x\sigma_0\right. \\ \left. + i\sqrt{\frac{\omega_\mathrm{B}}{2}}\xi\sigma_x\sigma_y\right]\Psi(\xi) = 0. \end{aligned} \tag{8}$$

Differentiating the above expression with respect to ξ, we obtain the following equation

$$\left[\left(\frac{\mathrm{d}^2}{\mathrm{d}\xi^2} + \left(\sqrt{\frac{2}{\omega_\mathrm{B}}}\epsilon_0 - \beta_\nu\xi\right)^2 - \xi^2\right)\sigma_0 + \mathbb{K}\right]\Psi(\xi) = 0, \tag{9}$$

where $\mathbb{K} = i\,(\sigma_x\beta_\nu + \sigma_x\sigma_y)$ is a complex symmetric matrix. The solutions of Eq. (9) can be expressed as $\Psi(\xi)_\eta = \psi_\eta(\xi)\chi_\eta$, where χ_η fulfills the eigenvalue equation $\mathbb{K}\chi_\eta = \eta\chi_\eta$, and $\psi_\eta(\xi)$ is a scalar function that satisfies the differential equation

$$\left[\frac{\mathrm{d}^2}{\mathrm{d}\xi^2} + \left(\sqrt{\frac{2}{\omega_\mathrm{B}}}\epsilon_0 - \beta_\nu\xi\right)^2 - \xi^2 + \eta\right]\psi_\eta(\xi) = 0. \tag{10}$$

In order to simplify the above equation, the variable ζ is defined as

$$\zeta = \xi(1 - \beta_\nu^2)^{1/4} + \sqrt{\frac{2}{\omega_\mathrm{B}}}\frac{\beta_\nu\,\epsilon_0}{(1 - \beta_\nu^2)^{3/4}}, \tag{11}$$

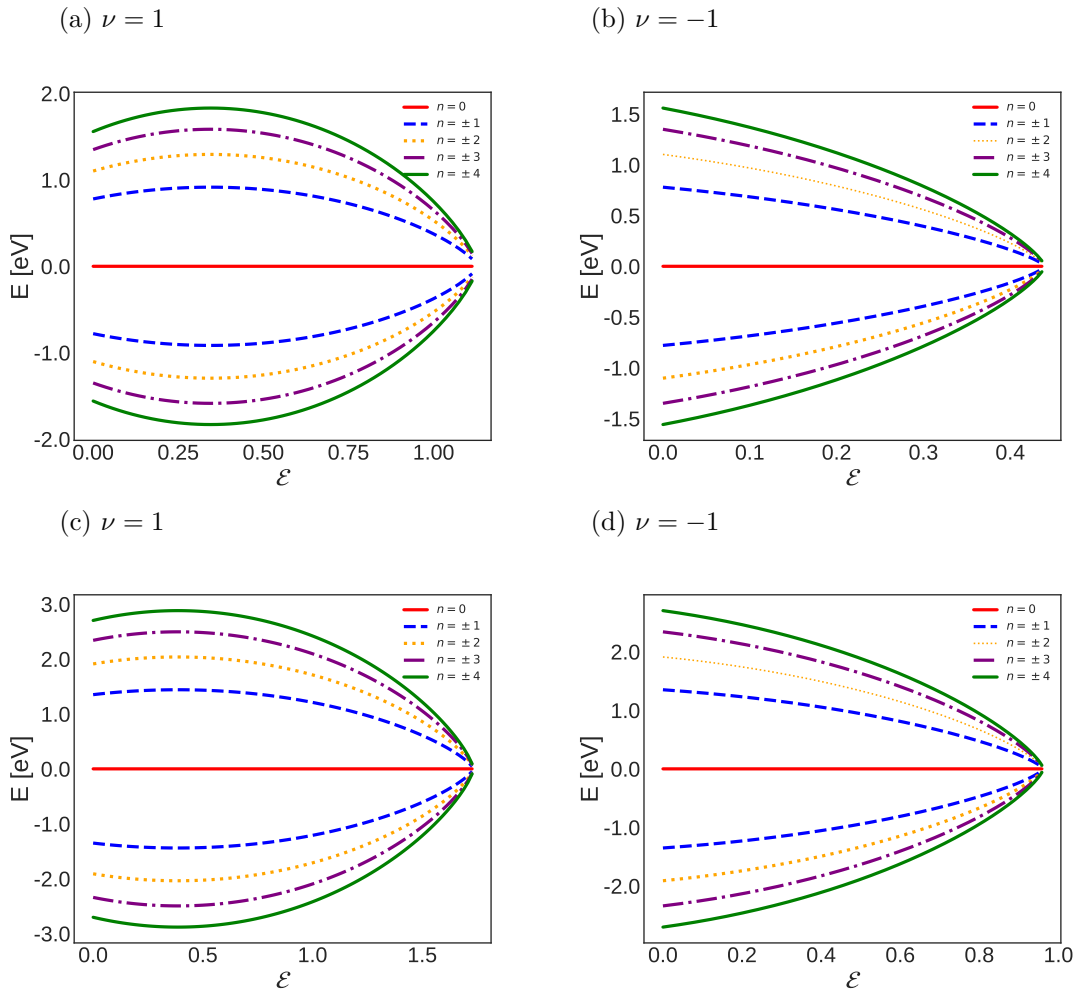

Figure 1. Energy spectrum in Eq. (15) with $k_y = 0$ and $B = 1$ as a function of the electric field $\mathcal{E}$ for 8B $-$ *pmmn* borophene (a, b) and 2BH $-$ *pmmn* (c, d) in each Dirac point ($\nu = \pm 1$).

where β_ν must fulfill the condition $|\beta_\nu| < 1$ for keeping real values of ζ. Hence, we obtain the Weber equation

$$\left[\frac{\mathrm{d}^2}{\mathrm{d}\zeta^2} - \zeta^2 + \frac{2\epsilon_0^2}{\omega_{\mathrm{B}}(1-\beta_\nu^2)^{3/2}} + \frac{\eta}{(1-\beta_\nu^2)^{1/2}}\right]\psi_\eta(\zeta) = 0. \tag{12}$$

On the other hand, the eigenvalues η of the matrix $\mathbb{K}$ turn out to be $\sigma(\mathbb{K}) = \{\eta_k = (-1)^k(1-\beta_\nu^2)^{1/2}\}$ with $k = 1, 2$, while the corresponding normalized eigenvectors are given by

$$\chi_{\eta_1} = \frac{1}{\sqrt{2}}\begin{pmatrix} \sqrt{C_+} \\ -i\sqrt{C_-} \end{pmatrix}, \quad \chi_{\eta_2} = \frac{1}{\sqrt{2}}\begin{pmatrix} -\sqrt{C_-} \\ i\sqrt{C_+} \end{pmatrix}, \tag{13}$$

where $C_\pm = 1 \pm \sqrt{1-\beta_\nu^2}$. Substituting the eigenvalues η_k in Eq. (12) and taking $\psi_\eta(\zeta) = \exp\left(-\zeta^2/2\right) f_\eta(\zeta)$, one gets the following ODE:

$$f_\eta''(\zeta) - 2\,\zeta f_\eta'(\zeta) = \left(1 - (-1)^k - \frac{2\epsilon_0^2/\omega_{\mathrm{B}}}{(1-\beta_\nu^2)^{3/2}}\right) f_\eta(\zeta), \tag{14}$$

with $k = 1, 2$. By solving the above ODE, the energy spectrum turns out to be [80] (see Figure 1):

$$E_{n,k_y} = \mathrm{sgn}(n)\sqrt{v_x v_y}(1-\beta_\nu^2)^{3/4}\sqrt{\omega_{\mathrm{B}}|n|} - k_y\, v_{\mathrm{d}}. \tag{15}$$

The Landau energy levels in Eq. (15) depend on valleys K and K' [43] via the amount β_ν in Eq. (6), which indicates whether the orbits are closed ($|\beta_\nu| < 1$) or opened ($|\beta_\nu| \geq 1$) [43, 80, 81]. Also, the critical values of $v_{\mathrm{d}}^c = \mathcal{E}_c$ for which $\beta_\nu = 1$ depend on each tilted anisotropic Dirac material (see again Figure 1). For instance, in Table 2 we summarize the critical values $\mathcal{E}_c$ in valleys K and K' for three monolayers of boron allotropes.

Borophene monolayer	$\mathcal{E}_c$ (K)	$\mathcal{E}_c$ (K')
$8 - pmmn$	0.37	1.01
8B $-$ *pmmn*	1.13	0.44
2BH $-$ *pmmn*	1.734	0.962

Table 2. The electric field critical value $\mathcal{E}_c = (v_y - \nu v_t)B$ for three boron allotropes according to the valley index ν. The data for $8 - pmmn$ borophene were obtained from [35].

Finally, the average velocity in the y-direction is given by [82, 83]

$$\langle v_y \rangle = \frac{\partial E_{n,ky}}{\partial k_y} = -v_{\rm d} = \left[\frac{\mathbf{E} \times \mathbf{B}}{B^2} \right]_y , \qquad (16)$$

that means the Dirac fermions move with an average velocity $v_{\rm d}$ in the negative y-direction.

2.1.2. Eigenstates

The eigenstates of the Hamiltonian in Eq. (4) can be written as

$$\Psi_n(x) = \frac{[(1-\delta_{0n})\chi_{\eta_1}\psi_{n-1}(x) + \lambda\chi_{\eta_2}\psi_n(x)]}{\sqrt{2^{(1-\delta_{0n})}}} = \mathbb{M}\Phi_n(x), \qquad (17)$$

where δ_{mn} denotes the Kronecker delta, the band index λ indicates the conduction ($\lambda = 1$) or ($\lambda = -1$) valence band, and

$$\mathbb{M} = \sqrt{\frac{1}{2}} \begin{pmatrix} \sqrt{C_+} & i\sqrt{C_-} \\ -i\sqrt{C_-} & \sqrt{C_+} \end{pmatrix}, \qquad (18a)$$

$$\Phi_n(x) = \frac{1}{\sqrt{2^{(1-\delta_{0n})}}} \begin{pmatrix} (1-\delta_{0n})\psi_{n-1}(x) \\ i\lambda\,\psi_n(x) \end{pmatrix}. \qquad (18b)$$

The components of the pseudo-spinor $\Phi_n(x)$ are given by the wave functions [79]

$$\psi_n(\zeta_n) = \frac{(1-\beta_\nu^2)^{1/8}}{\sqrt{n!}} \left(\frac{\omega_{\rm B} v_y}{2\pi v_x} \right)^{1/4} D_n(\sqrt{2}\,\zeta_n), \qquad (19)$$

where $D_n(\cdot)$ are the parabolic cylinder functions with n a non-negative integer, and the quantity ζ_n is given by Eq. (11) with $\epsilon_0 = (E_{n,k_y} + k_y v_{\rm d})/\sqrt{v_x v_y}$.

3. Coherent electron states

We start to obtain the CSs by first considering the set of ladder operators $\mathbb{A}^\pm$ given in [35] and acting on the Hilbert basis $\Phi_n(x) = \mathbb{M}^{-1}\Psi_n(x)$, namely,

$$\mathbb{A}^+\Phi_n(\zeta_n) = \sqrt{2^{(1-\delta_{0n})}}\sqrt{n+1}\,\Phi_{n+1}(\zeta_{n+1}), \qquad (20a)$$

$$\mathbb{A}^-\Phi_n(\zeta_n) = \sqrt{2^{(1-\delta_{1n})}}\sqrt{n}\,\Phi_{n-1}(\zeta_{n-1}), \qquad (20b)$$

and whose commutation relation reads

$$[\mathbb{A}^-, \mathbb{A}^+]\Phi_n(x) = c(n)\Phi_n(x), \quad c(n) = \begin{cases} 1, & n = 0, \\ 3, & n = 1, \\ 2, & n > 1. \end{cases} \qquad (21)$$

Now, we define the CSs as eigenstates of the annihilation operator $\mathbb{A}^-$:

$$\mathbb{A}^-\Phi_z(x) = z\,\Phi_z(x), \quad z \in \mathbb{C}, \qquad (22)$$

with complex eigenvalue, where

$$\Phi_z(x) = \sum_{n=0}^{\infty} a_n \Phi_n(x). \qquad (23)$$

Using Eq. (20a), the explicit expression for the CSs is given by

$$\Phi_z(x) = \mathcal{N}_\alpha \left[\Phi_0(x) + \sum_{n=1}^{\infty} \frac{\sqrt{2}\alpha^n}{\sqrt{n!}} \Phi_n(x) \right], \qquad (24)$$

where $\mathcal{N}_\alpha^{-2} = 2\exp\left(|\alpha|^2\right) - 1$ and $\alpha = z/\sqrt{2} = |\alpha|\exp(i\varphi)$. Here, the physical meaning of $|\alpha|$ is that it is the oscillation amplitude while the phase angle φ is identical to the angular rotation in the classical motion. It is worth to mention that the procedure described allows to obtain the so-called Barut-Girrardello CSs. However, this is not the only way to build CSs. In [27], the displacement-operator method has been implemented in order to construct such states in other honeycomb lattices.

Finally, defining the matrix operators

$$\mathbb{B}^- \equiv \mathbb{M}\,\mathbb{A}^-\mathbb{M}^{-1}, \quad \mathbb{B}^+ \equiv \mathbb{M}\,\mathbb{A}^+\mathbb{M}^{-1}, \qquad (25)$$

whose actions on the Landau states $\Psi_n(x)$ in Eq. (17) reads as

$$\mathbb{B}^+\Psi_n(\zeta_n) = \sqrt{2^{(1-\delta_{0n})}}\sqrt{n+1}\,\Psi_{n+1}(\zeta_{n+1}), \qquad (26a)$$

$$\mathbb{B}^-\Psi_n(\zeta_n) = \sqrt{2^{(1-\delta_{1n})}}\sqrt{n}\,\Psi_{n-1}(\zeta_{n-1}), \qquad (26b)$$

it is possible to verify that the states $\Psi_\alpha(x) = \mathbb{M}\,\Phi_z(x)$ are eigenfunctions of the annihilation operator $\mathbb{B}^-$ with the same eigenvalue z. Therefore, the states $\bar{\Psi}_\alpha(\mathbf{r}) = \exp(ik_y y)\,\Psi_\alpha(x)$ are the coherent electron states of the system. In addition, the commutation relation in Eq. (21) is also fulfilled writing $\mathbb{B}^\pm$ and Ψ_n instead of $\mathbb{A}^\pm$ and Φ_n, respectively.

3.1. Overcompleteness and resolution to the identity

The CSs satisfy the following relation

$$|\langle\bar{\Psi}_{\alpha'}|\bar{\Psi}_\alpha\rangle| = \left| \frac{2\exp(\alpha'^*\alpha) - 1}{\sqrt{(2\exp(|\alpha|^2) - 1)(2\exp(|\alpha'|^2) - 1)}} \right| \neq \delta(\alpha' - \alpha). \qquad (27)$$

Since the coherent electron states are not orthogonal for $\alpha \neq \alpha'$, we say the set of such states is overcomplete.

Besides, these CSs satisfy the following relation that can be considered as an unusual resolution to the identity:

$$\frac{|\bar{\Psi}_0\rangle\langle\bar{\Psi}_0|}{2} + \int_{\mathbb{C}} \frac{{\rm d}\rho(\alpha)}{\pi} |\bar{\Psi}_\alpha\rangle\langle\bar{\Psi}_\alpha| = \mathbb{I}_+, \qquad (28)$$

where $\mathbb{I}_+$ denotes the identity operator in the Hilbert space for Landau states in the conduction band, and ${\rm d}\rho(\alpha)$ is a positive measure defined as

$${\rm d}\rho(\alpha) = \frac{2\exp\left(|\alpha|^2\right) - 1}{2\exp\left(-|\alpha|^2\right)} |\alpha|\,{\rm d}|\alpha|\,{\rm d}\varphi. \qquad (29)$$

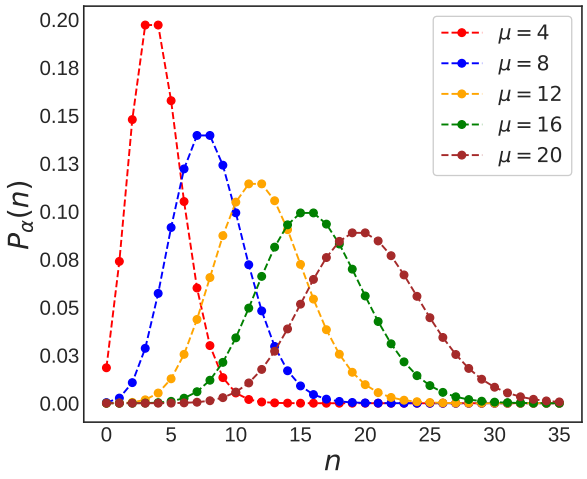

Figure 2. Occupation number distribution $P_\alpha(n)$ in Eq. (30) for the coherent electron states $\bar{\Psi}_\alpha$ for different values of $\mu = |\alpha|^2$.

3.2. Occupation number distribution

The CSs follow a Poisson-like distribution with mean $\mu = |\alpha|^2$, according to the occupation number distribution

$$P_\alpha(n) = |\langle \bar{\Psi}_n | \bar{\Psi}_\alpha \rangle| = \frac{1}{2\exp(\mu) - 1} \begin{cases} 1, & n = 0, \\ \frac{2\mu^n}{n!}, & n > 0, \end{cases} \tag{30}$$

which gives the probability of a CS of being in an Landau state $\bar{\Psi}_n$ (see Figure 2).

3.3. Mean energy value

On the another hand, the expectation value of the energy in the CS basis is given by

$$\langle H \rangle_\alpha = \mathcal{N}_\alpha^2 \Bigg[k_y v_\mathrm{d} \left(1 - 2\exp\left(|\alpha|^2\right)\right) + 2\sqrt{v_x v_y \omega_\mathrm{B}} \times (1 - \beta_\nu^2)^{3/4} \sum_{n=1}^{\infty} \mathrm{sgn}(n) \frac{|\alpha|^{2n}}{n!} \sqrt{|n|} \Bigg]. \tag{31}$$

The mean group velocity of the CSs is obtained as

$$\langle v_y \rangle_\alpha = \frac{\partial \langle H \rangle_\alpha}{\partial k_y} = -v_\mathrm{d}, \tag{32}$$

which agrees with Eq. (16).

3.4. Time evolution of the wave packet

Now, let us consider the time-evolution operator $U(t) = \exp(-iHt)$ applied on the expansion of CSs in terms of Landau states $\bar{\Psi}_n(\mathbf{r})$. Hence, the time-dependent coherent electron states are:

$$\bar{\Psi}_\alpha(\mathbf{r}, t) = \mathcal{N}_\alpha \exp(ik_y y)\, \mathbb{M} \begin{pmatrix} \psi_{\alpha,1}(x,t) \\ i\,\lambda\, \psi_{\alpha,2}(x,t) \end{pmatrix}, \tag{33}$$

where

$$\psi_{\alpha,1}(x,t) = \sum_{n=1}^{\infty} \frac{\alpha^n \mathrm{e}^{-iE_n t}}{\sqrt{n!}} \psi_{n-1}(x), \tag{34a}$$

$$\psi_{\alpha,2}(x,t) = \sum_{n=0}^{\infty} \frac{\alpha^n \mathrm{e}^{-iE_n t}}{\sqrt{n!}} \psi_n(x). \tag{34b}$$

The time-dependent probability density $|\bar{\Psi}_\alpha(\mathbf{r}, t)|^2$ is

$$|\bar{\Psi}_\alpha(\mathbf{r}, t)|^2 = \mathcal{N}_\alpha^2 \Big\{ |\psi_{\alpha,1}(x,t)|^2 + |\psi_{\alpha,2}(x,t)|^2 - 2\lambda\beta_\nu \Re\left[\psi_{\alpha,1}^*(x,t)\psi_{\alpha,2}(x,t)\right] \Big\}, \tag{35}$$

where $\Re(z)$ denotes the real part of a complex number z.

Figure 3 shows the time evolution of the probability distribution of the CSs for 8B and 2BH $-pmmn$ borophene. We can see that in both cases, the density probability in valley K evolves faster than that in valley K'. This means that Dirac fermions take less time to complete a loop around the equilibrium point. The function $|\bar{\Psi}_\alpha(\mathbf{r}, t)|^2$ shows maximum values close to the turning points in the x-axis. Besides, with the values chosen for the parameters $\alpha = 4i$, $k_y = 0$ and $B = 1$, the probability density of the CSs with $\nu = -1$ for 8B $-pmmn$ borophene shows a different behavior in time in comparison to the other cases. This is related to the fact for the electric field considered ($\mathcal{E} = 0.25$), the corresponding energy spectrum is near to collapse, indicating the classical orbits that the charge carriers in valley K' follow are more open compared with those in K for 8B $-pmmn$ borophene, and even for those ones in 2BH $-pmmn$ borophene.

3.5. Obtaining of the time-dependent Wigner function for coherent electron states

To calculate the Wigner matrix (WM) [84] for the coherent states in Eq. (33) in valleys K and K', we substitute them into the integral matrix representation in Eq. (1) to get [35]:

$$\mathbb{W}_\alpha(\mathbf{r}, \mathbf{p}) = \mathbb{M} W_\alpha(\mathbf{r}, \mathbf{p}) \mathbb{M}^\dagger. \tag{36}$$

Thus, the trace of this matrix provides us an expression of the time-dependent WF of the coherent states:

$$\mathrm{Tr}[\mathbb{W}_\alpha(\mathbf{r}, \mathbf{p}, t)] = \mathcal{N}_\alpha^2\, \delta(p_y - k_y) \Big\{ W_{11}(\chi, t) + W_{22}(\chi, t) - 2\lambda\beta_\nu \Re[W_{12}(\chi, t)] \Big\}, \tag{37}$$

where the components W_{11}, W_{22} and W_{12} are the corresponding Wigner functions of the terms in Eq. (34) and their product, and that in general involve sums

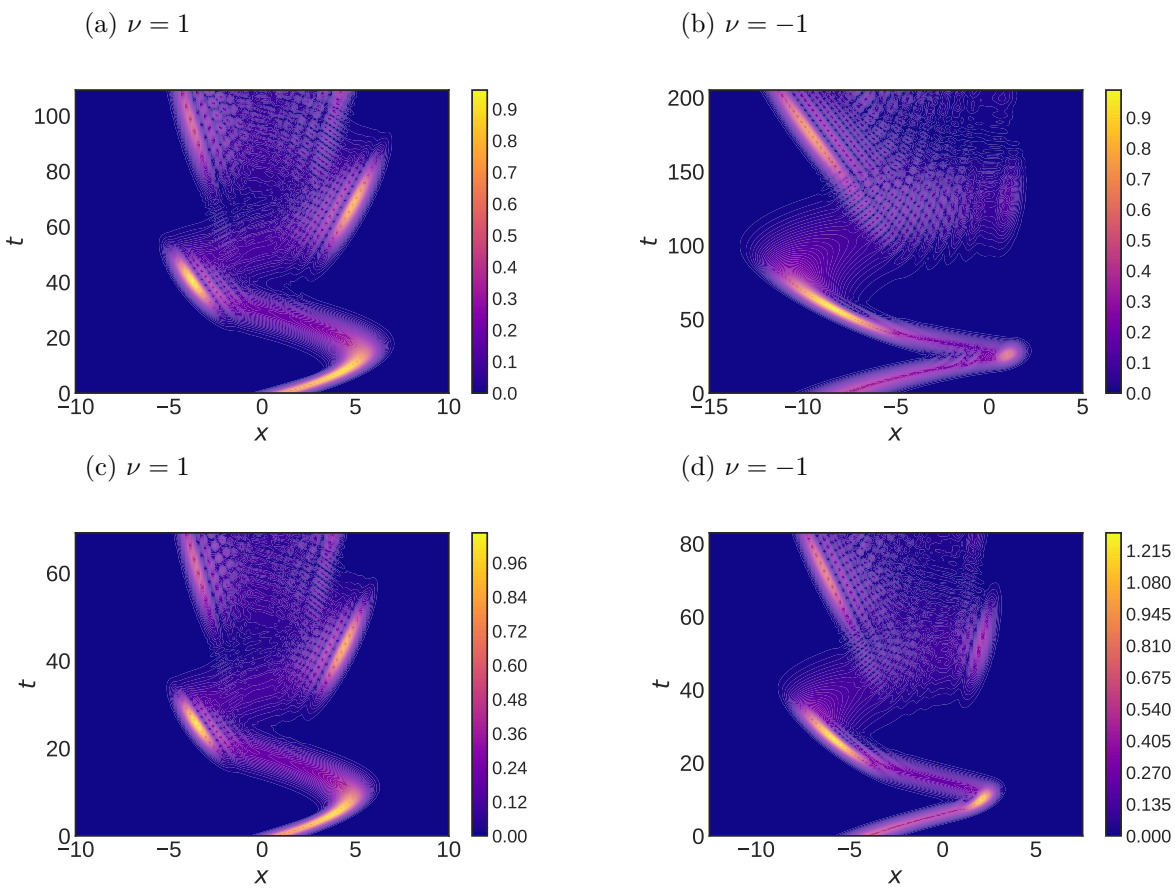

FIGURE 3. Time evolution of the probability density $|\Psi_\alpha(\mathbf{r},t)|^2$ in Eq. (35) with $k_y = 0$, $B = 1$, $\alpha = 4i$, $\mathcal{E} = 0.25$ and $\lambda = 1$ for 8B $-pmmn$ borophene (a, b) and 2BH $-pmmn$ borophene (c, d) in each Dirac point ($\nu = \pm 1$).

of functions of the form (see [35] for more details)

$$W_{u,v}(\chi_{n,m}) = \frac{1}{\pi}\exp\left(-\frac{1}{2}|\chi_{n,m}|^2 + i(\zeta_n - \zeta_m)s\right) \times \begin{cases} (-1)^u\sqrt{\frac{u!}{v!}}\chi_{n,m}^{v-u}L_u^{v-u}\left(|\chi_{n,m}|^2\right), & \text{if } u \le v, \\ (-1)^v\sqrt{\frac{v!}{u!}}\chi_{n,m}^{*u-v}L_v^{u-v}\left(|\chi_{n,m}|^2\right), & \text{if } u \ge v, \end{cases} \tag{38}$$

with $L_n^m(\cdot)$ denoting the associated Laguerre polynomials, and

$$\chi_{n,m} = \frac{\zeta_n + \zeta_m}{\sqrt{2}} + i\sqrt{2}\,s, \quad \chi_n \equiv \chi_{n,n}, \tag{39a}$$

$$s = \left(1 - \beta_\nu^2\right)^{-1/4}\sqrt{\frac{2v_x}{\omega_B v_y}}\,p_x. \tag{39b}$$

The time evolution of the WM trace for the CSs is shown in Figures 4 and 5 for 8B and 2BH $-pmmn$ borophene, respectively. In both cases, we observe that the WF in valley K propagates faster than in valley K'. As the state evolves in time, the trace of the WM takes negative values, which is an indication of the increasing of the CS quantumness and also of the uncertainty relations, as is discussed in [35]. For larger times, the WM traces become identical to that of the Landau state with n equal to the integer part of $|\alpha|^2$, in agreement to the number occupation distribution in Eq. (30).

3.5.1. PERIOD OF MOTION

Now, in order to provide an approximate period τ for the CSs, we proceed as follows [85]. First, we calculate the mean energy $\langle H\rangle_\alpha$ for the CSs $\bar{\Psi}_\alpha(\mathbf{r})$. Then, setting the eigenvalue z, we compute the energy interval in which $\langle H\rangle_\alpha$ lies, namely, $E_{j,k_y} < \langle H\rangle_\alpha < E_{j+1,k_y}$. Thus, the approximate period is determined as:

$$\tau = \frac{2\pi}{\Delta E} = \frac{2\pi}{E_{j+1,k_y} - E_{j,k_y}}, \tag{40}$$

that will be different for each valley since the energy spectrum depends on the tilting parameter ν. For instance, for the CSs with $\alpha = 4i$ and the same values used in Figures 3, 4 and 5, we have $E_{15} < \langle H\rangle_\alpha < E_{16}$. Note that $\langle H\rangle_\alpha$ is bounded by the Landau level with $n = |\alpha|^2 = 16$. Thus, the respective periods are reported in Table 3.

The period τ in Eq. (40) increases as $\Delta E \to 0$ close to the electric field critical value $\mathcal{E}_c$, since a Dirac fermion takes a longer time to complete a loop an opened orbit (see red and blue curves in Figure 6). In contrast, the orbits are closed for more separated energy levels resulting in a shorter period τ (see green curve in Figure 6).

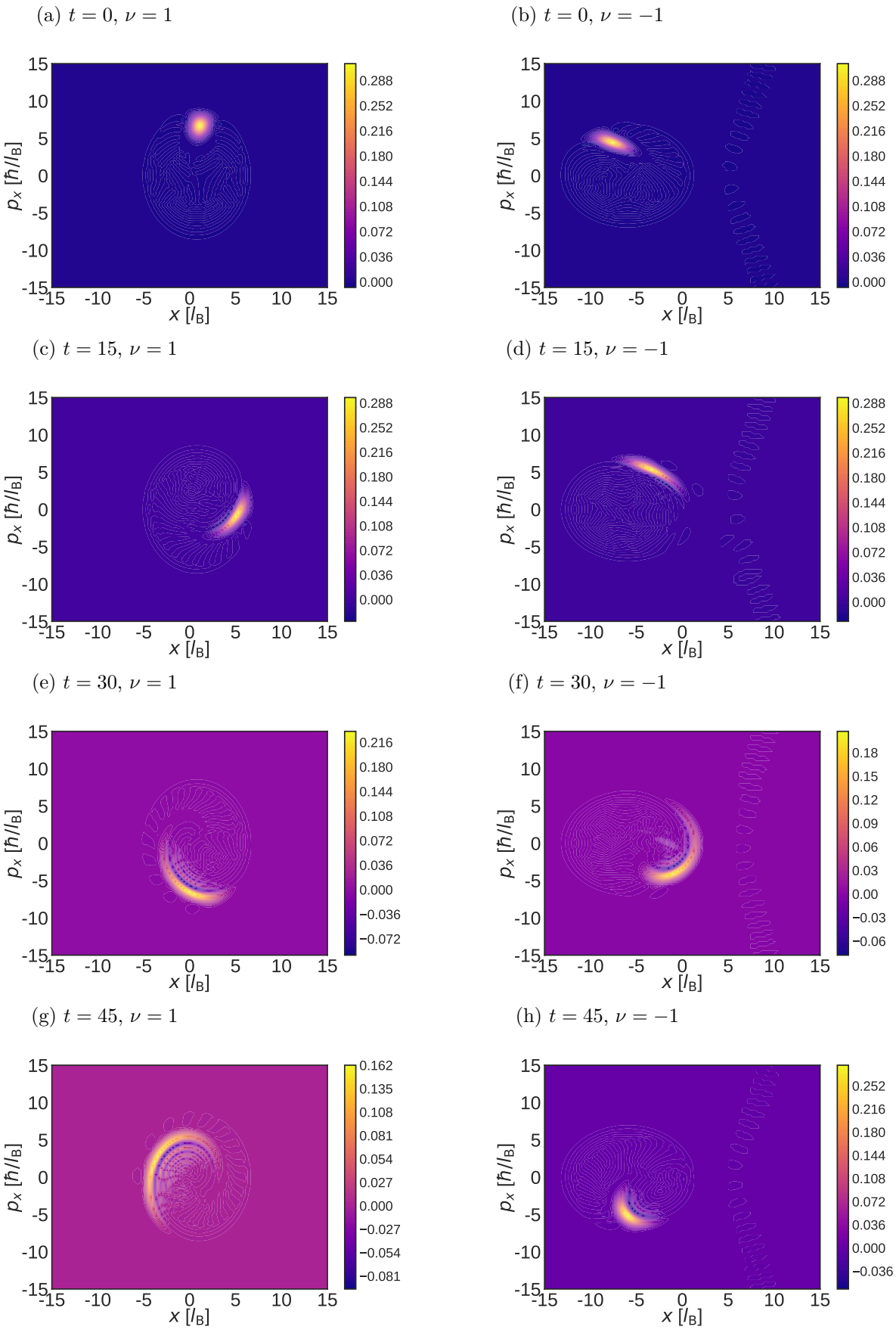

FIGURE 4. Time evolution of the trace of the Wigner matrix $\mathbb{W}_\alpha(\mathbf{r}, \mathbf{p})$ in Eq. (37) for different values of t in each Dirac point ($\nu = \pm 1$) of 8B $-pmmn$ borophene. $B = 1$, $k_y = 0$, $\alpha = 4i$, $\{v_x, v_y, v_t\} = \{0.534, 0.785, -0.345\}$, $\mathcal{E} = 0.25$, and $\lambda = 1$. In the figure labels, $l_B = 1/\sqrt{B}$.

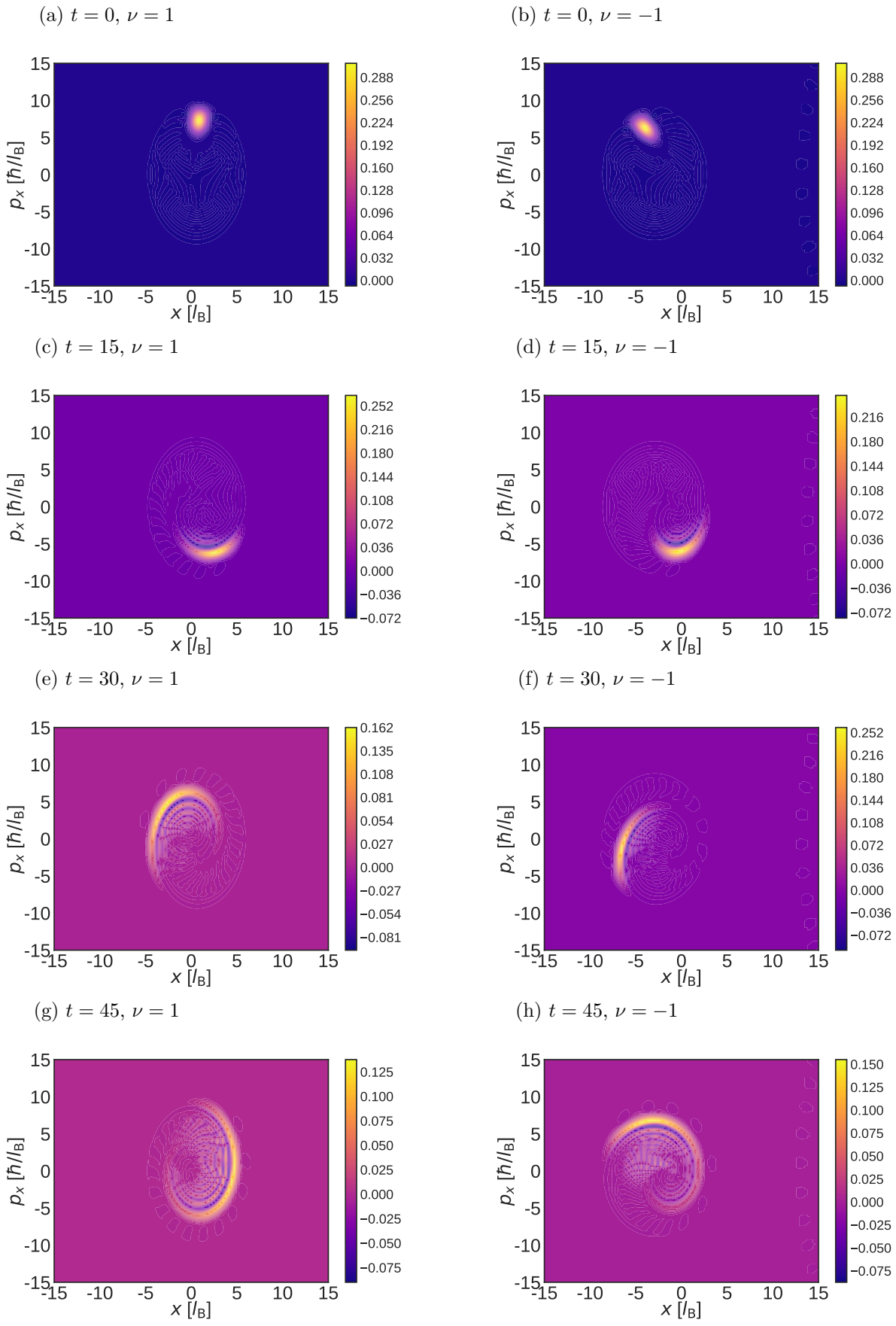

FIGURE 5. Time evolution of the trace of the Wigner matrix $\mathbb{W}_\alpha(\mathbf{r}, \mathbf{p})$ in Eq. (37) for different values of t in each Dirac point ($\nu = \pm 1$) of 2BH $-pmmn$ borophene. $B = 1$, $k_y = 0$, $\alpha = 4i$, $\{v_x, v_y, v_t\} = \{0.77, 1.348, -0.380\}$, $\mathcal{E} = 0.25$, and $\lambda = 1$. In the figure labels, $l_B = 1/\sqrt{B}$.

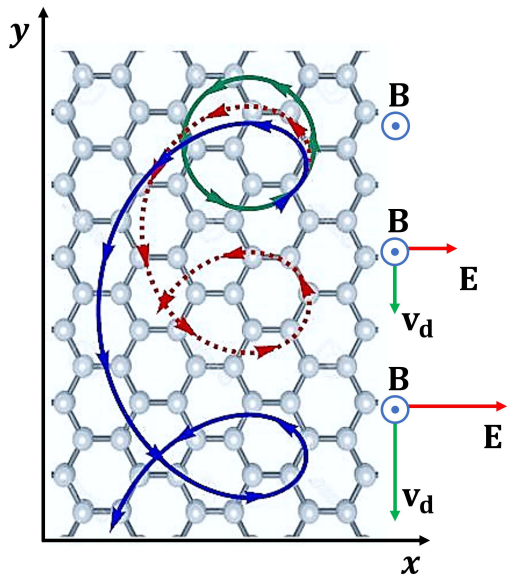

Figure 6. A generic honeycomb lattice interacts with crossed electric and magnetic fields directed along the x- and z-directions, respectively. In absence of electric field $\mathbf{E}$, a non-relativistic classical charged particle performs a circular trajectory (green curve), while if the strength $\mathbf{E}$ increases, the trajectory becomes into a trochoid (red and blue curves). The drift velocity $\mathbf{v}_\mathrm{d} = \mathbf{E} \times \mathbf{B}/B^2$ is directed along the y-direction.

Borophene monolayer	τ_+ (K)	τ_- (K')
$8-pmmn$	34.165π	14.566π
$8\mathrm{B}-pmmn$	17.388π	32.642π
$2\mathrm{BH}-pmmn$	11.012π	13.200π

Table 3. Valley-dependent period τ for the CSs with eigenvalue $\alpha = 4i = z/\sqrt{2}$ in three boron allotropes. The data for $8-pmmn$ borophene were obtained from [35].

3.6. Discussion

Anisotropic and tilted Dirac cone materials, such as 8B and $2\mathrm{BH}-pmmn$ borophene, possess valley-dependent electronic properties under the interaction with crossed electric and magnetic fields. The effective Hamiltonian depends on two anisotropic velocities and one tilt velocity (see Eq. (2)). In the case in which these materials interact with external crossed electric and magnetic fields (see Eq. (4)), it is possible to obtain the solutions to the physical problem in a simple algebraic way (see Eq. (15) and (17)).

We have constructed the CSs $\bar{\Psi}_\alpha(\mathbf{r})$ as a linear combination of the Landau eigenfunctions $\bar{\Psi}(\mathbf{r})$ of the Hamiltonian in Eq. (4), that also be eigenfunction of a matrix ladder operator $\mathbb{B}^-$ with a complex eigenvalue z. As the coherent electron states evolve in time, their probability density clearly shows maximum values only around the turning points in the x-axis, in which momentarily the velocity of charge carriers reduces. In turn, the emergence of negative values in the trace of the Wigner matrix for longer times is related to the increasing uncertainties of the position and momentum, as is studied in [35], in agreement to the probability distribution Eq. (30). Also, the increasing of the electric field to a critical value can delay the time-evolution of CSs in one of the valleys, allowing us to distinguish the Dirac fermions of one valley from those of another (see Figures 3, 4 and 5).

In Figure 6, we have showed the classical picture of a (valley-independent) non-relativistic charge carrier that follows a closed trajectory in the xy-plane in presence of an external magnetic field $\mathbf{B}$ along the z-direction. When an electric field $\mathbf{E}$ is applied along the x-axis, the trajectory becomes into a trochoid with velocity $\mathbf{v}_\mathrm{d}$ directed to the y-direction. In contrast, we observe that in the quantum picture of our problem, due to the Lorentz transformation into the reference frame and the energy [43], as well as the valley index, there is a factor $(1-\beta_\nu^2)^{3/4}$ that modifies the spacing between two adjacent Landau levels, and as a consequence also the period of motion in Eq. (40).

4. Conclusions

We studied the dynamics of massless Dirac fermions in two bidimensional monolayers of boron allotropes under the interaction with crossed external electric and magnetic fields. We analyzed the effect of the Dirac cone tilt in the time evolution of probability density of coherent electron states as well as the corresponding Wigner function. We conclude that the time evolution of the coherent electron states in these materials is valley dependent, and the presence of an in-plane external electric field reinforces such a dependency.

We consider that the findings here presented may contribute to the understanding of the effects of the tilting of the Dirac cones 8B and $2\mathrm{BH}-pmmn$ borophene on the charge carrier dynamics under the interaction of electromagnetic fields, with which these materials could be considered as viable valley splitters in experimental applications. Besides, the coherent state description developed through the phase-space representation may provide a satisfactory semi-classical description of similar quantum valley-dependent phenomena that occur in other tilted anisotropic Dirac materials interacting with external electromagnetic fields.

Acknowledgements

The author acknowledges T. Stegmann and Y. Betancur-Ocampo for their invaluable comments to improve this work, as well as the financial support from CONACYT Project FORDECYT-PRONACES/61533/2020 and SIP-IPN research grant 20210317.

References

[1] E. Schrödinger. Der stetige Übergang von der Mikro- zur Makromechanik. *Naturwissenschaften* **14**(28):664–666, 1926. https://doi.org/10.1007/BF01507634.

[2] R. J. Glauber. Coherent and incoherent states of the radiation field. *Physical Review* **131**:2766–2788, 1963. https://doi.org/10.1103/PhysRev.131.2766.

[3] J. Weinbub, D. K. Ferry. Recent advances in Wigner function approaches. *Applied Physics Reviews* **5**(4):041104, 2018. https://doi.org/10.1063/1.5046663.

[4] C. Gerry, P. Knight, C. C. Gerry. *Introductory Quantum Optics*. Cambridge University Press, 2010. ISBN 052152735X.

[5] E. Wigner. On the quantum correction for thermodynamic equilibrium. *Physical Review* **40**(5):749–759, 1932. https://doi.org/10.1103/physrev.40.749.

[6] M. Hillery, R. F. O'Connell, M. O. Scully, E. P. Wigner. Distribution functions in physics: Fundamentals. *Physics Reports* **106**(3):121–167, 1984. https://doi.org/10.1016/0370-1573(84)90160-1.

[7] A. Kenfack, K. Zyczkowski. Negativity of the Wigner function as an indicator of non-classicality. *Journal of Optics B: Quantum and Semiclassical Optics* **6**(10):396–404, 2004. https://doi.org/10.1088/1464-4266/6/10/003.

[8] D. T. Smithey, M. Beck, M. G. Raymer, A. Faridani. Measurement of the Wigner distribution and the density matrix of a light mode using optical homodyne tomography: Application to squeezed states and the vacuum. *Physical Review Letters* **70**(9):1244–1247, 1993. https://doi.org/10.1103/physrevlett.70.1244.

[9] C. Baune, J. Fiurášek, R. Schnabel. Negative Wigner function at telecommunication wavelength from homodyne detection. *Physical Review A* **95**(6):061802, 2017. https://doi.org/10.1103/physreva.95.061802.

[10] H.-W. Lee. Theory and application of the quantum phase-space distribution functions. *Physics Reports* **259**(3):147–211, 1995. https://doi.org/10.1016/0370-1573(95)00007-4.

[11] W. B. Case. Wigner functions and Weyl transforms for pedestrians. *American Journal of Physics* **76**(10):937–946, 2008. https://doi.org/10.1119/1.2957889.

[12] R. P. Rundle, P. W. Mills, T. Tilma, et al. Simple procedure for phase-space measurement and entanglement validation. *Physical Review A* **96**(2):022117, 2017. https://doi.org/10.1103/physreva.96.022117.

[13] M. V. Berry. Semi-classical mechanics in phase space: A study of Wigner's function. *Philosophical Transactions of the Royal Society of London Series A, Mathematical and Physical Sciences* **287**(1343):237–271, 1977. https://doi.org/10.1098/rsta.1977.0145.

[14] C. Jacoboni, P. Bordone. The Wigner-function approach to non-equilibrium electron transport. *Reports on Progress in Physics* **67**(7):1033, 2004. https://doi.org/10.1088/0034-4885/67/7/r01.

[15] C. Bäuerle, D. C. Glattli, T. Meunier, et al. Coherent control of single electrons: a review of current progress. *Reports on Progress in Physics* **81**(5):056503, 2018. https://doi.org/10.1088/1361-6633/aaa98a.

[16] E. Colomés, Z. Zhan, X. Oriols. Comparing Wigner, Husimi and Bohmian distributions: which one is a true probability distribution in phase space? *Journal of Computational Electronics* **14**(4):894–906, 2015. https://doi.org/10.1007/s10825-015-0737-6.

[17] D. J. Mason, M. F. Borunda, E. J. Heller. Revealing the flux: Using processed Husimi maps to visualize dynamics of bound systems and mesoscopic transport. *Physical Review B* **91**(16):165405, 2015. https://doi.org/10.1103/physrevb.91.165405.

[18] C. M. Carmesin, P. Kling, E. Giese, et al. Quantum and classical phase-space dynamics of a free-electron laser. *Physical Review Research* **2**(2):023027, 2020. https://doi.org/10.1103/physrevresearch.2.023027.

[19] O. Morandi, F. Schürrer. Wigner model for quantum transport in graphene. *Journal of Physics A: Mathematical and Theoretical* **44**(26):265301, 2011. https://doi.org/10.1088/1751-8113/44/26/265301.

[20] E. Díaz-Bautista, Y. Betancur-Ocampo. Phase-space representation of Landau and electron coherent states for uniaxially strained graphene. *Physical Review B* **101**(12):125402, 2020. https://doi.org/10.1103/physrevb.101.125402.

[21] E. Díaz-Bautista, Y. Concha-Sánchez, A. Raya. Barut–Girardello coherent states for anisotropic 2D-Dirac materials. *Journal of Physics: Condensed Matter* **31**(43):435702, 2019. https://doi.org/10.1088/1361-648x/ab2d18.

[22] E. Díaz-Bautista, D. J. Fernández. Graphene coherent states. *The European Physical Journal Plus* **132**(11):499, 2017. https://doi.org/10.1140/epjp/i2017-11794-y.

[23] D. J. Mason, M. F. Borunda, E. J. Heller. Semiclassical deconstruction of quantum states in graphene. *Physical Review B* **88**(16):165421, 2013. https://doi.org/10.1103/physrevb.88.165421.

[24] G. J. Iafrate, V. N. Sokolov, J. B. Krieger. Quantum transport and the Wigner distribution function for Bloch electrons in spatially homogeneous electric and magnetic fields. *Physical Review B* **96**(14):144303, 2017. https://doi.org/10.1103/physrevb.96.144303.

[25] P. Ghosh, P. Roy. Quasi coherent state of the Dirac oscillator. *Journal of Modern Optics* **68**(1):56–62, 2021. https://doi.org/10.1080/09500340.2021.1876261.

[26] D. K. Ferry, I. Welland. Relativistic Wigner functions in transition metal dichalcogenides. *Journal of Computational Electronics* **17**(1):110–117, 2017. https://doi.org/10.1007/s10825-017-1094-4.

[27] E. Díaz-Bautista, M. Oliva-Leyva. Coherent states for dispersive pseudo-Landau-levels in strained honeycomb lattices. *The European Physical Journal Plus* **136**(7):765, 2021. https://doi.org/10.1140/epjp/s13360-021-01753-w.

[28] J. R. Schaibley, H. Yu, G. Clark, et al. Valleytronics in 2D materials. *Nature Reviews Materials* **1**(11):16055, 2016. https://doi.org/10.1038/natrevmats.2016.55.

[29] A. Kundu, H. A. Fertig, B. Seradjeh. Floquet-engineered valleytronics in Dirac systems. *Physical Review Letters* **116**:016802, 2016. https://doi.org/10.1103/PhysRevLett.116.016802.

[30] Y. S. Ang, S. A. Yang, C. Zhang, et al. Valleytronics in merging Dirac cones: All-electric-controlled valley filter, valve, and universal reversible logic gate. *Physical Review B* **96**:245410, 2017. https://doi.org/10.1103/PhysRevB.96.245410.

[31] A. Lopez-Bezanilla, P. B. Littlewood. Electronic properties of 8−*Pmmn* borophene. *Physical Review B* **93**(24):241405, 2016. https://doi.org/10.1103/physrevb.93.241405.

[32] A. D. Zabolotskiy, Y. E. Lozovik. Strain-induced pseudomagnetic field in the Dirac semimetal borophene. *Physical Review B* **94**(16):165403, 2016. https://doi.org/10.1103/physrevb.94.165403.

[33] SK Firoz Islam, A. M. Jayannavar. Signature of tilted Dirac cones in weiss oscillations of 8 − *Pmmn* borophene. *Physical Review B* **96**(23):235405, 2017. https://doi.org/10.1103/physrevb.96.235405.

[34] SK Firoz Islam. Magnetotransport properties of 8-Pmmn borophene: effects of Hall field and strain. *Journal of Physics: Condensed Matter* **30**(27):275301, 2018. https://doi.org/10.1088/1361-648x/aac8b3.

[35] Y. Betancur-Ocampo, E. Díaz-Bautista, T. Stegmann. Valley-dependent time evolution of coherent electron states in tilted anisotropic Dirac materials. *Physical Review B* **105**(4):045401, 2022. https://doi.org/10.1103/PhysRevB.105.045401.

[36] M. Assili, S. Haddad, W. Kang. Electric field-induced valley degeneracy lifting in uniaxial strained graphene: Evidence from magnetophonon resonance. *Physical Review B* **91**(11):115422, 2015. https://doi.org/10.1103/physrevb.91.115422.

[37] D. Sabsovich, T. Meng, D. I. Pikulin, et al. Pseudo field effects in type II Weyl semimetals: new probes for over tilted cones. *Journal of Physics: Condensed Matter* **32**(48):484002, 2020. https://doi.org/10.1088/1361-648x/abaa7e.

[38] K. Das, A. Agarwal. Linear magnetochiral transport in tilted type-I and type-II Weyl semimetals. *Physical Review B* **99**(8):085405, 2019. https://doi.org/10.1103/physrevb.99.085405.

[39] A. Menon, B. Basu. Anomalous Hall transport in tilted multi-Weyl semimetals. *Journal of Physics: Condensed Matter* **33**(4):045602, 2020. https://doi.org/10.1088/1361-648x/abb9b8.

[40] P. P. Ferreira, A. L. R. Manesco, T. T. Dorini, et al. Strain engineering the topological type-II Dirac semimetal $NiTe_2$. *Physical Review B* **103**(12):125134, 2021. https://doi.org/10.1103/physrevb.103.125134.

[41] J. Sári, M. O. Goerbig, C. Tőke. Magneto-optics of quasirelativistic electrons in graphene with an inplane electric field and in tilted Dirac cones in α-(BEDT TTF)$_2$I$_3$. *Physical Review B* **92**(3):035306, 2015. https://doi.org/10.1103/physrevb.92.035306.

[42] M. O. Goerbig, J.-N. Fuchs, G. Montambaux, F. Piéchon. Tilted anisotropic Dirac cones in quinoid-type graphene and α-(BEDT-TTF)$_2$I$_3$. *Physical Review B* **78**(4):045415, 2008. https://doi.org/10.1103/physrevb.78.045415.

[43] M. O. Goerbig, J.-N. Fuchs, G. Montambaux, F. Piéchon. Electric-field–induced lifting of the valley degeneracy in α-(BEDT-TTF)$_2$I$_3$ Dirac-like Landau levels. *EPL Europhysics Letters* **85**(5):57005, 2009. https://doi.org/10.1209/0295-5075/85/57005.

[44] T. Morinari, T. Himura, T. Tohyama. Possible verification of tilted anisotropic Dirac cone in α-(BEDT-TTF)$_2$I$_3$ using interlayer magnetoresistance. *Journal of the Physical Society of Japan* **78**(2):023704, 2009. https://doi.org/10.1143/jpsj.78.023704.

[45] X.-F. Zhou, X. Dong, A. R. Oganov, et al. Semimetallic two-dimensional boron allotrope with massless Dirac fermions. *Physical Review Letters* **112**(8):085502, 2014. https://doi.org/10.1103/physrevlett.112.085502.

[46] A. J. Mannix, X.-F. Zhou, B. Kiraly, et al. Synthesis of borophenes: Anisotropic, two-dimensional boron polymorphs. *Science* **350**(6267):1513–1516, 2015. https://doi.org/10.1126/science.aad1080.

[47] B. Feng, J. Zhang, Q. Zhong, et al. Experimental realization of two-dimensional boron sheets. *Nature Chemistry* **8**(6):563–568, 2016. https://doi.org/10.1038/nchem.2491.

[48] W. Li, L. Kong, C. Chen, et al. Experimental realization of honeycomb borophene. *Science Bulletin* **63**(5):282–286, 2018. https://doi.org/10.1016/j.scib.2018.02.006.

[49] Z.-Q. Wang, T.-Y. Lü, H.-Q. Wang, et al. Review of borophene and its potential applications. *Frontiers of Physics* **14**(3):33403, 2019. https://doi.org/10.1007/s11467-019-0884-5.

[50] S.-H. Zhang, W. Yang. Oblique Klein tunneling in 8-*Pmmn* borophene $p-n$ junctions. *Physical Review B* **97**(23):235440, 2018. https://doi.org/10.1103/physrevb.97.235440.

[51] S.-H. Zhang, W. Yang. Anomalous caustics and Veselago focusing in 8-*pmmn* borophene p–n junctions with arbitrary junction directions. *New Journal of Physics* **21**(10):103052, 2019. https://doi.org/10.1088/1367-2630/ab4d8f.

[52] N. Tajima, K. Kajita. Experimental study of organic zero-gap conductor α-(BEDT-TTF)$_2$I$_3$. *Science and Technology of Advanced Materials* **10**(2):024308, 2009. https://doi.org/10.1088/1468-6996/10/2/024308.

[53] N. P. Armitage, E. J. Mele, A. Vishwanath. Weyl and Dirac semimetals in three-dimensional solids. *Reviews of Modern Physics* **90**(1):015001, 2018. https://doi.org/10.1103/revmodphys.90.015001.

[54] Y. Betancur-Ocampo, F. Leyvraz, T. Stegmann. Electron optics in phosphorene pn junctions: Negative reflection and anti-super-Klein tunneling. *Nano Lett* **19**(11):7760–7769, 2019. https://doi.org/10.1021/acs.nanolett.9b02720.

[55] Y. Betancur-Ocampo, E. Paredes-Rocha, T. Stegmann. Phosphorene pnp junctions as perfect electron waveguides. *Journal of Applied Physics* **128**(11):114303, 2020. https://doi.org/10.1063/5.0019215.

[56] N. Levy, S. A. Burke, K. L. Meaker, et al. Strain-induced pseudo-magnetic fields greater than 300 tesla in graphene nanobubbles. *Science* **329**(5991):544–547, 2010. https://doi.org/10.1126/science.1191700.

[57] F. Guinea, M. I. Katsnelson, A. K. Geim. Energy gaps and a zero-field quantum Hall effect in graphene by strain engineering. *Nature Physics* **6**(1):30–33, 2009. https://doi.org/10.1038/nphys1420.

[58] S. H. R. Sena, J. M. Pereira Jr, G. A. Farias, et al. The electronic properties of graphene and graphene ribbons under simple shear strain. *Journal of Physics: Condensed Matter* **24**(37):375301, 2012. https://doi.org/10.1088/0953-8984/24/37/375301.

[59] P. Ghosh, P. Roy. Collapse of Landau levels in graphene under uniaxial strain. *Materials Research Express* **6**(12):125603, 2019. https://doi.org/10.1088/2053-1591/ab52ad.

[60] V. M. Pereira, A. H. Castro Neto. Strain engineering of graphene's electronic structure. *Physical Review Letters* **103**(4):046801, 2009. https://doi.org/10.1103/physrevlett.103.046801.

[61] V. M. Pereira, A. H. Castro Neto, N. M. R. Peres. Tight-binding approach to uniaxial strain in graphene. *Physical Review B* **80**(4):045401, 2009. https://doi.org/10.1103/physrevb.80.045401.

[62] G. Cocco, E. Cadelano, L. Colombo. Gap opening in graphene by shear strain. *Physical Review B* **81**(24):241412, 2010. https://doi.org/10.1103/physrevb.81.241412.

[63] F. M. D. Pellegrino, G. G. N. Angilella, R. Pucci. Strain effect on the optical conductivity of graphene. *Physical Review B* **81**(3):035411, 2010. https://doi.org/10.1103/physrevb.81.035411.

[64] H. Rostami, R. Asgari. Electronic ground-state properties of strained graphene. *Physical Review B* **86**(15):155435, 2012. https://doi.org/10.1103/physrevb.86.155435.

[65] S. Barraza-Lopez, A. A. Pacheco Sanjuan, Z. Wang, M. Vanević. Strain-engineering of graphene's electronic structure beyond continuum elasticity. *Solid State Communications* **166**:70–75, 2013. https://doi.org/10.1016/j.ssc.2013.05.002.

[66] G. G. Naumis, S. Barraza-Lopez, M. Oliva-Leyva, H. Terrones. Electronic and optical properties of strained graphene and other strained 2D materials: a review. *Reports on Progress in Physics* **80**(9):096501, 2017. https://doi.org/10.1088/1361-6633/aa74ef.

[67] D.-N. Le, V.-H. Le, P. Roy. Graphene under uniaxial inhomogeneous strain and an external electric field: Landau levels, electronic, magnetic and optical properties. *The European Physical Journal B* **93**(8):158, 2020. https://doi.org/10.1140/epjb/e2020-10222-3.

[68] S. M. Cunha, D. R. da Costa, L. C. Felix, et al. Electronic and transport properties of anisotropic semiconductor quantum wires. *Physical Review B* **102**(4):045427, 2020. https://doi.org/10.1103/physrevb.102.045427.

[69] T. Stegmann, N. Szpak. Current flow paths in deformed graphene: from quantum transport to classical trajectories in curved space. *New Journal of Physics* **18**(5):053016, 2016. https://doi.org/10.1088/1367-2630/18/5/053016.

[70] T. Stegmann, N. Szpak. Current splitting and valley polarization in elastically deformed graphene. *2D Materials* **6**(1):015024, 2019. https://doi.org/10.1088/2053-1583/aaea8d.

[71] Y. Betancur-Ocampo. Partial positive refraction in asymmetric Veselago lenses of uniaxially strained graphene. *Physical Review B* **98**(20):205421, 2018. https://doi.org/10.1103/physrevb.98.205421.

[72] Y. Betancur-Ocampo, P. Majari, D. Espitia, et al. Anomalous floquet tunneling in uniaxially strained graphene. *Physical Review B* **103**(15):155433, 2021. https://doi.org/10.1103/physrevb.103.155433.

[73] T. Cheng, H. Lang, Z. Li, et al. Anisotropic carrier mobility in two-dimensional materials with tilted Dirac cones: theory and application. *Physical Chemistry Chemical Physics* **19**:23942–23950, 2017. https://doi.org/10.1039/C7CP03736H.

[74] B. Feng, J. Zhang, R.-Y. Liu, et al. Direct evidence of metallic bands in a monolayer boron sheet. *Physical Review B* **94**:041408, 2016. https://doi.org/10.1103/PhysRevB.94.041408.

[75] Y. Zhao, X. Li, J. Liu, et al. A new anisotropic Dirac cone material: A B_2S honeycomb monolayer. *The Journal of Physical Chemistry Letters* **9**(7):1815–1820, 2018. https://doi.org/10.1021/acs.jpclett.8b00616.

[76] D. Ferraro, B. Roussel, C. Cabart, et al. Real-time decoherence of Landau and Levitov quasiparticles in quantum hall edge channels. *Physical Review Letters* **113**(16):166403, 2014. https://doi.org/10.1103/physrevlett.113.166403.

[77] T. Jullien, P. Roulleau, B. Roche, et al. Quantum tomography of an electron. *Nature* **514**(7524):603–607, 2014. https://doi.org/10.1038/nature13821.

[78] J. Oertel. *Solutions of the Dirac equation in spacetime-dependent electric fields.* Master's thesis, University of Duisburg-Essen, Freiberg, Germany, 2014.

[79] M. Castillo-Celeita, E. Díaz-Bautista, M. Oliva-Leyva. Coherent states for graphene under the interaction of crossed electric and magnetic fields. *Annals of Physics* **421**:168287, 2020. https://doi.org/10.1016/j.aop.2020.168287.

[80] V. Lukose, R. Shankar, G. Baskaran. Novel electric field effects on Landau levels in graphene. *Physical Review Letters* **98**(11):116802, 2007. https://doi.org/10.1103/physrevlett.98.116802.

[81] N. Gu, M. Rudner, A. Young, et al. Collapse of Landau levels in gated graphene structures. *Physical Review Letters* **106**(6):066601, 2011. https://doi.org/10.1103/physrevlett.106.066601.

[82] J. M. Ziman. *Principles of the Theory of Solids.* Cambridge University Press, 2nd edn., 1972. https://doi.org/10.1017/CBO9781139644075.

[83] T. Huang, R. Chen, T. Ma, et al. Electronic Bloch oscillation in a pristine monolayer graphene. *Physics Letters A* **382**(42-43):3086–3089, 2018. https://doi.org/10.1016/j.physleta.2018.07.035.

[84] M. Kai, W. Jian-Hua, Y. Yi. Wigner function for the Dirac oscillator in spinor space. *Chinese Physics C* **35**(1):11–15, 2011. https://doi.org/10.1088/1674-1137/35/1/003.

[85] D. J. Fernández, D. I. Martínez-Moreno. Bilayer graphene coherent states. *The European Physical Journal Plus volume* **135**(9):739, 2020. https://doi.org/10.1140/epjp/s13360-020-00746-5.

GENERALIZED THREE-BODY HARMONIC OSCILLATOR SYSTEM: GROUND STATE

Adrian M. Escobar-Ruiz*, Fidel Montoya

Universidad Autónoma Metropolitana, Departamento de Física, Av. San Rafael Atlixco 186, 09340 Ciudad de México, CDMX, México

* corresponding author: admau@xanum.uam.mx

Abstract.

In this work we report on a 3-body system in a $d-$dimensional space $\mathbb{R}^d$ with a quadratic harmonic potential in the relative *distances* $r_{ij} = |\mathbf{r}_i - \mathbf{r}_j|$ between particles. Our study considers unequal masses, different spring constants and it is defined in the three-dimensional (sub)space of solutions characterized (globally) by zero total angular momentum. This system is exactly-solvable with hidden algebra $s\ell_4(\mathbb{R})$. It is shown that in some particular cases the system becomes maximally (minimally) superintegrable. We pay special attention to a physically relevant generalization of the model where eventually the integrability is lost. In particular, the ground state and the first excited state are determined within a perturbative framework.

Keywords: Three-body system, exact-solvability, hidden algebra, integrability.

1. Introduction

The two-body harmonic oscillator, i.e. two particles with masses m_1 and m_2 interacting via the translational invariant potential $V \propto |\mathbf{r}_i - \mathbf{r}_j|^2$, appears in all textbook in Classical Mechanics. In an arbitrary $d-$dimensional Euclidean space $\mathbb{R}^d$ this system admits separation of variables in the center-of-mass and relative coordinates as well as exact solvability. The relevance of such a system is obvious: any scalar potential $U = U(|\mathbf{r}_i - \mathbf{r}_j|)$ can be approximated by the two-body harmonic oscillator. In this case, the center-of-mass and relative coordinates are nothing but the normal coordinates. Therefore, in the n-body case of $n > 2$ particles interacting by a quadratic pairwise potential it is natural to ask the question about the existence of normal coordinates and the corresponding explicit exact solutions. Interestingly, even for the three-body case $n = 3$ a complete separation of variables can not be achieved in full generality.

Starting in 1935, the quantum $n-$body problem in $\mathbb{R}^3$ was studied by Zernike and Brinkman [1] using the so-called hyperspherical-harmonic expansion. Two decades later, this method possessing an underlying group-theoretical nature was then reacquainted and refined in the papers by Delves [2] and Smith [3]. Nevertheless, in practice the success of the method is limited to the case of highly symmetric systems, namely identical particles with equal masses and equal spring constants.

In a previous work [4], the most general quantum system of a three-body chain of harmonic oscillators, in $\mathbb{R}^d$, was explored exhaustively. For arbitrary masses and spring constants this problem possesses spherical symmetry. It implies that the total angular momentum is a well-defined Observable which allows to reduce effectively the number of degrees of freedom in the corresponding Schrödinger equation governing the states with zero angular momentum. In the sector of vanishing angular momentum, it turns out that this three-body quantum system is exactly solvable. The hidden algebra $s\ell(4,\mathbb{R})$ responsible of the exact solvability was exhibited in [4] using the ρ-representation. In the present work we consider a physically relevant generalization of the model where eventually the integrability properties are lost. Again, in our analysis we assume a system of arbitrary masses and spring constants with the total angular momentum identically zero.

In the current study we revisited the algebraic structure and solvability of the quantum 3-body quantum oscillator system in the special set of coordinates appearing in [5], [6]. Afterwards, a physically motivated generalization of the model is considered. The goal of the paper is two-fold. Firstly, in the (sub)-space of zero total angular momentum we will describe the reduced Hamiltonian operator which admits a hidden $s\ell(4;\mathbb{R})$ algebraic structure, hence, allowing exact-analytical eigenfunctions. Especially, at any $d \geq 1$ it is demonstrated the existence of an exactly-solvable model that solely depends on the moment of inertia of the system. This model, admits a quasi-exactly-solvable extension as well.

Secondly, we explore a physically relevant generalization of the model. Approximate solutions of the problem are presented just for the case of equal masses in the framework of standard perturbation theory and complemented by the variational method. The first excited state, thus the energy gap of the system, is briefly discussed.

2. Generalities

The quantum Hamiltonian in $\mathbb{R}^d$ $(d>1)$ for three non-relativistic spinless particles with masses m_1, m_2, m_3 and translationally invariant potential is given by

$$\mathcal{H} \;=\; -\sum_{i=1}^{3}\frac{1}{2\,m_i}\Delta_i^{(d)} \;+\; V(r_{12},\,r_{13},\,r_{23})\;, \qquad (1)$$

$(\hbar=1)$ see e.g. [4, 5], where $\Delta_i^{(d)}$ stands for the individual Laplace operator of the ith mass with $d-$dimensional position vector $\mathbf{r}_i$, and

$$r_{ij} \;=\; |\mathbf{r}_i-\mathbf{r}_j|\;, \qquad (2)$$

$(j=1,2,3)$ is the relative mutual distance between the bodies i and j. The eigenfunctions of (1) which solely depend on the ρ-variables, $\rho_{ij}=r_{ij}^2$, are governed by a three-dimensional reduced Hamiltonian [4]

$$\mathcal{H}_{\rm rad} \;\equiv\; -\Delta_{\rm rad} \;+\; V(\rho)\;, \qquad (3)$$

where

$$\begin{aligned}\Delta_{\rm rad} \;=\; &\frac{2}{\mu_{12}}\,\rho_{12}\,\partial^2_{\rho_{12}} \;+\; \frac{2}{\mu_{13}}\rho_{13}\,\partial^2_{\rho_{13}}\\ &+\frac{2}{\mu_{23}}\rho_{23}\,\partial^2_{\rho_{23}} \;+\; \frac{2(\rho_{13}+\rho_{12}-\rho_{23})}{m_1}\partial_{\rho_{13},\,\rho_{12}}\\ &+\frac{2(\rho_{13}+\rho_{23}-\rho_{12})}{m_3}\partial_{\rho_{13},\,\rho_{23}}+\frac{2(\rho_{23}+\rho_{12}-\rho_{13})}{m_2}\partial_{\rho_{23},\,\rho_{12}}\\ &+\;\frac{d}{\mu_{12}}\partial_{\rho_{12}}+\frac{d}{\mu_{13}}\partial_{\rho_{13}}+\frac{d}{\mu_{23}}\partial_{\rho_{23}}\;, \qquad (4)\end{aligned}$$

c.f. [5], and

$$\mu_{ij} \;=\; \frac{m_i\,m_j}{m_i+m_j}\;,$$

denotes a reduced mass. The operator (3) describes three-dimensional (radial) dynamics in variables $\rho_{12},\rho_{13},\rho_{23}$. This operator $\mathcal{H}_{\rm rad}$ is, in fact, equivalent to a Schrödinger operator, see [4]. We call it three-dimensional (radial) Hamiltonian. All the $d-$dependence in (3) occurs in the coefficients in front of the first derivatives.

2.1. Case of identical particles: τ-representation

Now, let us consider the case of identical masses

$$m_1 \;=\; 1\;;\; m_2 \;=\; 1\;;\; m_3 \;=\; 1\;,$$

thus, $\mu_{ij} \;=\; \frac{1}{2}$, and the operator (4) is S_3 permutationally-invariant in the ρ-variables. It suggests the change of variables $\rho\leftrightarrow\tau$ where

$$\begin{aligned}\tau_1 \;&=\; \rho_{12}+\rho_{13}+\rho_{23}\;,\\ \tau_2 \;&=\; \rho_{12}\,\rho_{13}+\rho_{12}\,\rho_{23}+\rho_{13}\,\rho_{23}\;, \qquad (5)\\ \tau_3 \;&=\; \rho_{12}\,\rho_{13}\,\rho_{23}\;,\end{aligned}$$

are nothing but the lowest elementary symmetric polynomials in ρ-coordinates.

In these variables (5), the coefficients of the operator $\Delta_{\rm rad}$ are also polynomials, hence, this operator is algebraic in both representations. Explicitly,

$$\begin{aligned}\Delta_{\rm rad} \;=\; &6\,\tau_1\partial_1^2 \;+\; 2\tau_1(7\tau_2-\tau_1^2)\partial_2^2 \;+\; 2\tau_3(6\tau_2-\tau_1^2)\partial_3^2\\ &+\;24\,\tau_2\partial^2_{1,2} \;+\; 36\tau_3\partial^2_{1,3} \;+\; 2\,[9\tau_3\tau_1+4\tau_2(\tau_2-\tau_1^2)]\partial^2_{2,3}\\ &+\;6\,d\,\partial_1 \;+\; 2\,(2d+1)\tau_1\,\partial_2 \;+\; 2\,[(d+4)\tau_2-\tau_1^2]\,\partial_3\\ \partial_i \;&\equiv\; \partial_{\tau_i},\; i=1,2,3.\end{aligned} \qquad (6)$$

3. Laplace-Beltrami operator

Now, as a result of calculations it is convenient to consider the following gauge factor

$$\Gamma^4 \;=\; \frac{\left(S^2_{\triangle}\right)^{2-d}}{M\,\mathcal{I}}\;, \qquad (7)$$

$M=m_1+m_2+m_3$, where

$$S^2_{\triangle}=\frac{2\rho_{12}\,\rho_{13}+2\rho_{12}\,\rho_{23}+2\rho_{23}\,\rho_{13}-\rho_{12}^2-\rho_{13}^2-\rho_{23}^2}{16}\,,$$

and

$$\mathcal{I} \;=\; \frac{m_1m_2\,\rho_{12} \;+\; m_1m_3\,\rho_{13} \;+\; m_2m_3\,\rho_{23}}{M}\;,$$

possess a geometrical meaning. The term $S^2_{\triangle}$ is the area (squared) of the triangle formed by the position vectors of the three bodies whilst the term $\mathcal{I}$ is the *moment of inertia* of the system with respect to its center of mass. The radial operator $\mathcal{H}_{\rm rad}$ (3) is gauge-transformed to a truly Schrödinger operator [4],

$$\mathcal{H}_{\rm LB} \;\equiv\; \Gamma^{-1}\,\mathcal{H}_{\rm rad}\,\Gamma \;=\; -\Delta_{\rm LB} \;+\; V \;+\; V^{(\rm eff)}\;, \qquad (8)$$

here $\Delta_{\rm LB}$ stands for the Laplace-Beltrami operator

$$\Delta_{LB}(\rho) \;=\; \sqrt{|\,g\,|}\;\partial_\mu\;\frac{1}{\sqrt{|\,g\,|}}\;g^{\mu\nu}\partial_\nu\;,$$

$(\nu,\mu=1,2,3)$ and $\partial_1=\frac{\partial}{\partial\rho_{12}},\partial_2=\frac{\partial}{\partial\rho_{13}},\partial_3=\frac{\partial}{\partial\rho_{23}}$. The corresponding co-metric in $\Delta_{LB}(\rho)$ reads

$$g^{\mu\nu} \;=\; \begin{pmatrix} \frac{2}{\mu_{12}}\rho_{12} & \frac{(\rho_{13}+\rho_{12}-\rho_{23})}{m_1} & \frac{(\rho_{23}+\rho_{12}-\rho_{13})}{m_2}\\ \frac{(\rho_{13}+\rho_{12}-\rho_{23})}{m_1} & \frac{2}{\mu_{13}}\rho_{13} & \frac{(\rho_{13}+\rho_{23}-\rho_{12})}{m_3}\\ \frac{(\rho_{23}+\rho_{12}-\rho_{13})}{m_2} & \frac{(\rho_{13}+\rho_{23}-\rho_{12})}{m_3} & \frac{2}{\mu_{23}}\rho_{23}\end{pmatrix}.$$

Its determinant

$$|\,g\,| \equiv\; {\rm Det}g^{\mu\nu} \;=\; 32\,\frac{M^2}{m_1^2m_2^2m_3^2}\,\mathcal{I}\,S^2_{\triangle}\;, \qquad (9)$$

admits factorization and is positive definite. The term $V^{(\rm eff)}$ denotes an *effective potential*

$$V^{(\rm eff)} \;=\; \frac{3}{8}\,\frac{1}{\mathcal{I}} \;+\; \frac{(d-2)(d-4)}{32}\;\frac{M\,\mathcal{I}}{m_1\,m_2\,m_3\,S^2_{\triangle}}\;,$$

which depends on the two variables $\mathcal{I}$ and $S^2_{\triangle}$ alone. Thus, the underlying geometry of the system emerges.

The classical analogue of the quantum Hamiltonian operator (8) describes an effective non-relativistic

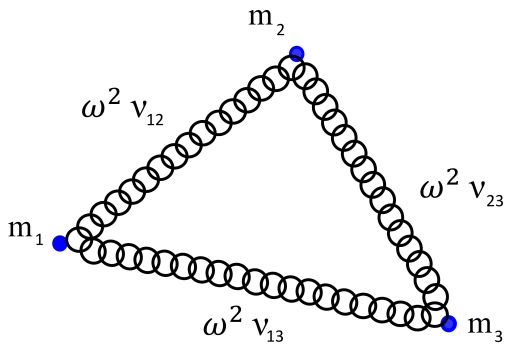

FIGURE 1. 3-body chain of harmonic oscillators.

classical particle in a three-dimensional curved space. Explicitly, the Hamiltonian function takes the form

$$\mathcal{H}_{\rm LB}^{\rm (classical)} \;=\; g^{\mu\nu}\,\Pi_\mu\,\Pi_\nu \;+\; V\;, \qquad (10)$$

where $\Pi_\mu\,,\ \mu = 12, 23, 13$ are the associated canonical conjugate momenta to the ρ-coordinates. The Hamilton-Jacobi equation, at vanishing potential $V = 0$ (free motion), is clearly integrable. However, a complete separation of variables is absent in the ρ-representation. The Poisson bracket between the kinetic energy $T = g^{\mu\nu}\,\Pi_\mu\,\Pi_\nu$ and the linear function in momentum variables

$$L_1^{(c)} \;=\; (\rho_{13}-\rho_{23})\Pi_{12}+(\rho_{23}-\rho_{12})\Pi_{13}+(\rho_{12}-\rho_{13})\Pi_{23}\;,$$

is zero.

4. THREE BODY HARMONIC OSCILLATOR SYSTEM

In the spectral problem with Hamiltonian (3) we take the harmonic potential

$$V^{(HO)}(\rho) \;=\; 2\,\omega^2\left[\nu_{12}\,\rho_{12}+\nu_{13}\,\rho_{13}+\nu_{23}\,\rho_{23}\right], \qquad (11)$$

$\omega > 0$ is frequency and ν_{12}, ν_{13}, $\nu_{23} > 0$ are constants with dimension of mass. This problem can be solved exactly [4]. In particular, in ρ-space the reduced operator (3) possesses multivariate polynomial eigenfunctions, see below. We call the above potential $V^{(HO)}(\rho)$ the 3-body oscillator system. We mention that in the case $d = 1$ (3 particles on a line), the corresponding spectral problem was studied in the paper [7]. In the current report, we analyze the $d-$dimensional case with $d > 1$.

In r-variables, $\rho = r^2$, the potential (11) can be interpreted as a three-dimensional (an)isotropic one-body oscillator. It is displayed in Figure 1. The configuration space is a subspace of the cube $\mathbb{R}^3_+(\rho)$ in E_3 ρ-space. The ρ-variables must obey the "triangle condition" $S^2_\triangle \geqslant 0$, namely the area of the triangle formed by the position vectors of the bodies is always positive.

4.1. SOLUTION FOR THE GROUND STATE

In the harmonic potential (11), the ground state eigenfunction reads

$$\Psi_0^{(HO)} \;=\; e^{-\omega\,(a_1\,\mu_{12}\,\rho_{12}\,+\,a_2\,\mu_{13}\,\rho_{13}\,+\,a_3\,\mu_{23}\,\rho_{23})}\;, \qquad (12)$$

where the parameters a_1, a_2, $a_3 \geq 0$ are introduced for convenience. They define the spring constants, see below. The associated ground state energy

$$E_0 \;=\; \omega\,d\,(a_1+a_2+a_3)\;, \qquad (13)$$

is mass-independent. There exists the following algebraic relations

$$\begin{aligned}
\nu_{12} &= a_1^2\,\mu_{12} \;+\; a_1\,a_2\;\frac{\mu_{12}\,\mu_{13}}{m_1} \;+\; a_1\,a_3\;\frac{\mu_{12}\,\mu_{23}}{m_2}\\
&\quad -\; a_2\,a_3\;\frac{\mu_{13}\,\mu_{23}}{m_3}\;,\\
\nu_{13} &= a_2^2\,\mu_{13} \;+\; a_1\,a_2\;\frac{\mu_{12}\,\mu_{13}}{m_1} \;+\; a_2\,a_3\;\frac{\mu_{13}\,\mu_{23}}{m_3}\\
&\quad -\; a_1\,a_3\;\frac{\mu_{12}\,\mu_{23}}{m_2}\;,\\
\nu_{23} &= a_3^2\,\mu_{23} \;+\; a_1\,a_3\;\frac{\mu_{12}\,\mu_{23}}{m_2} \;+\; a_2\,a_3\;\frac{\mu_{13}\,\mu_{23}}{m_3}\\
&\quad -\; a_1\,a_2\;\frac{\mu_{12}\,\mu_{13}}{m_1}\;.
\end{aligned}$$

5. LIE ALGEBRAIC STRUCTURE

Using the previous function $\Psi_0^{(HO)}$ (12) as a gauge factor, the transformed Hamiltonian $\mathcal{H}_{\rm rad}$ (3)

$$h^{\rm (algebraic)} \equiv \left(\Psi_0^{(HO)}\right)^{-1}\left[-\Delta_{\rm rad}+V-E_0\right]\Psi_0^{(HO)} \qquad (14)$$

is an algebraic operator, i.e. the coefficient are polynomials in the ρ-variables. The E_0 is taken from (13).

In addition, this algebraic operator (14) is of Lie-algebraic nature. It admits a representation in terms of the generators

$$\begin{aligned}
\mathcal{J}_i^- &= \frac{\partial}{\partial y_i}\;,\\
\mathcal{J}_{ij}^0 &= y_i\frac{\partial}{\partial y_j}\;,\\
\mathcal{J}^0(N) &= \sum_{i=1}^{3} y_i\frac{\partial}{\partial y_i}-N\,,\\
\mathcal{J}_i^+(N) &= y_i\,\mathcal{J}^0(N) \;=\; y_i\left(\sum_{j=1}^{3} y_j\frac{\partial}{\partial y_j}-N\right)\;,
\end{aligned}$$

$(i, j = 1, 2, 3)$ of the algebra $s\ell(4,\mathbb{R})$, see [8, 9] here N is a constant. The notation

$$y_1 \;=\; \rho_{12}\;, \qquad y_2 \;=\; \rho_{13}\;, \qquad y_3 \;=\; \rho_{23}\;,$$

was employed for simplicity. If N is a non-negative integer, a finite-dimensional representation space takes place,

$$\mathcal{V}_N \;=\; \langle y_1^{n_1}\,y_2^{n_2}\,y_3^{n_3}|\;0\leq n_1+n_2+n_3\leq N\rangle\;. \qquad (15)$$

6. Relation with the Jacobi oscillator

Now, we can indicate an emergent relation between the harmonic potential (11) and the Jacobi oscillator system

$$\mathcal{H}^{(\text{Jacobi})} \equiv \sum_{i=1}^{2}\left[-\frac{\partial^2}{\partial \mathbf{z}_i \partial \mathbf{z}_i} + 4\,\Lambda_i\,\omega^2\,\mathbf{z}_i\cdot\mathbf{z}_i\right] , \quad (16)$$

where $\omega > 0$, Λ_1, $\Lambda_2 \geq 0$, and

$$\begin{aligned}\mathbf{z}_1 &= \sqrt{\frac{m_1\,m_2}{m_1+m_2}}\,(\mathbf{r}_1 - \mathbf{r}_2)\\ \mathbf{z}_2 &= \sqrt{\frac{(m_1+m_2)\,m_3}{m_1+m_2+m_3}}\left(\mathbf{r}_3 - \frac{m_1\,\mathbf{r}_1+m_2\,\mathbf{r}_2}{m_1+m_2}\right)\end{aligned}$$

are standard Jacobi variables, see e.g. [10]. This Hamiltonian describes two decoupled harmonic oscillators in flat space, see [6]. Consequently, it is an exactly-solvable problem. The complete spectra and eigenfunctions can be calculated by pure algebraic means.

The solutions of the Jacobi oscillator that solely depend on the Jacoby distances $z_i = |\mathbf{z}_i|$ are governed by the operator,

$$\begin{aligned}\mathcal{H}^{(\text{Jacobi})}_{\text{rad}} &= \sum_{i=1}^{2}\left[-\frac{\partial^2}{\partial z_i \partial z_i} - \frac{(d-1)}{z_i}\frac{\partial}{\partial z_i}\right] \\ &+ 4\,\Lambda_1\,\omega^2\,z_1^2 + 4\,\Lambda_2\,\omega^2\,z_2^2 .\end{aligned} \quad (17)$$

In this case, the associated hidden algebra is given by $sl_2^{\otimes\,(2)}$ which acts on the two-dimensional space (z_1, z_2).

In particular, the eigenfunctions of $\mathcal{H}^{(\text{Jacobi})}$ (16) can be employed to construct approximate solutions for the n-body problem, for this discussion see [10].

Assuming any of the two conditions

$$\frac{m_2}{m_3} = \frac{\nu_{12}}{\nu_{13}} \quad ; \quad \frac{m_1}{m_2} = \frac{\nu_{13}}{\nu_{23}} ,$$

in the harmonic oscillator potential $V^{(HO)}$ (11), we obtain

$$\begin{aligned}U_J^{(HO)} &\equiv 4\,\Lambda_1\,\omega^2\,z_1^2 + 4\,\Lambda_2\,\omega^2\,z_2^2\\ &= 2\,\omega^2\left[\nu_{12}\,\rho_{12} + \nu_{13}\,\rho_{13} + \nu_{23}\,\rho_{23}\right]\\ &= V^{(HO)}\end{aligned} \quad (18)$$

with

$$\Lambda_1 = \Lambda_2 = \frac{m_1+m_2+m_3}{2\,m_1\,m_3}\,\nu_{13} ,$$

hence, in this case the three-body oscillator potential coincides with the two-body Jacobi oscillator potential. In fact, imposing the singly condition $m_2\,\nu_{13} = m_3\,\nu_{12}$ the equality (18) is still valid but $\Lambda_1 \neq \Lambda_2$ and the system is not maximally superintegrable any more.

6.1. Identical particles: hyperradious

A remarkable simplification occurs in the case of three identical particles with the same common spring constant, namely

$$m_1 = m_2 = m_3 = 1 \quad , \quad a_1 = a_2 = a_3 \equiv a . \quad (19)$$

Thus, the potential (11) reduces to

$$\begin{aligned}V^{(HO)} &= \frac{3}{2}\,a^2\,\omega^2\,(\rho_{12} + \rho_{13} + \rho_{23})\\ &= \frac{3}{2}\,a^2\,\omega^2\,\tau_1 .\end{aligned}$$

Consequently, the ground state solutions (12) and (13) read

$$\begin{aligned}\Psi_0^{(3a)} &= e^{-\frac{\omega}{2}\,a\,(\,\rho_{12}\,+\,\rho_{13}\,+\,\rho_{23}\,)}\\ &= e^{-\frac{\omega}{2}\,a\,\tau_1} ,\end{aligned} \quad (20)$$

$$E_0 = 3\,\omega\,d\,a , \quad (21)$$

respectively. Moreover, from (6) it follows that in this case there exists an infinite family of eigenfunctions

$$\Psi_N(\tau_1) = e^{-\frac{1}{2}\,a\,\omega\,\tau_1}\,L_N^{(d-1)}(a\,\omega\,\tau_1) ,$$

with energy

$$E_N = 3\,a\,\omega\,(\,d + 2\,N\,) ,$$

$N = 0, 1, 2, 3, \ldots$, that solely depend on the variable τ_1, the so called *hyperradious*, here $L_N^{(d-1)}(x)$ denotes the generalized Laguerre polynomial. These solutions are associated with a hidden $s\ell(2,\mathbb{R})$ Lie-algebra.

6.2. Arbitrary masses: moment of inertia

A generalization of the results presented in Section 6.1 can be derived from the decomposition of Δ_{rad} (4)

$$\Delta_{\text{rad}} = \Delta_{\mathcal{I}} + \tilde{\Delta} , \quad (22)$$

where $\Delta_{\mathcal{I}} = \Delta_{\mathcal{I}}(\mathcal{I})$ is an algebraic operator for arbitrary $d \geq 1$. It depends on the moment of inertial $\mathcal{I}$ only. Explicitly, we have

$$\Delta_{\mathcal{I}} = 2\,\mathcal{I}\,\partial^2_{\mathcal{I},\mathcal{I}} + 2\,d\,\partial_{\mathcal{I}} . \quad (23)$$

The operator $\tilde{\Delta} = \tilde{\Delta}(\mathcal{I}, q_1, q_2)$ depends on $\mathcal{I}$ and two more (arbitrary) variables q_1, q_2 for which the coordinate transformation $\{\rho_{ij}\} \to \{\mathcal{I}, q_1, q_2\}$ is invertible (not singular). Since such an operator $\tilde{\Delta}$ annihilates any function $F = F(\mathcal{I})$, i.e. $\tilde{\Delta}\,F = 0$, the splitting (22) indicates that for any potential of the form

$$V = V(\mathcal{I}) , \quad (24)$$

the eigenvalue problem for the operator $\mathcal{H}_{\text{rad}} = -\Delta_{\text{rad}} + V$ is further reduced to a one-dimensional spectral problem, namely

$$[\,-\Delta_{\mathcal{I}} + V(\mathcal{I})\,]\,\psi = E\,\psi , \quad (25)$$

which can be called the $\mathcal{I}-$representation.

In the case of equal masses $m_1 = m_2 = m_3$ the coordinate $\mathcal{I}$ is proportional to the hyperspherical radius (hyperradious). Also, $H_{\mathcal{I}}$ (25) is gauge-equivalent to a one-dimensional the Schrödinger operator.

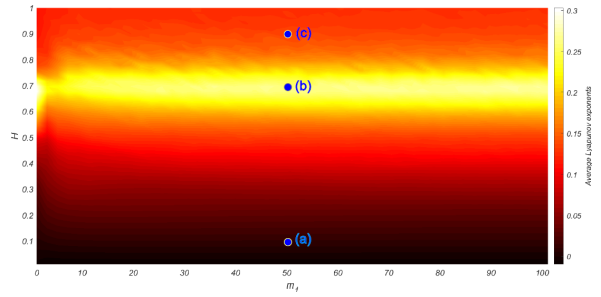

Figure 2. Classical generalized three-body harmonic oscillator system: average Lyapunov exponent in the space of parameters $(H,\, m_1)$. The values $m_2 = m_3 = 1$, $\omega = 1$, $\nu_{12} = \nu_{13} = \nu_{23} = 1$ and $R_{12} = R_{13} = R_{23} = 1$ were used.

7. Generalized three body harmonic oscillator system

Now, let us consider the following potential

$$V^{(R)} = 2\,\omega^2\Big[\nu_{12}\,(\sqrt{\rho_{12}} - R_{12})^2 + \nu_{13}\,(\sqrt{\rho_{13}} - R_{13})^2 + \nu_{23}\,(\sqrt{\rho_{23}} - R_{23})^2\Big]\,, \tag{26}$$

where $R_{12}, R_{13}, R_{23} \geqslant 0$ denote the rest lengths of the system. At $R_{12} = R_{13} = R_{23} = 0$ we recover the exactly solvable 3-body oscillator system, $V^{(R)} \to V^{(HO)}$. The relevance of $V^{(R)}$ comes from the fact that any arbitrary potential $V = V(r_{ij})$ can be approximated, near its equilibrium points, by this generalized 3-body harmonic potential.

However, the existence of non-trivial exact solutions is far from being evident. Even for the most symmetric case of equal masses and equal spring constants, we were not able to find a hidden Lie algebra in the corresponding spectral problem (3). Moreover, at the classical level such a system is chaotic. This can be easily seen by computing the average Lyapunov exponent in the space of parameters $(H,\, m_1)$, see Figure 2, where H is the value of the classical Hamiltonian (energy) with potential $V^{(R)}$ (26).

Also, for one-dimensional systems it is said (see [11]) that a classical orbit is $\mathcal{PT}$-symmetric if the orbit remains unchanged upon replacing $x(t)$ by $-x^*(-t)$. There are several classes of complex $\mathcal{PT}$-symmetric non-Hermitian quantum-mechanical Hamiltonians whose eigenvalues are real and with unitary time evolution [12, 13]. However, while the corresponding quantum three-body oscillator Hamiltonian is Hermitian, it can still have interesting complex classical trajectories.

7.1. Identical particles

In order to simplify the problem one can consider the simplest case of equal masses and equal spring constants (19) with $\omega = 1$. Also, we will assume equal rest lengths

$$R_{12} \;=\; R_{13} \;=\; R_{23} \;=\; R \,>\, 0\;.$$

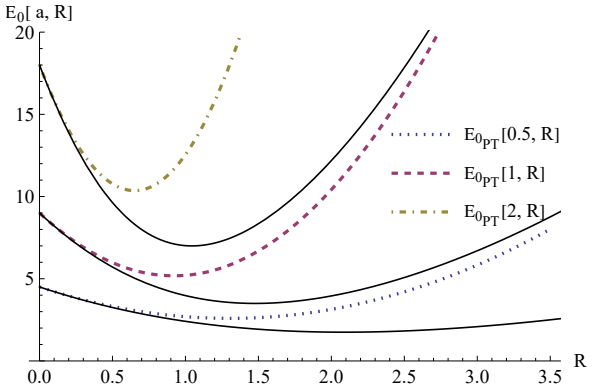

Figure 3. Ground state energy of the generalized 3-body harmonic oscillator *vs* R for different values of the parameter a which defines the spring constant, see text. The solid lines correspond to the variational result whilst the dashed ones refer to the value calculated by perturbation theory up to first order.

In this case, approximate solutions for the Schrödinger equation can be obtained using perturbation theory in powers of R.

7.1.1. Ground state

Taking the $R-$dependent terms in (26) as a small perturbation, the first correction $E_{1,0}$ to the ground state energy takes the form

$$E_{1,0} \;=\; \frac{3\,a}{2\,\pi}(\,3\,\pi\,a\,R^2 \;-\; 4\,R\sqrt{6\,\pi\,a}\,)\;.$$

The domain of validity of this perturbative approach is estimated by means of the variational method. The use of the simple trial function

$$\Psi_0^{\text{trial}} \;=\; e^{-\frac{\omega}{2}\,a\,\alpha\,(\,\rho_{12}\,+\,\rho_{13}\,+\,\rho_{23}\,)}$$

c.f. (20), where α is a variational parameter to be fixed by the procedure of minimization, leads to the results shown in Figure 3.

7.1.2. First excited state

It is important to mention that for the 3-body harmonic oscillator $(R = 0)$ the exact first excited state possesses a degeneracy equal to 3. For $R > 0$, the perturbation theory partially breaks this degeneracy. The energy of the approximate first excited state calculated by perturbation theory, up to first order, is displayed in Figure 4.

8. Conclusions

In this report for a 3-body harmonic oscillator in Euclidean space $\mathbb{R}^d$ we consider the Schrödinger operator in ρ-variables $\rho_{ij} = r_{ij}^2$,

$$\mathcal{H}_{\text{LB}} \;=\; -\Delta_{\text{LB}}(\rho_{ij}) + V^{(HO)}(\rho_{ij}) + V^{(\text{eff})}(\rho_{ij})\;, \tag{27}$$

where the kinetic energy corresponds to a 3-dimensional particle moving in a non-flat space. The

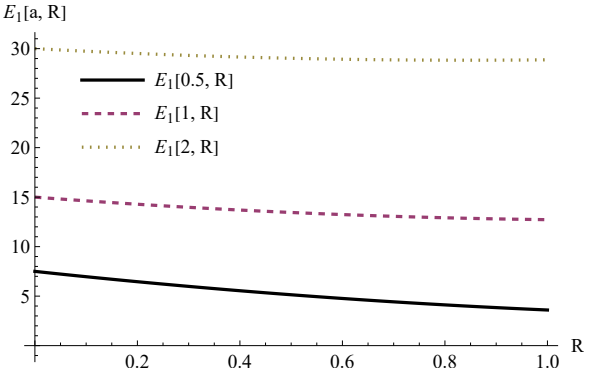

FIGURE 4. First excited state of the generalized 3-body harmonic oscillator *vs* R.

Schrödinger operator (27) governs the $\mathcal{S}$-states solutions of the original three-body system (1), in particular, it includes the ground state. It implies that the solutions of corresponding eigenvalue problem depend solely on three coordinates, contrary to the $(3d)$-dimensional Schrödinger equation. The reduced Hamiltonian $\mathcal{H}_{\rm LB}$ is an Hermitian operator, where the variational method can be more easily implemented (the energy functional is a 3-dimensional integral only). The classical analogue of (27) was presented as well. The operator (27) up to a gauge rotation is equivalent to an algebraic operator with hidden algebra $s\ell(4,\mathbb{R})$, thus, becoming a Lie-algebraic operator.

In the case of identical masses and equal frequencies the aforementioned model was generalized to a 3-body harmonic system with a non-zero rest length $R > 0$. In this case, no hidden algebra nor exact solutions seem to occur. An indication of the lost of integrability is the fact that the classical counterpart of this model exhibits chaotic motion. Using perturbation theory complemented by the variational method it was shown that the ground state energy *vs* R develops a global minimum, hence, defining a configuration of equilibrium.

ACKNOWLEDGEMENTS

AMER thanks the support through the Programa Especial de Apoyo a la Investigación 2021, UAM-I. FM and AMER are thankful to Mario Alan Quiroz for helping in the numerical computations.

REFERENCES

[1] F. Zernike, H. C. Brinkman. Hypersphärische Funktionen und die in sphärischen Bereichen orthogonalen Polynome. *Koninklijke Nederlandse Akademie van Wetenschappen* **38**:161–170, 1935.

[2] L. M. Delves. Tertiary and general-order collisions (I). *Nuclear Physics* **9**(3):391–399, 1958. https://doi.org/10.1016/0029-5582(58)90372-9.

[3] F. Smith. A symmetric representation for three-body problems. I. Motion in a plane. *Journal of Mathematical Physics* **3**(4):735, 1962. https://doi.org/10.1063/1.1724275.

[4] A. Turbiner, W. Miller Jr, M. A. Escobar-Ruiz. Three-body problem in d-dimensional space: ground state, (quasi)-exact-solvability. *Journal of Mathematical Physics* **59**(2):022108, 2018. https://doi.org/10.1063/1.4994397.

[5] A. Turbiner, W. Miller Jr, M. A. Escobar-Ruiz. Three-body problem in 3D space: ground state, (quasi)-exact-solvability. *Journal of Physics A: Mathematical and Theoretical* **50**(21):215201, 2017. https://doi.org/10.1088/1751-8121/aa6cc2.

[6] W. Miller Jr, A. Turbiner, M. A. Escobar-Ruiz. The quantum n-body problem in dimension $d \geq n-1$: ground state. *Journal of Physics A: Mathematical and Theoretical* **51**(20):205201, 2018. https://doi.org/10.1088/1751-8121/aabb10.

[7] F. M. Fernández. Born-Oppenheimer approximation for a harmonic molecule. ArXiv:0810.2210v2.

[8] A. V. Turbiner. Quasi-exactly-solvable problems and the $sl(2,R)$ algebra. *Communications in Mathematical Physics* **118**:467–474, 1988. https://doi.org/10.1007/BF01466727.

[9] A. V. Turbiner. One-dimensional quasi-exactly-solvable Schrödinger equations. *Physics Reports* **642**:1–71, 2016. https://doi.org/10.1016/j.physrep.2016.06.002.

[10] L. M. Delves. Tertiary and general-order collisions (II). *Nuclear Physics* **20**:275–308, 1960. https://doi.org/10.1016/0029-5582(60)90174-7.

[11] C. M. Bender, J.-H. Chen, D. W. Darg, K. A. Milton. Classical Trajectories for Complex Hamiltonians. *Journal of Physics A: Mathematical and General* **39**(16):4219–4238, 2006. https://doi.org/10.1088/0305-4470/39/16/009.

[12] C. M. Bender, S. Boettcher. Real spectra in Non-Hermitian Hamiltonians having $\mathcal{PT}$ symmetry. *Physical Review Letters* **80**(24):5243–5246, 1998. https://doi.org/10.1103/PhysRevLett.80.5243.

[13] P. Dorey, C. Dunning, R. Tateo. Supersymmetry and the spontaneous breakdown of $\mathcal{PT}$ symmetry. *Journal of Physics A: Mathematical and General* **34**(28):L391, 2001. https://doi.org/10.1088/0305-4470/34/28/102.

TIME-DEPENDENT STEP-LIKE POTENTIAL WITH A FREEZABLE BOUND STATE IN THE CONTINUUM

Izamar Gutiérrez Altamirano[a,*], Alonso Contreras-Astorga[b], Alfredo Raya Montaño[a,c]

[a] *Instituto de Física y Matemáticas, Universidad Michoacana de San Nicolás de Hidalgo, Edificio C-3, Ciudad Universitaria. Francisco J. Mújica s/n. Col. Felícitas del Río. 58040 Morelia, Michoacán, México*

[b] *CONACyT–Physics Department, Cinvestav, P.O. Box. 14-740, 07000 Mexico City, Mexico*

[c] *Centro de Ciencias Exactas, Universidad del Bío-Bío, Avda. Andrés Bello 720, Casilla 447, 3800708, Chillán, Chile*

[*] corresponding author: izamar.gutierrez@umich.mx

Abstract. In this work, we construct a time-dependent step-like potential supporting a normalizable state with energy embedded in the continuum. The potential is allowed to evolve until a stopping time t_i, where it becomes static. The normalizable state also evolves but remains localized at every fixed time up to t_i. After this time, the probability density of this state freezes becoming a Bound state In the Continuum. Closed expressions for the potential, the freezable bound state in the continuum, and scattering states are given.

Keywords: Bound states in the continuum, supersymmetric quantum mechanics, time-dependent quantum systems.

1. Introduction

The first discussion of Bound states In the Continuum (BICs) in quantum mechanics dates back to von Neumann and Wigner [1] who constructed normalizable states corresponding to an energy embedded in the continuum in a periodic potential $V(r) = E + \nabla^2\psi/\psi$ from a modulated free-particle wave function $\psi(r) = (\sin(r)/r)f(r)$, with twice the period of the potential. The localization of this state is interpreted as the result of its reflection in the Bragg mirror generated by the wrinkles of $V(r)$ as $r \to \infty$. The extended family of von-Neumann and Wigner potentials have been discussed and extended for many years [2–5] from different frameworks including the Gelfan-Levitan equation [6] also known as inverse scattering method [4, 7], Darboux transformations [8, 9] and supersymmetry (SUSY) [10–13], among others. Bound states In the Continuum are nowadays recognized as a general wave phenomenon and has been explored theoretically and experimentally in many different setups, see [14] for a recent review.

Exact solutions to the time-dependent Schrödinger equation are known only in a few cases, including the potential wells with moving walls [15, 16], which has been explored from several approaches (see, for instance, Ref. [17] and references therein) including the adiabatic approximation [18] and perturbation theory [16] and through point transformations [19–23], which combined with supersymmetry techniques allow to extend from the infinite potential well with a moving wall to the trigonometric Pöschl-Teller potential [24].

In this article, we present the construction of a time-dependent step-like potential. We depart from the standard stationary step potential and apply a second-order supersymmetric transformation to add a BIC. Then, by means of a point transformation, the potential and the state become dynamic and we allow them to evolve. After a certain time, we assume that all the time-dependence of the potential is frozen, such that the potential becomes stationary again and explore the behavior of the normalizable state. Intriguingly, it is seen that the freezable BIC is not an eigensolution of the stationary Schrödinger equation in the frozen potential, but rather solves an equation that includes a vector potential that does not generate a magnetic field whatsoever. Thus, by an appropriate gauge transformation, we gauge away the vector potential and observe the BIC that remains frozen as an eigenstate of the stationary Hamiltonian after the potential ceases to evolve in time.

In order to expose our results, we have organized the remaining of this article as follows: In Section 2 we describe the preliminaries of SUSY and a point transformation. Section 3 presents the construction of the time-dependent step-like potential and give explicit expressions for the freezable BIC and scattering states. Final remarks are presented in Section 4.

2. Supersymmetry and a point transformation

Point transformation is a successful technique to define a time-dependent Schrödinger equation with a full time-dependent potential from a known stationary problem [19, 20, 24]. In this section, we use a trans-

formation of this kind in combination with a confluent supersymmetry transformation to obtain a time-dependent step-like potential from the stationary case.

2.1. Confluent supersymmetry

Darboux transformation, intertwining technique or supersymmetric quantum mechanics (SUSY) is a method to map solutions ψ of a Schrödinger equation into solutions $\bar{\psi}$ of another Schrödinger equation [25–29]. It is based on an intertwining relation where two Hamiltonians and a proposed operator $L^\dagger$ must fulfill the relation

$$\bar{H}L^\dagger = L^\dagger H, \tag{1}$$

where

$$H = -\frac{d^2}{dy^2} + V_0(y), \quad \bar{H} = -\frac{d^2}{dy^2} + \bar{V}(y). \tag{2}$$

The main ingredient of SUSY are the *seed solutions*, which correspond to solutions of the initial differential equation $Hu = \epsilon u$, where ϵ is a real constant called *factorization energy*. In this work we focus on the so called *confluent supersymmetry*, where $L^\dagger$ is a second-order differential operator. Once a seed solution and a factorization energy are chosen, the next step is to construct the following auxiliary function

$$v = \frac{1}{u}\left(\omega + \int u^2(y)dz\right), \tag{3}$$

where ω is a real constant to be fixed. Then, one way to fulfill (1) is by selecting

$$L^\dagger = \left(-\frac{d}{dy} + \frac{v'}{v}\right)\left(-\frac{d}{dy} + \frac{u'}{u}\right), \tag{4}$$

and the potential term in $\bar{H}$ as

$$\bar{V}(y) = V_0(y) - 2\frac{d^2}{dy^2}\ln\left(\omega + \int_{y_0}^{y} u^2 dz\right). \tag{5}$$

Then, solutions of the differential equation $H\psi = E\psi$, where E is energy, can be mapped using $L^\dagger$ and the intertwining relation as follows:

$$\begin{aligned} H\psi &= E\psi, \\ &\Downarrow \qquad \text{times } L^\dagger \\ L^\dagger H\psi &= EL^\dagger\psi, \\ &\Downarrow \qquad \text{using (1)} \\ \bar{H}L^\dagger\psi &= EL^\dagger\psi, \\ &\Downarrow \qquad \text{defining } \bar{\psi} \propto L^\dagger\psi \\ \bar{H}\bar{\psi} &= E\bar{\psi}. \end{aligned}$$

We define $\bar{\psi}$ as

$$\bar{\psi} = \frac{1}{E-\epsilon}L^\dagger\psi. \tag{6}$$

The factor $(E-\epsilon)^{-1}$ is introduced for normalization purposes. Moreover, $\bar{H}$ could have an extra eigenstate that cannot be written in the form (6). This state is called *missing state* and plays an important role in this work. The missing state is obtained as follows: First we have seen that $L^\dagger$ maps solutions of $H\psi = E\psi$ into solutions of $\bar{H}\bar{\psi} = E\bar{\psi}$, by obtaining the adjoint equation of (1) $HL = L\bar{H}$, where $L = (L^\dagger)^\dagger$ we can construct the inverse mapping, but there is a solution $\bar{\psi}_\epsilon$ such that $L\bar{\psi}_\epsilon = 0$. This solution is explicitly:

$$\bar{\psi}_\epsilon = C_\epsilon\frac{1}{v} = C_\epsilon\frac{u}{\omega + \int u^2(y)dy}, \tag{7}$$

where C_ϵ is a normalization constant if $\bar{\psi}_\epsilon$ is square integrable. This state fulfills $\bar{H}\bar{\psi}_\epsilon = \epsilon\bar{\psi}_\epsilon$. Notice that the selection of u, ϵ and ω is very relevant, we must choose these carefully to avoid the introduction of singularities in the potential $\bar{V}$ that lead to singularities also in $\bar{\psi}$. The function $\omega + \int u^2 dy$ must be nodeless. We can satisfy this if either $\lim_{y\to\infty} u(y) = 0$ or $\lim_{y\to-\infty} u(y) = 0$ and if ω is appropriately chosen.

2.2. Point transformation

Given that we know the solution of the time independent Schrödinger equation

$$\frac{d^2}{dy^2}\bar{\psi}(y) + \left[E - \bar{V}(y)\right]\bar{\psi}(y) = 0 \tag{8}$$

with a potential defined in $y \in (-\infty, \infty)$, let us consider the following change of variable

$$y(x,t) = \frac{x}{4t+1}, \tag{9}$$

where $x \in (-\infty, \infty)$ is considered as a spatial variable and $t \in [0, \infty)$ a temporal one. Then, the wavefunction

$$\phi(x,t) = \frac{1}{\sqrt{4t+1}}\exp\left\{\frac{i(x^2 + \frac{E}{4})}{4t+1}\right\}\bar{\psi}\left(\frac{x}{4t+1}\right), \tag{10}$$

solves the time-dependent Schrödinger equation

$$i\frac{\partial}{\partial t}\phi(x,t) + \frac{\partial^2}{\partial x^2}\phi(x,t) - V(x,t)\phi(x,t) = 0, \tag{11}$$

where the potential term is

$$V(x,t) = \frac{1}{(4t+1)^2}\bar{V}\left(\frac{x}{4t+1}\right). \tag{12}$$

In other words, the change of variable (9) together with the replacements $\bar{V} \to V$ and $\bar{\psi} \to \phi$ transform a stationary Schrödinger equation into a time dependent solvable one.

3. Time dependent step-like potential with a freezable bound state in the continuum

In this section, we depart from the well-known step potential $V(y) = \hat{V}\Theta(-y)$ as time independent system. Then, using confluent supersymmetry we will

add a single BIC. Furthermore, with the point transformation previously introduced we transform the stationary system into a time-dependent system with an explicitly time-dependent potential. We will choose a stopping time or *freezing time* t_i after which the potential no longer evolves:

$$V_F(x,t) = \begin{cases} V(x,t) & 0 \le t < t_i, \\ V(x,t_i) & t \ge t_i. \end{cases} \tag{13}$$

Finally, the solutions of the Schrödinger equation will be presented.

Let us commence our discussion by considering the Step-Potential

$$V_0(y) = \begin{cases} \hat{V} & y \le 0, \\ 0 & y > 0, \end{cases} \tag{14}$$

defined along the axis $y \in (-\infty, \infty)$ and $\hat{V}$ is a positive constant. The solutions of this system are well known in the literature (see [30, 31]). Restricting ourselves to the case $0 < E_q < \hat{V}$, the solutions are:

$$\psi(y) = \begin{cases} \exp(\rho y) & y \le 0, \\ \cos(qy) + \frac{\kappa}{k}\sin(qy) & y > 0, \end{cases} \tag{15}$$

with energy $E_q = q^2$ and $\rho = \sqrt{\hat{V} - E_q}$.

Next, to perform the confluent supersymmetric transformation we choose a factorization energy such that $0 < \epsilon < \hat{V}$ and the corresponding seed solution $u(y)$ as

$$u(y) = \begin{cases} \exp(\kappa y) & y \le 0, \\ \cos(ky) + \frac{\kappa}{k}\sin(ky) & y > 0, \end{cases} \tag{16}$$

with $k^2 = \epsilon$ and $\kappa^2 = \hat{V} - \epsilon$. Note that $u(y) \to 0$ when $y \to -\infty$. Then, from (5) we obtain explicitly the SUSY partner $\bar{V}$:

$$\bar{V}(y) = \begin{cases} \hat{V} - \frac{16\exp(2\kappa y)\kappa^3\omega}{(\exp(2\kappa y)+2\kappa\omega)^2} & y \le 0 \\ 32k^2\left(k\cos(ky) + \kappa\sin(ky)\frac{\tilde{v}(y)}{\hat{v}(y)}\right) & y > 0, \end{cases} \tag{17}$$

where the functions $\tilde{v}(y)$ and $\hat{v}(y)$ are

$$\begin{aligned} \tilde{v}(y) = {} & \left[(k^2+\kappa^2)(k^2 x + \kappa) + 2k^4\omega\right]\sin(ky) \\ & - k\left[(k^2+\kappa^2)(\kappa y + 1) + 2k^2\kappa\omega\right], \\ \hat{v}(y) = {} & \left[2ky(k^2+\kappa^2) + 4k^3\omega - 2k\kappa\cos(2ky)\right. \\ & \left. + (k^2-\kappa^2)\sin(2ky)\right]^2. \end{aligned}$$

We can calculate directly from (7) the missing state associated to the factorization energy ϵ:

$$\bar{\psi}_\epsilon(y) = C_\epsilon \begin{cases} \frac{2\kappa\exp(\kappa y)}{2\kappa\omega+\exp(2\kappa y)} & y \le 0, \\ \frac{4k^3(\cos(ky)+\frac{\kappa}{k}\sin(ky))}{\hat{\psi}_\epsilon(y)} & y > 0, \end{cases} \tag{18}$$

where

$$\begin{aligned} \hat{\psi}_\epsilon(y) = {} & (k^2-\kappa^2)\sin(2ky) - 2\kappa k\cos(2ky) \\ & + 4\omega k^3 + 2ky\left(\kappa^2+k^2\right). \end{aligned}$$

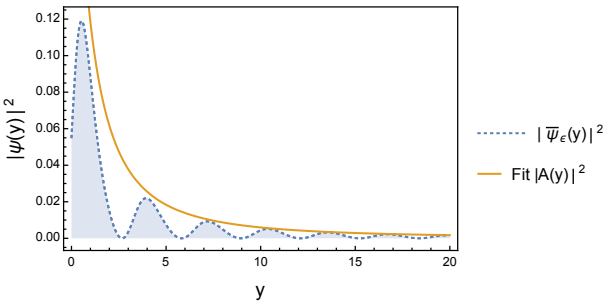

FIGURE 1. $|\bar{\psi}_\epsilon(y)|^2$ and an envelop function of the form $A(y) = \frac{a}{b+y}$, with $a = 2k(\kappa^2+k^2)^{-1/2}$, $b = 2\omega k^2(\kappa^2+k^2)^{-1}$. The scale of the graph is fixed with $\hat{V} = 5$, $k = 1$, $\kappa = 2$ and $C_\epsilon = 1$, in the appropriate units.

In order to confirm that $\bar{\psi}_\epsilon$ is square integrable, we proceed in the following way. First, we separate the integral $||\bar{\psi}_\epsilon||^2 = \int_{-\infty}^{\infty}|\bar{\psi}_\epsilon|^2 dy = \int_{-\infty}^{0}|\bar{\psi}_\epsilon|^2 dy + \int_0^\infty |\bar{\psi}_\epsilon|^2 dy$. The first integral can be directly calculated:

$$\int_{-\infty}^{0}|\bar{\psi}_\epsilon|^2 dy = |C_\epsilon|^2\sqrt{\frac{2}{\kappa\omega}}\tan^{-1}\left(\frac{1}{\sqrt{2\kappa\omega}}\right).$$

For the second integral, we can show that it is bounded by a square integrable function:

$$\begin{aligned} \frac{\int_0^\infty |\bar{\psi}_\epsilon|^2 dy}{|C_\epsilon|^2} &= \int_0^\infty \left|\frac{4k^3(\cos(ky)+\frac{\kappa}{k}\sin(ky))}{\hat{\psi}_\epsilon(y)}\right|^2 dy \\ &\le \int_0^\infty \left|\frac{4k^2\sqrt{k^2+\kappa^2}}{4\omega k^3 + 2ky\left(\kappa^2+k^2\right)}\right|^2 dy \\ &= \int_0^\infty \left|\frac{a}{b+y}\right|^2 dy = \frac{a^2}{b}, \end{aligned} \tag{19}$$

where $a = \frac{2k}{\sqrt{\kappa^2+k^2}}$, $b = \frac{2\omega k^2}{\kappa^2+k^2}$. Figure 1 shows a fair fit to the squared modulus of eq. (18) for $y > 0$.

For an energy $E = q^2 \neq \epsilon$, the wavefunction solving $\bar{H}\bar{\psi} = E\bar{\psi}$ is constructed using (6), and (15). It reads

$$\bar{\psi}(y) = \begin{cases} \left[\frac{(\kappa-\rho)\exp(\rho y)}{(q^2-k^2)}\right]\bar{\psi}_-(y) & y \le 0, \\ \frac{\hat{\psi}_+(y) - q^2\cos(qy) - q\rho\sin(qy)}{q^2-k^2} & y > 0, \end{cases} \tag{20}$$

where we abbreviated

$$\begin{aligned} \bar{\psi}_-(y) &= \frac{2\kappa\omega_0(\kappa+\rho) + (\rho-\kappa)\exp(2\kappa y)}{2\kappa\omega + \exp(2\kappa y)}, \\ \bar{\psi}_+(y) &= \frac{k^2(\rho\sin(qy) + q\cos(qy))}{q} \\ &+ \frac{4k(\kappa\sin(ky) + k\cos(ky))}{\hat{\psi}_\epsilon(y)} \\ &\times \left[\frac{k}{q}\left(\kappa\cos(ky) - k\sin(ky)\right)\left(\rho\sin(qy) + q\cos(qy)\right)\right. \\ &\left. + \left(\kappa\sin(ky) + k\cos(ky)\right)\left(q\sin(qy) - \rho\cos(qy)\right)\right]. \end{aligned}$$

In Figure 2 the potential $\bar{V}(y)$, along with the probability densities of the missing state $|\bar{\psi}_\epsilon(y)|^2$ and a scattering state $|\bar{\psi}(y)|^2$ are shown. We observe that the wavefunction of the BIC has an envelop function which tends to zero as $|y| \to \infty$, whereas the state $\bar{\psi}(y)$ is not localized.

The next step is to construct a time dependent potential from (17) using the point transformation presented in (9-12). Notice that $x = y$ at $t = 0$. Then $\bar{V}$ transforms as the piecewise potential:

$$V(x,t) = \frac{1}{(4t+1)^2}\left\{\hat{V} - \frac{16\kappa^3\omega\exp(\frac{2\kappa x}{4t+1})}{\left[2\kappa\omega + \exp(\frac{2\kappa x}{4t+1})\right]^2}\right\} \quad (21)$$

if $x \leq 0$, otherwise

$$V(x,t) = \frac{32k^2}{(4t+1)^2} \times \left[k\cos\left(\frac{kx}{4t+1}\right) + \kappa\sin\left(\frac{kx}{4t+1}\right)\frac{\tilde{v}(y(x,t))}{\hat{v}(y(x,t))}\right]. \quad (22)$$

In Figure 3 (top) we show the potential $V(x,t)$ at $t = 0$, $t = 0.1$ and $t = 0.2$. Its shape changes in time and its spatial profile oscillates as expected, vanishing as $x \to \infty$. Analogously, for the time-dependent BIC, the associated wavefunction for energy ϵ is explicitly

$$\phi_\epsilon(x,t) = \frac{1}{\sqrt{4t+1}}\exp\left\{\frac{i(x^2+\frac{k^2}{4})}{4t+1}\right\}\bar{\psi}_\epsilon\left(\frac{x}{4t+1}\right), \quad (23)$$

This function solves the time-dependent Schrödinger equation $i\partial_t\phi_\epsilon + \partial_{xx}\phi_\epsilon - V\phi_\epsilon = 0$ and its square integrability is guaranteed since $\bar{\psi}_\epsilon(y)$ is a square integrable function:

$$\begin{aligned} ||\phi_\epsilon||^2 &= \int_{-\infty}^{\infty}|\phi_\epsilon(x,t)|^2dx \\ &= \frac{1}{4t+1}\int_{-\infty}^{\infty}\left|\bar{\psi}_\epsilon\left(\frac{x}{4t+1}\right)\right|^2dx \\ &= \int_{-\infty}^{\infty}\left|\bar{\psi}_\epsilon(y)\right|^2dy = ||\bar{\psi}_\epsilon||^2. \end{aligned} \quad (24)$$

where we used the change of variable (9). Its probability density is shown in Figure 3 (center) at different times. This state is localized and the first peak in the probability density broadens and diminishes height as time increases.

For states with energy $E_q = q^2 \neq \epsilon$, the corresponding time-dependent wavefunction has the explicit form

$$\phi(x,t) = \frac{1}{\sqrt{4t+1}}\exp\left\{\frac{i(x^2+\frac{q^2}{4})}{4t+1}\right\}\bar{\psi}\left(\frac{x}{4t+1}\right), \quad (25)$$

The behavior of the probability density $|\phi(x,t)|^2$, for $E = 2$ at different times is shown in Figure 3 (bottom). This state is unlocalized at any time.

Finally, we choose the freezing or stopping time t_i. Then, we can consider a charge particle in a potential:

$$V_F(x,t) = \begin{cases} V(x,t) & 0 \leq t < t_i, \\ V(x,t_i) & t \geq t_i. \end{cases} \quad (26)$$

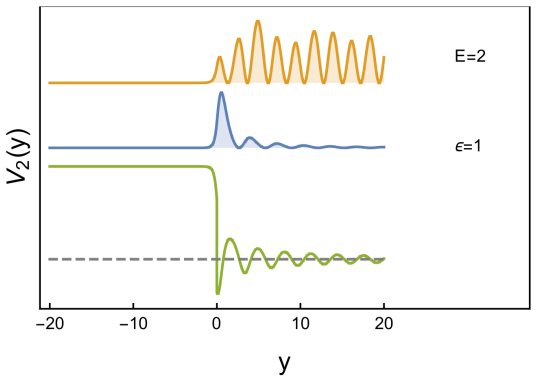

FIGURE 2. Potential $\bar{V}(y)$, along with the probability densities of the missing state $|\bar{\psi}_\epsilon(y)|^2$ and a scattering state $|\bar{\psi}(y)|^2$ are shown. The scale of the graph is fixed with $\hat{V} = 5$, $k = 1$, $\kappa = 2$, $q = \sqrt{2}$ and $\omega = 4$.

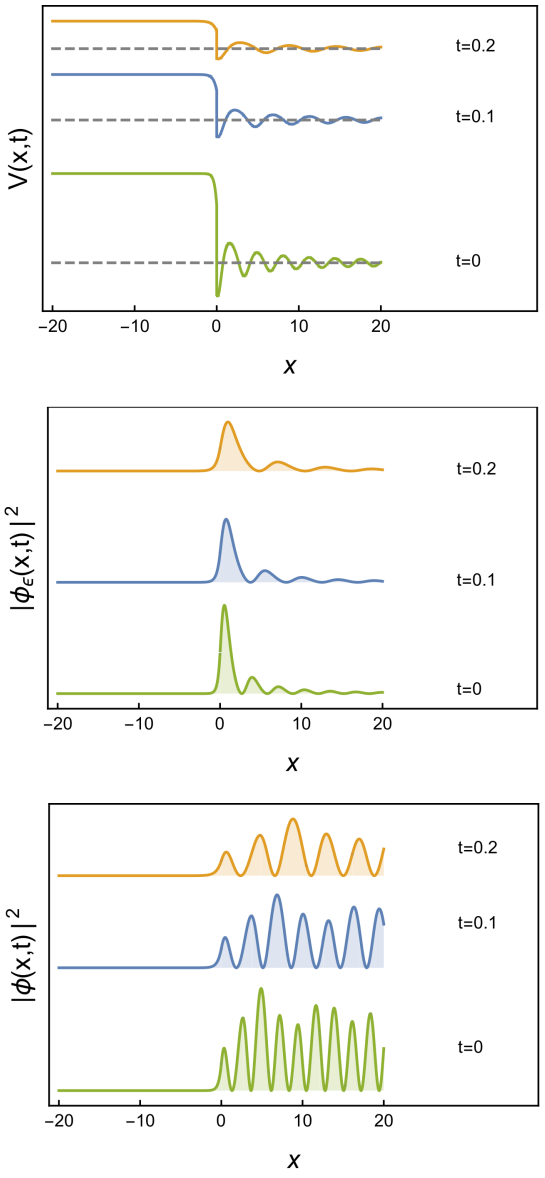

FIGURE 3. Behavior of the potential $V(x,t)$ (top), the BIC $\phi_\epsilon(x,t)$ (center) and the scattering state $\phi(x,t)$ (bottom) at the times $t = 0$, $t = 0.1$, and $t = 0.2$. The scale of the graphs is fixed by $\hat{V} = 5$, $k = 1$, $\kappa = 2$, $q = \sqrt{2}$ and $\omega = 4$.

where $V(x,t)$ is given by (21,22). Notice that when $t \in [0, t_i)$ the potential is changing in time, and when $t \geq t_i$ the potential is frozen. This potential is in fact a family, parametrized by $\omega > 0$, recall that ω was introduced by the confluent SUSY transformation.

Neither $\phi(x,t)$ nor $\phi_\epsilon(x,t)$ are stationary states, they evolve in time, and they are not eigenfunctions of the operator $-\partial_{xx} + V$. At any time $t \geq t_i$, the functions $\phi(x,t_i)$ and $\phi_\epsilon(x,t_i)$ satisfy the eigenvalue equation:

$$\left[\left(-\frac{\partial}{\partial x} + iA_x(x)\right)^2 + V(x,t_i)\right]\phi(x,t_i) = \frac{E}{(4t_i+1)^2}\phi(x,t_i), \quad t \geq t_i, \tag{27}$$

where $A_x(x) = -\partial_x\theta(x)$ and

$$\theta(x) = \frac{i}{4t_i+1}\left(x^2 + \frac{E}{4}\right). \tag{28}$$

Equation (27) is the Schrödinger equation for a charged particle under the influence of a vector potential $\mathbf{A} = (A_x, 0, 0)$ that, nevertheless, does not generate magnetic field since $\mathbf{B} = \nabla \times \mathbf{A} = 0$. Let us recall that the Schrödinger equation for a charged particle of charge q immersed in an external electromagnetic field is better written in terms of the scalar φ and vector potentials $\mathbf{A}$ through the Hamiltonian

$$H = (\hat{\mathbf{p}} + q\mathbf{A})^2 + q\varphi. \tag{29}$$

These electromagnetic potentials allow us to define the electric and magnetic fields as

$$\mathbf{E} = -\nabla\varphi - \frac{\partial \mathbf{A}}{\partial t}, \qquad \mathbf{B} = \nabla \times \mathbf{A}, \tag{30}$$

definition that does not change if the following transformations are performed simultaneously,

$$\mathbf{A} \to \mathbf{A}' = \mathbf{A} + \nabla\lambda, \qquad \varphi \to \varphi' = \varphi - \frac{\partial\lambda}{\partial t}, \tag{31}$$

where $\lambda = \lambda(x,t)$ is a scalar function. This is a statement of gauge invariance of Maxwell's equations. In quantum mechanics, the time-dependent Schrödinger equation

$$i\frac{\partial\psi}{\partial t} = H\psi \tag{32}$$

retains this feature if along the transformations in Eq. (31) in the Hamiltonian (29), the wavefunction changes according to the local phase transformation

$$\psi \to \psi' = e^{i\lambda}\psi. \tag{33}$$

In our example at hand, this freedom allows us to select λ in such a way that if at certain instant of time t_i the vector potential $\mathbf{A} \neq 0$ but before we had $\mathbf{A} = 0$, one can still have a Schrödinger equation without vector potential by tuning appropriately the scalar potential. In particular, by selecting

$$\lambda(x,t) = \ell(x)\Theta(t - t_i), \tag{34}$$

we can shift the scalar potential such that the time-dependent equation governing this state never develops a vector potential to begin with. Then, by choosing a vector potential $\mathbf{A}(x,t) = (A_x(x,t), 0, 0)$ where $A_x(x,t) = -\Theta(t-t_i)\partial_x\theta(x)$, we observe that the piecewise function

$$\phi_F(x,t) = \begin{cases} \phi(x,t) & 0 \leq t < t_i, \\ \bar{\psi}\left(\frac{x}{4t_i+1}\right) & t \geq t_i. \end{cases} \tag{35}$$

becomes a solution of

$$i\partial_t\phi_F(x,t) = \left[-\partial_{xx} + V_F(x,t)\right]\phi_F(x,t) = H\phi_F(x,t).$$

In particular, the function

$$\phi_{F\epsilon}(x,t) = \begin{cases} \phi_\epsilon(x,t) & 0 \leq t < t_i, \\ \bar{\psi}_\epsilon\left(\frac{x}{4t_i+1}\right) & t \geq t_i, \end{cases} \tag{36}$$

before the freezing time t_i is just a time dependent wave packet but for $t > t_i$ it becomes a Frozen Bound state In the Continuum satisfying the eigenvalue equation $H\phi_{F\epsilon} = \varepsilon\phi_{F\epsilon}$, where $\varepsilon = \epsilon/(4t_i+1)^2$. In Figure 4 we plot the potential V_F (top), the Freezable Bound State in the Continuum $\phi_{F\epsilon}$ (center) and a scattering state ϕ_F (bottom) at $t = 0.8$, $t = 1$ and $t = 1.8$, the freezing time is $t_i = 1$, note that after $t = 1$ neither the potential nor the wavefunctions evolve.

4. Final remarks

In this article, we apply a confluent supersymmetric transformation to the standard Step-Potential defined in the whole real axis. The seed solution that we use makes it possible to embed a localized squared integrable state in the continuum spectrum, a BIC. We have provided the system, potential, and states, with time evolution through a point transformation. Nevertheless, we notice that the wrinkles in the potential as $x \to \infty$ still localize a BIC at every fixed time.

Next, we allow the evolution of the system continue and at a given stopping time t_i, we freeze the potential and fix it stationary. Upon exploring the behavior of the BIC with this static potential after the freeze-out time, we surprisingly observe that it does not correspond to a solution of the stationary Schrödinger equation, but instead it develops a geometric phase encoded in a vector potential which does not generate any magnetic field. Thus, by gauging out this geometric phase, the resulting state becomes indeed an eigenstate of the frozen Hamiltonian. We call this state a Freezable Bound state In the Continuum.

Further examples are being examined under the strategy presented in this work, including vector potentials which might be relevant for pseudo-relativistic systems.

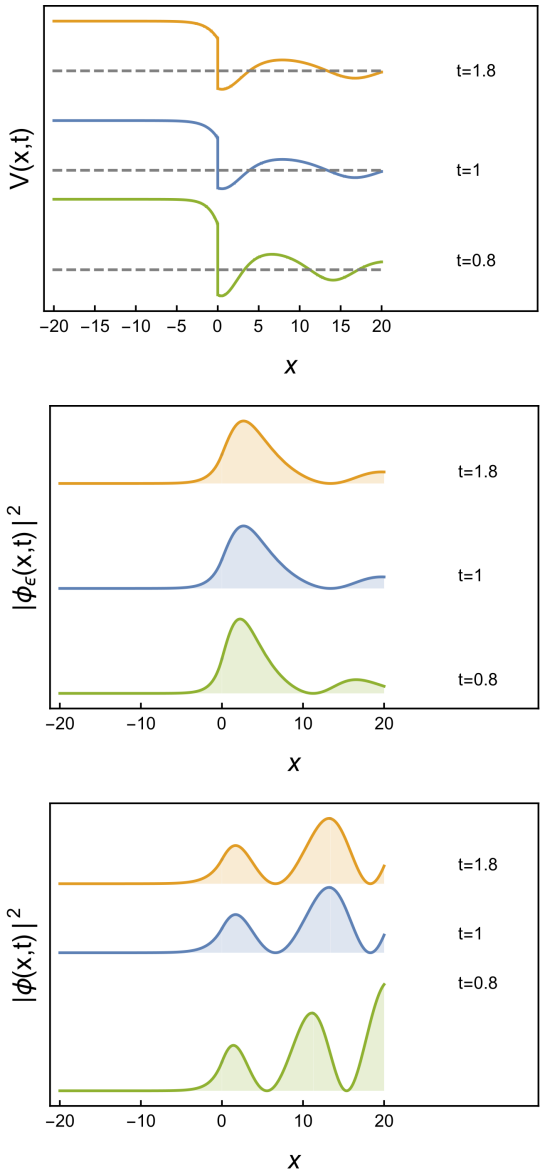

FIGURE 4. Behavior of the potential $V_F(x,t)$ (top), the FBIC $\phi_{F\epsilon}(x,t)$ (center) and the scattering state $\phi_F(x,t)$ (bottom) at the times $t = 0.8$, $t = 1$, and $t = 1.8$. The freezing time is $t_i = 1$. The scale of the graph is fixed by $\hat{V} = 5$, $k = 1$, $\kappa = 2$, $q = \sqrt{2}$ and $\omega = 4$.

ACKNOWLEDGEMENTS

The authors acknowledge Consejo Nacional de Ciencia y Tecnología (CONACyT-México) under grant FORDECYT-PRONACES/61533/2020. IG and AR acknowledge valuable discussions with Juan Angel Casimiro Olivares.

REFERENCES

[1] J. von Neuman, E. Wigner. Uber merkwürdige diskrete Eigenwerte. Uber das Verhalten von Eigenwerten bei adiabatischen Prozessen. *Physikalische Zeitschrift* **30**:467–470, 1929. https://ui.adsabs.harvard.edu/abs/1929PhyZ...30..467V Provided by the SAO/NASA Astrophysics Data System.

[2] B. Simon. On positive eigenvalues of one-body Schrödinger operators. *Communications on Pure and Applied Mathematics* **22**:531–538, 1969. https://doi.org/10.1002/cpa.3160220405.

[3] F. H. Stillinger, D. R. Herrick. Bound states in the continuum. *Physical Review A* **11**:446–454, 1975. https://doi.org/10.1103/PhysRevA.11.446.

[4] B. Gazdy. On the bound states in the continuum. *Physics Letters A* **61**(2):89–90, 1977. https://doi.org/10.1016/0375-9601(77)90845-3.

[5] M. Klaus. Asymptotic behavior of Jost functions near resonance points for Wigner–von Neumann type potentials. *Journal of Mathematical Physics* **32**:163–174, 1991. https://doi.org/10.1063/1.529140.

[6] I. M. Gel'fand, B. M. Levitan. On the determination of a differential equation from its spectral function. *Izvestiya Akademii Nauk SSSR Seriya Matematicheskaya* **15**(4):309–360, 1951.

[7] T. A. Weber, D. L. Pursey. Continuum bound states. *Physical Review A* **50**:4478–4487, 1994. https://doi.org/10.1103/PhysRevA.50.4478.

[8] A. A. Stahlhofen. Completely transparent potentials for the schrödinger equation. *Physical Review A* **51**:934–943, 1995. https://doi.org/10.1103/PhysRevA.51.934.

[9] D. Lohr, E. Hernandez, A. Jauregui, A. Mondragon. Bound states in the continuum and time evolution of the generalized eigenfunctions. *Revista Mexicana de Física* **64**(5):464–471, 2018. https://doi.org/10.31349/RevMexFis.64.464.

[10] J. Pappademos, U. Sukhatme, A. Pagnamenta. Bound states in the continuum from supersymmetric quantum mechanics. *Physical Review A* **48**:3525–3531, 1993. https://doi.org/10.1103/PhysRevA.48.3525.

[11] N. Fernández-García, E. Hernández, A. Jáuregui, A. Mondragón. Exceptional points of a Hamiltonian of von Neumann–Wigner type. *Journal of Physics A: Mathematical and Theoretical* **46**(17):175302, 2013. https://doi.org/10.1088/1751-8113/46/17/175302.

[12] L. López-Mejía, N. Fernández-García. Truncated radial oscillators with a bound state in the continuum via Darboux transformations. *Journal of Physics: Conference Series* **1540**:012029, 2020. https://doi.org/10.1088/1742-6596/1540/1/012029.

[13] A. Demić, V. Milanović, J. Radovanović. Bound states in the continuum generated by supersymmetric quantum mechanics and phase rigidity of the corresponding wavefunctions. *Physics Letters A* **379**(42):2707–2714, 2015. https://doi.org/10.1016/j.physleta.2015.08.017.

[14] C. W. Hsu, B. Zhen, A. D. Stone, et al. Bound states in the continuum. *Nature Reviews Materials* **1**(9):16048, 2016. https://doi.org/10.1038/natrevmats.2016.48.

[15] D. L. Hill, J. A. Wheeler. Nuclear constitution and the interpretation of fission phenomena. *Physical Review* **89**:1102–1145, 1953. https://doi.org/10.1103/PhysRev.89.1102.

[16] S. W. Doescher, M. H. Rice. Infinite square-well potential with a moving wall. *American Journal of Physics* **37**:1246–1249, 1969. https://doi.org/10.1119/1.1975291.

[17] K. Cooney. The infinite potential well with moving walls, 2017. arXiv:1703.05282.

[18] M. V. Berry. Quantal phase factors accompanying adiabatic changes. *Proceedings of the Royal Society Lond A* **392**:45–57, 1984. https://doi.org/10.1098/rspa.1984.0023.

[19] J. R. Ray. Exact solutions to the time-dependent Schrödinger equation. *Physical Review A* **26**:729–733, 1982. https://doi.org/10.1103/PhysRevA.26.729.

[20] G. W. Bluman. On mapping linear partial differential equations to constant coefficient equations. *SIAM Journal on Applied Mathematics* **43**(6):1259–1273, 1983. https://doi.org/10.1137/0143084.

[21] A. Schulze-Halberg, B. Roy. Time dependent potentials associated with exceptional orthogonal polynomials. *Journal of Mathematical Physics* **55**(12):123506, 2014. https://doi.org/10.1063/1.4903257.

[22] K. Zelaya, O. Rosas-Ortiz. Quantum nonstationary oscillators: Invariants, dynamical algebras and coherent states via point transformations. *Physica Scripta* **95**(6):064004, 2020. https://doi.org/10.1088/1402-4896/ab5cbf.

[23] K. Zelaya, V. Hussin. Point transformations: Exact solutions of the quantum time-dependent mass nonstationary oscillator. In M. B. Paranjape, R. MacKenzie, Z. Thomova, et al. (eds.), *Quantum Theory and Symmetries*, pp. 295–303. Springer International Publishing, Cham, 2021. https://doi.org/10.1007/978-3-030-55777-5_28.

[24] A. Contreras-Astorga, V. Hussin. *Infinite Square-Well, Trigonometric Pöschl-Teller and Other Potential Wells with a Moving Barrier*, pp. 285–299. Springer International Publishing, Cham, 2019. https://doi.org/10.1007/978-3-030-20087-9_11.

[25] V. B. Matveev, M. A. Salle. *Darboux Transformations and Solitons*. Springer Series in Nonlinear Dynamics. Springer, Berlin, Heidelberg, 1992. ISBN 9783662009246, https://books.google.com.mx/books?id=pJDjvwEACAAJ.

[26] F. Cooper, A. Khare, U. Sukhatme. Supersymmetry and quantum mechanics. *Physics Reports* **251**(5-6):267–385, 1995. https://doi.org/10.1016/0370-1573(94)00080-M.

[27] D. J. Fernández C., N. Fernández-García. Higher-order supersymmetric quantum mechanics. *AIP Conference Proceedings* **744**:236–273, 2004. https://doi.org/10.1063/1.1853203.

[28] A. Gangopadhyaya, J. V. Mallow, C. Rasinariu. *Supersymmetric Quantum Mechanics: An Introduction (Second Edition)*. World Scientific Publishing Company, 2017. ISBN 9789813221062.

[29] G. Junker. *Supersymmetric Methods in Quantum, Statistical and Solid State Physics*. IOP Expanding Physics. Institute of Physics Publishing, 2019. ISBN 9780750320245.

[30] C. Cohen-Tannoudji, B. Diu, F. Laloë. *Quantum mechanics*. 1st ed. Wiley, New York, NY, 1977. Trans. of : Mécanique quantique. Paris : Hermann, 1973, https://cds.cern.ch/record/101367.

[31] R. Shankar. *Principles of quantum mechanics*. Plenum, New York, NY, 1980. https://cds.cern.ch/record/102017.

ORTHONORMAL POLYNOMIAL PROJECTION QUANTIZATION: AN ALGEBRAIC EIGENENERGY BOUNDING METHOD

Carlos R. Handy

Texas Southern University, 3100 Cleburne St., Houston, Texas, U.S.A.

correspondence: carlos.handy@tsu.edu

Abstract. The ability to generate tight eigenenergy bounds for low dimension bosonic or ferminonic, hermitian or non-hermitian, Schrödinger operator problems is an important objective in the computation of quantum systems. Very few methods can simultaneously generate lower and upper bounds. One of these is the Eigenvalue Moment Method (EMM) originally introduced by Handy and Besssis, exploiting the use of semidefinite programming/nonlinear-convex optimization (SDP) techniques as applied to the positivity properties of the multidimensional bosonic ground state for a large class of important physical systems (i.e. those admitting a moments' representation). A recent breakthrough has been achieved through another, simpler, moment representation based quantization formalism, the *Orthonormal Polynomial Projection Quantization Bounding Method* (OPPQ-BM). It is purely algebraic and does not require any SDP analysis. We discuss its essential structure in the context of several one dimensional examples.

Keywords: Eigenvalue bounding methods, hermitian and non-hermitian linear operators.

1. Introduction

The eigenvalue bounding problem for linear ordinary differential equations, or linear partial differential equations (i.e. LODE/LPDE) has been an active area of research for many decades. In the context of quantum physical systems, as represented by the multidimensional Schrödinger equation,

$$-\frac{\hbar^2}{2m}\nabla^2\Psi(\overrightarrow{r})+V(\overrightarrow{r})\Psi(\overrightarrow{r})=E\Psi(\overrightarrow{r}), \qquad (1)$$

the generation of upper bounds to the individual discrete state energies is readily obtainable through such well known methods as that of Rayleigh-Ritz (RR) [1]. The challenge has been to find an equally effective lower bound method. A well known lower bound method is that associated with Temple [2]; however, its convergence rate is slow. Nevertheless, it has served as a spring board for other more effective lower bound formulations. Among these is the work by Marmorino et al. [3], and more recently, that of Martinazzo and Pollak [4]. The latter are able to improve upon the convergence rate of Temple's lower bound formulation.

Despite these successes, two important facts remain. The first is that all the above bounding methods require the use of two different bounding formulations. One for the upper bounds (RR), another for the lower bounds. That is, they do not define a unified theoretical framework for simultaneously generating lower and upper bounds. Additionally, these methods are based on a Hilbert space representation for quantum systems, dependent on the existence of hermitian hamiltonians. They are of little relevance for bounding the real/complex eigenenergies of non-hermitian systems, particularly those corresponding to PT-symmetry breaking systems [5–8].

In this work we present a novel approach that can generate tight bounds for the discrete states of bosonic or fermionic, low dimension, systems, regardless if they are hermitian or not. It is referred to as the Orthonormal Polynomial Projection Quantization Bounding Method (OPPQ-BM), as developed by Handy [9]; and based, in part, on a related method, the OPPQ-Approximation Method by Handy and Vrinceanu [10, 11]. Its general structure is outlined in the following sections, through representative one dimensional systems, both hermitian and non-hermitian. We outline the full OPPQ-BM theory within the context of the one dimensional, double well, sextic anharmonic oscillator; and then demonstrate the existence of the key structures necessary for its implementation to the PT symmetry breaking problem with potential $V(x)=ix^3+iax$.

Beyond the theoretical interest in bounds, they are also of practical importance for delicate systems where conventional computational methods may yield widely varying results. That is, the availability of tight bounds allows one to discriminate between competing theories.

One famous problem of this type corresponds to the Quadratic Zeeman (QZM) effect for superstrong magnetic fields. This problem was analyzed through many different types of computational methods, resulting in a wide range of values for the most challenging state to compute: the ground state binding energy. This was reviewed by Le Guillou and Zinn-Justin (LG-ZJ) in the context of their order dependent conformal transformation analysis [12]. Using novel, Moment Problem [13] related, computational methods, Handy, Bessis, et al. [14, 15]. were able to confirm the accuracy of the LG-ZJ analysis, by computing sufficiently

tight bounds to the ground state binding energy. Subsequent studies by Kravchenko et al. [16], and the more recent work by Schimerczek and Wunner [17], developed a different formulation that yielded vastly improved estimates (not bounds). The work by Handy extended OPPQ-BM to the QZM problem, yielding bounds that significantly improved upon, or were competitive with, the estimates by Kravchenko et al.

The QZM problem is an example of an important class of problems for which bounding methods are highly relevant. These are classified as *singular perturbation – strongly coupled* systems. Such systems involve quantum particles subjected to very strong forces, over relatively short length scales. This is inherently a multiscale problem, in keeping with the objectives of wavelet analysis [18, 19], etc.

Our original immersion into the eigenenergy bounding problem was through the study of strong coupling-singular perturbation type systems, such as QZM. The natural framework for regulating these systems is through the use of a non-local, extensive, representation. The power moments provide such a representation. As such, the types of systems studied here are those for which the Schrödinger operator configuration space problem can be transformed into a moments' equation counterpart for the power moments of the bound state solutions. We refer to these as MER type systems (i.e. those admitting a moment equation representation). This will become clear below. This condition can be relaxed, and essentially imposed on systems that do not admit such MER formulations, making the underlying OPPQ-BM principles applicable to many different types of systems. The details of this expanded analysis will be communicated shortly.

1.1. Singular-perturbation strong coupling problems and moment representations

It is not widely appreciated that power moments are relevant in understanding the multiscale structure of most systems. Thus, consider the scaling transform of a given wavefunction (i.e. signal, where we have simplified the notation to that of one dimension):

$$S\Psi(a,b) \equiv \frac{1}{a\nu}\int_{-\infty}^{+\infty} dx\ \mathcal{S}(\frac{x-b}{a})\Psi(x), \qquad (2)$$

where

$$Lim_{a\to 0^+} S\Psi(a,b) = \Psi(b), \qquad (3)$$

and $\nu \equiv \int dx\ \mathcal{S}(x) \neq 0$.

Physicists are biased in favor of attaining an analytical understanding of problems. Therefore the natural question to ask is, what is the analytical dependence in the inverse scale (i.e. $\frac{1}{a}$) for this scaling transform, if Ψ is a bounded, L^2 state? It will become clear from Eq. (4), that the power moments of the bound state solution, determine the analytic structure of the inverse scale expansion. These considerations underlie the analysis by Handy [20].

Alternatively, engineers are more oriented towards computational capabilities. If so, then it readily follows that the $a \to 0$ limit can be replaced by the integral $\int_0^\infty d\alpha \partial_\alpha \Big(\alpha \mathcal{S}\big(\alpha(x-b)\big)\Big)$, where $\alpha \equiv \frac{1}{a}$, which after a convolution substitution gives one the Continuous Wavelet Transform [19].

For bound state configurations, if $\lim_{|x|\to\infty} \Psi(|x|)\mathcal{S}(|x|e^{i\theta}) = 0$, exponentially, for arbitrary θ, then the scaling transform becomes analytic in the inverse scale, $\frac{1}{a}$. Under this assumption, the scaling transform's analytic expansion depends on the moments [20]

$$S\Psi(a,b) = \frac{1}{a\nu}\sum_{j=0}^{\infty}\frac{\sigma_j}{j!a^j}\sum_{p=0}^{j}\binom{j}{p}(-b)^{j-p}\mu(p), \qquad (4)$$

where $\partial_x^j \mathcal{S}(0) \equiv \sigma_j$, and

$$\mu(p) \equiv \int_{-\infty}^{+\infty} dx\ x^p \Psi(x). \qquad (5)$$

2. The moment equation representation

The natural extension of the above considerations is to study linear quantum systems whose differential form is transformable into a moment equation. Thus consider the sextic anharmonic oscillator potential, where the physical parameters have been re-scaled:

$$-\epsilon^2\partial_x^2\Psi(x) + (mx^2 + gx^6)\Psi(x) = E\Psi(x). \qquad (6)$$

The nature of physical quantum systems is that the discrete states decay exponentially, and therefore have finite power moments. The unphysical solutions become exponentially unbounded in one or both asymptotic directions, therefore their power moments are infinite.

We can multiply the above equation by x^p and integrate by parts, assuming the underlying wavefunction is that of a discrete state. We then obtain the *moment equation representation* (MER):

$$\begin{aligned} g\mu(p+6) =& -m\mu(p+2) + E\mu(p) \\ &+ p(p-1)\epsilon^2\mu(p-2), \qquad p \geq 0. \end{aligned} \qquad (7)$$

This homogeneous MER expression is a finite difference equation of effective order $1+m_s$ where $m_s = 5$. That is, for any E parameter value, the first six power moments $\{\mu_0, \mu_1, \ldots, \mu_5\}$ (i.e. $\mu(\ell) \equiv \mu_\ell$) are the initialization moments, or *missing moments*, and generate all the other power moments through closed form, energy dependent coefficients:

$$\mu(p) = \sum_{\ell=0}^{m_s} M_E(p,\ell)\ \mu_\ell, \qquad p \geq 0. \qquad (8)$$

If the coupling strength is large, $g >> 1$, the natural inclination is to attempt some kind of singular perturbation analysis involving expansions around the kinetic energy term; or, alternatively, a large perturbative expansion/resummation analysis.

In configurations space, kinetic energy expansions become singular (i.e. expanding in ϵ^2) because the order of the differential equation abruptly changes from zero to two. However, the order of the MER relation does not change as its kinetic energy counterpart is set to zero. This is one simple evidence that the MER transformation regulates singular perturbation expansions (i.e. kinetic energy expansions). That is, singular perturbation expansions in the moments' representation are better behaved.

3. Generating eigenenergy bounds within a moments' representation

There are two methods for generating bounds within a moment equation representation (MER). The first method, referred to as the Eigenvalue Moment Method (EMM), was developed by Handy and Bessis [14, 15], and is based on the Moment Problem [13]. Its theoretical-computational structure is based on what is now referred to as semidefnite programming (SDP) [21, 22]. As such, the SDP based formulation of Handy and Bessis is the first use of such methods for quantum operators [22]. Its computational implementation was done through the use of linear programming [23], since SDP algorithms were not known in the 1980s.

The second moment representation bounding formulation is that presented in this work, OPPQ-BM. Unlike EMM, OPPQ-BM is applicable to the low lying discrete states of any system, hermitian, or non-hermitian, bosonic, or fermionic, provided it admits a moment equation representation (MER). EMM is applicable only for the multidimensional bosonic ground state.

For systems admitting both EMM and OPPQ-BM, it is our belief that at its basic level, EMM produces faster converging bounds (as shown in this work through the analysis of the sextic anharmonic oscillator in Eq. (6)); however, if one optimizes the selection of the *reference/weight* function, then OPPQ-BM can yield significantly faster converging results.

The EMM formulation involves sophisticated, nonlinear, convex optimization analytical tools. However, OPPQ-BM is purely algebraic (i.e. eigenvalues, eigenvectors, and algebra). Given the power of Mathematica, with unlimited precision, it can produce spectacular results.

It is important to stress that EMM produces (when applicable) tight bounds ab initio. The OPPQ-BM is empirical. If the convergence of a particular parameter is numerically observed, then one can confidently generate bounds for the physical energies. We demonstrate this.

4. The eigenvalue moment method

The bosonic ground state must be a positive (nonnegative) configuration [24], $\Psi_{gr}(\overrightarrow{r}) \geq 0$. If the corresponding Schrödinger equation is transformable into MER form, then one can impose the Moment Problem positivity theorems and constrain the power moments, and in turn the energy and missing moments. This is the EMM-methodology. This was done, several decades ago, by Handy and Bessis (HB) [14, 15].

The Eigenvalue Moment Method (EMM), achieves geometric convergence rates for the bounds to the ground state energy. The only limitation is that it can only be applied to multidimensional bosonic systems, and then only to the ground state. As previously noted, it was used to solve the Quadratic Zeeman (QZM) problem [15]. The bounding of bosonic excited states, through a moment representation, could only be realized more recently through application of OPPQ-BM [9].

One can extend the EMM quantization philosophy to the probability density of one dimensional hermitian Schrödinger operators. This is because the probability density will satisfy a third order, linear, differential equation (LODE). If the LODE representation admits a MER formulation, then one can generate tight bounds to any discrete state. This is because all the discrete states are associated with nonnegative, L^2, configurations.

If the underlying Sturm-Liouville problem is non-hermitian, then the one dimensional Schrödinger equation can be transformed into a fourth order LODE for the probability density. This approach was used by Handy [8] in precisely computing the a-parameter regimes where the system $V(x) = ix^3 + iax$, violated PT symmetry (i.e. PT symmetry breaking). These results were confirmed through a faster, moment based, estimation procedure [25], that led to a more detailed understanding for the onset of PT symmetry breaking. These results significantly improved upon the predictions by Delabaere and Trinh [26], based on asymptotic analysis. We revisit this problem in this work.

The multidimensional probability density, $S(\overrightarrow{r}) \equiv \Psi^*(\overrightarrow{r})\Psi(\overrightarrow{r})$ will not generally satisfy a linear partial differential equation; therefore, no MER relation can be generated, and EMM cannot be applied. Nevertheless, through OPPQ-BM we can circumvent this difficulty.

5. THE ORTHONORMAL POLYNOMIAL PROJECTION QUANTIZATION FORMALISM

5.1. THE OPPQ NON-ORTHOGONAL BASIS EXPANSION

Let us expand the discrete state wavefunction in terms of some appropriate, complete, non-orthonormal basis, $\{\mathcal{B}_n(x) \equiv P_n(x)R(x)\}$:

$$\Psi(x) = \sum_{n=0}^{\infty} c_n P_n(x) R(x). \tag{9}$$

We require a weighted polynomial basis, involving orthonormal polynomials relative to some appropriate positive weight $R(x) > 0$ (we adopt the one dimensional notation for simplicity):

$$\langle P_m | R | P_n \rangle = \delta_{m,n}. \tag{10}$$

The weight is real, as are its orthonormal polynomials, involving real polynomial coefficients:

$$P_n(x) = \sum_{j=0}^{n} \Xi_j^{(n)} x^j. \tag{11}$$

For non-hermitian systems with complex bound state wavefunctions, it is the projection coefficients, $\{c_n\}$ that become complex.

The basis $\{\mathcal{B}_n(x)R(x)\}$ will be complete, but non-orthogonal (i.e. $\langle \mathcal{B}_m | \mathcal{B}_n \rangle \neq 0$, if $m \neq n$).

We can rewrite Eq. (10) as

$$\sum_{j_1=0}^{m} \sum_{j_2=0}^{n} \Xi_{j_1}^{(m)} \omega(j_1 + j_2) \Xi_{j_2}^{(n)} = \delta_{m,n}, \tag{12}$$

where $\omega(j_1 + j_2) = \int dx\ x^{j_1+j_2} R(x)$, the Hankel moment matrix of the weight, $W_{i,j} \equiv \omega(i + j)$.

Knowledge of the Hankel moment matrix allows us to generate the orthonormal polynomials through the Cholesky decomposition method, which involves decomposing the positive Hankel matrix into the form $W = CC^\dagger$. Let $\hat{e}_j$ correspond to a unit vector in the j-th component. We then solve for

$$\overrightarrow{\Xi}^{(j)} = (C^\dagger)^{-1} \hat{e}_j. \tag{13}$$

This generates the coefficient vector for $P_n(x)$, or $\overrightarrow{\Xi^{(n)}}$.

The projection coefficients are obtainable from the MER relation for the power moments of $\Psi(x)$:

$$\mu(p) \equiv \int_{\Re} dx\ x^p \Psi(x). \tag{14}$$

Assume that the corresponding MER relation exists

$$\mu(p) = \sum_{\ell=0}^{m_s} M_E(p, \ell) \mu_\ell. \tag{15}$$

It then follows that

$$\begin{aligned} c_n &= \langle P_n | \Psi \rangle, \\ &= \sum_{j=0}^{n} \Xi_j^{(n)} \mu(j) \\ &= \sum_{j=0}^{n} \Xi_j^{(n)} \sum_{\ell=0}^{m_s} M_E(j, \ell) \mu_\ell, \end{aligned} \tag{16}$$

$$c_n(\overrightarrow{\mu}) = \sum_{\ell=0}^{m_s} \Lambda_\ell^{(n)}(E) \mu_\ell, \tag{17}$$

where

$$\Lambda_\ell^{(n)}(E) = \sum_{j=0}^{n} \Xi_j^{(n)} M_E(j, \ell). \tag{18}$$

The MER relation suggested in Eq. (15) is a homogeneous relation for the power moments. Some normalization condition needs to be imposed:

$$\mathcal{C}(\overrightarrow{\mu}) = 1. \tag{19}$$

For one dimensional systems, the natural normalization is the unit (nonlinear) normalization: $|\overrightarrow{\mu}|^2 = 1$. However, it need not be chosen as such. Alternative choices [9] are linear normalizations such as $\mu_0 = 1$ or $\mu_0 + \mu_1 = 1$, etc.

5.2. THE OPPQ QUANTIZATION CONDITION

The OPPQ quantization condition requires that the weight be chosen so that the following positive integral is bounded for discrete solutions and infinite for unphysical solutions:

$$\mathcal{I}[\Psi, R] = \int_{\Re} dx\ \frac{|\Psi(x)|^2}{R(x)}, \tag{20}$$

$$= \sum_{j=0}^{\infty} |c_j(E, \overrightarrow{\mu})|^2, \tag{21}$$

where we have assumed Ψ is a bounded discrete state.

More generally, we note that depending on the asymptotic behavior of the physical or unphysical (i.e. unbounded) solutions, and the chosen asymptoic form for the weight, the integral in Eq. (20) will satisfy the quantization condition:

$$\mathcal{I}[\Psi, R] = \begin{cases} finite, \iff E = E_{phys}\ and\ \overrightarrow{\mu} = \overrightarrow{\mu}_{phys} \\ \infty, \iff E \neq E_{phys}\ or\ \overrightarrow{\mu} \neq \overrightarrow{\mu}_{phys}. \end{cases} \tag{22}$$

The OPPQ quantization condition essentially becomes a *shooting method* in the $E \times \overrightarrow{\mu}$, $1 + m_s$, parameter space (after imposing a normalization). This is the essence of the OPPQ-BM *bounding procedure*. The focus of the remaining OPPQ formalism is to reduce this shooting method to a minimization problem in the energy parameter space.

5.2.1. SELECTION OF THE OPPQ WEIGHT

The above formalism has two significant advantages.

The first is that it tells us that the weight should not be chosen so that it asymptotically vanishes much faster than the asymptotic form of the physical solutions.

Thus, given a physical, discrete state, Ψ, let $C(x)$ satisfy the asymptotic relation:

$$Lim_{|x|\to\infty}\frac{\Psi(x)}{R(x)} = C(x). \tag{23}$$

We then want

$$\int dx|\Psi(x)C(x)| < \infty. \tag{24}$$

In the works by Handy and Vrinceanu [10, 11], which introduce a particular version of the OPPQ formalism (i.e. to be referred to here to as the OPPQ-Approximation Method (OPPQ-AM)), they argued and demonstrated that the fastest convergence to the discrete states is associated with weights that mimic the asymptotic form of the desired discrete state:

$$Lim_{|x|\to\infty}C(x) = const. \tag{25}$$

The constant can be finite (i.e. zero), but not infinite in a manner that violates Eq. (24).

5.2.2. USE OF THE GROUND STATE AS A WEIGHT

Another advantage of the above formalism is that we can take $R(x) = \Psi_{gr}(x)$ even if we do not know the functional form for the ground state.

As long as one does not require that the discrete state wavefunction be reconstructed (i.e. one is only interested in the eigenenergies) then the only information required for the ground state is that its power moments be known accurately. This then allows us to generate the corresponding orthonormal polynomials, allowing for the generation of rapidly converging bounds to the discrete states. We demonstrate this in this work (i.e. Table 8).

One can determine the power moments of the ground state wavefunction either through EMM or OPPQ-BM. Note that for bosonic systems, this is an excellent use of EMM, since the ground state is usually the only state that can be determined.

Using the ground state as a weight usually yields the fastest convergence.

6. THE OPPQ-APPROXIMATION METHOD (OPPQ-AM)

From Eq. (21) and the OPPQ quantization condition in Eq. (22) it follows that the physical energy and missing moment values must satisfy

$$lim_{\to\infty}c_n(E_{phys}, \overrightarrow{\mu}_{phys}) = 0. \tag{26}$$

Since $c_n(E, \overrightarrow{\mu}) = \overrightarrow{\Lambda}^{(n)}(E)\cdot\overrightarrow{\mu}$, from Eq. (17), the $1+m_s$ linear equations

$$\sum_{\ell_2=0}^{m_s}\Lambda_{\ell_2}^{(N-\ell_1)}(E)\ \mu_{\ell_2} = 0, \tag{27}$$

$0 \le \ell_1 \le m_s$, can be used to approximate the physical energies through the determinantal secular equation

$$Det\Big(\Lambda_{\ell_2}^{(N-\ell_1)}(E)\Big) = 0. \tag{28}$$

This defines the OPPQ-Approximation Method (OPPQ-AM). As indicated earlier, Handy and Vrinceanu [10, 11] noted significant improvement in the convergence rates when the weight, R, mimics the asymptotic form of the desired physical states.

The OPPQ representation is very robust, and no convergence irregularities emerge so long as the weight does not decrease much faster than the asymptotic form of the physical states. Provided this is satisfied, the OPPQ-AM formalism will always converge to the true physical energies; however, the rate of convergence depends on the asymptotic properties of the chosen weight.

Despite these impressive results, there is no guarantee that, for hermitian systems, the energies generated through Eq. (28) will be real. Spurious, small imaginary parts may be produced from Eq. (28), that vanish in the $N \to \infty$ limit.

By way of contrast, the OPPQ-Bounding Method to be described below, will always generate real energies for hermitian systems. In addition, as its name suggests, converging bounds to the discrete state energies can be generated.

We make the last observation more explicit. As will be shown below, OPPQ-BM generates, to each order, an energy dependent function, $\mathcal{L}_N(E)$. The local minima, $\partial_E\mathcal{L}_N(E) = 0$ will approximate the physical energies. These local minima can, essentially, be bounded, through converging lower and upper bounds. We refer to the local minima in $\mathcal{L}_N(E)$ as the *OPPQ-BM estimates*, in order to distinguish them from the OPPQ-AM estimates from Eq. (28) and the OPPQ-BM generated bounds.

7. THE OPPQ-BOUNDING METHOD

We outline the structure of OPPQ-BM for one space dimension problems. The major difference between one dimensional and multidimensional MER type systems is that one dimensional problems have a fixed number of missing moments: $m_s < \infty$.

Multidimensional problems involve an infinite hierarchy of missing moment subspaces of increasing dimension. That is, $m_s \to \infty$. We develop the 1-space dimension OPPQ formalism in a manner that extends to multidimensions. How the normalization prescription is chosen, plays an important role in the formalism [9].

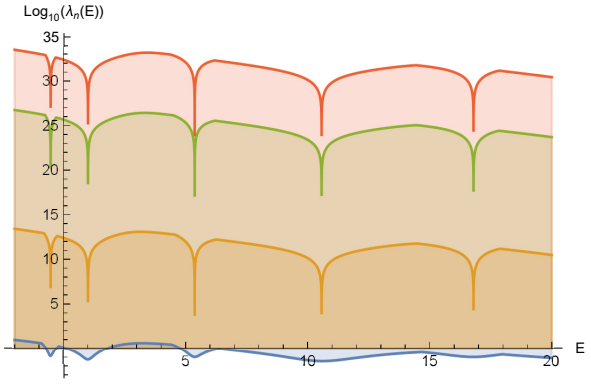

FIGURE 1. $Log_{10}(\lambda_N(E))$ for sextic anharmonic oscillator system in Eq. (47); $N = 20, 40, 100, 120$.

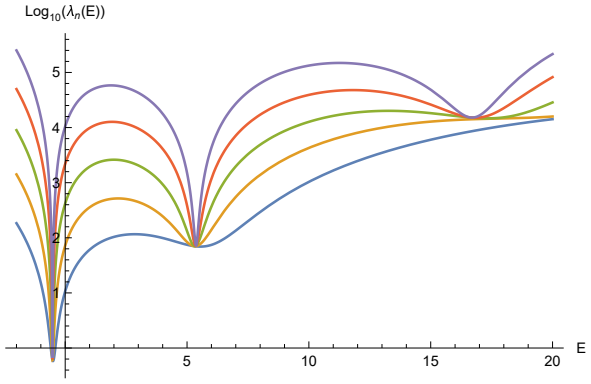

FIGURE 2. $Log_{10}(\lambda_N(E))$ for sextic anharmonic oscillator even states in Eq. (65); $N = 4, 6, 8, 10, 12$; based on the weight $R_L(\xi) = \xi^{-\frac{1}{2}} exp(-\xi)$.

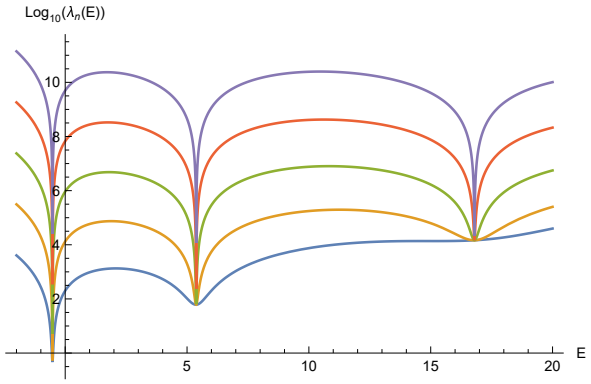

FIGURE 3. $Log_{10}(\lambda_N(E))$ for sextic anharmonic oscillator even states in Eq. (65); $N = 4, 6, 8, 10, 12$; based on the weight $R_G(\xi) = \xi^{-\frac{1}{2}} exp(-\xi^2/2)$.

The OPPQ quantization condition in Eq. (22) is dependent on the positive, (essentially) increasing, sequence, defined by the partial sums:

$$\mathcal{I}[\Psi, R] = Lim_{N\to\infty} S_N(E, \overrightarrow{\mu}), \tag{29}$$

where

$$S_N(E, \overrightarrow{\mu}) = \sum_{j=0}^{N} |c_j(E, \overrightarrow{\mu})|^2, \tag{30}$$

$$= \langle \overrightarrow{\mu} | \mathcal{P}_N(E) | \overrightarrow{\mu} \rangle, \tag{31}$$

where $\mathcal{P}_N(E)$ is an energy dependent, positive matrix (if $N \geq m_s$) of dimension $(1 + m_s) \times (1 + m_s)$:

$$\mathcal{P}_N(E) = \sum_{j=0}^{N} \left(\overrightarrow{\Lambda}^{(j)}(E)\right)^* \overrightarrow{\Lambda}^{(j)}(E), \tag{32}$$

involving the sum over dyad matrix expressions.

For non-hermitian systems, the "*bra*" missing moment vector in Eq. (31) requires the complex conjugate expression for positive norms on complex vector spaces.

It trivially follows, by definition, that

$$0 < S_N(E, \overrightarrow{\mu}) < S_{N+1}(E, \overrightarrow{\mu}) < \ldots < \mathcal{I}[E, \overrightarrow{\mu}]. \tag{33}$$

The OPPQ quantization condition in Eq. (22) tells us that the physical energy and corresponding missing moments correspond to $(E_{phys}, \overrightarrow{\mu}_{phys})$ points within the $E \times \overrightarrow{\mu}$ parameter space where the functional $\mathcal{I}[\Psi, R]$ has a local minimum. Also, for fixed E_{phys}, the corresponding physical missing moment values are those corresponding to a global minimum in the missing moment space. Therefore, to order N we can focus on the global minimum within the constrained (i.e. normalized) missing moment space:

$$\mathcal{L}_N(E) \equiv Inf_{\overrightarrow{\mu}}\{S_N(E, \overrightarrow{\mu}) | \mathcal{C}_{norm}(\overrightarrow{\mu}) = 1\}, \tag{34}$$

where some convenient normalization has been adopted, $\mathcal{C}(\overrightarrow{\mu}) = 1$.

An important result is that

$$\mathcal{L}_N(E) < \mathcal{L}_{N+1}(E). \tag{35}$$

This trivially follows from Eqs. (33-34).

An immediate consequence is that the counterpart to the quantization condition in Eq. (22) now becomes simpler:

$$\lim_{N\to\infty} \mathcal{L}_N(E) = \begin{cases} finite & \Longleftrightarrow \; E = E_{phys}, \\ \infty & \Longleftrightarrow \; E \neq E_{phys}. \end{cases} \tag{36}$$

Combining this with Eq. (35) we obtain:

$$0 < \mathcal{L}_N(E) < \mathcal{L}_{N+1}(E) < \ldots \begin{cases} finite, & \Longleftrightarrow \; E = E_{phys} \\ \infty, & \Longleftrightarrow \; E \neq E_{phys}. \end{cases} \tag{37}$$

Therefore, the $\mathcal{L}_N(E)$ functions form an increasing, nested, concaved upwards, sequence of positive functions. This is demonstrated for the sextic anharmonic harmonic oscillator problem (Figures 1-3), as well as the non-hermitian $ix^3 + iax$ potential (Figure 4), on the complex energy domain. Only at the exact physical energy will the limit be finite. Everywhere else it will become infinite.

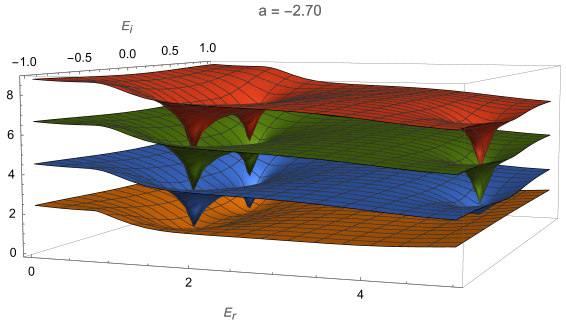

FIGURE 4. $Log_{10}(\lambda_N(E))$ for $N = 20, 30, 40, 50$, $V(x) = ix^3 + iax$, $a = -2.70$

Given the behavior of the $\mathcal{L}_N(E)$, it is clear that the local minima in the energy variable, at a given order "N", should approximate the physical energies. Thus, for each physical discrete state, its corresponding approximants, $E_{phys;N}$, will satisfy

$$\partial_E \mathcal{L}_N(E^{(min)}_{phys;N}) = 0, \tag{38}$$

resulting in

$$\lim_{N\to\infty} E^{(min)}_{phys;N} = E_{phys}. \tag{39}$$

More importantly, these local minima have a very important property. The expressions $\mathcal{L}_N(E^{(min)}_{phys;N})$ form an increasing, positive sequence, bounded from above by the physical counterpart. This follows from

$$\mathcal{L}_N(E^{(min)}_{phys;N}) < \mathcal{L}_{N+1}(E^{(min)}_{phys;N+1}), \tag{40}$$

which follows from:

$$\begin{aligned}\mathcal{L}_N(E^{(min)}_{phys;N}) &< \mathcal{L}_N(E^{(min)}_{phys;N+1}) \\ &< \mathcal{L}_{N+1}(E^{(min)}_{phys;N+1}).\end{aligned} \tag{41}$$

It now follows that the counterpart to the OPPQ quantization condition in Eq. (22) becomes

$$\begin{aligned}0 < \mathcal{L}_N(E^{(min)}_{phys;N}) < \mathcal{L}_{N+1}(E^{(min)}_{phys;N+1}) < \dots \\ < \mathcal{L}_\infty(E_{phys}).\end{aligned} \tag{42}$$

Thus, the $\{\mathcal{L}_N(E^{(min)}_{phys;N})\}$ form a monotonically increasing positive sequence bounded from above by the physical value. The minima do not necessarily converge monotonically.

8. The OPPQ-bounding method

Upon reviewing Eq. (42) a bounding strategy emerges. Assume that the sequence elements can be generated to sufficiently high expansion orders, and that a rough upper bound, $\mathcal{B}_U$ can be discerned:

$$\begin{aligned}\mathcal{L}_N(E^{(min)}_{phys;N}) < \mathcal{L}_{N+1}(E^{(min)}_{phys;N+1}) < \dots \\ < \mathcal{L}_\infty(E_{phys}) < \mathcal{B}_U.\end{aligned} \tag{43}$$

Given the behavior of the $\mathcal{L}_N(E)$ functions, as given in Eqs. (35-37), one can readily determine energy parameter values satisfying

$$\mathcal{L}_N(E^{(L)}_{phys;N}) = \mathcal{L}_N(E^{(U)}_{phys;N}) = \mathcal{B}_U, \tag{44}$$

such that

$$E^{(L)}_{phys;N} < E_{phys} < E^{(U)}_{phys;N}, \tag{45}$$

and

$$\lim_{N\to\infty} \left(E^{(U)}_{phys;N} - E^{(L)}_{phys;N}\right) = 0^+. \tag{46}$$

As a point of comparison, the Rayleigh-Ritz (RR) method solely produces upper bounds. Regardless of how rapidly these bounds converge from above (to the physical value), there is no theoretical criteria by which the RR results can suggest a lower bound to the physical energy. The OPPQ-BM method does.

9. The sextic anharmonic double well potential

The sextic anharmonic oscillator (double well) potential problem is defined by

$$-\partial_x^2\Psi(x) + (x^6 + mx^2)\Psi(x) = E\Psi(x), \tag{47}$$

where we will take $g \equiv 1$ and $m = -4$.

There are three different configuration space representations for the sextic anharmonic oscillator problem, each with different MER relations of varying order. The most immediate is simply working with Ψ as given in Eq. (47). This leads to a sixth order (i.e. $1 + m_s = 6$) finite difference MER relation, as given in Eq. (48). We examine both OPPQ-AM and OPPQ-BM as applied to this representation.

The next configuration space representation is that of the $\Psi^2(x)$ presentation. It leads to a MER relation of order 3 (i.e. $1 + m_s = 3$). We do not apply either OPPQ formulation to this case. However, one can use EMM to bound all the low lying discrete states; thereby providing a test for the effectiveness of OPPQ.

The third, and last, sextic configuration space representation is provided by the contact transformation, $\Phi(x) = exp(-\frac{x^4}{4})\Psi(x)$. This leads to the most efficient MER representation, corresponding to a first order (homogeneous) MER relation (i.e, $1 + m_s = 1$). It results in the fastest OPPQ and EMM convergence.

9.1. EMM-Ψ

The first MER representation to be considered, for the sextic anharmonic oscillator, results from a direct MER analysis of the Schrödinger equation representation in Eq. (47). The power moments along the entire real axis are referred to as the Hamburger moments $\mu(p) = \int_{\Re} dx\ x^p\Psi(x)$.

Upon multiplying both sides of Eq. (47) by x^p and implementing an integration by parts analysis, implicitly assuming that one is working with a discrete state,

there ensues a Hamburger moment equation relation (MER) of the form:

$$\mu(p+6) = -\ m\ \mu(p+2) + E\mu(p) + \ p(p-1)\mu(p-2), \qquad p \geq 0. \quad (48)$$

This is a MER equation of order $1 + m_s = 6$. The MER relation in Eq. (48) applies to both even and odd discrete states.

The generator form for the above MER becomes

$$M_E(p+6,\ell) = -\ m\ M_E(p+2,\ell) + EM_E(p,\ell) + \ p(p-1)M_E(p-2,\ell), \quad (49)$$

$p \geq 0$; and $0 \leq \ell \leq m_s = 5$. The initialization conditions becomes

$$M(\ell_1, \ell_2) = \delta_{\ell_1,\ell_2}, \quad (50)$$

for $0 \leq \ell_{1,2} \leq 5$.

The OPPQ representation becomes

$$\Psi(x) = \sum_{n=0}^{\infty} c_n P_n(x) R(x). \quad (51)$$

One can take the weight to be the Gaussian, $R_G(x) = exp(-x^2)$, or the asymptotic form for the physical states, $R_A(x) = exp(-\frac{x^4}{4})$. In the original formulation of the OPPQ-Approximation Method (OPPQ-AM) Handy and Vrinceanu examined both; and demonstrated the superiority of $R_A(x)$. Our interest here is to demonstrate this approach, and to implement the OPPQ-Bounding Method with regards to the R_A formulation.

The orthonormal polynomials for the Gaussian, $R_G(x)$, are determined by the Hermite polynomials

$$\langle \hat{H}_m | exp(-x^2) | \hat{H}_n \rangle = \delta_{m,n}, \quad (52)$$

or

$$\hat{H}_n(x) = \frac{1}{\sqrt{\sqrt{\pi} 2^n n!}} H_n(x). \quad (53)$$

The orthonormal polynomials (i.e. their coefficients) for $R_A(x)$ are determined through the Cholesky decomposition of the Hankel moment matrix

$$W_{m,n} \equiv \int_{\Re} dx\ x^{m+n} exp(-x^4/4), \quad (54)$$

or

$$W_{m,n} = \begin{cases} 0, \text{if } m+n = odd, \\ 2^{\eta - \frac{1}{2}} \Gamma(\frac{\eta + 1/2}{2}), \text{if } m+n = 2\eta, (\text{even}). \end{cases} \quad (55)$$

The projection coefficients are determined by

$$c_n(E, \mu_0, \ldots, \mu_5) = \sum_{\ell=0}^{m_s=5} \Lambda_\ell^{(n)}(E)\ \mu_\ell, \quad (56)$$

from Eq. (17-18), where

$$\Lambda_\ell^{(n)}(E) = \sum_{j=0}^{n} \Xi_j^{(n)} M_E(j,\ell). \quad (57)$$

The OPPQ-Approximation Method corresponds to solving the secular equation

$$c_{N-\ell_1}(E, \overrightarrow{\mu}) = 0, \quad (58)$$

for $0 \leq \ell \leq 5$ and $N \to \infty$, or

$$Det\Big(\Lambda_{\ell_2}^{(N-\ell_1)}(E)\Big) = 0, \quad (59)$$

a 6×6 determinantal secular equation.

In summary, having chosen N, we need to generate $\{\Lambda_\ell^{(n)}(E) | N - m_s \leq n \leq N\}$. This requires the orthonormal polynomials to order N and the generation of $M_E(p+6,\ell)$, for $0 \leq p \leq N-6$. The Hankel moment matrix for the weight are required up to order $2N$.

The results for both choices of weight are indicated in Tables 1 and 2, for the first ten discrete state energies. It is clear that the R_A choice for the weight is orders of magnitude faster than the simple Gaussian.

It is natural to normalize the missing moments according to a unit normalization $|\overrightarrow{\mu}|^2 = 1$, or

$$\sum_{\ell=0}^{5} \mu_\ell^2 = 1. \quad (60)$$

Accordingly, the energy functional whose minimization is part of the OPPQ-Bounding Method becomes:

$$\mathcal{L}_N(E) \to \lambda_N(E) \equiv \textit{Smallest Eigenvalue of } \mathcal{P}_N(E), \quad (61)$$

where the dyad matrix is given by

$$\Big(\mathcal{P}_N(E)\Big)_{\ell_1,\ell_2} = \sum_{j=0}^{N} \Lambda_{\ell_1}^{(j)}(E) \Lambda_{\ell_2}^{(j)}(E). \quad (62)$$

The $\lambda_N(E)$ form a family of nested, increasing functions, whose local minima approximate the eigenenergies, and serve to define a bounding formalism. We depict this behavior for the $R_A(x)$ weight, in Figure 1. The resolution is not too high and so it is difficult to appreciate that the downward spikes actually are very close to each other. This type of illustration becomes easier to recognize in a subsequent reformulation of the sextic anharmonic oscillator.

We can also apply EMM analysis to the system in Eq. (47). The EMM procedure essentially imposes the well known Hankel Hadamard Moment Problem constraints in order to bound the discrete state energies associated with nonnegative configuration space solutions. Since the only state of this type is the ground state, which must also be of even parity, we can further specialize the MER relation in Eq. (48) to

N	E_0	E_1	E_2	E_3	E_4
25	-0.530376450630854	0.985067365669966	5.28830977093027	10.4934190522107	15.8338485774860
50	-0.523284216533135	1.00560182885171	5.37480811122565	10.5699924952422	16.7909114406834
75	-0.523268805558542	1.00576819439460	5.37496683348150	10.5725844031665	16.7952741272760
100	-0.523268623704744	1.00576834791848	5.37496999430605	10.5725850991710	16.7953468181267
125	-0.523268622109697	1.00576834035184	5.37497000920767	10.5725850451529	16.7953468448794
150	-0.523268622126032	1.00576834023041	5.37497000886154	10.5725850446303	16.7953468331754
175	-0.523268622127498	1.00576834022567	5.37497000884083	10.5725850445874	16.7953468327220
200	-0.523268622127550	1.00576834022555	5.37497000884007	10.5725850445860	16.7953468327042
25	-0.523268576015852	1.00576828117312	5.37497437050670	10.5726072299740	16.7951977796668
50	-0.523268622127552	1.00576834022554	5.37497000884005	10.5725850445859	16.7953468327034
100	-0.523268622127552	1.00576834022554	5.37497000884004	10.5725850445859	16.7953468327036
200.	-0.523268622127552	1.00576834022554	5.37497000884004	10.5725850445859	16.7953468327036

TABLE 1. OPPQ-AM, for the first five states of $V(x) = x^6 - 4x^2$, $m_s = 5$, $R_{Gauss} = e^{-x^2}$ and $R_A = e^{-x^4/4}$.

N	E_5	E_6	E_7	E_8	E_9
25	23.5770262257055	46.5131514442214			
50	23.8599097864908	31.6506317849753	40.1684238879451	48.7083019153321	57.2184300245252
75	23.8838452220218	31.7416917119713	40.2993336329482	49.5062748750452	59.2851256940478
100	23.8839209143498	31.7425529172254	40.3026888622591	49.5114653542220	59.3258556535193
125	23.8839223617171	31.7425500612024	40.3027376770457	49.5115009782085	59.3262796515870
150	23.8839223760489	31.7425498440774	40.3027378004240	49.5115004143879	59.3262744628777
175	23.8839223758291	31.7425498374411	40.3027377924283	49.5115003807374	59.3262741019580
200	23.8839223758112	31.7425498371238	40.3027377918922	49.5115003775253	59.3262740863702
25	23.8828743775059	31.7384980035506	40.3209134822543	50.0634788389675	
50	23.8839223758082	31.7425498371192	40.3027377921622	49.5115003777545	59.3262740709658
100	23.8839223758101	31.7425498371122	40.3027377918721	49.5115003773799	59.3262740857373
150	23.8839223758101	31.7425498371122	40.3027377918721	49.5115003773799	59.3262740857373
200	23.8839223758101	31.7425498371122	40.3027377918721	49.5115003773799	59.3262740857373

TABLE 2. OPPQ-AM, for the sixth-tenth states of $V(x) = x^6 - 4x^2$, $m_s = 5$, $R_{Gauss} = e^{-x^2}$ and $R_A = e^{-x^4/4}$.

such states, yielding a reduced finite order difference equation for the power moments (i.e. $m_s = 2$). The results produced bounds to the 8th decimal place for the ground state energy. We obtain the EMM bounds: $-0.523268623844284 < E_{gr} < -0.523268619253327$, based on an expansion order of approximately 29 power moments (i.e. $\{\mu(p)|0 \leq p \leq 28\}$). This was done on a simple PC with about 14 place precision.

We note that the EMM bounds quoted above were accurate to approximately eight decimal places, based on approximately 28-29 power moments. The missing moment order used for the even state formulation was $m_s = 2$. The OPPQ-BM bounds quoted in Table 3, based on an $m_s = 5$ MER formulation, use an optimal weight, but only give us two decimal place accuracy on the basis of 25 power moments. Of course, the bounds quickly improve, as $N \to 125$. We continue these EMM versus OPPQ comparisons below.

By way of contrast, the OPPQ-BM procedure can produce bounds on all the low-lying states. To produce these, we must first generate the local minima, $\partial_E \lambda_N(E^{(min)}_{phys;N}) = 0$. Fortunately, these derivatives can be obtained algebraically through a recursion procedure. Following this, we must discern a crude upper bound (i.e. $\mathcal{B}^{(U)}_{phys}$) to the positive sequence $\{\lambda_N(E^{(min)}_{phys;N})|N > 0\} < \mathcal{B}^{(U)}_{phys}$. We then determine the energy interval whose endpoints satisfy $\lambda_N(E^{(L)}_{phys;N}) = \mathcal{B}^{(U)}_{phys} = \lambda_N(E^{(U)}_{phys;N})$. These become the lower and upper bound estimates for that physical energy.

The above bounding analysis is initiated in Table 4 for the ground and second excited state of the sextic anharmonic oscillator. Since the use of the R_A weight yields very rapid convergence, we see that the coarse upper bounds, $\mathcal{B}^{(U)}$ are easily determined. Using these we can generate the bounds for the ground state and first excited state, as given in Table 3. We note that the OPPQ-BM bounds generated in Table 3 (we could have continued tightening the bounds), for the ground state, used 125 power moments giving us bounds at the 18th decimal place. In Eq. (69) we quote the EMM bounds obtained on the basis of 61 power moments. The accuracy is at the 33rd decimal place. However, in Eq. (70), using an optimal (Stieljes representation) weight, the OPPQ-AM converged to 50 decimal places, using only 45 power moments.

N	$E^{(L)}_{0;N}$	$E^{(U)}_{0;N}$	$E^{(L)}_{2;N}$	$E^{(U)}_{2;N}$
25	-0.524852943468474	-0.521778245307431	5.368449680815753	5.384374689469648
50	-0.523268749143883	-0.523268495112775	5.374969291406036	5.374970726288986
75	-0.523268622134517	-0.523268622120587	5.374970008804361	5.374970008875728
100	-0.523268622127553	-0.523268622127552	5.3749700088400432	5.3749700088400468
125	-0.52326862212755223948	-0.52326862212755223934	5.3749700088400449937	5.3749700088400449945
		$\mathcal{B}^{(U)} = -0.876$		$\mathcal{B}^{(U)} = -0.990$

TABLE 3. OPPQ-BM upper and lower bounds for the ground and second excited states, using $R_A = e^{-x^4/4}$.

N	$\partial_E \lambda(E^{(min)}_{0;N}) = 0$	$Log_{10}\Big(\lambda(E^{(min)}_{0;N})\Big)$	$\partial_E \lambda(E^{(min)}_{2;N}) = 0$	$Log_{10}\Big(\lambda(E^{(min)}_{2;N})\Big)$
25	-0.523315367444853	-0.877054685910968	5.37640170043752	-0.991603081677466
50	-0.523268622128326	-0.877042389134943	5.37497000884746	-0.991530473233468
75	-0.523268622127552	-0.877042389134815	5.37497000884004	-0.991530473233135
100	-0.523268622127552	-0.877042389134815	5.37497000884004	-0.991530473233135
		$\mathcal{B}^{(U)} = -0.876$		$\mathcal{B}^{(U)} = -0.990$

TABLE 4. OPPQ-BM Analysis for determining coarse upper bounds, $\mathcal{B}^{(U)}$, for the ground and second excited states, using $R_A = e^{-x^4/4}$.

9.2. EMM-Ψ^2

Another MER representation for the sextic anharmonic oscillator is possible by working with the probability density, $S(x) = \Psi^2(x)$. It is easy to show that the probability density for real potentials satisfies a third order LODE. For the sextic anharmonic oscillator problem, this 3rd order LODE yields a MER relation of order 3 (i.e. $m_s = 2$). We do not give the details of this analysis, since the following MER representation offers the easiest OPPQ implementation. The value of EMM-Ψ^2 is that we can bound the discrete states and use the results to gauge the effectiveness of OPPQ. This is referenced below.

9.3. EMM $e^{-\frac{x^4}{4}}\Psi(x)$

The third MER representation is obtained through the contact transformation,

$$\Phi(x) = exp(-\frac{x^4}{4})\Psi(x). \tag{63}$$

Since this involves a factor identical to the dominant WKB asymptotic form for the physical states, the MER representation for Φ will involve fewer missing moments (i.e. none, after a normalization) than the MER for Ψ, as given in Eq. (48), involving five (5) missing moments (after imposing a normalization). This is desirable since the lower the missing moment order, the faster the convergence of either OPPQ or EMM. We provide the details of both approaches below.

9.4. OPPQ ANALYSIS OF THE $(m_s = 0)$ SEXTIC ANHARMONIC DOUBLE WELL OSCILLATOR

The double well anharmonic problem of interest is that for the potential $V(x) = x^6 - 4x^2$, where $x \in \Re$. The physical solutions must die off, asymptotically, according to the dominant WKB expression $\Psi(x) \sim exp(-\frac{x^4}{4})$.

If we work with the contact transformation in Eq. (63) $\Phi(x) = exp(-\frac{x^4}{4})\Psi(x)$, we note that the discrete states remain normalizable and exponentially bounded, in the Φ representation. Unphysical Ψ configurations (i.e. non-normalizable due to their exponentially unbounded form in one or both asymptotic directions) map into non-normalizable Φ configurations. The EMM formalism works in either representation, precisely because of this. We note that the power moments for exponentially bounded configurations exist; whereas they become infinite (or do not exist) for unphysical configurations.

The Φ configurations must satisfy the differential equation

$$\Phi''(x) + 2x^3\Phi'(x) + (7x^2 + E)\Phi(x) = 0. \tag{64}$$

The Hamburger moment (i.e. $\mu(p) \equiv \int_{\Re} dx\ x^p\Phi(x)$) equation becomes

$$(2p-1)\mu(p+2) = p(p-1)\mu(p-2) + E\mu(p).$$

The even parity states will admit a MER for the even order power moments, $\mu(2\rho) = u(\rho)$ or

$$(4\rho-1)u(\rho+1) = 2\rho(2\rho-1)u(\rho-1) + Eu(\rho). \tag{65}$$

The odd parity states $\mu(2\rho+1) \equiv \nu(\rho)$ will satisfy the MER :

$$(4\rho+1)\nu(\rho+1) = 2\rho(2\rho+1)\nu(\rho-1) + E\nu(\rho). \tag{66}$$

We note that the even order Hamburger moments satisfy: $\mu(2\rho) = u(\rho) = \int_0^{+\infty} d\xi\ \xi^{\rho-1/2}\Phi(\sqrt{\xi})$, where $x^2 = \xi$; however, the odd order Hamburger moments satisfy $\mu(2\rho+1) = \nu(\rho) = \int_0^{+\infty} d\xi\ \xi^{\rho}\Phi(\sqrt{\xi})$. The importance of these relations is that the respective

N	E_0	E_2	E_4	E_6	E_8
10	-0.5234534028	5.354166238	16.82887249		
20	-0.5232677208	5.375031586	16.79298386	31.63171200	49.94322409
30	-0.5232686293	5.374969341	16.79536744	31.74329539	49.45632020
40	-0.5232686220	5.374970019	16.79534604	31.74254727	49.51247497
50	-0.5232686221	5.374970009	16.79534686	31.74254902	49.51148774
60	-0.5232686221	5.374970009	16.79534683	31.74254987	49.51149946
70	-0.5232686221	5.374970009	16.79534683	31.74254984	49.51150043
80	-0.5232686221	5.374970009	16.79534683	31.74254984	49.51150038
90	-0.5232686221	5.374970009	16.79534683	31.74254984	49.51150038
100	-0.5232686221	5.374970009	16.79534683	31.74254984	49.51150038

TABLE 5. OPPQ-BM Estimates (i.e. $\partial_E \lambda_N(E^{(min)}_{phys;N}) = 0$), Φ representation, (Eq. 65) $R_L(\xi) = \xi^{-\frac{1}{2}} exp(-\xi)$.

moments, in the context of Eqs. (65, 66) allow us to implement a Stieltjes moment analysis through EMM.

We will only apply OPPQ on the even Ψ configurations, for simplicity. However, since the even order power moments are the moments of $\Upsilon(\xi) \equiv \frac{\Phi(\sqrt{\xi})}{\sqrt{\xi}}$, the OPPQ expansion must be relative to this configuration. Thus, the relevant OPPQ expansion will be

$$\Upsilon(\xi) = \sum_{n=0}^{\infty} c_n P_n(\xi) R(\xi), \tag{67}$$

where Φ's power moments will satisfy Eq. (65).

Since the physical configurations behave, asymptotically, as $\Psi(x) \sim exp(-\frac{x^4}{4})$, the transformed expressions behave as $\Phi(\xi) \sim exp(-\frac{\xi^2}{2})$.

Since the transformed system involves a Stieltjes configuration supported on the nonnegative axis, one might take the weight to be the exponential function, $\tilde{R}_L(\xi) = exp(-\xi)$, with Laguerre polynomials; or the Gaussian $\tilde{R}_G(\xi) = exp(-\xi^2/2)$, restricted to the nonnegative real axis. However, for the quantization integral in Eq. (20) to apply, particularly with regards to the generation of bounds, we need to take into account the $\xi^{-\frac{1}{2}}$ that is inherent to the transformed, even order, power moments.

Based on the previous arguments we will work with $R_L(\xi) = \xi^{-\frac{1}{2}} exp(-\xi)$ and $R_G(\xi) = \xi^{-\frac{1}{2}} exp(-\xi^2/2)$. The corresponding power moments for the weights, in order to generate the orthonormal polynomials are obtained as follows.

The power moments $w_L(p) \equiv \int_0^\infty d\xi\ \xi^p R_L(\xi)$ or $w_L(p) = \Gamma[p + \frac{1}{2}]$ satisfy the recursion relation $w_L(p+1) = (p + 1/2) w_L(p)$; whereas $w_G(p) \equiv \int_0^\infty d\xi\ \xi^p R_G(\xi)$, or $w_G[p] = 2^{\frac{2p-3}{4}} \Gamma[\frac{2p+1}{4}]$, satisfy the recursion relation $w_G(p+2) = (p + 1/2) w_G(p)$.

In their original work on the OPPQ-Approximation Method (i.e. Eq. (28)), Handy and Vrinceanu implemented OPPQ-AM with both of these types of weights (i.e. using their counterparts along the entire real axis, $x \in \Re$). They showed that superior (faster converging) results were obtained for weights that emulated the asymptotic form of the physical states.

The enhanced efficiency of working with $R_G(\xi)$ instead of $R_L(\xi)$ is evident in Figure 3 compared to Figure 2 (i.e. the functions for the former are converging much faster around the physical energies).

The numerical results for the $m_s = 0$ sextic anharmonic oscillator problem are given in the following section. We only give numerical results based on using $R_L(\xi)$. Instead of working with $R_G(\xi)$, we will use the actual ground state wavefunction (i.e. its power moments), $R_{gr}(\xi)$. The reason is that both have the same asymptotic behavior. That is, $R_{gr}(\xi) = \Phi_{gr}(\xi) \sim R_G(\xi)$; therefore, upon solving for the power moments of the ground state wavefunction (including the energy), we can use it to generate its orthonormal polynomials, and quantize the excited states, through OPPQ.

To be able to do this requires sufficient accuracy in the determination of the ground state power moments, since these must generate a positive Hankel matrix for the weight (before implementation of a Cholesky analysis). Although this can be done through OPPQ, EMM inherently works with positive matrices and therefore is more efficient for doing this type of analysis.

9.5. OPPQ RESULTS FOR THE $m_s = 0$, SEXTIC ANHARMONIC OSCILLATOR

The OPPQ-Φ formulation is a zero missing moment problem (i.e. $m_s = 0$) and converges very fast.

In Figure 2 we plot the nested sequence $\lambda_N(E)$, for $N = 4, 6, 8, 10, 12$. This calculation was done based on the $R_L(\xi)$ weight. A similar result holds for the $R_G(\xi)$ weight as depicted in Figure 3. It clearly reveals the faster convergence afforded by a weight that emulates the asymptotic form of the physical states.

In Table 5 we give the OPPQ-BM energy estimates (i.e. the local minima, $\partial_E \lambda_N(E^{(min)}_{phys.;N}) = 0$) for the low lying, even parity, discrete state energies, based on Eq. (65), using the inferior weight $R_L(\xi) = \xi^{-\frac{1}{2}} exp(-\xi)$.

Table 5 only cites results (to ten significant figures) for $N \leq 100$. Not shown in Table 5 are the OPPQ-BM estimation results for the ground state at $N = 120$:

N	$\partial_E S_N(E_N^{(min)}) = 0$	$Log(S_N(E_N^{(min)}))$	$c_N(E_N) = 0$	$E_N^{(L)}$	$E_N^{(U)}$
20	49.94322409213197	7.982552803	49.4426432537	48.893	50.857
30	49.45632020275004	7.997267757	49.4986057623	49.366	49.546
40	49.51247497421839	8.002499541	49.5123070944	49.504	49.520
50	49.51148774312169	8.002657778	49.5114731270	49.510	49.512
60	49.51149945726214	8.002665930	49.5115007312	49.51140	49.51159
70	49.51150043370514	8.002667120	49.5115003992	49.51148	49.51151
80	49.51150037650008	8.002667337	49.511500375879294	49.5114990	49.5115017
90	49.51150037729806	8.002667346	49.511500377394135	49.5115001949	49.5115005597
100	49.51150037738496	8.002667348	49.511500377382972	49.5115003518	49.5115004029
110	49.51150037737999	8.002667348	49.511500377379789	49.5115003736	49.5115003811
120	49.51150037737991	8.002667348	49.511500377379918	49.5115003768	49.5115003780
		$\mathcal{B} = 8.01$			

TABLE 6. OPPQ Results for E_8: $R_L = \frac{e^{-\xi}}{\sqrt{\xi}}$.

$E_{gr} = -.52326862212755224$. This result lies within the bounds generated through an EMM-Φ analysis (based on the first 29 power moments):

$$-.5232686221275616 < E_{gr} < -.5232686221275495. \quad (68)$$

We can infer that the EMM bounds in Eq. (68) predict the exact answer to 13 decimal places. This result, based on 29 moments, surpasses the OPPQ-BM estimation analysis in Table 5 ($N = 30$) of -0.5232712343, at the fourth-fifth decimal place. Thus EMM-Φ, by this comparison, is approximately three times more efficient.

Having said this, we remind the reader that whereas EMM involves sophisticated analysis (i.e. nonlinear convex optimization), OPPQ is purely algebraic, and implementable to arbitrary accuracy through algebraic software, such as Mathematica. Additionally, EMM is, in practice, only applicable to the (multidimensional) bosonic ground state; whereas OPPQ applies to any multidimensional bosonic or fermionic (low dimension) system, including non-hermitian systems.

9.5.1. GENERATING BOUNDS FOR E_8

We re-examine the results in Table 5 for E_8, the slowest converging energy. As with other methods, such as Rayleigh-Ritz (RR), the manifest convergence of the results (i.e. the $N \to 120$ sequence in Table 5) is no guarantee of the accuracy of the apparent limit in predicting the true energy. Whereas EMM produces converging bounds from first principles; OPPQ defines a procedure by which one can generate bounds provided a certain parameter is empirically determined, specifically the *coarse upper bound*, $\mathcal{B}^{(U)}$. Below we describe the OPPQ-BM bounding procedure in detail, although the same underlies the results in Tables 4 and 3, for the $m_s = 3$ MER formulation in Eq. (48). The only advantage of the current problem is that it is a zero missing moment problem, and therefore easier to implement.

In Table 6 we provide the OPPQ-BM eigenenergy estimate for E_8 (the second column). The third column contains the increasing, convergent, positive sequence from which a coarse upper bound, $\mathcal{B}^{(U)}$, is to be empirically determined. Using this coarse upper bound, we can generate arbitrarily tight bounds (i.e. the last two columns), as $N \to \infty$. Note that we continued generating these bounds in Table 7. This entire procedure is based on the assumption that the manifest convergence of the third column in Table 6 is correctly bounded, from above, by the empirically determined coarse upper bound, $\mathcal{B}^{(U)}$. The fourth column contains the OPPQ-AM estimate.

It is important to appreciate that the coarseness of $\mathcal{B}^{(U)}$ has nothing to do with the tightness of the bounds, in principle, assuming one can generate high OPPQ expansion orders.

Below we compare the accuracy of the OPPQ-BM formalism to order $N - 120$, both with respect to the OPPQ-BM energy estimate ($E_8 = 49.5115003774$, from Table 6) and the OPPQ-BM bounds ($49.5115003768 < E_8 < 49.5115003780$, also from Table 6), as compared to the bounds generated by an EMM analysis. The results are very good and consistent.

It is important to note that the OPPQ-BM estimate obtained at lower order, does not have to lie within the OPPQ-BM bounds obtained at higher order. Thus the entry in the second column in Table 6, corresponding to OPPQ-BM energy estimate (i.e. the local minima) of $E = 49.51148774312169$ (i.e. $N = 50$), lies outside of the bounds generated in the last two columns, for $N > 80$. However, all OPPQ-BM estimates must lie within the bounds calculated at lower order.

9.6. COMPARISON WITH EMM BOUNDS

Generally, the EMM analysis will be more efficient in generating bounds than OPPQ-BM. That is, fewer moments will be required to generate the same level of tightness of the bounds. However, this depends

N	$E_8^{(L)}$	$E_8^{(U)}$
150	49.511500377377302482	49.511500377382545933
160	49.511500377379459378	49.511500377380389040
170	49.511500377379839286	49.511500377380009132
180	49.511500377379908253	49.511500377379940166
190	49.511500377379921131	49.511500377379927287
200	49.511500377379923601	49.511500377379924818
210	49.511500377379924086	49.511500377379924333
220	49.511500377379924184	49.511500377379924235
230	49.511500377379924204	49.511500377379924215
240	49.511500377379924208	49.511500377379924210
250	49.51150037737992420904883O	49.51150037737992420955895 3
260	49.51150037737992420924685 1	49.51150037737992420936093 2
270	49.51150037737992420929091 4	49.51150037737992420931686 9
280	49.51150037737992420930089 0	49.51150037737992420930689 3
290	49.51150037737992420930318 6	49.51150037737992420930459 7
300	49.51150037737992420930372 3	49.51150037737992420930406 0
	$\mathcal{B} = 8.01$	

TABLE 7. Bounds for E_8 based on chosen $\mathcal{B}^{(U)}$.

N	E_0	E_2	E_4	E_6	E_8
1	-0.5232686221275529				
5	-0.5232686221276021	5.37847969429	16.78604192264		
10	-0.5232686221275522	5.37497046837	16.79542276464	31.74535880954	49.5248113799
20	-0.5232686221275523	5.37497000884	16.79534683270	31.74254983720	49.5115003841
30	-0.5232686221275523	5.37497000884	16.79534683270	31.74254983711	49.5115003772

TABLE 8. OPPQ-BM Estimates (i.e. $\partial_E S_N(E) = 0$) for $V(x) = x^6 - 4x^2$, $m_s = 0$, $R(x) = \Phi_{gr}(x)$ based on the first 61, EMM generated, ground state power moments $\{u_{gr}(p \leq 60)\}$.

on the choice of weight, as the following case exemplifies. Thus, with regards to the $m_s = 2$ missing moment formulation given earlier, the EMM bounds for the ground state $-0.523268623844284 < E_{gr} < -0.523268619253327$, were based on the first 29 power moments. The same (approximately) level of tightness was achieved with OPPQ-BM using more than 50 power moments, based on the results in Table 3. Thus, in this example EMM is vastly superior to OPPQ-BM. However, for the next example the situation significantly improves for OPPQ-BM over EMM.

For the $m_s = 0$ formulation being considered, using the first 62 Stieljes power moments (i.e. $\{u(p)|p \leq 61\}$), EMM achieves the bounds:

$$-.523268622127552239416169497190784061165647716306044 < E_{EMM} < -.523268622127552239416169497190784061165647716306035 \quad (69)$$

Using the weight R_L the OPPQ-AM estimate achieves this level of accuracy on the basis of approximately 220 power moments; whereas the weight R_G generates an OPPQ-AM estimate that surpasses the EMM accuracy based only on the use of 45 moments (OPPQ-AM):

$$E_{OPPQ-AM} = -0.523268622127552239416169497190784061165647716306044 \quad (70)$$

9.7. USING THE GROUND STATE AS A WEIGHT

In Table 8 we implement OPPQ-BM on a representation that uses the generated moments of the unknown ground state $R(x) = \Psi_{gr}(x)$. As expected, the convergence is very fast in comparison with results based on R_L.

9.8. EMM RESULTS FOR THE PROBABILITY DENSITY

Application of EMM to the probability density (i.e. EMM-Ψ^2, an $m_s = 2$ problem) yields the bounds $-.52326866 < E_0 < -.52326857$, $1.0057681 < E_1 < 1.0057685$, $5.3749699 < E_2 < 5.3749701$, $10.5725845 < E_3 < 10.5725855$, $16.795339 < E_4 < 16.795351$, $23.883886 < E_5 < 23.883961$, $31.74217 < E_6 < 31.74323$, $40.301 < E_7 < 40.305$, $49.506 < E_8 < 49.533$ all to the same moment expansion order of 28. We also note that an EMM-$\Psi\{m_s = 2\}$ bounding formulation on the ground state yields comparable bounds using the first 28 power moments: $-.5232686237 < E_{gr} < -.5232686193$. With regards

to E_8, extension of EMM-$\Psi^2\{m_s=2\}$ analysis to the first 48 moments (i.e. $\{u(p)|0\le p\le 47\}$) yields the bounds $49.5115003768 < E_8 < 49.5115003798$. These serve to further confirm some of the results previously cited.

10. A PT-symmetry breaking, non-hermitian, problem

Consider the non-hermitian system

$$-\partial_x^2\Psi(x)+(ix^3+iax)\Psi(x)=E\Psi(x), \quad (71)$$

which is known to break PT symmetry for negative values of the 'a' parameter ($a<-2.611809356$, and for $a<-5.375879629$) from Refs. [8, 25]. The case $a=0$ has purely real eigen-energies, as computed by Bender and Boettcher [5], and theoretically confirmed by Dorey et al. [6]. The EMM-$\Psi^*\Psi$ formulation also provided strong numerical evidence for this [27].

States that are PT symmetric satisfy $\Psi^*(-x)=\Psi(x)$, and have real energies, $E\in\Re$. States that break this symmetry have complex conjugate pairs for the energies (i.e. $\Psi^*(-x)\neq\Psi(x)$, with complex energies E^* and E, respectively).

We work with the MER-Ψ representation for which the complex power moments on the real axis satisfy

$$\begin{aligned}\mu(p+3)=&-a\mu(p+1)-iE\mu(p)\\&-ip(p-1)\mu(p-2),\qquad p\ge 0.\end{aligned} \quad (72)$$

The recursion relation for the energy dependent generator coefficients is

$$\begin{aligned}M_E(p+3,\ell)=&-aM_E(p+1,\ell)-iEM_E(p,\ell)\\&-ip(p-1)M_E(p-2,\ell),\end{aligned} \quad (73)$$

for $p\ge 0$, $0\le\ell\le 2$, and $M_E(\ell_1,\ell_2)=\delta_{\ell_1,\ell_2}$. This is an $m_s=2$ representation of order 3. Since the asymptotic form of the physical states goes as $\Psi(x)\sim exp(-\frac{2}{5}|x|^{\frac{5}{2}})$, we can use the Gaussian weight $R(x)=exp(-x^2/2)$. The OPPQ-BM formalism ensues as before:

$$\Psi(x)=\sum_{j=0}^{\infty}c_jP_j(x)R(x), \quad (74)$$

involving real weights and corresponding orthonormal polynomials. The complex projection coefficients are given by

$$c_j(E,\mu_0,\mu_1,\mu_2)=\langle P_j(x)|\Psi\rangle, \quad (75)$$

or

$$c_j(E,\mu_0,\mu_1,\mu_2)=\sum_{\ell=0}^{m_s=2}\Lambda_\ell^{(j)}(E)\ \mu_\ell, \quad (76)$$

where the coefficients depend on the orthonormal polynomial coefficients and the $M_E(p,\ell)$'s:

$$\Lambda_\ell^{(j)}(E)=\sum_{\eta=0}^{j}\Xi_\eta^{(j)}M_E(\eta,\ell). \quad (77)$$

The OPPQ-BM quantization condition is

$$\begin{aligned}\mathcal{I}[\Psi,R]&=\int_{\Re}dx\frac{\Psi^*(x)\Psi(x)}{R(x)}\\&=\begin{cases}finite \iff E=E_{phys}\ and\ \overrightarrow{\mu}=\overrightarrow{\mu}_{phys},\\ \infty \iff E\neq E_{phys}\ or\ \overrightarrow{\mu}\neq\overrightarrow{\mu}_{phys}.\end{cases}\end{aligned} \quad (78)$$

We adopt the vector notation for the missing moments $\overrightarrow{\mu}\equiv(\mu_0,\mu_1,\mu_2)$.

Substituting the OPPQ representation we obtain:

$$\mathcal{I}[\Psi,R]=\sum_{j=0}^{\infty}c_j^*(E,\overrightarrow{\mu})c_j(E,\overrightarrow{\mu}). \quad (79)$$

Once again, the focus is on :

$$\begin{aligned}&S_N(E,\overrightarrow{\mu})\\&\quad=\sum_{\ell_1=0}^{m_s}\sum_{\ell_2=0}^{m_s}\mu_{\ell_1}^*\Big(\sum_{j=0}^{N}\Lambda_{\ell_1}^{(j)}(E)^*\Lambda_{\ell_2}^{(j)}(E)\Big)\mu_{\ell_2},\end{aligned} \quad (80)$$

involving the positive definite matrix

$$\big(\mathcal{P}_N(E)\big)_{\ell_1,\ell_2}=\sum_{j=0}^{N}\Lambda_{\ell_1}^{(j)}(E)^*\Lambda_{\ell_2}^{(j)}(E). \quad (81)$$

If we adopt a unit missing moment vector normalization, then the focus for OPPQ-BM quantization is on the behavior of the smallest eigenvalue, $\lambda_N(E)\equiv$ Smallest Eigenvalue$\Big(\mathcal{P}_N(E)\Big)$, viewed as a function of the real and imaginary parts of the energy variable. The focus is on determining the local minima: $\partial_{E_r}\lambda_N(E_{N,phys}^{(min)})=\partial_{E_i}\lambda_N(E_{N,phys}^{(min)})=0$. These derivatives can be obtained algebraically.

We outline the essential steps for algebraically generating the partial derivatives. First of all, we have $\lambda_N(E)=\langle\overrightarrow{\mu}|\mathcal{P}_N(E)|\overrightarrow{\mu}\rangle$, involving the normalized missing moment (lowest) eigenvector. This is not an analytic function in E, so we must work with the partial derivatives with respects to $E_{r,i}$. Thus, we need $\partial_{E_{r,i}}\lambda_N(E)=\langle\overrightarrow{\mu}|\partial_{E_{r,i}}\mathcal{P}_N(E)|\overrightarrow{\mu}\rangle$. We can generate the required matrix expression from Eq. (80) or $\partial_{E_{r,i}}\mathcal{P}_N(E)=\sum_{j=0}^{N}\Big(\partial_{E_{r,i}}\Lambda^{(j)}(E)^*\Big)\Lambda^{(j)}(E)+c.c.$. From Eq. (77), so long as the Ξ's do not depend on the energy parameter, we need $\partial_{E_{r,i}}M_E(\eta,\ell)$. However, this can be obtained recursively through the expression in Eq. (72).

Our immediate interest is on the behavior of $\lambda_N(E)$ over the two dimensional complex energy plane, as the parameter 'a' is varied, and $N=40$. In Figures 5-12 we show the convergence of two PT-breaking (complex conjugate) energies (eventually becoming real) as we increase the a-parameter through

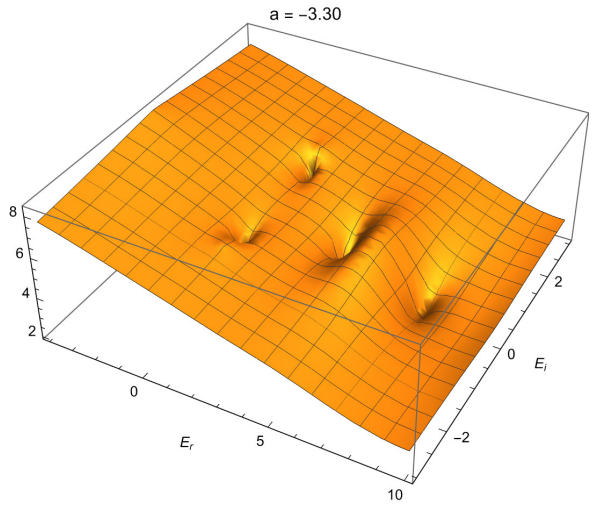

FIGURE 5. $Log_{10}(\lambda_{40}(E))$ for PT-breaking regime, $-3.30 \leq a \leq -1.70$ for $V(x) = ix^3 + iax$, $a = -3.30$

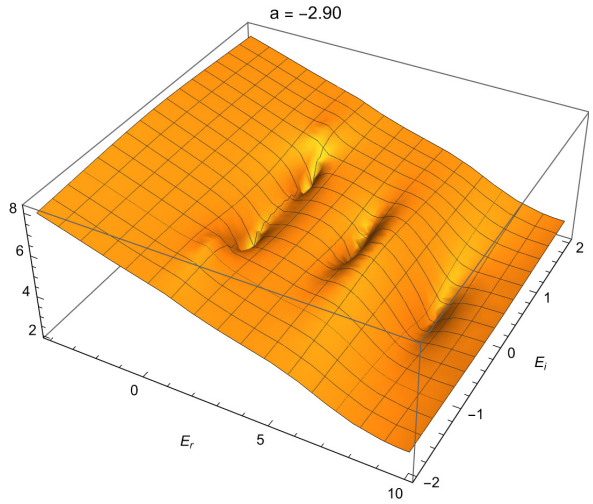

FIGURE 6. $Log_{10}(\lambda_{40}(E))$ for PT-breaking regime, $-3.30 \leq a \leq -1.70$ for $V(x) = ix^3 + iax$, $a = -2.90$

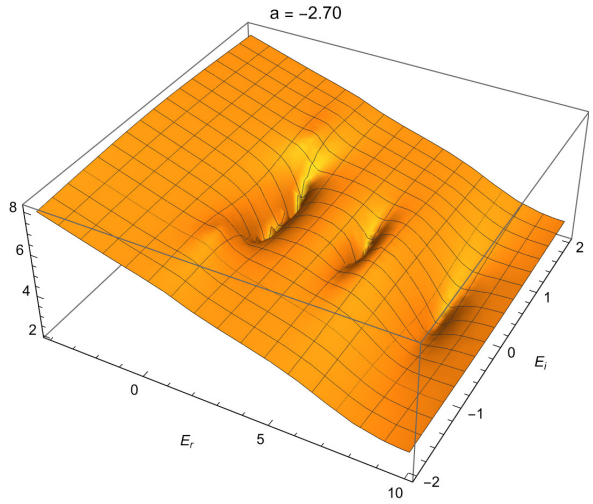

FIGURE 7. $Log_{10}(\lambda_{40}(E))$ for PT-breaking regime, $-3.30 \leq a \leq -1.70$ for $V(x) = ix^3 + iax$, $a = -2.70$

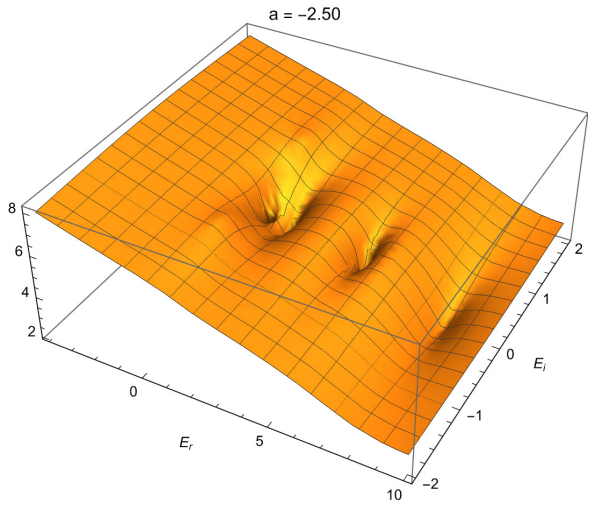

FIGURE 8. $Log_{10}(\lambda_{40}(E))$ for PT-breaking regime, $-3.30 \leq a \leq -1.70$ for $V(x) = ix^3 + iax$, $a = -2.50$

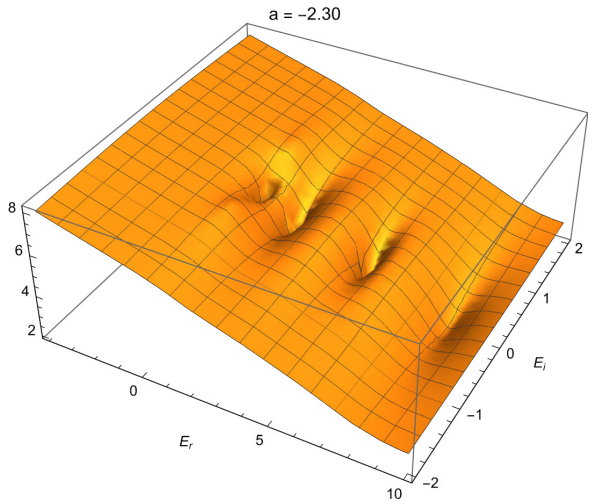

FIGURE 9. $Log_{10}(\lambda_{40}(E))$ for PT-breaking regime, $-3.30 \leq a \leq -1.70$ for $V(x) = ix^3 + iax$, $a = -2.30$

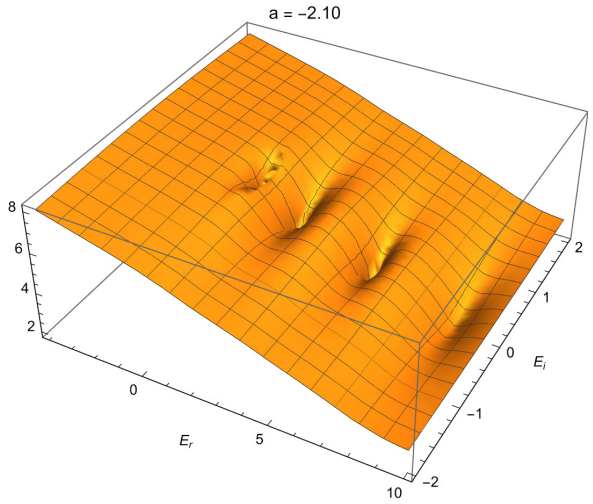

FIGURE 10. $Log_{10}(\lambda_{40}(E))$ for PT-breaking regime, $-3.30 \leq a \leq -1.70$ for $V(x) = ix^3 + iax$, $a = -2.10$

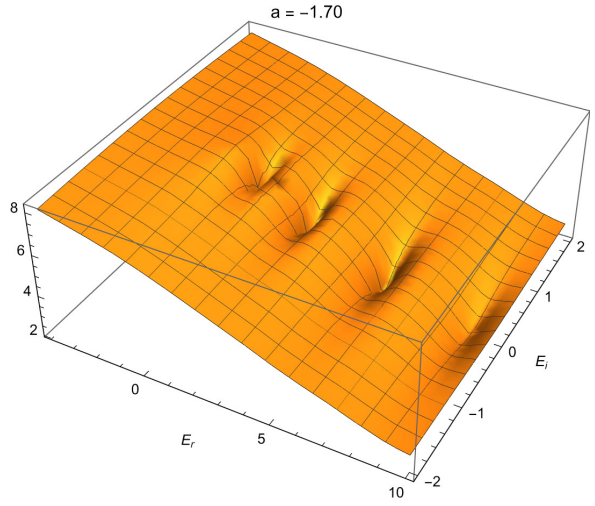

Figure 11. $Log_{10}(\lambda_{40}(E))$ for PT-breaking regime, $-3.30 \leq a \leq -1.70$ for $V(x) = ix^3 + iax$, $a = -1.70$

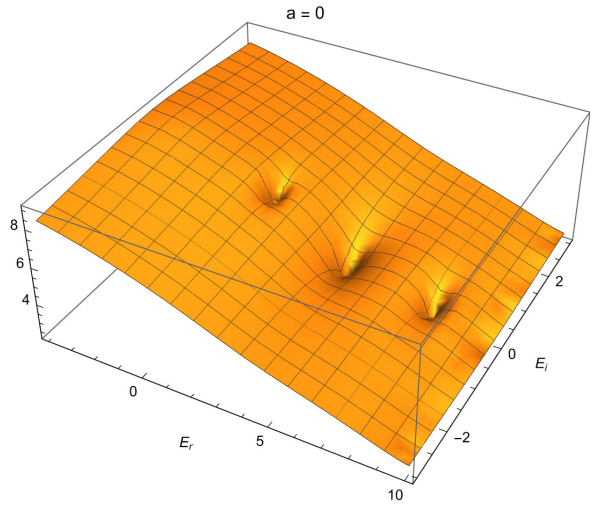

Figure 12. $Log_{10}(\lambda_{40}(E))$ for PT-breaking regime, $-3.30 \leq a \leq -1.70$ for $V(x) = ix^3 + iax$, $a = 0.00$

$-3.30, -2, 90, -2.70, -2.50, -2.30, -2.10, -1.70$ and 0. These parameter values were chosen since it is known that PT-symmetry breaking occurs at $a_{c_1} = -2.611809356$ (as well as at $a_{c_2} = -5.375879629$) [8, 25].

Figure 7 shows the behavior of the physical energies (i.e. defined by the local minima), for $a = -2.70 \approx a_{c_1}$, the critical value for the onset of symmetry breaking. For this same $a = -2.70$, Figure 4 shows the behavior of successive $\lambda_N(E)$ surfaces for $N = 20, 30, 40, 50$. Within the two dimensional graphical renderings, we see similar behaviors to that in Figures 1-3. We can implement the same OPPQ-BM bounding analysis used previously, for hermitian systems, to bound the real and imaginary parts of the *discrete state* real/complex energies. The nesting of the respecive $\lambda_N(E_r, E_i)$ in Figure 4 shows the viability of the previous OPPQ-BM analysis for bounding the real and imaginary parts of the complex-plane energies. This is the focus of a future work.

We note that for $a = 0$, the local minima in Figure 12 correspond, approximately (due to the low order, $N = 40$) to the PT-symmetric states with energies $E_0 = 1.15626707198811$, $E_2 = 4.10922875280956$, $E_3 = 7.56227385497590$ and $E_4 = 11.31442182025857$ (not shown). These were determined by EMM [8] and OPPQ-AM [10].

11. Conclusions

We have demonstrated the effectiveness of a new eigenenergy bounding procedure implementable for multidimensional discrete states regardless of the hermitian or non-hermitian character of the associated Schrödinger operator. The discussion centered on several one dimensional systems of this type. The extension to multidimensions have been given elsewhere [9]. The approach advocated here is purely algebraic.

Acknowledgements

The author is greatful to the organizers of the 2021 Conference on Analytic and Algebraic Methods In Physics XVIII, particularly Dr. Miloslav Znojil and Dr. Vit Jakubsky, and the support from the Doppler Institute of the Czech Academy of Sciences. Additional remarks from Dr. Daniel Bessis, Dr. John R. Klauder, Dr. Jerzy Cioslowski, and Dr. A. Turbiner are greatly appreciated. Technical support from Dr. Maribel Handy is also greatly appreciated.

References

[1] W. Ritz. Über eine neue Methode zur Lösung gewisser Variationsprobleme der mathematischen Physik. *Journal für die reine und angewandte Mathematik* **1909**(135):1–61, 1909. https://doi.org/10.1515/crll.1909.135.1.

[2] G. Temple. The theory of Rayleigh's principle as applied to continuous systems. *Proceedings of the Royal Society of London Series A, Containing Papers of a Mathematical and Physical Character* **119**(782):276–293, 1928. http://www.jstor.org/stable/95047.

[3] M. G. Marmorino, A. Almayouf, T. Krause, D. Le. Optimization of the temple lower bound. *Journal of Mathematical Chemistry* **50**(4):833–842, 2012. https://doi.org/10.1007/s10910-011-9927-z.

[4] R. Martinazzo, E. Pollak. Lower bounds to eigenvalues of the schrödinger equation by solution of a 90-y challenge. *Proceedings of the National Academy of Sciences* **117**(28):16181–16186, 2020. https://doi.org/10.1073/pnas.2007093117.

[5] C. M. Bender, S. Boettcher. Real spectra in non-Hermitian Hamiltonians having $\mathcal{PT}$ symmetry. *Physical Review Letters* **80**:5243–5246, 1998. https://doi.org/10.1103/PhysRevLett.80.5243.

[6] P. Dorey, C. Dunning, R. Tateo. Supersymmetry and the spontaneous breakdown of $\mathcal{PT}$ symmetry. *Journal of Physics A: Mathematical and General* **34**(28):L391–L400, 2001. https://doi.org/10.1088/0305-4470/34/28/102.

[7] C. M. Bender. Making sense of non-Hermitian Hamiltonians. *Reports on Progress in Physics* **70**(6):947–1018, 2007. https://doi.org/10.1088/0034-4885/70/6/r03.

[8] C. R. Handy. Generating converging bounds to the (complex) discrete states of $P^2+\mathrm{i}X^3+\mathrm{i}\alpha X$ Hamiltonian. *Journal of Physics A: Mathematical and General* **34**(24):5065–5081, 2001. https://doi.org/10.1088/0305-4470/34/24/305.

[9] C. R. Handy. Exact Christoffel-Darboux expansions: A new, multidimensional, algebraic, eigenenergy bounding method. *Physica Scripta* **96**(7):075201, 2021. https://doi.org/10.1088/1402-4896/abf67e.

[10] C. R. Handy, D. Vrinceanu. Orthogonal polynomial projection quantization: a new Hill determinant method. *Journal of Physics A: Mathematical and Theoretical* **46**(13):135202, 2013. https://doi.org/10.1088/1751-8113/46/13/135202.

[11] C. R. Handy, D. Vrinceanu. Rapidly converging bound state eigenenergies for the two dimensional quantum dipole. *Journal of Physics B: Atomic, Molecular and Optical Physics* **46**(11):115002, 2013. https://doi.org/10.1088/0953-4075/46/11/115002.

[12] J. Le Guillou, J. Zinn-Justin. The hydrogen atom in strong magnetic fields: Summation of the weak field series expansion. *Annals of Physics* **147**(1):57–84, 1983. https://doi.org/10.1016/0003-4916(83)90067-2.

[13] J. A. Shohat, J. D. Tamarkin. *The Problem of Moments*. American Mathematical Society, Providence, RI, 1963.

[14] C. R. Handy, D. Bessis. Rapidly convergent lower bounds for the Schrödinger-equation ground-state energy. *Physical Review Letters* **55**:931–934, 1985. https://doi.org/10.1103/PhysRevLett.55.931.

[15] C. R. Handy, D. Bessis, G. Sigismondi, T. D. Morley. Rapidly converging bounds for the ground-state energy of hydrogenic atoms in superstrong magnetic fields. *Physical Review Letters* **60**:253–256, 1988. https://doi.org/10.1103/PhysRevLett.60.253.

[16] Y. P. Kravchenko, M. A. Liberman, B. Johansson. Exact solution for a hydrogen atom in a magnetic field of arbitrary strength. *Physical Review A* **54**:287–305, 1996. https://doi.org/10.1103/PhysRevA.54.287.

[17] C. Schimeczek, G. Wunner. Accurate 2d finite element calculations for hydrogen in magnetic fields of arbitrary strength. *Computer Physics Communications* **185**(2):614–621, 2014. https://doi.org/10.1016/j.cpc.2013.09.023.

[18] A. Grossmann, J. Morlet. Decomposition of Hardy functions into square integrable wavelets of constant shape. *SIAM Journal on Mathematical Analysis* **15**(4):723–736, 1984. https://doi.org/10.1137/0515056.

[19] C. Handy, R. Murenzi. Moment-wavelet quantization: a first principles analysis of quantum mechanics through continuous wavelet transform theory. *Physics Letters A* **248**(1):7–15, 1998. https://doi.org/10.1016/S0375-9601(98)00645-8.

[20] C. R. Handy. Singular-perturbation–strong-coupling field theory and the moments problem. *Physical Review D* **24**:378–383, 1981. https://doi.org/10.1103/PhysRevD.24.378.

[21] S. Boyd, L. Vandenberghe. *Convex optimization*. Cambridge University Press, New York, 2004.

[22] J. B. Lasserre. *Moments, positive polynomials and their applications*. Imperial College Press, London, 2010.

[23] V. Chvátal. *Linear programming*. Freeman, New York, 1983.

[24] M. Reed, B. Simon. *Methods of modern mathematical physics. Vol. 1-3*. Academic Press, New York, 1972. https://doi.org/10.1016/B978-0-12-585001-8.X5001-6.

[25] C. R. Handy, D. Khan, X.-Q. Wang, C. J. Tymczak. Multiscale reference function analysis of the $\mathcal{PT}$ symmetry breaking solutions for $P^2+\mathrm{i}X^3+\mathrm{i}\alpha X$ Hamiltonian. *Journal of Physics A: Mathematical and General* **34**(27):5593–5602, 2001. https://doi.org/10.1088/0305-4470/34/27/309.

[26] E. Delabaere, D. T. Trinh. Spectral analysis of the complex cubic oscillator. *Journal of Physics A: Mathematical and General* **33**(48):8771–8796, 2000. https://doi.org/10.1088/0305-4470/33/48/314.

[27] C. R. Handy. Generating converging eigenenergy bounds for the discrete states of the ix^3 non-Hermitian potential. *Journal of Physics A: Mathematical and General* **34**(19):L271–L277, 2001. https://doi.org/10.1088/0305-4470/34/19/102.

ON THE WESS-ZUMINO MODEL: A SUPERSYMMETRIC FIELD THEORY

Daya Shankar Kulshreshtha[a,*], Usha Kulshreshtha[b]

[a] *University of Delhi, Department of Physics and Astrophysics, Delhi – 110007, India*

[b] *University of Delhi, Kirori Mal College, Department of Physics, Delhi – 110007, India*

[*] corresponding author: dskulsh@gmail.com

Abstract. We consider the free massless Wess-Zumino Model in 4D which describes a supersymmetric field theory that is invariant under the rigid or global supersymmetry transformations where the transformation parameter ϵ (or $\bar{\epsilon}$) is a constant Grassmann spinor. We quantize the theory using the Hamiltonian and path integral formulations.

Keywords: Wess-Zumino Model, supersymmetric field theories, Hamiltonian and path integral quantization.

1. Introduction

Supersymmetry (SUSY) is a symmetry that rotates bosons into fermions and fermions into bosons. It is one of the beautiful symmetries of nature. Also, a field theory (FT) which remains invariant under the rigid or global supersymmetry transformations (where the transformation paremeter is a constant Grassman spinor) and which also satisfies the super Poincare algebra (SPA) is usually referred to as a supersymmetric field theory (SFT). In this article, we consider the free massless Wess-Zumino Model (WZM) in 4D which describes a SFT. It may be important to mention here that the WZM is the first known example of an interacting 4D quantum field theory with linearly realised SUSY, studied by Wess and Zumino using the dynamics of a single chiral superfield (composed of a complex scalar and a spinor fermion). It may be important to mention that the WZM represents a typical SFT which is of central importance in the theory of SUSY, supergravity and superstring theory (SST) and for further details we refere to the work of Refs. [1–8].

The WZM describes an example of a non-manifest supersymmetry [5]. One could of course go to the formalism of superspace and superfields to construct a theory that has a manifest supersymmetry [5]. Taking this theory as an example, it is possible to formulate supersymmertic field theories in different dimensions including in higher dimensions. The WZM also provides a basic framework for the study of Ramond Nievue Schwarz (RNS) SST [8] which is an example of a SST with non-manifest SUSY. Further, starting with the WZM, it is also possible to construct a supergravity theory [1–6, 8].

SPA is a graded Lie algebra that includes anti-commutation relations (ACR's) involving the supercharge Q_a – the generator of the SUSY transformations. WZM is one of the simplest examples of a SFT. In this article, we discuss the supersymmetry of WZM and present some remarks with respect to the rigid or global supersymmetry versus the local supersymmetry (which happens to be a Supergravity theory). Finally we consider the constraint quantization of this theory [7]. It is important to mention that the supersymmetry has profound applications in conformal hadron physics from light-front holography where it even has some observational prospects [9–11].

As mentioned above, the supersymmetry is a symmetry that relates bosonic and fermionic variables (or the bosons and fermions) so that:

$$\delta B = \bar{\epsilon} F \ , \quad \delta F = \epsilon \ \partial B \ ; \quad \partial \equiv \partial_\mu \tag{1}$$

Here, δ is bosonic, B is bosonic and F is fermionic. The transformation parameter ϵ (or $\bar{\epsilon}$) is a constant Grassman spinor and is fermionic. Grassman variables are anti-commuting. Supergravity theory on the other hand is a theory that has "local supersymmetry" and it is invariant under local Susy transformations where the transformation parameter depends on the spacetime x^μ. So the transformation parameter for supergravity: $\epsilon(x^\mu)$ or $\bar{\epsilon}(x^\mu)$ depends on x^μ and hence supergravity is a "gauge theory" of gravity. In contrast to this the WZM is a supersymmetric FT with rigid or global (not local) Supersymmetry.

Let us us consider two consecutive infinitesimal rigid supersymmetry transformations of a bosonic field B:

$$\delta_1 \ B = \bar{\epsilon}_1 F \ , \quad \delta_2 F = \epsilon_2 \partial B \tag{2}$$

This then implies that the two internal SUSY transformations lead us to a spacetime translation:

$$\{\delta_1, \delta_2\} B = a^\mu \partial_\mu B \ ; \quad a^\mu = (\bar{\epsilon}_2 \gamma^\mu \epsilon_1) \tag{3}$$

Presence of a spacetime derivative of B on right hand side (RHS) of above equation suggests that the Susy is an extension of the Poincare spacetime symmetry:

$$\{Q_a, \bar{Q}_b\} = 2(\gamma^\mu)_{ab} P_\mu \tag{4}$$

Supercharge Q_a ($a = 1, 2, 3, 4$ in 4D) is the generator of SUSY transformations. It is related to the generator of spacetime translations P_μ and therefore is not an internal symmetry generator. The SUSY transformation is an extention of the Poincare spacetime symmetry. Supercharge Q_a is a spinor. It is fermionic and anti-commuting. Poincare algebra (PA) after including the supersymmetry becomes the SPA.

2. The Wess-Zumino Model

The WZM is defined (on-shell) by the Lagrangian density [5]:

$$\begin{aligned}\mathcal{L} :=\Big[&\frac{1}{2}(\partial_\mu A)\partial^\mu A - \frac{1}{2}m^2A^2 + \frac{1}{2}(\partial_\mu B)\partial^\mu B \\ &- \frac{1}{2}m^2B^2 - mgA(A^2+B^2) \\ &+ \bar\psi(i\gamma^\nu\partial_\nu - m)\psi - g\ (\bar\psi\psi\ A + i\bar\psi\gamma^5\psi B) \\ &- \frac{1}{2}g^2(A^2+B^2)^2\Big] \end{aligned} \tag{5}$$

Here A is a scalar field, B is a pseudoscalar field, ψ is a spin-1/2 Majorana field ($\psi = \psi^C = C\bar\psi^T$). C is the charge conjugation matrix and $A = A^\dagger$ and $B = B^\dagger$. All the fields here have the same mass m and they couple with the same strength g. This is in contrast to the non-SUSY FT's.

This is due to the fact that states of a particular representation of the super Poincare algebra (SPA) are characterized by the eigenvalue m^2 of P^2 ($= P_\mu P^\mu$) and different values of spin s. Actually, all the fields belong to the same mass multiplet in SPA.

Pauli-Ljubanski polarization vector is defined as:

$$W_\mu := \frac{1}{2}\epsilon_{\mu\nu\rho\sigma}P^\nu M^{\rho\sigma} \tag{6}$$

Here

$$\begin{aligned} P^2 &= P_\mu P^\mu \\ W^2 &= W_\mu W^\mu \end{aligned} \tag{7}$$

are Casimir operators of PA that satisfy:

$$\begin{aligned} \big[P^2, M_{\mu\nu}\big] &= 0 \\ \big[P^2, P_\mu\big] &= 0 \\ \big[W^2, M_{\mu\nu}\big] &= 0 \\ \big[W^2, P_\mu\big] &= 0 \end{aligned} \tag{8}$$

We further have:

$$\begin{aligned} P^2 &= m^2 > 0 \\ W^2 &= -m^2 s(s+1). \end{aligned} \tag{9}$$

Where, m^2 and $(-m^2 s(s+1))$ are the eigenvalues of P^2 and W^2. Here s denotes the spin of the representation which assumes discrete values: $s = 0, 1/2, 1, 3/2, \ldots$

This representation is specified in terms of the mass m and spin s. Physically a state in a representation (m, s) corresponds to a particle of rest mass m and spin s. Also, since the spin projection S_3 can take any value from $-s$ to $+s$, (massive particles fall into $(2s+1)$-dimensional multiplets).

In WZM, all the fields namely, A, B, ψ, $\bar\psi$ have the same mass m and they couple with the same strength g (in the unbroken SUSY) – in contrast to the non-supersymmetric field theories. States of a particular representation of SPA are characterized by the eigenvalue m^2 of Casimir operator P^2 and different values of spin s. W^μ is proportional to P^μ (generator of the Poincare group):

$$W^\mu = \lambda P^\mu \tag{10}$$

and

$$W_0 = \lambda P_0 = \overrightarrow{P}\cdot\overrightarrow{J} \tag{11}$$

where

$$P^\mu = (P_0\ , \overrightarrow{P}). \tag{12}$$

The constant of proportionality λ in $W_\mu = \lambda P_\mu$ is called Helicity and it is defined by:

$$\lambda := \frac{\overrightarrow{P}\cdot\overrightarrow{J}}{P_0} \tag{13}$$

for massless particles with $\lambda := \pm s$ where $s = 0, 1/2, 1, \ldots$ is the spin of representation. $N = 1$ is called as the Minimal Supersymmetry and $N > 1$ is called the Extended Supersymmetry.

For simplicity we set ($g = 0$) yielding the Lagrangian density of the free WZM [5]:

$$\begin{aligned}\mathcal{L} :=\Big[&\frac{1}{2}\partial_\mu A\partial^\mu A - \frac{1}{2}m^2A^2 + \frac{1}{2}\partial_\mu B\partial^\mu B \\ &- \frac{1}{2}m^2B^2 + \bar\psi(i\gamma^\nu\partial_\nu - m)\psi\Big] \end{aligned} \tag{14}$$

Theory is seen to be invariant (up to a total derivative) under the rigid SUSY transformation [5]:

$$\begin{aligned} \delta A &= \bar\epsilon\ \psi \\ \delta B &= -i\ \bar\epsilon\ \gamma^5\ \psi \\ \delta\psi &= -\ (i\gamma^\nu\partial_\nu + m)\ (A - i\gamma^5\ B)\ \epsilon \\ \delta\bar\psi &= \ \bar\epsilon\ (A - i\gamma^5\ B)\ (i\gamma^\nu\overleftarrow{\partial}_\nu - m) \end{aligned} \tag{15}$$

Here ϵ is a constant Grasmann variable (which does not depend on spacetime $x \equiv x^\mu$) implying a global or rigid SUSY transformations. However, $\delta\psi$ and $\delta\bar\psi$ here, are seen to depend on spacetime derivatives of A and B. This implies that this is an extention of Poincare spacetime symmetry (different than an internal symmetry).

Supercurrent j^μ of the theory could be easily calculated to be [5]:

$$\begin{aligned} j^\mu &= \Big[\frac{i}{2}\bar\epsilon(A - i\gamma^5\ B)\ (i\gamma^\nu\overleftarrow{\partial}_\nu - m)\gamma^\mu\ \psi\Big] \\ &\equiv \Big[\frac{1}{\beta}\ \bar\epsilon\ k^\mu\Big] \end{aligned} \tag{16}$$

Here β is a real constant which could be suitably choosen. The spinor charges Q_a are defined by [5]:

$$Q_a := \int d^3x\ k^0_a$$
$$k^0_a = \frac{i}{2}\beta\Big[\{(A - i\gamma^5\ B)(i\gamma^\nu \overleftarrow{\partial}_\nu - m)\}\gamma^0\psi\Big]_a \quad (17)$$

Here k^0_a are the spinor charge densities with $a = 1, 2, 3, 4$. Spinor charges and spinor charge densities being fermionic satisfy SPA and the spinor charges are seen to satisfy the anti-commutation relation (ACR) [5]:

$$\{Q_a, \bar{Q}_b\} = 2P_\mu(\gamma^\mu)_{ab} \quad (18)$$

This explicitly shows that the WZM obeys the SPA and it is a supersymmetric FT having a rigid or global SUSY. Also, the supersymmetry of the theory is a non-manifest supersymmetry.

We now set $m = 0$ for making the fields to be massless, so that the free massless WZM is defined by the Lagrangian density:

$$\mathcal{L} := \Big[\frac{1}{2}\partial_\mu A\partial^\mu A + \frac{1}{2}\partial_\mu B\partial^\mu B + \bar{\psi}(i\gamma^\nu\partial_\nu)\psi\Big] \quad (19)$$

This is the simplest example of a supersymmetric FT in 4D with a non-manifest supersymmetry.

We obtain the free WZM by setting $g = 0$ and it is seen to be invariant, up to a total derivative, under the rigid SUSY transformations [5]:

$$\begin{aligned}
\delta A &= \bar{\epsilon}\ \psi \\
\delta B &= -i\ \bar{\epsilon}\ \gamma^5\ \psi \\
\delta\psi &= -\ (i\gamma^\nu\partial_\nu)\ (A - i\gamma^5\ B)\ \epsilon \\
\delta\bar{\psi} &= \bar{\epsilon}\ (A - i\gamma^5\ B)\ (i\gamma^\nu \overleftarrow{\partial}_\nu)
\end{aligned} \quad (20)$$

Here ϵ is a constant Grasmann variable (which does not depend on spacetime $x \equiv x^\mu$). Here, $\delta\psi$ and $\delta\bar{\psi}$ are seen to depend on spacetime derivatives of A and B which implies that this is an extention or generalization of the Poincare spacetime symmetry. $(\epsilon, \bar{\epsilon})$ being constant, implies that the symmetry is a rigid or global Susy.

It is also possible to consider it as a theory of a single complex scalar field and a fermionic field by combining the fields A and B as follows:

$$\begin{aligned}
\phi(x) &:= (A + iB)/2 \\
\phi^\star(x) &= (A - iB)/2
\end{aligned} \quad (21)$$

implying therefore: $\delta\phi = \bar{\epsilon}\bar{\psi}$ and $\delta\phi^\star = \epsilon\psi$ and

$$\begin{aligned}
\delta\psi_A &= 2i(\sigma^\mu\bar{\epsilon})_A\partial_\mu\phi^\star(x) \\
\delta\bar{\psi}^{\dot{A}} &= -2i(\bar{\sigma}^\mu\epsilon)^{\dot{A}}\partial_\mu\phi(x)
\end{aligned} \quad (22)$$

Since A is a scalar field and B is a pseudoscalar field, the complex combination $\phi(x)$ transforms under the parity transformation like complex conjugation. Here, ψ and $\bar{\psi}$ are not independent fields as they are the Majorana spinor fields in the Weyl formulation. Hence the transformations of $\delta\psi$ and $\delta\bar{\psi}$ are not independent and one could be obtained from the other. Supercurrent j^μ of the theory is obtained as:

$$j^\mu = \Big[\frac{i}{2}\bar{\epsilon}(A - i\gamma^5\ B)\ (i\gamma^\nu \overleftarrow{\partial}_\nu)\gamma^\mu\ \psi\Big] \equiv \Big[\frac{1}{\beta}\ \bar{\epsilon}\ k^\mu\Big] \quad (23)$$

Here β is a real constant. Spinor charge Q_a are:

$$Q_a := \int d^3x\ k^0_a$$
$$k^0_a = \frac{i}{2}\beta\Big[\{(A - i\gamma^5\ B)\ (i\gamma^\nu \overleftarrow{\partial}_\nu)\}\gamma^0\ \psi\Big]_a \quad (24)$$

Here k^0_a are the spinor charge densities with $a = 1, 2, 3, 4$. WZM being a supersymmetric FT, spinor charges and the spinor charge densities are seen to satisfy SPA and the spinor charges satisfy the ACR:

$$\{Q_a, \bar{Q}_b\} = 2P_\mu(\gamma^\mu)_{ab} \quad (25)$$

This implies that the WZM obeys SPA and it is a supersymmetric FT with a rigid Susy. SPA reads [5]:

$$[P_\mu, P_\nu] = 0 \quad (26)$$

$$[M_{\mu\nu}, P_\rho] = -i\ (\eta_{\mu\rho}\ P_\nu - \eta_{\nu\rho}\ P_\mu) \quad (27)$$

$$\begin{aligned}
[M_{\mu\nu}, M_{\rho\sigma}] = &-i(\eta_{\mu\rho}M_{\nu\sigma} + \eta_{\nu\sigma}M_{\mu\rho}) \\
&+ i\ (\eta_{\mu\sigma}M_{\nu\rho} + \eta_{\nu\rho}M_{\mu\sigma})
\end{aligned} \quad (28)$$

$$[P_\mu, Q_a] = 0 \quad (29)$$

$$[M_{\mu\nu}, Q_a] = -(\sigma^4_{\mu\nu})_{ab}\ Q_b \quad (30)$$

$$\begin{aligned}
\sigma^4_{\mu\nu} &:= \frac{i}{4}[\gamma_\mu, \gamma_\nu] \\
\{Q_a, \bar{Q}_b\} &= 2(\gamma^\mu)_{ab}\ P_\mu \\
\{Q_a, Q_b\} &= -2\ (\gamma^\mu\ C)_{ab}\ P_\mu \\
\{\bar{Q}_a, \bar{Q}_b\} &= 2\ (C^{-1}\gamma^\mu)_{ab}\ P_\mu
\end{aligned} \quad (31)$$

SPA has 14 generators: 4 generators of Lorentz translations P_μ , 6 generators of Poincare transformations $M_{\mu\nu}$ and 4 spinor charges Q_a (the Majorana spinors). Here the indices a and b run from 1 to 4 in 4D.

3. Free massless WZM

We now set $m = 0$ for making the fields to be massless, so that the free massless WZM is defined by the Lagrangian density:

$$\mathcal{L} := \Big[\frac{1}{2}\partial_\mu A\partial^\mu A + \frac{1}{2}\partial_\mu B\partial^\mu B + \bar{\psi}(i\gamma^\nu\partial_\nu)\psi\Big] \quad (32)$$

We break up the Lagrangian density of the free massless WZM into bosonic and fermionic parts:

$$\begin{aligned}\mathcal{L} &= \mathcal{L}_B + \mathcal{L}_F \\ \mathcal{L}_B &= \frac{1}{2}\partial_\mu A \partial^\mu A + \frac{1}{2}\partial_\mu B \partial^\mu B \\ \mathcal{L}_F &= \bar{\psi}(i\gamma^\nu \partial_\nu)\psi \end{aligned} \tag{33}$$

Further, $\mathcal{L}_F$ $(= \mathcal{L}^F)$ could be written in two different looking but conceptually equivalent forms (which differ by a total derivative (t.d.)) as follows:

$$\begin{aligned}\mathcal{L}_1^F &= i\bar{\psi}\gamma^\mu \partial_\mu \psi \\ \mathcal{L}_2^F &= \frac{i}{2}\Big[\bar{\psi}\gamma^\mu(\partial_\mu\psi) - (\partial_\mu\bar{\psi})\gamma^\mu\psi\Big] \end{aligned} \tag{34}$$

$$\begin{aligned}\mathcal{L}_1^F - \mathcal{L}_2^F &= \frac{i}{2}\partial_\mu(\bar{\psi}\gamma^\mu\psi) = \frac{i}{2}\partial_\mu j^\mu \\ j^\mu &= (\bar{\psi}\gamma^\mu\psi) \end{aligned} \tag{35}$$

Theory described by $\mathcal{L}_1^F$ is seen to possess a set of two second class constraints:

$$\begin{aligned}\rho_1 &= (\pi + i\bar{\psi}\gamma^0) \approx 0 \\ \rho_2 &= \bar{\pi} \approx 0 \end{aligned} \tag{36}$$

Here, Fermi fields ψ and $\bar{\psi}$ are to be treated as independent fields. Theory described by $\mathcal{L}_2^F$ is also seen to possess a set of two second class constraints:

$$\begin{aligned}\chi_1 &= (\pi + \frac{i}{2}\bar{\psi}\gamma^0) \approx 0 \\ \chi_2 &= (\bar{\pi} + \frac{i}{2}\gamma^0\psi) \approx 0. \end{aligned} \tag{37}$$

The Fermi fields ψ and $\bar{\psi}$ in this later case are not independent fields. This is consistent with the definition of Majorana spinor fields (we remind ourselves here that in WZM, the fermionic fields are Majorana spinor fields).

We now study the Hamiltonian formulation of the theory [7]. The canonical momenta following from the Lagerangian density of WZM defined by $\mathcal{L} := (\mathcal{L}_B + \mathcal{L}_F)$ with $\mathcal{L}_F = \mathcal{L}_2^F$ (working with the signature $\eta_{\mu\nu} := \text{diag}(+1, -1, -1, -1)$) are:

$$\begin{aligned}\Pi_A &:= \frac{\partial\mathcal{L}}{\partial(\partial_0 A)} = \partial_0 A \\ \Pi_B &:= \frac{\partial\mathcal{L}}{\partial(\partial_0 B)} = \partial_0 B \end{aligned} \tag{38}$$

$$\begin{aligned}\pi &:= \frac{\partial\mathcal{L}}{\partial(\partial_0\psi)} = -\frac{i}{2}\bar{\psi}\gamma^0 \\ \bar{\pi} &:= \frac{\partial\mathcal{L}}{\partial(\partial_0\bar{\psi})} = -\frac{i}{2}\gamma^0\psi \end{aligned} \tag{39}$$

Theory thus has 2 primary constraints (PC's):

$$\begin{aligned}\chi_1 &= (\pi + \frac{i}{2}\bar{\psi}\gamma^0) \approx 0 \\ \chi_2 &= (\bar{\pi} + \frac{i}{2}\gamma^0\psi) \approx 0 \end{aligned} \tag{40}$$

In principle, χ_1, χ_2 represent an infinite number of PC's which could be labeled say by α, β (which run from one to infinity). We however, ignore these further labelings in our considerations. The canonical Hamiltonian density of the theory is obtained as:

$$\begin{aligned}\mathcal{H}_c =& (\partial_0 A)\ \Pi_A + (\partial_0 B)\ \Pi_B + (\partial_0\psi_\alpha)\ \pi_\alpha \\ &+ (\partial_0\bar{\psi}_\alpha)\ \bar{\pi}_\alpha - \mathcal{L}_B - \mathcal{L}_F \end{aligned} \tag{41}$$

$$\mathcal{H}_c = \frac{1}{2}\Big[\Pi_A^2 + \Pi_B^2 - i\bar{\psi}\gamma_k\partial^k\psi + i(\partial^k\bar{\psi})\gamma_k\psi\Big] \tag{42}$$

The total Hamiltonian density is:

$$\mathcal{H}_T := \mathcal{H}_c + \chi_1\ u + \chi_2\ v \tag{43}$$

Demanding that the constraints χ_1 and χ_2 are preserved in the course of time one does not get any secondary constraints and therefore these are the only 2 constraints that the theory possesses. Non-vanishing matrix elements of the 2×2 matrix of the PB's of these above constraints among themselves are:

$$R_{12} = -R_{21} = i\gamma^0\delta(x^1 - y^1)\delta(x^2 - y^2)\delta(x^3 - y^3). \tag{44}$$

The non-vanishing equal-time (ET) commutation relations (CR's) (denoted by a square bracket) and ET anti-commutation relations (ACR's) (denoted by a curly bracket) of the bosonic and ferminic variables of the theory are found to be:

$$[A(x,t), \Pi_A(y,t)] = i\ \delta(x-y) \tag{45}$$

$$[B(x,t), \Pi_B(y,t)] = i\ \delta(x-y) \tag{46}$$

$$\{\psi_\alpha(x,t), \bar{\psi}_\beta(y,t)\} = \gamma^0\delta_{\alpha\beta}\ \delta(x-y) \tag{47}$$

$$\delta(x-y) := \delta(x^1 - y^1)\delta(x^2 - y^2)\delta(x^3 - y^3) \tag{48}$$

These relations appear to be similar to the usual ones. However, the fermionic spinor field ψ here is not a Dirac spinor but it is a Majorana spinor having real components: $(\psi = \psi^C)$. We need to remember here that the Dirac spinor is a 4-component spinor which has complex elements and it could be expressed in terms of two, 2-component Weyl spinors having complex elements. However, if the elements of these Weyl spinors are taken as real $(\psi = \psi^C)$ then it becomes a Majorana spinor (having real elements).

In path integral quantization (PIQ) [7], transition to quantum theory is made by writing the vacuum to vacuum transition amplitude for the theory, called the generating functional $Z[J_k]$ of the theory which in the presence of the external sources J_k for the present theory is [7]:

$$\begin{aligned}Z[J_k] = \int [d\mu] \exp\Big[i \int dxdy[&J_k\Phi^k + \Pi_A\partial_0 A \\ &+ \Pi_B\partial_0 B + \pi\partial_0\psi + \bar{\pi}\partial_0\bar{\psi} \\ &+ \Pi_u\partial_0 u + \Pi_v\partial_0 v - \mathcal{H}_T]\Big] \end{aligned} \tag{49}$$

Here $\Phi^k \equiv (A, B, \psi, \bar{\psi}, u, v)$ are the phase space variables of the theory with the corresponding respective canonical conjugate momenta: $\Pi_k \equiv (\Pi_A, \Pi_B, \pi, \bar{\pi}, \Pi_u, \Pi_v)$. The functional measure $[d\mu]$ of the theory (with the above generating functional $Z[J_k]$) is:

$$\begin{aligned}[d\mu] = \Big[& [\delta(x^1 - y^1)\delta(x^2 - y^2)\delta(x^3 - y^3)][dA] \\ & [dB][d\psi][d\bar{\psi}][du][dv][d\Pi_A] \\ & [d\Pi_B][d\pi][d\bar{\pi}][d\Pi_u][d\Pi_v] \\ & \delta[(\pi + \frac{i}{2}\bar{\psi}\gamma^0) \approx 0] \\ & \delta[(\bar{\pi} + \frac{i}{2}\gamma^0\psi) \approx 0]\Big] \end{aligned} \tag{50}$$

4. Conclusions and summary

Some important remarks may be helpful. In relativistic quantum mechanics, the Dirac equation (DE) is a single particle relativistic wave equation where ψ represents a wave function. In FT, DE is an Euler-Lagrange field equation which is obtained from the Dirac action or the Dirac Lagrangian by using the variational principle.

WZM is the simplest example of a supersymmetric field theory in 4D. This is also an example of a FT with non-manifest supersymmetry. Taking the example of free massless WZM, one could study many important theories in different dimensions including in higher dimsimensions. The theory also provides a basic framework for the study of Ramond Nievue Schwarz (RNS) superstring theory (SST) which is an example of a SST with non-manifest SUSY. Starting with the WZM, it is possible to construct a supergravity theory by gauging its global (rigid) SUSY into a local SUSY through the Noether's procedure.

Just to summarize in brief, we have studied in this work, the WZM [5], which is a supersymmetric FT that has rigid or global supersymmetry. The theory has a supercharge Q_a ($a = 1, 2, 3, 4$ in 4D) which is a Grassmann spinor having anti-commuting properties. Theory is invariant under rigid supersymmetry transformations where the transformation parameter is a constant Grassmann spinor [5]. Finally, we have also studied the Hamiltonian and path integral quantization of the theory [7].

Acknowledgements

It is matter of great pleasure to thank the organizers of the International Conference on Analytic and Algebraic Methods in Physics XVIII (AAMP XVIII) – 2021 at Prague, Czechia, Prof. Vít Jakubský, Prof. Vladimir Lotoreichik, Prof. Matej Tusek, Prof. Miloslav Znojil and the entire team for a wonderful orgnization of the conference.

References

[1] J. Wess, B. Zumino. Supergauge transformations in four dimensions. *Nuclear Physics B* **70**(1):39–50, 1974. https://doi.org/10.1016/0550-3213(74)90355-1.

[2] S. Deser, B. Zumino. Consistent supergravity. *Physics Letters B* **62**(3):335–337, 1976. https://doi.org/10.1016/0370-2693(76)90089-7.

[3] D. Z. Freedman, P. van Nieuwenhuizen, S. Ferrara. Progress toward a theory of supergravity. *Physical Review D* **13**:3214–3218, 1976. https://doi.org/10.1103/PhysRevD.13.3214.

[4] P. van Nieuwenhuizen. Supergravity. *Physics Reports* **68**(4):189–398, 1981. https://doi.org/10.1016/0370-1573(81)90157-5.

[5] H. J. W. Müller-Kirsten, A. Wiedemann. *Introduction to Supersymmetry.* World Scientific, Singapore, 2nd edn., 2010. https://doi.org/10.1142/7594.

[6] J. Wess, J. Bagger. *Supersymmetry and Supergravity.* Princeton University Press, 1992. ISBN 9780691025308.

[7] H. J. W. Müller-Kirsten. *Introduction to Quantum Mechanics: Schrödinger Equation and Path Integral.* World Scientific, Singapore, 2006. ISBN 9789812566911.

[8] K. Becker, M. Becker, J. H. Schwarz. *String Theory and M-Theory: A Modern Introduction.* Cambridge University Press, 2007. ISBN 9780521860697.

[9] S. J. Brodsky. Supersymmetric and conformal features of hadron physics. *Universe* **4**(11):120, 2018. https://doi.org/10.3390/universe4110120.

[10] S. J. Brodsky, G. F. de Teramond, H. G. Dosch. Light-front holography and supersymmetric conformal algebra: A novel approach to hadron spectroscopy, structure, and dynamics, 2020. arXiv:2004.07756.

[11] S. J. Brodsky. Color confinement and supersymmetric properties of hadron physics from light-front holography. *Journal of Physics: Conference Series* **1137**:012027, 2019. https://doi.org/10.1088/1742-6596/1137/1/012027.

MAXWELL-CHERN-SIMONS-HIGGS THEORY

USHA KULSHRESHTHA[a,*], DAYA SHANKAR KULSHRESHTHA[b], BHEEMRAJ SIHAG[b]

[a] *University of Delhi, Kirori Mal College, Department of Physics, Delhi-110007, India*

[b] *University of Delhi, Department of Physics and Astrophysics, Delhi-110007, India*

[*] corresponding author: ushakulsh@gmail.com

ABSTRACT.

We consider the three dimensional electrodynamics described by a complex scalar field coupled with the U(1) gauge field in the presence of a Maxwell term, a Chern-Simons term and the Higgs potential. The Chern-Simons term provides a velocity dependent gauge potential and the presence of the Maxwell term makes the U(1) gauge field dynamical. We study the Hamiltonian formulation of this Maxwell-Chern-Simons-Higgs theory under the appropriate gauge fixing conditions.

KEYWORDS: Electrodynamics, Higgs theories, Chern-Simons-Higgs theories, Hamiltonian formulations, gauge-theories.

1. INTRODUCTION

We study the Hamiltonian formulation [1] of the three dimensional (3D) electrodynamics [2–22], involving a Maxwell term [20], a Chern-Simons (CS) term [19, 21, 22], and a term that describes a coupling of the U(1) gauge field with a complex scalar field in the presence of a Higgs potential [22]. Such theories in two-space one-time dimension ((2+1)D) can describe particles that satisfy fractional statistics and are referred to as the reletivistic field theoretic models of anyons and of the anyonic superconductivity [21, 22].

A remarkable property of the CS action [21, 22], is that it depends only on the antisymmetric tensor $\epsilon^{\mu\nu\lambda}$ and not on the metric tensor $g^{\mu\nu}$. As a result, the CS action in the flat spacetime and in the curved spacetime remains the same [21, 22]. Hence CS action, in both the Abelian and in the non-Abelian cases represents an example of a topological field theory [21, 22].

The systems in two-space, one-time dimensions (2+1)D (i.e., the planar systems, display a variety of peculiar quantum mechanical phenomena ranging from the massive gauge fields to soluble gravity [19–22]. These are linked to the peculiar structure of the rotation group and the Lorentz and Poincare groups in (2+1)D. The 3D electrodynamics models with a Higgs potential, namely, the Abelian Higgs models involving the vector guage field A^μ with and without the topological CS term in (2+1)D have been of a wide interest [19–22].

When these models are considered without a CS term but only with a Maxwell term accounting for the kinetic energy of the vector gauge field and they represent field-theoretical models which could be considered as effective theories of the Ginsburg-Landau-type [22] for superconductivity. These models in (2+1)D or in (3+1)D are known as the Nielsen-Olesen (vortex) models (NOM) [20]. These models are the relativistic generalizations of the well-known Ginsburg-Landau phenomenological field theory models of superconductivity [2, 20, 22].

The effective theories with excitations, with fractional statistics are supposed to be described by gauge theories with CS terms in (2+1)D and a study of these gauge field theories and the models of quantum electrodynamics involving the CS term represent a broad important area of investigation [21, 22].

The CS term provides a velocity dependent gauge potential [21, 22], and the presence of the Maxwell term in the action makes the gauge field dynamical [20]. We study the Hamiltonian formulation [1] of this Maxwell-Chern-Simons-Higgs theory under the appropriate gauge fixing conditions [20, 22].

The quantization of field theory models with constraints has always been a challenging problem [1]. Infact, any complete physical theory is a quantum theory and the only way of defining a quantum theory is to start with a classical theory and then to quantize it [1]. Theory presently under consideration is also a constrained system. In the present work, we quantize this theory using the Dirac's Hamiltonian formulation [1] in the usual instant-form (IF) of dynamics (on the hyperplanes defined by: $x^0 = t =$ constant) under appropriate gauge-fixing conditions (GFC's) [1, 19–22].

2. HAMILTONIAN FORMULATION

The Maxwell Chern-Simons Higgs Theory in two space one time is defined by the following action:

$$S = \int \mathcal{L}(\Phi, \Phi^*, A^\mu)\, d^3x, \tag{1}$$

where the Lagrangian density $\mathcal{L}$ (with $\kappa = \frac{\theta}{2\pi^2}$; θ being the CS parameter) is given by:

$$\mathcal{L} = \Big[-\frac{1}{4}F_{\mu\nu}F^{\mu\nu} + (\widetilde{D}_\mu\Phi^*)(D^\mu\Phi) - V(|\Phi|^2) + \frac{\kappa}{2}\epsilon^{\mu\nu\lambda}A_\mu\partial_\nu A_\lambda\Big] \quad (2)$$

$$V(|\Phi|)^2 = \gamma + \beta|\Phi|^2 + \alpha|\Phi|^4 = \lambda(|\Phi|^2 - \Phi_0^2)^2 \ ; \ \ (\Phi_0 \neq 0). \quad (3)$$

Where the covariant derivative is defined by:

$$\begin{aligned} D_\mu &= (\partial_\mu + i\ eA_\mu) \\ \widetilde{D}_\mu &= (\partial_\mu - i\ eA_\mu) \\ g_{\mu\nu} &= diag(+1,-1,-1) \\ \epsilon^{012} &= \epsilon_{012} = +1 \\ \mu,\nu &= 0,1,2. \end{aligned} \quad (4)$$

In the above Lagrangian density the first term is the kinetic energy term of the U(1) gauge field and second term represents the coupling of U(1) gauge field with the complex scalar field as well as kinetic energy for the complex scalar field. Third term describes Higgs potential and the last term is the CS term.

The model without the CS term describes an Abelian Higgs model and is defined by the Lagrangian density $\mathcal{L} = \mathcal{L}\big(\Phi, \Phi^*, A_\mu\big)$ where $\mathcal{L}$ is a function of a complex scalar field and an Abelian gauge vector field $A_\mu(x)$ defined by the above Lagrangian density. In (2+1)D this theory is called as the Nielsen Olsen (vortex) model (NOM). These models possesses stable, time independent (i.e., static), classical solutions (which could be called 2D solitons). In fact, the model admits the so-called topological solitons of the vortex type [4].

Further, in this model, if we choose the parameters of the Higgs potential to be such that the scalar and vector masses become equal i.e., if we set the Higgs boson and the vector boson (photon) masses to be equal i.e., if we set: $m_{Higgs} = m_{Photon} = e\Phi_0$ then that implies:

$$V(|\Phi|)^2 = \frac{1}{2}e^2(|\Phi|^2 - \Phi_0^2)^2. \quad (5)$$

The above model then reduces to the so-called Bogomol'nyi model which describes a system on the boundary between type-I and type-II superconductivity [4].

In component form, the above Lagrangian density can be written as:

$$\begin{aligned} \mathcal{L} = {} & \left(\frac{\kappa}{2}\right)\Big[A_0F_{12} + A_1(\partial_2A_0) - A_2(\partial_1A_0)\Big] \\ & + \left(\frac{\kappa}{2}\right)\Big[A_2(\partial_0A_1) - A_1(\partial_0A_2)\Big] - \frac{1}{2}F_{12}^2 \\ & + \Big[\frac{1}{2}(\partial_1A_0 - \partial_0A_1) + \frac{1}{2}(\partial_0A_2 - \partial_2A_0)\Big] \\ & + \Big[\ (\partial_0\Phi^*)(\partial_0\Phi) + i\ e(\partial_0\Phi^*)A_0\Phi \\ & - i\ e(\partial_0\Phi)A_0\Phi^* + e^2A_0^2\Phi^*\Phi\Big] \\ & + \Big[\ -(\partial_1\Phi^*)(\partial_1\Phi) - i\ e(\partial_1\Phi^*)A_1\Phi \\ & + i\ e(\partial_1\Phi)A_1\Phi^* - e^2A_1^2\Phi^*\Phi\Big] \\ & + \Big[\ -(\partial_2\Phi^*)(\partial_2\Phi) - i\ e(\partial_2\Phi^*)A_2\Phi \\ & + i\ e(\partial_2\Phi)A_2\Phi^* - e^2A_2^2\Phi^*\Phi\Big] \\ & - \ V(|\Phi|^2). \end{aligned} \quad (6)$$

Canonical momenta obtained from the above Lagrangian density are:

$$\begin{aligned} \Pi &= \frac{\partial\mathcal{L}}{\partial(\partial_0\Phi)} = (\partial_0\Phi^* - i\ eA_0\Phi^*) \\ \Pi^* &= \frac{\partial\mathcal{L}}{\partial(\partial_0\Phi^*)} = (\partial_0\Phi + i\ eA_0\Phi) \\ \Pi^0 &= \frac{\partial\mathcal{L}}{\partial(\partial_0A_0)} = 0 \end{aligned} \quad (7)$$

$$\begin{aligned} E_1(:=\Pi^1) &:= \frac{\partial\mathcal{L}}{\partial(\partial_0A_1)} \\ &= -(\partial_1A_0 - \partial_0A_1) + \frac{\kappa}{2}A_2 \\ E_2(:=\Pi^2) &= \frac{\partial\mathcal{L}}{\partial(\partial_0A_2)} \\ &= (\partial_0A_2 - \partial_2A_0) - \frac{\kappa}{2}A_1. \end{aligned} \quad (8)$$

Here $\Pi, \Pi^*, \Pi^0, E_1, E_2$ are the momenta canonically conjugate respectively to $\Phi, \Phi^*, A_0, A_1, A_2$. The theory is thus seen to possess only one primary constraint (PC):

$$\chi_1 = \Pi^0 \approx 0. \quad (9)$$

The canonical Hamiltonian density of the theory is obtained using the Legendre transformation from the Lagrangian density of the theory in the usual manner. Every term in the Lagrangian density (including the CS term) is equally important. The calculational details are omitted here for the sake of brevity. The total Hamiltonian density of the theory is then obtained from the canonical Hamiltonian density by including

in it the primary constraint of the theory with the help of the Lagrange multiplier field $u \equiv u(x^\mu)$ (which is dynamical) as follows:

$$\begin{aligned}\mathcal{H}_T &= \Pi^0 u + \Pi\,\Pi^* - ieA_0(\Pi\Phi - \Pi^*\Phi^*) \\ &+ \frac{1}{2}({E_1}^2 + {E_2}^2) \\ &+ \frac{1}{2}F_{12}^2 + \big[E_1(\partial_1 A_0) + E_2(\partial_2 A_0)\big] \\ &+ \frac{1}{2}\left(\frac{\kappa}{2}\right)^2({A_1}^2 + {A_2}^2) \\ &- \left(\frac{\kappa}{2}\right)\big[A_2E_1 - A_1E_2 + A_0F_{12}\big] \\ &+ \Big[\ (\partial_1\Phi^*)(\partial_1\Phi) + i\ e(\partial_1\Phi^*)A_1\Phi \\ &- i\ e(\partial_1\Phi)A_1\Phi^* + e^2A_1^2\Phi^*\Phi\Big] \\ &+ \Big[\ (\partial_2\Phi^*)(\partial_2\Phi) + i\ e(\partial_2\Phi^*)A_2\Phi \\ &- i\ e(\partial_2\Phi)A_2\Phi^* + e^2A_2^2\Phi^*\Phi\Big], \end{aligned} \tag{10}$$

where

$$H_T = \int \mathcal{H}_T d^2x, \tag{11}$$

with the total Hamiltonian density given by:

$$\mathcal{H}_T = \big[\mathcal{H}_c + \ \Pi^0 u\big]. \tag{12}$$

.

It is to be noted here that in the construction of the canonical Hamiltonian density of the theory, all the fields of the theory play an equally important role through the Legendre transformation and through the Lagrangian density of the theory that defines the theory. Also, it is worth mentioning here that the Hamilton's equations of motion of the theory (that are omitted here for the sake of brevity) obtained from the total Hamiltonian density of the theory preserve the constraints of the theory for all time. After preserving the Primary constraint χ_1 in the course of time, one obtains a secondary constraint

$$\begin{aligned}\chi_2 = \Big[&ie(\Pi\Phi - \Pi^*\Phi^*) + (\partial_1 E_1 + \partial_2 E_2) \\ &+ \frac{\kappa}{2}(\partial_1 A_2 - \partial_2 A_1)\Big] \approx 0. \end{aligned} \tag{13}$$

The matrix of Poisson Brackets (PB's) among the constraints χ_i is a null matrix and thereby theory is a gauge invariant theory and is invariant under the following local vector gauge transformations:

$$\begin{aligned}&\delta\Phi = i\beta\Phi, \quad \delta\Phi^* = -i\beta\Phi^*, \quad \delta\Pi^0 = 0 \\ &\delta A_0 = -\partial_0\beta\ ; \quad \delta A_1 = -\partial_1\beta\ ; \quad \delta A_2 = -\partial_2\beta \\ &\delta\Pi = -i\beta(\partial_0\Phi^*) - e\beta A_0\Phi^* + i(e-1)(\partial_0\beta)\Phi^* \\ &\delta\Pi^* = i\beta(\partial_0\Phi) - e\beta A_0\Phi - i(e-1)(\partial_0\beta)\Phi \\ &\delta E_1 = \frac{-\kappa}{2}\partial_2\beta;\ \delta E_2 = \frac{\kappa}{2}\partial_1\beta;\ \delta u = -\partial_0\partial_0\beta. \end{aligned} \tag{14}$$

Here, β is the gauge parameter $\beta \equiv \beta(x^\mu)$ and the vector gauge current satisfies: $\partial_\mu J^\mu = 0$. The components of J^μ are:

$$\begin{aligned}J^0 = J_0 = &(i\beta\Phi)\big[\partial_0\Phi^* - i\ eA_0\Phi^*\big] \\ &- (i\beta\Phi^*)\big[\partial_0\Phi + i\ eA_0\Phi\big] \\ &- (\partial_1\beta)\ F_{01} - (\partial_2\beta)\ F_{02} \\ &- \frac{\kappa}{2}\big[(\partial_1\beta)A_2 - (\partial_2\beta)A_1\ \big] \end{aligned}$$

$$\begin{aligned}J^1 = -J_1 = &(i\beta\Phi)\big[\ -\partial_1\Phi^* + i\ eA_1\Phi^*\big] \\ &- (i\beta\Phi^*)\big[\ -\partial_1\Phi - i\ eA_1\Phi\big] \\ &- (\partial_0\beta)\ F_{10} - (\partial_2\beta)\ F_{21} \\ &+ \frac{\kappa}{2}\big[(\partial_0\beta)A_2 - (\partial_2\beta)A_0\ \big] \end{aligned}$$

$$\begin{aligned}J^2 = -J_2 = &(i\beta\Phi)\big[\ -\partial_2\Phi^* + i\ eA_2\Phi^*\big] \\ &- (i\beta\Phi^*)\big[\ -\partial_2\Phi - i\ eA_2\Phi\big] \\ &- (\partial_0\beta)\ F_{20} - (\partial_1\beta)\ F_{12} \\ &- \frac{\kappa}{2}\big[(\partial_0\beta)A_1 - (\partial_1\beta)A_0\ \big]. \end{aligned} \tag{15}$$

For quantizing the theory using Dirac's procedure we choose the following two gauge-fixing conditions (GFC's):

$$\begin{aligned}\xi_1 &= \Pi \approx 0 \\ \xi_2 &= A_0 \approx 0. \end{aligned} \tag{16}$$

Here the gauge $A_0 \approx 0$ represents the time-axial or temporal gauge and the gauge $\Pi \approx 0$ represents the coulomb gauge. These gauges are acceptable and consistent with our quantization procedure and also physically more interesting. Corresponding to this set of gauge fixing conditions the total set of constraints now becomes:

$$\begin{aligned}\chi_1 &= \Pi^0 \approx 0 \\ \chi_2 &= \big[ie(\Pi\Phi - \Pi^*\Phi^*) + (\partial_1 E_1 + \partial_2 E_2) \\ &\quad + \frac{\kappa}{2}(\partial_1 A_2 - \partial_2 A_1)\big] \approx 0 \end{aligned}$$

$$\begin{aligned}\chi_3 = \xi_1 \ &= \ \Pi \approx 0 \\ \chi_4 = \xi_2 \ &= \ A_0 \approx 0. \end{aligned} \tag{17}$$

The non-vanishing matrix elements of the matrix $R_{\alpha\beta}$ ($:= \{\chi_1, \chi_2\}_P$) of the equal-time Poisson brackets of the above constraints are:

$$\begin{aligned}R_{14} = -R_{41} &= \ -\ \delta(x^1 - y^1)\delta(x^2 - y^2) \\ R_{23} = -R_{32} &= \ ie\Pi\ \delta(x^1 - y^1)\delta(x^2 - y^2). \end{aligned} \tag{18}$$

The above matrix is nonsingular and the set of constraints $\chi_i\ ;\ i = 1, 2, 3, 4$ is now second class and the theory is a gauge non-invariant theory. The non-vanishing matrix elements of the matrix $R^{-1}_{\alpha\beta}$ (which

is the inverse of the matrix $R_{\alpha\beta}$) are given by:

$$R_{14}^{-1} = -R_{41}^{-1} = \delta(x^1 - y^1)\delta(x^2 - y^2) \qquad (19)$$
$$(e\Pi)R_{23}^{-1} = -(e\Pi)R_{32}^{-1} = \ i\ \delta(x^1 - y^1)\delta(x^2 - y^2).$$

Following the standard Dirac quantisation procedure, the non-vanishing equal time Dirac Brackets (DB's) of the theory are obtained as:

$$(\Pi)\ \{\Pi^*(x^0, x^1, x^2)\ ,\ \Phi(x^0, y^1, y^2)\}_D = (-\Pi^*)\delta(x^1 - y^1)\delta(x^2 - y^2)$$

$$\{\Pi^*(x^0, x^1, x^2)\ ,\ \Phi^*(x^0, y^1, y^2)\}_D = \{\Pi^*(x^0, x^1, x^2)\ ,\ \Phi^*(x^0, y^1, y^2)\}_P = -\delta(x^1 - y^1)\delta(x^2 - y^2)$$

$$(ie\Pi)\ \{E_1(x^0, x^1, x^2)\ ,\ \Phi(x^0, y^1, y^2)\}_D = \left(\frac{\kappa}{2}\right)\ \delta(x^1 - y^1)\ \partial_2\delta(x^2 - y^2)$$

$$\{E_1(x^0, x^1, x^2)\ ,\ A_1(x^0, y^1, y^2)\}_D = \{E_1(x^0, x^1, x^2)\ ,\ A_1(x^0, y^1, y^2)\}_P = -\ \delta(x^1 - y^1)\delta(x^2 - y^2)$$

$$(ie\Pi)\ \{E_2(x^0, x^1, x^2)\ ,\ \Phi(x^0, y^1, y^2)\}_D = -\left(\frac{\kappa}{2}\right)\ \partial_1\delta(x^1 - y^1)\delta(x^2 - y^2)$$

$$\{E_2(x^0, x^1, x^2)\ ,\ A_2(x^0, y^1, y^2)\}_D = \{E_2(x^0, x^1, x^2)\ ,\ A_2(x^0, y^1, y^2)\}_P = -\delta(x^1 - y^1)\delta(x^2 - y^2)$$

$$(\Pi)\ \{\Phi(x^0, x^1, x^2)\ ,\ \Phi^*(x^0, y^1, y^2)\}_D = (-\Phi^*)\delta(x^1 - y^1)\delta(x^2 - y^2)$$

$$(\Pi)\ \{\Phi(x^0, x^1, x^2)\ ,\ A_0(x^0, y^1, y^2)\}_D = (\Phi)\ \delta(x^1 - y^1)\delta(x^2 - y^2)$$

$$(ie\Pi)\ \{\Phi(x^0, x^1, x^2)\ ,\ A_1(x^0, y^1, y^2)\}_D = \partial_1\delta(x^1 - y^1)\delta(x^2 - y^2)$$

$$(ie\Pi)\ \{\Phi(x^0, x^1, x^2)\ ,\ A_2(x^0, y^1, y^2)\}_D = \delta(x^1 - y^1)\ \partial_2\delta(x^2 - y^2). \qquad (20)$$

Here one finds that the product of the canonical variables appear in the expressions of the constraints as well as in the expressions of the DB's and therefore for achieving the canonical quantisation of the theory, one encounters the problem of operator ordering while going from DB's to the commutation relations, this problem could however be resolved by demanding that all the fields and the field momenta after quantisation become Hermitian operators and that all the canonical commutation relations need to be consistent with the Hermiticity of these operators. This completes the Hamiltonian formulation of the theory under the choosen gauge fixing conditions.

It may be worthwhile to mention here that our choice of GFC's is by no means unique. In principle, one can choose any set of GFC's that would convert the set of constraints of the theory from first-class into a set of second-class constraints. However, it is better to choose the GFC's that are physically more meaningful and nore relevant like the ones that we have choosen. In our case the gauge $A_0 \approx 0$ represents a time-axial or temporal gauge and the gauge $\Pi \approx 0$ represents a Culomb gauge and both of them are physically important GFC's. Another important point is that one can not choose covariant GFC's here simply because the constraints of the theory are not covariant and therefore it would not work.

In path integral quantization (PIQ) [23], transition to quantum theory is made by writing the vacuum to vacuum transition amplitude for the theory, called the generating functional $Z[J_k]$ of the theory which in the presence of the external sources J_k for the present theory is [23]:

$$Z[J_k] = \int [d\mu] \exp\left[i \int d^3x\ [J_k\Phi^k + \Pi\partial_0\Phi + \Pi^*\partial_0\Phi^* + \Pi^0\partial_0 A_0 + E_1\partial_0 A_1 + E_2\partial_0 A_2 + \Pi_u\partial_0 u - \mathcal{H}_T]\right]. \qquad (21)$$

Here $\Phi^k \equiv (\Phi, \Phi^*, A_0, A_1, A_2, u)$ are the phase space variables of the theory with the corresponding respective canonical conjugate momenta: $\Pi_k \equiv (\Pi, \Pi^*, \Pi^0, E_1, E_2, \Pi_u)$. The functional measure $[d\mu]$ of the theory (with the above generating functional $Z[J_k]$) is:

$$[d\mu] = \Big[(ie\Pi)\delta(x^1 - y^1)\delta(x^2 - y^2) [d\Phi][d\Phi^*][dA_0][dA_1][dA_2][du][d\Pi] [d\Pi^*][d\Pi^0][dE_1][dE_2][d\Pi_u]\delta[(\Pi^0) \approx 0] \delta[[ie(\Pi\Phi - \Pi^*\Phi^*) + (\partial_1 E_1 + \partial_2 E_2) + \frac{\kappa}{2}(\partial_1 A_2 - \partial_2 A_1)] \approx 0] \delta[\Pi \approx 0]\delta[A_0 \approx 0]\Big]. \qquad (22)$$

Acknowledgements

We thank the organizers of the International Conference on Analytic and Algebraic Methods in Physics XVIII (AAMP XVIII) – 2021 at Prague, Czechia, Prof. Vít Jakubský, Prof. Vladimir Lotoreichik, Prof. Matej Tusek, Prof. Miloslav Znojil and the entire team for a wonderful orgnization of the conference. One of us (Bheemraj Sihag) thanks the University of Delhi for the award of a Research Fellowship.

References

[1] P. A. M. Dirac. Generalized Hamiltonian dynamics. *Canadian Journal of Mathematics* **2**:129–148, 1950. https://doi.org/10.4153/cjm-1950-012-1.

[2] V. L. Ginzburg, L. D. Landau. On the theory of superconductivity (in Russian). *Zhurnal Eksperimental'noi i Teoreticheskoi Fiziki* **20**:1064–1082, 1950.

[3] A. A. Abrikosov. On the magnetic properties of superconductors of the second group. *Soviet Physics JETP* **5**:1174–1182, 1957.

[4] H. B. Nielson, P. Olsen. Vortex line models for dual strings. *Nuclear Physics B* **61**:45–61, 1973.

[5] C. Becchi, A. Rouet, R. Stora. The abelian Higgs Kibble model, unitarity of the S-operator. *Physics Letters B* **52**(3):344–346, 1974. https://doi.org/10.1016/0370-2693(74)90058-6.

[6] E. B. Bogomolnyi. The stability of classical solutions. *Soviet Journal of Nuclear Physics* **24**(4):449–458, 1976.

[7] S. Deser, R. Jackiw, S. Templeton. Three-dimensional massive gauge theories. *Physical Review Letters* **48**:975–978, 1982. *Annals of Physics*, **140**:372, 1982, https://doi.org/10.1103/PhysRevLett.48.975.

[8] F. Wilczek. Quantum mechanics of fractional-spin particles. *Physical Review Letters* **49**:957–959, 1982. https://doi.org/10.1103/PhysRevLett.49.957.

[9] A. J. Niemi, G. W. Semenoff. Axial-anomaly-induced fermion fractionization and effective gauge-theory actions in odd-dimensional space-times. *Physical Review Letters* **51**:2077–2080, 1983. https://doi.org/10.1103/PhysRevLett.51.2077.

[10] A. N. Redlich. Gauge noninvariance and parity nonconservation of three-dimensional fermions. *Physical Review Letters* **52**:18–21, 1984. https://doi.org/10.1103/PhysRevLett.52.18.

[11] K. Ishikawa. Chiral anomaly and quantized Hall effect. *Physical Review Letters* **53**:1615–1618, 1984. https://doi.org/10.1103/PhysRevLett.53.1615.

[12] G. W. Semenoff, P. Sodano. Non-Abelian adiabatic phases and the fractional quantum Hall effect. *Physical Review Letters* **57**:1195–1198, 1986. https://doi.org/10.1103/PhysRevLett.57.1195.

[13] L. Jacobs, C. Rebbi. Interaction energy of superconducting vortices. *Physical Review B* **19**:4486–4494, 1979. https://doi.org/10.1103/PhysRevB.19.4486.

[14] I. V. Krive, A. S. Rozhavskiĭ. Fractional charge in quantum field theory and solid-state physics. *Soviet Physics Uspekhi* **30**(5):370, 1987. https://doi.org/10.1070/PU1987v030n05ABEH002884.

[15] A. L. Fetter, C. B. Hanna, R. B. Laughlin. Random-phase approximation in the fractional-statistics gas. *Physical Review B* **39**:9679–9681, 1989. https://doi.org/10.1103/PhysRevB.39.9679.

[16] T. Banks, J. D. Lykken. Landau-Ginzburg description of anyonic superconductors. *Nuclear Physics B* **336**(3):500–516, 1990. https://doi.org/10.1016/0550-3213(90)90439-K.

[17] G. V. Dunne, C. A. Trugenberger. Self-duality and nonrelativistic Maxwell-Chern-Simons solitons. *Physical Review D* **43**:1323–1331, 1991. https://doi.org/10.1103/PhysRevD.43.1323.

[18] S. Forte. Quantum mechanics and field theory with fractional spin and statistics. *Reviews of Modern Physics* **64**:193–236, 1992. https://doi.org/10.1103/RevModPhys.64.193.

[19] U. Kulshreshtha. Hamiltonian and BRST formulations of the two-dimensional Abelian Higgs model. *Canadian Journal of Physics* **78**(1):21–31, 2000. https://doi.org/10.1139/p00-002.

[20] U. Kulshreshtha. Hamiltonian and BRST formulations of the Nielsen-Olesen model. *International Journal of Theoretical Physics* **41**(2):273–291, 2002. https://doi.org/10.1023/A:1014058806710.

[21] U. Kulshreshtha, D. S. Kulshreshtha. Hamiltonian, path integral, and BRST formulations of the Chern–Simons theory under appropriate gauge-fixing. *Canadian Journal of Physics* **86**(2):401–407, 2008. https://doi.org/10.1139/p07-176.

[22] U. Kulshreshtha, D. S. Kulshreshtha, H. J. W. Mueller-Kirsten, J. P. Vary. Hamiltonian, path integral and BRST formulations of the Chern–Simons–Higgs theory under appropriate gauge fixing. *Physica Scripta* **79**(4):045001, 2009. https://doi.org/10.1088/0031-8949/79/04/045001.

[23] H. J. W. Mueller-Kirsten. *Introduction to Quantum Mechanics: Schrödinger Equation and Path Integral*. World Scientific, Singapore, 2006. ISBN 9789814397735.

RATIONAL EXTENSION OF MANY PARTICLE SYSTEMS

Bhabani Prasad Mandal

Banaras Hindu University, Institute of Science, Physics Department, Lanka, 221005–Varanasi, Uttar Pradesh India

correspondence: bhabani.mandal@gmail.com

Abstract.

In this talk, we briefly review the rational extension of many particle systems, and is based on a couple of our recent works. In the first model, the rational extension of the truncated Calogero-Sutherland (TCS) model is discussed analytically. The spectrum is isospectral to the original system and the eigenfunctions are completely expressed in terms of exceptional orthogonal polynomials (EOPs). In the second model, we discuss the rational extension of a quasi exactly solvable (QES) N-particle Calogero model with harmonic confining interaction. New long-range interaction to the rational Calogero model is included to construct this QES many particle system using the technique of supersymmetric quantum mechanics (SUSYQM). Under a specific condition, infinite number of bound states are obtained for this system, and corresponding bound state wave functions are written in terms of EOPs.

Keywords: Exceptional orthogonal polynomials, rational extensions, many particle systems, SUSYQM.

1. Introduction

Orthogonal polynomials play very useful and important roles in studying physics, particularly in electrostatics and in quantum mechanics. In quantum mechanics, only a few of the commonly occuring bound states problems, which have a wide range of applications and/or extensions, are solvable. Such systems generally bring into physics a class of orthogonal polynomials.These classical orthogonal polynomials have many properties common, such as (i) each constitutes orthogonal polynomials of successive increasing degree starting from $m = 0$, (ii) each satisfy a second order homogeneous differential equations, (iii) they satisfy orthogonality over a certain interval and with a certain non-negative weight function, etc. In 2009, new families of orthogonal polynomials (known as exceptional orthogonal polynomials (EOP)) related to some of the old classical orthogonal polynomials were discovered [1–3]. Unlike the usual classical orthogonal polynomials, these EOPs start with degree $m = 1$ or higher integer values and still form a complete orthonormal set with respect to a positive definite inner product defined over a compact interval. Two of the well known classical orthogonal polynomials, namely Laguerre orthogonal polynomials and Jacobi orthogonal polynomials, have been extended to EOPs category. X_m Laguerre (Jocobi) EOP means the complete set of Laguerre (Jacobi) orthogonal polynomials with degree $\geq m$. m is positive integer and can have values of $1, 2, 3, \ldots$ Attempts were made to also extend the classical Hermite polynomials [4]. Soon after this remarkable discovery, the connection of EOPs with the translationally shape invariant potential were established [5–9]. The list of exactly solvable quantum mechanical systems is enlarged and the wave functions for the newly obtained exactly solvable systems are written in terms of EOPs. Such systems are known as rational extension of the original systems. The study for the exactly solvable potentials has been boosted greatly due to this discovery of EOPs over the past decade [10–37].

There are several commonly used approaches to build the rationally extended models, such as SUSYQM approach [38, 39], Point canonical transformation approach [40, 41], Darboux-Crum transformation approach [42, 43], group theoretical approach [44], etc. These approaches have been used to study different problems in this field leading to a discovery of a large number of new exactly solvable systems, which are isospectral to the original system and the eigenfunctions are written in terms of EOPs. Further, quasi-exactly solvable (QES) systems [45–49] and conditionally exactly solvable (CES) systems [50, 51] attracted attention in literature due to the lack of many exactly solvable systems. Several works have been devoted to the rational extension of these QES/ CES systems [22, 24, 37]. Nowadays, the parity time reversal (PT) symmetric non-Hermitian systems [52–62] are among the exciting frontier research areas. Rational extensions have also been carried out for non-Hermitian systems [6, 19, 29–32]. Even though most of the rational extensions are for the one dimensional and/or one particle exactly solvable systems, the research in this field has also been extended to many particle systems [24, 25, 27]. We have done several works on rational extensions for many particle systems. In one of the works, the well known Calogero-Wolfes type 3-body problem on a line was extended rationally to show that exactly solvable wave functions are written in terms of X_m Laguerre and X_m Jacobi EOPs [26]. However, this article is based on two of our earlier works on rational extension of many particle systems [24, 25], which

were central to the talk presented during the AAMP meeting. In the first work [25], we discuss the rational extension of the truncated Calogero-Sutherland model using a PCT approach. We indicate how to obtain rationally extended solutions, which are isospectral to the original system in terms of X_m Laguerre EOPs. In the second model [24], we discuss the rational extension of a QES N-particle Calogero model with a harmonic confining interaction. New long-range interactions to the rational Calogero model are included to construct this QES many particle system using SUSYQM. The wavefunctions are expressed, again, in terms of exceptional orthogonal Laguerre polynomials.

Now, we present the organisation of the article. In the next section, we present the TCS model and its solutions in brief to set the things for the section 3, where we consider the rational extension of the TCS model. In section 4, the QES solutions for the rationally extended Calogero type many particle system are presented. Section 5 is reserved for conclusions.

2. TCS MODEL

In his work, Jain-Khare (JK) [63] exactly solved some variant of Calogero-Sutherland model (CSM) on the full line by taking only the nearest and next-to-nearest neighbor interactions through 2-body and 3-body interactions. Later, Pittman et al. [64] generalized this model by considering an N-body problem on a line with harmonic confinement with tunable inverse square as well as the three-body interaction extends over a finite number of neighbors and were able to solve it exactly. This model is known as truncated Calogero-Sutherland model (TCS). N-body TCS model [64], where particles are interacting through 2-body and 3-body potentials, is given by

$$H=\sum_{i=1}^{N}\Big[-\frac{1}{2}\frac{\partial^2}{\partial x_i^2}+\frac{1}{2}\omega^2 x_i^2\Big]+\sum_{\substack{i<j\\ |i-j|\le r}}\frac{\lambda(\lambda-1)}{|\,x_i-x_j\,|^2}+\sum_{\substack{i<j<k\\ |i-j|\le r\\ |j-k|\le r}}\frac{\lambda^2(x_i-x_j)\mathbf{x}\cdot(x_j-x_k)\mathbf{x}}{|x_j-x_j|^2|x_j-x_k|^2} \tag{1}$$

with $\lambda\neq 0$ and $\mathbf{x}=(x_1,x_2,\ldots,x_N)\in R^N$. The 2- body interaction is attractive for $0<\lambda<1$ and is repulsive for $\lambda\geq 1$. Here, r is the integer parameter and for $r=1$, this system reduces to that of the Jain-Khare [63] model. However, for $r=N-1$, it corresponds to the CSM [65–67] model.

Using standard techniques in the case of many particle systems, the time independent Schrodinger equation (TISE) corresponding to the above system can be written in radial and angular parts as

$$\Phi''(\rho)+\Big(N+2s-1+\lambda r(2N-r-1)\Big)\frac{1}{\rho}\Phi'(\rho)+2(E-\frac{1}{2}\omega^2\rho^2)\Phi(\rho)=0\,, \tag{2}$$

(where $\rho=\sum_i^N x_i^2$, is the radial coordinate and the prime denotes the differentiation with respect to its arguments and this convention is adopted throughout this manuscript) and

$$\Big[\sum_{i=1}^{N}\frac{\partial^2}{\partial x_i^2}+2\lambda\sum_{i<j}^{N-1}\frac{1}{x_i-x_j}\Big(\frac{\partial}{\partial x_i}-\frac{\partial}{\partial x_j}\Big)\Big]P_s(\mathbf{x})=0. \tag{3}$$

(where the function P_s denotes the homogeneous polynomial of angular variables of degree $s=0,1,2,\ldots$). To obtaine these Eqs. we have substituted the wave function

$$\Psi(x)=\prod_{i<j}(x_i-x_j)^{\lambda}\,\Phi(\rho)\;P_s(x) \tag{4}$$

in the TISE, $H\Psi=E\Psi$.

This model is solved exactly and the solution is given by,

$$\text{the spectrum: } E_n=\omega\big(2n+s+\frac{N}{2}+\frac{\lambda r}{2}(2N-r-1)\big), \tag{5}$$

and the corresponding radial wave function in terms of classical Laguerre polynomials is given as

$$\Phi(\rho)\simeq\exp(-\frac{\omega\rho^2}{2})L_n^{(\alpha)}(\omega\rho^2);\quad n=0,1,2,\ldots \tag{6}$$

where $\alpha=\big(s-1+\frac{N}{2}+\frac{\lambda r}{2}(2N-r-1)\big)$. This result is consistent with JK and CSM models in the appropriate limit [64]. In the next section, we will extend this model by adding some interaction terms. Then, the extended model will be cast as a rational extension of the TCS model.

3. Extended TCS model (ETCS)

We would like to find another system related to the TCS model, which is isospectral to the TCS and possibly, its wave functions are written in terms of EOPs. To find the rational extension of the TCS model, we start by adding a new interaction term, [25]

$$H_e = H + \frac{(\alpha_1 + \alpha_2\omega^2\rho^2)}{(\beta_1 + \beta_2\omega^2\rho^2)^2} = H + V_{new}, \tag{7}$$

where $\alpha_{1,2}$ and $\beta_{1,2}$ are unknown constants and will be fixed later. We would like to show that this H_e will correspond to the rational extension of this TCS model for some specific values of the parameters $\alpha_{1,2}$ and $\beta_{1,2}$. Since V_{new} depends only on radial coordinate, ρ, only the radial equation will be modified and angular equation will be the same as in the case of the TCS model. The radial part is obtained having the same substitution as in Eq. (4) in the earlier section for the Hamiltonian H_e

$$\Phi''_{ext}(\rho) + \big(N + 2s - 1 + \lambda r(2N - r - 1)\big)\frac{1}{\rho}\Phi'_{ext}(\rho) + 2\big(E - (\frac{1}{2}\omega^2\rho^2 + V_{new})\big)\Phi_{ext}(\rho) = 0, \tag{8}$$

with $P_s(\mathbf{x})$ satisfying the same generalised Laplace equation as in Eq. (3). Note that here, a prime on $\Phi_{ext}(\rho)$ indicates a derivative with respect to ρ.
We further substitute,

$$\Phi_{ext}(\rho) = f(\rho)\zeta(g(\rho)), \tag{9}$$

in Eq. 8 where $f(\rho)$ and $g(\rho)$ are two undermined functions and $\zeta(g)$ is a special function to obtain

$$\zeta''(g) + \left(\frac{2f'(\rho)}{f(\rho)g'(\rho)} + \frac{g''(\rho)}{g'(\rho)^2} + \frac{\tau}{\rho g'(\rho)}\right)\zeta'(g) + \frac{1}{g'(\rho)^2}\left(\frac{f''(\rho)}{f(\rho)} + \frac{\tau f'(\rho)}{\rho f(\rho)} + 2(E_{ext} - V_{ext})\right)\zeta(g) = 0, \tag{10}$$

where, $\tau = \big(N + 2s - 1 + \lambda r(2N - r - 1)\big)$ and E_{ext} is exactly same as E_n given in Eq. (5)

We now compare this differential equation satisfied by $\zeta(g(\rho))$ with the differential equation satisfied by the X_1 Laguerre polynomial $\hat{L}_n^{(\alpha)}(g)$

$$\hat{L}_n^{''(\alpha)}(g(\rho)) - \frac{(g-\alpha)(g+\alpha+1)}{g(g+\alpha)}\hat{L}_n^{'(\alpha)}(g(\rho)) + \frac{1}{g}\left(\frac{(g-\alpha)}{(g+\alpha)} + n - 1\right)\hat{L}_n^{(\alpha)}(g(\rho)) = 0; \quad n \geq 1, \tag{11}$$

to obtain (with $n \to n+1$,)

$$V_{ext} = \frac{1}{2}\omega^2\rho^2 + \frac{4\omega}{(2\omega\rho^2 + \tau - 1)} - \frac{8\omega(\tau - 1)}{(2\omega\rho^2 + \tau - 1)^2}, \tag{12}$$

and

$$f(\rho) \simeq (g'(\rho))^{-\frac{1}{2}}\rho^{-\frac{\alpha}{2}}\exp\left(\frac{1}{2}\int^g [-\frac{(g-\alpha)(g+\alpha+1)}{g(g+\alpha)}]dg\right). \tag{13}$$

for a given $g(\rho)$ as defined in the case of a conventional model

$$g(\rho) = \omega\rho^2; \quad \alpha = \frac{\tau}{2} - \frac{1}{2}. \tag{14}$$

The energy eigenvalues E_{ext} for the new system with the potential in Eq. 12 turn out to be the same as that of the conventional TCS model as discussed in Section 2 and are given by Eq. (5). However, the corresponding eigenfunction $\Phi_{ext}(\rho)$ is completely different. Using $f(\rho)$ and replacing $\zeta(g) \to \hat{L}_{n+1}^{(\alpha)}(g)$ in Eq. (9), the expressions for the energy eigenfunctions are obtained in terms of X_1 exceptional orthogonal Laguerre polynomials ($\hat{L}_{n+1}^{(\alpha)}(g)$) as

$$\Phi_{ext}(\rho) \simeq \frac{\exp(-\frac{\omega\rho^2}{2})}{(2\omega\rho^2 + \alpha)}\hat{L}_{n+1}^{(\alpha)}(\omega\rho^2); \; n = 0, 1, 2, \ldots \tag{15}$$

Note that the X_1 Laguerre polynomial ($\hat{L}_{n+1}^{(\alpha)}(g)$) is related to the classical Laguerre polynomials by

$$\hat{L}_{n+1}^{(\alpha)}(g) = -(g + \alpha + 1)L_n^{(\alpha)}(g) + L_{n-1}^{(\alpha)}(g). \tag{16}$$

The constant parameters $\alpha_{1,2}$ and $\beta_{1,2}$ for which the Hamiltonian (7) is exactly solvable can easily be determined by comparing Eqs. (7) and (12), and one finds that

$$\begin{aligned} \alpha_1 &= -4\omega(\tau-1); \qquad \alpha_2 = 8, \\ \beta_1 &= \tau - 1; \quad \text{and} \quad \beta_2 = 2/\omega. \end{aligned} \tag{17}$$

In the special cases of $r = 1$ and $r = N - 1$, we then obtain the rational extension of the JK model and the CSM, respectively.

X_m **case:**

Similar to the X_1 case, we redefine Eqs. (8) and (9) by replacing $\Phi_{ext}(\rho) \to \Phi_{m,ext}(\rho)$ and $f(\rho) \to f_m(\rho), \zeta(g) \to \zeta_m(g)$, respectively. Now the differential Eq. (8) will also be m dependent and can be written as

$$\Phi''_{m,ext}(\rho) + \big(N + 2s - 1 + \lambda r(2N - r - 1)\big)\frac{1}{\rho}\Phi'_{m,ext}(\rho) + 2\big(E - (\frac{1}{2}\omega^2\rho^2 + V_{m,new})\big)\Phi_{m,ext}(\rho) = 0. \tag{18}$$

Now, we proceed with the steps as in the case of X_1, by substituting $\Phi_{m,ext}(\rho) = f_m(\rho)\zeta_m(g(\rho))$ in the above equation to obtain the differential equation for $\zeta_m(g)$, which is exactly same as in Eq. (10).Then, we compare that equation with the X_m exceptional Laguerre differential equation

$$\hat{L}^{''(\alpha)}_{n,m}(g(\rho)) + Q_m(g)\hat{L}^{'(\alpha)}_{n,m}(g(\rho)) + R_m(g)\hat{L}^{(\alpha)}_{n,m}(g(\rho)) = 0, \tag{19}$$

with

$$\begin{aligned} Q_m(g) &= \frac{1}{g}\left[(\alpha + 1 - g) - 2g\frac{L^{(\alpha)}_{m-1}(-g)}{L^{(\alpha-1)}_m(-g)}\right] \\ \text{and} \quad R_m(g) &= \frac{1}{g}\left[n - 2\alpha\frac{L^{(\alpha)}_{m-1}(-g)}{L^{(\alpha)}_m(-g)}\right] \end{aligned} \tag{20}$$

to get (replacing n by $n + m$)

$$V_{m,new} = -2\omega^2\rho^2\frac{L^{(\alpha+1)}_{m-2}(-g)}{L^{(\alpha-1)}_m(-g)} + 2\omega(\alpha + \omega\rho^2 - 1)\frac{L^{(\alpha)}_{m-1}(-g)}{L^{(\alpha-1)}_m(-g)} + 4\omega^2\rho^2\left(\frac{L^{(\alpha)}_{m-1}(-g)}{L^{(\alpha-1)}_m(-g)}\right)^2 - 2m\omega, \tag{21}$$

and

$$f(\rho) \simeq (g'(\rho))^{-\frac{1}{2}}\rho^{-\frac{\alpha}{2}}\exp\left(\frac{1}{2}\int^g Q_m(g)dg\right). \tag{22}$$

We note that the spectrum for the potential in Eq. (21) is exactly same as that for the potential in Eq. (12) and for a usual TCS system. However, the eigen functions in all three cases are different. For a usual TCS model, these are in terms of classical Laguerre polynomials, in case of the potential in Eq. (12), that is, in the X_1 case, these are in terms of X_1 Laguerre polynomials and finally the wave functions for the system with the potential in Eq. (21) are in terms of X_m Laguerre polynomials. The wave functions for the system described by the potential in Eq. (21) are given by

$$\Phi_{m,ext}(\rho) \simeq \frac{\exp(-\frac{\omega\rho^2}{2})}{\hat{L}^{(\alpha-1)}_m(-\omega\rho^2)}\hat{L}^{(\alpha)}_{n+m}(\omega\rho^2); \quad n, m = 0, 1, 2, \ldots \tag{23}$$

where the X_m Laguerre polynomial ($\hat{L}^{(\alpha)}_{n+m}(g)$) is related to the classical Laguerre polynomials by

$$\hat{L}^{(\alpha)}_{n+m}(g) = L^{(\alpha)}_m(-g)L^{(\alpha-1)}_n(g) + L^{(\alpha-1)}_m(-g)L^{(\alpha)}_{n-1}(g). \tag{24}$$

As expected, for $m = 1$, the above results reduce to the corresponding X_1-case, while for the $m = 0$ case one gets back the conventional TCS model. In the next section, we will consider a rational extension of Calogero like many particle systems.

4. QES many particle system

In this section, we would like to discuss a rational extension of Calogero like many particle systems [24]. We start with a many particle Calogero like Hamiltonian with an arbitrary potential $U(\sqrt{N}\rho)$, which depends only on the 'radial' coordinate ρ

$$H = -\sum_{i=1}^{N} \frac{\partial^2}{\partial x_i^2} + \sum_{i<j}^{N} \frac{\lambda}{(x_i - x_j)^2} + U(\sqrt{N}\rho);\ \lambda \geq -\frac{1}{2},\ \rho = \sqrt{\frac{1}{N}\sum_{i<j}^{N}(x_i - x_j)^2} \tag{25}$$

Our aim is to construct a possible structure of $U(\sqrt{N}\rho)$, for which the many particle model is exactly solvable. To this end, we follow the standard method [65–67] and take a trial wavefunction for $\psi(x)$ in a sector of the configuration space corresponding to a definite ordering of particles (e.g., $x_1 \geq x_2 \geq \cdots \geq x_N$) as

$$\psi(x) = \prod_{i<j}(x_i - x_j)^{a+\frac{1}{2}} P_{k,q}(x)\phi(\rho), \text{with } a = \frac{1}{2}\sqrt{1+2\lambda} \tag{26}$$

and obtain the radial part differential equation,

$$-[\phi''(\rho) + 2(k+b+1)\frac{1}{\rho}\phi'(\rho)] + [U(\sqrt{N}\rho) - E]\phi(\rho) = 0 \tag{27}$$

with $b = \frac{N(N-1)}{2}a + \frac{N(N+1)}{4} - 2$. The angular part is described by $P_{k,q}(x)$, which are translationally invariant, symmetric, k-th order homogeneous polynomials satisfying the differential equations

$$\sum_{j=1}^{N} \frac{\partial^2 P_{k,q}(x)}{\partial x_j^2} + \left(a + \frac{1}{2}\right) \sum_{j\neq k} \frac{1}{(x_j - x_k)} \left(\frac{\partial}{\partial x_j} - \frac{\partial}{\partial x_k}\right) P_{k,q}(x) = 0\,. \tag{28}$$

Note that the index q in $P_{k,q}(x)$ can take any integral value ranging from 1 to $\lambda(N,k)$, where $\lambda(N,k)$ is the number of independent polynomials. The existence of such translationally invariant, symmetric and homogeneous polynomial solutions of (28) has been discussed in the original work by Calogero [65, 66].

For our purpose, we will look for a solution of the radial part and proceed with the substitution

$$\phi(\rho) = \rho^{-(l+1)}\chi(\rho), \quad \text{with } l = k + b \tag{29}$$

in Eq. (27) to obtain

$$-\frac{d^2}{d\rho^2}\chi(\rho) + U_k(\sqrt{N}\rho)\chi(\rho) = E\chi(\rho) \tag{30}$$

where $U_k(\sqrt{N}\rho)$ is k dependent (through l) and is written as

$$U_k(\sqrt{N}\rho) = \frac{l(l+1)}{\rho^2} + U(\sqrt{N}\rho)\,. \tag{31}$$

Our aim here is to find a solution of Eq. (30) with a possible general structure of $U(\sqrt{N}\rho)$. This will provide an exact solution of a many particle system given in Eq. (25). This can be done in various ways, but we would like to use the technique of SUSYQM, details of which can be found in [38, 39]

We consider a specific superpotential of the form [22]

$$W(\rho) = \rho + \frac{2g_1\rho}{1+g_1\rho^2} + \frac{\alpha+1}{\rho}\,, g_1(\alpha) = \frac{2}{2\alpha+3}\,.\ \ \alpha \in \mathcal{R}^+ \tag{32}$$

for which one of the partner potentials is a radial oscillator. The partner potentials can be calculated as,

$$V_+(\rho) = \rho^2 + \frac{\alpha(\alpha+1)}{\rho^2} + 2\alpha + 7\,, \tag{33a}$$

$$V_-(\rho) = \rho^2 + \frac{(\alpha+1)(\alpha+2)}{\rho^2} - \frac{4g_1}{1+g_1\rho^2} + \frac{8g_1^2\rho^2}{(1+g_1\rho^2)^2} + 2\alpha + 5\,. \tag{33b}$$

The potential V_+ is the potential for a radial oscillator model with a constant term. The complete solution for this potential is given by

$$E_n^+ = 4\left(n+\alpha+\frac{5}{2}\right), \quad n=0,1,2,\ldots \tag{34}$$

$$\chi_n^+(\rho) = \sqrt{\frac{n!}{\Gamma(n+\alpha+\frac{3}{2})}}\,\rho^{\alpha+1}e^{-\rho^2/2}L_n^{\alpha+1/2}(\rho^2)\,. \tag{35}$$

Where $L_n^{\alpha+1/2}(\rho^2)$ is a usual Laguerre polynomial. Using the results of SUSYQM, we can obtained the solution for the partner potential $V_-(\rho)$ given in Eq. (33b) as

$$E_n^- = 4\left(n+\alpha+\frac{5}{2}\right), \tag{36}$$

which is the same as in the case of V_+, the radial oscillator potential. The radial part of the wave function is written as

$$\chi_n^-(\rho) = \sqrt{\frac{4(n!)}{E_n^+\Gamma(n+\alpha+\frac{3}{2})}}\rho^{\alpha+2}e^{-\rho^2/2}\frac{1}{L_1^{\alpha+1/2}(-\rho^2)}\hat{L}_{n+1,1}^{\alpha+3/2}(\rho^2). \tag{37}$$

This solution for $V_-(\rho)$ is possible only when the parameter g_1 depends on α in a particular fashion and hence, the model with V_- is conditionally exactly solvable. Note that $V_+(\rho)$ can be used to generate the exactly solvable Calogero model with a harmonic confining interaction as in this case

$$U(\sqrt{N}\rho) = U_k(\sqrt{N}\rho) - \frac{l(l+1)}{\rho^2} = \rho^2 + \frac{\alpha(\alpha+1)-l(l+1)}{\rho^2}, \tag{38}$$

apart from an overall constant term. Now, $l=k+b$ and α are free parameters and we can chose the parameter $\alpha=l$ such that $U(\sqrt{N}\rho)=\rho^2$ is independent of k. Calogero has shown that the many particle system (25) with $U(\sqrt{N}\rho)=\rho^2$ can be solved exactly for all possible values of k. However, unlike this case, $V_-(\rho)$ represents a QES many particle system as we explain below.

$$U(\sqrt{N}\rho) = \rho^2 + \frac{(\alpha+1)(\alpha+2)-l(l+1)}{\rho^2} - \frac{4g_1}{1+g_1\rho^2} + \frac{8g_1^2\rho^2}{(1+g_1\rho^2)^2} + 2\alpha + 5\,, \tag{39}$$

In this case, α depends on g_1 and hence can't be chosen as such that $U(\sqrt{N}\rho)$ is independent of k. Hence, the many particle system with $U(\sqrt{N}\rho)$ is QES as it is solvable only for a particular value of k. The eigenvalues are

$$E_n = 4\left(n+\alpha+\frac{5}{2}\right), \quad n=0,1,2,\ldots. \tag{40}$$

and the corresponding (unnormalized) QES eigenfunctions in terms of X_1 Laguerre polynomials are written as

$$\psi_n(x) = \rho^{\alpha-l+1}e^{-\rho^2/2}\frac{1}{L_1^{\alpha+1/2}(-\rho^2)}\hat{L}_{n+1,1}^{\alpha+3/2}(\rho^2)\prod_{i<j}(x_i-x_j)^{a+\frac{1}{2}}P_{\tilde{k},q}(x)\,. \tag{41}$$

Note that the solution of the angular part $P_{\tilde{k},q}(x)$ is only for a specific value of the degree of the polynomial, i.e. for $k=\tilde{k}$. We can't find the solution of the radial part for $k\neq\tilde{k}$. Thus, the solution is not complete, we have obtained a part of it and thus, in this sense, we called the solutions QES. Now, we have obtained another potential given in Eq. (33b), which is isospectral to a radial oscillator potential but the wave functions are completely different and are written in terms of X_1 Laguerre polynomials. Thus, we have achieved the rational extension of Calogero like many particle system with a $U(\sqrt{N}\rho)$ given in Eq. (39).

We would like to point out that exactly same result can also be obtained using the other method, like PCT method. Furthermore, using the PCT approach, one can obtain the most general rationally extended radial oscillator potential

$$V_m(\rho) = \rho^2 + \frac{l(l+1)}{\rho^2} - \frac{4\rho^2L_{m-2}^{l+3/2}(-\rho^2)}{L_m^{l-1/2}(-\rho^2)} + 2(2\rho^2+2l-1)\frac{4\rho^2L_{m-2}^{l+1/2}(-\rho^2)}{L_m^{l-1/2}(-\rho^2)} + 8\rho^2[\frac{4\rho^2L_{m-2}^{l+3/2}(-\rho^2)}{L_m^{l-1/2}(-\rho^2)}]^2 - 4 \tag{42}$$

whose bound state solutions for the energy eigenvalues $E_n = (4n + 2l + 3)$ $n = 0, 1, 2, \ldots$ and eigenfunctions are written in terms of X_m exceptional Laguerre Polynomials as

$$\chi_{n,m}(\rho^2) = [\frac{(n-m)!}{(l+1/2+n)\Gamma(l+1/2+n-m)}]^{1/2} \frac{x^{l+1}\exp(-\rho^2/2)}{L_m^{l-1/2}(-\rho^2)} \hat{L}_{n+m,m}^{l+1/2}(\rho^2) \tag{43}$$

Where $\hat{L}_{n+m,m}^{l+1/2}(\rho^2)$ is X_m exceptional orthogonal Laguerre polynomial, $m = 0$ corresponds to usual Laguerre polynomials. Now, we note that $m = 1$ corresponds to the case we discus, in the context of Calogero Model as the potential

$$V_1 = \rho^2 + \frac{l(l+1)}{\rho^2} - \frac{8}{2\rho^2 + 2l + 1} + \frac{32\rho^2}{(2\rho^2 + 2l + 1)^2} \tag{44}$$

calculated from Eq. (42) is the same as our $V_-(\rho)$ in Eq. (33b) when $l = (\alpha + 1)$ and $g_1 = \frac{2}{(2\alpha+3)}$ apart from an overall constant term. The solution obtained through the PCT approach in Eq. (43) for $m = 1$ is exactly the same as we obtained through the supersymmetric approach.

5. Conclusions

In this article, we have reviewed two of our old works [24, 25] on a rational extension of many particle systems. In the first model [25], we have considered the TCS model with pairwise 2-body and 3-body interactions, and using the well known PCT approach, we have extended the model rationally. The spectrum is isospectral to the original TCS system and the wave functions are written in terms of X_m Laguerre polynomials. This means that we have a family of isospectral systems for $m = 1, 2, \ldots$ related to the TCS model with different potentials. The eigen functions are different and are written in terms of EOPs. In the other model, we have considered the QES Calogero like many particle system, and using SUSYQM techniques, obtained the general structure of the QES potential for which we can find the QES solutions. The wave functions are written in terms of EOPs. We have considered broken SUSYQM in our approach. We feel it would be of interest to investigate similar many particle systems for which supersymmetry is unbroken.

Acknowledgements

The author acknowledges the support from MATRIX project (Grant No. MTR/2018/000611), SERB, DST Govt. of India and the Research Grant for Faculty under IoE Scheme (number 6031) of BHU.

References

[1] D. Gómez-Ullate, N. Kamran, R. Milson. An extended class of orthogonal polynomials defined by Sturm-Liouville problem. *Journal of Mathematical Analysis and Applications* **359**(1):352–367, 2009. https://doi.org/10.1016/j.jmaa.2009.05.052.

[2] D. Gómez-Ullate, N. Kamran, R. Milson. Exceptional orthogonal polynomials and the Darboux transformation. *Journal of Physics A: Mathematical and Theoretical* **43**(43):434016, 2010. https://doi.org/10.1088/1751-8113/43/43/434016.

[3] D. Gómez-Ullate, N. Kamran, R. Milson. On orthogonal polynomials spanning a non-standard flag. *Contemporary Mathematics* **563**:51, 2012.

[4] D. Gómez-Ullate, Y. Grandati, R. Milson. Rational extensions of the quantum harmonic oscillator and exceptional Hermite polynomials. *Journal of Physics A: Mathematical and Theoretical* **47**(1):015203, 2014. https://doi.org/10.1088/1751-8113/47/1/015203.

[5] C. Quesne. Exceptional orthogonal polynomials, exactly solvable potentials and supersymmetry. *Journal of Physics A: Mathematical and Theoretical* **41**(39):392001, 2008. https://doi.org/10.1088/1751-8113/41/39/392001.

[6] B. Bagchi, C. Quesne, R. Roychoudhary. Isospectrality of conventional and new extended potentials, second-order supersymmetry and role of $\mathcal{PT}$ symmetry. *Pramana* **73**:337, 2009. https://doi.org/10.1007/s12043-009-0126-4.

[7] S. Odake, R. Sasaki. Another set of infinitely many exceptional (X_l) Laguerre polynomials. *Physics Letters B* **684**(2-3):173–176, 2010. https://doi.org/10.1016/j.physletb.2009.12.062.

[8] C.-L. Ho, S. Odake, R. Sasaki. Properties of the exceptional (X_l) Laguerre and Jacobi polynomials. *SIGMA* **7**:107, 2011. https://doi.org/10.3842/SIGMA.2011.107.

[9] C.-L. Ho, R. Sasaki. Zeros of the exceptional Laguerre and Jacobi polynomials. *International Scholarly Research Notices* **2012**:920475, 2012. https://doi.org/10.5402/2012/920475.

[10] D. Gómez-Ullate, F. Marcellán, R. Milson. Asymptotic and interlacing properties of zeros of exceptional Jacobi and Laguerre polynomials. *Journal of Mathematical Analysis and Applications* **399**(2):480–495, 2013. https://doi.org/10.1016/j.jmaa.2012.10.032.

[11] C. Quesne. Rationally-extended radial oscillators and Laguerre exceptional orthogonal polynomials in kth-order SUSYQM. *International Journal of Modern Physics A* **26**(32):5337–5347, 2011. https://doi.org/10.1142/S0217751X11054942.

[12] Y. Grandati. Solvable rational extensions of the isotonic oscillator. *Annals of Physics* **326**(8):2074–2090, 2011. https://doi.org/10.1016/j.aop.2011.03.001.

[13] B. Midya, B. Roy. Exceptional orthogonal polynomials and exactly solvable potentials in position dependent mass Schrödinger Hamiltonian. *Physics Letters A* **373**(45):4117–4122, 2009. https://doi.org/10.1016/j.physleta.2009.09.030.

[14] B. Midya, P. Roy, T. Tanaka. Effect of position-dependent mass on dynamical breaking of type B and type X_2 $\mathcal{N}$-fold supersymmetry. *Journal of Physics A: Mathematical and Theoretical* **45**(20):205303, 2012. https://doi.org/10.1088/1751-8113/45/20/205303.

[15] K. Zelaya, V. Hussin. Time-dependent rational extensions of the parametric oscillator: quantum invariants and the factorization method. *Journal of Physics A: Mathematical and Theoretical* **53**(16):165301, 2020. https://doi.org/10.1088/1751-8121/ab78d1.

[16] S. E. Hoffmann, V. Hussin, I. Marquette, Y. Zhang. Ladder operators and coherent states for multi-step supersymmetric rational extensions of the truncated oscillator. *Journal of Mathematical Physics* **60**(5):052105, 2019. https://doi.org/10.1063/1.5091953.

[17] C. Quesne. Quantum oscillator and Kepler–Coulomb problems in curved spaces: Deformed shape invariance, point canonical transformations, and rational extensions. *Journal of Mathematical Physics* **57**(10):102101, 2016. https://doi.org/10.1063/1.4963726.

[18] S. Sree Ranjani, R. Sandhya, A. K. Kapoo. Shape invariant rational extensions and potentials related to exceptional polynomials. *International Journal of Modern Physics A* **30**(24):1550146, 2015. https://doi.org/10.1142/S0217751X15501468.

[19] B. Bagchi, C. Quesne. An update on the $\mathcal{PT}$-symmetric complexified Scarf II potential, spectral singularities and some remarks on the rationally extended supersymmetric partners. *Journal of Physics A: Mathematical and Theoretical* **43**(30):305301, 2010. https://doi.org/10.1088/1751-8113/43/30/305301.

[20] B. Bagchi, Y. Grandati, C. Quesne. Rational extensions of the trigonometric Darboux–Pöschl–Teller potential based on para-Jacobi polynomials. *Journal of Mathematical Physics* **56**(6):062103, 2015. https://doi.org/10.1063/1.4922017.

[21] I. Marquette, C. Quesne. New families of superintegrable systems from Hermite and Laguerre exceptional orthogonal polynomials. *Journal of Mathematical Physics* **54**(4):042102, 2013. https://doi.org/10.1063/1.4798807.

[22] D. Dutta, P. Roy. Conditionally exactly solvable potentials and exceptional orthogonal polynomials. *Journal of Mathematical Physics* **51**(4):042101, 2010. https://doi.org/10.1063/1.3339676.

[23] A. Ramos, B. Bagchi, N. Kumari, et al. A short note on "Group theoretic approach to rationally extended shape invariant potentials" [Ann. Phys. 359 (2015) 46-54]. *Annals of Physics* **382**:143–149, 2017. https://doi.org/10.1016/j.aop.2017.05.006.

[24] B. Basu-Mallick, B. P. Mandal, P. Roy. Quasi exactly solvable extension of Calogero model associated with exceptional orthogonal polynomials. *Annals of Physics* **380**:206–212, 2017. https://doi.org/10.1016/j.aop.2017.03.019.

[25] R. K. Yadav, A. Khare, N. Kumari, B. P. Mandal. Rationally extended many-body truncated Calogero–Sutherland model. *Annals of Physics* **400**:189–197, 2019. https://doi.org/10.1016/j.aop.2018.11.009.

[26] R. K. Yadav, S. R. Banerjee, A. Khare, et al. One parameter family of rationally extended isospectral potentials. *Annals of Physics* **436**:168679, 2022. https://doi.org/10.1016/j.aop.2021.168679.

[27] N. Kumari, R. K. Yadav, A. Khare, B. P. Mandal. A class of exactly solvable rationally extended Calogero-Wolfes type 3-body problems. *Annals of Physics* **385**:57–69, 2017. https://doi.org/10.1016/j.aop.2017.07.022.

[28] N. Kumari, R. K. Yadav, A. Khare, B. P. Mandal. A class of exactly solvable rationally extended non-central potentials in two and three dimensions. *Journal of Mathematical Physics* **59**(6):062103, 2018. https://doi.org/10.1063/1.4996282.

[29] B. Midhya, P. Roy. Infinite families of (non)-Hermitian Hamiltonians associated with exceptional X_m Jacobi polynomials. *Journal of Physics A: Mathematical and Theoretical* **46**(17):175201, 2013. https://doi.org/10.1088/1751-8113/46/17/175201.

[30] N. Kumari, R. K. Yadav, A. Khare, et al. Scattering amplitudes for the rationally extended $\mathcal{PT}$ symmetric complex potentials. *Annals of Physics* **373**:163–177, 2016. https://doi.org/10.1016/j.aop.2016.07.024.

[31] N. Kumari, R. K. Yadav, A. Khare, B. P. Mandal. Group theoretic approach to rationally extended shape invariant potentials. *Annals of Physics* **359**:46–54, 2015. https://doi.org/10.1016/j.aop.2015.04.002.

[32] R. K. Yadav, A. Khare, B. Bagchi, et al. Parametric symmetries in exactly solvable real and $\mathcal{PT}$ symmetric complex potentials. *Journal of Mathematical Physics* **57**(6):062106, 2016. https://doi.org/10.1063/1.4954330.

[33] R. K. Yadav, A. Khare, B. P. Mandal. The scattering amplitude for newly found exactly solvable potential. *Annals of Physics* **331**:313–316, 2013. https://doi.org/10.1016/j.aop.2013.01.006.

[34] R. K. Yadav, A. Khare, B. P. Mandal. The scattering amplitude for one parameter family of shape invariant potentials related to X_m Jacobi polynomials. *Physics Letter B* **723**(4-5):433–435, 2013. https://doi.org/10.1016/j.physletb.2013.05.036.

[35] R. K. Yadav, A. Khare, B. P. Mandal. Rationally extended shape invariant potentials in arbitrary D-dimensions associated with exceptional X_m polynomials. *Acta Polytechnica* **57**(6):477–487, 2017. https://doi.org/10.14311/AP.2017.57.0477.

[36] R. K. Yadav, A. Khare, B. P. Mandal. The scattering amplitude for rationally extended shape invariant Eckart potentials. *Physics Letter A* **379**(3):67–70, 2015. https://doi.org/10.1016/j.physleta.2014.11.009.

[37] C. Quesne. Revisiting (quasi-)exactly solvable rational extensions of the Morse potential. *International Journal of Modern Physics A* **27**(13):1250073, 2012. https://doi.org/10.1142/S0217751X1250073X.

[38] W. Witten. Dynamical breaking of supersymmetry. *Nuclear Physics B* **188**(3):513–554, 1981. https://doi.org/10.1016/0550-3213(81)90006-7.

[39] F. Cooper, A. Khare, U. Sukhatme. *Supersymmetric Quantum Mechanics*. World Scientific, Singapore, 2001. https://doi.org/10.1142/4687.

[40] A. Anderson. Canonical transformations in quantum mechanics. *Annals of Physics* **232**(2):292–331, 1994. https://doi.org/10.1006/aphy.1994.1055.

[41] A. Bhattacharjie, E. C. G. Sudarshan. A class of solvable potentials. *Nuovo Cimento* **25**:864–879, 1962. https://doi.org/10.1007/BF02733153.

[42] G. Darboux. *Theorie Generale des Surfaces, Vol. 2*. Gauthier-Villars, Paris, 1998.

[43] R. Sasaki, S. Tsujimoto, A. Zhedanov. Exceptional Laguerre and Jacobi polynomials and corresponding potentials through Darboux Crum transformations. *Journal of Physics A: Mathematical and Theoretical* **43**(31):315204, 2010. https://doi.org/10.1088/1751-8113/43/31/315204.

[44] Y. Alhassid, F. Gürsey, F. Iachello. Potential scattering, transfer matrix and group theory. *Physical Review Letters* **50**(12):873–876, 1983. https://doi.org/10.1103/PhysRevLett.50.873.

[45] A. Ushveridze. *Quasi-Exactly Solvable Models in Quantum Mechanics*. IOP, Bristol, 1994.

[46] A. Khare, B. P. Mandal. A number of quasi-exactly solvable $\mathcal{N}$-body problems. *Journal of Mathematical Physics* **39**(11):5789–5797, 1998. https://doi.org/10.1063/1.532593.

[47] A. Khare, B. P. Mandal. Do quasi-exactly solvable systems always correspond to orthogonal polynomials ? *Physics Letter A* **239**(4-5):197–200, 1998. https://doi.org/10.1016/S0375-9601(97)00897-9.

[48] A. Khare, B. P. Mandal. New QES Hermitian as well as non-Hermitian PT invariant potentials. *Pramana: Journal of Physics* **73**:387–395, 2009.

[49] A. Turbiner. Quasi-exactly-solvable problems and$sl(2)$ algebra. *Communications in Mathematical Physics* **118**:467–474, 1988. https://doi.org/10.1007/BF01466727.

[50] G. Junker, P. Roy. Conditionally exactly solvable problems and non-linear algebras. *Physics Letters A* **232**(3-4):155–161, 1997. https://doi.org/10.1016/S0375-9601(97)00422-2.

[51] G. Levai, P. Roy. Conditionally exactly solvable potentials and supersymmetric transformations. *Physics Letters A* **264**(2-3):117–123, 1999. https://doi.org/10.1016/S0375-9601(99)00778-1.

[52] C. M. Bender, S. Boettcher. Real spectra in non-Hermitian Hamiltonians having $\mathcal{PT}$ symmetry. *Physical Review Letters* **80**(24):5243–5246, 1998. https://doi.org/10.1103/PhysRevLett.80.5243.

[53] C. M. Bender. Making sense of non-Hermitian Hamiltonians. *Reports on Progress in Physics* **70**(6):947–1018, 2007. https://doi.org/10.1088/0034-4885/70/6/R03.

[54] A. Mostafazadeh. Pseudo-Hermitian representation of quantum mechanics. *International Journal of Geometric Methods in Modern Physics* **07**(07):1191–1306, 2010. https://doi.org/10.1142/S0219887810004816.

[55] M. Moiseyev. *Non-Hermitian quantum mechanics*. Cambridge University Press, 2011.

[56] F. Bagarallo, J.-P. Gazeau, F. H. Szafraniec, M. Znojil. *Non-Selfadjoint Operators in Quantum Physics: Mathematical Aspects*. Wiley, Hoboken, 2015.

[57] B. Basu-Mallick, B. P. Mandal. On an exactly solvable B_N type Calogero model with non-Hermitian PT invariant interaction. *Physics Letters A* **284**(6):231–237, 2001. https://doi.org/10.1016/S0375-9601(01)00310-3.

[58] A. Khare, B. P. Mandal. A PT-invariant potential with complex QES eigenvalues. *Physics Letters A* **272**(1-2):53–56, 2000. https://doi.org/10.1016/S0375-9601(00)00409-6.

[59] R. Modak, B. P. Mandal. Eigenstate entanglement entropy in a $\mathcal{PT}$-invariant non-Hermitian system. *Physical Review A* **103**(6):062416, 2021. https://doi.org/10.1103/PhysRevA.103.062416.

[60] R. Rawal, B. P. Mandal. Deconfinement to confinement as PT phase transition. *Nuclear Physics B* **946**:114699, 2019. https://doi.org/10.1016/j.nuclphysb.2019.114699.

[61] A. Dwivedi, B. P. Mandal. Higher loop β function for non-Hermitian PT symmetric $ig\phi^3$ theory. *Annals of Physics* **425**:168382, 2021. https://doi.org/10.1016/j.aop.2020.168382.

[62] B. Basu-Mallick, T. Bhattacharyya, B. P. Mandal. Phase shift analysis of PT-symmetric nonhermitian extension of AN-1 Calogero model without confining interaction. *Modern Physics Letters A* **20**(7):543–552, 2005. https://doi.org/10.1142/S0217732305015896.

[63] S. R. Jain, A. Khare. An exactly solvable many-body problem in one dimension and the short-range Dyson model. *Physics Letters A* **262**(1):35–39, 1999. https://doi.org/10.1016/S0375-9601(99)00637-4.

[64] S. M. Pittam, M. Beau, M. Olshanii, A. del Campo. Truncated Calogero-Sutherland models. *Physical Review B* **95**(20):205135, 2017. https://doi.org/10.1103/PhysRevB.95.205135.

[65] F. Calogero. Solution of a three-body problem in one dimension. *Journal of Mathematical Physics* **10**(12):2191–2196, 1969. https://doi.org/10.1063/1.1664820.

[66] F. Calogero. Ground state of a one dimensional N-body system. *Journal of Mathematical Physics* **10**(12):2197–2200, 1969. https://doi.org/10.1063/1.1664821.

[67] B. Sutherland. Quantum many-body problem in one dimension: Ground state. *Journal of Mathematical Physics* **12**(2):246–250, 1971. https://doi.org/10.1063/1.1665584.

QUANTIZATION OF RATIONALLY DEFORMED MORSE POTENTIALS BY WRONSKIAN TRANSFORMS OF ROMANOVSKI-BESSEL POLYNOMIALS

Gregory Natanson

AI-Solutions Silver Spring MD 20904, U.S.A.

correspondence: gregorynatanson@gmail.com

Abstract. The paper advances Odake and Sasaki's idea to re-write eigenfunctions of rationally deformed Morse potentials in terms of Wronskians of Laguerre polynomials in the reciprocal argument. It is shown that the constructed quasi-rational seed solutions of the Schrödinger equation with the Morse potential are formed by generalized Bessel polynomials with degree-independent indexes. As a new achievement we can point to the construction of the Darboux-Crum net of isospectral rational potentials using Wronskians of generalized Bessel polynomials with no positive zeros. One can extend this isospectral family of solvable rational potentials by including 'juxtaposed' pairs of Romanovski-Bessel polynomials into the aforementioned polynomial Wronskians which results in deleting the corresponding pairs of bound energy states.

Keywords: Translationally form-invariant Sturm-Liouville equation, generalized Bessel polynomials, Romanovski-Bessel polynomials, rational Darboux-Crum transformations, polynomial Wronskians.

1. Introduction

In recent publication [1] Alhaidari pointed to a new form of 'quasi-rational' [2] solutions (q-RSs) of the Schrödinger equation with the Morse potential in terms of generalized Bessel polynomials [3–6], instead of using the conventional q-RSs composed of weighted Laguerre polynomials [7–11]; though, to be more accurate, the possibility to quantize the Morse potential by Romanovski-Bessel (R-Bessel) polynomials [12, 13] has been already recognized by Quesne [14], with reference to Cotfas' papers [15, 16] (see also [17]). It should be also emphasized that Odake and Sasaki in their in-depth study [18, 19] on rational Darboux-Crum [20, 21] transforms (RDC$\mathscr{T}$s) of translationally shape-invariant (TSI) potentials did implicitly express eigenfunctions of the Morse potential in terms of R-Bessel polynomials with *degree-independent* indexes as a substitute for commonly used classical Laguerre polynomials [22]. (Though the Bochner-type differential equation for generalized Bessel polynomials was also listed in Table 1 in [7] on the line linked to the Morse potential the authors used the conventional representation for eigenfunctions [22] to construct rationally deformed Morse potentials.)

The remarkable feature of the new rational realization for the Morse oscillator is that the resultant rational canonical Sturm-Liouville equation (RCSLE) can be converted by an *energy-independent* gauge transformation to the Bochner-type eigenequation with a linear coefficient function of the first derivative *independent of degrees of sought-for polynomial solutions.* Using terminology of our recent study [23] on translationally form-invariant (TFI) CSLEs this implies that the given RCSLE belongs to TFI Group A and we should give full credit to Odake and Sasaki[18, 19] who initially came up with this breakthrough idea to treat the Morse oscillator as a rational TSI potential of Group A.

Keeping in mind that the TFI equation under consideration has only two basic solutions the net of its RDC$\mathscr{T}$s is uniquely specified by a single series of Maya diagrams [24] and therefore any rationally deformed Morse potential can be re-expressed in terms the Wronskian of generalized Bessel polynomials with a *common* degree-independent index, as it has been done in [19] though in slightly different terms. The novel representation of seed eigenfunctions [19] is in a sharp contrast with their conventional representation in terms of classical Laguerre polynomials with *degree-dependent* indexes [10, 11].

The main purpose of this work is to present new simplified expressions for eigenfunctions of the Schrödinger equation with a rationally deformed Morse potential by re-writing them in terms of *finite* exceptional orthogonal polynomial (EOP) sequences formed by Wronskian transforms of R-Bessel polynomials.

2. TFI Sturm-Liouville equations

2.1. Liouville-Darboux transformations

Let $\phi_\tau[\xi;Q]$ be a solution of the generic CSLE

$$\left\{\frac{d^2}{d\xi^2}+I^0[\xi;Q]+\varepsilon_\tau(Q)\rho[\xi]\right\}\phi_\tau[\xi;Q]=0 \tag{1}$$

at an energy $\varepsilon_\tau(Q)$, where the index τ specifies the factorization function (FF) in question. In the problems of our current interest $I^0[\xi;Q]$ is a rational function of ξ termed 'reference polynomial fraction' (RefPF). We prefer to keep this notation in the general case when $I^0[\xi;Q]$ is an arbitrarily chosen real function of ξ also dependent on some parameters Q. We will replace Q by $\vec{a},b$ after restricting the analysis solely to TFI CSLEs. In [23] we identified four families of RefPFs associated with rational TSI potentials termed 'Jacobi', 'Laguerre', 'Routh' and 'Bessel' (or $\mathscr{J}$Ref, $\mathscr{L}$Ref, $\mathscr{R}$Ref, and $\mathscr{B}$Ref for briefness) so the corresponding q-RSs are composed of polynomials (with degree-dependent indexes in general) from one of four conventional differential polynomial systems (DPSs) [25, 26]. The density function $\rho[\xi]$ plays a crucial role in our analysis because, as indicated by Eq. (4) below, it determines the change of variable converting CSLE (1) to the Schrödinger equation [27, 28].

It was Rudjak and Zakhariev [29] who extended the intertwining technique [30] from the Schrödinger equation to the CSLE. Here we however use a slightly different definition of the socalled [31, 32] 'generalized' Darboux transformations introducing them via the requirement that the function

$${}^*\phi_\tau[\xi;Q]\propto\rho^{-1/2}[\xi]/\phi_\tau[\xi;Q] \tag{2}$$

is a solution of the transformed CSLE at the same energy $\varepsilon_\tau(Q)$, i.e.,

$$\left\{\frac{d^2}{d\xi^2}+I^0[\xi;Q\mid\tau]+\varepsilon_\tau(Q)\rho[\xi]\right\}\ {}^*\phi_\tau[\xi;Q]=0. \tag{3}$$

Rudjak and Zakhariev's reciprocal formula (2) thus plays a crucial role in our approach to the theory of TFI CSLEs.

Since various authors give the term *'generalized Darboux transformation'* completely different meanings it seems preferable to refer to these operations as *'Liouville-Darboux'* transformations keeping in mind that they can be performed in three sequential steps:

(1.) The Liouville transformation $\xi(x)$:

$$\xi'(x)=\rho^{-1/2}[\xi(x)] \tag{4}$$

from the CSLE

$$\left\{\frac{d^2}{d\xi^2}+I^0[\xi;Q]+\varepsilon\rho[\xi]\right\}\Phi[\xi;Q;\varepsilon]=0 \tag{5}$$

to the stationary 1D Schrödinger equation with the potential [27, 28]

$$V[\xi(x);Q]=-\rho^{-1}[\xi(x)]I^0[\xi(x);Q]-1/2\,\{\xi,x\} \tag{6}$$

where $\{\xi,x\}$ stands for the 'Schwarzian derivative';

(2.) the Darboux deformation of Liouville potential (6) using the FF

$$\psi_\tau(x;Q)=\rho^{1/4}[\xi(x)]\phi_\tau[\xi(x);Q]; \tag{7}$$

(3.) reverse Liouville transformation from the Schrödinger equation to the new CSLE

$$\left\{\frac{d^2}{d\xi^2}+I^0[\xi;Q\mid\tau]+\varepsilon\rho[\xi]\right\}\Phi[\xi;Q;\varepsilon\mid\tau]=0. \tag{8}$$

Obviously any TFI theorem proven for Liouville-Darboux transformations of CSLE (5) can be directly applied to the resultant Liouville potential thus linking the new technique to the conventional Darboux-Crum theory of TSI potentials [11, 19, 33].

2.2. Translational from-invariance of Sturm-Liouville equation

We call a CSLE 'translationally form-invariant' if it has two 'basic' solutions $\phi_{+,0}[\xi, \vec{a}, b]$ and $\phi_{-,0}[\xi, \vec{a}, b]$

$$\left\{ \frac{d^2}{d\xi^2} + I^0[\xi; \vec{a}, b] + \varepsilon_{\pm,0}(\vec{a}, b)\rho[\xi] \right\} \phi_{\pm,0}[\xi; \vec{a}, b] = 0 \tag{9}$$

related via the following reciprocal formulas:

$$\phi_{\pm,0}[\xi; \vec{a} \pm \vec{1}, b] = \rho^{-1/2}[\xi]/\phi_{\pm,0}[\xi; \vec{a}, b]. \tag{10}$$

It has been proven [23] that

$$I^0[\xi; \vec{a}, b \mid \pm, 0] = I^0[\xi; \vec{a} \pm \vec{1}, b] + \mathscr{E}_{\pm 1}(\vec{a}, b)\rho[\xi], \tag{11}$$

where

$$\mathscr{E}_{\pm 1}(\vec{a}, b) \equiv \varepsilon_{\mp,0}(\vec{a} \pm \vec{1}, b) - \varepsilon_{\pm,0}(\vec{a}, b). \tag{12}$$

The Liouville transformations of the CSLEs with zero-energy free terms $I^0[\xi; \overline{a}, b]$ and $I^0[\xi; \overline{a}, b \mid \pm, 0]$ then brings us to Gendenshtein's conventional definition of a TSI potential [34]

$$V[\xi; \vec{a}, b \mid +, 0] = V[\xi; \vec{a} + \vec{1}, b] - \mathscr{E}_{+1}(\vec{a}, b) \tag{13}$$

or

$$V[\xi; \vec{a}, b \mid -, 0] = V[\xi; \vec{a} - \vec{1}, b] - \mathscr{E}_{-1}(\vec{a}, b) \tag{14}$$

depending on which basic solution $\phi_{+,0}[\xi; \vec{a}, b]$ or $\phi_{-,0}[\xi; \vec{a}, b]$ represents the lowest energy eigenfunction.

Note that the Russian word 'форма' used by Gendenshtein [34] has two meanings 'form' and 'shape'. The term 'form invariant' with reference to CSLEs was adopted by us from the English translation of Gendenshtein's joint paper with Kreve [35] while the commonly accepted term 'shape-invariance' is preserved for the corresponding Liouville potentials. The shift of the translational parameters $\vec{a}$ by 1 thus retains the analytical form of the TFI CSLE while preserving the 'shape' of its Liouville potential. It is true that the Liouville transformation of the TFI CSLE results in a 'translationally shape-invariant (TSI) potential. However the Class of TFI SLEs is defined via (10) with no reference to the associated Schrödinger equation.

2.3. Equivalence theorem for Darboux-Crum transforms of a TFI CSLE with two basic solutions

It has been proven [23] that any TFI CSLE has at least two infinite sets of solutions

$$\phi_{\pm,m+1}[\xi; \vec{a}, b] = \rho^{-1/2}[\xi] W[\xi; \vec{a} \pm \vec{1}, b \mid \mp, 0; \pm, m]/\phi_{\pm,0}[\xi; \vec{a} \pm \vec{1}, b], \tag{15}$$

where

$$W[\xi; \vec{a}, b \mid \pm, m; \mp, m'] \equiv W\left\{ \phi_{\pm,m}[\xi; \vec{a}, b] \phi_{\mp,m'}[\xi; \vec{a}, b] \right\}. \tag{16}$$

The cited 'raising' recurrence relations can be conveniently re-written as

$$f_{\pm,m+1}[\xi; \vec{a} \pm \vec{1}; b] = \dot{f}_{\pm,m}[\xi; \vec{a}, b], \tag{17}$$

where

$$f_{\pm,m+1}[\xi; \vec{a}, b] \equiv \phi_{\pm,m}[\xi; \vec{a}, b]/\phi_{\mp,0}[\xi; \vec{a}, b] \tag{18}$$

and dot denotes the first derivative with respect to ξ.

The solutions $\phi_{\pm,m}[\xi; \vec{a}, b]$ also obey the ´lovering´ recurrence relations:

$$\begin{aligned} &\phi_{\pm,m}[\xi; \vec{a}, b] \equiv \rho^{-1/2}[\xi] w[\xi; a, b \mid \pm\dot{:}0, m]/\phi_{\pm,0}[\xi; \vec{a}, b] = \\ &= -\mathscr{E}_{\pm,m-1}(\vec{a} \pm \vec{1}, b)\phi_{\pm,m-1}[\xi; \vec{a} \pm \vec{1}; \vec{b}] \quad \text{for} \quad m \geq 1, \end{aligned} \tag{19}$$

where

$$\mathscr{E}_{\pm,m}(\vec{a}, b) \equiv \varepsilon_{\pm,m}(\vec{a}, b) - \varepsilon_{\mp,0}(\vec{a}, b). \tag{20}$$

Solutions from both infinite sets can be then used as seed functions for Darboux-Crum transformations (DCTs) of the given TFI CSLE which results in an infinite net of solvable SLEs specified by a single series of Maya

diagrams [24]. Following the arguments presented in [33] for rationally deformed TSI potentials we [23] proved that any CSLE in this net can obtained using only seed solutions of the same type.

Let us parametrize a set of seed functions of the same type,

$$\overline{M}(\overline{\Delta}_{1\to L}) = m_1, \ldots, m_{|\overline{\delta}_{1\to L}|}, \tag{21}$$

by two partitions of an equal size L:

$$\overline{\Delta}_{1\to L} \equiv \overline{\delta}_{1\to L}; \overline{\delta'}_{1\to L} \tag{22}$$

such that

$$m_k = \delta'_1 + k - 1 \quad \text{for} \quad 1 < k \le \overline{\delta}_1, \tag{23}$$

$$m_{|\overline{\delta}_{1\to l-1}|+1} = m_{|\overline{\delta}_{1\to l-1}|} + \delta'_l + 1 = \mid \overline{\Delta}_{1\to l-1} \mid + \delta'_l + 1 \quad \text{for} \quad 1 < l \le L, \tag{24}$$

$$m_{|\overline{\delta}_{1\to l-1}|+k} = m_{|\overline{\delta}_{1\to l-1}|+1} + k - 1 \quad \text{for} \quad 1 < l \le L, 1 < k \le \overline{\delta}_l, \tag{25}$$

One can easily verify that the largest element in partition (21) coincides with the sum of the partition lengths $\mid \overline{\delta}_{1\to L} \mid$ and $\mid \overline{\delta'}_{1\to L} \mid$, i.e.,

$$m_{|\overline{\delta}_{1\to L}|} = \mid \overline{\Delta}_{1\to L} \mid \equiv \mid \overline{\delta}_{1\to L} \mid + \mid \overline{\delta'}_{1\to L} \mid . \tag{26}$$

It has been proved in [23] that use of the conjugated set of seed solutions of opposite type,

$$\overline{\Delta'}_{L\to 1} \equiv \overline{\delta'}_{L\to 1}; \overline{\delta}_{L\to 1} \equiv \delta'_L, \delta'_{L-1}, \ldots, \delta'_1; \delta_L, \delta_{L-1}, \ldots, \delta_1, \tag{27}$$

results in an equivalent CSLE so the corresponding Liouville potential $V[\xi; \vec{a}^{(\delta)}, b \mid \mp, \overline{M}(\overline{\Delta'}_{L\to 1})]$ computed at shifted values of the translational parameters,

$$\vec{a}^{(\delta)} \equiv \vec{a} + \delta \vec{1}, \tag{28}$$

where δ is a nonzero integer, differs from the Liouville potential $V[\xi; \vec{a}, b \mid \pm, \overline{M}(\overline{\Delta'}_{1\to L})]$ only by a zero-point energy.

In [23] we have derived the following relation between the Wronskians of two equivalent sets of seed solutions of the same type

$$\begin{aligned} &\frac{w[\xi; \vec{a}, b \mid +\vdots \overline{M}(\overline{\Delta}_{1\to L})]}{\rho^{1/4|\overline{\delta}_{1\to L}|(|\overline{\delta}_{1\to L}|-1)}[\xi] \prod_{l=1}^{L} \chi_{-\delta_l}[\xi; \vec{a}^{(|\overline{\Delta'}_{l\to 1}|-\delta_l)}, b]} \\ &\propto \frac{w[\xi; \vec{a}^{(|\overline{\Delta'}_{L\to 1}|)}, b \mid -\vdots \overline{M}(\overline{\Delta'}_{L\to 1})]}{\rho^{1/4|\overline{\delta'}_{L\to 1}|(|\overline{\delta'}_{L\to 1}|-1)}[\xi] \prod_{l=1}^{L} \chi_{\delta_l}[\xi; \vec{a}^{(|\overline{\Delta'}_{l-1\to 1}|+\delta'_l)}, b]}, \end{aligned} \tag{29}$$

where

$$\chi_{\mp|N|}[\xi; \vec{a}, b] \equiv \prod_{k=0}^{|N|-1} \phi_{\pm,0}[\xi; \vec{a}^{(\pm k)}, b]. \tag{30}$$

For any CSLE from Group A the derived relation turns into the equivalence relations between the Wronskians of the corresponding seed polynomials discovered in the breakthrough paper by Odake and Sasaki [19]. We illuminate these relations in more details in subsection 3.4 below using Wronskians of generalized Bessel polynomials as an example.

If the given rational TSI potential has only a finite number of eigenfunctions then the set of seed functions $+, m$ or $-, m$ which starts from these eigenfunctions ($-, m$ in case of our current interest) also contains infinitely many q-RSs vanishing at only one quantization end (*virtual state wavefunctions* in Odake and Sasaki's terms [18, 19]), with the Gendenshtein (Scarf II) potential [34] as the sole exception (including its symmetric limit represented by the sech-squared potential well). The DCTs using nodeless q-RSs of the selected type results in a net of isospectral potentials. Therefore, except for the Gendenshtein potential, we don't need to include '*state-inserting*' solutions (*'pseudo-virtual state wave functions*' in Odake and Sasaki's terms) into the given set of seed functions– a remarkable corollary of the 'extended' Krein-Adler theorem [11].

If the given partition $\overline{\Delta}_{1\to L}$ is composed of alternating even and odd integers staring from an even integer δ'_1 then all the integers

$$\delta'_l = m_{|\overline{\delta}_{1\to 1}|+1} - m_{|\overline{\delta}_{1\to 1}|} - 1 > 0 \quad \text{for any} \quad l < L \tag{31}$$

must be also even which implies that the set of seed solutions $\pm, \overline{M}(\overline{\Delta}'_{L\to 1})$ is composed of L segments of even lengths [11, 19] or in other words is formed by 'juxtaposed' [36–38] pairs of seed solutions $\pm, m', \pm, m'+1$. Similarly if the set of seed solutions, $\pm, \overline{M}(\overline{\Delta}')_{L\to 1}$ is formed by 'juxtaposed' pairs of seed solutions $\pm, m, \pm, m+1$ then the conjugated set is formed by seed solutions $\mp, m'$ with only even gap lengths, again starting from an even number. We refer the reader to subsection 3.4 below for a scrupulous analysis of this issue in connection with juxtaposed pairs of eigenfunctions of the Schrödinger equation with the Morse potential in the $\mathscr{B}$Ref representation [19].

3. Quantization of rationally deformed Morse potentials by Wronskian transforms of R-Bessel polynomials

3.1. Schrödinger equation with Morse potential in Bessel form

In this paper we focus solely on the TFI CSLE

$$\left\{\frac{d^2}{dy^2} + I^0[y;a] + \varepsilon_\infty \rho_\diamond[y]\right\}_\infty \Phi[y;a;\varepsilon] = 0 \tag{32}$$

with the RefPF

$$I^0[y;a] = 2ay^{-3} - y^{-4} + 1/4y^{-2} \tag{33}$$

and the density function

$${}_\infty\rho_\diamond[y] \equiv {}_\infty\sigma^{-1}[y] = y^{-2} \tag{34}$$

One can directly verify that CSLE (32) has a pair of 'basic' solutions

$${}_\infty\phi_{\pm,0}(y;a) = y^{1\pm a}e^{\pm 1/y} \ (y>0) \tag{35}$$

at the energies

$${}_\infty\varepsilon_{\pm,0}(a) = -(a\pm 1/2)^2. \tag{36}$$

Examination of solutions (35) shows that they obey the following symmetry relations

$${}_\infty\phi_{\pm,0}[y;a+k] = y^{\pm k}{}_\infty\phi_{\pm,0}[y;a] \tag{37}$$

for any integer k and

$${}_\infty\phi_{+,0}(y;a){}_\infty\phi_{-,0}(y;a) = y^2 \tag{38}$$

whereas the function

$$f_{\pm,0}[\xi;\overrightarrow{a},b] \equiv \phi_{\mp,0}[\xi;\overrightarrow{a},b]/\phi_{\pm,0}[\xi;\overrightarrow{a},b] \tag{39}$$

takes form

$${}_\infty f_{\pm,0}[\xi;a] \equiv y^{\mp 2a}e^{\mp 2/y}. \tag{40}$$

We thus proved that the pair of basic solutions in question satisfy the TFI condition [23]

$${}_\infty\phi_{\mp,0}[y;a\pm 1] = {}_\infty\rho_\diamond^{-1/2}[y]/{}_\infty\phi_{\pm,0}(y;a). \tag{41}$$

One can directly verify that

$${}_\infty\varepsilon_{\mp,0}(a\pm 1) = {}_\infty\varepsilon_{\pm,0}(a) \tag{42}$$

and thereby

$${}_\infty\mathscr{E}_{\pm 1}(a) \equiv {}_\infty\varepsilon_{\mp,0}(a\pm 1) - {}_\infty\varepsilon_{\pm,0}(a) = 0 \tag{43}$$

so the symmetry condition [23]

$$\mathscr{E}_{\mp 1}(a\pm 1) = -\mathscr{E}_{\pm 1}(a). \tag{44}$$

trivially holds.

The gauge transformations

$${}_\infty\Phi[y;a;\varepsilon] = {}_\varepsilon\phi_\pm[y;a]{}_\infty F_\pm[y;a;\varepsilon] \tag{45}$$

convert CSLE (32) to a pair of Bochner-type eigenequations

$$\left\{y^2\frac{d^2}{dy^2} + {}_\infty\tau_\pm[y;a]\frac{d}{dy} + [\varepsilon -_\infty \varepsilon_{\pm,0}(a)]\right\}_\infty F_\pm[y;a;\varepsilon] = 0, \tag{46}$$

with

$${}_\infty\tau^\pm[y;a] = 2(1\pm a)y \mp 2. \tag{47}$$

We define generalized Bessel polynomials as

$$Y_n^{(\alpha,\beta)}(y) \equiv Y_n^{(\alpha)}(y/\beta), \tag{48}$$

where the polynomial $Y_n^{(\alpha)}(x)$ is given by (2) in [4] and thereby coincides with polynomial (9.13.1) in [6]

$$Y_n^{(\alpha)}(x) \equiv y_n(x;\alpha). \tag{49}$$

Note that Chihara's relation (4.3) in [5] is apparently based on Brafman's definition [39] for the polynomial $y_n(x;\alpha,\beta)$ such that $y_n(x;\alpha+2,2) = y_n(x;\alpha)$. Adding the second index to the conventional notation [4, 5] allows us to avoid uncertainties in the definition of the variable used to differentiate a polynomial in the reflected argument, keeping in mind that

$$Y_n^{(\alpha)}(-y) \equiv Y_n^{(\alpha,-2)}(y). \tag{50}$$

Eq. (37) for the Bessel DPS in [40] thus corresponds to the polynomials $Y_n^{(\alpha-2,\beta)}(y)$ in our terms. (We prefer to preserve symbol 'B' for their orthogonal subset composed of R-Bessel polynomials [12, 13].) It is also worth mentioning that Alhaidari [1] introduced a slightly modified notation for generalized Bessel polynomials:

$$J_n^a(1/2y) \equiv Y_n^{(2a)}(y) = (2n+2a)_n (y/2)^n {}_1F_1(-n;-2a-n;2/y), \tag{51}$$

with the Pochhammer symbol $(a)_n$ standing for the *falling* factorial. And indeed it would be possibly more convenient to use the parameter a as the polynomial index keeping in mind that the forward and backward shift relations change the polynomial index by 1. However we prefer to stick to the more conventional notation.

The basic solution ${}_\infty\phi_{\pm,0}[y;a]$ is thus nothing but a constant solution of eigenequation (46) converted back by gauge transformation (45). Similarly the reverse gauge transformation of each of the DPSs composed of polynomials $Y_m^{(\pm 2a,\mp 2)}(y)$ results in pairs of infinite sequences of q-RSs of CSLE (32):

$${}_\infty\phi_{\pm,m}[y;a] = {}_\infty C_{\pm,m}(a)\, {}_\infty\phi_{\pm,0}[y;a] Y_m^{(\pm 2a,\mp 2)}(y). \tag{52}$$

The multiplier ${}_\imath C_{\pm,m}$ will be chosen below in such a way that q-RSs (52) satisfy recurrence relations (15). The crucial advantage of expressing q-RSs in terms of generalized Bessel polynomials, instead of Laguerre polynomials [7–11], is that the weight function ${}_\infty\phi_{\pm,0}[y;a]$ in the right-hand side of (52) does not depend on the polynomial degree – the direct consequence of the fact that the given TFI CSLE belongs to Group A [18, 19, 23], in contrast with the conventional representation of eigenfunctions of the Schrödinger equation with the Morse potential in terms of classical Laguerre polynomials [22].

According to the general theory of Bochner-type eigenequations [41] differential equation (46) has a polynomial solution of degree m at

$$\varepsilon = {}_\infty\varepsilon_{\pm,m}(a) = {}_\infty\varepsilon_{\pm,0}(a) - m[2(1\pm a)+m-1], \tag{53}$$

which, coupled with (36), gives

$${}_\infty\varepsilon_{\pm,m}(a) = -(m+1/2\pm a)^2. \tag{54}$$

This brings us to the simplified version of the raising ladder relations [23] for the energies of q-RSs (15):

$${}_\infty\varepsilon_{\pm,m+1}(a) = {}_\infty\varepsilon_{\pm,m}(a\pm 1) \tag{55}$$

with $\mathscr{E}_{\pm 1}(a) \equiv 0$.

To be historically accurate, it is worth mentioning that Cotfas' Eq. (10) in [16] with the leading coefficient $\sigma(s) = s^2$ does list Al-Salam's [4] formula

$$Y_n^{(\alpha)}(y) = n!\,(-y/2)^n L_n^{(-\alpha-2n-1)}(2/y) \tag{56}$$

for the generalized Bessel polynomials in terms of Laguerre polynomials in the reciprocal argument $2/y$ (though without mentioning the former polynomials by name). Actually Cotfas discusses only eigenfunctions of the corresponding Sturm-Liouville problem so the cited formula specifies R-Bessel polynomials expressed in terms of classical Laguerre polynomials in $2/y$:

$$B_n^{(A)}(y) \equiv Y_n^{(-2A-1)}(y) = n!\,(-y/2)^n L_n^{(2A-2n)}(2/y) \quad \text{for} \quad n<A, \tag{57}$$

with Cotfas' parameter α standing for $1-2A$ here. The remarkable feature of this finite subsequence of generalized Bessel polynomials is that the polynomials in question are orthogonal on the positive semi-axis as prescribed by orthonormality relations (9.13.2) in [6]:

$$\int_0^\infty {}_\infty\rho_\diamond[y]\, {}_\infty\phi^2_{-,0}[y;A+1/2] B_n^{(A)}(y) B_{\underset{\sim}{n}}^{(A)}(y)dy \equiv \int_0^\infty y^{-2A-1}e^{-2/y} B_n^{(A)}(y) B_{\underset{\sim}{n}}^{(A)}(y)dy = \frac{n!\,\Gamma(2A+1-n)}{2A-2n-1}\delta_{n\underset{\sim}{n}}. \tag{58}$$

Making use of (39) we can represent backward shift relation (9.13.8) in [6] as

$$\frac{d}{dy}\left[{}_\infty f_{+,0}[\,\xi;a]\; Y_m^{(-2a,2)}(y)\right] = 2\,{}_\infty f_{+,0}[\xi;a+1]Y_{m+1}^{(-2a-2,2)}(y) \tag{59}$$

so the functions

$${}_\infty f_{+,m}[\xi;a] = {}_\infty C_{-,m}(a)\,{}_\infty f_{\infty,0}[\xi;a]Y_m^{(-2a)}(y) \tag{60}$$

satisfy raising relation (17) provided we choose

$${}_\infty C_{-,m+1}(a) = 2\,{}_\infty C_{-,m}(a-1) \equiv 2^{m+1} \tag{61}$$

keeping in mind that ${}_\infty C_{-,0}(a) \equiv 1$.

Substituting (54) into (20) gives

$${}_\infty\mathscr{E}_{-,m-1}(a-1) = -m(m+1-2a) \tag{62}$$

so recurrence relation (19) can be re-written as

$$2^m y\dot{Y}_m^{(-2a,2)}(y) = m(m+1-2a)\,{}_\infty\phi_{-,m-1}[y;a-1]/{}_\infty\phi_{-,0}[y;a]. \tag{63}$$

Combining (52), (61), and (37) with $k=1$ brings us to 'forward shift operator' (9.13.6) in (6)

$$\dot{Y}_m^{(-2a,2)}(y) = 0.5m(m+1-2a)Y_{m-1}^{(2-2a,2)}(y). \tag{64}$$

To formulate the Sturm-Liouville problem of our interest it is worthy to convert CSLE (32) to its 'prime' [42] form at ∞ using the gauge transformation

$${}_\infty\Psi\,[y;a;\varepsilon] = y^{-1/2}\,{}_\infty\Phi[y;a;\varepsilon] \tag{65}$$

and then to solve the resultant RSLE

$$\left\{\frac{d}{dy}y\frac{d}{dy} - y^{-3} + 2ay^{-2} + \varepsilon y^{-1}\right\}{}_\infty\Psi\,[y;a;\varepsilon] = 0 \tag{66}$$

under the Dirichlet boundary conditions (DBCs):

$$\lim_{y\to 0}\,{}_\infty\Psi\,[y;a;\varepsilon_n] = \lim_{y\to\infty}\,{}_\infty\Psi\,[y;a;\varepsilon_n] = 0. \tag{67}$$

The main advantage of converting CSLE (32) to its prime form with respect to the *regular* singular point at infinity comes from our observation [42] that the characteristic exponents for this singular end have opposite signs and therefore the corresponding principal Frobenius solution is unambiguously selected by the DBC. Prime RSLE (66) can be also re-written in the form of the 'algebraic' [42] Schrödinger equation

$$\left\{y\frac{d}{dy}y\frac{d}{dy} - y^{-2} + 2ay^{-1} + \varepsilon\right\}{}_\infty\Psi\,[y;a;\varepsilon] = 0. \tag{68}$$

(As discussed in the following subsections this is the common remarkable feature of RCSLEs with density function (34) assuming that the singular point at infinity is regular.) Reformulating the given spectral problem in such a way allows us to take advantage of powerful theorems proven in [43] for zeros of principal solutions of SLEs solved under the DBCs at singular ends.

The eigenfunctions of RSLE (66) thus take form

$${}_\infty\psi_{-,n}\,[y;a] = y^{-1/2}\,{}_\infty\phi_{-,n}[y;a] = 2^n y^{1/2-a}e^{-1/y}B_n^{(a-1/2)}(y) \quad \text{for} \quad n=0,\ldots,N(a). \tag{69}$$

One can then directly verify that each eigenfunction obeys the DBC at both singular ends. Since R-Bessel polynomials (57) form an orthogonal sequence the eigenfunction ${}_\infty\psi_{-,n}\,[y;a]$ must have exactly n nodes and therefore [43] the sequence of eigenfunctions (69) corresponds to $\lceil A\rceil = N(a)+1$ lowest eigenvalues of RSLE (66) with

$$N(a) = \lfloor a-1/2\rfloor \equiv \lfloor A\rfloor. \tag{70}$$

Note also that eigenfunctions (69) are orthogonal with the weight y^{-1} and that any solution normalizable with this weight must vanish at infinity.

The presented argumentation does not exclude existence of eigenfunctions with the number of nodes larger than $N(a)-1$. To confirm that the problem in question is indeed *exactly* solvable one can simply take advantage of the conventional analysis of the Schrödinger equation with the Morse potential [22] in the $\mathscr{L}$Ref representation.

The reader can argue that the problem must be exactly solvable since the Morse potential is TSI. However the author [44] has an issue with this assertion. Though the Gendenshtein's claim [34] concerning the *exact* solvability of shape-invariant potentials is most likely correct it has been never accurately proven to our knowledge. The catch is that Gendenshtein's arguments decreasing the translational parameter a one by one bring us to the Sturm-Liouville problem with $\mid a \mid < 1/2$ and then we still need to prove that the resultant SLE has no discrete energy spectrum.

The change of variable $y(x) = e^x$ converts $\mathscr{B}$Ref CSLE (32) into the Schrödinger equation with the Morse potential ${}_\infty V[y(x); a]$, where

$$ {}_\infty V[y; a] = -y^2 I^0[y; a] + 1/4 \tag{71} $$

$$ = -2ay^{-1} + y^{-2}. \tag{72} $$

Comparing (72) with (1) in [10] shows that ${}_\infty V[y(x); A + 1/2] = V_{A,1}(x)$ in Quesne's notation.

According to the general theorem presented in [43] for *singular* SLEs solved under the DBCs any principal solution ${}_\infty \not\psi_{-,\mathbf{m}}[y; a]$ near the singular end point $y = 0$ has nodes at the positive semi-axis iff it lies above the ground energy level. Examination of the inequality

$$ {}_\infty\varepsilon_{-,\mathbf{m}}(a) < {}_\infty\varepsilon_{-,0}(a) \tag{73} $$

thus shows that the q-RS ${}_\infty \not\psi_{-,\mathbf{m}}[y; a]$ with $\mathbf{m} \neq 0$ preserves its sign on the positive semi-axis iff

$$ \mathbf{m} > 2a - 1 = 2A \tag{74} $$

(cf.(12) in [10]). It will be proven in next subsection that one can use any combination of admissible q-RSs ${}_\infty \not\psi_{-,\mathbf{m}}[y; a]$ as seed functions to construct an *exactly solvable* RDC$\mathscr{T}$ of the $\mathscr{B}$Ref CSLE.

According to (9.13.1) in [6]

$$ Y_m^{(-2a,+2)}(y) = 2^{-m}(2m - 2a)_m \hat{Y}_m^{(-2a,+2)}(y) \tag{75} $$

where, in following [5], we use hut to indicate that the polynomial in question is written in its monic form. It is essential that the multiplier

$$ (2m - 2a)_m = \prod_{l=0}^{m-1}(2m - 2a - l) = \prod_{l'=1}^{m}(m - 2a + l') \tag{76} $$

necessarily differs from 0 if either $2m - 2a < -1$ (R-Bessel polynomials) or $m = \mathbf{m} > 2a - 1$ (generalized Bessel polynomials with no positive zeros) so the polynomial degree is equal to m in both cases of our primary interest.

3.2. RDC$\mathscr{T}$s of principal solutions near singular end points

Using an arbitrary set $\overline{M}_p = m_1, \ldots, m_p$ of seed functions ${}_\infty\phi_{\pm,m_k}[y; a]$ of the same type ($0 < m_k < m_{k+1}$ for $k = 1, \ldots, p-1$) we can represent the corresponding RDC$\mathscr{T}$ of $\mathscr{B}$Ref CSLE (32) as

$$ \left\{ \frac{d^2}{dy^2} + {}_\infty I^0[y; a \mid \pm\dot{:}\overline{M}_p] + \varepsilon y^{-2} \right\} {}_\infty\Phi[y; a; \varepsilon \mid \pm\dot{:}\overline{M}_p] = 0, \tag{77} $$

where

$$ {}_\infty I^0[y; a \mid \dot{:}\overline{M}_p] = {}_\infty I^0[y; a] + \frac{2}{y}\frac{d}{dy}(y\ ld {}_\infty w[y; a \mid \pm\dot{:}\overline{M}_p]) \tag{78} $$

with

$$ {}_\infty w[y; a \mid \pm\dot{:}\overline{M}_1] \equiv {}_\infty\phi_{\pm,m_1}[y; a], \tag{79} $$

$$ {}_\infty w[y; a \mid \pm\dot{:}\overline{M}_p] \equiv W\left\{ {}_\infty\phi_{\pm,m_1}[y; a], \ldots, {}_\infty\phi_{\pm,m_p}[y; a] \right\} \quad \text{for} \quad p > 1, \tag{80} $$

and the symbolic expression ld standing for the logarithmic derivative. When deriving (78) we also took into account that the so-called [42] 'universal correction'

$$ \Delta I\left\{\rho(y)\right\} \equiv 0.5\sqrt{\rho(y)}\frac{d}{dy}\frac{ld\ \rho(y)}{\sqrt{\rho(y)}} \tag{81} $$

in Schulze-Halberg's [45] generic formula for zero-energy free term of the transformed CSLE vanishes in the case of our current interest: $\rho(y) = y^{-2}$.

The common remarkable feature of Wronskians (80) for TFI CSLEs from group A (originally noticed by Odake and Sasaki [19] in their scrupulous study on RDC$\mathscr{I}$s of the corresponding TSI potentials) is that each can be represented as the weighted polynomial Wronskian

$$ {}_\infty w[y;a \mid \pm\dot{:}\overline{M}_p] = {}_\infty\phi^p_{\pm,0}[y;a]\,{}_\infty\mathfrak{W}_{\mathfrak{N}_{\overline{M}_p}}[y;a \mid \pm\dot{:}\overline{M}_p], \tag{82} $$

where the Wronskian

$$ {}_\infty\mathfrak{W}_{\mathfrak{N}_{\overline{M}_p}}[y;a \mid \pm\dot{:}\overline{M}_p] \equiv W\left\{Y^{(\pm 2a,\mp 2)}_{m_1}(y),\dots,Y^{(\pm 2a,\mp 2)}_{m_p}(y)\right\} \tag{83} $$

is a polynomial of degree

$$ \mathfrak{N}_{\overline{M}_p} = \mid \overline{M}_p \mid -0.5p(p-1) \tag{84} $$

(see (61) in [19]). When it seems appropriate we will drop the index specifying the degree of polynomial Wronskians in question. Substituting (82) into (78), coupled with (33) and (35), one finds

$$ {}_\infty I^0[\, y;a \mid \pm\dot{:}\overline{M}_p] \;= 2(a\pm p)y^{-3} - y^{-4} + 1/4y^{-2} + \frac{2}{y}\frac{d}{dy}\left(\, y\; ld_\infty\mathfrak{W}[y;a \mid \pm\dot{:}\overline{M}_p]\right)\,. \tag{85} $$

Each RCSLE under consideration can be alternatively obtained via sequential RDTs with the FFs

$$ {}_\infty\Phi_{\pm,m_{\tilde{p}}}[y;a \mid \pm\dot{:}\overline{M}_{\tilde{p}-1}] = y^{p-1}\frac{{}_\infty w[y;a \mid \pm\dot{:}\overline{M}_{\tilde{p}}]}{{}_\infty w[y;a \mid \pm\dot{:}\overline{M}_{\tilde{p}-1}]} \qquad (\tilde{p}=1,\dots,p) \tag{86} $$

so RefPFs (85) can be determined via the following sequence of recurrence relations

$$ {}_\infty I^0[y;a \mid \pm\dot{:}\overline{M}_p] = {}_\infty I^0[y;a \mid \pm\dot{:}\overline{M}_{p-1}] + \frac{2}{y}\frac{d}{dy}\left(\, y\; ld_\infty\Phi_{\pm,m_p}[y;a \mid \pm\dot{:}\overline{M}_{p-1}]\right) \tag{87} $$

(a natural extension of the renown Crum formulas [21] to the CSLEs).

For an arbitrary choice of the partition $\overline{M}_p$ RefPF (85) generally has poles on the positive semi-axis and therefore RCSLE (77) cannot be quantized analytically. So let us choose a set $\overline{\mathbf{M}}^{\pm}_p = \mathbf{m}^{\pm}_1,\dots,\mathbf{m}^{\pm}_p$ of seed solutions of the sane type, ${}_\infty\phi_{\pm,\mathbf{m}_k}[y;a]$ $(0 < \mathbf{m}_k = \mathbf{m}^{\pm}_k < \mathbf{m}_{k+1} = \mathbf{m}^{\pm}_{k+1}$ for $k = 1,\dots,p-1)$, in such a way that the seed function ${}_\infty\phi_{\pm,\mathbf{m}_1}[y;a]$ and all Wronskians ${}_\infty w[y;a \mid \pm\dot{:}\overline{\mathbf{M}}^{\pm}_{\tilde{p}}]$ for $\tilde{p} = 2,\dots,p$ preserve their sign on the positive semi-axis. In particular Odake and Sasaki [19] and nearly the same time Gomez-Ullate et al [11] constructed the subnet of rationally deformed Morse potentials

$$ {}_\infty V[y;a \mid +\dot{:}\overline{\mathbf{M}}^{+}_p] \;= {}_\infty V[y;a] \;+ y^2\left\{{}_\infty I^0[y;a] \;- {}_\infty I^0[y;a \mid +\dot{:}\overline{\mathbf{M}}^{+}_p]\;\right\} \tag{88} $$

using seed solutions infinite at both quantization ends. In next subsection we will introduce another subnet of rationally deformed Morse potentials

$$ {}_\infty V[y;a \mid -\dot{:}\overline{\mathbf{M}}^{-}_p] \;= {}_\infty V[y;a] \;+ y^2\left\{{}_\infty I^0[y;a] \;- {}_\infty I^0[y;a \mid -\dot{:}\overline{\mathbf{M}}^{-}_p]\;\right\} \tag{89} $$

constructed by means of FFs vanishing at the origin. The subnet starts from the potential ${}_\infty V[y;a \mid -\dot{:}\mathbf{m}]$ with a positive integer $\mathbf{m} > 2a-1$ – potential function (16) in [10] with $A = a - 1/2, B = 1$.

Substituting (82) into (86) and also making use of (37) with $k = p$, shows that RCSLE (77) has an infinite set of q-RSs

$$ {}_\infty\Phi_{\pm,m}[y;a \mid \pm\dot{:}\overline{M}_p] \;= {}_\infty\phi_{\pm,0}[y;a\pm p]\;\frac{{}_\infty\mathfrak{W}[y;a \mid \pm\dot{:}\overline{M}_p,m]}{{}_\infty\mathfrak{W}[y;a \mid \pm\dot{:}\overline{M}_p]}. \tag{90} $$

Apparently q-RS (90) with the label '$-$' represents the principal solution approaching 0 as $y^{\delta_-(\overline{M}_p)}e^{-1/y}$ in the limit $y \to +0$. On other hand q-RS (90) labelled by '$+$' infinitely grows as $y^{\delta_+(\overline{M}_p)}e^{1/y}$ in this limit. In both cases

$$ ld_\infty\Phi_{\pm,m}[y;a \mid \pm\dot{:}\overline{M}_p] \;\approx \mp y^{-2} \tag{91} $$

and consequently

$$ld\ {}^{*}\Phi_{\pm,m}[y;a \mid \pm\dot{:}\overline{M}_p] \equiv ld\ y - ld_{\infty}\Phi_{\pm,m}[y;a \mid \pm\dot{:}\overline{M}_p] \approx \pm y^{-2} \tag{92}$$

for $0 < y << 1$, where we dropped subscript ∞ in the notation of the FF for the reverse RDT:

$${}^{*}\Phi_{\pm,m}[y;a \mid \pm\dot{:}\overline{M}_p] \equiv y/{}_{\infty}\Phi_{\pm,m}[y;a \mid \pm\dot{:}\overline{M}_p]\ . \tag{93}$$

Note that the last summand in sum (85) has a simple pole at $y = 0$ so an arbitrary principal solution of RCSLE (77) near its irregular singular point at $y = 0$ can be approximated as

$${}_{\infty}\Phi_0[y;a;\varepsilon \mid \pm\dot{:}\overline{M}_p] \propto y^{\Delta_{\pm}(a;\overline{M}_p)}e^{-1/y} \quad \text{for} \quad y << 1, \tag{94}$$

where $\Delta_{\pm}(a;\overline{M}_p)$ stands for a *finite* power exponent which particular value is non-essential for our discussion. Examination of the quasi-rational function

$$\begin{gathered}{}_{\infty}\Phi_0[y;a;\varepsilon \mid \pm\dot{:}\overline{M}_{p+1}] = \frac{y\ W\left\{{}_{\infty}\Phi_{\pm,m_{p+1}}[y;a \mid \pm\dot{:}\overline{M}_p]\ ,{}_{\infty}\Phi_0[y;a;\varepsilon \mid \pm\dot{:}\overline{M}_p]\right\}}{{}_{\infty}\Phi_{\pm,m_{p+1}}[y;a \mid \pm\dot{:}\overline{M}_p]} = \\ y\ {}_{\infty}\dot{\Phi}_0[y;a;\varepsilon \mid \pm\dot{:}\overline{M}_p] - y\ ld_{\infty}\Phi_{\pm,m_{p+1}}[y;a;\mid \dot{:}\overline{M}_p]\ {}_{\infty}\Phi_0[y;a;\varepsilon \mid \pm\dot{:}\overline{M}_p]\end{gathered} \tag{95}$$

representing the RD$\mathscr{T}$ of the principal solution of RCSLE (77) near its irregular singular point at $y = 0$ confirms that it is a principal solution of the transformed RCSLE near the singular point in question. Vice versa the quasi-rational function

$$\begin{gathered}\frac{y\ W\left\{{}^{*}\Phi_{\pm,m_p}[y;a \mid \pm\dot{:}\overline{M}_p]\ ,{}_{\infty}\Phi_0[y;a;\varepsilon \mid \pm\dot{:}\overline{M}_{p+1}]\right\}}{{}^{*}\Phi_{\pm,m_{p+1}}[y;a \mid \pm\dot{:}\overline{M}_p]} = \\ y\ {}_{\infty}\dot{\Phi}_0[y;a;\varepsilon \mid \pm\dot{:}\overline{M}_{p+1}] - y\ ld^{*}\Phi_{\pm,m_{p+1}}[y;a \mid \pm\dot{:}\overline{M}_{p+1}]\ {}_{\infty}\Phi_0[y;a;\varepsilon \mid \pm\dot{:}\overline{M}_{p+1}]\end{gathered} \tag{96}$$

representing the reverse RD$\mathscr{T}$ of the principal solution (95) is the principal solution of RCSLE (77) near its irregular singular point at $y = 0$.

To study a behavior of Frobenius solutions near a regular singular point of RCSLE (77) at infinity it is convenient to convert this equation to its 'prime' form [42] using the gauge transformation

$${}_{\infty}\ \Psi\!\!\!/\ [y;a;\varepsilon \pm \dot{:}\overline{M}_p] = y^{-1/2}{}_{\infty}\Phi[y;a;\varepsilon \mid \dot{:}\overline{M}_p] \tag{97}$$

which gives

$$\left\{\frac{d}{dy}y\frac{d}{dy} - y^{-3} + 2(a \pm 1)y^{-2} + 2\frac{d}{dy}(y\ ld_{\infty}\mathfrak{W}[y;a \mid \pm\dot{:}\overline{M}_p]\ ) + \varepsilon y^{-1}\right\}{}_{\infty}\ \Psi\!\!\!/\ [y;a;\varepsilon \mid \pm\dot{:}\overline{M}p] = 0 \tag{98}$$

As explained above the main advantage of this representation comes from the fact that the characteristic exponents of two Frobenius solutions of RSLE (98) near this singular end have opposite signs, with the principal Frobenius solution decaying as $y^{-\sqrt{-\varepsilon}}$ when $y \to \infty$. Again RSLE (98) is nothing but the 'algebraic' [42] form of the Schrödinger equation with the rationally deformed Morse potentials (88) or (89) accordingly – the common feature of RCSLEs with density function (34) as far as the given SLE has a regular singular point at infinity. Apparently

$$\begin{gathered}{}_{\infty}\ \Psi\!\!\!/\ [y;a;\varepsilon \mid \pm\dot{:}\overline{M}_{p+1}] \equiv y^{-1/2}{}_{\infty}\Phi[y;a;\varepsilon \mid \pm\dot{:}\overline{M}_{p+1}] = \\ \frac{y\ W\left\{{}_{\infty}\ \Psi\!\!\!/\ [y;a;\varepsilon_{\pm,m_{p+1}}(a) \mid \pm\dot{:}\overline{M}_p],\ {}_{\infty}\ \Psi\!\!\!/\ [y;a;\varepsilon \mid \pm\dot{:}\overline{M}_p]\right\}}{{}_{\infty}\ \Psi\!\!\!/\ [y;a;\varepsilon_{\pm,m_{p+1}}(a) \mid \pm\dot{:}\overline{M}_p]}\end{gathered} \tag{99}$$

Here we are only interested in cases when the FF appearing in the denominator of PF (99) is the non-principal Frobenius solution of RSLE (98) near the singular point at infinity so

$${}_{\infty}\ \Psi\!\!\!/\ [y;a;\varepsilon \mid \pm\dot{:}\overline{M}_{p+1}] \approx -[\sqrt{-\varepsilon} + \sqrt{-\varepsilon_{\pm,m_{p+1}}(a)}]y^{-\sqrt{-\varepsilon}} \quad \text{for} \quad y >> 1 \tag{100}$$

if ${}_\infty\Psi\,[y;a;\varepsilon \mid \pm\dot{:}\overline{M}_p]$ is an arbitrary principal Frobenius solution of this RSLE near the singular end in question. We thus proved that the RD$\mathscr{T}$ of any principal Frobenius solution for each of the singular end points is itself the *principal* Frobenius solution of the transformed RSLE near the singular point in question.

Suppose that RSLE (98) with $\overline{M}_p$ replaced for $\overline{\mathbf{M}}^{\pm}_{p+1}$ has an additional eigenfunction ${}_\infty\Psi\,[y;a;\varepsilon^*(a) \mid \pm\dot{:}\overline{\mathbf{M}}^{\pm}_{p+1}]$ at the energy $\varepsilon^*(a)<0$. Applying the reverse RDT with the FF

$$y^{1/2}/{}_\infty\Phi[y;a;\varepsilon_{\pm,\mathbf{m}_{p+1}}(a) \mid \pm\dot{:}\overline{\mathbf{M}}^{\pm}_{p}] = {}_\infty\Psi^{-1}\,[y;a;\varepsilon_{\pm,\mathbf{m}_{p+1}}(a) \mid \pm\dot{:}\overline{\mathbf{M}}^{\pm}_{p}] \tag{101}$$

to the new eigenfunction we would come to the solution which obeys the DBC at infinity:

$$\frac{W\left\{{}_\infty\Psi^{-1}\,[y;a;\varepsilon_{\pm,\mathbf{m}_{p+1}}(a) \mid \pm\dot{:}\overline{\mathbf{M}}^{\pm}_{p}],\,{}_\infty\Psi\,[y;a;\varepsilon^*(a) \mid \pm\dot{:}\overline{\mathbf{M}}^{\pm}_{p+1}]\right\}}{{}_\infty\Psi^{-1}\,[y;a;\varepsilon_{\pm,\mathbf{m}_{p+1}}(a) \mid \pm\dot{:}\overline{\mathbf{M}}^{\pm}_{p}]} \tag{102}$$

$$\approx [\sqrt{-\varepsilon_{\pm,\mathbf{m}_{p+1}}(a)} - \sqrt{-\varepsilon^*(a)}]y^{-\sqrt{-\varepsilon_{\pm,\mathbf{m}_{p+1}}(a)}} \quad \text{for} \quad y >> 1$$

assuming that $\varepsilon^*(a) \neq \varepsilon_{\pm,\mathbf{m}_{p+1}}(a)$. On other hand, the quasi-rational function on the left is related to principal solution (96) via gauge transformation (97) with $\varepsilon=\varepsilon^*(a)$ and therefore the solution in question would obey both DBCs which contradicts the assumption that $\varepsilon^*(a)$ is a new eigenvalue. The only exception corresponds to the case $\varepsilon^*(a)=\varepsilon_{\pm,\mathbf{m}_{p+1}}(a)$, when the RDT with FF (100) insert the new bound energy state below the ground energy level of rationally deformed Morse potential (88) or (89) accordingly.

3.3. Isospectral family of rationally deformed Morse potentials with a regular spectrum

Let us prove that any set $\overline{\mathbf{M}}^{-}_{p}$ of seed solutions $\phi_{-,\mathbf{m}_k}[y;a]$ $(0<\mathbf{m}_1<\mathbf{m}_k<\mathbf{m}_{k+1}\leq p)$ is admissible if the generalized Bessel polynomial $Y^{(-2a)}_{\mathbf{m}_k}(y)$ does not have positive zeros so each seed function ${}_\infty\phi_{-,\mathbf{m}_k}[y;a]$ preserves its sign on the positive semi-axis. According to (73), this is possible if $\mathbf{m}>2a-1$ for any $\mathbf{m}\in\overline{\mathbf{M}}^{-}_{p}$. In other words we have to prove that polynomial Wronskian (83) does not have positive zeros if this is true for each polynomial $Y^{(-2a)}_{\mathbf{m}_k}(y)$. This assertion is obviously trivial for $p=1$. It also directly follows from the arguments presented in previous subsection that the RDT of $\mathscr{B}$Ref CSLE (32) with the FF $\phi_{-,\mathbf{m}_1}[y;a]$ preserves the discrete energy spectrum so the prime RSLE

$$\left\{\frac{d}{dy}y\frac{d}{dy} + y_\infty I^0[y;a \mid -\dot{:}\mathbf{m}_1] + (\varepsilon+1/2)y^{-1}\right\}{}_\infty\Psi\,[y;a;\varepsilon \mid -\dot{:}\mathbf{m}_1] = 0 \tag{103}$$

solved under the DBCs

$$\lim_{y\to 0}{}_\infty\Psi\,[y;a;\varepsilon_n(a) \mid -\dot{:}\mathbf{m}_1] = \lim_{y\to\infty}{}_\infty\Psi\,[y;a;\varepsilon_n(a) \mid -\dot{:}\mathbf{m}_1] = 0 \tag{104}$$

has exactly $\mathrm{N}(a)$ eigenfunctions

$${}_\infty\Psi\,[y;a;\varepsilon_n(a) \mid -\dot{:}\mathbf{m}_1] \equiv {}_\infty\Psi_{-,n}\,[y;a \mid -\dot{:}\mathbf{m}_1] = y^{-1/2}{}_\infty\Phi_{-,n}[y;a \mid -\dot{:}\mathbf{m}_1] \tag{105}$$

at the energies ${}_\infty\varepsilon_{-,n}(a)$ with n varying from 0 to $N(a)-1$. Making use of (90) with $p=1$ and $m=n$, they can be also re-written in the quasi-rational form

$${}_\infty\Psi_{-,n}\,[y;a \mid -\dot{:}\mathbf{m}_1] = {}_\infty\psi_{-,0}\,[y;a-1]\frac{{}_\infty\mathfrak{W}[y;a \mid -\dot{:}\mathbf{m}_1,n]}{Y^{(-2a)}_{\mathbf{m}_1}(y)} \tag{106}$$

Keeping in mind that the PF in the right-hand side of the latter expression is proportional to y^{n-1} for $y>>1$ one can immediately confirm that eigenfunctions (105) vanish in the limit $y\to\infty$ for any $n<a-1/2$.

Let us now use the mathematical induction to prove that the polynomial ${}_\infty\mathfrak{W}[y;a \mid -\dot{:}\overline{\mathbf{M}}^{-}_{p+1}]$ does not have positive zeros if this assertion holds for the polynomial ${}_\infty\mathfrak{W}[y;a \mid -\dot{:}\overline{\mathbf{M}}^{-}_{p}]$. Again it is suitable to convert RCSLE (77) to its prime form

$$\left\{\frac{d}{dy}y\frac{d}{dy} + y_\infty I^0[y;a \mid -\dot{:}\overline{\mathbf{M}}^{-}_{p}] + (\varepsilon+1/2)y^{-1}\right\}{}_\infty\Psi\,[y;a;\varepsilon \mid -\dot{:}\overline{\mathbf{M}}^{-}_{p}] = 0 \tag{107}$$

solved under the DBCs

$$\lim_{y\to 0} {}_\infty\Psi\,[y;a;\varepsilon_n(a)\mid -\dot{:}\overline{\mathbf{M}}_{\underset{\sim}{p}}^{-}] = \lim_{y\to\infty} {}_\infty\Psi\,[y;a;\varepsilon_n(a)\mid -\dot{:}\overline{\mathbf{M}}_{\underset{\sim}{p}}^{-}] = 0. \tag{108}$$

Making use of (90) with $p = \underset{\sim}{p}$ we can again re-write the eigenfunctions

$${}_\infty\Psi_{-,n}\,[y;a\mid -\dot{:}\overline{\mathbf{M}}_{\underset{\sim}{p}}^{-}] \equiv {}_\infty\Psi\,[y;a;\varepsilon_n(a)\mid -\dot{:}\overline{\mathbf{M}}_{\underset{\sim}{p}}^{-}] = y^{-1/2}{}_\infty\Phi_{-,n}[y;a\mid -\dot{:}\overline{\mathbf{M}}_{\underset{\sim}{p}}^{-}] \tag{109}$$

in the quasi-rational form

$${}_\infty\Psi\,[y;a\mid -\dot{:}\overline{\mathbf{M}}_{\underset{\sim}{p}}^{-}] = {}_\infty\psi_{-,0}\,[y;a-\underset{\sim}{p}]\frac{{}_\infty\mathfrak{W}[y;a\mid -\dot{:}\overline{\mathbf{M}}_{\underset{\sim}{p}+1}^{-}]}{{}_\infty\mathfrak{W}[y;a\mid -\dot{:}\overline{\mathbf{M}}_{\underset{\sim}{p}}^{-}]} \tag{110}$$

Examination of q-RS (110) reveals that it vanishes at the origin and therefore represents a principal solution of prime SLE (103) near its irregular singular point. Since this solution lies below the lowest eigenvalue it must be nodeless [43] and therefore no Wronskian ${}_\infty\mathfrak{W}[y;a\mid -\dot{:}\overline{\mathbf{M}}_{p}^{-}]$ has positive zeros.

All the q-RSs

$${}_\infty\Psi_{-,n}\,[y;a\mid -\dot{:}\overline{\mathbf{M}}_{p}^{-}] = {}_\infty\psi_{-,0}\,[y;a-p]\frac{{}_\infty\mathfrak{W}[y;a\mid -\dot{:}\overline{\mathbf{M}}_{p}^{-},n]}{{}_\infty\mathfrak{W}[y;a\mid -\dot{:}\overline{\mathbf{M}}_{p}^{-}]} \tag{111}$$

vanish at infinity for $n < N(a) = \lfloor A \rfloor$ since the power exponent of the PF in the right-hand side of (111) is equal to $n-p$ in the limit $y\to\infty$. This confirms that the Direchlet problem for SLE (103) has exactly $N(a)$ eigenfunctions defined via (111) with $n < N(a)$. Since these eigenfunctions must be orthogonal [43] with the weight y^{-1} the polynomial Wronskians ${}_\infty\mathfrak{W}[y;a\mid -\dot{:}\overline{\mathbf{M}}_{p}^{-},n]$ with n varying from 0 to $N(a)-1$ are orthogonal with the positive weight

$${}_\infty W[y;a\mid -\dot{:}\overline{\mathbf{M}}_{p}^{-}] = \frac{{}_\infty\psi^2_{-,0}\,[y;a-p]}{y\;{}_\infty\mathfrak{W}^2[y;a\mid -\dot{:}\overline{\mathbf{M}}_{p}^{-}]}\;. \tag{112}$$

If the Morse potential has at least 2 energy levels the sequence starts from a polynomial of degree

$$\mid \overline{\mathbf{M}}_{p}^{-} \mid -0.5\;p(p+1) \geq 2p. \tag{113}$$

keeping in mind

$$\mid \overline{\mathbf{M}}_{p}^{-} \mid > (2a-1)p + 0.5p(p+1) > 2p + 0.5p(p+1) \tag{114}$$

in this case. The finite EOP sequence in question thus starts from a polynomial of at least second degree and therefore [46] does not obey the Bochner theorem [47].

Re-writing (85) with $\overline{M}_p = \overline{\mathbf{M}}_{p}^{-}$ as

$${}_\infty I^0[y;a\mid -\dot{:}\overline{\mathbf{M}}_{p}^{-}] = {}_\infty I^0[y;a-p] + \frac{2}{y}\frac{d}{dy}\left(y\;ld_\infty\mathfrak{W}[y;a\mid -\dot{:}\overline{\mathbf{M}}_{p}^{-}]\right) \tag{115}$$

we can then explicitly express corresponding Liouville potential (89) in terms of the admissible Wronskian ${}_\infty\mathfrak{W}[y;a\mid -\dot{:}\overline{\mathbf{M}}_{p}^{-}]$ as follows

$${}_\infty V[y;a\mid -\dot{:}\overline{\mathbf{M}}_{\underset{\sim}{p}}^{-}] = {}_\infty V[y;a-p] - 2y\frac{d}{dy}\left(y\;ld_\infty\mathfrak{W}[y;a\mid -\dot{:}\overline{\mathbf{M}}_{p}^{-}]\right) \tag{116}$$

As mentioned in previous subsection this net of isospectral rational potentials starts from potential function (16) in [10] with $A = a - 1/2\;,\;\; B = 1$, after the latter is expressed in terms of the variable $y = e^x$.

3.4. Subnet of rationally deformed Morse potentials quantized via Wronskians of R-Bessel polynomials

Another family of solvable RDC$\mathscr{T}$s of CSLE (32) can be constructed using juxtaposed pairs of eigenfunctions ${}_\infty\phi_{-,n_k}[y;a]$, ${}_\infty\phi_{-,n_k+1}[y;a]$ $(0 < n_k < n_{k+1} - 1 < N(a)$ for $k = 1,\dots,J)$. The simplest double-step representative of this finite family of rationally deformed Morse potentials with $n_1 = 1,\ J = 2$ was constructed by Bagrov and Samsonov [38, 48] in the late nineties based on the conventional $\mathscr{L}$Ref representation of the Schrödinger equation with the Morse potential. The extensions of their works to an arbitrary number of juxtaposed pairs of eigenfunctions in both $\mathscr{L}$Ref and $\mathscr{B}$Ref representations were performed more recently in [11] and [19] accordingly.

For any TFI RCSLE from Group A one can by-pass an analysis of the pre-requisites for the Krein-Adler theorem [49, 50] by taking advantage of the fact that the Wronskians of eigenfunctions are composed of weighted orthogonal polynomials with the common degree-independent weight and therefore the numbers of their positive zeros are controlled by the general Conjectures proven in [51] for Wronskians of positive definite orthogonal polynomials. In particular we conclude that any Wronskian formed by juxtaposed pairs of R-Bessel polynomials of non-zero degrees may not have positive zeros.

Let $\overline{\mathbf{N}}_{2J}$ be a set of R-Bessel polynomials of degrees

$$\begin{gathered}\overline{\mathbf{N}}_{2J} = \overline{M}(\overline{\mathbb{A}'}_{L\to 1}) = \\ n_1 : n_1 + 2j_1 - 1, n_{2j_1+1} : n_{2j_1+1} + 2j_2 - 1, \dots, n_{2J-2j_L+1} : n_{2J}(n_1 > 0, n_{2J} < N)\end{gathered} \tag{117}$$

with even

$$\mathbb{d}'_l = 2\mathrm{j}_l\ (l = 1,\dots,L). \tag{118}$$

Examination of the q-RS functions

$$\begin{gathered}{}_\infty\Psi_{-,n}[y;a \mid -\dot{:}\overline{\mathbf{N}}_{2J}] = y^{-1/2}{}_\infty\Phi_{-,n}[y;a \mid -\dot{:}\overline{\mathbf{N}}_{2J}] = \\ {}_\infty\psi_{-,0}[y;a-2J]\frac{{}_\infty\mathfrak{W}[y;a \mid -\dot{:}\overline{\mathbf{N}}_{2J},n]}{{}_\infty\mathfrak{W}[y;a \mid -\dot{:}\overline{\mathbf{N}}_{2J}]}\ (n \notin \overline{\mathbf{N}}_{2J})\end{gathered} \tag{119}$$

shows that they all represent principal solutions near the irregular singular point of the prime RSLE

$$\left\{\frac{d}{dy}y\frac{d}{dy} + y_\infty I^0[y;a \mid -\dot{:}\overline{\mathbf{N}}_{2J}] + (\varepsilon + 1/2)y^{-1}\right\}{}_\infty\Psi[y;a;\varepsilon \mid -\dot{:}\overline{\mathbf{N}}_{2J}] = 0 \tag{120}$$

assuming again that the latter equation is solved under DBCs

$$\lim_{y\to 0}{}_\infty\Psi[y;a;\varepsilon_n \mid -\dot{:}\overline{\mathbf{N}}_{2J}] = \lim_{y\to\infty}{}_\infty\Psi[y;a;\varepsilon_n \mid -\dot{:}\overline{\mathbf{N}}_{2J}] = 0. \tag{121}$$

Note that the PF in the right-hand side of (119) is proportional to y^{n-2J} for $y >> 1$ so each solution with $n \notin \overline{\mathbf{N}}_{2J} < N(a)$ represents an eigenfunction of RSLE (120).

Again these eigenfunctions must be orthogonal with the weight y^{-1} and therefore $N(a) - 2J$ Wronskians ${}_\infty\mathfrak{W}[y;a \mid -\dot{:}\overline{\mathbf{N}}_{2J},n]$ with $n \notin \overline{\mathbf{N}}_{2J} < N(a)$ form a polynomial set orthogonal with the positive weight

$${}_\infty W[y;a \mid -\dot{:}\overline{\mathbf{N}}_{2J}] = \frac{{}_\infty\psi^2_{-,0}[y;a-2J]}{y_\infty\mathfrak{W}^2[y;a \mid -\dot{:}\overline{\mathbf{N}}_{2J}]} \tag{122}$$

If sequence (117) starts from $n_1 = 1$ then the finite EOP sequence in question lacks the first-degree polynomial. Otherwise it always starts from a polynomial of non-zero degree

$$\mid \overline{\mathbf{N}}_{2J} \mid -J(2J+1) > (n_1 - 1)(\mathbb{d}'_1 - 1) \geq 1. \tag{123}$$

In both cases the pre-requisites of the Bochner theorem are invalid as expected [46].

The Liouville potentials in question can be thus expressed in terms of the admissible Wronskians ${}_\infty\mathfrak{W}[y;a \mid -\dot{:}\overline{\mathbf{N}}_{2J}]$ as follows

$${}_\infty V[y;a \mid -\dot{:}\overline{\mathbf{N}}_{2J}] = {}_\infty V[y;a-2J] - 2y\frac{d}{dy}(y\ ld_\infty\mathfrak{W}[y;a \mid -\dot{:}\overline{\mathbf{N}}_{2J}]). \tag{124}$$

We refer the reader to Conjectures in [51] to verify that the number of zeros of each Wronskian in the constructed orthogonal polynomial set changes exactly by 1 even if a jump in the polynomial degree is larger than 1. However

even if we take advantage of these elegant results we still need to prove that there are no additional eigenfunctions with a number of nodes larger than $N(a) - 2J - 1$. In contrast with the analysis presented in the previous section, this proof is complicated by the fact that the RDT at each odd step results in a non-solvable RSLE with singularities on the positive semi-axis. Luckily we deal with the TFI CSLE so its RDC $\mathscr{T}$ using juxtaposed pairs of eigenfunctions can be alternatively obtained via *sequential* RDTs with seed solutions from the second sequence $+, m$ [11, 19]. Namely, as already mentioned in the end of section 2 the conjugated partition

$$\overline{\mathbf{M}}^{+}_{|\overline{\delta}_{1\to L}|} = \overline{M}(\overline{\Delta}_{1\to L}) \tag{125}$$

is formed by alternating even and odd integers starting from an even integer $\overline{\delta'}_1$. The reverse is also true: if the partition

$$\overline{\mathbf{M}}^{+}_{p} = \overline{M}({}^{p}\overline{\delta}_{1\to L_p}; {}^{p}\overline{\delta'}_{1\to L_p}) \tag{126}$$

is composed of alternating even and odd integers starting from an even integer $\overline{\delta'}_1$ then each segment of the conjugated partition

$${}^{p}\overline{\mathbf{N}}_{2\mathrm{J}_p} = \overline{M}({}^{p}\overline{\delta}'_{L_p\to 1}; {}^{p}\overline{\delta}_{L_p\to 1}) \tag{127}$$

must have an even length, with the largest element

$$\mathbf{m}^{+}_{|{}^{p}\overline{\delta'}_{1\to L_p}|} = \mid {}^{p}\overline{\Delta}_{1\to L_p} \mid -1 = \mathbf{m}_{|{}^{p}\overline{\delta}_{L_p\to 1}|} \in {}^{p}\overline{\mathbf{N}}_{2J_p}, \tag{128}$$

where ${}^{p}\overline{\Delta}_{1\to L_p} \equiv {}^{p}\overline{\delta}_{1\to L_p}; {}^{p}\overline{\delta'}_{1\to L_p}$.

Making use of (37) one can verify that quasi-rational functions (30) can be decomposed as

$${}_{\infty}\chi_{\mp N}[y;a] = y^{1/2N(N-1)\mp N\delta}[\xi]\,{}_{\infty}\phi^{N}_{\pm,0}[y;a^{(\delta)}] \tag{129}$$

and therefore the denominators of the fractions in equivalence relations (29) take form

$$y^{-1/2|\overline{\delta}_L|(|\overline{\delta}_L|-1)}\prod_{l=1}^{L}{}_{\infty}\chi_{-\delta_l}[y;a^{(|\overline{\Delta'}_{l\to 1}|-\delta)}] = y^{\Sigma_L}\,{}_{\infty}\phi^{|\overline{\delta}_L|}_{-,0}[y;a] \tag{130}$$

$$y^{-1/2|\overline{\delta'}_L|(|\overline{\delta'}_L|-1)}\prod_{l=1}^{L}{}_{\infty}\chi_{-\delta'_l}[y;a^{(|\overline{\Delta'}_{l\to 1}|-\delta')}] = y^{\Sigma_L}\,{}_{\infty}\phi^{|\overline{\delta'}_L|}_{-,0}[y;a^{(|\overline{\Delta}_{1\to L}|)}] \tag{131}$$

accordingly, where $\mid \overline{\Delta}_{1\to L} \mid = \mid \overline{\Delta'}_{L\to 1} \mid$ and

$$\Sigma_L = \sum_{l=1}^{L}\delta'_l(\delta_l + \sum_{\underset{\sim}{l}=l+1}^{L}\delta_{\underset{\sim}{l}}) = \sum_{l=1}^{L}\delta_l(\delta'_l + \sum_{\underset{\sim}{l}=1}^{l-1}\delta'_{\underset{\sim}{l}}). \tag{132}$$

We thus come to the following equivalence theorem for the Wronskians of generalized Bessel polynomials

$${}_{\infty}\hat{\mathfrak{W}}[y;a \mid +\vdots\overline{M}(\overline{\Delta}_{1\to L})] = {}_{\infty}\hat{\mathfrak{W}}[y;a^{(|\Delta_{1\to L}|)} \mid -\vdots\overline{M}(\overline{\Delta'}_{L\to 1})]. \tag{133}$$

Note that decomposition (129) holds for any TFI CSLE of Group A provided that we replace y^2 for the leading coefficient ${}_{l}\sigma[y]$ of the corresponding counter-parts of differential eigenequations (46). This brings us to the equivalence relations for polynomial Wronskians discovered by Odake and Sasaki [19] in their pioneering analysis of TSI potentials from Group A.

If $a > 1/2$ then, according to (128), the largest element of the partition ${}^{p}\overline{\mathbf{N}}_{2\mathrm{J}_p}$ is smaller than $a+\mid {}^{p}\overline{\Delta}_{l\to L_p} \mid -1/2$ and therefore the Wronskian in the right-hand side of (133) with $\overline{\Delta'}_{L\to 1}$ replaced for ${}^{p}\overline{\Delta'}_{L_p\to 1}$ is formed by juxtaposed pairs of R-Bessel polynomials. This confirms that none of the polynomial Wronskians ${}_{\infty}\hat{\mathfrak{W}}[y;a \mid +\vdots\overline{\mathbf{M}}^{+}_{p}]$ has zeros on the positive semi-axis and therefore each partition $\overline{\mathbf{M}}^{+}_{p}$ specifies an admissible sequence of seed solutions ${}_{\infty}\phi_{+,\mathbf{m}_k}[y;a]$ ($\mathbf{m}_k \in \overline{\mathbf{M}}^{+}_{p}$ for $k = 1,\dots,p$). Based on the arguments presented in subsection 3.2 we thus assert that the RDTs in question may insert only one bound energy level at the energy ${}_{\infty}\varepsilon_{+,\mathbf{m}_{p+1}}(a)$ which by definition lies below the ground energy level ${}_{\infty}\varepsilon_{+,\mathbf{m}_p}(a)$ of the Liouville potential ${}_{\infty}V[a \mid \overline{\mathbf{M}}^{+}_{p}]$. On other hand all the existent energy levels remain unchanged.

As the simplest example we can cite the partition

$$1,2,\dots,2J = \overline{M}(2J,1) = \overline{M}^{\dagger}(1,2J) \quad \text{for} \quad 2J \le \lfloor A \rfloor \tag{134}$$

As a direct consequence of the equivalence theorem we find that

$$\hat{Y}_{2J}^{(2a-2J-1,-2)}(y) = {}_{\infty}\hat{\mathfrak{W}}[y; a \mid -\dot{:}1:2J] \ (2J \leq \lfloor A \rfloor), \tag{135}$$

where the Wronskian on the right is formed by $2J$ sequential R-Bessel polynomials of non-zero degrees smaller than A and therefore may not have positive zeros for $a > -1/2$ [51]. As initially proven in [7] and then illuminated in more details in [8] using the so-called 'Kienast-Lawton-Hahn's theorem' [52–54] the latter assertion holds for any positive J despite the fact that the seed functions ${}_{\infty}\not{\psi}_{-,m}[y; a^{(2J+1)}]$ have nodes on the positive semi-axis for

$$a^{(2J+1)} + 1/2 < m < 2A. \tag{136}$$

Indeed, representing (56) as

$$Y_m^{(2a,-2)}(y) \equiv Y_m^{(2a)}(-y/2) = m!\,(-y/2)^m L_m^{(-2a-2m-1)}(-2/y) \tag{137}$$

shows that the absolute value of the negative m-dependent Laguerre index

$$\alpha_m = -2a - 2m - 1 < 0 \tag{138}$$

is larger than the polynomial degree and therefore the polynomial in question may not have zeros at negative values of its argument.

3.5. Isospectral rational extensions of Krein-Adler SUSY partners of Morse potential

Since any RDCT of the Morse potentials using pairs of juxtaposed eigenfunctions $\overline{\mathbf{N}}_{2J}$ keeps unchanged the ground-energy level a set of seed functions ${}_{\infty}\phi_{+,\mathbf{m}}[y; a]$ is admissible iff all $\mathbf{m} \in \overline{\mathbf{N}}_{2J}, \overline{\mathbf{M}}_p^-$, where $\overline{\mathbf{M}}_p^-$ is an admissible set of seed polynomials specified in subsection 3.3. We can then use the same arguments as in subsection 3.3 to prove that any Liouville potential

$${}_{\infty}V[y; a \mid -\dot{:}\overline{\mathbf{N}}_{2J}, \overline{\mathbf{M}}_p^-] = {}_{\infty}V[y; a - 2J - p] - 2y\frac{d}{dy}\left(y\ ld_{\infty}\mathfrak{W}[y; a \mid -\dot{:}\overline{\mathbf{N}}_{2J}, \overline{\mathbf{M}}_p^-]\right) \tag{139}$$

has exactly the same discrete energy spectrum as rationally deformed Morse potential (124) constructed by means of juxtaposed pairs of R-Bessel polynomials of non-zero degrees. Its eigenfunctions expressed in terms of the variable $y = e^x$ can be represented as

$${}_{\infty}\not{\psi}_{-,n}[y; a \mid -\dot{:}\overline{\mathbf{N}}_{2J}, \overline{\mathbf{M}}_p^-] = {}_{\infty}\not{\psi}_{-,0}[y; a - 2J - p]\frac{{}_{\infty}\mathfrak{W}[y; a \mid -\dot{:}\overline{\mathbf{N}}_{2J}, n, \overline{\mathbf{M}}_p^-]}{{}_{\infty}\mathfrak{W}[y; a \mid -\dot{:}\overline{\mathbf{N}}_{2J}, \overline{\mathbf{M}}_p^-]} for\ n \notin \overline{\mathbf{N}}_{2J} < N(a) \tag{140}$$

keeping in mind that the corresponding prime RSLE is nothing but the Schrödinger equation re-written in its algebraic form.

4. Conclusions

The presented analysis illuminates the non-conventional approach [19] to the family of rationally deformed Morse potentials using seed solutions expressed in terms of Wronskians of generalized Bessel polynomials in the variable $y = e^x$. As a new achievement compared with Odake and Saski's [19] study on RDC$\mathscr{T}$s of the Morse potential (see also [11] where a similar analysis was performed within the conventional $\mathscr{L}$Ref framework) we constructed a new RDC net of *isospectral* potentials by expressing them in terms of the logarithmic derivative of Wronskians of generalized Bessel polynomials with no positive zeros. The constructed isospectral family of rationally deformed Morse potentials represents a natural extension of the isospectral RD$\mathscr{T}$s of the Morse potential discovered by Quesne [10]. An important element of our analysis often overlooked in the literature is the proof that the sequential RDTs in question do not insert new bound energy states. The widespread argumentation in support of this (usually taken-for-granted) presumption is based on the speculation that the theorems of the *regular* Sturm-Liouville theory [55] are automatically applied to singular SLEs. We can refer the reader to the scrupolous analysis performed in [43] for SLEs solved under the DBCs as an illustration that this is by no means a trivial issue. To be able to prove the aforementioned assertion we converted the given RCSLE to its prime form such that the characteristic exponents of Frobenius solutions for the regular singular point at ∞ have opposite signs and therefore the principal Frobenius solution near this singular end is unambiguously selected by the corresponding DBC. (In the particular case under consideration the prime RSLE accidently coincides with the Schrödinger equation re-written in the 'algebraic' [42] form but this is

not true in general.) Re-formulating the given spectral problem in such a very specific way allowed us to take advantage of powerful theorems proven in [43] for zeros of principal solutions of SLEs solved under the DBCs at singular ends. We [42] also used this simplified version of the conventional spectral theory to prove that any RD$\mathscr{T}$ of a principal (non-principal) Frobenius solution near the regular singular point at ∞ is itself a principal (non-principal) Frobenius solution of the transformed RSLE. This assertion plays a crucial role in our proof of the exact solvability of the constructed DC net of isospectral rational potentials. It is commonly presumed that the Krein-Adler theorem [49, 50] is applied to an arbitrary potential regardless its behavior near the singular end points. In [42] we examined this presumption more carefully for the Dirichlet problems of our interest again taking advantage of the theorems proven in [43] for zeros of juxtaposed eigenfunctions. However one can by-pass this analysis for any TFI RSLE from Group A keeping in mind that the Wronskians in questions are formed by orthogonal polynomials with degree-independent indexes and therefore the numbers of their positive zeros are controlled by the general Conjectures proven in [51]. In particular this implies that any Wronskian formed by juxtaposed pairs of R-Bessel polynomials of non-zero degrees may not have positive zeros.

Acknowledgements

I am grateful to A. D. Alhaidari for bringing my attention to the alternative representation of eigenfunctions of the Schrödinger equation with the Morse potential in terms of R-Bessel polynomials with *degree-independent* indexes. This alteration helped me to fully comprehend Odake and Sasaki's suggestion to place the Morse oscillator into Group A of rational TSI potentials.

References

[1] A. D. Alhaidari. Exponentially confining potential well. *Theoretical and Mathematical Physics volume* **206**:84–96, 2021. https://doi.org/10.1134/S0040577921010050.

[2] J. Gibbons, A. P. Veselov. On the rational monodromy-free potentials with sextic growth. *Journal of Mathematical Physics* **50**(1):013513, 2009. https://doi.org/10.1063/1.3001604.

[3] H. L. Krall, O. Frink. A new class of orthogonal polynomials: the Bessel polynomials. *Transactions of the American Mathematical Society* **65**:100–105, 1949. https://doi.org/10.1090/S0002-9947-1949-0028473-1.

[4] W. A. Al-Salam. The Bessel polynomials. *Duke Mathematical Journal* **24**(4):529–545, 1957. https://doi.org/10.1215/S0012-7094-57-02460-2.

[5] T. S. Chihara. *An Introduction to Orthogonal Polynomials.* Gordon and Breach, New York, 1978.

[6] R. Koekoek, P. A. Lesky, R. F. Swarttouw. *Hypergeometric Orthogonal Polynomials and Their q-Analogues.* Springer, Heidelberg, 2010.

[7] D. Gomez-Ullate, N. Kamran, R. Milson. The Darboux transformation and algebraic deformations of shape-invariant potentials. *Journal of Physics A: Mathematical and General* **37**(5):1789–1804, 2004. https://doi.org/10.1088/0305-4470/37/5/022.

[8] Y. Grandati. Solvable rational extensions of the Morse and Kepler-Coulomb potentials. *Journal of Mathematical Physics* **52**(10):103505, 2011. https://doi.org/10.1063/1.3651222.

[9] C.-L. Ho. Prepotential approach to solvable rational potentials and exceptional orthogonal polynomials. *Progress of Theoretical Physics* **126**(2):185–201, 2011. https://doi.org/10.1143/PTP.126.185.

[10] C. Quesne. Revisiting (quasi-)exactly solvable rational extensions of the Morse potential. *International Journal of Modern Physics A* **27**(13):1250073, 2012. https://doi.org/10.1142/S0217751X1250073X.

[11] D. Gomez-Ullate, Y. Grandati, R. Milson. Extended Krein-Adler theorem for the translationally shape invariant potentials. *Journal of Mathematical Physics* **55**(4):043510, 2014. https://doi.org/10.1063/1.4871443.

[12] V. I. Romanovski. Sur quelques classes nouvelles de polynomes orthogonaux. *Comptes Rendus de l'Académie des Sciences* **188**:1023–1025, 1929.

[13] P. A. Lesky. Einordnung der Polynome von Romanovski-Bessel in das Askey-Tableau. *Zeitschrift für Angewandte Mathematik und Mechanik* **78**(9):646–648, 1998. https://doi.org/10.1002/(SICI)1521-4001(199809)78:9<646::AID-ZAMM646>3.0.CO;2-W.

[14] C. Quesne. Extending Romanovski polynomials in quantum mechanics. *Journal of Mathematical Physics* **54**(12):122103, 2013. https://doi.org/10.1063/1.4835555.

[15] N. Cotfas. Systems of orthogonal polynomials defined by hypergeometric type equations with application to quantum mechanics. *Central European Journal of Physics* **2**(3):456–466, 2004. https://doi.org/10.2478/BF02476425.

[16] N. Cotfas. Shape-invariant hypergeometric type operators with application to quantum mechanics. *Central European Journal of Physics* **4**(3):318–330, 2006. https://doi.org/10.2478/s11534-006-0023-0.

[17] M. A. Jafarizadeh, H. Fakhri. Parasupersymmetry and shape invariance in differential equations of mathematical physics and quantum mechanics. *Annals of Physics* **262**(2):260–276, 1998. https://doi.org/10.1006/aphy.1997.5745.

[18] S. Odake, R. Sasaki. Extensions of solvable potentials with finitely many discrete eigenstates. *Journal of Physics A: Mathematical and Theoretical* **46**(23):235205, 2013. https://doi.org/10.1088/1751-8113/46/23/235205.

[19] S. Odake. Krein–Adler transformations for shape-invariant potentials and pseudo virtual states. *Journal of Physics A: Mathematical and Theoretical* **46**(24):245201, 2013. https://doi.org/10.1088/1751-8113/46/24/245201.

[20] G. Darboux. *Leçons sur la théorie générale des surfaces et les applications géométriques du calcul infinitésimal*. Gauthier-Villars, Paris, 1915.

[21] M. M. Crum. Associated Sturm-Liouville systems. *The Quarterly Journal of Mathematics* **6**(1):121–127, 1955. https://doi.org/10.1093/qmath/6.1.121.

[22] L. D. Landau, E. M. Lifshity. *Quantum Mechanics (Non-relativistic Theory)*. 3rd ed. Butterworth-Heinemann, 1977.

[23] G. Natanson. Equivalence relations for Darboux-Crum transforms of translationally form-invariant Sturm-Liouville equations, 2021. `https://www.researchgate.net/publication/353131294`.

[24] D. Gómez-Ullate, Y. Grandati, R. Milson. Durfee rectangles and pseudo-Wronskian equivalences for Hermite polynomials. *Studies in Applied Mathematics* **141**(4):596–625, 2018. https://doi.org/10.1111/sapm.12225.

[25] W. N. Everitt, L. L. Littlejohn. Orthogonal polynomials and spectral theory: a survey. In C. Brezinski, L. Gori, A. Ronveaux (eds.), *Orthogonal Polynomials and their Applications*, vol. 9, pp. 21–55. 1991. IMACS Annals on Computing and Applied Mathematics.

[26] W. N. Everitt, K. H. Kwon, L. L. Littlejohn, R. Wellman. Orthogonal polynomial solutions of linear ordinary differential equations. *Journal of Computational and Applied Mathematics* **133**(1-2):85–109, 2001. https://doi.org/10.1016/S0377-0427(00)00636-1.

[27] A. K. Bose. A class of solvable potentials. *Nuovo Cimento* **32**:679–688, 1964. https://doi.org/10.1007/BF02735890.

[28] G. A. Natanzon. Study of the one-dimensional Schrödinger equation generated from the hypergeometric equation. *Vestnik Leningradskogo Universiteta* **10**:22–28, 1971. English translation `https://arxiv.org/PS_cache/physics/pdf/9907/9907032v1.pdf`.

[29] B. V. Rudyak, B. N. Zakhariev. New exactly solvable models for Schrödinger equation. *Inverse Problems* **3**(1):125–133, 1987. https://doi.org/10.1088/0266-5611/3/1/014.

[30] L. D. Fadeev, B. Seckler. The inverse problem in the quantum theory of scattering. *Journal of Mathematical Physics* **4**(1):72–104, 1963. https://doi.org/10.1063/1.1703891.

[31] W. A. Schnizer, H. Leeb. Exactly solvable models for the Schrödinger equation from generalized Darboux transformations. *Journal of Physics A: Mathematical and General* **26**(19):5145–5156, 1993. https://doi.org/10.1088/0305-4470/26/19/041.

[32] W. A. Schnizer, H. Leeb. Generalized Darboux transformations: classification of inverse scattering methods for the radial Schrödinger equation. *Journal of Physics A: Mathematical and General* **27**(7):2605–2614, 1994. https://doi.org/10.1088/0305-4470/27/7/035.

[33] D. Gómez-Ullate, Y. Grandati, R. Milson. Shape invariance and equivalence relations for pseudo-Wronskians of Laguerre and Jacobi polynomials. *Journal of Physics A: Mathematical and Theoretical* **51**(34):345201, 2018. https://doi.org/10.1088/1751-8121/aace4b.

[34] L. E. Gendenshtein. Derivation of exact spectra of the Schrödinger equation by means of supersymmetry. *Journal of Experimental and Theoretical Physics Letters* **38**:356–359, 1983.

[35] L. E. Gendenshtein, I. V. Krive. Supersymmetry in quantum mechanics. *Soviet Physics Uspekhi* **28**(8):645–666, 1985. https://doi.org/10.1070/PU1985v028n08ABEH003882.

[36] B. F. Samsonov. On the equivalence of the integral and the differential exact solution generation methods for the one-dimensional Schrodinger equation. *Journal of Physics A: Mathematical and General* **28**(23):6989–6998, 1995. https://doi.org/10.1088/0305-4470/28/23/036.

[37] B. F. Samsonov. New features in supersymmetry breakdown in quantum mechanics. *Modern Physics Letters A* **11**(19):1563–1567, 1996. https://doi.org/10.1142/S0217732396001557.

[38] V. G. Bagrov, B. F. Samsonov. Darboux transformation and elementary exact solutions of the Schrödinger equation. *Pramana* **49**:563–580, 1997. https://doi.org/10.1007/BF02848330.

[39] F. Brafman. A set of generating functions for Bessel polynomials. *Proceedings of the American Mathematical Society* **4**:275–277, 1953. https://doi.org/10.1090/S0002-9939-1953-0054100-X.

[40] K. H. Kwon, L. L. Littlejohn. Classification of classical orthogonal polynomials. *Journal of the Korean Mathematical Society* **34**(4):973–1008, 1997.

[41] A. F. Nikiforov, V. B. Uvarov. *Special Functions of Mathematical Physics*. Birkhauser, Basel, 1988. https://doi.org/10.1007/978-1-4757-1595-8.

[42] G. Natanson. Darboux-Crum nets of Sturm-Liouville problems solvable by quasi-rational functions I. General theory, 2018. https://doi.org/10.13140/RG.2.2.31016.06405/1.

[43] F. Gesztesy, B. Simon, G. Teschl. Zeros of the Wronskian and renormalized oscillation theory. *American Journal of Mathematics* **118**(3):571–594, 1996. https://doi.org/10.1353/ajm.1996.0024.

[44] G. Natanson. Exact quantization of the Milson potential via Romanovski-Routh polynomials, 2015. https://doi.org/10.13140/RG.2.2.24354.09928.

[45] A. Schulze-Halberg. Higher-order Darboux transformations with foreign auxiliary equations and equivalence with generalized Darboux transformations. *Applied Mathematics Letters* **25**(10):1520–1527, 2012. https://doi.org/10.1016/j.aml.2012.01.008.

[46] D. Gomez-Ullate, N. Kamran, R. Milson. An extension of Bochner's problem: exceptional invariant subspaces. *Journal of Approximation Theory* **162**(5):987–1006, 2010. https://doi.org/10.1016/j.jat.2009.11.002.

[47] S. Bochner. Über Sturm-Liouvillesche Polynomsysteme. *Mathematische Zeitschrift* **29**:730–736, 1929. https://doi.org/10.1007/BF01180560.

[48] V. G. Bagrov, B. F. Samsonov. Darboux transformation of the Schrödinger equation. *Physics of Particles and Nuclei* **28**(4):374–397, 1997. https://doi.org/10.1134/1.953045.

[49] M. G. Krein. On a continuous analogue of the Christoffel formula from the theory of orthogonal polynomials. *Doklady Akademii Nauk SSSR* **113**(5):970–973, 1957.

[50] V. E. Adler. A modification of Crum's method. *Theoretical and Mathematical Physics* **101**:1381–1386, 1994. https://doi.org/10.1007/BF01035458.

[51] A. J. Durán, M. Pérez, J. L. Varona. Some conjecture on Wronskian and Casorati determinants of orthogonal polynomials. *Experimental Mathematics* **24**(1):123–132, 2015. https://doi.org/10.1080/10586458.2014.958786.

[52] A. Kienast. Untersuchungen über die Lösungen der Differentialgleichung $xy'' + (\gamma - x)y' - \beta y$. *Denkschriften der Schweizerischen Naturforschenden Gesellschaft* **57**:247, 79 pages, 1921.

[53] W. Lawton. On the zeros of certain polynomials related to Jacobi and Laguerre polynomials. *Bulletin of the American Mathematical Society* **38**:442–448, 1932. https://doi.org/10.1090/S0002-9904-1932-05418-0.

[54] W. Hahn. Bericht über die Nullstellen der Laguerreschen und der Hermiteschen Polynome. *Jahresbericht der Deutschen Mathematiker-Vereinigung* **1**:215–236, 1933.

[55] R. Courant, D. Hilbert. *Methods of Mathematical Physics, Vol. 1,*. Interscience, New York, 1953.

HOW TO UNDERSTAND THE STRUCTURE OF BETA FUNCTIONS IN SIX-DERIVATIVE QUANTUM GRAVITY?

Lesław Rachwał

Universidade Federal de Juiz de Fora, Departamento de Física–Instituto de Ciências Exatas, 33036-900, Juiz de Fora, MG, Brazil

correspondence: grzerach@gmail.com

Abstract. We extensively motivate the studies of higher-derivative gravities, and in particular we emphasize which new quantum features theories with six derivatives in their definitions possess. Next, we discuss the mathematical structure of the exact on the full quantum level beta functions obtained previously for three couplings in front of generally covariant terms with four derivatives (Weyl tensor squared, Ricci scalar squared and the Gauss-Bonnet scalar) in minimal six-derivative quantum gravity in $d = 4$ spacetime dimensions. The fundamental role here is played by the ratio x of the coupling in front of the term with Weyl tensors to the coupling in front of the term with Ricci scalars in the original action. We draw a relation between the polynomial dependence on x and the absence/presence of enhanced conformal symmetry and renormalizability in the models where formally $x \to +\infty$ in the case of four- and six-derivative theories respectively.

Keywords: Quantum Gravity, higher derivatives, beta functions, UV-finiteness, conformal symmetry.

1. Introduction and motivation

Six-derivative Quantum Gravity (QG) is a model of quantum dynamics of relativistic gravitational field with higher derivatives. It is a special case of general higher-derivative (HD) models which are very particular modifications of Einsteinian gravitational theory. The last one is based on the theory with up to two derivatives (an addition of the cosmological constant term brings terms with no derivatives on the metric field at all) and it is simply based on the action composed of the Ricci curvature scalar R understood as the function of the spacetime metric. In this setup, we consider that gravitational field is completely described by the symmetric tensor field $g_{\mu\nu}$ being the metric tensor of the pseudo-Riemannian smooth differential manifold of a physical spacetime. In Einstein's theory the scalar R contains precisely two ordinary (partial) derivatives of the metric. The action obtained by integrating over the spacetime volume the densitized Lagrangian $\sqrt{|g|}R$ we call as Einstein-Hilbert action. The QG models based on it were originally studied in [1–3]. Below we consider modifications of two-derivative gravitational theory, where the number of derivatives on the metric is higher than just two.

It must be remarked, however, that the kinematical framework of general relativity (GR) (like metric structure of the spacetime manifold, the form of Christoffel coefficients, the motion of probe particles, or geodesic and fluid dynamics equations) remains intact for these modifications. Therefore these higher-derivative (HD) models of gravitational field are still consistent with the physical basis of GR, the only difference is that their dynamics – the dynamics of the gravitational field – is described by classical equations of motion with higher-derivative character. Thence these modifications of standard Einsteinian gravitational theory are still in the set of generally relativistic models of the dynamics of the gravitational field. They could be considered both on the classical and quantum levels with the benefits of getting new and deeper insights in the theory of relativistic gravitational field. Our framework on the classical level can be summarized by saying that we work within the set of metric theories of gravity, where the metric and only the metric tensor characterizes fully the configurations of the gravitational fields which are here represented by pseudo-Riemannian differential manifolds of relativistic four-dimensional continuous spacetimes. Therefore, in this work we neglect other classical modifications of GR, like by adding torsion, non-metricity, other geometric elements or other scalars, vectors or tensor fields. This choice of the dynamical variables for the relativistic gravitational field bears impact both on the classical dynamics as well as on the quantum theory.

Theories with higher derivatives come naturally both with advantages and with some theoretical problems. This happens already on the classical level when they supposed to describe the modified dynamics of the gravitational field (metric field $g_{\mu\nu}(x)$ living on the spacetime manifold). These successes and problems get amplified even more on the quantum level. The pros for HD theories give strong motivations why to consider seriously these modifications of Einstein's gravitation. We will briefly discuss various possibilities of how to resolve the problems of higher-derivative field dynamics in one of the last sections of this contribution, while here we will consider more the motivations.

On the classical level, the set of HD gravitational theories can be viewed as one of the many possible modifications of two-derivative gravitational theory. It is true that now observations, mainly in cosmology and on the intergalactic scales, point to some possible failures of Einsteinian theory of gravity or to our lack in understanding the proper nature of the sources of gravity in these respective situations. There are various views possible on this situation and its explanations by gravitational theories. In the first view, researchers say that Einstein-Hilbert theory is still fine, but we need to add locally new exotic (meaning coming with some non-standard properties) matter source. Since we do not know what these sources for energy-momentum tensor (EMT) of matter are built out of (for example – from which quantum fields of particle physics as understood nowadays), we call the missing sources as dark energy and dark matter respectively. Contrary to this approach, in the other, the gravitational source is standard, that is we describe what we really see in the galaxies and in the universe, without any "dark" components, but the gravitational theory should be modified. In this second path, the internal dynamics of the gravitational field is changed and that is why it reacts differently to the same classical visible EMT source of standard matter. One of the promising options is to add higher derivatives of the metric on the classical level, but in such a way to still preserve the local Lorentz symmetry of the dynamics that is to be safe with respect to the general covariance. Hence all HD terms in the action of the theory must come from generally densitized scalars which are HD analogs of the Ricci scalar. They can be in full generality built as contractions of the metric tensors (both covariant $g_{\mu\nu}$ and contravariant $g^{\mu\nu}$), Riemann curvature tensor $R_{\mu\nu\rho\sigma}$ and also of covariant derivatives ∇_μ acting on these Riemann tensors[1]. Initially this may look as presumably unnecessary complication since classical equations of motion (EOM) with higher derivatives of the gravitational field are even more complicated than already a coupled system of non-linear partial differential equations for the components of the metric tensor field in Einstein's gravity. However, on the cosmological and galactic scales some gravitational models with higher derivatives give successes in explaining: the problem of dark matter halos, flat galactic rotation curves, cosmological dark energy (late-time exponential expansion of the universe) and also primordial inflation without a necessity of having the actual inflaton field. These are amongst all of observational pieces of evidence that can be taken for HD models.

Since our work is theoretical we provide below some conceptual and consistency arguments for HD gravities. First, still on the classical level, within the class of higher-derivative gravitational theories, there are models that are the first, which besides relativistic symmetries, enjoy also invariance under conformal symmetry understood in the GR framework. Properly this is called as Weyl symmetry of the rescaling of the covariant metric tensor, according to the law: $g_{\mu\nu} \to \Omega^2 g_{\mu\nu}$ with $\Omega = \Omega(x)$ being an arbitrary scalar parameter of these transformations. To understand better this fact, one may first recall that the metric tensor $g_{\mu\nu}$ is taken here as a dimensionless quantity and all energy dimensions are brought only by partial derivatives acting on it. Next, the prerequisite for full conformal symmetry is scale-invariance of the classical action, so the absence of any dimensionful parameter in the definition of the theory. From these facts, one derives that in four spacetime dimensions ($d = 4$) the gravitational conformal models must possess terms with precisely four derivatives acting on the metric. In general, in d dimensions, for conformal gravitational theory the classical action must be precisely with d derivatives on the metric. (One sees due to the requirement of general covariance that this consideration of conformal gravitational theories makes sense only in even dimensions d of spacetime.) Another interesting observation, is that the gravitational theory with Einstein-Hilbert action is classically conformally invariant only in two-dimensional framework. For 4-dimensional scale-invariant gravitational theory one must use a combination of the squares of the Riemann tensors and various contractions thereof. (The term $\Box R$ is trivially a total derivative term, so cannot be used.) Therefore for d-dimensional conformal gravitational theories ($d > 2$) we inevitably must consider HD metric theories. The conformally invariant gravitational dynamics is very special both on the classical level and also on the quantum level as we will see in the next sections.

The main arguments for higher-derivative gravitational theories in dimensions $d > 2$ come instead from quantum considerations. After all, it is not so surprising that it is the quantum coupling between quantum field theory (QFT) of matter fields and quantum (or semi-classical) gravity or self-interactions within pure quantum gravity that dictates what should be a consistent quantum theory of gravitational interactions. Our initial guess (actually Einstein's one) might not be the best one when quantum effects are taken fully into account. Since it is the classical theory that is emergent from the more fundamental quantum one working not only in the microworld, but at all energy scales (equivalent to various distances), then the underlying fundamental quantum theory must necessarily be mathematically consistent, while some different classical theories may not possess the same strong feature. Already here we turn the reader's attention to the fact that the purely mathematical requirement of the consistency on the quantum level of gravitational self-interactions is very strongly constraining the possibilities for quantum gravitational theories. It is more constraining than it was originally thought of. Moreover, not all macroscopic, so

[1] We do not need to consider covariant derivatives on the metric tensor because of the metricity condition, $\nabla_\mu g_{\nu\rho} = 0$.

long wavelength limit, classical theories are with these quantum correspondence features, only those which emerge as classical limits of consistent quantum gravity theories. Following this path, at the end, we must also correct our classical gravitational theory, and likely it will not be Einsteinian gravity any more.

From a different side, we know that matter fields are quantum, they interact and they are energetic, so they are "charged" under gravitation since energy-momentum content is what the gravity couples to. If we did not know nothing about gravity, then we could discover something about it from quantum considerations of gravitationally "charged" matter fields and their mutual interactions consistent with quantum mechanics. In this way we could make gravity dynamical and quantum with a proper form of graviton's propagation. Actually, it is the quantum consideration that makes the gauge bosons mediating the interactions between quantum charged particles dynamical. These gauge bosons are emanations or quantum realizations of classical dynamical gauge fields that must be introduced in the classical dynamics of matter fields or particles for the overall consistency. Below we will present a few detailed arguments why we need HD gravities in $d > 2$ giving rise to dynamical gravitational fields with HD form of the graviton's propagators in the quantum domain. They are all related and in a sense all touch upon the issue of coupling of a potential unknown dynamical quantum gravity theory to some energetic quantum matter fields moving under the influence of classical initially non-dynamical gravitational background field. (The background gravitational field does not have to be static, stationary or completely time-independent, what we only require here is that it is not a dynamical one.) These last classical fields can be understood as frozen expectation values of some dynamical quantum gravitational fields. As one can imagine for this process of quantum balancing of interactions the issue of back-reaction of quantum matter fields on the classical non-dynamical geometry is essential.

Firstly, we recall the argument of DeWitt and Utiyama [4]. Due to quantum matter loops some UV divergences in the gravitational sector are generated. This is so even if the original matter theory is with two-derivative actions (like for example standard model of particle physics). The reasons for these divergences are pictorially Feynman diagrams with quantum matter fields running in the perturbative loops, while the graviton lines are only external lines of the diagrams since they constitute classical backgrounds. In such a way we generate the dynamics to the gravitational field due to quantum matter interactions with gravity, so due to the back-reaction phenomena. If the latter was neglected we would have only the impact of classical gravitational field on the motion and interactions of quantum matter particles. We can be very concrete here, namely for example in $d = 4$ spacetime dimensions, the dynamical action that is generated for gravity takes the form

$$S_{\rm div} = \int d^4x \sqrt{|g|} \left(\alpha_C C^2 + \alpha_R R^2 \right), \qquad (1)$$

so we see that counterterms of the GR-covariant form of C^2 and R^2 are being generated. (In the equation above, the R^2 and C^2 terms denote respectively the square of the Ricci scalar and of the Weyl tensor, where the indices are contracted in the natural order, i.e. $C^2 = C_{\mu\nu\rho\sigma} C^{\mu\nu\rho\sigma}$. Collectively, we will denote these curvatures as $\mathcal{R}^2$, so $\mathcal{R}^2 = R^2, C^2$.) This is true no matter what was our intention of what was the dynamical theory of the gravitational field. We might have thought that this was described by the standard two-derivative Einstein-Hilbert action, but still the above results persist. One notices that in these two counterterms C^2 and R^2 one has four derivatives acting on a metric tensor, so these are theories of a general higher-derivative type, differently from originally intended E-H gravitational theory whose action is just based on the Ricci scalar R. These C^2 and R^2 terms appear in the divergent part of the dynamically induced action for the gravitational fields. We must be able to absorb these divergences to have a consistent quantum theory of the gravitational field coupled to the quantum matter fields present here on such curved (gravitational) backgrounds [5]. This implies that in the dynamics of the gravitational field we must have exactly these terms with higher derivatives as in (1). Finally, we can even abstract and forget about matter species and consider only pure gravitational quantum theory. The consistency of self-interactions there on the quantum level puts the same restriction on the form of the action of the theory. In such a situation in the language of Feynman diagrams, one considers also loops with quantum gravitons running inside. These graphs induce the same form of UV divergences as in (1). Then in such a model, we must still consider the dynamics of the quantum gravitational field with higher derivatives. Hence, from quantum considerations higher derivatives are inevitable.

We also remark here that in the special case, where the matter theory is classically conformally invariant with respect to classical gravitational background field (the examples are: massless fermion, massless Klein-Gordon scalar field conformally coupled to the geometry, electrodynamic field or non-Abelian Yang-Mills field in $d = 4$), then only the conformally covariant counterterm C^2 is generated, while the coefficient $\alpha_R = 0$ in (1). This is due to the fact that the quantization procedure preserves conformal symmetries of the original classical theory coupled to the non-trivial spacetime background. Such argument can be called as a conformal version of the original DeWitt-Utiyama argument. Then the R^2 counterterm is not needed but still the action of a quantum consistent coupled conformal system requires the higher-derivative dynamics in the gravitational sector [6]. Here this is clearly the gravitational dynamics only in the spin-2 sector of

metric fluctuations, which is contained entirely in the (conformal) C^2 sector of the generic four-derivative theory presented in (1).

An intriguing possibility for having higher derivatives in the gravitational action was first considered by Stelle in [7] and some exact classical solutions of such a theory were analyzed in [8–10]. In $d = 4$ spacetime dimensions, the minimal number of derivatives is exactly four, the same as the number of dimensions [11]. This reasoning coincides with the one presented earlier that we need to have in even number of dimensions d, precisely d derivatives in the gravitational action to have first scale-invariant model of gravitational dynamics (later possible to be promoted to enjoy also the full conformal invariance). However, as proven by Asorey, Lopez and Shapiro in [12], there are also possible theories with even higher number of derivatives, and they still have good properties on the quantum level and when coupled to quantum matter fields. Similarly, in the literature there are various known motivations for conformal gravity in $d = 4$ spacetime dimensions, one can consult representatives in [13, 14].

Secondly, we emphasize that to have a minimal (in a sense with the smallest number of derivatives) perturbatively renormalizable model of QG in dimensions d, one also has to consider actions with precisely d derivatives. The actions with smaller number are not scale-invariant and have problems on the quantum level to control all perturbative UV divergences, and not all of them are absorbable in the counterterms coming from the original classical actions of the theories – such models with less than d derivatives are not multiplicatively renormalizable. The first case for renormalizability is when the action contains all generic terms with arbitrary coupling coefficients with d (partial) derivatives on the metric for d dimensions. The special cases when some coefficients and some coupling parameters vanish may lead to restricted situations in which full renormalizability is not realized. We discuss such special limiting cases in further sections of this paper. The argument with the first renormalizable theory is a very similar in type to the quantum induced action from matter fields, but this time the particles which run in the perturbative loops of Feynman diagrams are quantum gravitons themselves. So this argument about renormalizability applies to pure quantum gravity cases. Unfortunately, the original Einstein-Hilbert action for QG model is not renormalizable (at least not perturbatively) in $d = 4$ dimensions [15–18]. The problems show up when one goes off-shell, couples some matter, or goes to the two-loop order, while at the first loop order with pure E-H gravitational action on-shell all UV divergences could be successfully absorbed [15] on Einstein vacuum backgrounds (so on Ricci-flat configurations). Actually, in such a case in vacuum configurations the theory at the one-loop level is completely UV-finite.

There are also other ways how one can on the quantum level induce the higher-derivative terms in the gravitational actions, although these further arguments are all related to the original one from DeWitt and Utiyama. One can, for example, consider integrating out completely quantum matter species on the level of functional integral which represents all accessible information of the quantum theory. In the situation, when these matter species are coupled to some background gravitational field, then the resulting partition function Z is a functional of the background gravitational field. Not surprisingly, this functional is of the higher-derivative nature in terms of number of derivatives of the fundamental metric field, if we work in the dimension $d > 2$. This reasoning was for example popularized by 't Hooft [19–21], especially since in $d = 4$ it can give rise to another motivations for conformal gravity as a quantum consistent model of conformal and gravitational interactions, when massless fields are integrated out in the path integral.

In this way we can discover the quantum consistent dynamics of the gravitational field even if we did not know that such quantum fields mediating gravitational interactions between particles existed in the first place. The graviton becomes a propagating particle and with higher-derivative form of the propagator, which translates in momentum space to the enhanced suppression of the fall-off of the propagator for large momenta in the UV regime. This is due to the additional higher powers of propagating momentum in the perturbative expression for the graviton's propagator. This enhanced UV decaying form of the propagator is what makes the UV divergences under perturbative control and what makes the theory at the end renormalizable. Besides a few (finite number of) controlled UV divergences the theory is convergent and gives finite perturbative answers to many questions one can pose about the quantum dynamics of the gravitational field, also in models coupled consistently to quantum matter fields.

Another way is to consider the theory of Einsteinian gravity and corrections to it coming from higher dimensional theories. One should already understood from the discussion above, that E-H action is a good quantum action for the QG model only in the special 2-dimensional case. There in $d = 2$ QG is very special renormalizable and finite theory, but without dynamical content resembling anything what is known from four dimensions (like for example the existence of gravitational waves, graviton spin-2 particles, etc.). This is again due to infinite power of conformal symmetry in $d = 2$ case. Instead, if one considers higher dimensions like 6, 8, etc. and then compactifies them to common 4-dimensional case, one finds that even if in the higher dimensions one had to deal with the two-derivative theory based on the Einstein-Hilbert action, then in the reduced case in four dimensions, one again finds effective (dimensionally reduced) action with four derivatives. These types of arguments were recently invoked by Maldacena [22] in order to study higher-derivative (and conformal) gravities from the

point of view of higher dimensions, when the process of integration out of quantum modes already took place and one derives a new dynamics for the gravitational field based on some compactification arguments.

All this above shows that many arguments from even various different directions lead to the studies of higher-derivative gravitational theories in dimensions of spacetime $d > 2$. Therefore, it is very natural to quantize such four-derivative theories (like it was first done by Stelle) and treat them as a starting point for discussion of QG models in $d = 4$ case. At the end, one can also come back and try to solve for exact solutions of these higher-derivative gravitational theories on the classical level, although due to increased level of nonlinearities this is a very difficult task [23].

Yet another argument is based on apparent similarity and symmetry seen in the action of quadratic gravity and action for a general Yang-Mills theory. Both these actions are quadratic in the corresponding field strengths (or curvatures). They are curvatures respectively in the external spacetime for the gravitational field and in the internal space for gauge degrees of freedom. The Einstein-Hilbert action is therefore *not similar* to the F^2 action of Yang-Mills theory and the system of Einstein-Maxwell or Einstein-Yang-Mills theory does not look symmetric since the number of curvatures in two sectors is not properly balanced. Of course, this lack of balance is later even amplified to the problematic level by quantum corrections and the presence of unbalanced UV divergences (non-renormalizability!). Still, already on the classical level, one sees some dichotomy, especially when one tries to define a common total covariant derivative D_μ (covariant both with respect to Yang-Mills internal group G and with respect to gravitational field). For such an object, one can define the curvature $\mathcal{F}_{\mu\nu}$ that is decomposed in its respective sectors into the gauge field strength $F_{\mu\nu}$ and the Riemann gravitational tensor $R_{\mu\nu\rho\sigma}$. But the most natural thing to do here is to consider symmetric action constructed with such a total curvature of the derivative D_μ and then the generalized $\mathcal{F}^2$ is the first consistent option to include both dynamics of the non-Abelian gauge field and also of the gravitational field. As we have seen this choice is also stable quantum-mechanically [24] since there are no corrections that would destabilize it and the only quantum corrections present they support this $\mathcal{F}^2$ structure of the theory, even if this was not there from the beginning. We emphasize that this was inevitably the higher-derivative structure for the dynamics of the quantum relativistic gravitational field studied here.

1.1. Motivations for and introduction to six-derivative gravitational theories

Now, we would like to summarize here on what is the general procedure to define the gravitational theory, both on the classical as well as on the quantum level. First, we decide what our theory is of – which fields are dynamical there. In our case these are gravitational fields entirely characterized by the metric tensor of gravitational spacetime. Secondly, we specify the set of symmetries (invariance group) of our theory. Again, in our setup these are, in general, invariances under general coordinate transformations also known as diffeomorphism symmetries of gravitational theories. In this sense, we also restrict the set of possible theories from general models considered in the gauge treatment of gravity, when the translation group or full Poincaré groups are gauged. Then finally following Landau we define the theory by specifying its dynamical action functional. In our case for a classical level, this is a GR-invariant scalar obtained by integrating some GR-densitized scalar Lagrangian over the full 4-dimensional continuum (spacetime). As emphasized above, for theoretical consistency, we must use Lagrangians (actions) which contain higher (partial) derivatives of the metric tensor, when the Lagrangian is completely expanded to a form where ordinary derivatives act on the metric tensors (contracted in various combinations). Specifying now, to the case motivated above, we shall use and study below the theories defined by classical action functionals which contain precisely six derivatives of the metric tensor field.

In order to define the theory on the quantum level, we use the standard functional integral representation of the partition function (also known as the vacuum transition amplitude) of the quantum theory. That is we construct, having the classical action functional $S_{\rm HD}$, being the functional of the classical metric field $S_{\rm HD}[g_{\mu\nu}]$, the following object

$$Z = \int \mathcal{D}g_{\mu\nu} \exp(iS_{\rm HD}), \tag{2}$$

where in the functional integral above we must be more careful than just on the formal level in defining properly the integration measure $\mathcal{D}g_{\mu\nu}$. For example, we should sum over all backgrounds and also over all topologies of the classical background gravitational field. One can hope that it is also possible to classify in four dimensions all gravitational configurations (all gravitational pseudo-Riemannian manifolds) over which we should integrate above. The functional integral, if properly defined, is the basis for quantum theory. One can even promote the point of view that by giving the functional Z one *defines* the quantum theory even without reference to any classical action S. However, it is difficult a priori to propose generating functionals Z, which are consistent with all symmetries of the theory (especially gauge invariances) and such that they possess sensible macroscopic (classical) limits. For practical purposes of evaluating various correlation functions between quantum fields and their fluctuations, one modifies this functional Z by adding a coupling of the quantum field (here this role of the integration variable is played by $g_{\mu\nu}$) to the classical external current J. And also for other theoretical rea-

sons, one can compute this functional in background field method, where the functional integration is over fluctuation fields, while the classical action functional is decomposed into background and parts quadratic, cubic and of higher order in quantum fluctuation fields. For this one defines that the full metric is decomposed as follows, $g_{\mu\nu} = \bar{g}_{\mu\nu} + h_{\mu\nu}$, where the background classical metric is denoted by $\bar{g}_{\mu\nu}$ and metric perturbations by $h_{\mu\nu}$. By computing variational derivatives of the partition function $Z[J]$ with respect to the classical current J one gets higher n-point functions with the accuracy of the full quantum level. One can compute them both perturbatively (in loop expansion) or non-perturbatively, and also on trivial backgrounds or in background field method. Finally, for spacetimes which asymptotically reach Riemann-flatness, from on-shell quantum Green functions dressed by wave functions of external classical states, one derives quantum matrix elements of scattering processes. Only in such conditions one can define general scattering problem in quantum gravitational theory.

In this article, we want to analyze the quantum gravitational model with six derivatives in the action. That the theory is with six derivatives can be seen, because of two related reasons. First, one can derive the classical equations of motion based on such an action. Then one will see that the number of partial derivatives acting on a metric tensor in a general term of such tensor of equations of motion is at most 6 in our model. Or similarly, one can compute the tree-level graviton's propagator for example around flat Minkowski background. And then one notices that some components of this propagator are suppressed in the UV regime by the power k^6 in Fourier space, when k is the propagating momentum of the quantum mode. Actually, for this last check one does not even have to invert and compute the propagator, one can perform a very much the same analysis on the level of the kinetic operator between gravitational fluctuations around some background (of course the flat background is here the easiest one). Later in the main text of this article, we discuss how to overcome the problems in defining the propagator in some special cases, but the situation with the terms of the kinetic operator is almost always well-defined and one can read the six-derivative character of the theory easily from there.

We have seen in the previous section that the four-derivative gravitational theories in $d = 4$ spacetime dimensions are scale-invariant (can be conformally invariant) on the classical level and that they are also first minimal renormalizable models of dynamical QG. This last assertion is proved by the power counting analysis. We will show below that it is possible to further extend the theory in such a way that the control over divergences is strengthened even more and this is again based on the analysis of the superficial degrees of divergences of any graph and also on the energy dimensionality arguments. In this way we will also explain why we can call generic six-derivative gravitational theories in $d = 4$ as perturbatively super-renormalizable theories.

The power counting analysis in the case of four-derivative Stelle gravity as in (1) (quadratic gravity of the schematic type $\mathcal{R}^2$ as in [7]) leads to the following equality

$$\Delta + d_\partial = 4, \tag{3}$$

where Δ is superficial degree of divergence of any Feynman graph G, d_∂ is the number of derivatives of the metric on the external lines of the diagram G, and for future use we define L as the number of loop order. For tree-level (classical level) we have $L = 0$, while for concreteness we shall assume $L \geqslant 1$. This theory is simply renormalizable since the needed GR-covariant counterterms (to absorb perturbative UV divergences) have the same form as the original action in (1)[2]. In general local perturbatively renormalizable HD model of QG in $d = 4$, the divergences at any loop order must take the form as in (1) with a potential addition of the topological Gauss-Bonnet term.

The change in the formula (3), when the six-derivative terms are leading in the UV regime, is as follows

$$\Delta + d_\partial = 6 - 2L. \tag{4}$$

The above formula can be also rewritten as a useful inequality (bound on the superficial degree Δ):

$$\Delta \leqslant 6 - 2L = 4 - 2(L - 1), \tag{5}$$

since $d_\partial \geqslant 0$. From this one sees an interesting feature that while in the case of four-derivative Stelle theory the bound was independent on the number of loops L, for the case of six derivatives (and higher too) the bound is tighter for higher number of loops. This is the basis for super-renormalizability properties. In particular, in the case of six-derivative theories there are no any loop divergences at the level of fourth loop, since for $L = 4$ we find that $\Delta < 0$, so all graphs are UV-convergent. We also emphasize that a super-renormalizable model is still renormalizable, but at the same time it is more special since infinities in the former do not show up at arbitrary loop order L, which is instead the case for merely renormalizable models. From the formula (4) at the $L = 3$ loop level the possible UV divergences are only of the form proportional to the cosmological constant Λ parameter, so completely without any partial derivatives acting on the metric tensor. Similarly for the case of $L = 2$, we have that divergences can be proportional to the Λ

[2]We remind for completeness that the Gauss-Bonnet scalar term GB $= E_4 = R^2_{\mu\nu\rho\sigma} - 4R^2_{\mu\nu} + R^2$ is a topological term, that is its variation in four spacetime dimensions leads to total derivative terms contributing nothing to classical EOM and also to quantum perturbation theory. It may however contribute non-perturbatively when the topology changes are expected. But for the sake of computing UV divergences we might simply neglect the presence of this term both in the original action as well as in the resulting one-loop UV-divergent part of the effective action.

(with no derivatives) and also to the first power of the Ricci scalar R of the manifold (with two derivatives on the metric, when it is expanded). In what follows we will not concentrate on these types of subleading in the UV divergences and our main attention in this paper will be placed on the four-derivative divergences as present in the action (1). Up to the presence of the Gauss-Bonnet term they are the same as induced from quantum matter loops. These types of divergences are only generated at the one-loop level since for them we must have $d_\partial = 4$ and $\Delta = 0$. The last information signifies that they are universal logarithmic divergences. Their names originate from the fact that they arise when the ultraviolet cutoff $\Lambda_{\rm UV}$ is used to cut the one-loop integrations over momenta of modes running in the loop in the upper limits.

The analysis of power counting implies that the theory has divergences only at the first, second and third loop order and starting from the fourth loop level it is completely UV-finite model of QG. Moreover, based on the above argumentation, the beta functions that we report below (in front of GR-covariant terms with four derivatives in the divergent effective action) receive contributions only at the one-loop level and higher orders (like two- and three-loop) do not have any impact on them. This means that the beta functions that we are interested in and that we computed at the one-loop level are all valid to all loop orders, hence our results for them are truly exact. They do not receive any perturbative contributions from higher loops. For other terms in the divergent action (like Λ or R) this is not true. The theory is four-loop finite, while the beta functions of R^2, C^2 and GB terms are one-loop exact. All these miracles are only possible to happen in very special super-renormalizable model since we have six derivatives in the gravitational propagator around flat spacetime. This number is bigger than the minimal for a renormalizable and scale-invariant QG theory in $d = 4$ spacetime dimensions and this is the origin of the facts above since we have a higher momentum suppression in the graviton's propagator.

According to what we have stated before, we decide to study the quantum theory described by the following classical Lagrangian,

$$\mathcal{L} = \omega_C C_{\mu\nu\rho\sigma}\Box C^{\mu\nu\rho\sigma} + \omega_R R\Box R + \theta_C C^2 + \theta_R R^2 + \theta_{\rm GB}{\rm GB} + \omega_\kappa R + \omega_\Lambda. \quad (6)$$

From this Lagrangian we construct the action of our HD quantum gravitational model, here with six derivatives as the leading number of derivatives in the UV regime, by the formula

$$S_{\rm HD} = \int d^4x\sqrt{|g|}\mathcal{L}. \quad (7)$$

Above by $C_{\mu\nu\rho\sigma}$ we denote the Weyl tensor (constructed from the Riemann $R_{\mu\nu\rho\sigma}$, Ricci tensor $R_{\mu\nu}$ and Ricci scalar R and with coefficients suitable for $d = 4$ case). Moreover, by GB we mean the Euler term which gives rise to Euler characteristic of the spacetime after integrating over the whole manifold. Its integrand is given by the term also known as the Gauss-Bonnet term and it has the following expansion in other terms quadratic in the gravitational curvatures,

$${\rm GB} = E_4 = R^2_{\mu\nu\rho\sigma} - 4R^2_{\mu\nu} + R^2. \quad (8)$$

Similarly, we can write for the "square" of the Weyl tensor in $d = 4$

$$C^2 = C^2_{\mu\nu\rho\sigma} = C_{\mu\nu\rho\sigma}C^{\mu\nu\rho\sigma} = R^2_{\mu\nu\rho\sigma} - 2R^2_{\mu\nu} + \frac{1}{3}R^2. \quad (9)$$

Finally, to denote the box operator we use the symbol $\Box$ with the definition $\Box = g^{\mu\nu}\nabla_\mu\nabla_\nu$, which is a GR-covariant analogue of the d'Alembertian operator ∂^2 known from the flat spacetime.

It is important to emphasize here that the Lagrangian (6) describes the most general six-derivative theory describing the propagation of gravitational fluctuations on flat spacetime. For this purpose it is important to include all terms that are quadratic in gravitational curvature. As it is obvious from the construction of the Lagrangian in (6) for six-derivative model we have to include terms which are quadratic in the Weyl tensor or Ricci scalar and they contain precisely one power of the covariant box operator $\Box$ (which is constructed using the GR-covariant derivative ∇_μ). These two terms exhaust all other possibilities since other terms which are quadratic and contain two covariant derivatives can be reduced to the two above exploiting various symmetry properties of the curvature Riemann tensor as well as cyclicity and Bianchi identities. Moreover, the basis with Weyl tensors and Ricci scalars is the most convenient when one wants to study the form of the propagator of graviton around flat spacetime. Other bases are possible as well but then they distort and entangle various contributions of various terms to these propagators. We also remark that the addition of the Gauss-Bonnet term is possible here (but it is a total derivative in $d = 4$); one could also add a generalized Gauss-Bonnet term, which is an analogue of the formula in (8), where the GR-covariant box operator in the first power is inserted in the middle of each of the tensorial terms there, which are quadratic in curvatures. Eventually, there is no contribution of the generalized Gauss-Bonnet term in any dimension to the flat spacetime graviton propagator, so for this purpose we do not need to add such term to the Lagrangian as it was written in (6).

In what follows we employ the pseudo-Euclidean notations and by $\sqrt{|g|}$ we will denote the square root of the absolute value of the metric determinant (always real in our conventions). The two most subleading terms in the Lagrangian (6) are with couplings ω_κ and ω_Λ respectively. The first one is related to the Newton gravitational constant G_N, while the last one ω_Λ to the value of the physical cosmological constant

parameter. The QG model with the Lagrangian (6) is definitely the simplest one that describes the most general form of the graviton propagator around flat spacetime, in four spacetime dimensions and for the theory with six derivatives.

We would like to already emphasize here, that there are two remarkable special limiting cases in the theory (6). In order to have a non-degenerate classical action and the well-defined Hessian operator of the second variational derivative, one needs to require that both coefficients of the UV-leading terms, namely ω_C and ω_R, should be non-zero. Only in this case the theory is renormalizable, moreover only in this case it also has nice additional features like super-renormalizability and that the fourth and higher perturbative loop contributions are completely finite. We want to say that the quantum calculations reported in the next section correspond only to this kind of well balanced model with both Weyl tensor and Ricci scalar squared terms and one power of the GR-covariant box operator inserted in the middle. (This is in order to have a six-derivative action, but also with terms that are precisely quadratic in gravitational curvatures.) In principle, there exist also models with non-balanced situations and dichotomy between different sectors of fluctuations. For example, in the special case of $\omega_C = 0$, $\theta_C \neq 0$ and $\omega_R \neq 0$, the theory has the propagating spin-two mode with four derivatives and the propagating spin-zero mode with six derivatives in the perturbative spectrum around flat spacetime. This has to be contrasted with the fact that interaction vertices have always six derivatives in both special and also in generic theories (with $\omega_C \neq 0$ and $\omega_R \neq 0$). For another special version of the model, with $\omega_C \neq 0$ and $\omega_R = 0$, the situation is quite opposite regarding the spectrum, but the negative conclusions are the same. According to the power counting arguments from [6, 25] and also from (3) in both special cases the theories are unfortunately non-renormalizable. (We also discuss in greater details the power counting for these two special limiting models in section 4.4.) Hence one should be very careful in performing computations in such cases and in trusting the results of limits there. These cases will be analyzed in more details in the next sections as it will be revealed that they are crucial for understanding the issue of the structure of perturbative divergences both in the four-derivative as well as also in six-derivative QG models in $d = 4$.

The other consequences of the formula for power counting as presented in (4) is that the subleading in the UV terms of the original action in (6) do not at all contribute to the four-derivative terms leading in the UV regime of the divergences in (1). That is we have that the coefficients α_C, α_R and $\alpha_{\rm GB}$ in (1) depend only on the ratio of the coefficient in front of the term with Weyl tensors and box inserted in the middle (i.e. $C\Box C$) to the coefficient in front of the corresponding term with two Ricci scalars (i.e. $R\Box R$), so only on the ratio ω_C/ω_R also to be analyzed later at length here. These coefficients of UV divergences α_C, α_R and $\alpha_{\rm GB}$ do not depend on θ_C, θ_R, $\theta_{\rm GB}$, ω_κ nor on ω_Λ. This is due to the energy dimensionality considerations of other UV-subleading terms in the action in (6). Only the terms having the same energy dimensionality as the leading in the UV regime (shaping the UV form of the perturbative propagator) may contribute to the leading form of UV divergences, which in the divergent action (1) are represented by dimensionless numbers (in $d = 4$) such as α_C, α_R and $\alpha_{\rm GB}$. For example, the terms with coefficients θ_C or θ_R have different energy dimensions and cannot appear there. This pertinent observation lets us for our computation to use just the reduced action, where we write only the terms that are important for the UV divergences we want to analyze in this paper. This action takes explicitly the following form

$$S_{\rm HD} = \int d^4x \sqrt{|g|}\,(\omega_C C_{\mu\nu\rho\sigma}\Box C^{\mu\nu\rho\sigma} + \omega_R R\Box R)\,. \quad (10)$$

We want to just remark here that the results in the theory with six-derivative gravitational action are discontinuous to the results one obtains for the similar type of computations in four-derivative Stelle quadratic QG models, which are usually analyzed in $d = 4$ as the first and the most promising models of higher-derivative QG. This discontinuity is based on the known fact (both for HD gauge and gravitational theories) that the cases with two and four more derivatives in the action of respective gauge fields (metric fields in gravity) than in the minimal renormalizable model are discontinuous and exceptional, while the general formula exists starting from action with six derivatives more in its definition (and then this formula could be analytically extended). All three cases of: first minimal renormalizable theory, and the models with two or four derivatives more are special and cannot be obtained by any limiting procedure from the general results which hold for higher-derivative regulated actions, which contain six or more derivatives than in the minimal renormalizable model. For the case of QG in $d = 4$ in the minimal model we have obviously four derivatives. Of course, this discontinuity is related to the different type of enhanced renormalizability properties of the models in question. As we have already explained above the gravitational model with six derivatives in $d = 4$ is the first super-renormalizable model of QG, where from the fourth loop on the perturbative UV divergences are completely absent. The case of Stelle theory gives just the renormalizable theory, where the divergences are present at any loop order (they are always the same divergences, always absorbable in the same set of counterterms since the theory is renormalizable). One sees the discontinuity already in the behaviour of UV divergences as done in the analysis of power counting. When the number of derivatives is increased in steps (by two), then the level of loops when one does not see divergences at all decreases but in some discontinuous jumps. And for example for the QG theory with ten or more derivatives the UV divergences are only at

the one-loop level. (For gravitational theories with 8 derivatives the last level which is divergent is the second loop.)

There exist also analytic formulas, which combine the results for UV divergences for the cases of theories with four or more derivatives more compared to the minimal renormalizable model with four derivatives in $d = 4$. Again one sees from such formulas, that the correct results for the minimal renormalizable model and the one with six derivatives are discontinuous. Then the case with 8-derivative gravitational theory is the first one for which the analytic formulas hold true. However, this has apparently nothing to do with the strengthened super-renormalizability properties at some loop level as it was emphasized above.

The six-derivative gravitational theory is therefore 3-loop super-renormalizable since the 3-loop level is the last one, when one needs to absorb infinities and renormalize anew the theory. These jumps from 3-loop super-renormalizability to 2-loop and finally to one-loop super-renormalizability are from their nature discontinuous and hence also the results for divergences inherit this discontinuity. For theories with ten or more derivatives we have one-loop super-renormalizability and the results for even higher number of derivatives $2n$ must be continuous in the parameter of the number of derivatives $2n$, which could be analytically extended to the whole complex plane from the even integer values $2n \geqslant 10$, which it originally had. In this analytically extended picture, the cases with eight, six and four derivatives are special isolated points, which are discontinuous and cannot be obtained from the general analytic formula valid for any $n \geqslant 5$. The origin of this is again in power counting of divergences, when some integrals over loop momenta are said to be convergent, when the superficial degree of divergence is smaller than zero, and when this is non-negative, then one meets non-trivial UV divergences. These infinities are logarithmic in the UV cutoff $k_{\rm UV}$ for loop integration momenta for the degree Δ vanishing, and power-law type for the degree Δ positive. This sharp distinction between what is convergent and what is divergent (based on the non-negativity of the degree of divergences Δ of any diagram) introduces the discontinuity, which is the main source of the problems here.

In this contribution, we mainly discuss and analyze the results which were first obtained in our recent publication [26]. The details of the methods used to obtain them were presented to some extent in this recent article. The method consists basically of using the Barvinsky-Vilkovisky trace technology [27] applied to compute functional traces of differential operators giving the expression for the UV-divergent parts of the effective action at the one-loop level. The main results were obtained in background field method and from UV divergences in [26] we read the beta functions of running dimensionless gravitational couplings. The results for them in six-derivative gravitational theory in $d = 4$ spacetime dimensions were the main results there. They are also described in section 2 here. Instead, in the present contribution, we decided to include an extended discussion of the theoretical checks done on these results in section 3. However, the main novel contribution is in section 4, where we present the analysis of the structure of these obtained results for the beta functions. Our main goal here is to show an argumentation that provides an explanation why the structure of the beta function is unique and why it depends in this particular form on the ratio x (to be defined later in the main text in (36)). These comments were not initially included in the main research article [26] and they constitute the main new development of the present paper.

We remind to the reader that in this paper, in particular, we will spend some time on attempts to explain the discontinuity of such results for UV divergences, when one goes from six- to four-derivative gravitational theories. So, in other words, when one reduces 3-loop super-renormalizability to just renormalizability. Or equivalently, when the situation at the fourth perturbative loop gets modified from not having divergences at all, because all loop integrations give convergent results (with negative superficial degree $\Delta < 0$), to the situation when at this loop level still UV divergences are present (since their degree Δ is zero for logarithmic UV divergences in the cutoff). This clearly sharp contrast in the sign of the superficial degree of divergences is one of the reasons, why the discontinuity between the cases of six- and four-derivative gravitational theories in $d = 4$ persists.

1.2. Addition of killer operators

As a matter of fact, we can also add other terms (cubic in gravitational curvatures $\mathcal{R}^3$) to the Lagrangian in (6). These terms again will come with the coefficients of the highest energy dimensionality, equal to the dimensionality of the coefficients ω_C and ω_R. Hence they could contribute to the leading four-derivative terms with UV divergences of the theory. The general form of them is given by the following list of six GR-covariant terms

$$\begin{aligned}\mathcal{L}_{\mathcal{R}^3} = {} & s_1 R^3 + s_2 R R_{\mu\nu} R^{\mu\nu} + s_3 R_{\mu\nu} R^{\mu}{}_{\rho} R^{\nu\rho} \\ & + s_4 R R_{\mu\nu\rho\sigma} R^{\mu\nu\rho\sigma} + s_5 R_{\mu\nu} R_{\rho\sigma} R^{\mu\rho\nu\sigma} \\ & + s_6 R_{\mu\nu\rho\sigma} R^{\mu\nu}{}_{\kappa\lambda} R^{\rho\sigma\kappa\lambda} \,. \end{aligned} \quad (11)$$

Actually, these terms can be very essential for making the gravitational theory with six-derivative actions completely UV-finite. However, for renormalizability or super-renormalizability properties these terms are not necessary, e.g., they do not make impact on the renormalizability of the theory and therefore should be regarded as non-minimal. In the analysis below we did not take their contributions into account and made already a technically demanding computation in a simplest minimal model with six-derivative actions. The set of terms in (11) is complete in $d = 4$ for all

what regards terms cubic in gravitational curvatures. This non-trivial statement is due to various identities as proven in [28].

These cubic terms are also sometimes called "killers" of the beta functions since they may have profound effects on the form of the beta functions of all terms in the theory. This is roughly very simple to explain. These killer terms are generally of the type $s\mathcal{R}^3$ and are to be added to the original Lagrangian in (6) of six-derivative theories, where the UV-leading terms were of the type $\omega\mathcal{R}\Box\mathcal{R}$. It is well known that to extract UV divergences at the one-loop level one has to compute the second variational derivative operator (Hessian $\hat{H}$) from the full action. The contributions from cubic killers to it will be of the form of at least $s\mathcal{R}$, when counted in powers of generalized curvature $\mathcal{R}$. Next, when computing the trace of the functional logarithm of the Hessian operator for the form of the one-loop UV-divergent effective action one uses the expansion of the logarithm in a series according to

$$\ln(1+z) = z - \frac{1}{2}z^2 + \dots . \tag{12}$$

Hence we need to take maybe up to the square of the contribution $s\mathcal{R}$ to the Hessian from the cubic killer term. The third power would be too much. We must remember that we are looking for terms of the general type $\mathcal{R}^2$ in the UV-divergent part of the effective action. Hence the contribution of the cubic killer in curvatures would produce addition to the covariant terms with UV divergences of the general type $f(s)\mathcal{R}^2$, where the yet unknown functions $f(s)$ can be polynomials up to the second order in the coefficients s_i of these killers. Now, requiring the total beta functions vanish (for complete UV-finiteness) we need in general to solve the system of the quadratic equations in the coefficients s_i. The only obstacle for finding coefficients of the killers can be that some solutions of this system reveal to be complex numbers, not real, but we need to require all s_i coefficients to be real for the definiteness of the action (for example in the Euclidean case of the signature of the metric). Therefore this issue requires a more detailed mathematical analysis, but the preliminary results based on [26, 29] show that in most of the cases the UV-finiteness is possible and easily can be achieved by adding the cubic killer operators from (11) with real coefficients s_i.

One can compare the situation here with cubic killers to the more known situation where the quartic killers are used to obtain UV-finiteness. Unfortunately, such quartic killers cannot be added to the six-derivative gravitational theory from (6) since they would have too many partial derivatives and would destroy the renormalizability of the model. Quartic killers can be included in theories with at least 8 derivatives. Such approach seems to be preferred one since the contribution of quartic killers (of the type schematically as $\mathcal{R}^4$) is always linear in $d = 4$ to UV divergences proportional to $\mathcal{R}^2$ schematically. And to solve linear system of equations with linear coefficients is always doable and one always finds solutions and they are always real. This approach was successfully applied to gravity theories in [29], to gauge theories in [30], to the theories on de Sitter and anti-de Sitter backgrounds [31] and also in general non-local theories [32]. One could show that the UV-finiteness may be an universal feature of quantum field-theoretical interactions in nature [33]. Moreover, this feature of the absence of perturbative UV divergences is related to the quantum conformality as advocated in [34, 35].

1.3. Universality of the results

Finally, one of the most important features of the expression for the UV-divergent part of the effective action in the six-derivative gravitational theories is its complete independence of any parameter used in the computation. This parameter can be gauge-fixing parameter, or it can appear in gauge choice, or in details of some renormalization scheme, etc.. This bold fact of complete universality of the results for the effective action was proven by the theorem by Kallosh, Tarasov and Tyutin (KTT) [36–38], applied here to the six-derivative QG theories. The theorem expresses the difference between two effective actions of the same theory but computed using different set of external parameters. Basically, this difference is proportional to the off-shell tensor of classical equation of motion of the original theory. And this difference disappears on-shell. However, in our computation we want to exploit the case when the effective action and various Green functions are computed from it understood as the off-shell functional.

But in super-renormalizable theories there is still some advantage of using this theorem, namely for this one notices the difference in number of derivatives on the metric tensor between the original action and Lagrangian of the theory as it is in the form (10) (and resulting from it classical EOM) and between the same counting of derivatives done in the divergent part of the effective action. We remind the reader that in the former case we have six derivatives on the metric, while in the latter we count up to four derivatives. This mismatch together with the theorem of KTT implies that the difference between the two UV-divergent parts of the effective actions (only for these parts of the effective actions) computed using two different schemes or methods must vanish in super-renormalizable QG theories with six-derivative actions for whatever change of the external parameters that are used for the computation of these UV-divergent functionals. This means that our results for divergences are completely universal and cannot depend on any parameter. Hence we derive the conclusion that our found divergences do not depend on the gauge-fixing parameters, gauge choices nor on other parametrization ambiguities. We remark that this situation is much better than for example in E-H

gravity, where the dependence on a gauge is quite strong, or even in Stelle four-derivative theory, where four-derivative UV-divergent terms also show up some ambiguous dependence on gauge parameters off-shell. Here we are completely safe from such problems and such cumbersome ambiguities.

In this way such beta functions are piece of genuine observable quantity that can be defined in super-renormalizable models of QG. They are universal, independent of spurious parameters needed to define the gauge theory with local symmetries, and moreover they are exact, but still being computed at the one-loop level in perturbation calculus. They are clearly very good candidates for the observable in QG models. Therefore all these nice features gives us even more push towards analyzing the structure of such physical quantities and to understand this based on some theoretical considerations. This is what we are trying to attempt in this contribution.

Another important feature is that in theories with higher derivatives in their defining classical action, on the full quantum level there is no need for perturbative renormalization of the graviton‘s wave function. This is also contrary to the case of two-derivative theory, when one has to take this phenomena into account, although its expression is not gauge-invariant and depends on the gauge fixing. These nice properties of no need for wave function renormalization can be easily understood in the Batalin-Vilkovisky formalism for quantization of gauge theories (or in general theories with differential constraints) [39, 40]. This important feature is also shared by other, for example, four-derivative QG models. Since the wave function of the graviton does not receive any quantum correction, then one can derive the form of the beta functions for couplings just from reading the UV divergences of the dressed two-point functions with two external graviton lines. We can simplify our computation drastically since for this kind of one-loop computation we do not have to bother ourselves with the three- or higher n-point function to independently determine the wave function renormalization. Unfortunately, the latter is the case, for example, for standard gauge theory (Yang-Mills model) or for E-H gravity, where the renormalization of the coupling constant of interactions has to be read from the combination of the two- and three-point functions of the quantum theory, while the wave function renormalization of gauge fields or graviton field respectively can be just read from quantum dressed two-point Green function. For the case of six-derivative theories, just from the two-point function we can read everything about the renormalization of the coupling parameters of gravitons' interactions. Additionally, we have that on the first quantum loop level we do not need to study effective interaction vertices dressed by quantum corrections. Hence, here at the one-loop level there is no quantum renormalization of the graviton's wave function and UV divergences related to interactions are derived solely from propagation of free modes (here of graviton fields) around the flat spacetime and corrected (dressed) at the first quantum loop. Effective vertices of interactions between gravitons do not matter for this, but that situation may be changed at higher loop orders. At the one-loop level this is a great simplification for our algorithm of derivation of the covariant form of UV divergences since we just need to extract them from the expression for one-loop perturbative two-point correlators of the theory, both in cases of four- and six-derivative QG models.

All these nice features of the six-derivative QG model makes it further worth studying as an example of non-trivial RG flows in QG. Here we have exactness of one-loop expressions for running $\theta_C(t)$, $\theta_R(t)$ and $\theta_{\rm GB}(t)$ coupling parameters in (6), together with super-renormalizability. This is one of the most powerful and beautiful features of the super-renormalizable QG theory analyzed here. Therefore, this model gives us a good and promising theoretical laboratory for studying RG flows in general quantum gravitational theories understood in the field-theoretical framework.

We remark that from a technical point of view, the one-loop calculations in super-renormalizable models of QG are more difficult when compared to the ones done in the four-derivative just renormalizable gravitational models [27, 41–43]. The level of complexity of such calculations depends strongly on the number of derivatives in the classical action of the model as well as on the type of one-loop counterterms one is looking for. The counterterm for the cosmological constant is actually very easy to obtain and this was done already in [12]. Next, the derivation of the divergence linear in the scalar curvature R requires really big efforts and was achieved only recently in our collaboration in [44]. In the present work, we comment on the next step, and we show the results of the calculations of the simply looking one-loop UV divergences for the four-derivative sector in the six-derivative minimal gravity model. In our result, we have now full answers to the beta functions for the Weyl-squared C^2, Ricci scalar-squared R^2 and the Gauss-Bonnet GB scalar terms. The calculation is really tedious and cumbersome and it was done for the simplest possible six-derivative QG theory without cubic terms in the classical action, which here would be third powers of the generalized curvature tensor $\mathcal{R}^3$. Even in this simplest minimal case, the intermediate expressions are too large for the explicit presentation here, hence they will be mostly omitted. Similar computations in four-, six- and general higher-derivative gauge theory were also performed in [30, 45, 46].

As it was already mentioned above, the derivation of zero- and two-derivative ultraviolet divergences has been previously done in Refs. [12] and [44]. Below we will show the results for the complete set of beta functions for the theory (10). This we will achieve by deriving the exact and computed at one-loop beta function coefficients for the four-derivative gravitational

couplings, namely θ_C, θ_R and $\theta_{\rm GB}$, extracted as the coefficients of the UV-divergent part of the effective action in (1). Without loss of generality, the calculation will be performed in the reduced model (10), so without terms subleading in the number of partial derivatives acting on the metric tensor after the proper expansion here. (We will not need to include terms like R^2, C^2 or even R in (10).) This is clearly explained by the arguments from dimensional analysis since the divergences with four derivatives of the metric, in (1), are of our biggest interest here. Moreover, numerical coefficients of those subleading terms cannot in any way combine with coefficients of propagators (shaped in the UV regime by the leading terms with six derivatives in the action (10)) to form dimensionless ratios in front of terms in (1) in $d = 4$ spacetime dimensions.

2. Brief description of the technique for computing UV divergences

An essential part of the calculations is pretty much the same as usually done in any higher-derivative QG model, especially in the renormalizable or super-renormalizable models [26, 44] as considered here. In what follows, we can skip a great part of the explanations. We will focus on the calculation of the fourth derivative terms of the divergent part of the effective action.

First, to perform pure computation we use the background field method, which is defined by the following splitting of the metric

$$g_{\mu\nu} \longrightarrow \bar{g}_{\mu\nu} + h_{\mu\nu} \tag{13}$$

to the background $\bar{g}_{\mu\nu}$ and the quantum fluctuation parts given by the spin-2 symmetric tensor $h_{\mu\nu}$.

The next step is to define the gauge-fixing condition. Since our theory with six derivatives still possesses gauge invariance due to diffeomorphism symmetry we have to fix the gauge to make the graviton propagator non-degenerate. For this we will make some choice of the gauge-fixing parameters, here represented by numerical α, β and γ parameters. First, we choose the parameter β in the harmonic background gauge-fixing condition χ_μ, according to

$$\chi_\mu = \nabla^\lambda h_{\lambda\mu} - \beta\,\nabla_\mu h, \qquad h = h^\nu{}_\nu\,, \tag{14}$$

in the most simple "minimal" form, as will be indicated below. The same concerns the parameters α and γ. Finally, we select a general form of the weighting operator, $\hat{C} = \tilde{C}^{\mu\nu}$, which is defined by the formula below:

$$\hat{C} = \tilde{C}^{\mu\nu} \;=\; -\frac{1}{\alpha}\left(g^{\mu\nu}\Box^2 + (\gamma-1)\nabla^\mu\Box\nabla^\nu\right). \tag{15}$$

This together with the gauge-fixing condition, that is χ^μ, defines the gauge-fixing action [41] in the following form,

$$S_{\rm gf} = \int d^4x\sqrt{|g|}\;\chi_\mu\,\tilde{C}^{\mu\nu}\,\chi_\nu. \tag{16}$$

The action of the complex Faddeev-Popov (FP) ghost fields (respectively $\bar{C}^\mu$ and C_μ) has in turn the form

$$S_{\rm gh} \;=\; \int d^4x\sqrt{|g|}\;\bar{C}^\mu M_\mu{}^\nu C_\nu, \tag{17}$$

where the bilinear part between the anti-ghost $\bar{C}^\mu$ and ghost fields C_μ, the so called FP-matrix $\hat{M}$, depends differentially on χ_μ gauge-fixing conditions and also on the contracted form of the generator of gauge transformations $\hat{R}$,

$$\hat{M} \;=\; M_\mu{}^\nu \;=\; \frac{\delta\chi_\mu}{\delta g_{\alpha\beta}}\,R_{\alpha\beta}{}^\nu \;=\; \delta^\mu_\nu\Box + \nabla^\nu\nabla_\mu - 2\beta\nabla_\mu\nabla^\nu. \tag{18}$$

In the above equation by the matrix-valued operator $R_{\alpha\beta}{}^\nu$ we mean the generator of infinitesimal diffeomorphism (local gauge) transformations in any metric theory of gravity.

Since as proven and explained at the end of section 1.3, our final results for UV divergences are here completely universal and they are independent of any parameter used to regularize, compute and renormalize the effective action of the theory, then we can take the following philosophy at work here. We choose some specific gauge choice in order to simplify our calculation, but then we are sure that the final results will be still correct, if obtained consistently within this computation done in a particular gauge choice. It is true that intermediate steps of the computation may be different in different gauges, but the final results must be unique and it does not matter which way we arrive to them. We think we could choose one of the simplest path to reach this goal. A posteriori this method is justified, but the middle steps of the processing of the Hessian operator will not have any invariant objective physical meaning. These are just steps in the calculational procedure in some selected gauge.

One knows that in such a case, for example, for a formalism due to Barvinsky-Vilkovisky (BV) [27] of functional traces of differential operators applied in the background field method framework, all intermediate results are manifestly gauge-independent. Then still such partial contributions (any of them) separately do not have any sensible physical meaning, although such results are gauge-independent and look superficially physical – any physical meaning cannot be properly associated to them, if all these terms are not taken in total and only in the final sum. On the contrary, if the computation is performed using Feynman diagrams, momentum integrals and around flat spacetime, then the intermediate results are not gauge-invariant, as it is well known for partial contributions of some graphs, and only in the final sum they acquire such features of gauge-independence.

We also need to distinguish here two different features. Some partial results may be still gauge-dependent and their form may not show up gauge symmetry (for example, using Feynman diagram approach, a contribution from a subset of divergent

diagrams may not be absorbed by a gauge-covariant counterterm: F^2 in gauge theories, or $\mathcal{R}^2$ in gravity in $d = 4$). This feature should be however regained when the final results are obtained. This is actually a good check of the computation. But another property is independence of the gauge-fixing parameters, which are spurious non-physical parameters. At the same time, a counterterm might be gauge-covariant (built with F^2 or $\mathcal{R}^2$ terms), but its front coefficient may depend on these gauge parameters α, β, γ, etc.. This should not happen for the final results and they should be both gauge-covariant (so gauge-independent or gauge-invariant) and also gauge-fixing parameters independent. These two necessary properties, to call the result physical, must be realized completely independently and they are a good check of the correctness of the calculation.

Unfortunately, it seems that using the BV computational methods even in the intermediate results for traces of separate matrix-valued differential operators (like $\hat{H}$, $\hat{M}$ and $\hat{C}$), we see already both gauge-independence and gauge-fixing parameters independence provided that such parameters were not used in the definition of these operators. Only in some cases, the total result is only gauge-fixing parameter independent. This means that within this formalism of computation this check is not very valuable and one basically has to be very careful to get the correct results at the end. Instead, we perform a bunch of other rigorous checks of our results as it is mentioned, for example, in section 3.

Finally, let us here give briefly a few details concerning the choice of the gauge-fixing parameters α, β and γ. The bilinear form of the action is defined from the second variational derivative (giving rise to the Hessian operator $\hat{H}$)

$$\hat{H} = H^{\mu\nu,\rho\sigma} = \frac{1}{\sqrt{|g|}}\,\frac{\delta^2\,(S+S_{\rm gf})}{\delta h_{\mu\nu}\,\delta h_{\rho\sigma}} \;=\; H^{\mu\nu,\rho\sigma}_{\rm lead} + \mathcal{O}(\nabla^4), \tag{19}$$

where the first term $H^{\mu\nu,\rho\sigma}_{\rm lead}$ contains six-derivative terms, which are leading in the UV regime. By $\mathcal{O}(\nabla^4)$ we denote the rest of the bilinear form, with four or less derivatives and with higher powers of gravitational curvatures $\mathcal{R}$. The energy dimension of this expression is compensated by the powers of curvature tensor $\mathcal{R}$ and its covariant derivatives, hence in this case, we can also denote $\mathcal{O}(\nabla^4) = O(\mathcal{R})$. The corresponding full expression for the Hessian operator $\hat{H}$ is very bulky, and we will not include it here.

The highest derivative part (leading in the UV regime) of the $\hat{H}$ operator, after adding the gauge-fixing term (16) that we have selected, has the form

$$\begin{aligned} H^{\mu\nu,\rho\sigma}_{\rm lead} &= \Big[\omega_C\,\delta^{\mu\nu,\rho\sigma} + \Big(\frac{\beta^2\gamma}{\alpha} - \frac{\omega_C}{3} + 2\omega_R\Big) g^{\mu\nu} g^{\rho\sigma}\Big]\Box^3 \\ &+ \Big(\frac{\omega_C}{3} - 2\omega_R - \frac{\beta\gamma}{\alpha}\Big)\Big(g^{\rho\sigma}\nabla^\mu\nabla^\nu + g^{\mu\nu}\nabla^\rho\nabla^\sigma\Big)\Box^2 \\ &+ \Big(\frac{1}{\alpha}g^{\mu\rho} - 2\omega_C g^{\mu\rho}\Big)\nabla^\nu\nabla^\sigma\Box^2 \\ &+ \Big(\frac{2\omega_C}{3} + 2\omega_R + \frac{\gamma-1}{\alpha}\Big)\nabla^\mu\nabla^\nu\nabla^\rho\nabla^\sigma\Box. \end{aligned} \tag{20}$$

In this expression, we do not mark explicitly the symmetrization in and between the pairs of indices (μ,ν) and (ρ,σ) for the sake of brevity.

To make the UV-leading part of the Hessian operator $H^{\mu\nu,\rho\sigma}_{\rm lead}$ minimal, one has to choose the following values for the gauge-fixing parameters [44]:

$$\alpha = \frac{1}{2\omega_C}, \quad \beta = \frac{\omega_C - 6\omega_R}{4\omega_C - 6\omega_R}, \quad \gamma = \frac{2\omega_C - 3\omega_R}{3\omega_C}. \tag{21}$$

We previously explained that this choice does not affect the values and the form of one-loop divergences in super-renormalizable QG. Thus, we assume it as the most simple option.

One notices that the expressions for gauge-fixing parameters in (21) are singular in the limit $\omega_C \to 0$ and also when $\omega_C = \frac{3}{2}\omega_R$. While the first one is clearly understandable, because then we are losing one term $\omega_C C\Box C$ in the action (10) and the theory is degenerate and non-generic, the second condition is not easily understandable in the Weyl basis of writing terms in the action in (10) (with R^2 and C^2 terms). To explain this other spurious degeneracy one rather goes to the Ricci basis of writing terms (with R^2 and $R^2_{\mu\nu} = R_{\mu\nu}R^{\mu\nu}$ elements and also properly generalized to the six-derivative models by inserting one power of the box operator in the middle). There one sees that the absence of the coefficient in front of the $R^2_{\mu\nu}$ leads to the pathology in the case of $\omega_C = \frac{3}{2}\omega_R$ and also formal divergence of the β gauge-fixing parameter. We remark that in the final results there is no any trace of this denominator and this divergence, hence the condition for non-vanishing of the coefficient in front of the covariant term $R^2_{\mu\nu}$ in the Ricci basis does not have any sensible and crucial meaning – this is only a spurious intermediate dependence on $(4\omega_C - 6\omega_R)^{-1}$. Contrary, the singular dependence on ω_C coefficient is very crucial and will be analyzed at length here. Actually, to verify that the denominators with $(4\omega_C - 6\omega_R)^{-1}$ completely cancel out in the final results is a powerful check of our method of computation.

Now we can collect all the necessary elements to write down the general formula for the UV-divergent part of the one-loop contribution to the effective action of the theory [41],

$$\bar{\Gamma}^{(1)} \;=\; \frac{i}{2}{\rm Tr}\ln\hat{H} \;-\; i{\rm Tr}\ln\hat{M} \;-\; \frac{i}{2}{\rm Tr}\ln\hat{C}. \tag{22}$$

The calculation of the divergent parts of the first two expressions in (22) is very standard. One uses for this the technique of the generalized Schwinger-DeWitt method [27], which was first introduced by Barvinsky and Vilkovisky. For this reason we shall skip most of the standard technical details here. We use the Barvinsky-Vilkovisky trace technology related to the covariant heat kernel methods together with methods of dimensional regularization (DIMREG) to evaluate the functional traces present in (22) and to

have under control the general covariance of the final results. Due to this we cannot check it because all three contributions in (22) gives results which look covariant and sensible. We remind the reader that here we work with the minimal gauge choice and in general all three terms separately will show the gauge dependence and also spurious dependence on gauge-fixing parameters α, β and γ. However, only the final results, so the weighted sum as in (22) is properly gauge-independent and gauge-fixing independent and gives rise to a physical observable of the beta functional of the theory at the one-loop level.

The computational method that we adopt here consists basically of using the Barvinsky-Vilkovisky trace technology to compute functional traces of differential operators giving the expression for the UV-divergent parts of the effective action at the one-loop level. The main results are obtained in background field method and from UV divergences in [26] we read the beta functions of running gravitational couplings. We also present here below an illustrative scalar example of the techniques by which these results were obtained.

2.1. Example of the BV method of computation for the scalar case

The simplest example to use the technique of computation presented here can be based on the analysis of the scalar case given by the action

$$S=\int d^4x\left(-\frac{1}{2}\phi\Box\phi-\frac{\lambda}{4!}\phi^4\right). \tag{23}$$

From this action one reads the second variational derivative operator (also known as the Hessian) given by the formula

$$H=\frac{\delta^2 S}{\delta\phi^2}=-\Box-\frac{\lambda}{2}\phi^2. \tag{24}$$

Next, one needs to compute the following functional trace $\mathrm{Tr}\ln H$ to get the UV-divergent part of the one-loop effective action

$$\begin{aligned}\mathrm{Tr}\ln H&=\mathrm{Tr}\ln\left(-\Box-\frac{\lambda}{2}\phi^2\right)\\&=\mathrm{Tr}\ln\left(-\Box\left(1+\frac{\lambda}{2}\phi^2\Box^{-1}\right)\right)\\&=\mathrm{Tr}\ln\left(-\Box\right)+\mathrm{Tr}\ln\left(1+\frac{\lambda}{2}\phi^2\Box^{-1}\right).\end{aligned} \tag{25}$$

In the above expression, one concentrates on the second part which contains the λ coupling. One expands the logarithm, as in (12), in the second trace to the second order in λ. This yields

$$\begin{aligned}\mathrm{Tr}\ln\left(1+\frac{\lambda}{2}\phi^2\Box^{-1}\right)&=\mathrm{Tr}\left(\frac{\lambda}{2}\phi^2\Box^{-1}\right)\\&\quad-\frac{1}{2}\mathrm{Tr}\left(\frac{\lambda}{2}\phi^2\Box^{-1}\right)^2+\ldots\end{aligned} \tag{26}$$

and one picks up from it only the expression quadratic in λ and quartic in the background scalar field ϕ, which is also formally quadratic in the inverse box operator $\Box^{-1}$, that is the part

$$\mathrm{Tr}\ln H\supset-\frac{1}{2}\frac{\lambda^2}{4}\phi^4\mathrm{Tr}\,\Box^{-2}=-\frac{\lambda^2}{8}\phi^4\mathrm{Tr}\,\Box^{-2}. \tag{27}$$

Precisely this expression is relevant for the UV divergence proportional to the quartic interaction term $-\frac{\lambda}{4!}\phi^4$ in the original scalar field action (23). Noticing that the functional trace of the $\Box^{-2}$ scalar operator in $d=4$ is given by

$$\mathrm{Tr}\,\Box^{-2}=i\frac{\ln L^2}{(4\pi)^2}, \tag{28}$$

where L is a dimensionless UV-cutoff parameter related to the Λ_{UV} dimensionful momentum UV-cutoff and the renormalization scale μ via $\Lambda_{\mathrm{UV}}=L\mu$, one finds for the UV-divergent and interesting us part of the one-loop effective action here

$$\Gamma^{(1)}_{\mathrm{div}}=\frac{i}{2}\mathrm{Tr}\ln H\supset\int d^4x\frac{\ln L^2}{(4\pi)^2}\frac{\lambda^2}{16}\phi^4. \tag{29}$$

Now, one can compare this to the original action terms in (23) describing quartic interactions of the scalar fields ϕ: $-\int d^4x\frac{\lambda}{24}\phi^4$. The counterterm action (to absorb UV divergences) is opposite to Γ_{div} and the form of the terms in the counterterm action is expressed via perturbative beta functions of the theory. That is in the counterterm action Γ_{ct} we expect terms

$$\Gamma_{\mathrm{ct}}=-\Gamma_{\mathrm{div}}=-\frac{1}{2}\frac{\ln L^2}{24}\int d^4x\beta_\lambda\phi^4 \tag{30}$$

with the front coefficient exactly identical to the one half of the one in front of the quartic interactions in the original action in (23) (being equal to $-\frac{1}{4!}=-\frac{1}{24}$). From this one reads that (identifying that effectively $\ln L^2\to 1$ for comparison)

$$-\frac{1}{48}\beta_\lambda=-\frac{\lambda^2}{16(4\pi)^2} \tag{31}$$

and finally that

$$\beta_\lambda=\frac{3\lambda^2}{(4\pi)^2}, \tag{32}$$

which is a standard result for the one-loop beta function of the quartic coupling λ in $\frac{1}{4!}\lambda\phi^4$ scalar theory in $d=4$ spacetime dimensions.

One sees that even in the simplest framework, the details of such a computation are quite cumbersome, and we decide not to include in this manuscript other more sophisticated illustrative examples of such derivation of the explicit results for beta functions of the theory. The reader, who wants to see some samples can consult more explicit similar calculations as presented in references [26, 30, 44]. In particular, the appendix of [30] compares two approaches to the computation of UV divergences in gauge theory (simpler than gravity

but with non-Abelian gauge symmetry) – using BV heat kernel technique and using standard Feynman diagram computation using graphs and Feynman rules around flat space and in Fourier momentum space.

2.2. Results in six-derivative gravity

The final results for this computation of all UV divergences of the six-derivative gravitational theory are

$$\Gamma^{(1)R,C}_{\rm div} = -\frac{\ln L^2}{2(4\pi)^2}\int d^4x\sqrt{|g|}\left\{\left(\frac{397}{40}+\frac{2x}{9}\right)C^2 + \frac{1387}{180}{\rm GB} - \frac{7}{36}R^2\right\} \quad (33)$$

for the case of six-derivative pure QG model in $d = 4$ spacetime dimensions and

$$\Gamma^{(1)R,C}_{\rm div} = -\frac{\ln L^2}{2(4\pi)^2}\int d^4x\sqrt{|g|}\left\{-\frac{133}{20}C^2 + \frac{196}{45}{\rm GB} + \left(-\frac{5}{2}x^{-2}_{4-{\rm der}} + \frac{5}{2}x^{-1}_{4-{\rm der}} - \frac{5}{36}\right)R^2\right\} \quad (34)$$

for the case of four-derivative pure Stelle quadratic model of QG to the one-loop accuracy. This last result was first reported in [42]. The result in six-derivative gravity is freshly new [26]. Here we define the covariant cut-off regulator L [27], which stays in the following relations to the dimensional regularization parameter ϵ [27, 43],

$$\ln L^2 \equiv \ln\frac{\Lambda^2_{\rm UV}}{\mu^2} = \frac{1}{\epsilon} = \frac{1}{2-\omega} = \frac{2}{4-n}\,, \quad (35)$$

where we denoted by n the generalized dimensionality of spacetime in the DIMREG scheme of regularization (additionally $\Lambda_{\rm UV}$ is the dimensionful UV cutoff energy parameter and μ is the quantum renormalization scale). Moreover, to write compactly our finite results for the six-derivative theory we used the definition of the fundamental ratio of the theory x as

$$x = \frac{\omega_C}{\omega_R}, \quad (36)$$

while for Stelle four-derivative theory in (34) we use analogously but now with the theta couplings instead of omegas, namely

$$x_{4-{\rm der}} = \frac{\theta_C}{\theta_R}. \quad (37)$$

It is worth to describe briefly here also the passage from UV divergences of the theory at the one-loop level to the perturbative one-loop beta functions of relevant dimensionless couplings. Using the divergent contribution to the quantum effective action, derived previously, we can define the beta functions of the theory. Let us first fix some definitions.

The renormalized Lagrangian $\mathcal{L}_{\rm ren}$ is obtained starting from the classical Lagrangian written in terms of the renormalized coupling constants and then adding the counterterms to subtract the divergences,

$$\mathcal{L}_{\rm ren} = \mathcal{L}(\alpha_b(t)) = \mathcal{L}\left(Z_{\alpha_i(t)}\alpha_i(t)\right) = \mathcal{L}(\alpha_i(t)) + \mathcal{L}_{\rm ct} = \mathcal{L}(\alpha_i(t)) + (Z_C - 1)\,\theta_C(t)\,C^2 + (Z_R - 1)\,\theta_R(t)\,R^2 + (Z_{\rm GB} - 1)\,\theta_{\rm GB}(t)\,{\rm GB}, \quad (38)$$

where we have that $\mathcal{L}_{\rm ct} = -\mathcal{L}_{\rm div}$ and $\alpha_i(t) = \{\theta_C(t), \theta_R(t), \theta_{\rm GB}(t)\}$. Above we denoted by $\alpha_b(t)$ the RG running bare values of coupling parameters, by $\mathcal{L}_{\rm ct}$ and $\mathcal{L}_{\rm div}$ the counterterm and divergent Lagrangians respectively, by $Z_{\alpha_i}(t)$ renormalization constants for all dimensionless couplings and finally by $\alpha_i(t)$ these running couplings. Here and above we neglect writing terms which are UV-divergent but subleading in the number of derivatives in the UV regime. From (38), the full counterterm action reads, already in dimensional regularization,

$$\Gamma^{(1)}_{\rm ct} = -\Gamma^{(1)}_{\rm div} = \frac{1}{2\epsilon}\frac{1}{(4\pi)^2}\int d^4x\sqrt{|g|}\left\{\left(\frac{397}{40}+\frac{2x}{9}\right)C^2 - \frac{7}{36}R^2 + \frac{1387}{180}{\rm GB}\right\} \equiv \frac{1}{2\epsilon}\frac{1}{(4\pi)^2}\int d^4x\sqrt{|g|}\left\{\beta_C C^2 + \beta_R R^2 + \beta_{\rm GB}{\rm GB}\right\}. \quad (39)$$

Comparing the last two formulas we can identify the beta functions and finally get the renormalization group equations for the six derivative theory,

$$\beta_C = \mu\frac{d\theta_C}{d\mu} = \frac{1}{(4\pi)^2}\left(\frac{397}{40}+\frac{2x}{9}\right), \quad (40)$$

$$\beta_R = \mu\frac{d\theta_R}{d\mu} = -\frac{1}{(4\pi)^2}\,\frac{7}{36}\,, \quad (41)$$

$$\beta_{\rm GB} = \mu\frac{d\theta_{\rm GB}}{d\mu} = \frac{1}{(4\pi)^2}\,\frac{1387}{180}\,, \quad (42)$$

The three lines above constitute the main results of this work. Their structure, mainly the x-dependence is the main topic of discussion in the next sections. Above we denoted by t the so called logarithmic RG time parameter related in the following way: $t = \log\frac{\mu}{\mu_0}$ to the renormalization scale μ, where μ_0 is some reference energy scale.

As we will show below the differences between the cases of four-derivative theory and six-derivative one are significant and the dependence on the ratio x is with quite opposite pattern and in completely different sectors of ultraviolet divergences of the two respective theories. In the main part of this contribution we will try an attempt to explain the mentioned difference, which is now clearly noticeable, using some general principles and arguments about renormalizability of the quantum models. We will also study some limiting cases of the non-finite (infinite or zero) values of the x parameter and motivate that in such cases the QG model is non-renormalizable and this leads to characteristic patterns in the structure of beta functions mentioned above for six-derivative theories. This is also why we can call the ratio x as the fundamental parameter of the gravitational theory.

3. Some theoretical checks of the results (33)

Let us say that regardless of the simplicity of the final formulas with the final result in [26], the intermediate calculations were quite big and this is why we cannot present these intermediate steps here. This was not only because of the size of the algebraic expressions, where we used Mathematica for help with symbolic algebra manipulations, but also due to the complexity of all the steps of the computation starting from the quadratic expansions of the action of six-derivative classical theory. The ultimate validity of the calculations has been checked in several different ways. This is also briefly described below.

The following checks were performed to ensure the correctness of the intermediate results of the computation of UV divergences, which was the main task of the work presented here.

(1.) First, the validity of the expression for the Hessian operator from the classical action with six derivatives was verified in the following way. The covariant divergence of the second variational derivative operator (Hessian) with respect to gravitational fluctuations $h_{\mu\nu}$, from each GR-covariant term $S_{\mathrm{grav},i}$ in the gravitational action must be separately zero, namely

$$\nabla_\mu \left(\frac{\delta^2 S_{\mathrm{grav},i}}{\delta h_{\mu\nu} \delta h_{\rho\sigma}} \right) = 0 + O\left(\nabla^k \mathcal{R}^l, k + 2l > 4 \right), \quad (43)$$

where $S_{\mathrm{HD}} = \sum_i S_{\mathrm{grav},i}$. This formula was explicitly checked for each term in the action in (10) to the order quadratic in curvatures and up to total of four covariant derivatives acting on the general gravitational curvature $\mathcal{R}$.

(2.) The computation of the functional trace of the logarithm of the gauge weighting operator $\hat{C}$, namely of $\mathrm{Tr}\ln\hat{C}$ was checked using three methods. Since the $\hat{C}$ operator is a non-minimal four-derivative differential operator and matrix-valued (so with vector indices), then the computation of its trace of the logarithm is a bit troublesome. One has to be more careful here. Therefore, we performed additional verifications of our partial results for this trace. Our three methods consist basically of transforming the problem to computing the same trace of logarithm but of new operators (with higher number of derivatives). Next, by selecting some adjustable parameters present in the construction of these new operators, these morphed operators could be put into a minimal form and easily traced (under the functional logarithm operation) using standard methods and prescriptions of Barvinsky-Vilkovisky trace technology [27]. This construction of new operators was achieved by an operatorial multiplication by some two-derivative spin-one operator $\hat{Y}$ containing one free adjustable parameter. For details one can look up the section III of [26].

In the first variant of the method, we multiplied $\hat{C}$ from the right by $\hat{Y}$ one time, in the second method we multiplied by $\hat{Y}$ from the left also once, and in the final third method we used the explicitly symmetric form of multiplication $\hat{Y}\hat{C}\hat{Y}$. (This last form of multiplication is presumably very important for the manifest self-adjointness property of the resulting 8-derivative differential operator $\hat{Y}\hat{C}\hat{Y}$.) For these operatorial multiplications, $\hat{Y}$ was a two-derivative operator, whose trace of the logarithm is known and can be easily verified. (This was also checked independently below.) We emphasize that in the first two methods the resulting operators ($\hat{Y}\hat{C}$ and $\hat{C}\hat{Y}$ respectively) were six-derivative ones, while in the last one with double multiplication from both sides, $\hat{Y}\hat{C}\hat{Y}$ was an eight-derivative matrix-valued differential operator. At the end, all three described above methods of computation of $\mathrm{Tr}\ln\hat{C}$ agree for terms quadratic in curvatures. These terms are only important for us here since they appear in the form of UV divergences of the theory (and are composed from GR-invariants: R^2, $R_{\mu\nu}^2$, and $R_{\mu\nu\rho\sigma}^2$).

(3.) Similarly, the computation of $\mathrm{Tr}\ln\hat{Y}$ for the two-derivative operator $\hat{Y}$ was verified using three analogous methods. We used multiplication from both sides by the operator $\hat{A}$ and also the symmetric form of multiplication $\hat{A}\hat{Y}\hat{A}$, where $\hat{Y}$ is a two-derivative operator, whose functional trace of the logarithm we searched here. Above, $\hat{A}$ was another two-derivative non-minimal spin-one vector gauge (massless) operator, whose trace of the logarithm is well known [41] and can be easily found. Again, for the final results for $\mathrm{Tr}\ln\hat{Y}$ all three methods presented here agree to the order of terms quadratic in curvatures $\mathcal{R}$.

(4.) In total divergent part Γ_{div} of the quantum effective action, we checked a complete cancellation of terms with poles in $y = 2\omega_C - 3\omega_R$ variable, namely all terms with $\frac{1}{y}$ and $\frac{1}{y^2}$ in denominators (originating from the expression for the gauge-fixing parameter β in (21)) completely cancel out. This is not a trivial cancellation between the results of the following traces: $\mathrm{Tr}\ln\hat{H}$ and $\mathrm{Tr}\ln\hat{M}$.

(5.) Finally, using the same code written in Mathematica [47] a similar computation in four-derivative gravitational theory (Stelle theory in four dimensions) was repeated. We easily were able to reproduce all results about one-loop UV divergences there [42]. To our satisfaction, we found a complete agreement for all the coefficients and the same non-trivial dependence on the parameter $x_{4-\mathrm{der}}$, which was already defined above for Stelle gravity. This was the final check.

4. Structure of beta functions in six-derivative quantum gravity

4.1. Limiting cases

In this subsection, we discuss various limiting cases of higher-derivative gravitational theories (both with

four and six derivatives). We study in detail the situation when some of the coefficients of action terms in the Weyl basis tend to zero. We comment whether in such cases our method of computation is still valid and whether the final results for UV divergences are correct in that cases and whether they could be obtained by continuous limit procedures.

First, we discuss the situation with a possible degeneracy of the kinetic operator of the theory acting between quantum metric fluctuations $h_{\mu\nu}$ on the level of the quadratized action. If the action of a theory in the UV regime has the following UV-leading terms

$$S_{\rm grav} = \int d^d x \sqrt{|g|} \left(\omega_{C,N} C \Box^N C + \omega_{R,N} R \Box^N R \right), \quad (44)$$

with $\omega_{C,N} \neq 0$ and also $\omega_{R,N} \neq 0$ and after adding the proper gauge-fixing functional, then the kinetic operator can be defined, so in these circumstances it is not degenerate. Then it constitutes the operatorial kernel of the part of the action which is quadratic in the fluctuation fields. It can be well-defined not only for the cases when $\omega_{C,N} \neq 0$ and $\omega_{R,N} \neq 0$, but also when $\omega_{R,N} = 0$. This last assertion one can check by explicit inspection, but due to the length of the resulting expression we decided not to include such a bulky formula here. However, in the case $\omega_{C,N} = 0$, a special procedure must be used to define the theory of perturbations and to extract UV divergences of the model. We remark that in the last case the theory is non-renormalizable. We also emphasize that the addition of the gauge-fixing functional here is necessary since without it the kinetic operator (Hessian) is automatically degenerate as the result of gauge invariance of the theory (here in gravitational setup represented by the diffeomorphism gauge symmetry).

In general, as emphasized in [26], in four spacetime dimensions, the general UV divergences depend only on the coefficients appearing in the following UV-leading part of the gravitational HD action,

$$\begin{aligned} S_{\rm grav} = \int d^4 x \sqrt{|g|} \, & \left(\omega_{C,N} C \Box^N C + \omega_{R,N} R \Box^N R \right. \\ & + \omega_{C,N-1} C \Box^{N-1} C + \omega_{R,N-1} R \Box^{N-1} R \\ & \left. + \omega_{C,N-2} C \Box^{N-2} C + \omega_{R,N-2} R \Box^{N-2} R \right), \quad (45) \end{aligned}$$

where the last two lines contain subleading terms in the UV regime. However, they are the most relevant for the divergences proportional to the Ricci curvature scalar and also to the cosmological constant term [44]. Below for notational convenience, we adopt the following convention specially suited for six-derivative gravitational theories, so in the case when $N = 1$. We will call coupling coefficients in front of the leading terms as respective omega coefficients (like $\omega_C = \omega_{C,1}$ and analogously $\omega_R = \omega_{R,1}$), while the coefficients of the subleading terms with four derivatives we will denote as theta coefficients (like $\theta_C = \omega_{C,0}$ and analogously $\theta_R = \omega_{R,0}$). Eventually, for the most subleading terms with subindex values of $(N-2)$ equal formally to -1 here, we have just one term contributing to the cosmological constant type of UV divergence. We denote this coefficient as $\omega_{-1} = \omega_{R,-1}$ and it is in front of the Ricci scalar term in the original classical action of the theory (6). Simply this coefficient ω_{-1} is related to the value of the 4-dimensional gravitational Newton's constant G_N.

The expressions for the RG running of the cosmological constant and the Newton's constant in [26, 44] contain various fractions of parameters of the theory appearing in the action (45). Still, for a generic value of the integer N, giving roughly the half of the order of higher derivatives in the model, we have the following schematic structure of these fractions:

$$\frac{\omega_{R,N-1}}{\omega_{R,N}}, \quad \frac{\omega_{C,N-1}}{\omega_{C,N}}, \quad \frac{\omega_{R,N-2}}{\omega_{R,N}}, \quad \frac{\omega_{C,N-2}}{\omega_{C,N}}. \quad (46)$$

The structure of the UV divergences and of these fractions can be easily understood from the energy dimensionality arguments. We notice that in the Weyl basis with terms in (45) written with Weyl tensors $C_{\mu\nu\rho\sigma}$ and Ricci scalars R the only fractions, which appear in such subleading UV divergences are "diagonal" and do not mix terms from the spin-2 (Weyl) sector with terms from the spin-0 (Ricci scalar) sector. If in any of the above fractions, we take the limits: $\omega_{R,N-1} \to 0$, $\omega_{C,N-1} \to 0$, $\omega_{R,N-2} \to 0$, or $\omega_{C,N-2} \to 0$, then the corresponding fractions and also related UV divergences (and resulting beta functions in question) simply vanish, provided that the coefficients in their denominators $\omega_{R,N}$ and $\omega_{C,N}$ are non-zero.

On the other hand, if $\omega_{C,N} = 0$, then we cannot rely on this limiting procedure. In this case, on the level of the quadratized action the operator between quantum fluctuations is degenerate even after adding the gauge-fixing terms. This means that in this situation a special procedure has to be used to extract the UV divergences of the model. This is possible, but we will not discuss it here.

It is worth to notice that in turn, if $\omega_{R,N} = 0$, then the kinetic operator for small fluctuations and after adding the gauge fixing is still well-defined, as emphasized also above. For this case a special additional kind of gauge fixing has to be used, which fixes the value also of the trace of the metric fluctuations $h = g^{\mu\nu} h_{\mu\nu}$ and this last one in the theory with $N = 0$ resembles the conformal gauge fixing of the trace.

If $\omega_{R,N} = 0$ and additionally $\omega_{R,N-1}$ or $\omega_{R,N-2}$ are non-zero, then the corresponding beta functions for the cosmological constant and Newton's gravitational constant are indeed infinite and ill-defined as viewed naively from the expressions in (46). This situation could be understood as that there is an additional new divergence not absorbed in the adopted renormalization scheme and the renormalizability of such a theory is likely lost. But if the model is with $\omega_{R,N} = 0$ and at the same time $\omega_{R,N-1} = \omega_{R,N-2} = 0$, then the contributions of corresponding fractions in (46) are vanishing, because the limits $\omega_{R,N-1} \to 0$ or $\omega_{R,N-2} \to 0$

must be taken as the first respectively. Only after this, the final limiting procedure $\omega_{R,N} \to 0$ should be performed. Therefore, in this limiting situation, the proper sequence of limits on respective fractions is as follows:

$$\lim_{\omega_{R,N}\to 0}\left(\lim_{\omega_{R,N-1}\to 0}\frac{\omega_{R,N-1}}{\omega_{R,N}}\right)=0 \tag{47}$$

and

$$\lim_{\omega_{R,N}\to 0}\left(\lim_{\omega_{R,N-2}\to 0}\frac{\omega_{R,N-2}}{\omega_{R,N}}\right)=0\,. \tag{48}$$

In this case, there are no contributions to the beta functions from these fractions, so the R^2 sector does not contribute anything to the mentioned UV divergences, while it is expected that the terms in the C^2 sector make some impact on beta functions.

However, the similar procedure cannot be applied in the sector with Weyl square terms (C^2 sector), so to the model with $\omega_{C,N} = 0$ and at the same time $\omega_{C,N-1} = \omega_{C,N-2} = 0$ since these cases have to be treated specially and separately. In the last case, after the limit, only the pure sector with Ricci scalar square terms (R^2 sector) survives and the theory is likely non-renormalizable. Then we expect contributions to UV divergences only from terms in the R^2 sector.

Regarding the divergences proportional to expressions quadratic in curvatures (R^2, C^2, and the Gauss-Bonnet term GB), we have found the following generic structure in four-derivative gravity [42]:

$$\frac{A_{-2}}{x^2_{4-\mathrm{der}}}+\frac{A_{-1}}{x_{4-\mathrm{der}}}+A_0, \tag{49}$$

where in this case of four-derivative gravity the fundamental ratio of the theory is defined as

$$x_{4-\mathrm{der}}=\frac{\omega_{C,0}}{\omega_{R,0}}=\frac{\theta_C}{\theta_R}. \tag{50}$$

The numerical coefficients A_{-2}, A_{-1} and A_{-0} are different for different types of UV divergences (here they are given by terms with four derivatives, namely by R^2, C^2 and GB terms respectively). The explicit numerical values are given in the formula (34). One observes negative powers of the ratio $x_{4-\mathrm{der}}$ in (49) and in (34), implying also negative powers of the coupling θ_C in the final results for these UV divergences. This result signifies that the theory with $\theta_C = 0$ should be treated separately and then we do not have well-defined kinetic operator in a standard scheme of computation. The naive results with the limit $\theta_C \to 0$ of the above formula in (49) do not exist. Such theories with $\theta_C = 0$ entail complete absence of gravitational terms in the C^2 sector. They are again very special and perturbatively non-renormalizable models. The above remarks apply both to pure R^2 Starobinsky theory as well as to theories in the R^2 sector with addition of the Einstein-Hilbert R or the cosmological constant ω_Λ terms.

On the other side, the limit $\theta_R \to 0$ in pure C^2 gravity seems not to produce any problem with the degeneracy of the kinetic operator, nor with the final expression (49). The naive answer would be just A_0 for (49) for each of the UV divergences in this case. But this is an *incorrect* answer since for pure four-derivative gravity with $\theta_R = 0$ in the Weyl basis of terms, we have an enhancement of the symmetry in the model, beyond the case where θ_R was non-zero. In this situation, the theory enjoys also conformal symmetry and a more specialized and delicate computation must be performed to cover this case. This is the case of four-dimensional conformal (Weyl) gravity. (We decided for simplicity not to analyze here the cases when besides the C^2 action for four-dimensional conformal gravity, there are also some subleading terms from the almost "pure" R^2 sector, that is $\omega_{-1} \neq 0$ or when we allow for non-vanishing cosmological constant term $\omega_\Lambda \neq 0$ – these terms in the action would cause breaking of classical conformality.)

The computation in this case should reflect the fact that also the conformal symmetry should be gauge-fixed. We remark that the conformal symmetry does not require dynamical FP ghosts, because the conformal transformations of gravitational gauge potentials (not the conformal Weyl gauge potentials b_μ) are without derivatives. At the end, when the more sophisticated method is employed, the eventual result is different than A_0 for each type out of three types of four-derivative UV-divergent GR-invariant terms in the quantum effective action of the model. The strict result A_0 is still correct only for theories in which conformality is violated by inclusion of other non-conformal terms like the Einstein-Hilbert R term or the cosmological constant ω_Λ term. We conclude that in the four-derivative theory, the two possible extreme cases of $\theta_R = 0$ or $\theta_C = 0$ are not covered by the general formula (49). But in each of these cases the reasons for this omission are different. In both these cases the separate more adapted methods of computation of UV divergences have to be used.

In the case of six-derivative theory studied in [26], we have the following structure of UV divergences quadratic in gravitational curvatures

$$B_0 + B_1 x, \tag{51}$$

with new values for the constants B_0 and B_1. The explicit numerical values are given in our formula (33) with the results. We also remark that the values of the constant terms B_0 are different than the values of A_0 in the previous four-derivative gravity case. Moreover, the numerical coefficients B_0 and B_1 are different for different types of UV divergences of the effective action (R^2, C^2 and GB terms respectively). When the leading dynamics in the UV regime is governed by the theory with six derivatives, then the fundamental ratio x we define as

$$x=\frac{\omega_{C,1}}{\omega_{R,1}}=\frac{\omega_C}{\omega_R}. \tag{52}$$

We emphasize that in such a case, we cannot continuously take the limit $\omega_C \to 0$. Although, naively this would mean the limit $x \to 0$, the result just B_0 from (51) would be incorrect. This is because in this case we cannot trust the method of the computation. When $\omega_C = 0$ the kinetic operator is degenerate (the same as it was in the four-derivative gravity case) and needs non-standard treatment, that we will not discuss here.

Moreover, looking at the last formula (51), the other limit $\omega_R \to 0$ is clearly impossible too, because it gives divergent results. However, in this case ($\omega_R = 0$) and on the contrary to the previous case ($\omega_C = 0$), we could trust the computation at least on the level of the kinetic operator (Hessian) and its subsequent computation of the functional trace of the logarithm of. In this case, the final divergent results in (51) signify that the theory likely is non-renormalizable and that there are new UV divergences besides those ones derived from naive power counting analysis[3]. We conclude that in the case of six-derivative gravity, both cases $\omega_R = 0$ or $\omega_C = 0$ require special treatment and the type of formula like in (51) or (33) does not apply there and the limiting cases are not continuous. More discussion of these limits is contained also in the further subsection 4.4.

4.2. Dependence of the final results on the fundamental ratio x

Here we just want to understand the x-dependence in the result for the beta functions in six-derivative gravitational theory. We first try to analyze the situation for simpler theory (with four derivatives), prepare the ground for the theory with six derivatives, and then eventually draw some comparison between the two. We look for singular $\frac{1}{\omega_R}$ or $\frac{1}{\omega_C}$ dependence (corresponding to positive or negative powers of the fundamental ratio $x = \frac{\omega_C}{\omega_R}$ respectively) in functional traces of the fundamental operators defining the dynamics of quantum perturbations important to the one-loop perturbative level. We note that the two definitions for the ratio x in (50) and in (52) respectively for four- and six-derivative gravities are compatible with each other and the proper use of them (with theta or omega couplings) is obvious in the specific contexts they are used in. Below, when we will refer to features shared by both four- and six-derivative gravitational theories, we will use common notation with general ω_C, ω_R and x coefficients and we will not distinguish and not change it to the special notation originally adequate only to Stelle quadratic theory (with θ_C, θ_R and $x_{4-\mathrm{der}}$). We hope that this will not lead to any confusion.

We emphasize, that when we have one of the two terms missing – with ω_R or ω_C front couplings – in the leading in UV part of the action of the model, then the theory is badly non-renormalizable and degenerate. For example, one cannot define even at the tree-level the flat spacetime graviton propagator since the parts proportional to $P^{(0)}$ or $P^{(2)}$ projectors do not exist in cases when $\omega_R = 0$ or $\omega_C = 0$ respectively. However, there we can still use the Barvinsky-Vilkovisky (BV) trace technology to compute the new UV divergences. The fact that they are not possible to be absorbed in counterterms of the original theory is another story related to the non-renormalizability of the model that we will not discuss further here. We think that, for example, using the BV technique one can fast compute UV divergences in Einstein-Hilbert (E-H) theory in $d = 4$ (which is a non-renormalizable model) and this method still gives a definite result (besides that these divergences are gauge-fixing dependent and valid only for one gauge choice). Moreover, using the BV traces machinery and the minimal form of the kinetic operator is essential to get final results for the unique effective action (as introduced by Barvinsky [27, 48]), also in perturbatively non-renormalizable models.

In quadratic gravity (four-derivative theory) in $d = 4$, setting $\theta_C = 0$ is highly problematic. The same regards taking the limit $\theta_C \to 0$, because then the pure R^2 theory can be fully gauge-fixed. And for example, this means that on flat spacetime background, the kinetic operator vanishes, perturbative modes are not dynamical and there is no graviton propagator. Using the standard technique of the one-loop effective action one sees that the traces of the functional logarithms of $\hat{H}$ and of $\hat{C}$ operators both contain singular expressions $\frac{1}{\theta_C}$, and there is no final cancellation between them. In this case of four-derivative gravity, in final results for UV divergences, we really see inverse powers of the fundamental ratio of the theory $x_{4-\mathrm{der}}$.

The results in quadratic Stelle gravity, when we set $\theta_R = 0$, are not continuous either. Because in this case the local gauge symmetry of the theory is enhanced. We have also conformal symmetry there. The model is identical to the Weyl gravity in $d = 4$ described by the action C^2. As emphasized in [41], this case of $\theta_R = 0$ has to be treated specially. Also, in this model, the conformal symmetry has to be gauge-fixed and in this special case the operators $\hat{H}$ and $\hat{C}$ are different than their limiting versions under $\theta_R \to 0$ limit from the generic four-derivative theory case. Hence also the results for the beta functions are different than the limits of the corresponding beta functions in the situation with $\theta_R \neq 0$.

If we start with the theory with $\theta_C = 0$ from the beginning, then there are serious problems with the kinetic operator. We checked that it cannot be put by standard fixing of the gauge to the minimal form with four-derivative leading operator. Moreover, as the result of this process one of the typical gauge-fixing parameters remains undetermined. Here one can try to compute the trace of the logarithm of the Hessian using the method proposed in [44] consisting of multiplying by some two-derivative non-minimal

[3] We remark that the generic power counting analysis of UV divergences in six-derivative quantum gravity, as presented in section 1.1, applies only in cases when $\omega_C \neq 0$ and $\omega_R \neq 0$.

operator and getting a six-derivative operator, whose trace can be easily found. But it is hard to believe that one has any chance to get a non-singular answer for all the beta functions in pure R^2 theory since it is known that this theory is non-renormalizable (because it lacks the C^2 counterterm in the bare action).

Actually, here (for the $\theta_C = 0$ case) one could choose the $\hat{C}$ matrix-valued differential operator different from the standard minimal prescription and choose different values for the γ gauge-fixing parameter. In the standard minimal choice for the gauge-fixing parameters and in this model, the $\hat{C}$ matrix contains an irregular part in θ_C coupling ($\frac{1}{\theta_C}$ pole), because of the dependence of γ on θ_C. This last dependence originates from the conditions forced on gauge-fixing parameters in order to put the kinetic operator in the minimal form, in the standard case $\theta_C \neq 0$. However, knowing that in the case with $\theta_C = 0$, this procedure is anyhow unsuccessful, we have the freedom to choose the value of γ different than the standard one and at our wish.

In principle, similar considerations can be repeated verbatim for the case of six-derivative theory (with $N = 1$ power exponent on the box operator in the defining the theory action in (45)). But we remark here that the theory with $\omega_R = 0$ and $N = 1$ is *not* conformally invariant in $d = 4$ dimensions. And the above problems with the gauge fixing of the Hessian operator $\hat{H}$ and non-minimality of it in the case $\omega_C = 0$ still persist. This is because here for six-derivative gravitational theories the box operator $\Box$ acting between two gravitational curvatures is only a spectator from the point of view of the UV-leading part of the $\hat{H}$ operator (with the highest number of derivatives and with the zeroth powers in gravitational curvatures) or from the point of view of flat spacetime kinetic operator and flat spacetime graviton's propagator. The box operator in momentum space gives only one additional factor of $-k^2$ to the kinetic operator and additional suppression by $-k^{-2}$ to the propagator. The Hessian in the six-derivative theory with $\omega_R = 0$ must possess the same definitional issues as the one in the four-derivative theory (with $\theta_R = 0$), because for the kinetic terms box operator again plays only the role of the spectator. Hence the difference on this level between four- and six-derivative theories is only in some overall multiplicative coefficient (like flat spacetime d'Alembertian operator ∂^2 is $-k^2$ in Fourier space). So then, if we know that the Hessian $\hat{H}$ is almost well-defined for the conformal gravity case (up to the need for additional gauge fixing of the conformal symmetry), then the same will be true for the Hessian in the six-derivative theory with the $\omega_R = 0$ condition in $d = 4$ spacetime dimensions, although then the theory ceases to be conformal anymore. In conformal gravity in $d = 4$, when $\theta_R = 0$, we have almost well-defined Hessian, because we know that it gives rise to a good renormalizable theory at least to the one-loop perturbative level of computations.

Now, also in the case of six-derivative theories, setting $\omega_R = 0$ does not create any problem for the form of neither $\hat{H}$ nor $\hat{C}$ operators. Only the final results for the beta functions show $\frac{1}{\omega_R}$ poles as this was manifest from the results in [26]. In turn, in six-derivative theories, the limit $\omega_C \to 0$ seems regular, but it is questionable that now we can trust the results of this limit. In the pure $R\Box R$ theory, we expect to get some discontinuous results for the beta functions not obtainable by the limit $\omega_C \to 0$ since this model is non-renormalizable. In this model, there is still an open problem that one cannot make the kinetic operator of fluctuations a minimal 6-derivative one. Furthermore, taking the limit $\omega_C \to 0$ on the kinetic operator from the generic case $\omega_C \neq 0$ produces a Hessian $\hat{H}$ that vanishes on flat spacetime. Hence it seems that in this case the intermediate steps of the process of computing the divergent part of the effective action are not well-defined, while the final result is amenable to taking the limit $\omega_C \to 0$, but exactly because of this former reason, we should not trust these apparently continuously looking limits.

One should analyze deeper the form of the leading in the number of derivatives (and also in the UV regime) part of the kinetic operator $\hat{H}$ of the theory between graviton fluctuations. The insertions of box operators, like any power or functions of the box operator $\Box$, are only the immaterial differences between the cases of four- and six-derivative theories here. These operators are only spectators for getting the leading part of the Hessian, which is with the highest number of derivatives and also considered on flat spacetime, so with the condition that $\mathcal{R} = 0$. Using formula (20) with solutions for gauge-fixing parameters as in (21), one finds in the generic case $\omega_C \neq 0$ and $\omega_R \neq 0$, that the kinetic operator (leading part of the Hessian) is indeed minimal and of the form

$$H^{\mu\nu,\rho\sigma}_{\text{lead}} = \frac{\omega_C}{2}\Box\left(g^{\mu\rho}g^{\nu\sigma} + g^{\mu\sigma}g^{\nu\rho}\right) - \omega_C\frac{\omega_C - 6\omega_R}{4\omega_C - 6\omega_R}\Box g^{\mu\nu}g^{\rho\sigma}\,. \quad (53)$$

In the above formula, one does not see any singularity when ω_C is vanishing (one saw ω_C^{-1} divergences in the expressions for α and γ parameters in (21)), but in this case the above treatment was not justified. When $\omega_C = 0$, one can solve the system for gauge-fixing parameters for β and $\gamma' = \frac{\gamma}{\alpha}$ and assume that formally $\frac{1}{\alpha} = 0$ and $\frac{1}{\gamma} = 0$, but in the ratio $\frac{\gamma}{\alpha}$ the limit is finite. One then finds that $\beta = 1$ and $\gamma' = -2\omega_R$ and after substitution to the original Hessian, one gets that its leading part explicitly vanishes. The same one gets by plugging the naive limit $\omega_C \to 0$ in (53). One also sees from the explicit solutions in (21) and resulting general expression for γ' (i.e. $\gamma' = \frac{4}{3}\omega_C - 2\omega_R$) that by plugging $\omega_C = 0$ one finds again that $\beta = 1$ and $\gamma' = -2\omega_R$ as derived exactly above. The highest derivative level of the gravitational action is then completely gauge-fixed.

In the opposite case, when $\omega_R = 0$, the leading part of the Hessian does not vanish, but it is degenerate and in the form

$$H^{\mu\nu,\rho\sigma}_{\rm lead} = \frac{\omega_C}{2}\Box\left(g^{\mu\rho}g^{\nu\sigma} + g^{\mu\sigma}g^{\nu\rho}\right) - \frac{\omega_C}{4}\Box g^{\mu\nu}g^{\rho\sigma}, \quad (54)$$

because this operator does not possess a well-defined inverse, precisely in $d = 4$ dimensions. An addition of a new conformal-like type of gauge-fixing here $\tau h\Box^3 h$ with a new (fourth) gauge-fixing parameter τ and where the trace of metric fluctuations $h = h^\mu{}_\mu$ is used, removes the degeneracy provided that $\tau \neq 0$ is selected. Then the kinetic operator takes the form

$$H^{\mu\nu,\rho\sigma}_{\rm lead} = \frac{\omega_C}{2}\Box\left(g^{\mu\rho}g^{\nu\sigma} + g^{\mu\sigma}g^{\nu\rho}\right) + \left(\tau - \frac{\omega_C}{4}\right)\Box g^{\mu\nu}g^{\rho\sigma}. \quad (55)$$

Moreover, for any non-zero value of τ the Hessian is still a minimal operator. For $\tau \neq 0$ the inverse exists and also the propagator can be defined around flat spacetime. The only question is whether the final results are τ-independent since this is a spurious gauge-fixing parameter. The reason for such independence is obvious in the four-derivative case, since τ is a gauge-fixing parameter for conformal symmetry (conformal gauge-fixing parameter, so this is then in such circumstances a symmetry argument). But in the case of six-derivative model in $d = 4$, the reasoning with conformal symmetry is not adequate since this model is not conformal anymore. Only the explicit computation may show that τ parameter drops out from final results as it should for them to be physical and τ gauge choice independent.

In four-derivative gravitational theory, one can see the dependence on the $x_{4-\rm der}$ ratio only in the coefficient of the R^2 counterterm. This dependence is with the general schematic form $A_{-2}x^{-2}_{4-\rm der} + A_{-1}x^{-1}_{4-\rm der} + A_0 x^0_{4-\rm der}$ like in (49) and in (34). We remark that for other counterterms (namely for C^2 and GB in this Weyl basis), the coefficients of UV divergences are numbers completely independent of $x_{4-\rm der}$. One could try to explain here this quadratic dependence in the inverse ratio $x^{-1}_{4-\rm der}$ in front of the R^2 counterterm in a spirit similar to the argumentation presented in [44], where we counted active degrees of freedom contributing to the corresponding beta functions of the theory. It is well known by the examples of beta functions in QED coupled to some charged matter and in Yang-Mills theory, that the beta function at the one-loop level expresses weighted counting of degrees of freedom and their charges in interactions with gauge bosons in question (minimal couplings in three-leg vertices are enough to be considered here due the gauge symmetry). The similar counting could be attempted here, but in gravity, especially in HD gravity, there is a plenty of other gravitational degrees of freedom, so this is quite a difficult task to enumerate all of them and their strength of interactions in cubic vertices when they interact with background gravitational potentials. Therefore, this task of explaining x-dependence and numbers present in the expressions for all the beta functions both in four- and six-derivative theories, now seems to be too ambitious and we leave it for some further future considerations.

Instead, we comment briefly on the general dependence on the $x_{4-\rm der}$ ratio in four-derivative theory and compare this with six-derivative theory. In the case of $N = 1$ (six-derivative gravitational theory), it was found as a main result in [26], that the dependence on x is only in front of the C^2 counterterm and this is a linear dependence $B_1x^1 + B_0x^0$ like in (51) with non-negative powers of the x ratio. The other counterterms R^2 and GB are with constant coefficients (only B_0 terms present) (cf. with (33)). If the other than the Weyl basis is used to write counterterms, then the x-dependence is linear in coefficients in front of each basis term (like in the basis with R^2, $R^2_{\mu\nu}$, and $R^2_{\mu\nu\rho\sigma}$ terms). These explicit dissimilarities between $N = 0$ and $N = 1$ models certainly require deeper investigations.

It is interesting also to analyze a special value of the fundamental ratio x of the six-derivative gravitational theory, which makes the C^2 sector of UV divergences completely finite. This value is exactly $x = -\frac{3573}{80} = -44.6625$. The R^2 sector of UV divergences cannot be made finite this way. We remind for comparison that in the case of quadratic gravity with four derivatives in $d = 4$, the special values for $x_{4-\rm der}$, which made *contrary* the R^2 sector UV-finite, were two and they were $x_{4-\rm der} = 3(3 \pm \sqrt{7})$ (their numerical approximations are as follows: $x_{4-{\rm der},-} \approx 1.0627$ and $x_{4-{\rm der},+} \approx 16.937$) as solutions of some non-degenerate quadratic algebraic equation. Again, contrary to the previous case with six derivatives, here the divergences in the C^2 sector cannot be made vanish.

Now, we discuss the differences between the two extreme cases $\omega_C = 0$ and $\omega_R = 0$. In six-derivative model or when we have even more derivatives, superficially these two couplings and their roles for the computation of UV divergences may look symmetric. This is however not true due to the different impact of these two conditions on the form of the kinetic operator $\hat{H}$. In the case when $\omega_R = 0$, the Hessian operator still exists, while for $\omega_C = 0$ we lose its form. This observation has profound implications as we explain below. First, it is a fact that both these conditions lead to badly non-renormalizable theories, in which the flat spacetime propagator cannot be simply defined. Moreover, if $N > 0$ in none of these two reduced models we have an enhancement of symmetries and none of them has anything to do with conformal gravity models, which are present only for $N = 0$ and $\omega_R = 0$ case, despite that in constructions of these six-derivative models we might use only terms with Weyl tensor. (However, here we use the term $C\Box C$, where it is known that the GR-covariant box operator $\Box$ is not conformal.)

Our explanation of the x-dependence is as follows. First, in the generic model with $N > 0$, since it happens that it is the $N = 0$ scale-invariant gravitational model which is here the exceptional one. For six-derivative theory (or any one with $N > 0$) the two reduced models with conditions that $\omega_C = 0$ or $\omega_R = 0$ respectively are not renormalizable and likely even at the one-loop level higher types of divergences (besides C^2 and R^2 from (1)) will be generated. From this we expect that there must be some problems with UV divergences obtained from naive power counting arguments here. The problems must show up somehow in the final numerical values for divergent terms or in the intermediate steps of the process of computing these divergences. These problems then signal that we are working with non-renormalizable theory, which do not have a good control over perturbative divergences showing up at the one-loop level.

First, in the case $\omega_C = 0$, we see that the problems are already there with the definition of the kinetic operator (Hessian) between quantum metric fluctuation fields. This implies that further processing with this operator is ill-defined, we cannot trust it and even if it would give us some final results for divergences, then they are not reliable at all since the theory is non-renormalizable. But we already found here the instance of the problem, which makes our final limiting results (in the $\omega_C \to 0$ limit) not trustable. This means that from the expression in (51), we do not expect any additional obstacles, like $\frac{1}{\omega_C}$ poles since the price for non-renormalizability was already paid and we have already met dangerous problems, which signal the incorrectness of the naive limit $\omega_C \to 0$. This should already take away our trust in the limit $\omega_C \to 0$ of expressions for UV divergences in (33). Then this line of thought in the case $\omega_C = 0$ does not put any constraints at all on the final form of the x-dependence in (51) since these results like in (51) in the limit $\omega_C \to 0$ will anyway be likely incorrect.

Now, in the other case with $N > 0$ and $\omega_R = 0$, we do not have the problem with the definition of the Hessian $\hat{H}$. Formally, we can process it till the end of taking the functional trace of the logarithm and adding contributions from $\mathrm{Tr}\ln\hat{M}$ and $\mathrm{Tr}\ln\hat{C}$. But somehow, we must find the occurrence of the problem, because the theory is non-renormalizable! So the only place in which the problem may sit is in the final x-dependence of the results for UV divergences. These results should be ill-defined, when the limit $\omega_R \to 0$ is attempted. And this implies that they must be with poles in the ω_R coefficient, so they must be instead with positive powers of the x ratio of the theory. Hence, we conclude that the x-dependence must be linear or quadratic, but always with positive powers of the ratio x. This is now confirmed by explicit form as in (33) for UV divergences of six-derivative theory. The problems with renormalizability of the pure theory $C\Box C$ show up in the last possible moment in the procedure for obtaining the result, namely when one wants to take the limit $\omega_R \to 0$ or equivalently $x \to \infty$. This is the generic situation for any super-renormalizable theory and for any $N > 0$. There are still some mysterious things here, like why the dependence is only linear in x and why only for the C^2 type of UV counterterm, while two other counterterms R^2 and GB are numbers completely independent of x. Right now we cannot provide satisfactory mathematical explanations for these facts.

Using this argumentation in the theory models with $N = 1$, we get an explanation for the x-dependence in formula for UV divergences in (51). The logical chain for the explanation should be as follows. Firstly, in the pure theory $C\Box C$, one concludes that the problems of non-renormalizability shows only in the final results as impossibility to take the limit $\omega_R \to 0$ or equivalently $x \to \infty$ of formula in (51) for divergences of the model. Hence the dependence must be on non-negative powers of the ratio x in formula (51), as it is clearly confirmed by explicit inspection of this formula. This settles the issue of the structure of exact beta functions for $N = 1$ models (and also for higher $N \geqslant 1$ cases too). Now, the same formula is a starting point for an attempt to take the other limit $x \to 0$ of the also non-renormalizable model of the type $R\Box R$. But in such a model we have already found a source of the problem caused by non-renormalizability earlier, that it is here connected with the impossibility to properly define non-degenerate Hessian operator in the model. But this limiting case of $x \to 0$ must follow the same structure as already established in formula (51). Simply, theoretically speaking, there is no need to see more instances of problems due to non-renormalizability in the $R\Box R$ model. Hence, the first explanation based on the $C\Box C$ model is sufficient and the results in the model $R\Box R$ must be consistent with it. Moreover, from just the analysis of the case $x \to \infty$, we have concluded what is the structure in a generic renormalizable case, when we have both $\omega_R \neq 0$ and $\omega_C \neq 0$ (so $x \neq 0$ and $x \neq \infty$). This structure is beautifully confirmed by the formula (51) or (33) explicitly for the generic case.

As emphasized above, it is in turn the $N = 0$ case, which is extraordinary and it changes the pattern of $x_{4-\mathrm{der}}$-dependencies described above. This all can be traced back to the fact that for $N = 0$ we have the possibility of reducing the generic HD scale-invariant model to the conformal one, when the full conformal symmetry is preserved (at least on the classical level of the theory). This happens, when one takes the isolated case of $\theta_R = 0$ and $\theta_C \neq 0$ for the four-derivative theory (for positive-definiteness we may also assume that $\theta_C > 0$). This case is discontinuous and cannot be taken as the naive limit $x_{4-\mathrm{der}} \to \infty$ of the formula (49) for the R^2 type of UV divergences, which would leave us effectively only with the A_0 coefficient. It is well known that the conformal gravity model is renormalizable one (at least to the one-loop level), contrary to the case of the theory $C\Box C$, which was

discussed above. This means that we shall not find any source of the problem when computing and getting results for UV divergences of this C^2 model. We do not find problems with the Hessian or the propagator provided we also gauge-fix the conformal local symmetry of Weyl conformal gravity. We shall not find the problem with the final expression of UV divergences, so there we shall not expect poles with θ_R coefficient. But some $x_{4-\mathrm{der}}$-dependence up to the quadratic order could be present (this is due to the one-loop character of the computation here; one can understand this easily from contributing Feynman diagrams). So then, we conclude that this dependence may be only in positive powers of the inverse ratio, namely of $x^{-1}_{4-\mathrm{der}} = \theta_R/\theta_C$. This is again confirmed in the formula (49) and (34), where we indeed find the quadratic dependence but in the inverse ratio $x^{-1}_{4-\mathrm{der}}$.

Simply, the final results for the generic case $x_{4-\mathrm{der}} \neq 0$ and $x_{4-\mathrm{der}} \neq \infty$ cannot depend on positive powers of $x_{4-\mathrm{der}}$ since then the limit of conformal gravity in $d = 4$ (i.e. $x_{4-\mathrm{der}} \to \infty$) would produce divergent results, but we know that Weyl gravity is renormalizable with a good control over one-loop UV divergences. However, this does not mean that the results for conformal gravity are continuous and obtainable from the generic ones in (34) by taking the limit $x_{4-\mathrm{der}} \to \infty$ there. We admit the fact that the coefficients there may show some finite discontinuities. However, both in the true and naive $x_{4-\mathrm{der}} \to \infty$ limiting forms they must be finite – we only exclude the case when they would be divergent in the $x_{4-\mathrm{der}} \to \infty$ limit. In this way, the results in renormalizable 4-dimensional conformal gravity for UV divergences may be expressed via finite numbers multiplying just one common overall divergence (like $1/\epsilon$ parameter in dimensional regularization (DIMREG) scheme). The theory is renormalizable and there are no new divergences inside coefficients of established form of UV divergences in generic HD Stelle theory in $d = 4$ spacetime dimensions, as in (1).

The significant difference between the cases of $N = 0$ and $N \geqslant 1$ is that in the former case the theory with $\theta_R = 0$ is conformal on the classical tree-level as well as on the first quantum loop, since we know that Weyl conformal quantum gravity is one-loop renormalizable. This is why the pattern of the x-dependence in these two cases is diametrically different. In both these cases of $N = 0$ and $N \neq 0$, one can derive the general structure of beta functions in generic HD theory with any finite value of the fundamental ratio x ($x \neq 0$ and $x \neq \infty$) by just analyzing the limit $x \to \infty$ (or respectively $x_{4-\mathrm{der}} \to \infty$) and its divergences which should or should not appear there respectively for the cases of $N \neq 0$ or $N = 0$.

The inverse quadratic dependence on the ratio $x_{4-\mathrm{der}}$ in the case of four-derivative Stelle theory can be easily understood as well. It is up to the quadratic order and the same dependence we would expect in the case of six-derivative gravitational theory in the C^2 sector of UV divergences. However, there as a surprise we find only up to linear dependence on the fundamental ratio x and only in one distinguished sector of C^2 divergences. In general, we can have up to quadratic dependence on x in six-derivative models or on $x^{-1}_{4-\mathrm{der}}$ in the Stelle gravity case in $d = 4$ spacetime dimensions. The UV divergences of some renormalizable HD gravity models in $d = 4$ spacetime dimensions are all at most quadratic in the general gravitational curvature (schematically they are $\mathcal{R}^2$). Hence they can be all read from the one-loop perturbative quantum corrections to the two-point graviton Green function, so equivalently from the quantum dressed graviton's propagator around flat spacetime background. We remind that here there is no quantum divergent renormalization of the graviton wave function. Moreover, higher orders in graviton fields (appearing in interaction vertices) are completely determined here due to the gauge invariance (diffeomorphism) present in any QG model, so we can concentrate below only on these two-point Green functions.

As it is known from diagrammatics, here the contributing Feynman diagrams may have either one propagator (topology of the bubble attached to the line) or two propagators (sunset diagrams) at the one-loop order and for corrections to the two-point function. In the most difficult case, there are here two perturbative propagators. Since in our higher-derivative theory we have two leading terms shaping the UV form of the graviton's propagator, namely the terms $\omega_C C\Box C$ and $\omega_R R\Box R$, then the corresponding propagator may be either with the front coefficient ω_C^{-1} or ω_R^{-1} respectively as the leading term. To change between the two expansions (in ω_C or in ω_R) one needs to use one power of the ratio x. Since we have two such propagators in the one-loop diagrams considered here, then dependence is up to the quadratic power in x. Sometimes we need to change back from ω_C to ω_R as the leading coefficient of the tree-level propagator, and then we need to multiply by inverse powers of the ratio x. The quadratic dependence is what we can have here in the most complicated case, which is actually realized in Stelle generic theory with both $\theta_C \neq 0$ and $\theta_R \neq 0$. (The argumentation above can be repeated very similarly for quadratic gravity in $d = 4$ forgetting about one power of box operator $\Box$ and changing corresponding omega coefficients to theta coefficients and x to $x_{4-\mathrm{der}}$.) Apparently, in the case of six-derivative gravitational theories there is some, for the moment, unexplained cancellation, and we see there only the dependence up to the first power on the ratio x of that theory.

One should acknowledge here the speciality of the case of $d = 4$ and one-loop type of computation. For higher loop orders the powers of the x ratio may appear higher in the final expressions for UV divergences of the theory. Similarly, if one goes to higher dimensional QG models, then even in renormalizable models at the one-loop level, one needs to compute higher

n-point Green function. This is because in even dimension d one needs in renormalizable theory not only to renormalize terms of the type $\mathcal{R}\Box^{(d-4)/2}\mathcal{R}$ but also others with more curvatures (and correspondingly less powers of covariant derivatives) down to the term of the type $\mathcal{R}^{d/2}$, where we do not find covariant derivatives acting on curvature at all. In the middle, the general terms can be schematically parametrized as $\nabla^{d-2i}\mathcal{R}^i$ for $i = 2, \ldots, \frac{d}{2}$ – all these terms have the energy dimensionality equal to the dimensionality of spacetime d. For the last term of the type $\mathcal{R}^{d/2}$ one needs to look at the quantum dressed $n = \frac{d}{2}$-point function at the one-loop order. In conclusion, in higher dimensions one should consider not only two-point functions with one-loop diagrams with the two topologies described above, but up to quantum dressed $\frac{d}{2}$-point functions. And even for one-loop perturbative level these additional diagrams may have more complicated topology meaning more vertices and more propagators and this means that also powers of the ratio x or x^{-1} respectively will be higher and higher. They are expected to be up to the upper bound given by the maximal power exponent equal to $\frac{d}{2}$ – this can be derived from the expression of quantum dressed $\frac{d}{2}$-point function, which is built exactly with $\frac{d}{2}$ propagators joining precisely $\frac{d}{2}$ 3-leg the same perturbative vertices. Then the topology of such a diagram is this one of the main one-loop ring and $\frac{d}{2}$ external legs attached to it, with each one separately and each one emanating from one single 3-leg vertex. Again the situation at the one-loop and in $d = 4$ is quite special and simple since the ratio x appears here only up to the maximal power exponent given by $\frac{d}{2} = 2$.

As a side result, one also sees that the situation in four-derivative model with the condition $\theta_C = 0$ is somehow "doubly" bad. First, the Hessian is not well-defined to start with and this takes away our trust in this type of computation. Moreover, if we would attempt to take the limit $\theta_C \to 0$ (or equivalently $x_{4-\mathrm{der}} \to 0$) in the final result like in (49), then we get a second problem since such limit gives infinite results. This means that we somehow doubly confirmed the problem with the perturbative and multiplicative renormalizability of such a model. It is not that the two instances of the problem support each other – they appear somehow independently and are not related, nor they cancel out. Above, we have seen that in the six-derivative (or general $N > 0$) case, they could occur completely independently for two completely different types of non-renormalizable theories (with the conditions of $\omega_R = 0$ or $\omega_C = 0$ respectively). Here, we see that since conformal gravity at one-loop must be without any problem of this type (no problem with the Hessian and no problem with getting infinite results of the limits $x_{4-\mathrm{der}} \to \infty$), then the occurrence of these two problems at the same time must happen in badly non-renormalizable model with $\theta_C = 0$ condition. In other words, since conformal gravity is a safe model, then the model with $\theta_C = 0$ must suffer twice since all these two problems must inevitably appear in one model or the other, if some extreme special cases like $\theta_R = 0$ or $\theta_C = 0$ are being considered.

Again, we remark that in generic quadratic gravity model we see up to quadratic dependence on the inverse ratio $x^{-1}_{4-\mathrm{der}}$, but a precise location where this dependence shows up is still not amenable for an easy explanation. We do not know why this happens in the R^2 sector only, while the C^2 and GB sectors are free from any $x_{4-\mathrm{der}}$-dependence. But at least the dependence on the inverse ratio $x^{-1}_{4-\mathrm{der}}$, rather than on its original form $x_{4-\mathrm{der}} = \frac{\theta_C}{\theta_R}$, in the exceptional case of $N = 0$ can be explained by the miraculous one-loop perturbative renormalizability of the conformal gravity model in $d = 4$.

4.3. Case of conformal gravity

Here we continue the discussion of related issues, but now in the framework of conformal gravity, so within the model with the reduced HD action with $N = 0$ and formally with $\theta_R = 0$. There are various motivations for conformal gravity in $d = 4$ spacetime dimensions [13, 14]. As it is well known the reason for the multiplicative renormalizability of such a reduced model, when we have from the beginning that $\theta_R = 0$ is the presence of conformality – conformal symmetry both on the tree level and also on the level of the first loop. Unfortunately, the story with conformal gravity in $d = 4$ is even more complicated than what we argued above. First, already at the one-loop level one discovers the presence of conformal anomaly, which is typically thought as not so harmful on the first loop level. However, it heralds the soon breaking of conformal symmetry like for example via the appearance of the R^2 counterterm at the two-loop level. Such term as a counterterm is not fully invariant under local conformal transformations – it is only invariant under so called restricted conformal transformations that is such transformations whose parameters satisfy the source-free background GR-covariant d'Alembert equation ($\Box\Omega = 0$) on a general spacetime. Hence the R^2 term is still scale-invariant but it breaks full conformal symmetry of the quantum conformal gravity. It seems the only way out of this conformal anomaly problem is to include and couple to conformal gravity specific matter sector to cancel in effect the anomaly. This is, for example, done in $\mathcal{N} = 4$ conformal supergravity coupled to two copies of $\mathcal{N} = 4$ super-Yang-Mills theory, first proposed by Fradkin and Tseytlin [49]. In such a coupled supergravity model, we have vanishing beta functions, implying complete UV-finiteness and conformality present also on the quantum level. This is conformal symmetry in the local version (not a rigid one) with Weyl conformal transformations in the gravitational setup and on the quantum field theory level.

If not in the framework of $\mathcal{N} = 4$ Fradkin and Tseytlin supergravity, the conformal anomaly of local conformal symmetry signals breaking of conformal symmetry, while scale-invariance (global part of it) still may remain intact. In the long run, besides the presence of non-conformal R^2 counterterm, this breaking will put conformal Ward identities in question and also the constraining power of the quantum conformality in question too. It will not constrain any more the detailed form of gravitational correlation functions of the quantum theory. The conformal symmetry will not be there and it will not protect the spectrum from the emergence of some spurious ghost states in it. This last thing will endanger the perturbative unitarity of the theory (and we do not speak here about the danger of unitarity breaking due to the HD nature of conformal gravity). Without the power of quantum conformal symmetry, we may have unwanted states in the spectrum corresponding to the states from generic Stelle gravity, and not from the tree-level spectrum of conformal gravity, so we can see mismatch in counting number of degrees of freedom and also in their characters, namely whether they are spin-1 or spin-0, ghosts or healthy particles, etc.

Moreover, in pure conformal gravity described by the action simply C^2 without any supergravitational extension, we notice the somehow nomenclature problem with the presence of quantum conformality. Even barring the issue of conformal anomaly, the general pure gravitational theory has non-vanishing beta functions, so there is no UV-finiteness there. This implies that there is an RG running and scale-dependence of couplings and of various correlators on the renormalization energy scale. Hence already at the one-loop level one could say that scale-invariance is broken, which implies violation of conformal symmetry too. However, one can live with this semantic difference provided that there are no disastrous consequences of the conformal anomaly. One can adopt the point of view that the theory at the one-loop level is still good provided that the UV-divergent action is conformally invariant too, that is when one has only conformally invariant UV counterterms. (Although in the strict meaning having them implies non-vanishing beta function, RG running, loss of UV-finiteness and of scale-invariance.) In our case the conformally invariant counterterms are only of the type C^2 and GB, so if the R^2 counterterm is not present at the one-loop level, then we can speak about this preserved quantum conformality in the second sense. It happens this is exactly the situation we meet for quantum conformal gravity in $d = 4$ at the one-loop level.

In order to see quantum conformality of one-loop level conformal gravity in $d = 4$ described by the action, one first naively may try to take the limit $x \to +\infty$ from the expression for the R^2 sector of UV divergences from formula in (34). One would end up with the results, just a constant A_0, which is generally not zero. The whole story is again more subtle, since the limits in this case are again not continuous, although as we advocated above they are luckily also not divergent, when we want to send $\theta_R \to 0$. In the end, we have only a finite discrepancy in numbers, which can be easily explained. As emphasized above in this case of the special reduced model we have the enhancement of symmetries and this new emergent conformal symmetry in the local version must be gauge-fixed too. This means that the kinetic operator needs to be modified and some new conformal gauge-fixing functional must be added to it for the consistency of the generalized Faddeev-Popov quantization prescription of theories with local gauge symmetries. This means that we will also have a new conformal gauge-fixing parameter (the fourth one), which can be suitably adjusted to provide again the minimality of the Hessian operator. Although, of course, the whole details of the covariant quantization procedure for conformal gravity are more delicate and more subtle, here we can just take a shortcut and pinpoint the main points of attention. When computing UV divergences using generally covariant methods like BV trace technology and functional traces of logarithms of operators, one also necessarily needs to add here the contribution of the third conformal ghosts, which are scalars from the point of view of Lorentz symmetry but they come with anti-commuting statistics. They are needed here because the conformal gravity theory is a natural HD theory and then third ghosts are necessary for covariant treatment of any gauge symmetry in the local form. It is true that for conformal local symmetry we do not need FP ghost fields (because of the reasons elucidated above), but we need a new third conformal ghost, which is moreover independent from the third ghost of diffeomorphism symmetry. Each symmetry with local realization comes with its own set of third ghosts, when the theory is with higher derivatives. It is also well known that classically conformal fields (like massless gauge fields of electromagnetism and also of Yang-Mills theory) give contribution to divergences which is conformally invariant counterterm, so only of the type C^2 or GB terms. This can be understood easily as a kind of conformal version of the DeWitt-Utiyama argument used before. Hence, if the scalars of the anti-commuting type that we have to subtract were conformally coupled, then they will not contribute anything to the R^2 type of the counterterm. But we see from the formula in (34) that the A_0 coefficient there is non-zero, so only this one survives after the limit $x \to \infty$ is taken. To cancel the R^2 counterterm is crucial for the hypothesized conformal invariance of the conformal gravity also on the first loop quantum level. And this must be done by explicitly non-conformal fields with non-conformal contributions to divergences. They cannot be massless gauge fields, but they can be minimally, so not conformally coupled scalar fields. Here for the consistency of the whole formalism of the FP covariant quantization

of conformal gravity, this role is played by the one real conformal third ghost with the kinetic operator $\Box^2$.

The contribution of the third conformal ghosts is what we actually need to complete the whole process of the computation of the UV divergences in the conformal gravity model. We need them for the overall consistency since in this covariant framework we cannot a posteriori check the presence of all gauge invariances. Here we assume that on the first quantum loop level, the conformal gravity model enjoys fully diffeomorphism as well as conformal symmetry. The terms given in the covariant BV framework of computation all satisfy these requirements, so only we must be careful to take all these contributions into account. The contribution of the third conformal ghosts is like that of two real scalars coupled minimally (but not conformally to one's surprise) to the background gravitational metric, but of the ghost type. Indeed this means that we have to subtract the contribution of two scalars, which is of course, UV-divergent but after extracting the overall divergence there is only a finite number. This is the number that when subtracted now matches with number obtained after the naive limit $x \to \infty$ of the generic results from (49). We explain that we need to subtract two real scalars each one coming with the standard two-derivative GR-covariant box operator as the kinetic operator since in HD conformal gravity the operator between third conformal ghosts is of the $\Box^2$ type as for the four-derivative theory. The limit to conformal gravity is discontinuous, but only in this sense that one has to take out also contribution of real scalar fields minimally coupled to gravitation. The first part of the limiting procedure, namely $x \to \infty$ is only a partial step and to complete the whole limiting procedure one must also deal properly with conformal symmetry. This applies not only to the coefficients in front of the R^2 term, where we see the mysterious but explainable x-dependence, but also to other coefficients in front of terms like C^2 and GB terms. Of course, for the last two terms the limits $x \to \infty$ do not change anything, but the contribution of third conformal ghosts makes impact and change the numerical results, which are luckily still finite in conformal gravity. The coefficients in front of the R^2 and GB counterterms are also finite in generic four-derivative gravity (cf. with (34)), however by these types of arguments with conformal gravity we cannot at present understand why the x-dependence happens only in front of the R^2 counterterm. Of course, in conformal gravity model, there is not any x-dependence at all.

At the end, when one accounts for all these numerical contributions, one indeed finds that at the one-loop level in conformal gravity, the coefficient of the R^2 term is vanishing, so the quantum conformality is present in the second sense. And we have only conformally invariant counterterms in pure conformal gravity without any conformal matter, but there is still interesting RG flow of couplings there. This also signifies that there is conformally invariant but non-trivial divergent part of the effective action with finite numerical constant coefficients, when the overall divergence is extracted. These finite coefficients arise in the two-step process. First as the limit $x \to \infty$ of a generic HD gravity and then by subtraction of UV-divergent contributions of two real scalars minimally coupled to gravitational field. Since these last contributions are known to be finite numbers multiplying the overall UV divergence, then this implies that the limit $x \to \infty$ of the generic expression in (49) must also give finite numbers. This explains why in perturbatively one-loop renormalizable model of conformal gravity in $d = 4$ there are standard UV divergences, although this is a reduced model with $\theta_R = 0$ and $N = 0$ case. So the x-dependence in (34) must be as emphasized above that is with inverse powers of the fundamental ratio x of the theory and in accord with what was schematically displayed in formula (49). Hopefully now the dissimilarities between the cases with $N = 0$ and $N > 0$ are more clear.

In short, we think that the only sensible reason, why we see completely different behaviour when going from $N = 0$ to $N = 1$ class of theories is that the theory with $\omega_R = 0$ and $N = 1$ ceases to be conformally invariant in $d = 4$. In a different vein, the degeneracy of the kinetic operator $\hat{H}$ in the $\omega_C = 0$ cases, for both $N = 0$ and $N = 1$, remains always the same.

This proves again and again that the case of conformal gravity is very special among all HD theories, in $d = 4$ among all theories quadratic in gravitational curvatures. One can also study the phenomenological applications of the Weyl conformal gravity models to the evaporation process of black holes [50, 51] and also use the technology of RG flows (and also functional RG flows) in the quantum model of conformal gravity to derive some interesting consequences for the cosmology (like for example for the presence of dark components of the universe in [52–54]). Finally, the conformal symmetry realized fully on the classical level (and as we have seen also to the first loop level and perhaps also beyond) is instrumental in solving the issue with spacetime singularities [34, 55, 56], which are otherwise ubiquitous problems in any other model of generally covariant gravitational physics (both on the classical and quantum level). To resolve all singularities one must be sure that the conformality (Weyl symmetry) is present also on the full quantum level (and it is not anomalous there), so the resolution of singularities from the classical level (by some compensating conformal transformations) is not immediately destroyed by some dangerous non-conformal quantum fluctuations and corrections.

4.4. More on limiting cases

Here again we analyze closer the situation with various limits, when some coefficients in the gravitational action (45) disappear.

In a generic six-derivative theory, the trace of the logarithm of the FP ghosts kinetic operator $\hat{M}$ and of the standard minimal $\hat{C}$ matrix are regular in the limit $\omega_R \to 0$, but not in the limit $\omega_C \to 0$. For the $\hat{C}$ matrix this is understandable, because the γ parameter contains factor ω_C^{-1} in the minimal gauge. However, for the FP ghosts kinetic operator $\hat{M}$, this dependence was unexpected, because in the explicit definition of the $\hat{M}$ operator there was never any singularity in ω_C. Moreover, this singularity is even quadratic in ω_C coefficient.

We also emphasize that in the general six-derivative theory the trace of the logarithm of the Hessian operator $\hat{H}$ is irregular both in the limits $\omega_R \to 0$ and $\omega_C \to 0$ separately. It seems that in the total sum of contributions to the beta functions of the theory the singularity in ω_C cancels completely between $\mathrm{Tr}\ln\hat{H}$, $\mathrm{Tr}\ln\hat{C}$, and $\mathrm{Tr}\ln\hat{M}$, while the poles in ω_R remain and this is what is seen as a dependence of the final results on the non-negative powers of the fundamental ratio x. For the definition of the $\hat{H}$ operator, if the limit $\omega_R \to 0$ is taken, nothing bad is seen. This may be a partial surprise. Of course, when the limit $\omega_C \to 0$ is taken, then this operator does vanish on flat spacetime, so then its degeneracy is clearly visible.

The situation with limits ($\theta_R \to 0$ or $\theta_C \to 0$) in four-derivative theory we see as follows. The functional trace $\mathrm{Tr}\ln\hat{C}$ is regular in both limits. It actually does not depend on any gauge-fixing parameters here, despite that in its formal definition we used the γ parameter, which shows the $\frac{1}{\theta_C}$ singularity. The situation with the FP operator $\hat{M}$ is the same as previously, because the operator is identical as in the six-derivative theory case. The operator $\hat{H}$ shows the problem with its definition only when the limit $\theta_C \to 0$ is considered. The same is true for its trace of the functional logarithm, which shows singularity in θ_C coupling coefficient up to the quadratic order. In this case and in the total sum of all contributions, we see only $\frac{1}{\theta_C}$ singularity to the quadratic order. However, here the limit $\theta_R \to 0$ is not continuous either, because the theory reaches a critical point in the theory space with enhanced symmetry for $\theta_R = 0$ (conformal enhancement of local symmetries) as it was explained in subsection 4.3.

Let us also comment on what special happens in the computation of UV divergences for quadratic theory from the perspective of problems that we have initially encountered in six-derivative theory for the same computation. First, we established, in the middle steps of our computation for the results published in [26], that in the traces $\mathrm{Tr}\ln\hat{H}$ and $\mathrm{Tr}\ln\hat{C}$ in Stelle gravity there are no any dangerous $\frac{1}{y} = \frac{1}{2\omega_C - 3\omega_R}$ poles (cf. [42]). The cancellations happen separately within each trace. Second thing is that we found that the trace $\mathrm{Tr}\ln\hat{C}$ surprisingly completely does not depend on the gauge-fixing parameter γ, which was needed and used in the initial definition of the $\hat{C}$ operator in (15). Finally, one can notice that the addition of the Gauss-Bonnet term in $d = 4$ spacetime dimension, does not change anything for R^2, $R_{\mu\nu}^2$, and $R_{\mu\nu\rho\sigma}^2$ divergences (as it was expected), because its variation is a topological term in $d = 4$.

In this last part, we use the schematic notation for various gravitational theories, when we do not write, for simplicity, the coupling coefficients in front of various terms since they are not the most important for the considerations here. In the case of six-derivative theories, it is impossible to obtain the results for the cases with $\omega_C = 0$ or $\omega_R = 0$ by any limiting procedures of the corresponding results obtained for the general six-derivative theory with $\omega_R \neq 0$ and $\omega_C \neq 0$. These reduced theories have different bilinear parts, with degenerate forms of the kinetic operator and our calculation methods break down here. Similarly, one can calculate the beta functions in a theory with R^2 only and this was done indirectly many times. One can also calculate UV divergences in $C\Box C + R^2$ theory or in an analogous $R\Box R + C^2$ theory, but this is actually not easy to do. But then we cannot easily extract these results from our general calculation done in $C\Box C + R\Box R$ six-derivative theory. The simple reason is that all these theories have different amount and characteristics of degrees of freedom and the transition from one to another at quantum level is complicated (and to some extent unknown).

Moreover, we remark, that the results for beta functions in models $C\Box C + R^2$ (or $C\Box C + R^2 + C^2$) or in $R\Box R + C^2$ (or $R\Box R + C^2 + R^2$) could be obtained by though different computations than what we have done here. We summarize that the six-derivative gravitational theory to be renormalizable must contain both terms of the type $C\Box C$ and $R\Box R$. Then the kinetic operator (Hessian) between gravitational fluctuations and the graviton's propagator are well-defined. In all other models, there is not a balance between the number of derivatives in the vertices of the theory and in all gauge-invariant pieces of the propagator, so the theory behaves badly regarding perturbative UV divergences at higher loops. This does not mean that the computation of UV divergences at one-loop level is forbidden, just only that usually these are not all divergences in the theory, they may not be the UV-leading ones anymore or the theory does not have decent control over all of them.

For the strictly non-renormalizable theory with the leading in the UV term $C\Box C$ we can have additions of various subleading terms which do not change the fact of non-renormalizability. We can add terms (separately or in conjunction) of the following types: ω_Λ (cosmological constant term), R (E-H term), R^2 (Starobinsky's term), C^2 (Weyl square term). The UV-leading part of the Hessian still is defined as it contains six-derivative differential operator understood on flat spacetime and between tensorial fluctuations, so derived from the terms quadratic in curvatures. The Hessian is non-degenerate. (It has to be non-degenerate here, because the GR-covariant box oper-

ator is here only a spectator, and the Hessian must be "almost" non-degenerate for the case of conformal gravity with the action C^2.) The flat spacetime propagator can be defined only if we make addition of ω_Λ, or R or R^2 terms – this is because of the problematic part of it proportional to the projector $P^{(0)}$ which must for the consistency of the inverting procedure for the whole propagator be non-zero. This scalar part (spin-0 part) is sourced from any scalar term or from the cosmological constant term. If only the C^2 term is added, then the propagator still is ill-defined. Still these additions do not change the fact that the theory is non-renormalizable, if there is not an accompanying six-derivative term of the form $R\Box R$. As for the final results for UV divergences in these extended models, naively one would think that there are no additional UV divergences proportional to terms with four derivatives of the metric (namely to terms R^2, C^2 and GB), because of the limit $\omega_R \to 0$ and the dependence on the x ratio in (33) in the linear way. We would naively think that divergences with R^2 and GB terms are the same as in (33). The only problematic one could be this proportional to the C^2 term since the limit gives already divergent results (so "doubly" divergent) – this would mean that the coefficient of the C^2 divergence is further divergent and renormalization of just C^2 does not absorb everything at the one-loop level. Since the model is non-renormalizable we cannot trust this computation and these limits at the end, especially if they give divergent results. But this probably means that we cannot sensibly define the C^2 counterterm needed for the UV renormalization in these theories. In a sense an attempt of adding ω_Λ or R, or R^2 terms to regularize the theory $C\Box C + C^2$, or even the simplest one, just $C\Box C$, is unsuccessful so we perhaps still cannot trust there in the final results just given by two B_0 coefficients of UV divergences proportional to terms R^2 and GB, while the C^2 divergences are never well-defined in this class of models.

Instead, in the case of the reduced model with $R\Box R$ UV-leading action, one may keep some hope that the results for the C^2 counterterms will be finite at the end, but maybe still discontinuous, despite the non-renormalizability of the model with $R\Box R$ action (plus possible lower derivative additions to regularize it as it was mentioned above). Maybe in this reduced models the results of the projection procedure of the UV-divergent functional of the effective action of the theory onto the sector with only C^2 terms will result here in giving sense to pure C^2 divergences in this limiting model. (Here we may try to resort to some projection procedure for the functional with UV divergences since in these non-renormalizable models, one may expect to find more divergences than just of the form of C^2 and R^2 as presented initially in (1). There could exist new UV divergences, which contain even more than four derivatives on the background metric tensor, even in $d = 4$ case.) But the final finite value may be discontinuous and may not be obtainable by the naive limit $x \to 0$ of the expression for the divergent term in the C^2 sector of UV divergences, so it may not be just B_0 there. This remark about possible discontinuities may apply also to coefficients in front of divergent terms of the type R^2 and GB. They may still end up with some finite definite values for this model, but probably they are not the same as the coefficients B_0 of these terms from (51), so we probably will be able to see here another discontinuities in taking the naive limit $x \to 0$.

These above results about discontinuities and negative consequences due to the overall non-renormalizability of the two considered above reduced models, are also enforced by the analysis of power counting of UV divergences. One can try to perform the "worst case scenario" analysis of one-loop integrals and the results show complete lack of control over perturbative UV divergences in such reduced models. This is even worse that in the case of off-shell E-H gravity considered in $d = 4$ dimensions, which is known to be one-loop off-shell perturbatively non-renormalizable theory. In the latter case the superficial divergence of the divergence Δ is bounded at the one-loop level ($L = 1$) in formula (4) by the value 4. In general, at the arbitrary loop order we have the formula for power counting reads then

$$\Delta + d_\partial = 4 + 2(L - 1), \tag{56}$$

which if we concentrate on logarithmic UV divergences only (with $\Delta = 0$), we get that at the one-loop level for all Green functions we need counterterms with up to $d_\partial = 4$ partial derivatives on the metric tensor. At the two-loop level we instead need to absorb the divergence term with $d_\partial = 6$ partial derivatives as this was famously derived by Goroff and Sagnotti [17, 18]. The counterterm that they have found was of the form of the C^3 GR-covariant term and its perturbative coefficient at the two-loop order does not vanish, and this implies that the whole UV-divergent term does not vanish even in the on-shell situation. But still we know which counterterms to expect at the given loop order and the absorption of UV divergences works for all divergent Green functions of the QG model.

The situation in the reduced models of the type $C\Box C$ or $R\Box R$ in the leading UV terms is much worse even at the one-loop level from naive power counting there. One sees that different GR-covariant counterterms are needed to absorb divergences in different divergent Green functions of the quantum model at the one-loop level, so the counting does not stop at the two-point function level. We think that despite these tremendous difficulties, one still can compute the divergent parts of the effective action and the actual computations are very tedious and still possible. This is provided that one can invert the propagator, so one has some non-vanishing parts in both gauge-invariant parts of it with the spin-0 and spin-2 projectors. So,

it is at present practically impossible to do computation in the pure models $C\Box C$ or $R\Box R$ only. We know that they give contributions in momentum space proportional to k^6 in the spin-2 and spin-0 parts of the propagator respectively, while other parts are not touched. In order to regularize the theory and to give sense to the perturbative propagator around flat spacetime, one has to add the regulator terms as this was mentioned above. Let us assume that they give contributions to the other sector of the spin projectors in the graviton's propagator of the form k^{-m}, where m is some integer and $m < 6$, they may likely also give additional subleading contributions to the main respective part of the propagator which was there with six derivatives in the UV regime correspondingly to the spin-2 sector in $C\Box C$ theory and to the spin-0 sector in $R\Box R$ model. The values of m are respectively: $m = 0$ for the cosmological constant addition (it still regularizes the propagator but very, very weakly), $m = 2$ when E-H term is added (it contributes both to the spin-0 and spin-2 parts), $m = 4$ when either R^2 or C^2 terms are added (they contribute exclusively in their respective sectors).

Since now after the regularization of the graviton's propagator, its behaviour is still very unbalanced in the UV regime between different components, then one sees the following results of the analysis of UV divergences at the one-loop order. First, the general gravitational vertex is still with six derivatives, while the propagator is k^{-6} in the best (most suppressed) behaviour and k^{-m} is the worst behaviour in the other components. For the most dangerous situation we have to assume that the overall behaviour of the propagator is in the worst case, so with the UV scaling of the form k^{-m}. Then the relation between the number of derivatives in a general gravitational vertex and in the propagator is broken and this is a reason for very bad behaviour with UV divergences here. Such relation is typically present even in non-renormalizable models, like in E-H gravity. The lack of this relation means that now the result for d_∂ of any Feynman graph G depends on the number of external graviton lines n_g emanating from the one-loop diagram. Previously in the analysis of power counting there was never any dependence on this n_g parameter. This is a source for problems even bigger when one increases n_g. For definiteness we can assume that $n_g > 1$ since here we will not be interested in vacuum or tadpole diagrams and quantum corrections to them. Now, for a general diagram G with n_g external graviton lines, the worst situation from the point of view of UV divergences is for the following topology of the diagram, namely there is one loop of gravitons (so called "ring of gravitons") in the middle with n_g 3-leg vertices joined by n_g propagators. In the case when we concentrate on logarithmic divergences $D = 0$, we get the following results for the quantity d_∂ which tells us how many derivatives we must have in the corresponding counterterm to absorb the divergence,

$$d_\partial = 4 + n_g(6 - m) \tag{57}$$

for the graph contributing one-loop quantum corrections to the n_g-point Green function. One sees that this d_∂ grows without a bound even at the one-loop level, when n_g grows, so in principle to renormalize the theory at the one-loop level one would need already infinitely many GR-covariant terms, if one does not bound the number of external legs of Green functions that must be considered here. A few words about explanation of numbers appearing in the formula (57). The 4 there is the number of spacetime dimensions (integration over all momenta components at the one-loop level), while the $(6 - m)$ factor comes from the difference between the highest number of derivatives in the vertex, i.e. 6 compensated by the worst behaviour in some propagator components given in the UV by k^{-m} only.

Moreover, there are precisely n_g segments of the structure propagator joined with 3-leg vertex to create a big loop. This behaviour signals complete lack of control over perturbative one-loop divergences even at the one-loop level. Moreover, they have to be absorbed in the schematic terms of the type

$$\nabla^{4+4n_g-n_gm+2i}\mathcal{R}^{n_g-i}, \tag{58}$$

for the index i running over integer values in the range $i = 0, 1, 2, \ldots n_g - 2$, where we only mentioned the total number of covariant derivatives not specifying how they act on these general gravitational curvatures. This is because this is an expression for the quantum dressed one-loop Green function with n_g graviton legs on the flat spacetime, so terms with more curvatures than n_g will not contribute to absorb these divergence of flat Green n_g-point function. We only mentioned here the really the worst situation, where the divergence may be finally absorbable not only by the highest curvature terms of the type $\nabla^{4+4n_g-n_gm}\mathcal{R}^{n_g}$ but also for terms with smaller number of curvatures (up to $\mathcal{R}^2$ terms and in the precise form $\mathcal{R}\Box^{\frac{1}{2}n_g(6-m)}\mathcal{R}$). We neglect writing counterterms here which are total derivatives and which are of the cosmological constant type. These are then the needed counterterms off-shell at the one-loop level in such general reduced model.

To make it more concrete, we will analyze the cases of $m = 0, 2$ and 4 with special attention here in these badly non-renormalizable models for some small numbers of legs of quantum dressed Green functions. We have that at $m = 0$ to absorb UV divergences from the 2-point function we need generic counterterms of the form: $\mathcal{R}\Box^j\mathcal{R}$ with the exponent j running over values $j = 0, 1, 2, 3, 4, 5, 6$, while to renormalize a three-point function one needs previous terms and possibly new terms of the type $\nabla^j\mathcal{R}^3$ with $j = 0, \ldots, 16$ and for four-point functions new terms are of the type $\nabla^j\mathcal{R}^4$ with $j = 0, \ldots, 20$, etc. for higher Green functions (for n_g-leg correlators one needs j up to $j_{\max} = 4n_g + 4$).

When we regularize by adding the E-H term with $m = 2$ the situation is slightly better, but then to absorb UV divergences from the 2-point function we need generic counterterms of the form: $\mathcal{R}\Box^j\mathcal{R}$ with the exponent j running over values $j = 0, 1, 2, 3, 4$, while to renormalize a three-point function one needs previous terms and possibly new terms of the type $\nabla^j\mathcal{R}^3$ with $j = 0, \ldots, 10$ and for four-point functions new terms are of the type $\nabla^j\mathcal{R}^4$ with $j = 0, \ldots, 12$, etc. for higher Green functions (for n_g-leg correlators one needs j up to $j_{\max} = 2n_g+4$). Finally, we can add terms of the type R^2 and C^2 for the regularization purposes. In such final case to be considered here one has that to absorb UV divergences from the 2-point function we need generic counterterms of the form: $\mathcal{R}\Box^j\mathcal{R}$ with the exponent j running over values $j = 0, 1, 2$, while to renormalize a three-point function one needs previous terms and possibly new terms of the type $\nabla^j\mathcal{R}^3$ with $j = 0, \ldots, 4$ and for four-point functions new terms are of the type $\nabla^j\mathcal{R}^4$ with $j = 0, \ldots, 4$, etc. for higher Green functions (for n_g-leg correlators one needs j up to $j_{\max} = 4$ here independently on the number of legs n_g). Still in this last case one sees that one needs infinitely many counterterms to renormalize the theory at the one-loop level, although the index j of added covariant derivative is bounded by the values 4, still one needs more terms with more powers of gravitational curvatures $\mathcal{R}$.

This shows how badly non-renormalizable are these models already at the one-loop level and that any control over perturbative UV divergence is likely lost, when the number of external legs is not bounded here from above. These reduced models are examples of theories when the dimensionality and the number of derivatives one can extract from the vertices and propagators of the theory differ very much. Previously in quantum gravity models these two numbers were identical which leads to good properties of control over perturbative divergences (renormalizability, super-renormalizability and even UV-finiteness). With these reduced models we are on the other bad extreme of vast possibilities of QG models. But seeing them explicitly proves to us how precious is the renormalizability property and why we strongly need them in HD models of QG, in particular how we need super-renormalizability in six-derivative QG models.

The arguments above convince us to think that there is no hope to get convergent results for the front coefficient coming with the C^2 counterterm in the UV-divergent part of the effective action in the considered here model with the only presence of the $C\Box C$ as the leading one in the UV. This may signify that here there exists another UV-divergent term (perhaps of the structure like $C\Box^n C$), which contains more derivatives, and this could be a reason why the coefficient in front of the C^2 term is itself a divergent one. The presence of such new needed counterterms with more derivatives can be motivated by the analysis of power counting of UV divergences in this reduced unbalanced model, which is also presented below. Even if the higher $C\Box^n C$ type of UV divergence is properly extracted and taken care of, then we can still be unable to properly define and see as convergent the divergence proportional to the four-derivative term C^2. Even such a projection of the UV-divergent functional of the theory onto the sector with only C^2 terms will not help here in giving sense to pure C^2 divergences in this limiting model. However, this remark does not need necessarily to apply to coefficients in front of divergent terms of the type R^2 and GB. They may still end up with some finite definite values for this model, but probably they are not the same as the coefficients B_0 of these terms from (51), so we could be able to see here another discontinuity in taking the limit $x \to +\infty$.

On the other hand, for the strictly non-renormalizable theory with the leading in the UV term $R\Box R$ we can have additions of similar various subleading terms which do not change the fact of non-renormalizability. We can add terms (separately or in conjunction) of the following types: ω_Λ, R, R^2, or C^2. The UV-leading part of the Hessian still is not well-defined as it should contain six-derivative differential operator understood on flat spacetime and between tensorial fluctuations, while from the term $R\Box R$ we get only operator between traces of metric fluctuations $h = \eta^{\mu\nu}h_{\mu\nu}$ (between spin-0 parts), so derived from the terms quadratic in curvatures present in the UV regime. Probably the degeneracy of the Hessian operator can be easily lifted out, if we add one of the ω_Λ, or R or C^2 terms. If only the R^2 term is added, then the Hessian still is degenerate. Similarly, the flat spacetime propagator can be defined only if we make addition of ω_Λ, or R or C^2 terms – this is because of the problematic part of it proportional to the projector $P^{(2)}$ which must for the consistency of the inverting procedure for the whole propagator be non-zero. This tensorial part (spin-2 part) is sourced exclusively from any GR-invariant term built out with Weyl tensors in adopted here Weyl basis of terms or from the E-H term or from the cosmological constant term. If only the R^2 term is added, then the propagator still is ill-defined. Still these additions do not change the fact that the theory is formally non-renormalizable, if there is not an accompanying six-derivative term of the form $C\Box C$.

As for the final results for UV divergences in these extended models, naively one would think that there are no new UV divergences proportional to terms with four derivatives of the metric (namely to terms R^2, C^2 and GB), because of the limit $\omega_C \to 0$ and the dependence on the x ratio in (33) in the linear way. We would naively think that divergences with R^2 and GB terms are the same as in (33). The only problematic one could be this proportional to the C^2 term since the limit gives already constant result, namely the B_0 coefficient. Since the model is non-renormalizable we cannot trust this computation and these limits at the

end, even if they give here convergent results. But this probably means that we cannot sensibly define the C^2 counterterm needed for the renormalization of these theories. When we include additions to the action, which remove the degeneracy of the flat spacetime graviton's propagator, then at least the perturbative computation using Feynman diagrams can be attempted in such a theory. Although of course, in this case the different parts of the propagator have different UV scalings, so the situation for one-loop integrals is a bit unbalanced and there is not a stable control over perturbative UV divergences, when for example one goes to the higher loop orders. Probably new counterterms (with even higher number of derivatives) will be at need here. Making additions of some subleading terms from the point of view of the UV regime, may help in defining the unbalanced perturbative propagator, but still one expects (due to energy dimension considerations) that these additions do not at all influence the quantitative form of UV divergences with four-derivative terms, so these ones which are leading in the UV. These additions are needed here only quantitatively and on the formal level to let the computation being done for example using Feynman diagrams with some mathematically existing expressions for the graviton's propagator. In a sense adding ω_Λ or R, or C^2 terms regularizes the theory $R\Box R+R^2$ or even the simplest one, just $R\Box R$, so we can perhaps trust there in the final results just given by all three B_0 coefficients of UV divergences proportional to terms R^2, C^2 and GB. This can be motivated by the observation that here the limits $\omega_C \to 0$ or $\theta_C \to 0$ respectively do not enhance any symmetry of the model in question, so they can be naively and safely taken. But we agree that this case requires a special detailed and careful computation to prove this conjectural behaviours.

In the general case of badly non-renormalizable theories, with both $\omega_C = 0$ or $\omega_R = 0$, one trusts more the computation using Feynman diagrams and around flat spacetime than of the fully GR-covariant BV method of computation. For the former one only needs to be able to define properly the propagator – all physical sectors of it, and for this purpose one can regularize the theory by adding the term $\omega_\kappa R$, which is a dynamical one with the smallest number of derivatives and for which flat spacetime is an on-shell vacuum background. (In this way, we exclude adding the cosmological constant term ω_Λ, which would require adding some source and the flat spacetime propagator could not be considered anymore in vacuum there.) Then in such regulated non-renormalizable theory one can get results around flat spacetime and in Fourier momentum space, and then at the end one can take the limit $\omega_\kappa \to 0$. The results for some UV divergences in these non-renormalizable models must be viewed as projected since higher-derivative (like 6-derivative and even higher) infinities may be present as well. These last results must coincide with the ones we obtained in (33), when the proper limits of $\omega_C \to 0$ or $\omega_R \to 0$ are taken. We notice that adding the E-H term, which is always a good regulator, changes the dynamics very insignificantly for these higher-derivative models and the results from Feynman diagram computations can be always derived. Instead for the leading in the UV regime part of the Hessian operator, which is a crucial element for the BV method of computation, addition of just $\omega_\kappa R$ does not help too much and the operator is still degenerate since it is required that all its sectors are with six-derivative differential operators: are non-vanishing and non-degenerate there.

We propose the following procedure for the derivation of correct limiting cases analyzed here. First the theory with $\omega_C \neq 0$, $\omega_R \neq 0$ and $\omega_\kappa \neq 0$ is analyzed using Feynman diagram approach. The results for UV divergences must be identical to the ones found in (33) using the BV technique. They do not show any singularity at this moment. In Feynman diagram computation one can take the limit $\omega_C \to$ or $\omega_R \to 0$, while the propagator and perturbative vertices are still well-defined. In these circumstances we have that still $\omega_\kappa \neq 0$. We admit that the theory loses now its renormalizability properties, but we just want to project the UV-divergent action onto the terms with the structure of three GR-covariant terms C^2, R^2 and GB. For this the method of Feynman graph computation is still suitable since it only requires the well-defined propagator, but it can work even in badly non-renormalizable theories. This is like taking the naive limits of $\omega_C \to$ or $\omega_R \to 0$ in the results from (33) respectively, regardless which way they were obtained. One justifies the step of taking these limits by recalling that we are still working in the Feynman diagram approach, and not with the BV technique. Finally, one sends $\omega_\kappa \to 0$ hoping that this does not produce any finite discontinuity in the results for four-derivative UV divergences. This is justified by dimensional analysis arguments provided also earlier in this article and by the fact that except in the case of conformal gravity theory in $d = 4$, there is no any enhancement of local symmetries in the limit $\omega_\kappa \to 0$. Then one gets the sense for the limits considered in these sections.

This analysis concludes the part with special limiting cases of extended six-derivative theories, where one of the coefficients ω_R or ω_C is to be set to zero. Probably the same considerations of some limits can be repeated very similarly (with the exception of the conformal gravity case) for the Stelle quadratic gravity models, but we will skip this analysis here since it can be found in the literature.

5. Stability of HD theories

Above we have seen that HD theories of gravitation are inevitable due to quantum considerations. They also come with a lot of benefits that we have discussed at length before like super-renormalizability and the possibility for UV-finiteness. However, it is also well

known that they have their own drawbacks and problems. One of the most crucial one is the issue of unitarity of the scattering (S-matrix) in perturbative framework. This is of course in the situation when we can discuss the scattering problems, so when we can define asymptotic states in interacting gravitational background, so when the gravitational spacetime is asymptotically flat. In more generality, the related issue is of quantum stability of the theory.

In general, in literature about general HD theories there exist various proposals for solutions of these perennial problems. We can mention here a few of them: PT-symmetric quantum theory, Anselmi-Piva fakeon prescription, non-local HD theories, benign ghosts as proposed by Smilga, etc. Below we will try to describe some of their methods and show that the problems with unitarity or with the stability of the quantum theory can be successfully solved. We also provide arguments thanks to Mannheim [57, 58] that the gravitational coupled theory must be without problems of this type, if the original matter theory was completely consistent.

We first express the view that the stability of the quantum theory is fundamental, while the classical theory may emerge from it only in some properly defined limits. Hence we should care more about the full even non-linear stability on the quantum level and some instabilities on the classical level may be just artifacts of using classical theory which cannot be defined by itself without any reference to the original fundamental quantum theory. An attempt to understand the stability entirely in classical terms may be doomed to clearly fail since forgetting about the quantum origin may be here detrimental for the limiting process. If the quantum theory is stable and unitarity is preserved, then this is the only thing we should require since the world is in its nature quantum and physically we know that it is true that $\hbar = 1$ in proper units, rather than $\hbar \to 0$, so the classical limit may be only some kind of illusion. If there are problems with classical stability analysis like this done originally by Ostrogradsky, then this may only mean that the classical theory obtained this way neglects some important features that were relevant on the quantum level for the full quantum stability of the system.

First, in Anselmi-Piva prescription one solves completely the unitarity issue for HD theories by invoking fakeon prescription to take properly into account the contribution of particles which in the spectrum are related to higher derivatives theories and which typically are considered as dangerous for the unitarity of the theory. The presence of a particle with negative residue called a ghost at the classical level makes the theory not unitary in its original quantization based on the standard Feynman prescription [7] of encircling the poles for the loop integrals. A new quantum prescription, as recently introduced by Anselmi and Piva [59–61] was based on the earlier works by Cutkosky, Landshoff, Olive, and Polkinghorne [62]. The former authors invented a procedure for the Lee-Wick theories [63, 64], which allow them to tame the effects typically associated to the presence of ghosts in the Stelle's theory. In this picture, the ghost problem (also known as unitarity problem) is solved consequently at any perturbative order in the loop expansion [61] done for the loop integrals which need to be computed in any QFT, if one requires higher order accuracy.

At the classical level, the ghost particle (or what Anselmi and Piva define as "fakeon", because this particle understood as a quantum state can only appear as a virtual particle and inside perturbative loops) is removed from the perturbative spectrum of the theory. This is done by solving the classical equations of motion for the fakeon field by the mean of a very specific combination of advanced plus retarded Green's functions and by fixing to zero the homogeneous solution of resulting field equations [65, 66]. This is then equivalent to removing the complex ghosts in the quantum theory from the spectrum of asymptotic quantum states by hand. However, this choice and this removal decision is fully preserved and protected by quantum corrections, hence it does not invalidate the unitarity of the S-matrix at higher loop orders.

Such prescription of how to treat virtual particles arising due to HD nature of the theories is very general and can be applied to both real and complex ghosts, and also to normal particles, if one wishes to. (Every particle can be made fake, so without observable effects on the unitarity of the theory.) In particular, this prescription is crucial in order to make perturbatively unitary the theory proposed by Modesto and Shapiro in [67, 68] which comes under the name of "Lee-Wick quantum gravity". The latter class of theories is based on the general gravitational higher-derivative actions as proposed by Asorey, Lopez, and Shapiro [12]. In this range of theories, we can safely state to have a class of super-renormalizable or UV-finite and unitary higher-derivative theories of QG. In order to guarantee tree-level unitarity, the theory in [67, 68] has been constructed in such a way that it shows up only complex conjugate poles in the graviton's propagator, besides the standard spin-2 pole typically associated with the normal massless graviton particle with two polarizations. Afterwards, the new prescription by Anselmi and Piva [61] guarantees the unitarity of this theory at any perturbative order in the loop expansion.

We also emphasize that the Stelle's quadratic theory in gravitational curvatures [7] with the Anselmi-Piva prescription is the only strictly renormalizable theory of gravity in $d = 4$ spacetime dimensions, while the theories proposed in [67, 68] are from a large (in principle infinite) class of super-renormalizable or UV-finite models for quantum gravity.

Next, in the other approach pioneered by Bender and Mannheim to higher-derivative theories and to non-symmetric and non-Hermitian quantum mechan-

ics [69, 70], one exploits the power of non- Hermitian PT-symmetric quantum gravity. Here, the basic idea is that the gravitational Hamiltonian in such theories (if it can be well-defined), is not a Hermitian operator on the properly defined Hilbert space of quantum states, rather it is only PT-symmetric Hamiltonian. Then some eigenstates of such a Hamiltonian may correspond to non-stationary solutions of the original classical wave equations. They would indeed correspond in the standard classical treatment to the Ostrogradsky instabilities. The famous example are cosmological run-away solutions or asymptotically non-flat gravitational potentials for the black hole solutions. The problem of ghosts manifests itself already on the classical level of equations of motion, where one studies the linear perturbations and its evolution in time. For unstable theories, the perturbations growth is without a bound in time. But in some special solutions, like for example present in models of conformal gravity, these instabilities are clearly avoided and then one can speak that ghosts are benign in opposition to them being malign in destroying the unitarity of the theory. Such benign ghosts [71, 72] are then innocent for the issues of perturbative stability.

In the PT-symmetric approach to HD theories at the beginning, one cannot determine the Hilbert space by looking at the c-number propagators of quantum fields. In this case, one has to from the start quantize the theory and construct from the scratch the Hilbert space, which is different than the original naive construction based on the extension of the one used normally for example for two-derivative QFT's. With this new Hilbert space and with the non-Hermitian (but PT-symmetric) Hamiltonian the theory revealed to be quantum-mechanically stable. This is dictated by the construction of the new Hilbert space and the structure of the Hamiltonian operator. In that case the procedure of taking the classical limit, results in the definition of the theory in one of the Stokes wedges and in such a region the Hamiltonian is not real-definite and the corresponding classical Hamiltonian is not a Hermitian operator. Therefore, the whole discussion of Ostrogradsky analysis is correct as far as the theory with real functions and real-valued Hamiltonians is concerned, but it is not correct for the theory which corresponds to the quantum theory which was earlier proven to be stable quantum-mechanically. The whole issue is transmitted and now there is not any problem with unitarity or classical stability of the theory, but one has to be very careful in attempts to define the classical limiting theory.

We also repeat here arguments proposed by Mannheim about stability of the resulting gravitation-matter coupled theory [57, 58]. First we take some matter two-derivative model (like for example standard model of particle physics, where we have various scalars, fermions and spin-1 gauge bosons). This theory as considered on flat Minkowski background is well known to be unitary so it gives S-matrix of interactions with these properties. The model can be said that it is also stable on the quantum level. Now, we want to couple it to gravity, or in other words put it on gravitational spacetime with non-trivial background in such a way that the mutual interactions between gravitational sector and matter sector are consistent. This, in particular, implies that the phenomena of back-reaction of matter species on geometry are not to be neglected. The crucial assumption here is that this procedure of coupling to gravity is well behaved and for example, it will not destroy the unitarity properties present in the matter sector. We know that the theory in the matter sector is stable and also its coupling to geometry should be stable on the full quantum level. After all, this is just simple coupling procedure (could be minimal coupling) to provide mutual consistent interactions with the background configurations of the gravitational field.

Next, on the quantum level described, for example, by functional path integral, we can decide to completely integrate out matter species still staying on the general gravitational background. As emphasized in section 1, such procedure in $d = 4$ spacetime dimensions generate effective quantum gravitational dynamics of background fields with higher derivatives, precisely in this case there are terms of the type C^2 and R^2 (the latter term is absent when the matter theory is classically conformally invariant). In other words, the resulting functional of the quantum partition function of the total coupled model is a functional of only background gravitational fields. This last reduced or "effective" functional is given by the functional integral over quantum fluctuations of gravitational field of the theory given classically by the action with these HD above terms. Let us recall now what we have done, namely we have simply integrated out all quantum matter fields, which is an identity transformation for the functional integral representation of the partition function Z of the quantum coupled theory. Since this transformation does not change anything, then also the resulting theory of gravitational background must necessarily possess the same features as the original coupled theory we started with. Since the first theory was unitary, then also the last one theory of pure gravity but with higher-derivative terms must be unitary too. We emphasized that both theories give the same numerical values of the partition function Z understood here as the functional of the background spacetime metric. In the first theory the integration variables under functional integrals are quantum matter fields, while in the second case we are dealing with pure gravity so we need to integrate over quantum fluctuations of the gravitational fields. In the last case the model, which gives the integrand of the functional integral is given by the classical action $S_{\rm HD}$, so it contains necessarily higher derivatives of the gravitational metric field.

There also exist possibilities that ghosts or classical instabilities one sees on the classical level thanks to

Ostrogradsky analysis disappear. This may happen if for example, some very specific (or fine-tuned) initial or boundary conditions are used for solving non-linear higher-derivative classical equations of motion of the theory. It is not excluded as proven by Smilga that some instabilities may go away if one analyzes such special situations.

Various cures have been proposed in the literature for dealing with the ghosts-tachyon issue: Lee-Wick prescription [63, 64], fakeons [61, 65, 66, 73], non-perturbative numerical methods [71, 72, 74–78], ghost instabilities [79–81], non- Hermitian PT-symmetric quantum gravity based on PT-symmetric quantum mechanics [69, 70], etc (see also [82–87]). One might even entertain the idea that unitarity in quantum gravity is not a fundamental concept. So far, there is no a consensus in the community which solutions is the correct one. The unfortunate prevalent viewpoint is that none of the proposed solutions solves conclusively and completely the problem. And it seems that sadly the solutions proposed in the literature are not compatible and are unrelated to each other.

Therefore all the arguments given above should convince the reader that the HD (gravitational) theories are stable on the full quantum level. In particular, this means that for situations in which we can define asymptotic states (like for asymptotically flat spacetimes) the scattering matrix between fluctuations of the gravitational field is unitary on the quantum level and both perturbatively and non-perturbatively.

6. Conclusions

In this contribution, we have discussed the HD gravitational theories, in particular six-derivative gravitational theories. First, we motivated them by emphasizing their various advantages as for the models of consistent Quantum Gravities. We showed that six-derivative theories are even better behaved on the quantum level than just four-derivative theories, although the latter ones are very useful regarding scale- and conformal invariance of gravitational models. Moreover, the models with four-derivative actions serve as good starting examples of HD theories and they are reference points for consideration of six- and higher order gravitational theories. We first tried to explain the dependence of the beta functions in six-derivative theories by drawing analogies exactly to these prototype theories of Stelle gravity. We also emphasize that only in six-derivative gravitational models we have the very nice features of super-renormalizability and the narrow but still viable option for complete UV-finiteness. This is why we think super-renormalizable six-derivative theories have better control over perturbative UV divergences and give us a good model of QG, where this last issue with perturbative divergences is finally fully under our control and theoretical understanding.

In the main part of this paper, we analyzed the structure of perturbative one-loop beta functions in six-derivative gravity for couplings in front of terms containing precisely four-derivative in the UV-divergent part of the effective actions. These terms can be considered as scale-invariant term since couplings in front of them are all dimensionless in $d = 4$ spacetime dimensions. Our calculation for these divergences was done originally in the Euclidean signature using the so-called Barvinsky-Vilkovisky trace technology. However, the results are the same also in the Minkowskian signature independently which prescription one uses to rotate back to the physical relativistic Lorentz signature case, whether this is standard Wick rotation, or the one using Anselmi-Piva prescription using fakeons. This is because they are the leading divergences in the UV regime, and hence they do not completely depend how the rotation procedure is done from Euclidean to Minkowskian and how for example the contributions of arcs on the complex plane is taken into account since the last ones give subleading contributions to the UV-divergent integrals. Moreover, the calculations of beta functions that we presented in this paper has very nice and important features of being renormalization scheme-independent since they are done at the one-loop, but the expressions we get for them are valid universally. These are exact beta functions since they do not receive any perturbative corrections at the higher loop orders since the six-derivative gravitational theory is super-renormalizable in $d = 4$. Another part of good properties of the beta functions obtained here are the complete gauge independence and also independence on the gauge-fixing parameters one can use in the definition of the gauge-fixing functional. These last two properties are very important since in general gravitational theory we have the access to perturbative computation only after introducing some spurious element to the formalism which are related to gauge freedoms (in this case these are diffeomorphism symmetries). We modify the original theory (from the canonical formalism) by adding various additional fields and various spurious nonphysical (gauge) polarizations of mediating gauge bosons (in our case of gravitons) in order also to preserve relativistic invariances. These are redundancies that have to be eliminated when at the end one wants to compute some physical observables. Therefore, it is very reassuring that our final results are completely insensitive to these gauge-driven modifications of original theories.

Our beta functions being exact and with a lot of nice other properties, constitute one significant part of the accessible observables in the QG model with six-derivative actions. Their computation is a nice theoretical exercise, which of course from the sense of algebraic and analytic methods used in mathematical physics has its own sake of interest. However, as we emphasized above these final results for the beta functions may have also meaning as true physical observables in the model of six-derivative QG theories.

We described in greater detail the analysis of the structure of beta functions in this model. First we used arguments of energy dimensionality and the dependence of couplings on the dimensionless fundamental ratio of the theory x. Next, we tried to draw a comparison between the structure of 4-derivative gravitational Stelle theory and six-derivative theory in $d = 4$ dimensions. We showed the dependence on the parameters x is quite opposite in two cases. The case with four-derivative theory is exceptional because the model without any R term in the action (and also without the cosmological constant term) enjoys enhanced symmetry and then the quantum conformal gravity is renormalizable at the one-loop order, so then it is a special case of a sensible quantum physical theory (up to conformal anomaly problems discussed earlier). We also remark that in the cases of $x \to 0$ and $x \to \infty$ the generic six-derivative theories are badly non-renormalizable. This was the source of the problem with attempts to obtain sensible answers in these two limits. Non-renormalizability problem must show in some place in the middle or at the end of the computation to warn us that at the end we cannot trust in the final results for the beta functions in these cases. In these two cases this problem showed indeed in two different places and the logical consequences of this were strongly constraining the possible form of the rational x-dependence of these results. Thanks to these considerations we were able finally to understand whether the positive or inverse powers of the ratio x must appear in the final results for beta functions in question. Of course, we admit that this analysis is a posteriori since we first derived the results for the divergences and only later tried to understand the reasons behind these results. But eventually we were able to find a satisfactory explanation.

And there are a few of additional spin-offs of the presented argumentation. First, we can make predictions about the structure of beta functions in 8-derivative and also of other higher-derivative gravitational theories with the number of derivatives in the action which is bigger than 4 and 6 (analyzed in this paper). We conjecture that the structure should be very similar to what we have seen already in the generic case with six derivatives, so only positive powers of the corresponding fundamental ratio x of the theory, and probably only in the sector with C^2 type of UV divergences. Another good side effect is that we provide first (to our knowledge) theoretical explanation of the structure of beta functions as seen in four-derivative case of Stelle theory in $d = 4$ spacetime dimensions. It is not only that the theory with C^2 action is exceptional in $d = 4$ dimensions; we also "explained" these differences based on an extension of the theory to include higher-derivative terms like with 6-derivative and quantify to which level the theory with C^2 action is special and how this reflects on the structure of its one-loop beta functions. We remark that in Stelle gravity (or even in its subcase model with conformal symmetry based on the C^2 action), there are contributions to beta functions originating from higher perturbative loops since the super-renormalizability argument based on power counting analysis does not apply here. Our partial explanation of the structure of the one-loop beta functions in Stelle theory in $d = 4$ uses a general philosophy that to "explain" some numerical results in theoretical physics, one perhaps has to generalize the original setup and in this new extended framework looks for simplifying principles, which by reduction to some special cases show explicitly how special are these cases not only qualitatively but also quantitatively and what this reduction procedure implies on the numbers one gets as the results of the reduction. For example, one typically extend the original framework from $d = 4$ spacetime dimension fixed condition to more general situation with arbitrary d and then draw the general conclusion as a function of d based on some general simple principles. Then finally, the case of $d = 4$ is recovered as a particular value one gets when the function is evaluated for $d = 4$. And this should explain its speciality. In our case, we extended the four-derivative theory by adding terms with six derivatives and in this way we were able to study a more generic situation. This was in order to understand and explain the structure of divergences in the special reduced case of conformal gravity in $d = 4$ and of still generic four-dimensional Stelle theory. We think that this is a good theoretical explanation which sheds some light on the so far mysterious issue of the structure of beta functions. One can also see this as another advantage of why it is worth to study generalizations of higher-derivative gravitational actions to include terms with even more higher number of derivatives, like 6-derivative, 8-derivative actions, etc.

Finally, here we can comment on the issue of experimental bounds on the values of the ratio x. Since it appears in six-derivative gravitational theory the constraints on its possible values are very weak. Slightly stronger constraints apply now for the corresponding value of the ratio in four-derivative Stelle gravitational theory in $d = 4$ case. Since the main reason for higher-derivative modifications of gravity comes because of consistency of the coupled quantum theory, then one would expect that the stringent bounds would come from experimental measurement in the real domain of true quantum gravity. Of course, right now this is very, very far, if possible at all, future for experimental gravitational physics. This is all due to smallness of gravitational couplings characterized by G_N proportional inversely to the Planck mass $M_P \sim 10^{19}\,\mathrm{GeV}$. And in the quantum domain of elementary particle physics this scale is bigger than any energy scale of interactions between elementary quanta of matter. This implies that also quantum gravitational interactions are very weak in strength. Hence the only experimental/observational bounds we have on the coefficients in front of higher-derivative terms come from the classi-

cal/astrophysical domain of gravitational physics and they are still very weak. To probe the values of the coefficients in front of six-derivative terms, one would have to really perform a gravitational experiment to the increased level of accuracy between elementary particles in the full quantum domain, which is now completely unfeasible. Hence, we have to be satisfied with already existing very weak bounds, but this lets us to freely consider theoretical generic situation with arbitrary values of the ratio x since maybe only (very far) future experiments can force us theoreticians to consider some more restricted subset or interval for the values of the x ratio as consistent with observed situation in the Nature. For the moment it is reasonable to consider and explore theoretically all possible range of values for the x ratio and also both possible signs. (Only the case with $x = 0$ is excluded as a non-renormalizable theory that we have discussed before.)

In the last section of this contribution, we commented on the important issue of stability of higher-derivative theories. We touched both the classical and quantum levels, while the former should not be understood as a standalone level on which we can initially (before supposed quantization) define the classical theory of the relativistic gravitational field. We followed the philosophy that the quantum theory is more fundamental and it is a starting point to consider various limits, if it is properly quantized (in a sense that the quantum partition function is consistently defined, regardless of how we get there to its form, no matter which formal quantization procedure we have been following). One of such possible limit is the classical limit where the field expectation values are large compared to characteristic values as found in the microworld of elementary particles. And also the occupation number for bosonic states are large number (of the order of Avogadro number for example). Then we could speak about coherent states which could define well classical limit of the theory. Such procedure has to be followed in order to define HD classical gravitational theory. We emphasized that quantum theory is the basis and classical theory is the derived concept, not vice versa. On the quantum level we shortly discussed various approaches present in the literature to solve the problems with unwanted ghost-like particle states. They were classified in two groups: theories with PT-symmetric Hamiltonian and theories with Anselmi-Piva prescription instead of the Feynman prescription to take into account contributions of the poles of the ghost but without spoiling the unitarity issue. On the quantum level, we considered mainly the issue with unitarity of the scattering matrix since this seems the most problematic one. The violation of unitarity would signal the problem with conservation of the probability of quantum processes. Something that we cannot allow to happen in quantum-mechanical framework for the isolated quantum system (non-interacting with the noisy decohering and dissipative or some thermal environment). Of course, such an analysis was tailor-made for the cases of gravitational backgrounds on which we can define properly the scattering process.

In general, the scattering processes are not everything we can talk about in quantum field theories even for on-shell quantities. The analysis of some on-shell dressed Green functions may also show some problems with quantum stability of the system. Therefore, we briefly also described the results of the stability analysis, both on the classical and quantum level and to the various loop accuracy in QG models. This analysis is in principle applicable to the case of any gravitational background, more general than the one coming with the requirement of asymptotic flatness. We also mentioned that in some cases of classical field theory the analysis of classical exact solutions shows that the very special and tuned solutions are without classical instabilities and they are well-defined for any time starting with very special initial or boundary conditions. For example, here we can mention the case of so-called benign ghosts of higher-derivative gravitational theories as proposed by Smilga some time ago. This should prove to the reader that we are dealing with the theories which besides a very interesting structure of perturbative beta functions, are also amenable to solve the stability and unitarity issues in these theories, both on the quantum as well as on the classical level. With some special care we can exert control and HD gravitational theories are stable quantum-mechanically and this is what matters fundamentally.

Acknowledgements

We would like to thank I. L. Shapiro, L. Modesto and A. Pinzul for initial comments and encouragement about this work. L. R. thanks the Department of Physics of the Federal University of Juiz de Fora for kind hospitality and FAPEMIG for a technical support. Finally, we would like to express our gratitude to the organizers of the "Algebraic and analytic methods in physics" – AAMP XVIII conference for accepting our talk proposal and for creating a stimulating environment for scientific online discussions.

References

[1] B. S. DeWitt. Quantum theory of gravity. 1. The canonical theory. *Physical Review* **160**(5):1113–1148, 1967. https://doi.org/10.1103/PhysRev.160.1113.

[2] B. S. DeWitt. Quantum theory of gravity. 2. The manifestly covariant theory. *Physical Review* **162**(5):1195–1239, 1967. https://doi.org/10.1103/PhysRev.162.1195.

[3] B. S. DeWitt. Quantum theory of gravity. 3. Applications of the covariant theory. *Physical Review* **162**(5):1239–1256, 1967. https://doi.org/10.1103/PhysRev.162.1239.

[4] R. Utiyama, B. S. DeWitt. Renormalization of a classical gravitational field interacting with quantized matter fields. *Journal of Mathematical Physics* **3**(4):608–618, 1962. https://doi.org/10.1063/1.1724264.

[5] N. D. Birrell, P. C. W. Davies. *Quantum Fields in Curved Space*. Cambridge Monographs on Mathematical Physics. Cambridge Univ. Press, Cambridge, UK, 1984. ISBN 978-0-521-27858-4, 978-0-521-27858-4, https://doi.org/10.1017/CBO9780511622632.

[6] I. L. Buchbinder, S. D. Odintsov, I. L. Shapiro. *Effective action in quantum gravity*. 1992.

[7] K. S. Stelle. Renormalization of higher derivative quantum gravity. *Physical Review D* **16**(4):953–969, 1977. https://doi.org/10.1103/PhysRevD.16.953.

[8] K. S. Stelle. Classical gravity with higher derivatives. *General Relativity and Gravitation* **9**:353–371, 1978. https://doi.org/10.1007/BF00760427.

[9] H. Lü, A. Perkins, C. N. Pope, K. S. Stelle. Spherically symmetric solutions in higher-derivative gravity. *Physical Review D* **92**(12):124019, 2015. https://doi.org/10.1103/PhysRevD.92.124019.

[10] H. Lu, A. Perkins, C. N. Pope, K. S. Stelle. Black holes in higher-derivative gravity. *Physical Review Letters* **114**(17):171601, 2015. https://doi.org/10.1103/PhysRevLett.114.171601.

[11] L. Modesto. Super-renormalizable quantum gravity. *Physical Review D* **86**(4):044005, 2012. https://doi.org/10.1103/PhysRevD.86.044005.

[12] M. Asorey, J. L. Lopez, I. L. Shapiro. Some remarks on high derivative quantum gravity. *International Journal of Modern Physics A* **12**(32):5711–5734, 1997. https://doi.org/10.1142/S0217751X97002991.

[13] P. D. Mannheim. Making the case for conformal gravity. *Foundations of Physics* **42**:388–420, 2012. https://doi.org/10.1007/s10701-011-9608-6.

[14] P. D. Mannheim. Conformal invariance and the metrication of the fundamental forces. *International Journal of Modern Physics D* **25**(12):1644003, 2016. https://doi.org/10.1142/S021827181644003X.

[15] G. 't Hooft, M. J. G. Veltman. One loop divergencies in the theory of gravitation. *Annales de l' Inst H Poincare Physique Théorique A* **20**(1):69–94, 1974.

[16] S. Deser, P. van Nieuwenhuizen. One loop divergences of quantized Einstein-Maxwell fields. *Physical Review D* **10**(2):401–410, 1974. https://doi.org/10.1103/PhysRevD.10.401.

[17] M. H. Goroff, A. Sagnotti. Quantum gravity at two loops. *Physics Letters B* **160**(1-3):81–86, 1985. https://doi.org/10.1016/0370-2693(85)91470-4.

[18] M. H. Goroff, A. Sagnotti. The ultraviolet behavior of Einstein gravity. *Nuclear Physics B* **266**(3-4):709–736, 1986. https://doi.org/10.1016/0550-3213(86)90193-8.

[19] G. 't Hooft. Local conformal symmetry: the missing symmetry component for space and time, 2014. arXiv:1410.6675.

[20] G. 't Hooft. Local conformal symmetry: The missing symmetry component for space and time. *International Journal of Modern Physics D* **24**(12):1543001, 2015. https://doi.org/10.1142/S0218271815430014.

[21] G. 't Hooft. Local conformal symmetry in black holes, standard model, and quantum gravity. *International Journal of Modern Physics D* **26**(03):1730006, 2016. https://doi.org/10.1142/S0218271817300063.

[22] J. Maldacena. Einstein gravity from conformal gravity, 2011. arXiv:1105.5632.

[23] Y.-D. Li, L. Modesto, L. Rachwał. Exact solutions and spacetime singularities in nonlocal gravity. *Journal of High Energy Physics* **2015**:1–50, 2015. https://doi.org/10.1007/JHEP12(2015)173.

[24] I. L. Buchbinder, O. K. Kalashnikov, I. L. Shapiro, et al. The stability of asymptotic freedom in grand unified models coupled to R^2 gravity. *Physics Letters B* **216**(1-2):127–132, 1989. https://doi.org/10.1016/0370-2693(89)91381-6.

[25] I. L. Buchbinder, I. Shapiro. *Introduction to Quantum Field Theory with Applications to Quantum Gravity*. Oxford Graduate Texts. Oxford University Press, 2021.

[26] L. Rachwał, L. Modesto, A. Pinzul, I. L. Shapiro. Renormalization group in six-derivative quantum gravity. *Physical Review D* **104**(8):085018, 2021. https://doi.org/10.1103/PhysRevD.104.085018.

[27] A. O. Barvinsky, G. A. Vilkovisky. The generalized Schwinger-Dewitt technique in gauge theories and quantum gravity. *Physics Reports* **119**(1):1–74, 1985. https://doi.org/10.1016/0370-1573(85)90148-6.

[28] R. Mistry, A. Pinzul, L. Rachwał. Spectral action approach to higher derivative gravity. *The European Physical Journal C* **80**(3):266, 2020. https://doi.org/10.1140/epjc/s10052-020-7805-1.

[29] L. Modesto, L. Rachwal. Super-renormalizable and finite gravitational theories. *Nuclear Physics B* **889**:228–248, 2014. https://doi.org/10.1016/j.nuclphysb.2014.10.015.

[30] L. Modesto, M. Piva, L. Rachwal. Finite quantum gauge theories. *Physical Review D* **94**(2):025021, 2016. https://doi.org/10.1103/PhysRevD.94.025021.

[31] A. S. Koshelev, K. Sravan Kumar, L. Modesto, L. Rachwał. Finite quantum gravity in dS and AdS spacetimes. *Physical Review D* **98**(4):046007, 2018. https://doi.org/10.1103/PhysRevD.98.046007.

[32] L. Modesto, L. Rachwał. Nonlocal quantum gravity: A review. *International Journal of Modern Physics D* **26**(11):1730020, 2017. https://doi.org/10.1142/S0218271817300208.

[33] L. Modesto, L. Rachwał. Universally finite gravitational and gauge theories. *Nuclear Physics B* **900**:147–169, 2015. https://doi.org/10.1016/j.nuclphysb.2015.09.006.

[34] L. Modesto, L. Rachwal. Finite conformal quantum gravity and nonsingular spacetimes, 2016. arXiv:1605.04173.

[35] L. Modesto, L. Rachwał. Finite quantum gravity in four and extra dimensions. In *14th Marcel Grossmann Meeting on Recent Developments in Theoretical and Experimental General Relativity, Astrophysics, and Relativistic Field Theories*, vol. 2, pp. 1196–1203. 2017. https://doi.org/10.1142/9789813226609_0084.

[36] R. E. Kallosh, O. V. Tarasov, I. V. Tyutin. One loop finiteness of quantum gravity off mass shell. *Nuclear Physics B* **137**(1-2):145–163, 1978. https://doi.org/10.1016/0550-3213(78)90055-X.

[37] M. Y. Kalmykov. Gauge and parametrization dependencies of the one loop counterterms in the Einstein gravity. *Classical and Quantum Gravity* **12**(6):1401–1412, 1995. https://doi.org/10.1088/0264-9381/12/6/007.

[38] I. L. Shapiro, A. G. Zheksenaev. Gauge dependence in higher derivative quantum gravity and the conformal anomaly problem. *Physics Letters B* **324**(3-4):286–292, 1994. https://doi.org/10.1016/0370-2693(94)90195-3.

[39] I. A. Batalin, G. A. Vilkovisky. Quantization of gauge theories with linearly dependent generators. *Physical Review D* **28**(10):2567–2582, 1983. [Erratum: Phys.Rev.D 30, 508 (1984)], https://doi.org/10.1103/PhysRevD.28.2567.

[40] I. A. Batalin, G. A. Vilkovisky. Gauge algebra and quantization. *Physics Letters B* **102**(1):27–31, 1981. https://doi.org/10.1016/0370-2693(81)90205-7.

[41] E. S. Fradkin, A. A. Tseytlin. Renormalizable asymptotically free quantum theory of gravity. *Nuclear Physics B* **201**(3):469–491, 1982. https://doi.org/10.1016/0550-3213(82)90444-8.

[42] I. G. Avramidi, A. O. Barvinsky. Asymptotic freedom in higher derivative quantum gravity. *Physics Letters B* **159**(4-6):269–274, 1985. https://doi.org/10.1016/0370-2693(85)90248-5.

[43] L. S. Brown, J. P. Cassidy. Stress tensor trace anomaly in a gravitational metric: General theory, Maxwell field. *Physical Review D* **15**(10):2810–2829, 1977. https://doi.org/10.1103/PhysRevD.15.2810.

[44] L. Modesto, L. Rachwał, I. L. Shapiro. Renormalization group in super-renormalizable quantum gravity. *The European Physical Journal C* **78**(7):555, 2018. https://doi.org/10.1140/epjc/s10052-018-6035-2.

[45] M. Asorey, F. Falceto. On the consistency of the regularization of gauge theories by high covariant derivatives. *Physical Review D* **54**(8):5290–5301, 1996. https://doi.org/10.1103/PhysRevD.54.5290.

[46] M. Asorey, F. Falceto, L. Rachwał. Asymptotic freedom and higher derivative gauge theories. *Journal of High Energy Physics* **2021**:75, 2021. https://doi.org/10.1007/JHEP05(2021)075.

[47] Wolfram Research, Mathematica, Version 9.0, Champaign, IL (2012). https://www.wolfram.com/.

[48] A. O. Barvinsky, G. A. Vilkovisky. Covariant perturbation theory. 2: Second order in the curvature. General algorithms. *Nuclear Physics B* **333**(2):471–511, 1990. https://doi.org/10.1016/0550-3213(90)90047-H.

[49] E. S. Fradkin, A. A. Tseytlin. Conformal supergravity. *Physics Reports* **119**(4-5):233–362, 1985. https://doi.org/10.1016/0370-1573(85)90138-3.

[50] C. Bambi, L. Modesto, S. Porey, L. Rachwał. Black hole evaporation in conformal gravity. *Journal of Cosmology and Astroparticle Physics* **2017**(9):033, 2017. https://doi.org/10.1088/1475-7516/2017/09/033.

[51] C. Bambi, L. Modesto, S. Porey, L. Rachwał. Formation and evaporation of an electrically charged black hole in conformal gravity. *The European Physical Journal C* **78**(2):116, 2018. https://doi.org/10.1140/epjc/s10052-018-5608-4.

[52] P. Jizba, L. Rachwał, J. Kňap. Infrared behavior of Weyl gravity: Functional renormalization group approach. *Physical Review D* **101**(4):044050, 2020. https://doi.org/10.1103/PhysRevD.101.044050.

[53] P. Jizba, L. Rachwał, S. G. Giaccari, J. Kňap. Dark side of Weyl gravity. *Universe* **6**(8):123, 2020. https://doi.org/10.3390/universe6080123.

[54] L. Rachwał, S. Giaccari. Infrared behavior of Weyl Gravity. *Journal of Physics: Conference Series* **1956**(1):012012, 2021. https://doi.org/10.1088/1742-6596/1956/1/012012.

[55] C. Bambi, L. Modesto, L. Rachwał. Spacetime completeness of non-singular black holes in conformal gravity. *Journal of Cosmology and Astroparticle Physics* **2017**(05):003, 2017. https://doi.org/10.1088/1475-7516/2017/05/003.

[56] L. Rachwał. Conformal symmetry in field theory and in quantum gravity. *Universe* **4**(11):125, 2018. https://doi.org/10.3390/universe4110125.

[57] P. D. Mannheim. Mass generation, the cosmological constant problem, conformal symmetry, and the Higgs boson. *Progress in Particle and Nuclear Physics* **94**:125–183, 2017. https://doi.org/10.1016/j.ppnp.2017.02.001.

[58] P. D. Mannheim. *PT* symmetry, conformal symmetry, and the metrication of electromagnetism. *Foundations of Physics* **47**(9):1229–1257, 2017. https://doi.org/10.1007/s10701-016-0017-8.

[59] D. Anselmi, M. Piva. Perturbative unitarity of Lee-Wick quantum field theory. *Physical Review D* **96**(4):045009, 2017. https://doi.org/10.1103/PhysRevD.96.045009.

[60] D. Anselmi, M. Piva. A new formulation of Lee-Wick quantum field theory. *Journal of High Energy Physics* **2017**:66, 2017. https://doi.org/10.1007/JHEP06(2017)066.

[61] D. Anselmi. Fakeons and Lee-Wick models. *Journal of High Energy Physics* **2018**:141, 2018. https://doi.org/10.1007/JHEP02(2018)141.

[62] R. E. Cutkosky, P. V. Landshoff, D. I. Olive, J. C. Polkinghorne. A non-analytic $\mathcal{S}$-matrix. *Nuclear Physics B* **12**(2):281–300, 1969. https://doi.org/10.1016/0550-3213(69)90169-2.

[63] T. D. Lee, G. C. Wick. Negative metric and the unitarity of the $\mathcal{S}$-matrix. *Nuclear Physics B* **9**(2):209–243, 1969. https://doi.org/10.1016/0550-3213(69)90098-4.

[64] T. D. Lee, G. C. Wick. Finite theory of quantum electrodynamics. *Physical Review D* **2**(6):1033–1048, 1970. https://doi.org/10.1103/PhysRevD.2.1033.

[65] D. Anselmi. Fakeons, microcausality and the classical limit of quantum gravity. *Classical and Quantum Gravity* **36**(6):065010, 2019. https://doi.org/10.1088/1361-6382/ab04c8.

[66] D. Anselmi, M. Piva. Quantum gravity, fakeons and microcausality. *Journal of High Energy Physics* **11**:21, 2018. https://doi.org/10.1007/JHEP11(2018)021.

[67] L. Modesto, I. L. Shapiro. Superrenormalizable quantum gravity with complex ghosts. *Physics Letters B* **755**:279–284, 2016. https://doi.org/10.1016/j.physletb.2016.02.021.

[68] L. Modesto. Super-renormalizable or finite Lee–Wick quantum gravity. *Nuclear Physics B* **909**:584–606, 2016. https://doi.org/10.1016/j.nuclphysb.2016.06.004.

[69] C. M. Bender, P. D. Mannheim. No-ghost theorem for the fourth-order derivative Pais-Uhlenbeck oscillator model. *Physical Review Letters* **100**(11):110402, 2008. https://doi.org/10.1103/PhysRevLett.100.110402.

[70] C. M. Bender, P. D. Mannheim. Exactly solvable $\mathcal{PT}$-symmetric Hamiltonian having no Hermitian counterpart. *Physical Review D* **78**(2):025022, 2008. https://doi.org/10.1103/PhysRevD.78.025022.

[71] A. V. Smilga. Benign versus malicious ghosts in higher-derivative theories. *Nuclear Physics B* **706**(3):598–614, 2005. https://doi.org/10.1016/j.nuclphysb.2004.10.037.

[72] A. V. Smilga. Supersymmetric field theory with benign ghosts. *Journal of Physics A: Mathematical and Theoretical* **47**(5):052001, 2014. https://doi.org/10.1088/1751-8113/47/5/052001.

[73] D. Anselmi, A. Marino. Fakeons and microcausality: light cones, gravitational waves and the Hubble constant. *Classical and Quantum Gravity* **37**(9):095003, 2020. https://doi.org/10.1088/1361-6382/ab78d2.

[74] V. I. Tkach. Towards ghost-free gravity and standard model. *Modern Physics Letters A* **27**(22):1250131, 2012. https://doi.org/10.1142/S0217732312501313.

[75] M. Kaku. Strong coupling approach to the quantization of conformal gravity. *Physical Review D* **27**(12):2819–2834, 1983. https://doi.org/10.1103/PhysRevD.27.2819.

[76] E. Tomboulis. 1N expansion and renormalization in quantum gravity. *Physics Letters B* **70**(3):361–364, 1977. https://doi.org/10.1016/0370-2693(77)90678-5.

[77] E. Tomboulis. Renormalizability and asymptotic freedom in quantum gravity. *Physics Letters B* **97**(1):77–80, 1980. https://doi.org/10.1016/0370-2693(80)90550-X.

[78] E. T. Tomboulis. Unitarity in higher derivative quantum gravity. *Physical Review Letters* **52**(14):1173–1176, 1984. https://doi.org/10.1103/PhysRevLett.52.1173.

[79] F. d. O. Salles, I. L. Shapiro. Do we have unitary and (super)renormalizable quantum gravity below the Planck scale? *Physical Review D* **89**(8):084054, 2014. [Erratum: Phys.Rev.D 90, 129903 (2014)], https://doi.org/10.1103/PhysRevD.89.084054.

[80] P. Peter, F. de O. Salles, I. L. Shapiro. On the ghost-induced instability on de Sitter background. *Physical Review D* **97**(6):064044, 2018. https://doi.org/10.1103/PhysRevD.97.064044.

[81] F. de O. Salles, I. L. Shapiro. Recent progress in fighting ghosts in quantum gravity. *Universe* **4**(9):91, 2018. https://doi.org/10.3390/universe4090091.

[82] M. Christodoulou, L. Modesto. Note on reflection positivity in nonlocal gravity. *JETP Letters* **109**(5):286–291, 2019. https://doi.org/10.1134/S0021364019050011.

[83] F. Briscese, L. Modesto. Cutkosky rules and perturbative unitarity in Euclidean nonlocal quantum field theories. *Physical Review D* **99**(10):104043, 2019. https://doi.org/10.1103/PhysRevD.99.104043.

[84] J. F. Donoghue, G. Menezes. Unitarity, stability and loops of unstable ghosts. *Physical Review D* **100**(10):105006, 2019. https://doi.org/10.1103/PhysRevD.100.105006.

[85] M. Asorey, L. Rachwal, I. L. Shapiro. Unitarity issues in some higher derivative field theories. *Galaxies* **6**(1):23, 2018. https://doi.org/10.3390/galaxies6010023.

[86] F. Briscese, L. Modesto. Nonlinear stability of Minkowski spacetime in nonlocal gravity. *Journal of Cosmology and Astroparticle Physics* **2019**(07):009, 2019. https://doi.org/10.1088/1475-7516/2019/07/009.

[87] F. Briscese, G. Calcagni, L. Modesto. Nonlinear stability in nonlocal gravity. *Physical Review D* **99**(8):084041, 2019. https://doi.org/10.1103/PhysRevD.99.084041.

SWANSON HAMILTONIAN REVISITED THROUGH THE COMPLEX SCALING METHOD

MARTA REBOIRO[a,b,*], ROMINA RAMÍREZ[c,d], VIVIANO FERNÁNDEZ[c]

[a] *University of La Plata, Faculty of Exact Science, Department of Physics, 49 & 115, 1900 La Plata, Argentine*

[b] *CONICET, Institute of Physics of La Plata. 63 & diag. 113, 1900 La Plata, Argentine*

[c] *University of La Plata, Faculty of Exact Science, Department of Mathematics, 50 & 115, 1900 La Plata, Argentine*

[d] *CONICET, Institute Argentine of Mathematics. Saavedra 15 3º, C1083ACA Buenos Aires, Argentine*

[*] corresponding author: reboiro@fisica.unlp.edu.ar

ABSTRACT. In this work, we study the non-hermitian PT-symmetry Swanson Hamiltonian in the framework of the Complex Scaling Method. We show that by applying this method we can work with eigenfunctions that are square-integrable both in the PT and in the non-PT symmetry phase.

KEYWORDS: PT-symmetric Hamiltonians, Swanson model, Complex Scaling Method.

1. INTRODUCTION

The Swanson Model has been introduced in [1] as an example of a PT-symmetry hamiltonian [2–8]. Since then it has been extensively studied, allowing for several interesting extensions [9–25]. Among recent works, let us mention an extension of the Swanson model with complex parameters [23, 25], this work introduces bicoherent-state path integration as a method to quantify non-Hermitian systems. Though the Swanson model is described by quadratic operators, the underlying physics is nevertheless very rich. Depending on the region in the model parameter space, the Swanson model is similar to the hamiltonian of a parabolic barrier or the hamiltonian of a harmonic oscillator [26]. From the mathematical point of view, it is an example of a hamiltonian with eigenfunctions that do not belong to $\mathcal{L}^2(\mathbb{R})$ in some regions of the space of parameters.

Among the methods that are employed to describe the physics of resonances with complex energy, the Complex Scaling Method (CSM) [27–32] is one of the most powerful. It has been extensively used in the description of many-body resonant states and non-resonant continuum states observed in unstable nuclei [32]. In this work, we propose the use of the CSM to describe the dynamics of the Swanson model, particularly in the region of non-PT-symmetry.

The work is organized as follows. In Section 2 we describe the application of the CSM to the Swanson Hamiltonian. We establish a similarity transformation between the transformed hamiltonian and its adjoint operator. We discuss, according to the space of parameters of the model, the possibility of having square-integrable eigenfunctions. We present the mean values of some observables. In Section 3, we analyse with an example, the survival probability as a function of time for an initial coherent state. Conclusions are drawn in Section 4.

2. FORMALISM

The hamiltonian of Swanson [1] is given by

$$H = \hbar\omega \left(a^\dagger a + \frac{1}{2}\right) + \hbar\alpha\ a^2 + \hbar\beta\ {a^\dagger}^2, \qquad (1)$$

with $\omega,\ \alpha,\ \beta \in \mathbb{R}$. The hamiltonian of Eq. (1) can be written in terms of the coordinate operator, $\hat{x}$, and the momentum operator, $\hat{p}$, by implementing the following representation

$$\begin{aligned} a &= \frac{1}{\sqrt{2}}\left(\frac{\hat{x}}{b_0} + \mathbf{i}\frac{b_0}{\hbar}\hat{p}\right), \\ a^\dagger &= \frac{1}{\sqrt{2}}\left(\frac{\hat{x}}{b_0} - \mathbf{i}\frac{b_0}{\hbar}\hat{p}\right), \end{aligned} \qquad (2)$$

being b_0 the characteristic length of the non-interacting system. The hamiltonian in Eq. (1) reads

$$\begin{aligned} \mathrm{H}(\omega,\alpha,\beta) &= \frac{1}{2}\hbar(\omega+\alpha+\beta)\left(\frac{\hat{x}}{b_0}\right)^2 \\ &\quad + \frac{1}{2}\hbar(\omega-\alpha-\beta)\left(\frac{b_0\,\hat{p}}{\hbar}\right)^2 \\ &\quad + \hbar\frac{(\alpha-\beta)}{2}\left(2\,\hat{x}\frac{\mathbf{i}}{\hbar}\hat{p} + 1\right). \end{aligned} \qquad (3)$$

The adjoint hamiltonian of $\mathrm{H}(\omega,\alpha,\beta)$ is $\mathrm{H}_c = \mathrm{H}(\omega,\beta,\alpha)$.

As we showed in [26], some of the eigenfunctions of Eq. (3) do not belong to the usual Hilbert space, $\mathcal{H} = \mathcal{L}^2(\mathbb{R})$, so that we have to work in a Rigged Hilbert Space [33, 34].

An alternative approach to solve the eigenvalue problem of the hamiltonian of Eq. (1), is the use of the CSM method [27–32] . The aim of the CSM is to make a similarity transformation from the original hamiltonian to a hamiltonian which has eigenfunctions

that belong to $\mathcal{L}^2(\mathbb{R})$. In the framework of the CSM, we shall introduce the transformation operator $\hat{V}(\theta) = \mathrm{e}^{-\frac{\theta}{2\hbar}(\hat{x}\hat{p}+\hat{p}\hat{x})}$ with a real scaling parameter θ:

$$\begin{aligned} \hat{V}(\theta)\hat{x}\hat{V}^{-1}(\theta) &= \mathrm{e}^{\,\mathbf{i}\theta}\,\hat{x}, \\ \hat{V}(\theta)\hat{p}\hat{V}^{-1}(\theta) &= \mathrm{e}^{-\mathbf{i}\theta}\,\hat{p}. \end{aligned} \tag{4}$$

The hamiltonian of Eq. (3) is transformed as $\mathrm{H}(\theta) = \hat{V}(\theta)\mathrm{H}\hat{V}^{-1}(\theta)$:

$$\begin{aligned} \mathrm{H}(\theta) &= \mathrm{H}(\theta,\omega,\alpha,\beta) \\ &= \frac{1}{2}\hbar(\omega+\alpha+\beta)\left(\frac{e^{\,\mathbf{i}\theta}\,\hat{x}}{b_0}\right)^2 \\ &\quad +\frac{1}{2}\hbar(\omega-\alpha-\beta)\left(\frac{b_0\;e^{-\mathbf{i}\theta}\,\hat{p}}{\hbar}\right)^2 \\ &\quad +\hbar\frac{(\alpha-\beta)}{2}\left(2\,\hat{x}\frac{\mathbf{i}}{\hbar}\hat{p}+1\right). \end{aligned} \tag{5}$$

It is straightforward to observe that

$$\mathrm{H}^\dagger(\theta) = \mathrm{H}(-\theta,\omega,\beta,\alpha). \tag{6}$$

Notice that $\mathrm{H}(\theta)$ is not invariant under the usual PT-symmetry given by $\hat{x} \to -\hat{x}$, and $\hat{p} \to \hat{p}$, and $\mathbf{i} \to -\mathbf{i}$.

We shall introduce the following similarity transformation induced by the operator $\Upsilon(\theta) = \mathrm{e}^{-\frac{\alpha-\beta}{\omega-\alpha-\beta}\frac{\mathrm{e}^{2\mathbf{i}\theta}\mathrm{x}^2}{2\mathrm{b}_0^2}}$. It reads

$$\Upsilon(\theta)\;\mathrm{H}(\theta)\Upsilon(\theta)^{-1} = \mathfrak{h}(\theta), \tag{7}$$

where $\mathfrak{h}(\theta)$ is given by

$$\mathfrak{h}(\theta) = \frac{1}{2m}\left(\mathrm{e}^{-\mathbf{i}\theta}\hat{p}\right)^2 + \frac{1}{2}k\left(\mathrm{e}^{\mathbf{i}\theta}\hat{x}\right)^2. \tag{8}$$

We have defined [26] $k = m\,\Omega^2$ and

$$\begin{aligned} m = m(\omega,\alpha,\beta,b_0) &= \frac{\hbar}{(\omega-\alpha-\beta)b_0^2} \\ \Omega = \Omega(\omega,\alpha,\beta) &= \sqrt{\omega^2-4\alpha\beta} = |\Omega|\mathrm{e}^{\mathbf{i}\phi}. \end{aligned} \tag{9}$$

Though $\mathfrak{h}(\theta)$ is a non-hermitian operator, $\mathfrak{h}^\dagger(\theta) = \mathfrak{h}(-\theta) = V(-2\theta)\mathfrak{h}(\theta)V(-2\theta)^{-1}$. Consequently

$$\begin{aligned} \Upsilon(-\theta)^{-1}\mathrm{H}^\dagger(\theta)\Upsilon(-\theta) &= \mathfrak{h}(\theta)^*, \\ (\Upsilon(-\theta)V(-2\theta))^{-1}\mathrm{H}^\dagger(\theta)(\Upsilon(-\theta)V(-2\theta)) &= \mathfrak{h}(\theta). \end{aligned} \tag{10}$$

From Eqs. (7) and (10), it results $\mathrm{H}^\dagger(\theta)S = S\mathrm{H}(\theta)$, with $S = \Upsilon(-\theta)V(-2\theta)\Upsilon(\theta)$ [35–37].

The eigenfunctions and eigenvalues of $\mathfrak{h}(\theta)$, $\phi(\theta)$ and $E(\theta)$, are related to that of H and $\mathrm{H}^\dagger$ as follows.

Given $\mathfrak{h}(\theta)\phi(\theta,x) = E(\theta)\phi(\theta,x)$:

$$\begin{aligned} \mathrm{H} \quad \phi(\theta,x) &= \widetilde{E}(\theta) \quad \phi(\theta,x), \\ \mathrm{H}^\dagger \quad \psi(\theta,x) &= \overline{E}(\theta) \quad \psi(\theta,x), \end{aligned} \tag{11}$$

with

$$\begin{aligned} \widetilde{\phi}(\theta,x) &= \Upsilon(\theta)^{-1}\phi(\theta,x), \qquad E(\theta) = E(\theta), \\ \overline{\psi}(\theta,x) &= \Upsilon(-\theta)(\phi(\theta,x))^*, \quad E(\theta) = E(\theta)^*. \end{aligned} \tag{12}$$

Thus, the eigenfunctions of $\mathrm{H}(\theta)$ with eigenvalue $\widetilde{E}_\nu(\theta) = E_\nu(\theta)$ are given by

$$\widetilde{\phi}_\nu(\theta,x) = \mathrm{e}^{\;\frac{\alpha-\beta}{\omega-\alpha-\beta}\frac{\mathrm{e}^{2\mathbf{i}\theta}\mathrm{x}^2}{2\mathrm{b}_0^2}}\;\mathcal{N}_\nu\phi_\nu(\theta,x) \tag{13}$$

with $\mathcal{N}_\nu$ a normalization constant.

It can be shown that the eigenfunctions of $\mathrm{H}^\dagger(\theta)$ are

$$\overline{\psi}_\nu(\theta,x) = \mathrm{e}^{\;-\frac{\alpha-\beta}{\omega-\alpha-\beta}\frac{\mathrm{e}^{-2\mathbf{i}\theta}\mathrm{x}^2}{2\mathrm{b}_0^2}}\;\left(\mathcal{N}_\nu\phi_\nu(\theta,x)\right)^*, \tag{14}$$

and the corresponding eigenvalue is given by $\overline{E}_\nu(\theta) = \widetilde{E}_\nu(\theta)^*$. A similar structure for Eqs. (10)-(14) can be found in [38, 39]. Moreover, the relation between the eigenvalues, Eq. (12), is a typical feature for operators which are self-adjoint in Krein spaces [39–41].

It should be mentioned that the Hamiltonian of Eq. (5), for $\alpha = \beta = 0$ and $\omega = 1/\cos(2\theta)$, reduces to the one introduced in [23–25]. Particularly, in [25] the dynamics under the action of this hamiltonian is described for values of $\theta \in (-\pi/4, \pi/4)$. For further results, the reader is kindly referred to [23–25].

In what follows, we aim to determine the range of values of θ for which $\phi(\theta,x)$ belongs to the Hilbert space $\mathcal{L}^2(\mathbb{R})$.

2.1. Eigenfunctions and eigenvectors

For $\omega - (\alpha+\beta) \neq 0$, Eq. (8) can be also written as

$$-\frac{\mathrm{d}^2\phi(y)}{\mathrm{d}y^2} + \left(\frac{1}{4}y^2 - \epsilon\right)\;\phi(y) = 0, \tag{15}$$

with

$$\epsilon = \frac{E}{\hbar\Omega} = \frac{E}{\hbar|\Omega|}\mathrm{e}^{\mathbf{i}\phi} \tag{16}$$

and

$$y = \sqrt{2}\;|\sigma|\mathrm{e}^{\mathbf{i}(\theta+\gamma)}\,\frac{x}{b_0}, \tag{17}$$

where we have defined

$$\sigma = \left(\frac{m\Omega}{\hbar}\right)^{1/2} b_0 = \mathrm{e}^{\mathbf{i}\gamma}|\sigma|. \tag{18}$$

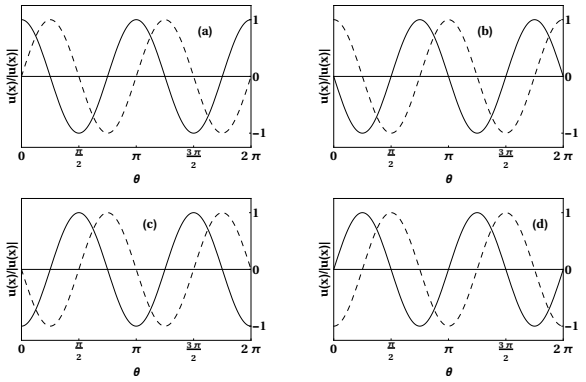

FIGURE 1. Effective potential of Eq. (19), $\frac{u(\theta,x)}{|u(\theta,x)|}$, for a fixed x in the regions determined by the signs of the parameters $m(\omega,\alpha,\beta,b_0)$ and $\Omega^2(\omega,\alpha,\beta,b_0)$. In Panel (a), $(sg(m),sg(\Omega^2))=(+,+)$, Region I. For Panel (b),$(sg(m),sg(\Omega^2))=(+,-)$, Region II. While, $(sg(m),sg(\Omega^2))=(-,+)$ in Panel (c), Region III. In Region IV $(sg(m),sg(\Omega^2))=(-,-)$, for Panel (d). The real part of the effective potential, $\mathrm{Re}\left(\frac{u(\theta,x)}{|u(\theta,x)|}\right)$, is displayed in solid lines, while the imaginary part of the effective potential, $\mathrm{Im}\left(\frac{u(\theta,x)}{|u(\theta,x)|}\right)$, is drawn with dashed lines.

Eq. (15) is the Schrödinger equation corresponding to the effective potential

$$u(\theta,x)=\frac{U(\theta,x)}{\hbar\Omega}=\mathrm{e}^{2\mathbf{i}(\theta+\gamma)}\frac{1}{2}|\sigma|^2\frac{x^2}{b_0^2}. \tag{19}$$

Solutions corresponding to Eq. (15) represent different physical systems according to the signs of $m(\omega,\alpha,\beta,b_0)$ and $\Omega^2(\omega,\alpha,\beta,b_0)$ [26]. In what follows, we shall refer to Region I when $(sg(m),sg(\Omega^2))=(+,+)$, Region II for the case $(sg(m),sg(\Omega^2))=(+,-)$, Region III for $(sg(m),sg(\Omega^2))=(-,+)$, and Region IV for $(sg(m),sg(\Omega^2))=(-,-)$, respectively.

In Figure 1 we present the behaviour of the effective potential of Eq. (19), $\frac{u(x)}{|u(x)|}$, as a function of θ, for x, $|\sigma|$ and $|\Omega|$ fixed, in the different regions of the parameter model-space. The real part of the effective potential, $\mathrm{Re}\left(\frac{u(x)}{|u(x)|}\right)$, is displayed in solid lines, while the imaginary part of the effective potential, $\mathrm{Im}\left(\frac{u(x)}{|u(x)|}\right)$, is drawn with dashed lines.

2.1.1. Discrete spectrum

For the discrete sector of the spectrum, eigenvalues and the eigenfunctions are given by

$$\begin{aligned} E_n &= \hbar\,\Omega\,[n]=\hbar\,|\Omega|\mathrm{e}^{\mathbf{i}\phi}\,[n],\\ \widetilde{\phi}_m(\theta,x) &= \mathrm{e}^{\frac{\alpha-\beta}{\omega-\alpha-\beta}\mathrm{e}^{2\mathbf{i}\theta}\frac{x^2}{2b_0^2}}\,\phi_m(\theta,x), \qquad (20)\\ \overline{\psi}_m(\theta,x) &= \mathrm{e}^{-\frac{\alpha-\beta}{\omega-\alpha-\beta}\mathrm{e}^{-2\mathbf{i}\theta}\frac{x^2}{2b_0^2}}\,(\phi_m(\theta,x))^*, \qquad (21)\end{aligned}$$

where $\phi_n(\theta,x)$ can be written as

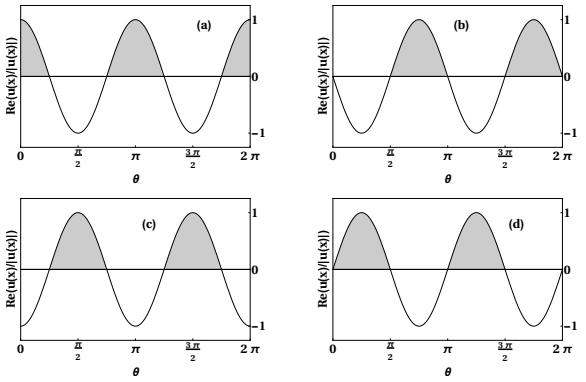

FIGURE 2. Real part of the effective potential of Eq. (19), $\frac{u(\theta,x)}{|u(\theta,x)|}$. The shadowed sectors correspond to the values of θ for which the solutions of Eq. (15) are square-integrable. In Panels (a), (b), c) and (d) we present the results for Regions I, II, III and IV, respectively.

$$\begin{aligned}\phi_n(\theta,x) &= \mathcal{N}_n\mathrm{e}^{-\mathrm{e}^{2\mathbf{i}(\theta+\gamma)}\frac{x^2}{2b_0^2}|\sigma|^2}\,H_n\left(\mathrm{e}^{\mathbf{i}(\theta+\gamma)}\,\frac{x}{b_0}|\sigma|\right).\\ \mathcal{N}_n{}^2 &= \frac{\mathrm{e}^{\mathbf{i}(\theta+\gamma)}}{\sqrt{\pi}n!2^n}\frac{|\sigma|}{b_0}, \qquad (22)\end{aligned}$$

being $H_n(z)$ the Hermite Polynomial of order n, and $[n]=n+1/2$.

Eigenfunctions $\phi_n(\theta,x)$ are square-integrable for θ-intervals where $\mathrm{Re}(u(\theta,x))$ takes positive values. In Figure 2, we plot $\mathrm{Re}(u(\theta,x)/|u(\theta,x)|)$ for every region, the gray regions correspond to the intervals for which the eigenfunctions are square integrable.

In Table (1), we summarize the sign of the parameter m and Ω^2, which characterize the different regions of the model, and for each region we present the values of phases γ and ϕ, and the interval where the eigenfunctions are square-integrable.

In Regions (I) and (III), we can define two well-defined $\theta-$domains: $I_1=[-\pi,-3\pi/4)\cup(-\pi/4,\pi/4)\cup(3\pi/4,\pi]$ and $I_2=(-3\pi/4,-\pi/4)\cup(\pi/4,3\pi/4)$. While, in Regions (II) and (IV), the θ-domains are: $I_3=(-\pi,-\pi/2)\cup(0,\pi/2)$ and $I_4=(-\pi/2,0)\cup(\pi/2,\pi)$. The intervals repeat themselves periodically, with period π.

In the domains summarized in Table 1, eigenfunctions $\{\overline{\psi}_\nu(\theta,x),\widetilde{\phi}_\nu(\theta,x)\}$ form a biorthogonal complete set.

$$\int_{-\infty}^{\infty}(\overline{\psi}_m(\theta,x))^*\widetilde{\phi}_n(\theta,x)\,\mathrm{d}x=\int_{-\infty}^{\infty}\phi_m(\theta,x)\phi_n(\theta,x)\,\mathrm{d}x=\delta_{mn}. \tag{23}$$

It should be noticed that in all regions, the $\theta-$domains of positive spectrum are different from the domains with negative spectrum. They represent different physical boundary conditions.

	sg(m)	sg(Ω^2)	γ	ϕ	I	θ_c
I	+	+	0	0	I_1	$\pm\pi/4$
			$\pi/2$	π	I_2	
III	-	+	$\pi/2$	0	I_2	
			0	π	I_1	
II	+	-	$\pi/4$	$\pi/2$	I_4	0
			$-\pi/4$	$-\pi/2$	I_3	$\pm\pi/2$
IV	-	-	$-\pi/4$	$\pi/2$	I_3	π
			$\pi/4$	$-\pi/2$	I_4	

TABLE 1. Values of the characteristic parameters for the different model-space regions. In columns 2 and 3 we give the sign of m and Ω^2, respectively. Phases γ and ϕ, for the different regions, are given in columns 4 and 5, respectively. In column 6 we present the θ-interval for which the different eigenfunctions are square-integrable. In the Table $I_1 = [-\pi, -3\pi/4) \cup (-\pi/4, \pi/4) \cup (3\pi/4, \pi]$, $I_2 = (-3\pi/4, -\pi/4) \cup (\pi/4, 3\pi/4)$, $I_3 = (-\pi, -\pi/2) \cup (0, \pi/2)$ and $I_4 = (-\pi/2, 0) \cup (\pi/2, \pi)$. In the last column, we give the values of θ_c for which the eigenfunctions of the continuous spectrum are square-integrable. The intervals repeat themselves periodically, with period π.

2.1.2. CONTINUOUS SPECTRUM

The eigenfunctions associated to the continuous spectrum [26, 42–45] are given, in terms of the eigenfunctions of $\mathfrak{h}(\theta)$ of Eq. (8), $\phi^E_\pm(\theta, x)$, by

$$\widetilde{\phi}^E_\pm(\theta, x) = \mathrm{e}^{\frac{\alpha-\beta}{\omega-\alpha-\beta}\mathrm{e}^{2\mathbf{i}\theta}\frac{x^2}{2b_0^2}}\ \phi^E_\pm(\theta, x), \quad (24)$$

$$\overline{\psi}^E_\pm(\theta, x) = \mathrm{e}^{-\frac{\alpha-\beta}{\omega-\alpha-\beta}\mathrm{e}^{-2\mathbf{i}\theta}\frac{x^2}{2b_0^2}}\ (\phi^E_\pm(\theta, x))^*, \quad (25)$$

with

$$\phi^E_\pm(\theta, x) = \mathcal{C}\ \Gamma(\nu+1) D_{-\nu-1}\left(\mp\sqrt{-2}\mathrm{e}^{\mathbf{i}(\theta+\gamma)}|\sigma|\tfrac{x}{b_0}\right). \quad (26)$$

being $D_{-\nu-1}(y)$ the parabolic cylinder functions and $\nu = \epsilon - \frac{1}{2}$. The normalization constant takes the value $\mathcal{C} = \frac{e^{\mathbf{i}\pi/8}\mathbf{i}^{\nu/2}}{\left(\frac{|\sigma|}{b_0}\mathrm{e}^{\mathbf{i}(\theta+\gamma)}\right)^{1/2}\pi 2^{3/4}}$.

The biorthogonality and the completeness relation can be written as

$$\int_{-\infty}^{\infty} (\overline{\psi}^E_\pm(\theta, x))^* \widetilde{\phi}^{E'}_\pm(\theta, x)\mathrm{dx} = \delta(E - E'),$$
$$\sum_{s=\pm}\int_{-\infty}^{\infty} (\overline{\psi}^E_s(\theta, x))^* \widetilde{\phi}^E_s(\theta, x)\mathrm{dE} = \delta(x - x'). \quad (27)$$

The possible values that the parameter θ can take to fulfill the requirements of biorthogonality and completeness of Eq. (27), θ_c, are presented in the last column of Table 1.

In the framework of the CSM, the continuous spectrum lies along the line 2θ. In Regions II and IV, the $2\theta_c = \pm\,\pi$ so that $E \in (-\infty, +\infty)$ Meanwhile, in Region I and III, $2\theta_c = \pm\,\frac{\pi}{2}$, so that E takes imaginary values. Consequently, the parameter ν associated to the order of the eigenfunctions of Eq. (26) takes the value $\nu = -\mathbf{i}|\epsilon| - \frac{1}{2}$.

If we look at the effective potential $u(\theta, x)$, the values of θ_c correspond to the values of θ for which $Re(u(\theta, x)) = 0$.

2.1.3. PARTICULAR CASES

Case (a): $\Omega = 0$.

When $\Omega = 0$ and $\omega - (\alpha + \beta) \neq 0$, the problem reduces to that of a free particle of energy $E = \varepsilon\ \mathrm{e}^{-2\mathbf{i}\theta}$. Eq. (8) reduces to

$$-\frac{\hbar^2}{2m\ \mathrm{e}^{2\mathbf{i}\theta}}\frac{\mathrm{d}^2 f(x)}{\mathrm{d}x^2} = E\ f(x), \quad (28)$$

the wave function can be written as $f(x) = A\mathrm{e}^{ikx} + A\mathrm{e}^{-ikx}$, with $k = \sqrt{\frac{2\varepsilon}{\hbar(\omega-\alpha-\beta)b_0^2}}$.

Case (b): $\omega - (\alpha + \beta) = 0,\ \alpha \neq \beta$.

To study this case we have to look at Eq. (5). If $\omega - (\alpha + \beta) = 0$, it reads

$$H(\theta) = \hbar(\alpha+\beta)\left(\frac{\mathrm{e}^{\ \mathbf{i}\theta}\ \hat{x}}{b_0}\right)^2 + \hbar\frac{(\alpha-\beta)}{2}\left(2\ \hat{x}\frac{\mathbf{i}}{\hbar}\hat{p} + 1\right), \quad (29)$$

$$f(x) = \mathrm{e}^{-\mathrm{e}^{2\mathbf{i}\theta}\frac{\hat{x}^2}{4b_0^2}\frac{\alpha+\beta}{\alpha-\beta}} x^{-\frac{1}{2}+\frac{\varepsilon\mathrm{e}^{-2\mathbf{i}\theta}}{\hbar(\alpha-\beta)}}. \quad (30)$$

In Table 2 we present the values of E for which the wavefunction $f(x)$ is square-integrable.

$(\alpha+\beta)/(\alpha-\beta)$	$(\alpha-\beta)$	$\cos(2\theta)$	ε
+	+	I_1	$\frac{\varepsilon\lvert\cos(2\theta)\rvert}{\hbar\lvert\alpha-\beta\rvert} < \frac{1}{2}$
-	-	I_2	
+	-	I_1	$\frac{\varepsilon\lvert\cos(2\theta)\rvert}{\hbar\lvert\alpha-\beta\rvert} > \frac{1}{2}$
-	+	I_2	

TABLE 2. Regions for which the wave function of Eq. (30) is square-integrable.

2.2. MEAN VALUES OF OBSERVABLES

To compute the mean values, we use operators $\hat{P}$ and $\hat{X}$ defined as [19, 46, 47]

$$\hat{P} = \Upsilon^{-1}V(\theta+\gamma)\hat{p}V(\theta+\gamma)^{-1}\Upsilon = \mathrm{e}^{-\mathbf{i}(\theta+\gamma)}\hat{p} + \mathbf{i}\hbar\mathrm{e}^{\mathbf{i}(\theta+\gamma)}\frac{\alpha-\beta}{(\omega-\alpha-\beta)b_0^2}\hat{x},$$
$$\hat{X} = \Upsilon^{-1}V(\theta+\gamma)\hat{x}V(\theta+\gamma)^{-1}\Upsilon = \mathrm{e}^{\mathbf{i}(\theta+\gamma)}\hat{x}, \quad (31)$$

that satisfy

$$[\hat{X},\hat{P}] = \mathbf{i}\hbar. \tag{32}$$

For the discrete spectrum of H, it can be proved that

$$\begin{aligned}
\langle m|\hat{P}|n\rangle &= \int_{-\infty}^{\infty} (\overline{\psi}_m(\theta,x))^*\ \hat{P}\ \widetilde{\phi}_n(\theta,x)\mathrm{dx} \\
&= \int_{-\infty}^{\infty} \phi_m(\theta,x)\ \mathrm{e}^{-\mathbf{i}(\theta+\gamma)\hat{p}}\ \phi_n(\theta,x)\mathrm{dx} \\
&= \frac{\mathbf{i}\hbar}{\sqrt{2}b_{0r}}\left(\sqrt{n+1}\delta_{m,n+1} - \sqrt{n}\delta_{m,n-1}\right), \\
\langle m|\hat{P}^2|n\rangle &= \int_{-\infty}^{\infty} (\overline{\psi}_m(\theta,x))^*\ \hat{P}^2\ \widetilde{\phi}_n(\theta,x)\mathrm{dx} \\
&= \int_{-\infty}^{\infty} \phi_m(\theta,x)\ \mathrm{e}^{-2\mathbf{i}(\theta+\gamma)\hat{p}^2}\ \phi_n(\theta,x)\mathrm{dx} \\
&= \frac{\mathbf{i}\hbar}{\sqrt{2}b_{0r}}\left(\sqrt{n+1}\delta_{m,n+1} - \sqrt{n}\delta_{m,n-1}\right) \\
&= -\frac{\hbar^2}{2b_{0r}^2}\Big(\sqrt{(n+2)(n+1)}\delta_{m,n+2} \\
&\qquad -(2n+1)\delta_{m,n} \\
&\qquad +\sqrt{n(n-1)}\delta_{m,n-2}\Big),
\end{aligned} \tag{33}$$

and

$$\begin{aligned}
\langle m|\hat{X}|n\rangle &= \int_{-\infty}^{\infty} (\overline{\psi}_m(\theta,x))^*\ \hat{X}\ \widetilde{\phi}_n(\theta,x)\mathrm{dx} \\
&= \int_{-\infty}^{\infty} \phi_m^{\pm}(\theta,x)\ \mathrm{e}^{\mathbf{i}(\theta+\gamma)\hat{x}}\ \phi_n^{\pm}(\theta,x)\mathrm{dx} \\
&= \frac{b_{0r}}{\sqrt{2}}\left(\sqrt{n+1}\delta_{m,n+1} + \sqrt{n}\delta_{m,n-1}\right), \\
\langle m|\hat{X}^2|n\rangle &= \int_{-\infty}^{\infty} (\overline{\psi}_m(\theta,x))^*\ \hat{X}^2\ \widetilde{\phi}_n(\theta,x)\mathrm{dx} \\
&= \int_{-\infty}^{\infty} \phi_m(\theta,x)\ \mathrm{e}^{2\mathbf{i}(\theta+\gamma)\hat{x}^2}\ \phi_n(\theta,x)\mathrm{dx} \\
&= \frac{b_{0r}^2}{2}\Big(\sqrt{(n+2)(n+1)}\delta_{m,n+2} \\
&\qquad +(2n+1)\delta_{m,n} \\
&\qquad +\sqrt{n(n-1)}\delta_{m,n-2}\Big),
\end{aligned} \tag{34}$$

with $b_{0r} = b_0/|\sigma|$.

2.3. Time dependent mean values

From the Schrödinger equation

$$\mathbf{i}\hbar\frac{\partial}{\partial t}\widetilde{\Phi}_n(\theta,x,t) = H(\theta)\widetilde{\Phi}_n(\theta,x,t), \tag{35}$$

it results

$$\widetilde{\Phi}_n(\theta,x,t) = \mathrm{e}^{-\mathbf{i}\widetilde{E}_n\frac{t}{\hbar}}\widetilde{\phi}_n(\theta,x). \tag{36}$$

In the same way

$$\mathbf{i}\hbar\frac{\partial}{\partial t}\overline{\Psi}_n(\theta,x,t) = H(\theta)^{\dagger}\overline{\psi}_n(\theta,x,t), \tag{37}$$

it results

$$\overline{\Psi}_n(\theta,x,t) = \mathrm{e}^{-\mathbf{i}\overline{E}_n\frac{t}{\hbar}}\overline{\psi}_n(\theta,x). \tag{38}$$

2.3.1. Reigions I and III: Real spectrum

In Regions I and III, the discrete eigenvalues of $H(\theta)$ take the values $E_n^{\pm} = \pm\hbar|\Omega|[n]$, with eigenfunctions $\widetilde{\phi}_n^{\pm}(\theta,x)$. In Region I, the eigenfunctions of the positive (negative) are square integrable in interval I_1 (I_2), see Table 1. Meanwhile, in Region III, tthe eigenfunctions of the positive (negative) are square integrable in interval I_2 (I_1). Consequently the time evolution of the states is given by

$$\begin{aligned}
\widetilde{\Phi}_n^{\pm}(\theta,x,t) &= \mathrm{e}^{-\mathbf{i}\frac{\widetilde{E}_n t}{\hbar}}\widetilde{\phi}_n(\theta,x), \\
&= \mathrm{e}^{\mp\mathbf{i}(n+\frac{1}{2})|\Omega|t}\widetilde{\phi}_n^{\pm}(\theta,x). \\
\overline{\Psi}_n^{\pm}(\theta,x,t) &= \mathrm{e}^{-\mathbf{i}\frac{\overline{E}_n t}{\hbar}}\overline{\psi}_n(\theta,x), \\
&= \mathrm{e}^{\mp\mathbf{i}(n+\frac{1}{2})|\Omega|t}\overline{\psi}_n^{\pm}(\theta,x),
\end{aligned} \tag{39}$$

and then

$$\langle m|\hat{O}|n\rangle = \mathrm{e}^{\mp\mathbf{i}(n-m)|\Omega|t}\int_{-\infty}^{\infty} (\overline{\psi}_m^{\pm}(\theta,x))^*\hat{O}\widetilde{\phi}_n^{\pm}(\theta,x)\mathrm{dx}. \tag{40}$$

2.3.2. Region II and IV: Complex spectrum

In Regions II and IV, the discrete eigenvalues of $H(\theta)$ take the values $E_n^{\pm} = \pm\mathbf{i}\hbar|\Omega|[n]$, with eigenfunctions $\widetilde{\phi}_n^{\pm}(\theta,x)$. In Region II, the eigenfunctions of the positive (negative) are square integrable in interval I_4 (I_3). Meanwhile, in Region III, the eigenfunctions of the positive (negative) are square integrable in interval I_3 (I_4). So that the time evolution of the eigenfunctions are given by

$$\begin{aligned}
\widetilde{\Phi}_n^{\pm}(\theta,x,t) &= \mathrm{e}^{-\mathbf{i}\frac{E_n t}{\hbar}}\widetilde{\phi}_n^{\pm}(\theta,x), \\
&= \mathrm{e}^{\pm(n+\frac{1}{2})|\Omega|t}\widetilde{\phi}_n(\theta,x).
\end{aligned} \tag{41}$$

and

$$\begin{aligned}
\overline{\Psi}_n^{\pm}(\theta,x,t) &= \mathrm{e}^{-\mathbf{i}\frac{E_n^* t}{\hbar}}\overline{\psi}_n(\theta,x), \\
&= \mathrm{e}^{\mp(n+\frac{1}{2})|\Omega|t}\overline{\psi}_n^{\pm}(\theta,x).
\end{aligned} \tag{42}$$

As a result

$$\langle m|\hat{O}|n\rangle = \mathrm{e}^{\pm(n-m)|\Omega|t}\int_{-\infty}^{\infty} (\overline{\psi}_m^{\pm}(\theta,x))^*\hat{O}\widetilde{\phi}_n^{\pm}(\theta,x)\mathrm{dx}. \tag{43}$$

3. Results and discussion

In order to evaluate the benefits of the present approach, let us consider the time evolution of a given initial state when the parameters of the model correspond to Region II.

In [26] we have analysed the Swanson model by solving its eigenvalue problem in the Rigged Hilbert Space. We have found that in Region II the hamiltonian was similar to the one of a particle in a parabolic barrier. In the framework of the CSM, we model the effective interaction by a complex potential. This fact resembles the spirit of the Optical Potential in Nuclear Physics [48, 49], as the potential seen by an incident nucleon on a nucleus is modeled by a complex effective potential accounting for the loss of flux due to the interaction of an incident particle with the nucleons of the nucleus.

We shall consider the solutions with eigenvalues $E_n = -\mathbf{i}\hbar|\Omega|(n+1/2)$, which evolve in time as $\mathrm{e}^{-|\Omega|(n+1/2)t}$. They correspond to the boundary problem for $0 < t < \infty$. In this case $\gamma = -\pi/4$ and $\theta \in I_3$.

For simplicity, let us assume that the initial state is a coherent state of the form

$$\phi_I(z,\theta,x) = \mathrm{e}^{-|z|^2/2} \sum_{k=0}^{\infty} \frac{z^k}{\sqrt{k!}} \phi_k(\theta,x), \qquad (44)$$

where $\widetilde{\phi}_k(\theta,x)$ is the k-eigenfunction of $\mathrm{H}(\theta)$. The survival probability of the state can be computed as

$$\begin{aligned} p(t) &= \left| \int_{-\infty}^{\infty} (\overline{\psi}_I(z,\theta,x))^* \mathrm{e}^{-\mathbf{i}\mathrm{H}(\theta)\mathrm{t}/\hbar} \phi_{\mathrm{I}}(\mathrm{z},\theta,\mathrm{x})\mathrm{dx} \right|^2 \\ &= \left| \mathrm{e}^{-|z|^2-|\Omega|t/2} \sum_{k=0}^{\infty} \frac{(|z|^2 \mathrm{e}^{-|\Omega|\mathrm{t}})^{\mathrm{k}}}{k!} \right|^2 \\ &= \mathrm{e}^{-|\Omega|t+2|z|^2(\mathrm{e}^{-|\Omega|\mathrm{t}}-1)}. \qquad (45) \end{aligned}$$

Notice that, in this particular case, $p(t)$ is independent of the parameter θ.

4. Conclusions

In this work we analyse the advantages of the CSM for describing the dynamics of a non-hermitian system when the eigenfunctions of the problem do not belong to $\mathcal{L}^2(\mathbb{R})$. We have shown that we can cast the original problem into a complex potential, which includes absorption and dissipation effects according to the sign of its imaginary component. We have shown that for a range of values of θ in the different regions of the model, the resulting eigenfunctions are square-integrable. This feature facilitates the study of the dynamics of the system from the computational point of view. The price we have to pay is the lack of PT-symmetry invariance of the transformed hamiltonian.

Work is in progress concerning the application of the CSM to a more involved problem as the one presented in [50].

Acknowledgements

This work was partially supported by the National Research Council of Argentine (CONICET) (PIP 0616) and by the Agencia Nacional de Promoción Científica (ANPCYT) of Argentina.

References

[1] M. S. Swanson. Transition elements for a non-Hermitian quadratic Hamiltonian. *Journal of Mathematical Physics* **45**(2):585–601, 2004. https://doi.org/10.1063/1.1640796.

[2] C. M. Bender, S. Boettcher. Real spectra in non-Hermitian Hamiltonians having $\mathcal{PT}$ symmetry. *Physical Review Letters* **80**(24):5243–5246, 1998. https://doi.org/10.1103/PhysRevLett.80.5243.

[3] C. M. Bender, M. V. Berry, A. Mandilara. Generalized PT symmetry and real spectra. *Journal of Physics A: Mathematical and General* **35**(31):L467–L471, 2002. https://doi.org/10.1088/0305-4470/35/31/101.

[4] C. Bender, B. Berntson, D. Parker, E. Samuel. Observation of $\mathcal{PT}$ phase transition in a simple mechanical system. *American Journal of Physics* **81**(3):173–179, 2013. https://doi.org/10.1119/1.4789549.

[5] C. M. Bender, M. Gianfreda, Ş. K. Özdemir, et al. Twofold transition in $\mathcal{PT}$-symmetric coupled oscillators. *Physical Review A* **88**(6):062111, 2013. https://doi.org/10.1103/PhysRevA.88.062111.

[6] A. Beygi, S. P. Klevansky, C. M. Bender. Coupled oscillator systems having partial $\mathcal{PT}$ symmetry. *Physical Review A* **91**(6):062101, 2015. https://doi.org/10.1103/PhysRevA.91.062101.

[7] Z. Wen, C. M. Bender. $\mathcal{PT}$-symmetric potentials having continuous spectra. *Journal of Physics A: Mathematical and Theoretical* **53**(37):375302, 2020. https://doi.org/10.1088/1751-8121/aba468.

[8] C. M. Bender, H. F. Jones. Interactions of Hermitian and non-Hermitian Hamiltonians. *Journal of Physics A: Mathematical and Theoretical* **41**(24):244006, 2008. https://doi.org/10.1088/1751-8113/41/24/244006.

[9] A. Sinha, R. Roychoudhury. Isospectral partners of a complex PT-invariant potential. *Physics Letters A* **301**(3-4):163–172, 2002. https://doi.org/10.1016/S0375-9601(02)00736-3.

[10] A. Sinha, P. Roy. Generalized Swanson models and their solutions. *Journal of Physics A: Mathematical and Theoretical* **40**(34):10599–10610, 2007. https://doi.org/10.1088/1751-8113/40/34/015.

[11] A. Sinha, P. Roy. Pseudo supersymmetric partners for the generalized Swanson model. *Journal of Physics A: Mathematical and Theoretical* **41**(33):335306, 2008. https://doi.org/10.1088/1751-8113/41/33/335306.

[12] H. F. Jones. On pseudo-Hermitian Hamiltonians and their Hermitian counterparts. *Journal of Physics A: Mathematical and General* **38**(8):1741–1746, 2005. https://doi.org/10.1088/0305-4470/38/8/010.

[13] Ö. Yeşiltaş. Quantum isotonic nonlinear oscillator as a Hermitian counterpart of Swanson Hamiltonian and pseudo-supersymmetry. *Journal of Physics A: Mathematical and Theoretical* **44**(30):305305, 2011. https://doi.org/10.1088/1751-8113/44/30/305305.

[14] P. E. G. Assis, A. Fring. Metrics and isospectral partners for the most generic cubic $\mathcal{PT}$-symmetric non-Hermitian Hamiltonian. *Journal of Physics A: Mathematical and Theoretical* **41**(24):244001, 2008. https://doi.org/10.1088/1751-8113/41/24/244001.

[15] B. Midya, P. P. Dube, R. Roychoudhury. Non-isospectrality of the generalized Swanson Hamiltonian and harmonic oscillator. *Journal of Physics A: Mathematical and Theoretical* **44**(6):062001, 2011. https://doi.org/10.1088/1751-8113/44/6/062001.

[16] A. Mostafazadeh. Metric operators for quasi-Hermitian Hamiltonians and symmetries of equivalent Hermitian Hamiltonians. *Journal of Physics A: Mathematical and Theoretical* **41**(24):244017, 2008. https://doi.org/10.1088/1751-8113/41/24/244017.

[17] A. Mostafazadeh. Pseudo-Hermitian representation of quantum mechanics. *International Journal of Geometric Methods in Modern Physics* **07**(07):1191–1306, 2010. https://doi.org/10.1142/S0219887810004816.

[18] M. Znojil. Complete set of inner products for a discrete $\mathcal{PT}$-symmetric square-well Hamiltonian. *Journal of Mathematical Physics* **50**(12):122105, 2009. https://doi.org/10.1063/1.3272002.

[19] B. Bagchi, A. Fring. Minimal length in quantum mechanics and non-Hermitian Hamiltonian systems. *Physics Letters A* **373**(47):4307–4310, 2009. https://doi.org/10.1016/j.physleta.2009.09.054.

[20] A. Sinha, P. Roy. Generalized Swanson model and its pseudo supersymmetric partners. In *Recent Developments in Theoretical Physics*, pp. 222–234. Indian Statistical Institute, India, 2009. https://doi.org/10.1142/9789814287333_0010.

[21] B. Bagchi, I. Marquette. New 1-step extension of the Swanson oscillator and superintegrability of its two-dimensional generalization. *Physics Letters A* **379**(26-27):1584–1588, 2015. https://doi.org/10.1016/j.physleta.2015.04.009.

[22] S. Dey, A. Fring, L. Gouba. Milne quantization for non-Hermitian systems. *Journal of Physics A: Mathematical and Theoretical* **48**(40):40FT01, 2015. https://doi.org/10.1088/1751-8113/48/40/40ft01.

[23] J. da Providência, N. Bebiano, J. P. da Providência. Non-Hermitian Hamiltonians with real spectrum in quantum mechanics. *Brazilian Journal of Physics* **41**:78–85, 2011. https://doi.org/10.1007/s13538-011-0010-9.

[24] F. Bagarello. Examples of pseudo-bosons in quantum mechanics. *Physics Letters A* **374**(37):3823–3827, 2010. https://doi.org/10.1016/j.physleta.2010.07.044.

[25] F. Bagarello, J. Feinberg. Bicoherent-state path integral quantization of a non-hermitian hamiltonian. *Annals of Physics* **422**:168313, 2020. https://doi.org/10.1016/j.aop.2020.168313.

[26] V. Fernández, R. Ramírez, M. Reboiro. Swanson Hamiltonian: non-PT-symmetry phase. *Journal of Physics A: Mathematical and Theoretical* **55**(1):015303, 2022. https://doi.org/10.1088/1751-8121/ac3a35.

[27] J. Aguilar, J. M. Combes. A class of analytic perturbations for one-body Schrödinger Hamiltonians. *Communications in Mathematical Physics* **22**:269–279, 1971. https://doi.org/10.1007/BF01877510.

[28] E. Balslev, J. M. Combes. Spectral properties of many-body Schrödinger operators with dilatation-analytic interactions. *Communications in Mathematical Physics* **22**:280–294, 1971. https://doi.org/10.1007/BF01877511.

[29] B. Simon. Quadratic form techniques and the Balslev-Combes theorem. *Communications in Mathematical Physics* **27**:1–9, 1972. https://doi.org/10.1007/BF01649654.

[30] H. Feshbach. A unified theory of nuclear reactions. II. *Annals of Physics* **19**(2):287–313, 1962. https://doi.org/10.1016/0003-4916(62)90221-X.

[31] Y. Ho. The method of complex coordinate rotation and its applications to atomic collision processes. *Physics Reports* **99**(1):1–68, 1983. https://doi.org/10.1016/0370-1573(83)90112-6.

[32] T. Myo, K. Katō. Complex scaling: Physics of unbound light nuclei and perspective. *Progress of Theoretical and Experimental Physics* **2020**(12):12A101, 2020.

[33] I. M. Gel'fand, G. Shilov. *Generalized Functions Vol. I.* Academic Press, New York and London, 1964.

[34] A. Bohm, J. D. Dollard, M. Gadella. *Dirac Kets, Gamow vectors and Gelfand Triplets.* Lecture Notes in Physics Vol. 348. Springer, 1989.

[35] A. Mostafazadeh. Pseudo-Hermiticity versus PT-symmetry. II. A complete characterization of non-Hermitian Hamiltonians with a real spectrum. *Journal of Mathematical Physics* **43**(5):2814–2816, 2002. https://doi.org/10.1063/1.1461427.

[36] F. Bagarello, J. P. Gazeau, F. H. Szafraniec, M. Znojil. *Non-selfadjoint operators in quantum physics: Mathematical Aspects.* John Wiley & Sons, USA, 2015.

[37] T. Y. Azizov, I. S. Iokhvidov. *Linear Operators in spaces with an indefinite metric.* John Wiley & Sons, USA, 1989.

[38] U. Günther, B. F. Samsonov. Naimark-dilated $\mathcal{PT}$-symmetric brachistochrone. *Physical Review Letters* **101**:230404, 2008. https://doi.org/10.1103/PhysRevLett.101.230404.

[39] U. Günther, S. Kuzhel. $\mathcal{PT}$-symmetry, Cartan decompositions, Lie triple systems and Krein space-related Clifford algebras. *Journal of Physics A: Mathematical and Theoretical* **43**(39):392002, 2010. https://doi.org/10.1088/1751-8113/43/39/392002.

[40] A. Dijksma, H. Langer. *Operator theory and ordinary differential operators.* American Mathematical Society, Providence, RI, 1996.

[41] F. S. U. Günther. IR-truncated $\mathcal{PT}$-symmetric ix^3 model and its asymptotic spectral scaling graph. arXiv:1901.08526.

[42] D. Chruściński. Quantum mechanics of damped systems. *Journal of Mathematical Physics* **44**(9):3718–3733, 2003. https://doi.org/10.1063/1.1599074.

[43] D. Chruściński. Quantum mechanics of damped systems. II. Damping and parabolic potential barrier. *Journal of Mathematical Physics* **45**(3):841–854, 2004. https://doi.org/10.1063/1.1644751.

[44] G. Marcucci, C. Conti. Irreversible evolution of a wave packet in the rigged-Hilbert-space quantum mechanics. *Physical Review A* **94**:052136, 2016. https://doi.org/10.1103/PhysRevA.94.052136.

[45] D. Bermudez, D. J. Fernández C. Factorization method and new potentials from the inverted oscillator. *Annals of Physics* **333**:290–306, 2013. https://doi.org/10.1016/j.aop.2013.02.015.

[46] S. Dey, A. Fring. Squeezed coherent states for noncommutative spaces with minimal length uncertainty relations. *Physical Review D* **86**:064038, 2012. https://doi.org/10.1103/PhysRevD.86.064038.

[47] S. Dey, A. Fring, B. Khantoul. Hermitian versus non-Hermitian representations for minimal length uncertainty relations. *Journal of Physics A: Mathematical and Theoretical* **46**(33):335304, 2013. https://doi.org/10.1088/1751-8113/46/33/335304.

[48] L. L. Foldy, D. Walecka. On the theory of the optical potential. *Annals of Physics* **54**(2):403, 1969. https://doi.org/10.1016/0003-4916(69)90161-4.

[49] J. Rotureau, P. Danielewicz, G. Hagen, et al. Optical potential from first principles. *Physical Review C* **95**:024315, 2017. https://doi.org/10.1103/PhysRevC.95.024315.

[50] R. Ramírez, M. Reboiro. Squeezed states from a quantum deformed oscillator Hamiltonian. *Physics Letters A* **380**(11-12):1117–1124, 2016. https://doi.org/10.1016/j.physleta.2016.01.027.

ON GENERALIZED HEUN EQUATION WITH SOME MATHEMATICAL PROPERTIES

Nasser Saad

University of Prince Edward Island, Department of Mathematics and Statistics, 550 University Avenue, Charlottetown, PEI, Canada C1A 4P3.

correspondence: nsaad@upei.ca

Abstract. We study the analytic solutions of the generalized Heun equation, $\left(\alpha_0+\alpha_1\,r+\alpha_2\,r^2+\alpha_3\,r^3\right)y''+\left(\beta_0+\beta_1\,r+\beta_2\,r^2\right)y'+\left(\varepsilon_0+\varepsilon_1\,r\right)y=0$, where $|\alpha_3|+|\beta_2|\neq 0$, and $\{\alpha_i\}_{i=0}^{3}$, $\{\beta_i\}_{i=0}^{2}$, $\{\varepsilon_i\}_{i=0}^{1}$ are real parameters. The existence conditions for the polynomial solutions are given. A simple procedure based on a recurrence relation is introduced to evaluate these polynomial solutions explicitly. For $\alpha_0=0$, $\alpha_1\neq 0$, we prove that the polynomial solutions of the corresponding differential equation are sources of finite sequences of orthogonal polynomials. Several mathematical properties, such as the recurrence relation, Christoffel-Darboux formulas and the norms of these polynomials, are discussed. We shall also show that they exhibit a factorization property that permits the construction of other infinite sequences of orthogonal polynomials.

Keywords: Heun equation, confluent forms of Heun's equation, polynomial solutions, sequences of orthogonal polynomials.

1. Introduction

It seems as a simple question to ask: *Under what conditions does the differential equation*

$$\pi_3(r)\,y''+\pi_2(r)\,y'+\pi_1(r)\,y=(\lambda_n+\mu_n\pi_0(r))\,y,$$

where λ_n and μ_n are constants and $\pi_j(r), j=0,1,2,3$ are polynomials of unknown degree to be found, has n-degree monic polynomial solutions $y_n=\sum_{k=0}^{n}c_k\,r^k$, $c_0\neq 0$, $c_k=1$?

A simple approach to deduce the possible degrees of $\pi_j, j=0,1,2,3$, is to examine the degrees for the (possible) polynomial solutions y_n:

For $n=0$, $y_0(r)=1$, we must have $\pi_1(r)=\lambda_0+\mu_0\pi_0(r)$ and the degree of the polynomial $\pi_1(r)$ must have the same degree as that of $\pi_0(r)$, so we may combine the same degree polynomial coefficients of y and write the equation as

$$\pi_3(r)y''+\pi_2(r)y'+\pi_1(r)y=0.$$

Next, for a polynomial solution of degree one, say $y_1(r)=r+\alpha$, the differential equation reduces to

$$\pi_2(r)+\pi_1(r)(r+\alpha)=0$$

and the degree of π_2 should be the degree of $\pi_1(r)$ plus one.

Similarly, for a second-order polynomial solution, say $y(r)=r^2+\alpha\,r+\beta$, it follows by substitution that

$$\pi_3(r)+\pi_2(r)(2r+\alpha)+\pi_1(r)(r^2+\alpha r+\beta)=0$$

which indicates that the degree of $\pi_3(r)$ should be the degree of π_2 plus one, which, in turn, is a polynomial of π_1 degree plus one.

This simple argument shows that for the polynomial solutions of the linear second-order differential equation with polynomial coefficients, the degree of the polynomial coefficients $\pi_j(r), j=3,2,1$ must be of degree n, $n-1$

and $n-2$, respectively. So, without the loss of generality, we may direct out attention to the following: *Under what conditions on the equation parameters α_k, β_k, and ε_k, for $k = 0, 1, \ldots, n$, does the differential equation*

$$\left(\sum_{k=0}^{n} \alpha_k\, r^k\right) y''(r) + \left(\sum_{k=0}^{n-1} \beta_k\, r^k\right) y'(r) + \left(\sum_{k=0}^{n-2} \varepsilon_k\, r^k\right) y(r) = 0,\ n \geq 2 \tag{1}$$

has polynomial solutions $y = \sum_{k=0}^{m} \mathcal{C}_j r^j$?

A logical approach is to examine the differential equation using the series solution

$$\begin{cases} y = \sum\limits_{j=0}^{\infty} \mathcal{C}_j\, r^j, \\ y' = \sum\limits_{j=0}^{\infty} j\, \mathcal{C}_j\, r^{j-1}, \\ y'' = \sum\limits_{j=0}^{\infty} j\,(j-1) \mathcal{C}_j\, r^{j-2} \end{cases}$$

in (1) and enforce the coefficients $\mathcal{C}_j = 0$ for all $j \geq m+1,\ m = 0, 1, 2, \cdots$ to find the condition so that $\mathcal{C}_m \neq 0$. This approach leads to a conclusion that for equation (1) to have m degree polynomial solution, it is necessary that

$$\varepsilon_{n-2} = -m\,(m-1)\,\alpha_n - m\,\beta_{n-1},\ n = 2, 3, \cdots . \tag{2}$$

Did this answer the question? Indeed, no. Consider, for example, this simple equation

$$r^3 y'' + 2\, r^2 y' + (-2\, r + 5) y = 0.$$

Clearly, the necessary condition (2) is satisfied for $m = 1$ and one expects the existence of a first degree polynomial solution, say $y = r + b$, for an arbitrary value of $b \in \mathbb{R}$, however, $2\, r^2 + (-2r + 5)(r + b) \neq 0$ for any real value of b.

Therefore, for $n \geq 3$, the condition (2) is *necessary* but not *sufficient* for the existence of polynomial solutions of the differential equation (1).

Note, for $n = 2$, equation (1) is the classical hypergeometric-type differential equation [1–4]

$$(\alpha_2\, r^2 + \alpha_1\, r + \alpha_0)\, y'' + (\beta_1\, r + \beta_0)\, y' + \varepsilon_0\, y = 0 \tag{3}$$

with the necessary and sufficient condition [2] for the polynomial solutions

$$\varepsilon_0 = -m\,(m-1)\,\alpha_2 - m\,\beta_1,\ m = 0, 1, 2, \cdots .$$

For $n = 3$, the differential equation (1) assumes the form

$$\begin{gathered} p_3(r)\, y'' + p_2(r)\, y' + p_1(r)\, y = 0, \\ \begin{cases} p_3(r) = \sum\limits_{j=0}^{3} \alpha_j r^j, \\ p_2(r) = \sum\limits_{j=0}^{2} \beta_j\, r^j, \\ p_1(r) = \sum\limits_{j=0}^{1} \varepsilon_j r^j, \qquad \alpha_j, \beta_j, \varepsilon_j \in \mathbb{R}\,, \end{cases} \end{gathered} \tag{4}$$

which includes as a special case or with elementary substitutions, the classical Heun differential equation [5, 6]

$$y'' + \left(\frac{\gamma}{r} + \frac{\delta}{r-1} + \frac{\varepsilon}{r-a}\right) y' + \frac{\alpha\,\beta\, r - q}{r(r-1)(r-a)}\, y = 0, \tag{5}$$

subject to the regularity (at infinity) condition

$$\alpha + \beta + 1 = \gamma + \delta + \varepsilon,$$

and its four confluent forms (Confluent, Doubly-Confluent, Biconfluent and Triconfluent Heun Equations). These equations are indispensable from the point of view of a mathematical analysis [5–11] and for its valuable applications in many areas of theoretical physics [5, 6, 12–20].

In the present work

- From equation (4), we will extract the possible differential equations that can be solved using two-term recurrence formulas.
- From equation (4), we will extract all the differential equations whose series solutions can be evaluated with a three-term recurrence formula.
- For $a_0 \neq 0$, we shall devise a procedure based on the Asymptotic Iteration Method [21] to find the series and polynomial solutions of the differential equation (4).
- In the neighbordhoud of a singular point $r = 0$, i.e., with $a_0 = 0$, we will prove that the series solution can be written as
$$y(r) = \sum_{k=0}^{\infty} (-1)^k \frac{P_{k;s}(\varepsilon_0)}{\alpha_1^k \left(\frac{\beta_0}{\alpha_1} + s\right)_k (1+s)_k} r^{k+s},$$
where s is a root of the indicial equation. Also, we show that $\{P_{k;s}(\varepsilon_0)\}_{k=0}^{\infty}$ is an infinite sequence of orthogonal polynomials with several interesting properties.
- By imposing the termination conditions, we study the mathematical properties of the finite sequences of the orthogonal polynomials $\{P_{k;s}(\varepsilon_0)\}_{k=0}^{n}$ and explore the factorization property associated with these polynomials.

2. Elementary observations

The classical approach to study the analytical solutions of equation (4) relies on the nature of the singular points of the leading polynomial coefficients

$$\mathfrak{L} \equiv \alpha_0 + \alpha_1 r + \alpha_2 r^2 + \alpha_3 r^3$$

in addition to the point $r = \infty$ in the extended plane. For real coefficients and $\alpha_0 \neq 0$, the odd-degree polynomial $\mathfrak{L}$ is factored into either a product of a linear polynomial and an irreducible quadratic polynomial or a product of three linear factors.

In the first case, the polynomial $\mathfrak{L}$ can be written as

$$\mathfrak{L} = \alpha_3 (r - \xi)(r^2 + br + c)$$

where $r^2 + br + c$ is an irreducible polynomial. In this case, ξ is regular, real, singular point and ∞ is irregular for otherwise, the differential equation can be solved in terms of elementary functions according to the classical theory of ordinary differential equations. In this case, the differential equation can be written as

$$\frac{d^2y}{dr^2} + \left(\frac{\mu_1}{r-\xi} + \frac{\mu_2}{r^2+br+c}\right)\frac{dy}{dr} + \frac{\varepsilon_1 r + \varepsilon_0}{\alpha_3 (r-\xi)(r^2 + b\, r + c)} y = 0. \tag{6}$$

The second case, the polynomial $\mathfrak{L}$ can be written as

$$\mathfrak{L} = \alpha_3 (r - \xi_1)(r - \xi_2)(r - \xi_3)$$

where $\xi_j, j = 1, 2, 3$ and ∞ are all regular singular points, i.e., the differential equation of Fushsian type,

$$\frac{d^2y}{dr^2} + \left(\sum_{j=1}^{3} \frac{\mu_j}{r-\xi_j}\right)\frac{dy}{dr} + \frac{\varepsilon_1 r + \varepsilon_0}{\alpha_3 (r-\xi_1)(r-\xi_2)(r-\xi_3)} y = 0. \tag{7}$$

where μ_j are constants depending on the differential equation parameters. One can then study the series solutions of equations (6) and (7) using the classical Frobenius method.

Another approach, recently adopted, to study (4), depends on the possible combination of the parameters $\alpha_j, j = 0, 1, 2, 3$ such that the polynomial $\mathfrak{L}$ does not vanish identically. There are fifteen possible combinations in total. These fifteen combinations can be classified into two main classes: the first class is characterized by $\alpha_0 \neq 0$, which has eight equations in total, the second class characterized by $\alpha_0 = 0$ includes the remaining seven equations. Each of these two classes will be studied in the next sections. First, we consider some elementary observations regarding the differential equation (4).

We assume no common factor among the polynomial coefficients $p_j(r),\ j=1,2,3$, we start our study of equation (4) by asking the following simple question: *Under what conditions the series solutions of the differential equation (4) can be evaluated using a two-term recurrence relation [22]?* For, in this case, the two linearly independent series solutions can be found explicitly.

Theorem 2.1. *The necessary and sufficient conditions for the linear differential equation*

$$p_2(r)\,u''(r)+p_1(r)\,u'(r)+p_0(r)\,u(r)=0, \tag{8}$$

to have a two-term recurrence relationship that relates the successive coefficients in its series solution is that in the neighbourhood of the singular regular point r_0 (where $p_2(r_0)=0$), the equation (8) can be written as:

$$\underbrace{[q_{2,0}+q_{2,h}\,(r-r_0)^h]}_{q_2(r)}\,(r-r_0)^{2-m}\,u''(r)+\underbrace{[q_{1,0}+q_{1,h}\,(r-r_0)^h]}_{q_1(r)}\,r^{1-m}\,u'(r)$$
$$+\underbrace{[q_{0,0}+q_{0,h}\,(r-r_0)^h]}_{q_0(r)}\,(r-r_0)^{-m}\,u(r)=0, \tag{9}$$

where, for $m\in\mathbb{Z}$, $h\in\mathbb{Z}^+$, $j=0,1,2$,

$$q_j(r)\equiv\sum_{k=0}^{\infty}q_{j,k}(r-r_0)^k=p_j(r)\,(r-r_0)^{m-j}, \tag{10}$$

when at least one of $q_{j,0}, j=0,1,2$ and $q_{j,h}, j=0,1,2$, is different from zero. In this case, the two-term recurrence formula is given by

$$\frac{c_k}{c_{k-h}}=-\frac{(k+\lambda-h)[q_{2,h}\,(k+\lambda-h-1)+q_{1,h}\,]+q_{0,h}}{(k+\lambda)[q_{2,0}\,(k+\lambda-1)+q_{1,0}]+q_{0,0}}, \tag{11}$$

where $c_0\neq 0$, and $\lambda=\lambda_1,\lambda_2$ are the roots of the indicial equation

$$q_{2,0}\,\lambda\,(\lambda-1)+q_{1,0}\,\lambda+q_{0,0}=0. \tag{12}$$

The closed form of the series solution generated by (11) can be written in terms of the generalized hypergeometric function as

$$\begin{aligned}u(r;\lambda)=&z^{\lambda}\sum_{k=0}^{\infty}c_{hk}r^{hk}=r^{\lambda}{}_3F_2\Big(1,\,\tfrac{2\lambda-1}{2h}+\tfrac{q_{1,h}}{2\,h\,q_{2,h}}-\tfrac{\sqrt{(q_{1,h}-q_{2,h})^2-4q_{0,h}q_{2,h}}}{2\,h\,q_{2,h}},\\ &\tfrac{2\lambda-1}{2h}+\tfrac{q_{1,h}}{2\,h\,q_{2,h}}+\tfrac{\sqrt{(q_{1,h}-q_{2,h})^2-4q_{0,h}q_{2,h}}}{2\,h\,q_{2,h}};1+\tfrac{2\lambda-1}{2\,h}+\tfrac{q_{1,0}}{2\,h\,q_{2,0}}-\tfrac{\sqrt{(q_{1,0}-q_{2,h})^2-4q_{0,0}q_{2,0}}}{2\,h\,q_{2,0}},\\ &1+\tfrac{2\lambda-1}{2h}+\tfrac{q_{1,0}}{2\,h\,q_{2,0}}+\tfrac{\sqrt{(q_{1,0}-q_{2,h})^2-4q_{0,0}q_{2,0}}}{2\,h\,q_{2,0}};-\tfrac{q_{2,h}}{q_{2,0}}\,r^h\Big).\end{aligned} \tag{13}$$

Applying this theorem, equation (4) generates the following solvable equations:

- Differential equation:

$$r^2\,(\alpha_2+\alpha_3\,r)\,u''(r)+r\,(\beta_1\,+\beta_2\,r)\,u'(r)+(\varepsilon_0+\varepsilon_1\,r)\,u(r)=0,\quad \varepsilon_0\neq 0, \tag{14}$$

Recurrence relation: For $k=1,2,\cdots$, and $c_0=1$,

$$\frac{c_k}{c_{k-1}}=-\frac{(k+\lambda-1)[\alpha_3\,(k+\lambda-2)+\beta_2]+\varepsilon_1}{(k+\lambda)[\alpha_2\,(k+\lambda-1)+\beta_1\,]+\varepsilon_0}, \tag{15}$$

where $\lambda=\lambda_+,\lambda_-$ are the roots of the indical equation

$$\alpha_2\,\lambda\,(\lambda-1)+\beta_1\,\lambda+\varepsilon_0=0,$$

namely

$$\lambda_{\pm}=\frac{\alpha_2-\beta_1\pm\sqrt{(\alpha_2-\beta_1)^2-4\alpha_2\varepsilon_0}}{2\alpha_2}.$$

The two linearly independent solutions generated by (15), in terms of the Gauss hypergeometric functions, are:

$$u_{\pm} = r^{\frac{\alpha_2-\beta_1\pm\sqrt{(\alpha_2-\beta_1)^2-4\alpha_2\varepsilon_0}}{2\alpha_2}}\,{}_2F_1\left(\frac{\beta_2}{2\alpha_3}-\frac{\beta_1}{2\alpha_2}\pm\frac{\sqrt{(\alpha_2-\beta_1)^2-4\alpha_2\varepsilon_0}}{2\alpha_2}-\frac{\sqrt{(\alpha_3-\beta_2)^2-4\alpha_3\varepsilon_1}}{2\alpha_3},\right.$$
$$\left.\frac{\beta_2}{2\alpha_3}-\frac{\beta_1}{2\alpha_2}\pm\frac{\sqrt{(\alpha_2-\beta_1)^2-4\alpha_2\varepsilon_0}}{2\alpha_2}+\frac{\sqrt{(\alpha_3-\beta_2)^2-4\alpha_3 c_1}}{2\alpha_3};\frac{\alpha_2\pm\sqrt{(\alpha_2-\beta_1)^2-4\alpha_2\varepsilon_0}}{\alpha_2};-\frac{\alpha_3}{\alpha_2}\,r\right). \tag{16}$$

- Differential equation:

$$(\alpha_1\,r+\alpha_3\,r^3)\,u''(r)+(\beta_0\,+\beta_2\,r^2)\,u'(r)+\varepsilon_1\,r\,u(r)=0,\qquad(\beta_0\neq 0), \tag{17}$$

Recurrence relation:

$$\frac{c_k}{c_{k-2}}=-\frac{(k+\lambda-2)[\alpha_3\,(k+\lambda-3)+\beta_2]+\varepsilon_1}{(k+\lambda)[\alpha_1(k+\lambda-1)+\beta_0]},\qquad(c_0,c_1\neq 0,\ k=2,3,\cdots), \tag{18}$$

where $\lambda=\lambda_+,\lambda_-$ are the roots of the indicial equation

$$\alpha_1\,\lambda(\lambda-1)+\beta_0\,\lambda=0,$$

i.e $\lambda_+=0,\lambda_-=1-\beta_0/\alpha_1$.

The two linearly independent series solutions generated by (18) are:

$$u_+(r)={}_2F_1\left(\frac{\beta_2}{4\alpha_3}-\frac{1}{4}-\frac{\sqrt{(\alpha_3-\beta_2)^2-4\alpha_3\varepsilon_1}}{4\alpha_3},\right.$$
$$\left.\frac{\beta_2}{4\alpha_3}-\frac{1}{4}+\frac{\sqrt{(\alpha_3-\beta_2)^2-4\alpha_3\varepsilon_1}}{4\alpha_3};\frac{1}{2}+\frac{\beta_0}{2\alpha_1};-\frac{\alpha_3}{\alpha_1}r^2\right), \tag{19}$$

and

$$u_-(r)=r^{1-\frac{\beta_0}{\alpha_1}}\times\,{}_2F_1\left(\frac{1}{4}+\frac{\beta_2}{4\alpha_3}-\frac{\beta_0}{2\alpha_1}-\frac{\sqrt{(\alpha_3-\beta_2)^2-4\alpha_3\varepsilon_1}}{4\alpha_3},\right.$$
$$\left.\frac{1}{4}+\frac{\beta_2}{4\alpha_3}-\frac{\beta_0}{2\alpha_1}+\frac{\sqrt{(\alpha_3-\beta_2)^2-4\alpha_3\varepsilon_1}}{4\alpha_3};\frac{3}{2}-\frac{\beta_0}{2\alpha_1};-\frac{\alpha_3}{\alpha_1}r^2\right). \tag{20}$$

- Differential equation

$$(\alpha_0+\alpha_3\,r^3)\,u''(r)+\beta_2\,r^2\,u'(r)+\varepsilon_1 r\,u(r)=0,\ \alpha_0\neq 0, \tag{21}$$

Recurrence relation:

$$\frac{c_k}{c_{k-3}}=-\frac{(k+\lambda-3)[\alpha_3(k+\lambda-4)+\beta_2]+\varepsilon_1}{\alpha_0\,(k+\lambda)(k+\lambda-1)},\qquad(c_0\neq 0), \tag{22}$$

where $\lambda=\lambda_1,\lambda_2$ are the roots of the indicial equation $\alpha_0\,\lambda\,(\lambda-1)=0$, namely, $\lambda_1=0$, $\lambda_2=1$.

The two linearly independent series solutions are:

$$u_1(r)=\,{}_2F_1\left(-\frac{\alpha_3-\beta_2+\sqrt{(\alpha_3-\beta_2)^2-4\alpha_3\varepsilon_1}}{6\alpha_3},\ \frac{-\alpha_3+\beta_2+\sqrt{(\alpha_3-\beta_2)^2-4\alpha_3\varepsilon_1}}{6\alpha_3};\frac{2}{3};-\frac{\alpha_3}{\alpha_0}\,r^3\right), \tag{23}$$

and

$$u_2(r)=r\,{}_2F_1\left(\frac{\alpha_3+\beta_2-\sqrt{(\alpha_3-\beta_2)^2-4\alpha_3\varepsilon_1}}{6\alpha_3},\ \frac{\alpha_3+\beta_2+\sqrt{(\alpha_3-\beta_2)^2-4\alpha_3\varepsilon_1}}{6\alpha_3};\frac{4}{3};-\frac{\alpha_3}{\alpha_0}\,r^3\right). \tag{24}$$

Out of the three generic equations (14), (17) and (21), five exactly solvable differential equations (Cases 1, 4, 5, 8, and 10) of the type (4) follows and other five (Cases 2, 3, 6, 7, 9) that can be derived directly from them by taking the limits of the equation parameters. For direct use, the ten equations are listed in Table 1.

	DEs and their linearly independent solutions
1	$\alpha_2\, r^2 u'' + (\beta_1 r + \beta_2 r^2)\, u' + (\varepsilon_0 + \varepsilon_1 r)\, u = 0$ $u = r^{\frac{1}{2} - \frac{\beta_1}{2\alpha_2} + \frac{1}{2\alpha_2}\sqrt{(\alpha_2-\beta_1)^2 - 4\alpha_2\varepsilon_0}}\, {}_1F_1\left(\frac{1}{2} - \frac{\beta_1}{2\alpha_2} + \frac{\varepsilon_1}{\beta_2} + \frac{\sqrt{(\alpha_2-\beta_1)^2-4\alpha_2\varepsilon_0}}{2\alpha_2}; 1 + \frac{\sqrt{(\alpha_2-\beta_1)^2-4\alpha_2\varepsilon_0}}{\alpha_2}; -\frac{\beta_2}{\alpha_2} r\right),$ $u =$ $r^{-\frac{1}{2} + \frac{\beta_1}{2\alpha_2} - \frac{1}{2\alpha_2}\sqrt{(\alpha_2-\beta_1)^2 - 4\alpha_2\varepsilon_0}}\, {}_1F_1\left(\frac{1}{2} - \frac{\beta_1}{2\alpha_2} + \frac{\varepsilon_1}{\beta_2} - \frac{\sqrt{(\alpha_2-\beta_1)^2-4\alpha_2\varepsilon_0}}{2\alpha_2}; 1 - \frac{\sqrt{(\alpha_2-\beta_1)^2-4\alpha_2\varepsilon_0}}{\alpha_2}; -\frac{\beta_2}{\alpha_2} r\right).$
2	$\alpha_2\, r^2 u'' + \beta_1 r\, u' + (\varepsilon_0 + \varepsilon_1 r)\, u = 0$ $u = r^{\frac{1}{2} - \frac{\beta_1}{2\alpha_2} + \frac{1}{2\alpha_2}\sqrt{(\alpha_2-\beta_1)^2 - 4\alpha_2\varepsilon_0}}\, {}_0F_1\left(-; 1 + \frac{\sqrt{(\alpha_2-\beta_1)^2-4\alpha_2\varepsilon_0}}{\alpha_2}; -\frac{\varepsilon_1}{\alpha_2} r\right),$ $u = r^{-\frac{1}{2} + \frac{\beta_1}{2\alpha_2} - \frac{1}{2\alpha_2}\sqrt{(\alpha_2-\beta_1)^2 - 4\alpha_2\varepsilon_0}}\, {}_0F_1\left(-; 1 - \frac{\sqrt{(\alpha_2-\beta_1)^2-4\alpha_2\varepsilon_0}}{\alpha_2}; -\frac{\beta_2}{\alpha_2} r\right).$
3	$\alpha_2\, r^2 u'' + \beta_2 r^2 u' + (\varepsilon_0 + \varepsilon_1 r)\, u = 0$ $u = r^{\frac{1}{2} - \frac{\sqrt{\alpha_2 - 4\varepsilon_0}}{2\sqrt{\alpha_2}}}\, {}_1F_1\left(\frac{1}{2} + \frac{\varepsilon_1}{\beta_2} - \frac{\sqrt{\alpha_2-4\varepsilon_0}}{2\sqrt{\alpha_2}}; 1 - \frac{\sqrt{\alpha_2-4\varepsilon_0}}{\sqrt{\alpha_2}}; -\frac{\beta_2}{\alpha_2} r\right),$ $u = r^{\frac{1}{2} + \frac{\sqrt{\alpha_2 - 4\varepsilon_0}}{2\sqrt{\alpha_2}}}\, {}_1F_1\left(\frac{1}{2} + \frac{\varepsilon_1}{\beta_2} + \frac{\sqrt{\alpha_2-4\varepsilon_0}}{2\sqrt{\alpha_2}}; 1 + \frac{\sqrt{\alpha_2-4\varepsilon_0}}{\sqrt{\alpha_2}}; -\frac{\beta_2}{\alpha_2} r\right).$
4	$(\alpha_2\, r^2 + \alpha_3\, r^3)u'' + \beta_1\, r\, u' + (\varepsilon_0 + \varepsilon_1 r)\, u = 0$ $u = r^{\frac{1}{2} - \frac{\beta_1}{2\alpha_2} + \frac{1}{2\alpha_2}\sqrt{(\alpha_2-\beta_1)^2 - 4\alpha_2\varepsilon_0}}\, {}_2F_1\left(\frac{1}{2}\sqrt{\frac{\alpha_3-4\varepsilon_1}{\alpha_3}} - \frac{\beta_1}{2\alpha_2} + \frac{\sqrt{(\alpha_2-\beta_1)^2-4\alpha_2\varepsilon_0}}{2\alpha_2},\right.$ $\left. -\frac{1}{2}\sqrt{\frac{\alpha_3-4\varepsilon_1}{\alpha_3}} - \frac{\beta_1}{2\alpha_2} + \frac{\sqrt{(\alpha_2-\beta_1)^2-4\alpha_2\varepsilon_0}}{2\alpha_2}; 1 + \frac{\sqrt{(\alpha_2-\beta_1)^2-4\alpha_2\varepsilon_0}}{\alpha_2}; -\frac{\alpha_3}{\alpha_2} r\right),$ $u = r^{\frac{1}{2} - \frac{\beta_1}{2\alpha_2} - \frac{1}{2\alpha_2}\sqrt{(\alpha_2-\beta_1)^2 - 4\alpha_2\varepsilon_0}}\, {}_2F_1\left(\frac{1}{2}\sqrt{\frac{\alpha_3-4\varepsilon_1}{\alpha_3}} - \frac{\beta_1}{2\alpha_2} - \frac{\sqrt{(\alpha_2-\beta_1)^2-4\alpha_2\varepsilon_0}}{2\alpha_2},\right.$ $\left. -\frac{1}{2}\sqrt{\frac{\alpha_3-4\varepsilon_1}{\alpha_3}} - \frac{\beta_1}{2\alpha_2} - \frac{\sqrt{(\alpha_2-\beta_1)^2-4\alpha_2\varepsilon_0}}{2\alpha_2}; 1 - \frac{\sqrt{(\alpha_2-\beta_1)^2-4\alpha_2\varepsilon_0}}{\alpha_2}; -\frac{\alpha_3}{\alpha_2} r\right).$
5	$(\alpha_2\, r^2 + \alpha_3\, r^3)u'' + \beta_2 r^2\, u' + (\varepsilon_0 + \varepsilon_1 r)\, u = 0$ $u = r^{\frac{1}{2} - \frac{1}{2\sqrt{\alpha_2}}\sqrt{\alpha_2 - 4\varepsilon_0}}\, {}_2F_1\left(\frac{\beta_2}{2\alpha_3} - \frac{1}{2}\sqrt{\frac{\alpha_2-4\varepsilon_0}{\alpha_2}} + \frac{\sqrt{(\alpha_3-\beta_2)^2-4\alpha_3\varepsilon_1}}{2\alpha_3},\right.$ $\left. \frac{\beta_2}{2\alpha_3} - \frac{1}{2}\sqrt{\frac{\alpha_2-4\varepsilon_0}{\alpha_2}} - \frac{\sqrt{(\alpha_3-\beta_2)^2-4\alpha_3\varepsilon_1}}{2\alpha_3}; 1 - \frac{\sqrt{\alpha_2-4\varepsilon_0}}{\sqrt{\alpha_2}}; -\frac{\alpha_3}{\alpha_2} r\right),$ $u = r^{\frac{1}{2} + \frac{1}{2\sqrt{\alpha_2}}\sqrt{\alpha_2 - 4\varepsilon_0}}\, {}_2F_1\left(\frac{\beta_2}{2\alpha_3} + \frac{1}{2}\sqrt{\frac{\alpha_2-4\varepsilon_0}{\alpha_2}} - \frac{\sqrt{(\alpha_3-\beta_2)^2-4\alpha_3\varepsilon_1}}{2\alpha_3},\right.$ $\left. \frac{\beta_2}{2\alpha_3} + \frac{1}{2}\sqrt{\frac{\alpha_2-4\varepsilon_0}{\alpha_2}} + \frac{\sqrt{(\alpha_3-\beta_2)^2-4\alpha_3\varepsilon_1}}{2\alpha_3}; 1 + \frac{\sqrt{\alpha_2-4\varepsilon_0}}{\sqrt{\alpha_2}}; -\frac{\alpha_3}{\alpha_2} r\right).$
6	$(\alpha_2\, r^2 + \alpha_3\, r^3)u'' + (\varepsilon_0 + \varepsilon_1\, r)\, u = 0$ $u = r^{\frac{1}{2} - \frac{1}{2\sqrt{\alpha_2}}\sqrt{\alpha_2 - 4\varepsilon_0}}\, {}_2F_1\left(-\frac{1}{2}\sqrt{\frac{\alpha_2-4\varepsilon_0}{\alpha_2}} - \frac{\sqrt{\alpha_3-4\varepsilon_1}}{2\sqrt{\alpha_3}}, -\frac{1}{2}\sqrt{\frac{\alpha_2-4\varepsilon_0}{\alpha_2}} - \frac{\sqrt{\alpha_3-4\varepsilon_1}}{2\sqrt{\alpha_3}}; 1 - \frac{\sqrt{\alpha_2-4\varepsilon_0}}{\sqrt{\alpha_2}}; -\frac{\alpha_3}{\alpha_2} r\right),$ $u = r^{\frac{1}{2} + \frac{1}{2\sqrt{\alpha_2}}\sqrt{\alpha_2 - 4\varepsilon_0}}\, {}_2F_1\left(\frac{1}{2}\sqrt{\frac{\alpha_2-4\varepsilon_0}{\alpha_2}} - \frac{\sqrt{\alpha_3-4\varepsilon_1}}{2\sqrt{\alpha_3}}, \frac{1}{2}\sqrt{\frac{\alpha_2-4\varepsilon_0}{\alpha_2}} + \frac{\sqrt{\alpha_3-4\varepsilon_1}}{2\sqrt{\alpha_3}}; 1 + \frac{\sqrt{\alpha_2-4\varepsilon_0}}{\sqrt{\alpha_2}}; -\frac{\alpha_3}{\alpha_2} r\right).$
7	$\alpha_2\, r^2\, u'' + (\varepsilon_0 + \varepsilon_1\, r)\, u = 0$ $u = r^{\frac{1}{2} + \frac{1}{2}\sqrt{1 - \frac{4\varepsilon_0}{\alpha_2}}}\, {}_0F_1\left(; 1 + \sqrt{1 + \frac{4\varepsilon_0}{\alpha_2}}; -\frac{\varepsilon_1}{\alpha_2} r\right), \qquad u = r^{\frac{1}{2} - \frac{1}{2}\sqrt{1 - \frac{4\varepsilon_0}{\alpha_2}}}\, {}_0F_1\left(; 1 - \sqrt{1 - \frac{4\varepsilon_0}{\alpha_2}}; -\frac{\varepsilon_1}{\alpha_2} r\right)$
8	$\alpha_1\, r\, u'' + (\beta_0 + \beta_2 r^2)\, u' + \varepsilon_1\, r\, u = 0,$ $u = {}_1F_1\left(\frac{\varepsilon_1}{2\beta_2}; \frac{1}{2} + \frac{\beta_0}{2\alpha_1}; -\frac{\beta_2}{2\alpha_1} r^2\right), \qquad u = r^{1 - \frac{\beta_0}{\alpha_1}}\, {}_1F_1\left(\frac{1}{2} - \frac{\beta_0}{2\alpha_1} + \frac{\varepsilon_1}{2\beta_2}; \frac{3}{2} - \frac{\beta_0}{2\alpha_1}; -\frac{\beta_2}{2\alpha_1} r^2\right).$
9	$\alpha_1\, r\, u'' + \beta_0\, u' + \varepsilon_1\, r\, u = 0,$ $u = {}_0F_1\left(-; \frac{1}{2} + \frac{\beta_0}{2\alpha_1}; -\frac{\varepsilon_1}{4\alpha_1} z^2\right), \qquad u = r^{1 - \frac{\beta_0}{\alpha_1}}\, {}_0F_1\left(-; \frac{3}{2} - \frac{\beta_0}{2\alpha_1}; -\frac{\varepsilon_1}{4\alpha_1} r^2\right).$
10	$\alpha_0\, u'' + \beta_2\, r^2 u' + \varepsilon_1\, r\, u = 0,$ $u = {}_1F_1\left(\frac{\varepsilon_1}{3\beta_2}; \frac{2}{3}; -\frac{\beta_2}{3\alpha_0} r^3\right), \qquad u = r\, {}_1F_1\left(\frac{1}{3} + \frac{\varepsilon_1}{3\beta_2}; \frac{4}{3}; -\frac{\beta_2}{3\alpha_0} r^3\right).$

TABLE 1. Ten solvable equations of the type (4) that follows from the generic equations (14), (17), and (21).

3. The solutions in the neighbourhood of an ordinary point

3.1. Series solutions

In the case of $\alpha_0 \neq 0$, $r = 0$, there is an ordinary point for the differential equations (4). The classical theory of differential equation ensure that the (4) has two linearly independent power series solutions in the neighbourhood of $r = 0$ and valid to the nearest real singular point of the leading polynomial coefficient $\mathfrak{L} \equiv \alpha_0 + \alpha_1\, r + \alpha_2\, r^2 + \alpha_3\, r^3 = 0$. Indeed, the polynomial $\mathfrak{L} = 0$ has the discriminate [23]:

$$\Delta = 18\,\alpha_3\,\alpha_2\,\alpha_1\,\alpha_0 - 4\,\alpha_2^3\,\alpha_0 + \alpha_2^2\,\alpha_1^2 - 4\,\alpha_3\,\alpha_1^3 - 27\,\alpha_3^2\,\alpha_0^2. \tag{25}$$

The nature of the $\mathfrak{L}$ roots as given by (25) along with the corresponding eight differential equations are summarized in Table 2.

For these differential equations, the following theorem, that can be easily proved using Frobenius method, holds.

Theorem 3.1. *(Formal series solutions) In the neighbourhood of the ordinary point $r = 0$, the coefficients of the series solution $y(r) = \sum_{k=0}^{\infty} \mathcal{C}_k\, r^k$ to the differential equation (4) satisfy the four-term recurrence relation*

$$\begin{aligned}&((k-1)\,((k-2)\,\alpha_3 + \beta_2) + \varepsilon_1)\,\mathcal{C}_{k-1} + (k((k-1)\,\alpha_2 + \beta_1) + \varepsilon_0)\,\mathcal{C}_k \\ &\quad + (k+1)(k\alpha_1 + \beta_0)\,\mathcal{C}_{k+1} + (k+2)\,(k+1)\,\alpha_0\,\mathcal{C}_{k+2} = 0,\end{aligned} \tag{26}$$

where $k = 0, 1, 2, \cdots$, with $\mathcal{C}_{-1} = 0$ and arbitrary nonzero constants $\mathcal{C}_0$ and $\mathcal{C}_1$. The radius of convergence of these series solutions is extended from $r = 0$ to the nearest singular point of the leading polynomial coefficient $\mathfrak{L} = 0$.

The first few terms of the series solution are given explicitly by

$$\begin{aligned}&\mathcal{C}_2 = -\tfrac{\varepsilon_0}{2\alpha_0}\,\mathcal{C}_0 - \tfrac{\beta_0}{2\alpha_0}\,\mathcal{C}_1, \\ &\mathcal{C}_3 = \tfrac{(\alpha_1+\beta_0)\,\varepsilon_0 - \alpha_0\,\varepsilon_1}{6\alpha_0^2}\,\mathcal{C}_0 + \tfrac{\beta_0(\alpha_1+\beta_0) - \alpha_0(\beta_1+\varepsilon_0)}{6\,\alpha_0^2}\,\mathcal{C}_1, \\ &\cdots.\end{aligned}$$

For $\alpha_0 \neq 0$, using (26), we can extract the following differential equations with series solution from (4) using a three-term recurrence relation:

- Differential equation:

$$\left(\alpha_0 + \alpha_1\, r + \alpha_3\, r^3\right) u''(r) + \left(\beta_0 + \beta_2\, r^2\right) u'(r) + \varepsilon_1\, r\, u(r) = 0. \tag{27}$$

  Recurrence formula:

$$C_{k+2} = -\frac{(k+1)(k\,\alpha_1 + \beta_0)}{(k+1)\,(k+2)\,\alpha_0} C_{k+1} - \frac{(k-1)((k-2)\,\alpha_3 + \beta_2) + \varepsilon_1}{(k+1)\,(k+2)\,\alpha_0} C_{k-1}. \tag{28}$$

- Differential equation:

$$\left(\alpha_0 + \alpha_2 r^2 + \alpha_3 r^3\right)\, u''(r) + (\beta_1\, r + \beta_2\, r^2) u'(r) + \varepsilon_1\, r\, u(r) = 0. \tag{29}$$

  Recurrence formula:

$$C_{k+2} = -\frac{k(k-1)\alpha_2 + k\,\beta_1}{(k+1)\,(k+2)\,\alpha_0} C_k - \frac{(k-1)(k-2)\alpha_3 + (k-1)\beta_2 + \varepsilon_1}{(k+1)(k+2)\,\alpha_0} C_{k-1}. \tag{30}$$

- Differential equation:

$$\left(\alpha_0 + \alpha_2\, r^2\right)\, u''(r) + (\beta_1\, r + \beta_2\, r^2)\, u'(r) + \varepsilon_1\, r\, u(r) = 0. \tag{31}$$

  Recurrence formula:

$$C_{k+2} = -\frac{k\,(k-1)\alpha_2 + k\,\beta_1}{(k+1)\,(k+2)\,\alpha_0} C_k - \frac{(k-1)\beta_2 + \varepsilon_1}{(k+1)\,(k+2)\,\alpha_0} C_{k-1}. \tag{32}$$

DE	α_3	α_2	α_1	α_0	**Discriminant**	**Roots of $\mathfrak{L}$**	**Domain definition**
I					$\Delta_3 > 0$	$\xi_1 \neq \xi_2 \neq \xi_3$	$\lvert r\rvert < \min_{i=1,2,3} \xi_i$
	α_3	α_2	α_1	α_0	$\Delta_3 = 0$	$\xi_1 = \xi_2 = \xi_3 = \xi$	$\lvert r\rvert < \xi$
					$\Delta_3 < 0$	$\xi \in \mathbb{R}$	$\lvert r\rvert < \xi$
	Differential equation:				$(\alpha_0 + \alpha_1 r + \alpha_2 r^2 + \alpha_3 r^3) y'' + (\beta_0 + \beta_1 r + \beta_2 r^2) y' + (\varepsilon_0 + \varepsilon_1 r) y = 0$		
	Discriminant:				$\Delta_3 = 18\,\alpha_3\,\alpha_2\,\alpha_1\,\alpha_0 - 4\,{\alpha_2}^3\,\alpha_0 + {\alpha_2}^2{\alpha_1}^2 - 4\,\alpha_3\,{\alpha_1}^3 - 27\,{\alpha_3}^2\,{\alpha_0}^2$		
II					$\Delta_3 > 0$	$\xi_1 \neq \xi_2$	$\lvert r\rvert < \min_{i=1,2} \xi_i$
	0	α_2	α_1	α_0	$\Delta_3 = 0$	$\xi_1 = \xi_2 = \xi$	$\lvert r\rvert < \xi$
					$\Delta_3 < 0$	None	$\lvert r\rvert < \infty$
	Differential Equation:				$(\alpha_0 + \alpha_1 r + \alpha_2 r^2) y'' + (\beta_0 + \beta_1 r + \beta_2 r^2) y' + (\varepsilon_0 + \varepsilon_1 r) y = 0$		
	Discriminant:				$\Delta_3 = \alpha_2^2(-4\,\alpha_2\,\alpha_0 + {\alpha_1}^2)$		
III	0	0	α_1	α_0	$\alpha_1\alpha_0 > 0$	$r = -\alpha_0/\alpha_1$	$-\infty < r < -\alpha_0/\alpha_1$
					$\alpha_1\alpha_0 < 0$	$r = -\alpha_0/\alpha_1$	$-\alpha_0/\alpha_1 < r < \infty$
	Differential Equation:				$(\alpha_0 + \alpha_1 r) y'' + (\beta_0 + \beta_1 r + \beta_2 r^2) y' + (\varepsilon_0 + \varepsilon_1 r) y = 0$		
	Discriminant:				$\Delta_3 = 0$		
IV	0	0	0	α_0	None	None	$-\infty < r < \infty$
	Differential Equation:				$\alpha_0 y'' + (\beta_0 + \beta_1 r + \beta_2 r^2) y' + (\varepsilon_0 + \varepsilon_1 r) y = 0$		
	Discriminant:				$\Delta_3 = 0$		
V					$\Delta_3 > 0$	$\xi_1 \neq \xi_2 \neq \xi_3$	$\lvert r\rvert < \min_{i=1,2,3} \xi_i$
	α_3	0	α_1	α_0	$\Delta_3 = 0$	$\xi_1 = \xi_2 = \xi_3 = \xi$	$\lvert r\rvert < \xi$
					$\Delta_3 < 0$	$\xi \in \mathbb{R}$	$\lvert r\rvert < \xi$
	Differential Equation:				$(\alpha_0 + \alpha_1 r + \alpha_3 r^3) y'' + (\beta_0 + \beta_1 r + \beta_2 r^2) y' + (\varepsilon_0 + \varepsilon_1 r) y = 0$		
	Discriminant:				$\Delta_3 = -4\,\alpha_3\,{\alpha_1}^3 - 27\,{\alpha_3}^2\,{\alpha_0}^2$		
VI					$\Delta_3 > 0$	$\xi_1 \neq \xi_2 \neq \xi_3$	$\lvert r\rvert < \min_{i=1,2,3} \xi_i$
	α_3	α_2	0	α_0	$\Delta_3 = 0$	$\xi_1 = \xi_2 = \xi_3 = \xi$	$\lvert r\rvert < \xi$
					$\Delta_3 < 0$	$\xi \in \mathbb{R}$	$\lvert r\rvert < \xi$
	Differential Equation:				$(\alpha_0 + \alpha_2 r^2 + \alpha_3 r^3) y'' + (\beta_0 + \beta_1 r + \beta_2 r^2) y' + (\varepsilon_0 + \varepsilon_1 r) y = 0$		
	Discriminant:				$\Delta_3 = -4\,{\alpha_2}^3\,\alpha_0 - 27\,{\alpha_3}^2\,{\alpha_0}^2$		
VII	α_3	0	0	α_0	$\alpha_0\,\alpha_3 < 0$ or $\alpha_0\,\alpha_3 > 0$	$\xi = \sqrt[3]{-\alpha_0/\alpha_3}$	$\lvert r\rvert < \xi$
	Differential Equation:				$(\alpha_0 + \alpha_3 r^3) y'' + (\beta_0 + \beta_1 r + \beta_2 r^2) y' + (\varepsilon_0 + \varepsilon_1 r) y = 0$		
	Discriminant:				$\Delta_3 = -27\,{\alpha_3}^2\,{\alpha_0}^2$		
VIII	0	α_2	0	α_0	$\alpha_2\alpha_0 < 0$	$r = \pm\sqrt{-\frac{\alpha_0}{\alpha_2}}$	$-\sqrt{-\frac{\alpha_0}{\alpha_2}} < r < \sqrt{-\frac{\alpha_0}{\alpha_2}}$
					$\alpha_2\alpha_0 > 0$	None	$-\infty < r < \infty$
	Differential Equation:				$(\alpha_0 + \alpha_2 r^2) y'' + (\beta_0 + \beta_1 r + \beta_2 r^2) y' + (\varepsilon_0 + \varepsilon_1 r) y = 0$		
	Discriminant:				$\Delta_3 = -4\,{\alpha_2}^3\,\alpha_0$		

TABLE 2. Tabulating the eight different types of differential equations, which apply to Theorem 3.1.

- Differential equation:

$$\left(\alpha_0+\alpha_3\,r^3\right)u''(r)+\left(\beta_1\,r+\beta_2\,r^2\right)u'(r)+r\,\varepsilon_1\,u(r)=0. \tag{33}$$

Recurrence formula:

$$C_{k+2}=-\frac{k\,\beta_1}{(k+1)\,(k+2)\,\alpha_0}C_k-\frac{(k-1)(k-2)\alpha_3+(k-1)\beta_2+\varepsilon_1}{(k+1)\,(k+2)\,\alpha_0}C_{k-1}. \tag{34}$$

- Differential equation:

$$\alpha_0\,u''(r)+\left(\beta_1\,r+\beta_2\,r^2\right)u'(r)+\varepsilon_1\,r\,u(r)=0. \tag{35}$$

Recurrence formula:

$$C_{k+2}=-\frac{k\,\beta_1}{(k+1)\,(k+2)\,\alpha_0}C_k-\frac{(k-1)\,\beta_2+\varepsilon_1}{(k+1)\,(k+2)\,\alpha_0}C_{k-1}. \tag{36}$$

- Differential equation:

$$\left(\alpha_0+\alpha_2\,r^2+\alpha_3\,r^3\right)\,u''(r)+\beta_1\,r\,u'(r)+\varepsilon_1\,r\,u(r)=0. \tag{37}$$

Recurrence formula:

$$C_{k+2}=-\frac{k\,(k-1)\alpha_2\,+k\,\beta_1}{(k+1)\,(k+2)\,\alpha_0}C_k-\frac{(k-2)(k-1)\alpha_3+\varepsilon_1}{(k+1)\,(k+2)\,\alpha_0}C_{k-1}. \tag{38}$$

- Differential equation:

$$\left(\alpha_0+\alpha_3\,r^3\right)u''(r)+\beta_1\,r\,u'(r)+\varepsilon_1\,r\,u(r)=0. \tag{39}$$

Recurrence formula:

$$C_{k+2}=-\frac{k\,\beta_1}{(k+1)(k+2)\,\alpha_0}C_k-\frac{(k-2)\,(k-1)\,\alpha_3+\varepsilon_1}{(k+1)(k+2)\,\alpha_0}C_{k-1}. \tag{40}$$

- Differential equation:

$$\left(\alpha_0+\alpha_2\,r^2\right)u''(r)+\beta_1\,r\,u'(r)+\varepsilon_1\,r\,u(r)=0. \tag{41}$$

Recurrence formula:

$$C_{k+2}=-\frac{k(k-1)\alpha_2+k\,\beta_1}{(k+1)(k+2)\alpha_0}C_k-\frac{\varepsilon_1}{(k+1)(k+2)\,\alpha_0}C_{k-1}. \tag{42}$$

- Differential equation:

$$\left(\alpha_0+\alpha_2\,r^2\right)\,u''(r)+(\beta_1+\beta_2\,r^2)u'(r)+\varepsilon_1\,r\,u(r)=0. \tag{43}$$

Recurrence formula:

$$C_{k+2}=-\frac{k(k-1)\alpha_2+\beta_1\,k)}{(k+1)\,(k+2)\,\alpha_0}C_k-\frac{(k-1)\beta_2+\varepsilon_1}{(k+1)\,(k+2)\,\alpha_0}C_{k-1}. \tag{44}$$

- Differential equation:

$$u''(r)+\beta_1\,r\,u'(r)+\varepsilon_1\,r\,u(r)=0, \tag{45}$$

Recurrence formula:

$$C_{k+2}=-\frac{k\,\beta_1}{(k+1)\,(k+2)}\,C_k-\frac{\varepsilon_1}{(k+1)\,(k+2)}\,C_{k-1}. \tag{46}$$

3.2. Polynomial solutions

The series solution $y(r)=\sum_{k=0}^{\infty}\mathcal{C}_k\,r^k$ terminates to an n^{th}-degree polynomial if $\mathcal{C}_n\neq 0$ and $\mathcal{C}_j=0$ for all $j\geq n+1$. It is not difficult to show by direct substitution that for polynomial solutions of $\mathbf{P}_n(r)=\sum_{k=0}^{n}\mathcal{C}_k\,r^k$, it is necessary that

$$\varepsilon_1=-n\,(n-1)\,\alpha_3-n\,\beta_2,\qquad n=0,1,2,\cdots. \tag{47}$$

Furthermore, the polynomial solution coefficients $\{\mathcal{C}_k\}_{k=0}^{n}$ satisfy a four-term recurrence relation, see (26),

$$\begin{aligned}&\big((k-1)\big((k-2)\alpha_3+\beta_2\big)+\varepsilon_{1;n}\big)\,\mathcal{C}_{k-1}+\big(k\big((k-1)\alpha_2+\beta_1\big)+\varepsilon_{0;n}\big)\,\mathcal{C}_k\\&\qquad+(k+1)(k\alpha_1+\beta_0)\,\mathcal{C}_{k+1}+(k+1)(k+2)\alpha_0\,\mathcal{C}_{k+2}=0\,,\quad k=0,\,1,\,\ldots,\,n+1\,,\end{aligned}\tag{48}$$

that generates a system of $(n+2)$ linear equations in $\{\mathcal{C}_k\}_{k=0}^{n}$: $\overbrace{\underbrace{\cdots\cdots\cdots}_{n-equations}}^{(n+2)-equations}$.

The first n equations are

$$\begin{cases}k=0, & \to \varepsilon_0\mathcal{C}_0+\beta_0\mathcal{C}_1+2\,\alpha_0\,\mathcal{C}_2=0\\ k=1, & \to \varepsilon_1\mathcal{C}_0+(\beta_1+\varepsilon_0)\mathcal{C}_1+2(\alpha_1+\beta_0)\mathcal{C}_2+6\,\alpha_0\,\mathcal{C}_3=0\\ k=2, & \to (\beta_2+\varepsilon_1)\mathcal{C}_1+(2\,\alpha_2+2\,\beta_1+\varepsilon_0)\mathcal{C}_2+3(2\,\alpha_1+\beta_0)\mathcal{C}_3+12\,\alpha_0\,\mathcal{C}_4=0\\ k=3, & \to (2\alpha_3+2\,\beta_2+\varepsilon_1)\mathcal{C}_2+(6\,\alpha_2+3\,\beta_1+\varepsilon_0)\mathcal{C}_3+4(3\,\alpha_1+\beta_0)\mathcal{C}_4+20\,\alpha_0\,\mathcal{C}_5=0\\ & \qquad\vdots\\ k=n-1, & \to \big((n-2)\,\big((n-3)\,\alpha_3+\beta_2\big)+\varepsilon_{1;n}\big)\mathcal{C}_{n-2}+\big((n-1)\big((n-2)\,\alpha_2+\beta_1\big)+\varepsilon_{0;n}\big)\mathcal{C}_{n-1}\\ & \qquad +n\big((n-1)\,\alpha_1+\beta_0\big)\mathcal{C}_n=0.\end{cases}\tag{49}$$

These equations permit the evaluation, using say Cramer's rule, of the coefficients $\{\mathcal{C}_k\}_{k=1}^{n}$ of the polynomial solution in terms of the non-zero constant $\mathcal{C}_0$.

The $(n+1)^{th}$ equation

$$\big((n-1)\,(n-2)\,\alpha_3+(n-1)\,\beta_2+\varepsilon_1\big)\,\mathcal{C}_{n-1}+\big(n(n-1)\,\alpha_2+n\,\beta_1+\varepsilon_0\big)\,\mathcal{C}_n=0\,,\tag{50}$$

gives our *sufficient condition* that relates $\varepsilon_0\equiv\varepsilon_{0;n}$ to the remaining parameters of the differential equation.

Finally, the $(n+2)^{th}$ equation

$$\varepsilon_{1;n}=-n\,(n-1)\,\alpha_3-n\,\beta_2\,,\quad n=0,\,1,\,\cdots\,,\tag{51}$$

re-establishes *the necessary condition* ($\varepsilon_1\equiv\varepsilon_{1;n}$) for the existence of the n-degree polynomial solution, see (47).

For a non-zero solution, the $n+1$ linear equations generated by the recurrence relation (48) require the vanishing of the $(n+1)\times(n+1)$-determinant (with four main diagonals and all other entries being zeros)

$$\Delta_{n+1}=\begin{vmatrix}S_0 & T_1 & \eta_1 & & & & \\ \gamma_1 & S_1 & T_2 & \eta_2 & & & \\ & \gamma_2 & S_2 & T_3 & \eta_3 & & \\ & & \ddots & \ddots & \ddots & \ddots & \\ & & & \gamma_{n-2} & S_{n-2} & T_{n-1} & \eta_{n-1}\\ & & & & \gamma_{n-1} & S_{n-1} & T_n\\ & & & & & \gamma_n & S_n\end{vmatrix},$$

where

$$\begin{aligned}&S_k=\varepsilon_{0;n}+k\big((k-1)\alpha_2+\beta_1\big)\,,\\&T_k=k\big((k-1)\alpha_1+\beta_0\big)\,,\\&\gamma_k=\varepsilon_{1;n}+(k-1)\big((k-2)\alpha_3+\beta_2\big)\,,\\&\eta_k=k(k+1)\alpha_0\,,\end{aligned}$$

and for fixed n,

$$\varepsilon_{1;n}=-n\,(n-1)\,\alpha_3-n\,\beta_2\,.\tag{52}$$

A simple relation to evaluate this determinant in terms of lower-degree determinants is given by

$$\Delta_{k+1} = S_k\,\Delta_k - \gamma_k\,T_k\,\Delta_{k-1} + \gamma_k\,\gamma_{k-1}\,\eta_{k-1}\,\Delta_{k-2}\,, \quad (\Delta_{-2} = \Delta_{-1} = 0,\ \Delta_0 = 1,\ k = 0,\,1,\,\ldots,\,n). \tag{53}$$

Although there is a classical theorem [24] that guarantees the simple distinct real roots of the three diagonal matrix, to the best of our knowledge, there is no such theorem available for the matrix-type (52). However, we shall assume, in the following example, that the matrix entries allow for the distinct real roots of the resulting polynomial of $\varepsilon_{0;n}$.

Illustrative example:

- For the zero-degree polynomial solution $\mathbf{P}_0\,(r) = 1$, i.e., $n = 0$, the coefficients $\mathcal{C}_j = 0$ for all $j \geq 1$ and the recurrence relation (28) for $k = 0, 1$ gives, respectively, the necessary and sufficient conditions

$$\varepsilon_{1;0} = 0\,, \qquad \varepsilon_{0;0} = 0. \tag{54}$$

- For a first-degree polynomial solution, $n = 1$, the coefficients $\mathcal{C}_j = 0$ for all $j \geq 2$ where $k = 0, 1, 2$ give the following three equations

$$\begin{cases} \varepsilon_{0;1}\,\mathcal{C}_0 + \beta_0\,\mathcal{C}_1 = 0, \\ \varepsilon_{1;1}\,\mathcal{C}_0 + (\beta_1 + \varepsilon_{0;1})\,\mathcal{C}_1 = 0, \\ (\beta_2 + \varepsilon_{1;1})\,\mathcal{C}_1 = 0. \end{cases} \tag{55}$$

So, for $\mathcal{C}_0 = 1$, it is necessary that $\varepsilon_{1;1} = -\beta_2$ and therefore, $\mathcal{C}_1 = -\varepsilon_{0;1}/\beta_0$ where $\varepsilon_{0;1}$ are now the roots of the quadratic equation

$$\beta_0\,\beta_2 + \beta_1\varepsilon_{0;1} + \varepsilon_{0;1}^2 = 0.$$

Let $\varepsilon_{0;1}^{\ell}, \ell = 1, 2$, denote, if any, the two distinct real roots $\varepsilon_{0;1}^{0} \neq \varepsilon_{0;1}^{1}$ of this quadratic equation. Then, for the two (distinct) differential equations

$$\begin{aligned} &\left(\alpha_0 + \alpha_1\,r + \alpha_2\,r^2 + \alpha_3\,r^3\right)\mathbf{P}''_{1;\ell}\,(r) + \left(\beta_0 + \beta_1\,r + \beta_2\,r^2\right)\mathbf{P}'_{1;\ell}\,(r) \\ &\quad + \left(\varepsilon_{0;1}^{\ell} - \beta_2\,r\right)\mathbf{P}_{1;\ell}\,(r) = 0\,, \quad \ell = 1,\,2\,, \end{aligned} \tag{56}$$

the first-order polynomial solutions are

$$\begin{cases} \mathbf{P}_{1;\ell}\,(r) = 1 - \dfrac{\varepsilon_{0;1}^{\ell}}{\beta_0}\,r, \\ \beta_0\,\beta_2 + \beta_1\,\varepsilon_{0;1}^{\ell} + (\varepsilon_{0;1}^{\ell})^2 = 0, \qquad \ell = 1,\,2\,. \end{cases} \tag{57}$$

- For a second-degree polynomial solution, $n = 2$, the coefficients $\mathcal{C}_j = 0$ for all $j \geq 3$ where $k = 0,\,1,\,2,\,3$ give the four linear equations

$$\begin{cases} \varepsilon_{0;2}\,\mathcal{C}_0 + \beta_0\,\mathcal{C}_1 + 2\,\alpha_0\,\mathcal{C}_2 = 0, \\ \varepsilon_{1;2}\,\mathcal{C}_0 + (\beta_1 + \varepsilon_{0;2})\,\mathcal{C}_1 + 2(\alpha_1 + \beta_0)\,\mathcal{C}_2 = 0, \\ (\beta_2 + \varepsilon_{1;2})\,\mathcal{C}_1 + (2\,\alpha_2 + 2\,\beta_1 + \varepsilon_{0;2})\,\mathcal{C}_2 = 0, \\ (2\alpha_3 + 2\,\beta_2 + \varepsilon_{1;2})\mathcal{C}_2 = 0. \end{cases} \tag{58}$$

The very last equation of (58), correspondent to $k = 3$, gives the necessary condition

$$\varepsilon_{1;2} = -2\,\alpha_3 - 2\,\beta_2\,, \tag{59}$$

and for $k = 0, 1$, the coefficients of the polynomial solution $y(r) = 1 + \mathcal{C}_1\,r + \mathcal{C}_2\,r^2$ read

$$\begin{cases} \mathcal{C}_1 = \dfrac{\begin{vmatrix} -\varepsilon_{0;2} & 2\alpha_0 \\ 2\,\alpha_3 + 2\,\beta_2 & 2\alpha_1 + 2\beta_0, \end{vmatrix}}{\begin{vmatrix} \beta_0 & 2\alpha_0 \\ \beta_1 + \varepsilon_{0;2} & 2\alpha_1 + 2\beta_0 \end{vmatrix}}, \\ \mathcal{C}_2 = \dfrac{\begin{vmatrix} \beta_0 & -\varepsilon_{0;2} \\ \beta_1 + \varepsilon_{0;2} & 2\,\alpha_3 + 2\,\beta_2 \end{vmatrix}}{\begin{vmatrix} \beta_0 & 2\alpha_0 \\ \beta_1 + \varepsilon_{0;2} & 2\alpha_1 + 2\beta_0 \end{vmatrix}}. \end{cases} \tag{60}$$

The equation corresponding to $k=2$ and $n=2$ establishes the sufficient condition

$$\begin{vmatrix} \varepsilon_{0;2}^{\ell} & \beta_0 & 2\alpha_0 \\ -2\,\alpha_3 - 2\,\beta_2 & \beta_1 + \varepsilon_{0;2}^{\ell} & 2\alpha_1 + 2\beta_0 \\ 0 & \beta_2 - 2\,\alpha_3 - 2\,\beta_2 & 2\,\alpha_2 + 2\,\beta_1 + \varepsilon_{0;2}^{\ell} \end{vmatrix} = 0, \tag{61}$$

where $\ell = 1, 2, 3$ refers to the three distinct simple roots $\varepsilon_{0;2}^{\ell},\ \ell = 1, 2, 3$, if any, of the polynomial generated by the determinant (61). Hence, for each index $\ell = 1, 2, 3$, the differential equation

$$\begin{aligned} &\left(\alpha_0 + \alpha_1\, r + \alpha_2\, r^2 + \alpha_3\, r^3\right) \mathbf{P}''_{2;\ell}\,(r) + \left(\beta_0 + \beta_1\, r + \beta_2\, r^2\right) \mathbf{P}'_{2;\ell}\,(r) \\ &\quad + \left(\varepsilon_{0;2}^{\ell} - (2\alpha_3 + 2\beta_2)\, r\right) \mathbf{P}_{2;\ell}\,(r) = 0\,, \end{aligned} \tag{62}$$

has the polynomial solution (for $\ell = 1,\ 2,\ 3\,.$)

$$\mathbf{P}_{2;\ell}\,(r) = 1 + \frac{\begin{vmatrix} -\varepsilon_{0;2}^{\ell} & 2\alpha_0 \\ 2\,\alpha_3 + 2\,\beta_2 & 2\alpha_1 + 2\beta_0 \end{vmatrix}}{\begin{vmatrix} \beta_0 & 2\alpha_0 \\ \beta_1 + \varepsilon_{0;2}^{\ell} & 2\alpha_1 + 2\beta_0 \end{vmatrix}}\, r + \frac{\begin{vmatrix} \beta_0 & -\varepsilon_{0;2}^{\ell} \\ \beta_1 + \varepsilon_{0;2}^{\ell} & 2\,\alpha_3 + 2\,\beta_2 \end{vmatrix}}{\begin{vmatrix} \beta_0 & 2\alpha_0 \\ \beta_1 + \varepsilon_{0;2}^{\ell} & 2\alpha_1 + 2\beta_0 \end{vmatrix}}\, r^2, \tag{63}$$

The above constructive approach can be continued to generate higher-order polynomial solutions of an arbitrary degree.

Theorem 3.2. *Suppose the polynomial in $\varepsilon_{0;n}^{\ell}$ generated by the determinant (52) has $n+1$ distinct real roots arranged in ascending order $\varepsilon_{0;n}^{0} < \varepsilon_{0;n}^{1} < \varepsilon_{0;n}^{2} < \cdots < \varepsilon_{0;n}^{n}$, then, the eigenvalue problem*

$$\begin{aligned} &\left(\alpha_0 + \alpha_1\, r + \alpha_2\, r^2 + \alpha_3\, r^3\right) \frac{d^2 \boldsymbol{P}_{n;\ell}}{dr^2} + \left(\beta_0 + \beta_1\, r + \beta_2\, r^2\right) \frac{d\boldsymbol{P}_{n;\ell}}{dr} \\ &\quad - n\big(\,(n-1)\,\alpha_3 + \beta_2\big)\, r\, \boldsymbol{P}_{n;\ell} = -\varepsilon_{0;n}^{\ell}\, \boldsymbol{P}_{n;\ell}, \end{aligned} \tag{64}$$

has a polynomial solution of the degree n, for $\ell = 1,\ 2,\ \ldots,\ n+1$.

This theorem is illustrated by Figure 1, for $n = 0, 1, 2, 3$,

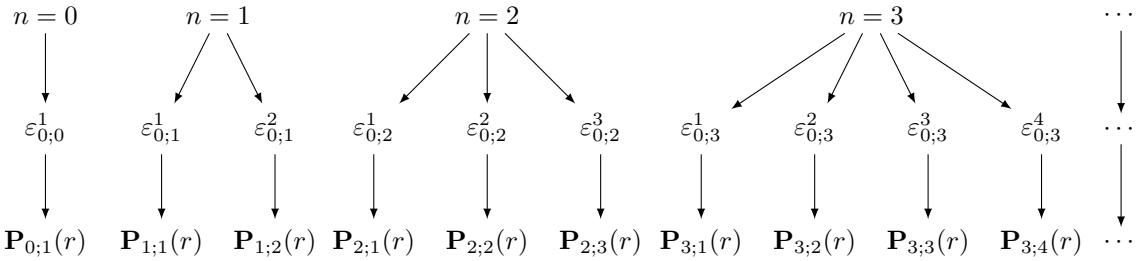

FIGURE 1. A graphical representation of Theorem 3.2

Open problem: *It is an open question to establish the condition(s) on the parameters so that the polynomial generated by the determinant (32) has simple and real distinct roots.*

4. The solutions in the neighbourhood of a singular point

4.1. Series Solution and infinite sequence of orthogonal polynomials $\{\mathcal{P}_k(\varepsilon_0)\}_{k=0}^{\infty}$

As mentioned earlier, if $\alpha_0 = 0$, there are seven subclasses characterized by the equation

$$r\left(\alpha_1 + \alpha_2\, r + \alpha_3 r^2\right) y'' + \left(\beta_0 + \beta_1\, r + \beta_2\, r^2\right) y' + \left(\varepsilon_0 + \varepsilon_1\, r\right) y = 0\,. \tag{65}$$

The classification of these seven equations along with their singularities and the associated domains are summarized in Table 3. From this Table, it is noted that if $\alpha_1 \neq 0$, there are four subclasses where the point $r = 0$ is a regular singular point, while if $\alpha_1 = 0$, the condition $\beta_0 = 0$ is necessary to ensure that $r = 0$ is a regular singular point for two additional subclasses and the last equation is a class where $r = 0$ is irregular singular point unless we reduce to Euler's type ($\alpha_1 = \alpha_2 = \beta_1 = \beta_0 = \varepsilon_0 = 0$).

In the neighbourhood of the regular singular point $r = 0$, the formal series solution $y(r) = r^s \sum_{k=0}^{\infty} \mathcal{C}_k r^k$ is then valid within the interval $(0, \zeta)$ where ζ is the nearest singular point obtained via the roots of the quadratic equation $\alpha_1 + \alpha_2\, r + \alpha_3 r^2 = 0$. Here, s are the roots of the indicial equation $\alpha_1\, s(s-1) + \beta_0\, s = 0$, i.e. $s_1 = 0$ and $s = 1 - \beta_0/\alpha_1$.

Using Frobenius method, it is straightforward to show that the coefficients $\{\mathcal{C}_k\}_{k=0}^{\infty}$ satisfy the three-term recurrence relation

$$\begin{aligned}(k+s+1)\big(\alpha_1(k+s)+\beta_0\big)\mathcal{C}_{k+1} + \big((k+s)[\alpha_2\,(k+s-1)+\beta_1]+\varepsilon_0\big)\mathcal{C}_k \\ + \big((k+s-1)[\alpha_3(k+s-2)+\beta_2]+\varepsilon_1\big)\mathcal{C}_{k-1} = 0\,,\end{aligned} \tag{66}$$

where $k = 1, 2, \ldots$. For

$$\begin{cases} \mathcal{C}_{-1} = 0, \\ \\ \mathcal{C}_0 = 1, \\ \\ \mathcal{C}_1 = -\dfrac{s(\alpha_2\,(s-1)+\beta_1)+\varepsilon_0}{(\alpha_1\, s+\beta_0)(s+1)} = -\dfrac{P_{1;s}(\varepsilon_0)}{\alpha_1\left(s+\frac{\beta_0}{\alpha_1}\right)(s+1)}, \end{cases}$$

this equation can be written as

$$\mathcal{C}_{k+2} = \lambda_0(k)\,\mathcal{C}_{k+1} + s_0(k)\,\mathcal{C}_k,$$

where

$$\begin{cases} \lambda_0(k) = -\dfrac{(\alpha_2\,(k+s)+\beta_1)\;(k+s+1)+\varepsilon_0}{(\alpha_1(k+s+1)+\beta_0)\,(k+s+2)}, \\ \\ s_0(k) = -\dfrac{(\alpha_3(k+s-1)+\beta_2)\,(k+s)+\varepsilon_1}{(\alpha_1(k+s+1)+\beta_0)\,(k+s+2)}, \end{cases}$$

From this equation, we note that

$$\mathcal{C}_{k+3} = \lambda_1(k)\,\mathcal{C}_{k+1} + s_1(k)\,\mathcal{C}_k, \qquad \begin{cases} \lambda_1(k) = \lambda_0(k+1)\,\lambda_0(k) + s_0(k+1) \\ s_1(k) = \lambda_0(k+1)\,s_0(k), \end{cases}$$

$$\mathcal{C}_{k+4} = \lambda_2(k)\,\mathcal{C}_{k+1} + s_2(k)\,\mathcal{C}_k, \qquad \begin{cases} \lambda_2(k) = \lambda_1(k+1)\lambda_0(k) + s_1(k+1) \\ s_2(k) = \lambda_1(k+1)s_0(k), \end{cases}$$

$$\mathcal{C}_{k+5} = \lambda_3(k)\,\mathcal{C}_{k+1} + s_3(k)\,\mathcal{C}_k, \qquad \begin{cases} \lambda_3(k) = \lambda_2(k+1)\lambda_0(k) + s_2(k+1) \\ s_3(k) = \lambda_2(k+1)s_0(k), \end{cases}$$

and in general

$$\mathcal{C}_{k+m} = \lambda_{m-2}(k)\,\mathcal{C}_{k+1} + s_{m-2}(k)\,\mathcal{C}_k, \qquad \begin{cases} \lambda_m(k) = \lambda_{m-1}(k+1)\lambda_0(k) + s_{m-1}(k+1) \\ s_m(k) = \lambda_{m-1}(k+1)s_0(k), \end{cases}$$

and therefore

$$\mathcal{C}_2 = \frac{(s+1)(\alpha_2\, s+\beta_1)+\varepsilon_0}{(\alpha_1(s+1)+\beta_0)(s+2)}\left(\frac{s(\alpha_2\,(s-1)+\beta_1)+\varepsilon_0}{(\alpha_1\, s+\beta_0)(s+1)}\right) - \frac{s(\alpha_3(s-1)+\beta_2)+\varepsilon_1}{(\alpha_1(s+1)+\beta_0)(s+2)} = \frac{P_{2;s}(\varepsilon_0)}{\alpha_1^2\left(s+\frac{\beta_0}{\alpha_1}\right)_2 (s+1)_2}. \tag{67}$$

DE	α_3	α_2	α_1	Condition	Roots of LPC	Domain definition
I	α_3	α_2	α_1	$a_2^2-4a_1a_3>0$	$r=0,\quad \xi_+\neq\xi_-$	$r\in(0,\min\xi_\pm)$ if $\xi_\pm>0$ $r\in(\max\xi_\pm,0)$ if $\xi_\pm<0$ $r\in(0,\xi_+)$ if $\xi_-<0<\xi_+, \lvert\xi_-\rvert>\xi_+$ $r\in(\xi_-,0)$ if $\xi_-<0<\xi_+, \lvert\xi_-\rvert<\xi_+$
				$a_2^2-4a_1a_3=0$	$r=0,\quad \xi_+=\xi_-=\xi$	$r\in(0,\xi)$
	Differential Equation:			$r\,(\xi_1-r)(\xi_2-r)\,y''+(\beta_0+\beta_1\,r+\beta_2\,r^2)\,y'+(\varepsilon_0+\varepsilon_1\,r)\,y=0$		
	Roots:			$r=0;\quad r=\xi_\pm\equiv(-\alpha_2\pm\sqrt{\alpha_2^2-4\alpha_1\alpha_3})/(2\alpha_3)$		
	Singularity:			$r=0,\xi_\pm,\infty$: Regular		
	Differential Equation:			$r\,(\xi-r)^2\,y''+(\beta_0+\beta_1\,r+\beta_2\,r^2)\,y'+(\varepsilon_0+\varepsilon_1\,r)\,y=0$		
	Roots:			$r=0;\quad r=\xi\equiv-\alpha_2/(2\alpha_3)$		
	Singularity:			$r=0,\xi$: Regular; $r=\infty$: Irregular		
II	0	α_2	α_1		$r=0,\quad r=-\alpha_1/\alpha_2$	$r\in(0,-\alpha_1/\alpha_2)$ if $\alpha_1/\alpha_2<0$ $r\in(-\alpha_1/\alpha_2,0)$ if $\alpha_1/\alpha_2>0$
	Differential Equation:			$r(\alpha_1+\alpha_2\,r)\,y''+(\beta_0+\beta_1\,r+\beta_2\,r^2)\,y'+(\varepsilon_0+\varepsilon_1\,r)\,y=0$		
	Singularity:			$r=0,-\alpha_1/\alpha_2$: Regular; $r=\infty$: Irregular		
III	α_3	0	α_1	$a_1a_3<0$	$r=0,\pm\sqrt{-\alpha_1/\alpha_3}$	$r\in(0,\sqrt{-\alpha_1/\alpha_3})$
				$\alpha_1\alpha_3>0$	$r=0,$	$r\in(0,\infty)$
	Differential Equation:			$r\,(\alpha_3r^2+\alpha_1)\,y''+(\beta_0+\beta_1\,r+\beta_2\,r^2)\,y'+(\varepsilon_0+\varepsilon_1\,r)\,y=0,\quad \alpha_3\alpha_1<0$		
	Singularity:			$r=0,\pm\sqrt{-\alpha_1/\alpha_3},\infty$: Regular		
	Differential Equation:			$r\,(\alpha_3r^2+\alpha_1)\,y''+(\beta_0+\beta_1\,r+\beta_2\,r^2)\,y'+(\varepsilon_0+\varepsilon_1\,r)\,y=0,\quad \alpha_3\alpha_1>0$		
	Singularity:			$r=0$: Regular; $r=\infty$: Irregular		
IV	α_3	α_2	0	$\beta_0=0$	$r=0,\quad -\alpha_2/\alpha_3$	$r\in(0,-\alpha_2/\alpha_3)$ if $\alpha_2/\alpha_3<0$ $r\in(-\alpha_2/\alpha_3,0)$ if $\alpha_2/\alpha_3>0$
	Differential Equation:			$r^2(\alpha_3r+\alpha_2)\,y''+r(\beta_1+\beta_2\,r)\,y'+(\varepsilon_0+\varepsilon_1\,r)\,y=0$		
	Singularity:			$r=0,-\alpha_2/\alpha_3$: Regular; $r=\infty$: Irregular		
V	0	0	α_1		$r=0$	$r\in(0,\infty)$
	Differential Equation:			$\alpha_1\,r\,y''+(\beta_0+\beta_1\,r+\beta_2\,r^2)\,y'+(\varepsilon_0+\varepsilon_1\,r)\,y=0$		
	Singularity:			$r=0$: Regular; $r=\infty$: Irregular		
VI	0	α_2	0	$\beta_0=0$	$r=0$	$r\in(0,\infty)$
	Differential Equation:			$\alpha_2\,r^2\,y''+r(\beta_1+\beta_2\,r)\,y'+(\varepsilon_0+\varepsilon_1\,r)\,y=0$		
	Singularity:			$r=0$: Regular; $r=\infty$: Irregular		
VII	α_3	0	0		$r=0$	$r\in(0,\infty)$
	Differential Equation:			$\alpha_3\,r^3\,y''+(\beta_0+\beta_1\,r+\beta_2\,r^2)\,y'+(\varepsilon_0+\varepsilon_1\,r)\,y=0$		
	Singulaity:			$r=0,\infty$: Irregular		

TABLE 3. Tabulating the seven different types of differential equations, which apply to Theorem 4.1.

initiated with

$$P_{2,s}(\varepsilon) = ((s+1)(\alpha_2\, s+\beta_1)+\varepsilon_0)P_{1;s}(\varepsilon_0) - (\alpha_1\, s+\beta_0)(s+1)(s(\alpha_3(s-1)+\beta_2)+\varepsilon_1)$$

Continuing with this process, it is straightforward to conclude that the series solution can be written as

$$y(r) = r^s \sum_{k=0}^{\infty} \mathcal{C}_k\, r^k = \sum_{k=0}^{\infty} (-1)^k \frac{P_{k;s}(\varepsilon_0)}{\alpha_1^k \left(\frac{\beta_0}{\alpha_1}+s\right)_k (1+s)_k}\, r^{k+s}, \tag{68}$$

where the k-degree polynomials of the parameter ε_0, namely $\{P_{k;s}(\varepsilon_0)\}_{k=0}^{\infty}$, satisfy the following three-term recurrence relation:

$$\begin{aligned} P_{k+1;s}(\varepsilon_0) = \big((k+s)\big[(k+s-1)\alpha_2+\beta_1\big]+\varepsilon_0\big)P_{k;s}(\varepsilon_0) - (k+s)\big((k+s-1)\alpha_1+\beta_0\big)\big((k+s-1) \\ \times \big[(k+s-2)\alpha_3+\beta_2\big]+\varepsilon_1\big)P_{k-1;s}(\varepsilon_0), \end{aligned} \tag{69}$$

initiated with $P_{-1;s}(\varepsilon_0) = 0$ and $P_{0;s}(\varepsilon_0) = 1$.

For the classes I-IV in Table 3, including, of course, the classical Heun equation, $r = 0$ is a regular singular point with one of the exponents of singularities being $s = 0$, in which case, the coefficients $\{\mathcal{C}_k\}_{k=0}^{\infty}$ of the series solution $y(r) = \sum_{k=0}^{\infty} \mathcal{C}_k r^k$ satisfy the three-term recurrence relation

$$\big((k+1)(k\,\alpha_1+\beta_0)\big)\mathcal{C}_{k+1} + \big(k\big((k-1)\alpha_2+\beta_1\big)+\varepsilon_0\big)\mathcal{C}_k + \big((k-1)\big((k-2)\alpha_3+\beta_2\big)+\varepsilon_1\big)\mathcal{C}_{k-1} = 0, \tag{70}$$

and we have the following general result concerning the series solutions of the equation (65):

Theorem 4.1. *In the neighbourhood of the regular singular point $r = 0$, the series solution $y(r) = \sum_{k=0}^{\infty} \mathcal{C}_k r^k$ of the differential equation (65), with $\alpha_1 \neq 0$, is explicitly given by*

$$y(r) = \sum_{k=0}^{\infty} (-1)^k \frac{\mathcal{P}_k(\varepsilon_0)}{k!\, \alpha_1^k \left(\frac{\beta_0}{\alpha_1}\right)_k} r^k, \tag{71}$$

where the infinite sequence $\{\mathcal{P}_k(\varepsilon_0)\}_{k=0}^{\infty}$ is evaluated using the three-term recurrence relation

$$\begin{aligned} \mathcal{P}_{k+1}(\varepsilon_0) = \big(k(k-1)\alpha_2 + k\beta_1 + \varepsilon_0\big)\mathcal{P}_k(\varepsilon_0) - k\big((k-1)\alpha_1+\beta_0\big) \\ \times \big((k-1)(k-2)\alpha_3 + (k-1)\beta_2 + \varepsilon_1\big)\mathcal{P}_{k-1}(\varepsilon_0), \end{aligned} \tag{72}$$

where $\mathcal{P}_{-1}(\varepsilon_0) = 0$, and $\mathcal{P}_0(\varepsilon_0) = 1$.

Here, $(\alpha)_n$ refers to the Pochhammer symbol $(\alpha)_n = \alpha(\alpha+1)\cdots(\alpha-n+1) = \Gamma(\alpha+n)/\Gamma(\alpha)$ which is defined in terms of Gamma functions and satisfies the identity $(-n)_k = 0$ for any positive integers $k \geq n+1$. Equation (72) in Theorem follows directly by substituting the coefficients of (71) in the recurrence relation (65) and eliminates the common terms.

Corollary 4.2. *In the neighbourhood of the regular singular point $r = 0$, the series solution $y(r) = \sum_{k=0}^{\infty} \mathcal{C}_k r^k$ of the differential equation*

$$r\,(\alpha_1+\alpha_3 r^2)\,y'' + (\beta_0+\beta_1\, r+\beta_2\, r^2)\,y' + (\varepsilon_0+\varepsilon_1\, r)\,y = 0, \tag{73}$$

is given, explicitly, by

$$y(r) = \sum_{k=0}^{\infty} (-1)^k \frac{\mathfrak{P}_k(\varepsilon_0)}{k!\, \alpha_1^k \left(\frac{\beta_0}{\alpha_1}\right)_k} r^k, \tag{74}$$

where

$$\mathfrak{P}_{k+1}(\varepsilon_0) = (k\,\beta_1+\varepsilon_0)\,\mathfrak{P}_k(\varepsilon_0) - k\,((k-1)\alpha_1+\beta_0) \times ((k-1)(k-2)\alpha_3 + (k-1)\beta_2 + \varepsilon_1)\,\mathfrak{P}_{k-1}(\varepsilon_0), \tag{75}$$

initiated with $\mathfrak{P}_{-1}(\varepsilon_0) = 0,\ \mathfrak{P}_0(\varepsilon_0) = 1$.

Corollary 4.3. *In the neighbourhood of the regular singular point $r = 0$, the series solution $y(r) = \sum_{k=0}^{\infty} C_k r^k$ of the differential equation*

$$r\,(\alpha_1 + \alpha_2\,r)\,y'' + (\beta_0 + \beta_1\,r + \beta_2\,r^2)\,y' + (\varepsilon_0 + \varepsilon_1\,r)\,y = 0, \tag{76}$$

is given, explicitly, by

$$y(r) = \sum_{k=0}^{\infty}(-1)^k\,\frac{\mathcal{P}_k(\varepsilon_0)}{k!\,\alpha_1^k\left(\dfrac{\beta_0}{\alpha_1}\right)_k}\,r^k, \tag{77}$$

where

$$\mathcal{P}_{k+1}(\varepsilon_0) = (k(k-1)\alpha_2 + k\beta_1 + \varepsilon_0)\mathcal{P}_k(\varepsilon_0) - k((k-1)\alpha_1 + \beta_0)((k-1)\beta_2 + \varepsilon_1)\mathcal{P}_{k-1}(\varepsilon_0), \tag{78}$$

initiated with $\mathcal{P}_{-1}(\varepsilon_0) = 0,\ \mathcal{P}_0(\varepsilon_0) = 1$.

Corollary 4.4. *In the neighbourhood of the regular singular point $r = 0$, the series solution $y(x) = \sum_{k=0}^{\infty} C_k r^k$ of the differential equation*

$$\alpha_1\,r\,y'' + (\beta_0 + \beta_1\,r + \beta_2\,r^2)\,y' + (\varepsilon_0 + \varepsilon_1\,r)\,y = 0, \tag{79}$$

is given, explicitly, by

$$y(r) = \sum_{k=0}^{\infty}(-1)^k\,\frac{\mathbb{P}_k(\varepsilon_0)}{k!\,\alpha_1^k\left(\dfrac{\beta_0}{\alpha_1}\right)_k}\,r^k, \tag{80}$$

where

$$\mathbb{P}_{k+1}(\varepsilon_0) = (k\beta_1 + \varepsilon_0)\mathbb{P}_k(\varepsilon_0) - k\,((k-1)\,\alpha_1 + \beta_0)((k-1)\beta_2 + \varepsilon_1)\mathbb{P}_{k-1}(\varepsilon_0), \tag{81}$$

initiated with $\mathbb{P}_{-1}(\varepsilon_0) = 0,\ \mathbb{P}_0(\varepsilon_0) = 0$.

Corollary 4.5. *In the neighbourhood of the regular singular point $x = 0$, the series solution $y(x) = \sum_{k=0}^{\infty} C_k x^k$ of the differential equation*

$$\alpha_1 r\,y'' + (\beta_0 + \beta_2\,r^2)\,y' + (\varepsilon_0 + \varepsilon_1\,r)\,y = 0, \tag{82}$$

is given, explicitly, by

$$y(r) = \sum_{k=0}^{\infty}(-1)^k\,\frac{\mathbf{P}_k(\varepsilon_0)}{k!\,\alpha_1^k\left(\dfrac{\beta_0}{\alpha_1}\right)_k}\,r^k, \tag{83}$$

where

$$\mathbf{P}_{k+1}(\varepsilon_0) = \varepsilon_0\mathbf{P}_k(\varepsilon_0) - k((k-1)\alpha_1 + \beta_0)((k-1)\beta_2 + \varepsilon_1)\mathbf{P}_{k-1}(\varepsilon_0), \tag{84}$$

initiated with $\mathbf{P}_{-1}(\varepsilon_0) = 0, \mathbf{P}_1(\varepsilon_0) = 1$.

Remark 4.6. If, in addition to $\alpha_0 = 0$, we also have $\alpha_1 = 0$, then $r = 0$ is a regular singular point only if $\beta_0 = 0$, in which case the differential equation reduces to an equation that resembles Euler's equation, namely

$$r^2\left(\alpha_2 + \alpha_3 r\right)y'' + r\big(\beta_1 + \beta_2\,r\big)\,y' + \big(\varepsilon_0 + \varepsilon_1\,r\big)\,y = 0. \tag{85}$$

The exponents of the singularity $r = 0$ are

$$s_\pm = \big(\alpha_2 - \beta_1 \pm \sqrt{(\alpha_2 - \beta_1)^2 - 4\alpha_2\varepsilon_0}\big)/(2\alpha_2).$$

From the relation (66), the coefficients of the formal series solution $y(r) = r^s \sum_{k=0}^{\infty} \mathcal{C}_k\,r^k$ satisfy the two-term recurrence relation ($k = 1, 2, \ldots,\ \mathcal{C}_0 = 1$),

$$\mathcal{C}_k = -\tfrac{(k-1+s_\pm)(k-2+s_\pm)\alpha_3+(k-1+s_\pm)\beta_2+\varepsilon_1}{(k+s_\pm)(k-1+s_\pm)\alpha_2+(k+s_\pm)\beta_1+\varepsilon_0}\mathcal{C}_{k-1}, = \prod_{j=1}^{k}(-1)^j\,\tfrac{(j-1+s_\pm)(j-2+s_\pm)\alpha_3+(j-1+s_\pm)\beta_2+\varepsilon_1}{(j+s_\pm)(j-1+s_\pm)\alpha_2+(j+s_\pm)\beta_1+\varepsilon_0}, \tag{86}$$

that allows to obtain a closed form of the series solution of (71) in terms of the generalized hypergeometric function as

$$\begin{aligned} y(r) =& r^{s_\pm}\,{}_3F_2\left(1, s_\pm - \tfrac{1}{2} + \tfrac{\beta_2}{2\alpha_3} - \tfrac{\sqrt{(\alpha_3-\beta_2)^2-4\alpha_3\varepsilon_1}}{2\alpha_3},\ s_\pm + \tfrac{1}{2} + \frac{\beta_2}{2\alpha_3} - \tfrac{\sqrt{(\alpha_3-\beta_2)^2-4\alpha_3\varepsilon_1}}{2\alpha_3};\right. \\ & \left. s_\pm + \tfrac{1}{2} + \tfrac{\beta_1}{2\alpha_2} - \tfrac{\sqrt{(\alpha_2-\beta_1)^2-4\alpha_2\varepsilon_0}}{2\alpha_2},\ s_\pm + \tfrac{1}{2} + \tfrac{\beta_1}{2\alpha_2} + \tfrac{\sqrt{(\alpha_2-\beta_1)^2-4\alpha_2\varepsilon_0}}{2\alpha_2};\ -\frac{\alpha_3}{\alpha_2}\,r\right). \end{aligned} \tag{87}$$

4.2. Polynomial Solution and finite sequence of orthogonal polynomials

Theorem 4.7. *The necessary condition for the second-order linear differential equation (65) to have an n^{th}-degree polynomial solution $y_n(r) = \sum_{k=0}^{n} \mathcal{C}_k\, r^k\,, n = 0,\, 1,\, 2,\, \ldots$, in the neighbourhood of the regular singular point $r = 0$ with one of the indicial equation exponents $s = 0$, is*

$$\varepsilon_{1;n} = -n\,(n-1)\;\alpha_3 - n\;\beta_2\,, \quad n = 0,\, 1,\, 2,\, \ldots\,, \tag{88}$$

along with the sufficient condition, relating the remaining coefficients, given by the vanishing of the tridiagonal $(n+1)\times(n+1)$-determinant $\Delta_{n+1} \equiv 0$ given by

$$\Delta_{n+1} = \begin{vmatrix} S_0 & T_1 & & & & & & \\ \gamma_1 & S_1 & T_2 & & & & & \\ & \gamma_2 & S_2 & T_3 & & & & \\ & & \ddots & \ddots & \ddots & & & \\ & & & \gamma_{n-2} & S_{n-2} & T_{n-1} & & \\ & & & & \gamma_{n-1} & S_{n-1} & T_n & \\ & & & & & \gamma_n & S_n & \end{vmatrix}, \tag{89}$$

where, for fixed n : $\varepsilon_{1;n} = -n\,(n-1)\,\alpha_3 - n\,\beta_2$,

$$\begin{cases} S_k = \varepsilon_{0;n} + k\big((k-1)\alpha_2 + \beta_1\big), \\ T_k = -k\big((k-1)\alpha_1 + \beta_0\big), \\ \gamma_k = -\varepsilon_{1;n} - (k-1)\big((k-2)\alpha_3 + \beta_2\big), \end{cases}$$

and all other entries are zeros. In this case, the polynomial solutions are given explicitly by

$$y_n(r) = \sum_{k=0}^{n} (-1)^k\, \frac{\mathcal{P}_k^n(\varepsilon_{0;n})}{k!\,\alpha_1^k \left(\dfrac{\beta_0}{\alpha_1}\right)_k}\, r^k\,, \tag{90}$$

where the finite orthogonal sequences $\{\mathcal{P}_k^n(\varepsilon_{0;n})\}_{k=0}^n$ are evaluated using the three-term recurrence relation

$$\mathcal{P}_{k+1}^n(\varepsilon_{0;n}) = \big(S_k + \varepsilon_{0;n}\big)\mathcal{P}_k^n(\varepsilon_{0;n}) - \gamma_k T_k \mathcal{P}_{k-1}^n(\varepsilon_{0;n})\,,$$

or, more explicitly,

$$\begin{aligned} \mathcal{P}_{k+1}^n(\varepsilon_{0;n}) = {} & \big(k(k-1)\alpha_2 + k\beta_1 + \varepsilon_{0;n}\big)\mathcal{P}_k^n(\varepsilon_{0;n}) + k(n-k+1)\big((k-1)\alpha_1 + \beta_0\big) \\ & \times \big(\beta_2 + \alpha_3(k+n-2)\big)\mathcal{P}_{k-1}^n(\varepsilon_{0;n})\,, \end{aligned} \tag{91}$$

where $\mathcal{P}_{-1}^n(\varepsilon_{0;n}) = 0$, and $\mathcal{P}_0^n(\varepsilon_{0;n}) = 1$ for the non-negative integer n.

Expanding Δ_{k+1} with respect to the last column, it is clear that the determinant (89) satisfies a three-term recurrence relation

$$\begin{cases} \Delta_{k+1} = (S_k + \varepsilon_{0;n})\,\Delta_k - \gamma_k\, T_k\, \Delta_{k-1}, \\ \Delta_0 = 1, \quad \Delta_{-1} = 0, \quad k = 0,\, 1,\, \ldots,\, n\,, \end{cases} \tag{92}$$

that allow to compute the determinant Δ_k recursively in terms of lower-order determinants. We now show, by induction on k, that

$$\Delta_{k+1} = P_{k+1}(\varepsilon_{0;n}). \tag{93}$$

For $k = 0$, we find by (89) that $\Delta_1 = (S_0 + \varepsilon_{0;n})$ where the right hand side equals to $P_1^n(\varepsilon_{0;n})$ using (91). Next, suppose that $\Delta_j = P_j(\varepsilon_{0;n})$, for $j = 0, 1, 2, \cdots, k$, then from (91)

$$\mathcal{P}_{k+1}^n(\varepsilon_{0;n}) = \big(S_k + \varepsilon_{0;n}\big)\,\mathcal{P}_k^n(\varepsilon_{0;n}) - \gamma_k\, T_k\, \mathcal{P}_{k-1}^n(\varepsilon_{0;n}) = \big(S_k + \varepsilon_{0;n}\big)\,\Delta_k - \gamma_k\, T_k\, \Delta_{k-1} = \Delta_{k+1}$$

and the induction step is reached. These results can be represented by the graphical representation (Figure 2).

Some of the mathematical properties of the finite sequence of polynomials $\{\mathcal{P}_k^n(\varepsilon_{0;n})\}_{k=0}^n$ will be explored in later sections.

$$\Delta_{k+1}=\det\begin{pmatrix}
\overset{\mathcal{P}_1^n}{\uparrow} & \overset{\mathcal{P}_2^n}{\uparrow} & \overset{\mathcal{P}_3^n}{\uparrow} & & \overset{\mathcal{P}_n^n}{\uparrow}\\
S_0 & T_1 & 0 & \vdots & 0\\
\gamma_1 & S_1 & T_2 & \vdots & 0\\
0 & \gamma_2 & S_2 & \vdots & 0\\
\cdots & \cdots & \cdots & \ddots & \vdots\\
0 & 0 & 0 & \cdots & S_n
\end{pmatrix}$$

FIGURE 2. A demonstration of how the polynomials $\{\mathcal{P}_k^n(\varepsilon_{0;n})\}_{k=0}^n$ may be obtained from the $(k+1)$-determinant Δ_{k+1} for $k=0,\,1,\,2,\,\ldots,\,n$.

Remark 4.8. For $\alpha_3+\alpha_2+\alpha_1=0$, the canonical form of Heun's equation can be deduced from (65) by means of the following substitutions:

$$y''(r)+\left(\frac{\frac{\beta_0+\beta_1+\beta_3}{\alpha_3-\alpha_1}}{r-1}+\frac{\frac{\beta_0}{\alpha_1}}{r}+\frac{\frac{\alpha_3^2\beta_0+\alpha_1\alpha_3\beta_1+\alpha_1^2\beta_2}{\alpha_1\alpha_3(\alpha_1-\alpha_3)}}{(r-\frac{\alpha_1}{\alpha_3})}\right)y'(r)+\frac{\frac{\varepsilon_1}{\alpha_3}r+\frac{\varepsilon_0}{\alpha_3}}{r\,(r-1)\left(r-\frac{\alpha_1}{\alpha_3}\right)}\,y(r)=0. \tag{94}$$

or, simply in the standard form as

$$y''(r)+\left(\frac{\gamma}{r}+\frac{\delta}{r-1}+\frac{\varepsilon}{r-b}\right)y'(r)+\frac{\alpha\,\beta\;r-q}{r(r-1)(r-b)}y(r)=0, \tag{95}$$

where

$$\begin{array}{ccccccc}
\gamma & \delta & \varepsilon & \alpha & \beta & q & b\\
\Downarrow & \Downarrow & \Downarrow & \Downarrow & \Downarrow & \Downarrow & \\
\frac{\beta_0}{\alpha_1} & \frac{\beta_2+\beta_1+\beta_0}{\alpha_3-\alpha_1} & \frac{\beta_2\alpha_1^2+\beta_1\alpha_1\alpha_3+\beta_0\alpha_3^2}{\alpha_3\alpha_1(\alpha_1-\alpha_3)} & \frac{\beta_2+(n-1)\alpha_3}{\alpha_3} & -n & -\frac{\varepsilon_0}{\alpha_3} & \frac{\alpha_1}{\alpha_3}\\
\Uparrow & \Uparrow & \Uparrow & \Uparrow & \Uparrow & \Uparrow & \\
\gamma & \delta & \varepsilon & \beta & \alpha & q & b
\end{array}$$

where, in either case, it follows

$$\gamma+\delta+\varepsilon=\alpha+\beta+1$$

that ensures the regularity of the singular point ∞. With these parameters, the Sturm-Liouville form of the differential equation (65) is

$$-\frac{d}{dr}\left(r^\gamma\,(r-1)^\delta\,(r-b)^\varepsilon\,\frac{dy}{dr}\right)+\alpha\,\beta\,r^\gamma\,(r-1)^{\delta-1}(r-b)^{\varepsilon-1}y=q\,r^{\gamma-1}(r-1)^{\delta-1}(r-b)^{\varepsilon-1}\,y \tag{96}$$

where, for $b\geq 1$, $\gamma\geq 0$, $\delta\geq 1$, $r\in(0,1)$.

Corollary 4.9. *The second-order linear differential equation*

$$r^2(\alpha_3\,r+\alpha_2)y''(r)+r\,(\beta_2\,r+\beta_1)\;y'+(-(n(n-1)\;\alpha_3+n\;\beta_2)\,r+\varepsilon_0)\;y=0, \tag{97}$$

where $r\in(-\alpha_2/\alpha_3,0)$ if $\alpha_2\alpha_3>0$ or $r\in(0,\alpha_2/\alpha_3)$ if $\alpha_2\alpha_3<0$, has a polynomial solution of degree n subject to

$$\begin{cases}\prod\limits_{k=0}^{n}(\varepsilon_0+k((k-1)\alpha_2+\beta_1)=0\\ \Longrightarrow\\ \varepsilon_0=-n\,(n-1)\,\alpha_2-n\,\beta_1,\quad n=0,1,2,\cdots.\end{cases} \tag{98}$$

In particular, the differential equation

$$r^2(\alpha_3 r+\alpha_2)\; y''(r)+r(\beta_2\, r+\beta_1)\; y'(r)-\Big((n\,(n-1)\;\alpha_3+n\;\beta_2)\,r+n\,(n-1)\;\alpha_2+n\;\beta_1\Big)\; y(r)=0, \tag{99}$$

has the polynomial solutions

$$y_n(r)=r^n,\quad n=0,1,2,\ldots. \tag{100}$$

Proof. Follows immediately from Theorem 4.7 with $\alpha_1=\beta_0=0$.

■

5. Mathematical properties of the orthogonal polynomials $\{\mathcal{P}_k(\varepsilon_0)\}_{k=0}^{\infty}$

As pointed out by Theorem 4.1, in the neighbourhood of the singular point $r=0$ with an indicial exponent root zero, the series solution of the differential equation with four singular points, see (65),

$$r\left(\alpha_1+\alpha_2\, r+\alpha_3 r^2\right) y''+\left(\beta_0+\beta_1\, r+\beta_2\, r^2\right) y'+\left(\varepsilon_0+\varepsilon_1\, r\right) y=0\,.$$

can be written as

$$y(r)=\sum_{k=0}^{\infty}(-1)^k\,\frac{\mathcal{P}_k(\varepsilon_0)}{k!\,\alpha_1^k\left(\dfrac{\beta_0}{\alpha_1}\right)_k}r^k\,, \tag{101}$$

where the infinite sequence of polynomials $\{\mathcal{P}_k(\varepsilon_0)\}_{k=0}^{\infty}$ in the real variable ε_0 satisfies the three-term recurrence relation

$$\mathcal{P}_{k+1}(\varepsilon_0)=(\varepsilon_0-\mathcal{A}_k)\mathcal{P}_k(\varepsilon_0)-\mathcal{B}_k\mathcal{P}_{k-1}(\varepsilon_0), \tag{102}$$

initiated with

$$\mathcal{P}_{-1}(\varepsilon_0)=0,\quad \mathcal{P}_0(\varepsilon_0)=1,\ k=1,2,3,\cdots.$$

where

$$\begin{aligned}\mathcal{A}_k&=-k(k-1)\alpha_2-k\beta_1,\\ \mathcal{B}_k&=k\big((k-1)\alpha_1+\beta_0\big)\big((k-1)((k-2)\alpha_3+\beta_2)+\varepsilon_1\big).\end{aligned}$$

For $\mathcal{A}_k,\mathcal{B}_k\in\mathbb{R}$ and if $\mathcal{B}_k>0$, then according to Favard Theorem [25], see also [26, Theorem 2.14], there exists a positive Borel measure μ such that $\{\mathcal{P}_k\}_{k=0}^{\infty}$ is orthogonal with respect to the inner product

$$\langle P_k,P_{k'}\rangle=\int_{\mathbb{R}}P_k(\varepsilon_0)P_{p'}(\varepsilon_0)d\mu \tag{103}$$

such that

$$\int_{\mathbb{R}}P_k(\varepsilon_0)P_{k'}(\varepsilon_0)d\mu=p_k p_{k'}\delta_{kk'},\quad \int_{\mathbb{R}}d\mu=1, \tag{104}$$

where $\delta_{kk'}$ is the Kronecker symbol. In particular,

$$\int_{\mathbb{R}}\varepsilon_0^k P_{k'}(\varepsilon_0)d\mu=0\quad for\ all\ 0<k<k'. \tag{105}$$

The norm p_k can be found using the recurrence relations (102) by multiplying with ε_0^{k-1} and taking the integral over ε_0 with respect to μ that yields

$$\int_{\mathbb{R}}\varepsilon_0^k\mathcal{P}_k(\varepsilon_0)d\mu=\mathcal{B}_k\int_{\mathbb{R}}\varepsilon_0^{k-1}\mathcal{P}_{k-1}(\varepsilon_0)d\mu=\mathcal{B}_k\mathcal{B}_{k-1}\int_{\mathbb{R}}\varepsilon_0^{k-2}\mathcal{P}_{k-2}(\varepsilon_0)d\mu=\cdots=\left(\prod_{j=2}^{k}\mathcal{B}_j\right)\int_{\mathbb{R}}d\mu \tag{106}$$

and

$$\int_{\mathbb{R}} \mathcal{P}_k(\varepsilon_0)\mathcal{P}_{k'}(\varepsilon_0)\, d\mu = \frac{k!\,(\alpha_1\,\alpha_3)^k}{\beta_0\varepsilon_1}\left(\frac{\beta_0}{\alpha_1}\right)_k \times \left(\frac{-\alpha_3+\beta_2-\sqrt{(\alpha_3-\beta_2)^2-4\alpha_3\varepsilon_1}}{2\alpha_3}\right)_k \times \left(\frac{-\alpha_3+\beta_2+\sqrt{(\alpha_3-\beta_2)^2-4\alpha_3\varepsilon_1}}{2\alpha_3}\right)_k \delta_{kk'}. \tag{107}$$

Using the recurrence relation (102), it also follows that

$$\int_{\mathbb{R}} \varepsilon_0[\mathcal{P}_k(\varepsilon_0)]^2 d\mu = -\frac{k((k-1)\alpha_2+\beta_1)k!\,(\alpha_1\,\alpha_3)^k}{\beta_0\varepsilon_1}\left(\frac{\beta_0}{\alpha_1}\right)_k \left(\frac{-\alpha_3+\beta_2-\sqrt{(\alpha_3-\beta_2)^2-4\alpha_3\varepsilon_1}}{2\alpha_3}\right)_k \times \left(\frac{-\alpha_3+\beta_2+\sqrt{(\alpha_3-\beta_2)^2-4\alpha_3\varepsilon_1}}{2\alpha_3}\right)_k. \tag{108}$$

Further, for $k = 0, 1, 2, \cdots$,

$$\int_{\mathbb{R}} \varepsilon_0\mathcal{P}_{k+1}(\varepsilon_0)\mathcal{P}_k(\varepsilon_0)d\mu = \frac{(k+1)!\,(\alpha_1\,\alpha_3)^{k+1}}{\beta_0\varepsilon_1} \times \left(\frac{\beta_0}{\alpha_1}\right)_{k+1} \left(\frac{-\alpha_3+\beta_2-\sqrt{(\alpha_3-\beta_2)^2-4\alpha_3\varepsilon_1}}{2\alpha_3}\right)_{k+1} \left(\frac{-\alpha_3+\beta_2+\sqrt{(\alpha_3-\beta_2)^2-4\alpha_3\varepsilon_1}}{2\alpha_3}\right)_{k+1}. \tag{109}$$

Other integrals can be evaluated similarly, for example $\int_{\mathbb{R}}[\varepsilon_0\mathcal{P}_k(\varepsilon_0)]^2 d\mu$ can be evaluated by multiplying (102) by $\varepsilon_0\mathcal{P}_k(\varepsilon_0)$ and integrate with respect to the measure μ using (107), (108), and (109) and we continue similarly for

$$\int_{\mathbb{R}} \varepsilon_0^m[\mathcal{P}_k(\varepsilon_0)]^2 d\mu, \qquad m = 0, 1, 2, \cdots.$$

The recurrence relations (102) for $x = \varepsilon_0$ and $y = \varepsilon_0'$ read

$$\begin{aligned}\mathcal{P}_{k+1}(x) &= \big(x - \mathcal{A}_k\big)\mathcal{P}_k^n(x) - \mathcal{B}_k\mathcal{P}_{k-1}^n(x)\,,\\ \mathcal{P}_{k+1}(y) &= \big(y - \mathcal{A}_k\big)\mathcal{P}_k^n(y) - \mathcal{B}_k\mathcal{P}_{k-1}^n(y),\end{aligned}$$

respectively. By multiplying the first by $\mathcal{P}_k(y)$ and the second by $\mathcal{P}_k(x)$ and subtracting, the resulting equation becomes

$$(x-y)\mathcal{P}_k(y)\mathcal{P}_k(x) = Q_{k+1}(x,y) - \mathcal{B}_k\, Q_k(x,y) \tag{110}$$

where $Q_{k+1}(x,y) = \mathcal{P}_{k+1}(x)\mathcal{P}_k(y) - \mathcal{P}_k(x)\mathcal{P}_{k+1}(y)$. Thus, recursively over k, we have

$$\begin{aligned}(x-y)\mathcal{P}_k(x)\mathcal{P}_k(y) &= Q_{k+1}(x,y) - \mathcal{B}_k\, Q_k(x,y)\\ (x-y)\mathcal{P}_{k-1}(x)\mathcal{P}_{k-1}(y) &= Q_k(x,y) - \mathcal{B}_{k-1}\, Q_{k-1}(x,y)\\ &\vdots\\ (x-y)\mathcal{P}_0^n(x)\mathcal{P}_0^n(y) &= Q_1(x,y)\,,\end{aligned}$$

from which it is straightforward to obtain

$$(x-y)\Big[\mathcal{P}_k(x)\mathcal{P}_k(y) + \mathcal{B}_k\mathcal{P}_{k-1}(x)\mathcal{P}_{k-1}(y) + \mathcal{B}_k\mathcal{B}_{k-1}\mathcal{P}_{k-2}(x)\mathcal{P}_{k-2}(y) + \mathcal{B}_k\mathcal{B}_{k-1}\mathcal{B}_{k-2}\mathcal{P}_{k-3}(x)\mathcal{P}_{k-3}(y) + \cdots + \lambda_{k+1}\lambda_k\lambda_{k-1}\lambda_{k-2}\ldots\lambda_2\mathcal{P}_0(x)\mathcal{P}_0(y)\Big] = Q_{k+1}(\varepsilon_0, y)\,.$$

Dividing both sides by $(x-y)\mathcal{B}_k\mathcal{B}_{k-1}\mathcal{B}_{k-2}\ldots\mathcal{B}_2$ and summing over k results in

$$\sum_{j=0}^{k}\frac{\mathcal{P}_j(x)\mathcal{P}_j(y)}{\mathcal{B}_j\mathcal{B}_{j-1}\mathcal{B}_{j-2}\ldots\mathcal{B}_2} = (\mathcal{B}_k\mathcal{B}_{k-1}\mathcal{B}_{k-2}\ldots\mathcal{B}_2)^{-1} \times \frac{\mathcal{P}_{k+1}(x)\mathcal{P}_k(y) - \mathcal{P}_k^n(x)\mathcal{P}_{k+1}(y)}{x-y}\,.$$

(101) then follows using

$$\mathcal{B}_k\mathcal{B}_{k-1}\mathcal{B}_{k-2}\ldots\mathcal{B}_2=\prod_{i=2}^{k}\mathcal{B}_i$$
$$=\frac{k!\,(\alpha_1\,\alpha_3)^k}{\beta_0\varepsilon_1}\left(\frac{\beta_0}{\alpha_1}\right)_k\times\left(\frac{-\alpha_3+\beta_2-\sqrt{(\alpha_3-\beta_2)^2-4\alpha_3\varepsilon_1}}{2\alpha_3}\right)_k\times\left(\frac{-\alpha_3+\beta_2+\sqrt{(\alpha_3-\beta_2)^2-4\alpha_3\varepsilon_1}}{2\alpha_3}\right)_k$$

and finally, we have, for $k\geq 0$, Christoffel-Darboux identities:

$$\sum_{j=0}^{k}\frac{\mathcal{P}_j(x)\mathcal{P}_j(y)}{j!\,(\alpha_1\,\alpha_3)^j\left(\frac{\beta_0}{\alpha_1}\right)_j(\xi_+)_j\,(\xi_-)_j}=\frac{\mathcal{P}_{k+1}(x)\mathcal{P}_k(y)-\mathcal{P}_k(x)\mathcal{P}_{k+1}(y)}{k!\,(\alpha_1\,\alpha_3)^k\left(\frac{\beta_0}{\alpha_1}\right)_k(\xi_+)_k\,(\xi_-)_k\,(x-y)},\tag{111}$$

where

$$\xi_\pm=\frac{-\alpha_3+\beta_2\pm\sqrt{(\alpha_3-\beta_2)^2-4\alpha_3\varepsilon_1}}{2\alpha_3}$$

and by evaluating the limit of both sides as $y\to x$, its confluent form

$$\sum_{j=0}^{k}\frac{[\mathcal{P}_j(x)]^2}{j!\,(\alpha_1\,\alpha_3)^j\,(\xi_+)_j\,(\xi_-)_j}=\frac{\mathcal{P}'_{k+1}(x)\mathcal{P}_k(x)-\mathcal{P}'_k(x)\mathcal{P}_{k+1}(x)}{k!\,(\alpha_1\,\alpha_3)^k\left(\frac{\beta_0}{\alpha_1}\right)_k(\xi_+)_k\,(\xi_-)_k}\tag{112}$$

follows. Here, the prime refers to the derivative with respect to the variable x. As a direct consequence of the Christoffel-Darboux formula (112), all the zeros of the n-degree polynomial $\mathcal{P}_n(\varepsilon)$ are simple. To prove that they are also real, we note that the recurrence relation (102) can be written in a matrix form as

$$x\begin{pmatrix}\mathcal{P}_0(x)\\ \mathcal{P}_1(x)\\ \mathcal{P}_2(x)\\ \vdots\\ \mathcal{P}_{k-1}(x)\end{pmatrix}=\begin{pmatrix}\mathcal{A}_0 & 1 & 0 & \cdots & 0 & 0\\ \mathcal{B}_1 & \mathcal{A}_1 & 1 & \cdots & 0 & 0\\ 0 & \mathcal{B}_2 & \mathcal{A}_2 & \cdots & 0 & 0\\ \vdots & \vdots & \vdots & \ddots & \vdots & \vdots\\ 0 & 0 & 0 & \cdots & \mathcal{B}_{k-1} & \mathcal{A}_{k-1}\end{pmatrix}\begin{pmatrix}\mathcal{P}_0(x)\\ \mathcal{P}_1(x)\\ \mathcal{P}_2(x)\\ \vdots\\ \mathcal{P}_{k-1}(x)\end{pmatrix}+\mathcal{P}_k(x)\begin{pmatrix}0\\0\\0\\\vdots\\1\end{pmatrix}\tag{113}$$

Thus, if x_i is a zero of $\mathcal{P}_k(x)$, it is an eigenvalue of the given tridiagonal matrix. Since, by the hypothesis of (102), $\mathcal{B}_k>0$ for all $k\geq 1$, the results of Arscott [24] confirm that (i) the zeros of $\mathcal{P}_{k-1}(x)$ and $\mathcal{P}_k(x)$ interlace – that is, between two consecutive zeros of either polynomial lies precisely one zero of the other (ii) at the zeros of $\mathcal{P}_k(x)$ the values of $\mathcal{P}_{k-1}(x)$ are alternately positive and negative, (iii) all the zeros of $\mathcal{P}_k(x)$ – i.e. all the eigenvalues of tridiagonal matrix are real and different.

6. Mathematical properties of the finite orthogonal polynomials $\{\mathcal{P}_k^n(\varepsilon_0)\}_{k=0}^n$

In this section, we shall study some of the mathematical properties of the orthogonal polynomials $\{\mathcal{P}_k^n(\varepsilon_{0;n})\}_{k=0}^n$. First, the zeros of the polynomial generated by the aforementioned determinant are all simple. This fact can be confirmed by establishing the Christoffel-Darboux formula. Denote $x=\varepsilon_{0;k}$ and $y=\varepsilon_{0;k'}$, where $k\neq k'$ and $k,k'=0,1,2,\cdots,n-1$: For $x\neq y$

$$\sum_{j=0}^{k}\frac{\mathcal{P}_j^n(x)\mathcal{P}_j^n(y)}{j!(\alpha_1\alpha_3)^j(-n)_j\left(\frac{\beta_0}{\alpha_1}\right)_j\left(\frac{\beta_2}{\alpha_3}+n-1\right)_j}=\frac{\mathcal{P}_{k+1}^n(x)\mathcal{P}_k^n(y)-\mathcal{P}_k^n(x)\mathcal{P}_{k+1}^n(y)}{k!(\alpha_1\alpha_3)^k(-n)_k\left(\frac{\beta_0}{\alpha_1}\right)_k\left(\frac{\beta_2}{\alpha_3}+n-1\right)_k(x-y)},\tag{114}$$

while, for the limit $y\to x$,

$$\sum_{j=0}^{k}\frac{\left(\mathcal{P}_j^n(x)\right)^2}{j!(\alpha_1\alpha_3)^j(-n)_j\left(\frac{\beta_0}{\alpha_1}\right)_j\left(\frac{\beta_2}{\alpha_3}+n-1\right)_j}=\frac{[\mathcal{P}_{k+1}^n(x)]'\mathcal{P}_k^n(x)-[\mathcal{P}_k^n(x)]'\mathcal{P}_{k+1}^n(x)}{k!(\alpha_1\alpha_3)^k(-n)_k\left(\frac{\beta_0}{\alpha_1}\right)_k\left(\frac{\beta_2}{\alpha_3}+n-1\right)_k}.\tag{115}$$

Here, the prime refers to the derivative with respect to the variable x. If $x = x_k$ is a zero of the polynomial $\mathcal{P}_k^n(x)$ with multiplicity > 1, then $\mathcal{P}_k^n(x_k) = 0$ and (115) yields the contradiction

$$0 < \sum_{j=0}^{k-1} \frac{\left(\mathcal{P}_j^n(x_i)\right)^2}{j!(\alpha_1\alpha_3)^j(-n)_j \left(\frac{\beta_0}{\alpha_1}\right)_j \left(\frac{\beta_2}{\alpha_3}+n-1\right)_j} = 0, \tag{116}$$

and the zeros of the polynomial $P_k^n(x)$, $k = 1, 2, \cdots n$ are distinct.

6.1. Norms of the orthogonal polynomials

Denote $\varepsilon_{0;n} = x$, the general theory of orthogonal polynomials [27] guarantees that the finite sequence of polynomials $\{\mathcal{P}_k(x)\}_{k=0}^n$ form a set of orthogonal polynomials for each n. This implies the existence of a certain weight function, $\mathcal{W}(x)$, which can be normalized as

$$\int d\mathcal{W} = 1\,, \tag{117}$$

for which

$$\int \mathcal{P}_k(x)\mathcal{P}_{k'}(x)d\mathcal{W} = p_k\, p_{k'}\, \delta_{kk'}\,, \qquad 0 \le k,\, k' \le n\,, \tag{118}$$

where p_k denotes the norms of polynomials $\mathcal{P}_k(x)$. These norms can be found from the recurrence relations (36) by multiplying with $x^{k-1}\mathcal{W}(x)$ and taking the integral over x yields the recurrence formula

$$\int x^k\, \mathcal{P}_k^n(x)\, \mathcal{W}(x)\, dx = -k(n-k+1)\big((k-1)\alpha_1+\beta_0\big) \times \big(\beta_2+\alpha_3(k+n-2)\big) \int x^{k-1}\mathcal{P}_{k-1}^n(x)\mathcal{W}(x)dx\,, \tag{119}$$

and thus

$$\int \mathcal{P}_k^n(x)\, x^k\, \mathcal{W}(x)\, dx = k!\,(\alpha_1\alpha_3)^k\,(-n)_k \left(\frac{\beta_0}{\alpha_1}\right)_k \left(\frac{\beta_2}{\alpha_3}+n-1\right)_k. \tag{120}$$

From which it follows

$$\int [\mathcal{P}_k^n(x)]^2\mathcal{W}(x)dx = p_k^2 = k!\,(\alpha_1\alpha_3)^k\,(-n)_k \left(\frac{\beta_0}{\alpha_1}\right)_k \left(\frac{\beta_2}{\alpha_3}+n-1\right)_k \tag{121}$$

for all $0 \le k \le n$.

Because of the Pochhammer identity $(-n)_k = 0$ for $k > n$, it follows from (71) that the norms of all polynomials $\mathcal{P}_k^n(x)$ with $k \ge n+1$ vanish. Thus

$$p_k = 0\,, \qquad k \ge n+1\,. \tag{122}$$

We may also note, using the recurrence relation, that

$$\int x[\mathcal{P}_k(x)]^2\mathcal{W}(x)dx = -k((k-1)\alpha_2+\beta_1)\; k!\,(\alpha_1\alpha_3)^k\,(-n)_k \left(\frac{\beta_0}{\alpha_1}\right)_k \left(\frac{\beta_2}{\alpha_3}+n-1\right)_k. \tag{123}$$

6.2. The zeros of the polynomials $\{\mathcal{P}_k^n(\varepsilon_{0;n})\}_{k=0}^n$

One of the important properties of the polynomials $\mathcal{P}_{n+1}^n(\varepsilon_{0;n})$ concerns their zeros. An argument provided by Arscott [24] proves that if the product $(\gamma_k \cdot T_k) > 0$ for all $k = 1, 2, \ldots, n$, then the polynomials that satisfy the tri-diagonal determinant (67) are real and simple. Let us denote that the roots of the polynomials $\mathcal{P}_{n+1}^n(\varepsilon_{0;n}) = 0$ by $\varepsilon_{0;n}^\ell$, $\ell = 0, 1, \ldots, n$ such that

$$\mathcal{P}_{n+1}^n(\varepsilon_{0;n}^\ell) = 0\,, \tag{124}$$

where

$$\varepsilon_{0;n}^0 < \varepsilon_{0;n}^1 < \cdots < \varepsilon_{0;n}^n\,.$$

In particular, since $\mathcal{P}^n_{n+1}(\varepsilon_{0;n})$ is of degree $n+1$ and all the roots are simple and different, it follows that

$$\mathcal{P}^n_{n+1}(\varepsilon_{0;n}) = \prod_{\ell=0}^{n}(\varepsilon_{0;n} - \varepsilon^{\ell}_{0;n})\,. \tag{125}$$

The 'discrete' weight function $\mathcal{W}$ can be computed numerically [28] using (118), (119) and (125) for the given n. Denote $\mathcal{P}_\ell(\varepsilon_0) = \mathcal{P}^n_\ell(\varepsilon_0)$, and let the roots of $\mathcal{P}^n_{n+1}(\varepsilon_{0;n}) = 0$ be $\varepsilon^j_{0;n}$ arranged in ascending order for $j = 0, 1, 2, \cdots, n$. The weights $\mathcal{W}_j, j = 0, 1, \cdots, n$, for the orthogonal polynomials $\{\mathcal{P}^n_\ell(\varepsilon_{0;n})\}^n_{k=0}$ can be computed by solving the linear system

$$\sum_{j=0}^{n} \mathcal{W}_j\, \mathcal{P}^n_\ell(\varepsilon^j_{0;n}) = 0 \tag{126}$$

for $\ell = 0, 1, \cdots, n$.

6.3. Factorization property

Another interesting property of the polynomials $\{\mathcal{P}^n_k(x)\}^n_{k=0}$, aside from being an orthogonal sequence, is that when the parameter n takes positive integer values, the polynomials exhibit a factorization property. Clearly, the factorization occurs because the third term in the recursion relation (36) vanishes when $k = n+1$, so that all subsequent polynomials have a common factor $\mathcal{P}^n_{n+1}(\zeta)$ called a *critical polynomial*. Indeed, all the polynomials $\mathcal{P}^n_{k+n+1}(x)$, beyond the critical polynomial $\mathcal{P}^n_{n+1}(x)$ are factored into the product

$$\mathcal{P}^n_{k+n+1}(x) = \mathcal{Q}^n_k(x)\,\mathcal{P}^n_{n+1}(x),\ k = 0,\, 1,\, \ldots\,, \tag{127}$$

where the sequence $\{\mathcal{Q}^n_k(x)\}$ are polynomials of degree $k = 0,\, 1,\, \ldots$. Interestingly, the quotient polynomials $\{\mathcal{Q}^n_k(x)\}^\infty_{k=0}$ form an infinite sequence of orthogonal polynomials. To prove this claim, we substitute (128) into (36) and re-index the polynomials to eliminate the common factor $\mathcal{P}^n_{n+1}(\zeta)$ from both sides. The recurrence relation (36) then reduces to a three-term recurrence relation for the polynomials $\{\mathcal{Q}^n_k(\zeta)\}_{k\geq 0}$ that reads

$$\begin{aligned}\mathcal{Q}^n_k(x) = {}& \big((k+n)(k+n-1)\alpha_2 + (k+n)\beta_1 + x\big)\mathcal{Q}^n_{k-1}(x) - (k+n)(k-1)\big((k+n-1)\alpha_1 + \beta_0\big)\\ & \times \big(\beta_2 + \alpha_3(k+2n-2)\big)\mathcal{Q}^n_{k-2}(x)\,,\end{aligned} \tag{128}$$

where $\mathcal{Q}^n_{-1}(\zeta) = 0$, and $\mathcal{Q}^n_0(\zeta) = 1$. Hence, the quotient polynomials $\mathcal{Q}^n_k(\zeta)$ also form a new sequence of orthogonal polynomials for each value of n. For example, if $n = 2$, the critical polynomial is

$$\begin{aligned}\mathcal{P}^2_3(x) = {}& x^3 + (2\alpha_2 + 3\beta_1)x^2 + 2\big((3\alpha_3 + 2\beta_2)\beta_0 + \beta_1(\alpha_2 + \beta_1) + \alpha_1(2\alpha_3 + \beta_2)\big)x\\ & + 4\beta_0(\alpha_2 + \beta_1)(\alpha_3 + \beta_2)\,.\end{aligned} \tag{129}$$

and

$$\begin{aligned}
\mathcal{P}^2_4(x) &= \big(x + 6\alpha_2 + 3\beta_1\big)\,\mathcal{P}^2_3(x)\,,\\
\mathcal{P}^2_5(x) &= \big(x^2 + (18\alpha_2 + 7\beta_1)x - 4\big((3\alpha_1 + \beta_0)(4\alpha_3 + \beta_2) - 3(2\alpha_2 + \beta_1)(3\alpha_2 + \beta_1)\big)\big)\,\mathcal{P}^2_3(x)\,,\\
\mathcal{P}^2_6(x) &= \Big(x^3 + (38\alpha_2 + 12\beta_1)x^2 + \big(432\alpha_2^2 + 290\alpha_2\beta_1 + 47\beta_1^2 - 2(124\alpha_1\alpha_3 + 33\alpha_3\beta_0 + 26\alpha_1\beta_2 + 7\beta_0\beta_2)\big)\,x\\
&\quad - 10\big(\beta_1(84\alpha_1\alpha_3 + 23\alpha_3\beta_0 - 6\beta_1^2 + 18\alpha_1\beta_2 + 5\beta_0\beta_2) + 2\alpha_2\big(31\alpha_3\beta_0 - 27\beta_1^2 + 7\beta_0\beta_2 + 12\alpha_1(9\alpha_3 + 2\beta_2)\big)\\
&\quad - 144\alpha_2^3 - 156\alpha_2^2\beta_1\big)\Big)\mathcal{P}^2_3(x)\,,\\
&\ \ \vdots
\end{aligned}$$

from which we have

$$\begin{aligned}
\mathcal{Q}_0(x) &= 1\,,\\
\mathcal{Q}_1(x) &= x + 6\alpha_2 + 3\beta_1\,,\\
\mathcal{Q}_2(x) &= x^2 + (18\alpha_2 + 7\beta_1)x - 4\big((3\alpha_1 + \beta_0)(4\alpha_3 + \beta_2) - 3(2\alpha_2 + \beta_1)(3\alpha_2 + \beta_1)\big)\,,\\
\mathcal{Q}_3(x) &= x^3 + (38\alpha_2 + 12\beta_1)x^2 + \big(432\alpha_2^2 + 290\alpha_2\beta_1 + 47\beta_1^2 - 2(124\alpha_1\alpha_3 + 33\alpha_3\beta_0 + 26\alpha_1\beta_2 + 7\beta_0\beta_2)\big)\,x\\
&\quad - 10\big(\beta_1(84\alpha_1\alpha_3 + 23\alpha_3\beta_0 - 6\beta_1^2 + 18\alpha_1\beta_2 + 5\beta_0\beta_2) + 2\alpha_2\big(31\alpha_3\beta_0 - 27\beta_1^2 + 7\beta_0\beta_2 + 12\alpha_1(9\alpha_3 + 2\beta_2)\big)\\
&\quad - 144\alpha_2^3 - 156\alpha_2^2\beta_1\big)\,,\\
&\ \ \vdots
\end{aligned}$$

and so on. The Christoffel-Darboux formula for this infinite sequence of orthogonal polynomials reads

$$\sum_{j=0}^{k}\frac{\mathcal{Q}_j^n(x)\mathcal{Q}_j^n(y)}{j!\,(\alpha_1\alpha_3)^j(n+2)_j\left(\frac{\beta_0}{\alpha_1}+n+1\right)_j\left(\frac{\beta_2}{\alpha_3}+2n\right)_j}=\frac{\mathcal{Q}_{k+1}^n(x)\mathcal{Q}_k^n(y)-\mathcal{Q}_k^n(x)\mathcal{Q}_{k+1}^n(y)}{k!\,(\alpha_1\alpha_3)^k(n+2)_k\left(\frac{\beta_0}{\alpha_1}+n+1\right)_k\left(\frac{\beta_2}{\alpha_3}+2n\right)_k(x-y)}\,, \tag{130}$$

and as $y\to x$

$$\sum_{j=0}^{k}\frac{\left(\mathcal{Q}_j^n(x)\right)^2}{j!\,(\alpha_1\alpha_3)^j(n+2)_j\left(\frac{\beta_0}{\alpha_1}+n+1\right)_j\left(\frac{\beta_2}{\alpha_3}+2n\right)_j}=\frac{[\mathcal{Q}_{k+1}^n(x)]'\mathcal{Q}_k^n(x)-[\mathcal{Q}_k^n(x)]'\mathcal{Q}_{k+1}^n(x)}{k!\,(\alpha_1\alpha_3)^k(n+2)_k\left(\frac{\beta_0}{\alpha_1}+n+1\right)_k\left(\frac{\beta_2}{\alpha_3}+2n\right)_k}\,. \tag{131}$$

Theorem 6.1. *The norms of all polynomials $\mathcal{Q}_k^n(\xi)$ are given by*

$$\mathcal{G}_k^{\mathcal{Q}}=k!\,(\alpha_1\alpha_3)^k(n+2)_k\left(\frac{\beta_0}{\alpha_1}+n+1\right)_k\left(\frac{\beta_2}{\alpha_3}+2n\right)_k\,. \tag{132}$$

Proof. The proof follows by multiplying the recurrence relation (128) by $x^{k-2}\rho(x)$, with the normalized weight function $\int\rho(x)dx=1$, and integrating over x. This procedure yields a two-term recurrence relation

$$\mathcal{G}_k^{\mathcal{Q}}=k\,(k+n+1)\,((k+n)\alpha_1+\beta_0)\,(\beta_2+\alpha_3(k+2n-1)))\,\mathcal{G}_{k-1}^{\mathcal{Q}}\,,$$

where $\mathcal{G}_k^{\mathcal{Q}}=\int|\mathcal{Q}_k^n(x)|^2\rho(z)dz=\int x^kQ_k^n(x)\rho(x)dx$ with a solution given by (132). We see that, in general, the norm of the polynomials $Q_k^n(x)$ does not vanish. ∎

Acknowledgements

Partial financial support of this work under grant number GP249507 from the Natural Sciences and Engineering Research Council of Canada is gratefully acknowledged.

References

[1] A. F. Nikiforov, V. B. Uvarov. *Special functions of mathematical physics.* Birkhäuser Verlag, Basel, 1988. https://doi.org/10.1007/978-1-4757-1595-8.

[2] E. J. Routh. On some properties of certain solutions of a differential equation of the second order. *Proceedings of the London Mathematical Society* **16**:245–262, 1884/85. https://doi.org/10.1112/plms/s1-16.1.245.

[3] N. Saad, R. L. Hall, H. Ciftci. Criterion for polynomial solutions to a class of linear differential equations of second order. *Journal of Physics A: Mathematical and General* **39**(43):13445–13454, 2006. https://doi.org/10.1088/0305-4470/39/43/004.

[4] N. Saad, R. L. Hall, V. A. Trenton. Polynomial solutions for a class of second-order linear differential equations. *Applied Mathematics and Computation* **226**:615–634, 2014. https://doi.org/10.1016/j.amc.2013.10.056.

[5] A. Ronveaux (ed.). *Heun's differential equations.* Oxford University Press, New York, 1995.

[6] S. Y. Slavyanov, W. Lay. *Special functions: a unified theory based on singularities.* Oxford University Press, Oxford, 2000. ISBN 0-19-850573-6.

[7] A. Decarreau, M.-C. Dumont-Lepage, P. Maroni, et al. Formes canoniques des équations confluentes de l'équation de Heun. *Annales de la Societé Scientifique de Bruxelles Série I Sciences Mathématiques, Astronomiques et Physiques* **92**(1-2):53–78, 1978.

[8] A. Decarreau, P. Maroni, A. Robert. Sur les équations confluentes de l'équation de Heun. *Annales de la Societé Scientifique de Bruxelles Série I Sciences Mathématiques, Astronomiques et Physiques* **92**(3):151–189, 1978.

[9] K. Heun. Zur Theorie der Riemann'schen Functionen zweiter Ordnung mit vier Verzweigungspunkten. *Mathematische Annalen* **33**(2):161–179, 1888. https://doi.org/10.1007/BF01443849.

[10] F. Beukers, A. van der Waall. Lamé equations with algebraic solutions. *Journal of Differential Equations* **197**(1):1–25, 2004. https://doi.org/10.1016/j.jde.2003.10.017.

[11] A. Turbiner. On polynomial solutions of differential equations. *Journal of Mathematical Physics* **33**(12):3989–3993, 1992. https://doi.org/10.1063/1.529848.

[12] R. V. Craster, V. H. Hoàng. Applications of Fuchsian differential equations to free boundary problems. *Proceedings of the Royal Society A Mathematical, Physical and Engineering Sciences* **454**(1972):1241–1252, 1998. https://doi.org/10.1098/rspa.1998.0204.

[13] P. P. Fiziev. The Heun functions as a modern powerful tool for research in different scientific domains, 2015. arXiv:1512.04025v1.

[14] Mathematical physics. In U. Camcı, I. Semiz (eds.), *Proceedings of the 13th Regional Conference held in Antalya, October 27–31, 2010*, pp. 23–39. World Scientific Publishing Co. Pte. Ltd., Hackensack, NJ, 2013. https://doi.org/10.1142/8566.

[15] H. Ciftci, R. L. Hall, N. Saad, E. Dogu. Physical applications of second-order linear differential equations that admit polynomial solutions. *Journal of Physics A: Mathematical and Theoretical* **43**(41):415206, 14, 2010. https://doi.org/10.1088/1751-8113/43/41/415206.

[16] Y.-Z. Zhang. Exact polynomial solutions of second order differential equations and their applications. *Journal of Physics A: Mathematical and Theoretical* **45**(6):065206, 2012. https://doi.org/10.1088/1751-8113/45/6/065206.

[17] B.-H. Chen, Y. Wu, Q.-T. Xie. Heun functions and quasi-exactly solvable double-well potentials. *Journal of Physics A: Mathematical and Theoretical* **46**(3):035301, 2013. https://doi.org/10.1088/1751-8113/46/3/035301.

[18] F. Caruso, J. Martins, V. Oguri. Solving a two-electron quantum dot model in terms of polynomial solutions of a Biconfluent Heun equation. *Annals of Physics* **347**:130–140, 2014. https://doi.org/10.1016/j.aop.2014.04.023.

[19] A. V. Turbiner. One-dimensional quasi-exactly solvable Schrödinger equations. *Physics Reports A Review Section of Physics Letters* **642**:1–71, 2016. https://doi.org/10.1016/j.physrep.2016.06.002.

[20] H. Karayer, D. Demirhan, F. Büyükkılıç. Solution of Schrödinger equation for two different potentials using extended Nikiforov-Uvarov method and polynomial solutions of biconfluent Heun equation. *Journal of Mathematical Physics* **59**(5):053501, 2018. https://doi.org/10.1063/1.5022008.

[21] H. Ciftci, R. L. Hall, N. Saad. Asymptotic iteration method for eigenvalue problems. *Journal of Physics A: Mathematical and General* **36**(47):11807–11816, 2003. https://doi.org/10.1088/0305-4470/36/47/008.

[22] H. Scheffé. Linear differential equations with two-term recurrence formulas. *Journal of Mathematics and Physics* **21**(1-4):240–249, 1942. https://doi.org/10.1002/sapm1942211240.

[23] R. S. Irving. *Integers, polynomials, and rings*. Springer-Verlag, New York, 2004. https://doi.org/10.1007/b97633.

[24] F. M. Arscott. Latent roots of tri-diagonal matrices. *Edinburgh Mathematical Notes* **44**:5–7, 1961. https://doi.org/10.1017/S095018430000330X.

[25] J. Favard. Sur les polynômes de Tchebicheff. *Comptes Rendus Hebdomadaires des Séances de l'Académie des Sciences, Paris* **200**:2052–2053, 1935.

[26] F. Marcellán, R. Álvarez Nodarse. On the "Favard theorem" and its extensions. *Journal of Computational and Applied Mathematics* **127**(1-2):231–254, 2001. https://doi.org/10.1016/S0377-0427(00)00497-0.

[27] M. E. H. Ismail. *Classical and quantum orthogonal polynomials in one variable*. Cambridge University Press, Cambridge, 2009.

[28] A. Krajewska, A. Ushveridze, Z. Walczak. Bender-Dunne orthogonal polynomials general theory. *Modern Physics Letters A* **12**(16):1131–1144, 1997. https://doi.org/10.1142/S0217732397001163.

MODIFIED KORTEWEG-DE VRIES EQUATION AS A SYSTEM WITH BENIGN GHOSTS

Andrei Smilga

University of Nantes, SUBATECH, 4 rue Alfred Kastler, BP 20722, Nantes 44307, France
correspondence: smilga@subatech.in2p3.fr

Abstract. We consider the modified Korteweg-de Vries equation, $u_{xxx} + 6u^2u_x + u_t = 0$, and explore its dynamics in *spatial* direction. Higher x derivatives bring about the *ghosts*. We argue that these ghosts are benign, i.e., the classical dynamics of this system does not involve a blow-up. This probably means that the associated quantum problem is also well defined.

Keywords: Benign ghosts, KdV equation, integrability.

1. Introduction

A system with ghosts is, by definition, a system where the quantum Hamiltonian has no ground state so its spectrum involves the states with arbitrarily low and arbitrarily high energies. In particular, all non-degenerate theories with higher derivatives in the Lagrangian (but not only them!) involve ghosts. The ghosts show up there already at the classical level: the Ostrogradsky Hamiltonians of higher derivative systems [1] include the linear in momenta terms and are thus not positive definite [2]. This brings about the ghosts in the quantum problem [3, 4].

In many cases, ghost-ridden systems are sick – the Schrödinger problem is not well posed and unitarity is violated. Probably, the simplest example of such a system is a system with the Hamiltonian describing the 3-dimensional motion of a particle in an attractive $\frac{1}{r^2}$ potential:

$$H = \frac{\vec{p}^2}{2m} - \frac{\kappa}{r^2}\,. \qquad (1)$$

For certain initial conditions, the particle falls to the center in a finite time, as is shown in Figure 1.

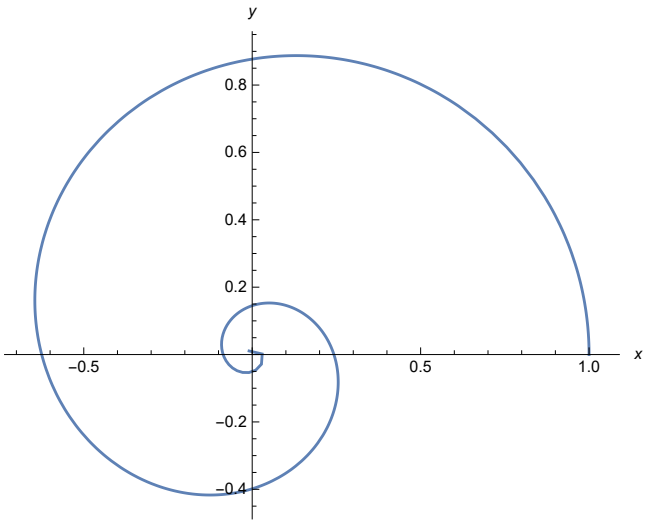

Figure 1. Falling on the center for the Hamiltonian (1) with $m = 1$ and $\kappa = .05$. The energy is slightly negative. The particles with positive energies escape to infinity.

The quantum dynamics of this system depends on the value of κ. If $m\kappa < 1/8$, the ground state exists and unitarity is preserved. If $m\kappa > 1/8$, the spectrum is not bounded from below and, what is worse, the quantum problem cannot be well posed until the singularity at the origin is smoothed out [5–7]. One can say that for $m\kappa < 1/8$, the quantum fluctuations cope successfully with the attractive force of the potential and prevent the system from collapsing.

The latter example suggests that quantum fluctuations can only make a ghost-ridden system better, not worse. We, therefore, *conjecture* that, if the classical dynamics of the system is benign, i.e., the system does not run into singularity in finite time,[1] its quantum dynamics will also be benign, irrespectively of whether the spectrum has, or does not have, a bottom.

This all refers to ordinary mechanical or field theory systems, where energy is conserved and the notion of Hamiltonian exists. The ghosts in gravity (especially, in higher-derivative gravity) are special issue that we are not discussing here.

Besides malignant ghost-ridden systems, of which the system (1) with $m\kappa > 1/8$ represents an example, there are also many systems with ghosts, which are *benign* – unitarity is preserved and the quantum Hamiltonian is self-adjoint with a well-defined real spectrum. To begin with, such is the famous *Pais-Uhlenbeck oscillator* [10] – a higher derivative system

[1] We still call a system benign if it runs into a singularity at $t = \infty$. Such systems have well-defined quantum dynamics. This refers, for example, to the problem of motion in a uniform electric field (see e.g. [8], §24) and also to the inversed oscillator with the Hamiltonian $H = (p^2 - x^2)/2$. In the latter problem, the classical trajectories $x(t)$ grow exponentially with time, but the quantum problem is still benign (see e.g. [9], Ch. 3, corollary 13). The spectrum in this case is continuous, as it is for the uniform field problem.

with the Lagrangian

$$L = \frac{1}{2}\left[\ddot{x}^2 - (\omega_1^2+\omega_2^2)\dot{x}^2 + \omega_1^2\omega_2^2 x^2\right]. \qquad (2)$$

This system is free, its canonical Hamiltonian can be reduced to the difference of the two oscillator Hamiltonians by a canonical transformation [11]. The first example of a nontrivial benign ghost system involving nonlinear interactions was built up in [12]. For other such examples, see Refs. [13–17].

In recent [18], we outlined two wide classes of benign ghost systems: *(i)* the systems obtained by a variation of ordinary systems and involving, compared to them, a double set of dynamic variables and *(ii)* the systems describing geodesic motion over Lorenzian manifolds. In addition, we noticed that the evolution of the modified Korteweg-de Vries (MKdV) system (9) in the *spatial* direction also exhibits a benign ghost dynamics. This report is mostly based on section 4 of [18] that deals with MKdV dynamics.

2. Spatial dynamics of KdV and MKdV equations

First, consider the ordinary KdV equation,

$$u_{xxx} + 6uu_x + u_t = 0\,, \qquad (3)$$

where $u_x = \partial u/\partial x, u_t = \partial u/\partial t$ etc. It has an infinite number of integrals of motion and is exactly soluble.[2] The KdV equation is derived from the field Lagrangian

$$L[\psi(t,x)] = \frac{1}{2}\psi_{xx}^2 - \psi_x^3 - \frac{1}{2}\psi_t\psi_x \qquad (4)$$

if one denotes $u(t,x) \equiv \psi_x$ after having varied over $\psi(t,x)$. This Lagrangian involves higher spatial derivatives, but not higher time derivatives and does not involve ghosts in the ordinary sense. We can, however, simply *rename*

$$t \to X, \qquad x \to T\,, \qquad (5)$$

in which case the equation acquires the form

$$u_{TTT} + 6uu_T + u_X = 0 \qquad (6)$$

and higher time derivatives appear. According to our conjecture, to study the question of whether the quantum Hamiltonian corresponding to the thus rotated Lagrangian (4) is Hermitian and unitarity is preserved, it is sufficient to study its classical dynamics: if it does not involve a blow-up and all classical trajectories exist at all times T, one can be sure that the quantum system is also benign.

Note that the question whether or not blowing up trajectories are present is far from being trivial. The ordinary Cauchy problem for the equation (4) consists in setting the initial value of $u(t_0,x)$ at a given time moment, say, $t_0 = 0$. And we are now interested [staying with Eq. (4) and not changing the name of the variables according to (5)] in the Cauchy problem in x direction. The presence of third spatial derivatives in (4) makes it necessary to define, at the line $x = x_0$, *three* different functions: $u(t,x_0), u_x(t,x_0)$ and $u_{xx}(t,x_0)$. The presence of three arbitrary functions makes the space of solutions to the spatial Cauchy problem much larger than for the ordinary Cauchy problem. The solutions to the latter represent a subset of measure zero in the set of the solutions in the former, and the fact that the solutions to the ordinary Cauchy problem are all benign does not mean that it is also the case for the rotated x-directed problem.

And, indeed, for the ordinary KdV equation (4), the problem is *not* benign. It is best seen if we choose a t-independent Ansatz $u(t,x) \to u(x)$ and plug it into (3). The equation is reduced to

$$\partial_x(u_{xx} + 3u^2) = 0 \quad \Longrightarrow \quad u_{xx} + 3u^2 = C\,. \qquad (7)$$

This equation describes the motion in the cubic potential $V(u) = u^3 - Cu$. It has blow-up solutions. If $C = 0$, they read

$$u(x) = -\frac{2}{(x-x_0)^2}\,. \qquad (8)$$

However, the situation is completely different for the *modified* KdV equation,[3]

$$u_{xxx} + 6u^2u_x + u_t = 0\,. \qquad (9)$$

This equation admits an infinite number of integrals of motion, as the ordinary KdV equation does. The first three local conservation laws are

$$\partial_t u = -\partial_x(u_{xx} + 2u^3)\,, \qquad (10)$$

$$\partial_t u^2 = -2\partial_x\left[\frac{3}{2}u^4 + uu_{xx} - \frac{1}{2}u_x^2\right], \qquad (11)$$

$$\partial_t\left(\frac{1}{2}u^4 - \frac{1}{2}u_x^2\right) = \partial_x\left[u_x(2u^2u_x + \frac{1}{2}u_{xxx}) - \frac{1}{2}u_{xx}^2 - 2u^3u_{xx} - 2u^6\right] \qquad (12)$$

For the time-independent Ansatz, we obtain, instead of (7),

$$\partial_x(u_{xx} + 2u^3) = 0 \quad \Longrightarrow \quad u_{xx} + 2u^3 = C\,. \qquad (13)$$

This describes the motion in a *quartic* potential $V(u) = u^4/2 - Cu$. This motion is bounded, the solutions being elliptic functions.

[2] Exact solvability always makes the behaviour of a system more handy. In particular, many mechanical models including benign ghosts, which were mentioned above, are exactly solvable.

[3] In Ref. [18], we wrote this equation as

$$u_{xxx} + 12\kappa u^2u_x + u_t = 0$$

and kept κ in all subsequent formulas. But here, we have chosen, for simplicity, to fix $\kappa = 1/2$.

This observation presents an argument that the rotated Cauchy problem for the equation (9) with arbitrary initial conditions on the line $x = const$ might be benign.

Note that this behaviour is specific for the equation (9) with the positive sign of the middle term (the so-called *focusing* case). Plugging the time-independent Ansatz in the *defocusing* MKdV equation,[4]

$$u_{xxx} - 6u^2 u_x + u_t = 0\,, \tag{14}$$

the problem would be reduced to the motion in the potential $V(u) = -u^4/2 - Cu$ characterized by a blow-up. This conforms to the well-known fact that any solution $u(t,x)$ of the ordinary KdV equation is related to a solution $v(t,x)$ of the defocusing MKdV equation by the Miura transformation,

$$u \;=\; -(v^2 + v_x)\,. \tag{15}$$

A different (though related) analytic argument indicating the absence of real blow-up solutions for the focusing MKdV equation comes from the analysis of its scaling properties. It is easily seen that Eq. (9) is invariant under the rescalings $u = \lambda_u \bar{u}$, $x = \lambda_x \bar{x}$, $t = \lambda_t \bar{t}$ if

$$\lambda_t = \lambda_x^3, \qquad \lambda_u = \lambda_x^{-1}\,. \tag{16}$$

The quantities xu and $x/t^{1/3}$ are invariant under these rescalings. Using also the space and time translational invariance of the MKdV equation, we can look for scaling solutions of the type

$$u(t,x) = \frac{1}{[3(t-t_0)]^{1/3}} w(z)\,, \tag{17}$$

where

$$z \;=\; \frac{x - x_0}{[3(t-t_0)]^{1/3}}\,. \tag{18}$$

Inserting the ansatz (17) in Eq. (9), one easily verifies that the function $w(z)$ satisfies the equation

$$0 = w''' + (6w^2 - z)w' - w = \frac{d}{dz}\left[w'' + 2w^3 - zw\right] \tag{19}$$

Denoting the constant value of the bracket in the last right-hand side as C, we conclude that $w(z)$ satisfies a second-order equation,

$$w'' = -2w^3 + zw + C\,. \tag{20}$$

For the equation (14), the same analysis would give the equation

$$w'' = 2w^3 + zw + C\,. \tag{21}$$

These are Painlevé II equations [19]. In general, Painlevé equations have pole singularities. And indeed, a local analysis of Eq. (21) (keeping the leading-order terms $w'' \approx 2w^3$) shows that (21) admits simple poles, $w(z) \approx \pm 1/(z - z_0)$. The existence of a real simple pole at $z = z_0$ would then correspond to a singular (blow-up) behavior of $u(t,x)$ of the form $u(t,x) \propto \left[x - x_0 - z_0[3(t-t_0)]^{1/3}\right]^{-1}$. But for the equation (20) [and hence for (9)], the singularities are absent.

[4] The coefficient 6 is a convention. It can be changed by rescaling t and x. But the sign stays invariant under rescaling.

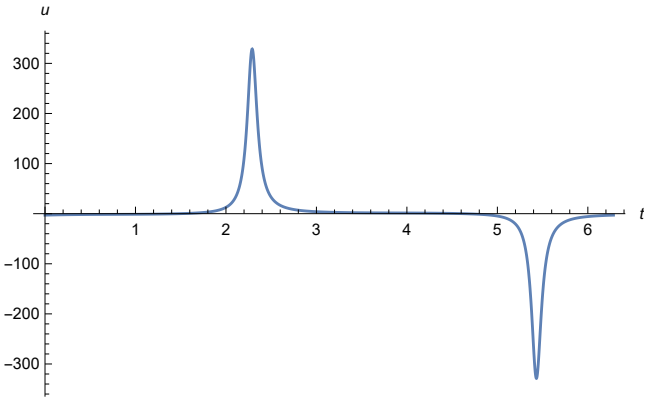

Figure 2. $u(t, x = 2.26)$ for the defocusing MKdV.

The third argument in favor of the conjecture that the x evolution of sufficiently smooth Cauchy data on the line $x = const$ for the MKdV equation (9) does not bring about singularities in $u(t,x)$ comes from numerical simulations. To simplify the numerical analysis, we considered the problem on the band $0 \leq t \leq 2\pi$, where we imposed [as is allowed by Eq. (9)] periodic boundary conditions:

$$u(t + 2\pi, x) \;=\; u(t,x)\,. \tag{22}$$

We have chosen the Cauchy data

$$u(t,0) \;=\; \sin t,\; u_x(t,0) \;=\; u_{xx}(t,0) \;=\; 0\,. \tag{23}$$

We first checked that the use of such Cauchy data for the defocusing MKdV equation (14) was leading to a blow-up rather fast (at $x = 2.2630\ldots$). This is illustrated in Figure 2, where the function $u(t,x)$ is plotted just before the blow-up, at $x = 2.26$.

By contrast, our numerical simulations of the x evolution of the focusing MKdV equation showed that $u(t,x)$ stayed bounded for all the values of x that we explored. We met, however, another problem associated with the *instability* of Eq. (9) under high-frequency (HF) perturbations.

Suppressing the nonlinear term in the KdV or MKdV equations, we obtain

$$u_{xxx} + u_t = 0\,. \tag{24}$$

This equation describes the fluctuations around the solution $u(t,x) = 0$. Its analysis gives us an idea about the behaviour of fluctuations around other solutions. Decomposing $u(t,x)$ as a Fourier integral, in plane waves $e^{\mathrm{i}(\omega t + kx)}$, we obtain the dispersion law

$$\omega = k^3\,. \tag{25}$$

If one poses the conventional Cauchy problem with some Fourier-transformable initial data

$$u(0,x) = v(x) \equiv \int \frac{dk}{2\pi}\, v(k) e^{\mathrm{i}kx}\,, \tag{26}$$

the time evolution of the initial data $v(x)$ yields the solution

$$u(t,x) = \int \frac{dk}{2\pi}\, v(k) e^{\mathrm{i}(k^3 t + kx)}\,. \tag{27}$$

The important point here is that $u(t,x)$ is obtained from $v(k)$ by a purely oscillatory complex kernel $e^{\mathrm{i}(k^3t+kx)}$ of unit modulus. It has been shown that this oscillatory kernel has *smoothing* properties (see, e.g., [20]). This allows one to take the initial data in low-s Sobolev spaces H^s (describing pretty rough initial data).

However, if one considers the x-evolution Cauchy problem, one starts from three independent functions of t along the $x = 0$ axis: $u(t,0) = u_0(t)$, $u_x(t,0) = u_1(t)$ and $u_{xx}(t,0) = u_2(t)$, as in (23). Assuming that the three Cauchy data $u_a(t)$, $a = 0,1,2$, are Fourier-transformable, we can represent them as

$$u_a(t) \;=\; \int \frac{d\omega}{2\pi}\, u_a(\omega) e^{\mathrm{i}\omega t}\,. \tag{28}$$

The three Cauchy data determine a unique solution which, when decomposed in plane waves, satisfies the same dispersion law (25) as before. However, the dispersion law (25) must now be solved for k in terms of ω. As it is a cubic equation in k, it has *three different roots*:

$$k_a(\omega) \;=\; \omega^{\frac{1}{3}} e^{2\pi i a/3} \qquad a = 0,1,2\,. \tag{29}$$

This yields a solution for $u(t,x)$ of the form

$$u(t,x) = \sum_{a=0,1,2} \int \frac{d\omega}{2\pi}\, v_a(\omega) e^{\mathrm{i}(\omega t + k_a x)}\,, \tag{30}$$

where the three coefficients $v_a(\omega)$ are uniquely determined by the three initial conditions at $x = 0$. The point of this exercise was to exhibit the fact that, when considering the x evolution with arbitrary Cauchy data $u_0(t)$, $u_1(t)$, $u_2(t)$, the solution involves *exponentially growing* modes in the x direction, linked to the imaginary parts of $k_1(\omega)$ and $k_2(\omega)$.

This can be avoided if the initial data are sufficiently smooth, not involving HF modes. As a minimum condition for a local existence theorem, one should require the Fourier transforms $v_a(\omega)$ to decrease like $e^{-\alpha|\omega|^{\frac{1}{3}}}$ for some positive constant α.[5]

However, it is difficult to respect these essential smoothness constraints on the behavour of $u(t,x)$ in the numerical calculations. The standard Mathematica algorithms do not do so, and that is why we, starting from some values of x, observe the HF noise in our results.

[5]See Ref. [18] for more detailed discussion.

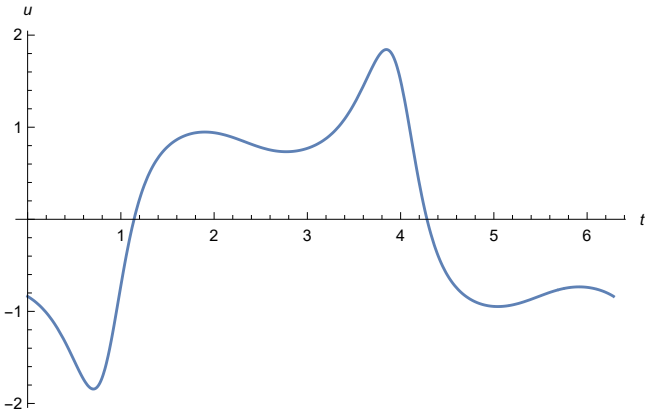

FIGURE 3. $u(t, x = 3)$ for the focusing MKdV.

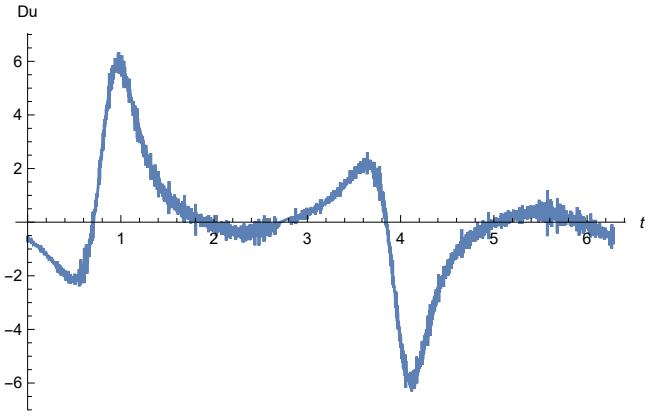

FIGURE 4. $u_x(t, x = 3)$ for the focusing MKdV.

In Figures 3, 4, we present the results of numerical calculations of $u(t,x)$ and $u_x(t,x)$ for $x = 3$. There is no trace of a blow-up. For the plot of $u(t,x)$, one also does not see a HF noise, but it is seen in the plot for $u_x(t,x)$. For larger values of x, the noise also shows up in the plot of $u(t,x)$. At $x \gtrsim 3.8$, the noise overwhelms the signal.

The observed noise is a numerical effect associated with a finite computer accuracy. To confirm this, we performed a different calculation choosing the initial conditions which correspond to the exact solitonic solution to Eq. (9).

The soliton is a travelling wave, $u(t,x) = u(x-ct) \equiv u(\bar{x})$. Plugging this Ansatz into (9), we obtain an ordinary differential equation

$$\frac{\partial}{\partial \bar{x}} \left[u_{\bar{x}\bar{x}} + 2u^3 - cu \right] = 0\,. \tag{31}$$

Denoting the constant quantity within the bracket as C', we then get the following second-order equation for the function $u(\bar{x})$:

$$u_{\bar{x}\bar{x}} = -\frac{d}{du}\mathcal{V}(u)\,, \tag{32}$$

with a potential function $\mathcal{V}(u)$ now given by

$$\mathcal{V}(u) \;=\; \frac{u^4 - cu^2}{2} - C'u\,. \qquad (33)$$

As was also the case for the time-independent Ansatz, the problem is reduced to the dynamics of a particle moving in the confining quartic potential $\mathcal{V}(u)$. The trajectory of the particle depends on three parameters: the celerity c, the constant C', and the particle energy,

$$E = \frac{1}{2}u_{\bar{x}}^2 + \mathcal{V}(u)\,. \qquad (34)$$

The usually considered solitonic solutions (such that $u(\bar{x})$ tends to zero when $\bar{x} \to \pm\infty$) are obtained by taking $c > 0$, $C' = 0$ (so that the potential represents a symmetric double-well potential) and $E = 0$. The zero-energy trajectory describes a particle starting at "time" $\bar{x} = -\infty$, at $u = 0$ with zero "velocity" $u_{\bar{x}}$, gliding down, say, to the right, reflecting on the right wall of the double well and then turning back to end up, again, at $u = 0$ when $\bar{x} = +\infty$. The explicit form of the corresponding solution defined on the infinite (t, x) plane is

$$u(t,x) \;=\; \frac{\sqrt{c}}{\cosh[\sqrt{c}\,(x - ct)]}\,. \qquad (35)$$

However, to make contact with our numerical calculations, we need a *periodic* soliton solution. Such solutions can be easily constructed by considering bounded mechanical motions in the potential $\mathcal{V}(u)$ having a *non-zero energy*. Periodic solutions exist both for positive and negative c. The trajectories are the elliptic functions. It was more convenient for us to assume $c = -|c|$, in which case we could make contact with Ref. [12], where the expressions for the trajectories of motion in the same quartic potential were explicitly written, one only had to rename the parameters. Choosing $E = 1$ and $c = -1$, we obtain the following solution:

$$u(t,x) \;=\; \mathrm{cn}\left[\sqrt{3}(x+t), m\right], \qquad (36)$$

where $\mathrm{cn}(z)$ is the Jacobi elliptic cosine function with the elliptic modulus $m = 1/3$. The function (36) is periodic both in t and x with the period

$$T \;=\; L \;=\frac{4}{\sqrt{3}}K\left(\frac{1}{3}\right) \;\approx 4\,. \qquad (37)$$

We fixed the initial conditions for $x = 0$ and periodic conditions in time as is dictated by (36), and then numerically solved (9). The numerical solution should reproduce the exact one, and it does for $x \lesssim 4$. However, at larger values of x, the HF noise appears. The result of the calculation for $x = 4.5$ is given in Figure 5.

One can suppress the HF noise by increasing the step size, but then the form of the soliton is distorted. To find a numerical procedure that suppresses the noise and gives correct results for large values of x remains a challenge for future studies.

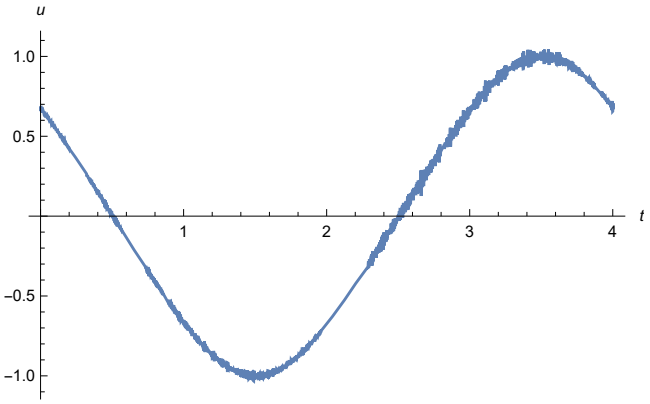

Figure 5. HF noise for the periodic soliton evolution. $x = 4.5$.

3. Discrete models with benign ghosts

One of the possible solutions to this numerical problem could consist in discretizing the model in time direction and assuming that the variable t takes only the discrete values $t = h, 2h, \cdots, Nh$, for some integer $N \geq 3$ and by replacing the continuous time derivative ψ_t by a discrete (symmetric) time derivative $[\psi(t+h,x) - \psi(t-h,x)]/(2h)$. Then the Lagrangian[6]

$$L[\psi(t,x)] \;=\; \frac{\psi_{xx}^2 - \psi_x^4 - \psi_x\psi_t}{2} \qquad (38)$$

acquires the form

$$L_N = \sum_{k=1}^{N}\left\{\frac{[\psi_{xx}(kh,x)]^2 - [\psi_x(kh,x)]^4}{2} - \right.$$
$$\left.\frac{1}{2}\psi_x(kh,x)\frac{\psi[(k+1)h,x] - \psi[(k-1)h,x]}{2h}\right\}, \qquad (39)$$

where we impose the periodicity: $\psi(0,x) \equiv \psi(Nh,x)$ and $\psi[(N+1)h,x] \equiv \psi(h,x)$.[7]

The Lagrangian (39) includes a finite number of degrees of freedom and represents a mechanical system. This system involves higher derivatives in x (playing the role of time) and hence involves ghosts. Defining the new dynamical variables $a^k(x) = \psi_x(kh,x)$, the equations of motion derived from the Lagrangian (39) read

$$a^k_{xxx} + 6(a^k)^2 a^k_x \;+\; \frac{a^{k+1} - a^{k-1}}{2h} \;=\; 0\,. \qquad (40)$$

There are two integrals of motion: the energy

$$E \;=\; \sum_{k=1}^{N}\left[\frac{(a^k_x)^2 - 3(a^k)^4}{2} - a^k a^k_{xx}\right] \qquad (41)$$

[6] It is quite analogous to (4). After variation with respect to $\psi(t,x)$, one gets Eq. (9) after posing $u(t,x) = \psi_x(t,x)$.

[7] It is also possible to impose the Dirichlet-type boundary conditions, $\psi(0h,x) = \psi[(N+1)h,x] = 0$. For $N = 2$, periodicity cannot be imposed and Dirichlet conditions are the only option.

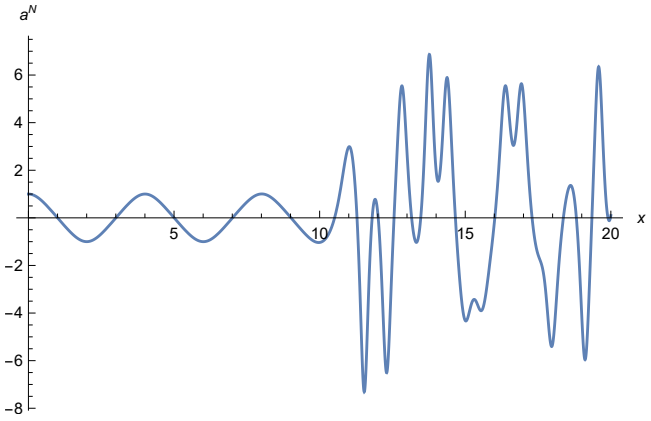

FIGURE 6. The solution of the system (40) for $a^N(x)$ ($N = 350,\ h = T/N$).

and

$$Q \;=\; \sum_{k=1}^{N} \left[a^k_{xx} + 2(a^k)^3\right] . \tag{42}$$

The expression (41) is the discretized version of the integral

$$\int dt \left[\frac{(u_x)^2 - 3u^4}{2} - uu_{xx}\right] \tag{43}$$

in the continuous MKdV system, which is conserved during the x evolution, as follows from the local conservation law (11). The second integral of motion is related to the conservation law (10). By contrast, the currents in the higher conservation laws of the MKdV equation, starting with Eq.(12), do not translate into integrals of motion of the discrete systems. We have only two integrals of motion and many variables, which means that the equation system (40) is not integrable and exhibits a chaotic behaviour.

We fed these equations to Mathematica and found out that their solution stays bounded up to $x = 10000$ and more – the ghosts are benign! This represents a further argument in favour of the conjecture that in the continuous theory the evolution in spatial direction is also benign. Indeed, one may expect that taking larger and larger values of N would allow one to simulate better and better the continuous theory (though the presence of chaos might make such a convergence non uniform in x).

Anyway, we tried the solitonic initial conditions and found out that the discrete system for large $N = 350$ (the limit of Mathematica skills) behaves better than the PDE. As is seen from Figure 6, the discrete solution stays close to the exact soliton solution up to $x \approx 10$, to be compared to $x \approx 4.5$, which was the horizon of the numerical procedure of the previous section. Hopefully, a clever mathematician, an expert in numerical calculations, would be able to increase the horizon even more...

Lastly, we note that, irrespectively to the relationship of the systems (39) to the MKdV equation, these systems represent an interest by their own because they provide a set of nontrivial interacting higher derivative systems with benign ghosts. Such systems were not known before.

ACKNOWLEDGEMENTS

I am grateful to the organizers of the AAMP conference for the invitation to make a talk there. Working on our paper [18], we benefited a lot from illuminating discussions with Piotr Chrusciel, Alberto De Sole, Victor Kac, Nader Masmoudi, Frank Merle and Laure Saint-Raymond.

REFERENCES

[1] M. Ostrogradsky. Mémoire sur les équations differéntielles relatives au problème des isopérimètres. *Mem Acad St Petersbourg* **VI**(4):385, 1850.

[2] R. P. Woodard. Ostrogradsky's theorem on Hamiltonian instability. *Scholarpedia* **10**(8):32243, 2015. https://doi.org/10.4249/scholarpedia.32243.

[3] M. Raidal, H. Veermae. On the quantisation of complex higher derivative theories and avoiding the Ostrogradsky ghost. *Nuclear Physics B* **916**:607–626, 2017. https://doi.org/10.1016/j.nuclphysb.2017.01.024.

[4] A. V. Smilga. Classical and quantum dynamics of higher-derivative systems. *International Journal of Modern Physics A* **32**(33):1730025, 2017. https://doi.org/10.1142/S0217751X17300253.

[5] K. M. Case. Singular potentials. *Physical Review* **80**(5):797–806, 1950. https://doi.org/10.1103/PhysRev.80.797.

[6] K. Meetz. Singular potentials in non-relativistic quantum mechanics. *Il Nuovo Cimento* **34**:690–708, 1964. https://doi.org/10.1007/BF02750010.

[7] A. M. Perelomov, V. S. Popov. "Fall to the center" in quantum mechanics. *Theoretical and Mathematical Physics* **4**:664–677, 1970. https://doi.org/10.1007/BF01246666.

[8] L. D. Landau, E. M. Lifshitz. *Quantum Mechanics*. Elsevier, 1981.

[9] M. Combescure, D. Robert. *Coherent States and Applications in Mathematical Physics*. Springer, 2012. https://doi.org/10.1007/978-94-007-0196-0.

[10] A. Pais, G. E. Uhlenbeck. On field theories with non-localized action. *Physical Review* **79**(1):145–165, 1950. https://doi.org/10.1103/PhysRev.79.145.

[11] P. D. Mannheim, A. Davidson. Dirac quantization of Pais-Uhlenbeck fourth order oscillator. *Physical Review A* **71**:042110, 2005. https://doi.org/10.1103/PhysRevA.71.042110.

[12] D. Robert, A. V. Smilga. Supersymmetry versus ghosts. *Journal of Mathematical Physics* **49**(4):042104, 2008. https://doi.org/10.1063/1.2904474.

[13] M. Pavšič. Stable self-interacting Pais-Uhlenbeck oscillator. *Modern Physics Letters A* **28**(36):1350165, 2013. https://doi.org/10.1142/S0217732313501654.

[14] I. B. Ilhan, A. Kovner. Some comments on ghosts and unitarity: The Pais-Uhlenbeck oscillator revisited. *Physical Review D* **88**(4):044045, 2013. https://doi.org/10.1103/PhysRevD.88.044045.

[15] A. V. Smilga. Supersymmetric field theory with benign ghosts. *Journal of Physics A: Mathematical and Theoretical* **47**(5):052001, 2014. https://doi.org/10.1088/1751-8113/47/5/052001.

[16] A. V. Smilga. On exactly solvable ghost-ridden systems. *Physics Letters A* **389**:127104, 2021. https://doi.org/10.1016/j.physleta.2020.127104.

[17] C. Deffayet, S. Mukohyama, A. Vikman. Ghosts without runaway instabilities. *Physical Review Letters* **128**(4):041301, 2022. https://doi.org/10.1103/PhysRevLett.128.041301.

[18] T. Damour, A. V. Smilga. Dynamical systems with benign ghosts. *Physical Review D* (in press), arXiv:2110.11175.

[19] P. A. Clarkson. Painlevé equations – nonlinear special functions. *Journal of Computational and Applied Mathematics* **153**(1-2):127–140, 2003. https://doi.org/10.1016/S0377-0427(02)00589-7.

[20] C. E. Kenig, G. Ponce, L. Vega. Well-posedness of the initial value problem for the Korteweg-de Vries equation. *Journal of the American Mathematical Society* **4**(2):323–347, 1991. https://doi.org/10.1090/S0894-0347-1991-1086966-0.

COMPLEX TOPOLOGICAL SOLITON WITH REAL ENERGY IN PARTICLE PHYSICS

Takanobu Taira

City, University of London, Department of Mathematics, Northampton Square, London EC1V 0HB, UK
correspondence: takanobu.taira@city.ac.uk

Abstract. We summarise the procedure used to find the classical masses of Higgs particle, massive gauge boson and t'Hooft-Polyakov monopole in non-Hermitian gauge field theory. Their physical regions are explored, and the mechanism of the real value of the monopole solution is analysed in different physical regions.

Keywords: t'Hooft-Polyakov monopole, quantum field theory, non-Hermitian quantum field theory.

1. Introduction

Quantum field theory is a key tool to analyse particle physics. The most modern physical description of the fundamental particle interaction is described by the model called the Standard Model. However, the model possesses several problems such as incompatibility with the general relativity, hierarchy problem, etc. Therefore, it is an active area to extend the standard model.

Recently a growing number of research papers started exploring the non-Hermitian extension of the Standard Model [1–14]. We have contributed to this development by analysing the Goldstone theorem [8, 10], The Higgs mechanism [9] and t'Hooft-Polyakov monopoles [11]. The classical masses of Higgs particles, massive gauge boson and monopoles were analysed. However, a detailed analysis of their intersecting physical regions and the mechanism of the real value of the energy of monopole was not explored. The main aim of this contribution is to fill this gap.

There are two separate mechanisms that guarantee the real value of the particle masses in question. First, the masses of Higgs particles are given by a non-Hermitian mass matrix M. Assume that the matrix possess anti-linear symmetry, which we refer to as $\mathcal{PT}$ symmetry, that satisfies $[\mathcal{PT}, M] = 0$, $Mv = \lambda v$, $\mathcal{PT}v = e^{i\theta}v$, where $\{v, \lambda\}$ are eigenvectors and eigenvalues of the mass matrix. From this, it is trivial to show that the eigenvalues are real

$$\begin{aligned} \mathcal{PT}Mv_i &= \mathcal{PT}\lambda_i v_i = \lambda_i^* \mathcal{PT}v_i = \lambda_i^* e^{i\theta_i} v_i, \\ \mathcal{PT}Mv_i &= M\mathcal{PT}v_i = Me^{i\theta_i} v_i = \lambda_i e^{i\theta_i} v_i. \end{aligned}$$

It was shown in [8] that this $\mathcal{PT}$ symmetry is related to the $\mathcal{CPT}$ symmetry of the field-theoretic action.

On the other hand, the classical energy of the soliton solution is found by inserting the solution into the Hamiltonian $E = H[\phi] = \int d^3x \mathcal{H}(\phi)$. Therefore, the techniques from $\mathcal{PT}$ symmetric quantum mechanics shown above can not be applied.

We will show below that the energy of the soliton solutions are real when the three conditions stated below holds. Therefore they are *sufficient* conditions to guarantee the real value of particles in the model. However, we do not claim that these are *necessary* conditions.

Let $\{\phi_1, \phi_2\}$ be a set of distinct (or identical) solutions to the equations of motion $\delta\mathcal{L}/\delta\phi - \partial_\mu(\delta\mathcal{L}/\delta\partial_\mu\phi) = 0$, where $\mathcal{L}(\phi)$ is the field-theoretic Lagrangian density. The classical energies of the solution are given by inserting the solution into the Hamiltonian, $E_i = H[\phi_i] = \int d^3x \mathcal{H}(\phi_i)$, for $i \in \{1, 2\}$. The classical mass of the solution ϕ_1 and ϕ_2 are real if there exist some anti-linear symmetry $\mathcal{CPT}$ (note that is it not the standard $\mathcal{CPT}$ symmetry in quantum field theory) such that three conditions are satisfied:

(1.) $\mathcal{CPT} : \mathcal{H}[\phi(x)] \to \mathcal{H}[\mathcal{CPT}\phi(x)] = \mathcal{H}^\dagger[\phi(-x)]$.

(2.) $\mathcal{CPT} : \phi_1(x) \to \phi_2(-x)$.

(3.) $H[\phi_1] = H[\phi_2]$.

If two solutions are identical $\phi_1 = \phi_2$, then the above condition reduces to the reality condition of the soliton solution already derived in [15]. Using the above three conditions, the real value of the classical mass can easily be shown by the following argument

$$\begin{aligned} \int d^3x \mathcal{H}[\mathcal{CPT}\phi(x)] &\overset{(1)}{=} \int d^3x \mathcal{H}^\dagger[\phi(-x)] = M_1^\dagger, \\ &\overset{(2)}{=} \int d^3x \mathcal{H}[\phi_2(-x)] = M_2, \\ \implies M_1^\dagger = M_2 &\overset{(3)}{\implies} M_1^\dagger = M_1, \end{aligned}$$

where numbers above the equal signs indicate the condition number.

The above analysis can be performed directly on the complex model. However, the non-Hermitian theory is only well-defined once the inner-product is identified. The modern way of the well-defined non-Hermitian quantum mechanics was first realised by Frederik Scholtz, Hendrik Geyer, and Fritz Hahne in 1992, [16]. The authors used the mathematical condition on the operator called the *quasi-Hermiticity* (the term was first coined in [17], but the metric was

not given) to define the positive definite inner product. The quasi-Hermiticity is defined as a condition on the bounded linear operator of the Hilbert space $A : \mathcal{H} \to \mathcal{H}$, which satisfies

(i)$\langle v|\rho v\rangle > 0$ for all $|v\rangle \in \mathcal{H}$ and $|v\rangle \neq 0$.

(ii)$\rho A = A^\dagger \rho$.

Where the bounded Hermitian linear operator $\rho : \mathcal{H} \to \mathcal{H}$ is often called the metric operator because the inner product is defined by the operator $\langle\cdot|\cdot\rangle_\rho := \langle\cdot|\rho\cdot\rangle$ restores the Hermiticity of the operator. This result can be shown by using the condition(ii)

$$\langle v|Aw\rangle_\rho \equiv \langle v|\rho Aw\rangle = \langle v|A^\dagger \rho w\rangle = \langle Av|\rho w\rangle = \langle Av|w\rangle_\rho ,$$

for all $|v\rangle , |w\rangle \in \mathcal{H}$. Note that the quasi-Hermiticity alone does not guarantee the real energy spectrum of the Hamiltonian. In fact, one requires two extra conditions.

(iii)The metric operator is invertible.

(iv)$\rho = \eta^\dagger \eta$.

The operator which satisfies only conditions (ii) and (iv) is referred to as the *pseudo-Hermitian* operator, which was first introduced in [18]. These extra conditions were considered in [16] to prove that, given a set of pseudo-Hermitian operators $\mathcal{A} = \{A_i\}$, the metric operator $\rho_\mathcal{A}$ which satisfies conditions (i), (ii), (iii) and (iv) for all operators of set $\mathcal{A}$ is uniquely determined if and only if all operators of the set $\mathcal{A}$ are irreducible on the Hilbert space $\mathcal{H}$. This procedure is analogous to the Dyson mapping first introduced by Freeman Dyson [19] used in the study of nuclear reaction [20–22], which maps the non-Hermitian operator A to Hermitian operator $\eta^{-1}A\eta$ via *Dyson map* η. The relation between the metric operator and the Dyson map is found by utilising the Hermiticity of the expression $\eta^{-1}A\eta$ in the following way

$$\eta^{-1}A\eta = (\eta^{-1}A\eta)^\dagger \implies A\eta^\dagger\eta = \eta^\dagger\eta A^\dagger \implies \eta^\dagger\eta = \rho. \tag{1}$$

We will utilise this mapping to transform the non-Hermitian field-theoretic Hamiltonian to a Hermitian Hamiltonian. This procedure will resolve the issue of complex vacuum solution and Derrick's scaling argument, as we will see below. However, we note that the Dyson map used here introduces a negative kinetic sign in the kinetic term of one of the fields, indicating the ghost field problem. This issue is removed if one further diagonalise the Hamiltonian. Such diagonalisation can be realised via field-redefinition or via another Dyson map. A more detailed discussion of this is found in [23], and a Dyson map which diagonalise the free part of the non-Hermitian Hamiltonian is found in [12].

2. Methods

In this section, we will summarise the method used in [8–11] to find the masses of the Higgs particles, massive gauge particles and t'Hooft-Polyakov monopoles in non-Hermitian gauge field theory. We note that the explicit forms of the similarity transformation will not be discussed in this paper as non-Hermitian and Hermitian theories are isospectral as long as the $\mathcal{CPT}$ symmetry is preserved for Hamiltonian, Higgs particles and monopole solution.

We begin with the non-Hermitian local $SU(2)$ gauge theory with matter fields in the adjoint representation

$$\begin{aligned}\mathcal{L}_2^{\rm ad} &= \frac{1}{4}\mathrm{Tr}\left(D\phi_1\right)^2 + \frac{m_1^2}{4}\mathrm{Tr}(\phi_1^2) \\ &\quad -i\frac{\mu^2}{2}\mathrm{Tr}(\phi_1\phi_2) - \frac{g}{64}\left[\mathrm{Tr}(\phi_1^2)\right]^2 \\ &\quad +\frac{1}{4}\mathrm{Tr}\left(D\phi_2\right)^2 + \frac{m_2^2}{4}\mathrm{Tr}(\phi_2^2) - \frac{1}{8}\mathrm{Tr}\left(F^2\right).\end{aligned} \tag{2}$$

Here we take $g, \mu \in \mathbb{R}$, $m_i \in \mathbb{R}$ and discrete values $c_i \in \{-1, 1\}$. The two fields $\{\phi_i\}_{i=1,2}$ are Hermitian matrices $\phi_i(t,\vec{x}) \equiv \phi_i^a(t,\vec{x})T^a$, where $\phi_i^a(t,\vec{x})$ is a real-valued field. The three generators $\{T^a\}_{a=1,2,3}$ of $SU(2)$ in the adjoint representation are defined by three Hermitian matrices of the form $(T^a)_{bc} = -i\epsilon_{abc}$, satisfying the commutation relation $[T^a, T^b] = i\epsilon^{abc}T^c$. One can check that $Tr(T^aT^b) = 2\delta^{ab}$. The field strength tensor is defined as $F_{\mu\nu} = \partial_\mu A_\nu - \partial_\nu A_\mu - ie[A_\mu, A_\nu]$, where the gauge fields are $A_\mu = A_\mu^a T^a$. The partial derivative is replaced with the covariant derivative $(D_\mu\phi_i)^a := \partial_\mu\phi_i^a + e\varepsilon_{abc}A_\mu^b\phi_i^c$ to compensate for the local symmetry group $SU(2)$.

This action is invariant under the local $SU(2)$ transformation of the matter fields $\phi_i \to e^{i\alpha^a(x)T^a}\phi_i e^{-i\alpha^a(x)T^a}$ and gauge fields $A_\mu \to e^{i\alpha^a(x)T^a}A_\mu e^{-i\alpha^a(x)T^a} + \frac{1}{e}\partial_\mu\alpha^a(x)T^a$. It is also symmetric under modified $\mathcal{CPT}$ symmetry, which transforms two fields, ϕ_1 and ϕ_2 as

$$\begin{aligned}\mathcal{CPT} &: \phi_1(t,\vec{x}) \to \phi_1(-t,-\vec{x}) \\ &: \phi_2(t,\vec{x}) \to -\phi_2(-t,-\vec{x}) \\ &: i \to -i.\end{aligned} \tag{3}$$

The equations of motion for the fields ϕ_i and A_μ of the Lagrangian (2) are

$$\begin{aligned}\left(D_\mu D^\mu\phi_i\right)^a + \tfrac{\delta V}{\delta\phi_i^a} = 0, \\ D_\nu F_a^{\nu\mu} - e\epsilon_{abc}\phi_1^b(D^\mu\phi)^c + e\epsilon_{abc}\phi_2^b(D^\mu\phi)^c = 0,\end{aligned} \tag{4}$$

where repeated indices are summed over. We perform the similarity transformation of the complex Lagrangian (2) by momentary resorting to a quantum theory where we assume an equal time commutation relation between the fields ϕ_i^a and their canonical momenta $\Pi_i^a = \partial_0\phi_i^a$, satisfying the commutation relation $[\phi_i^a(t,\vec{x}), \Pi_j^b(t,\vec{y})] = \delta(\vec{x}-\vec{y})\delta_{ij}\delta_{ab}$. Using this relation, we can transform the corresponding complex Hamiltonian of the Lagrangian (2) by

$$\begin{aligned}H \to e^{\eta_\pm}He^{-\eta_\pm}, \\ \eta_\pm = \textstyle\prod_{a=1}^3 \exp\left(\pm\frac{\pi}{2}\int d^3x\Pi_2^a\phi_2^a\right),\end{aligned} \tag{5}$$

where H is the field-theoretic Hamiltonian of our model (2), obtained via Legendre transformation. This non-uniqueness of the metric is analogous to

the non-uniqueness of the metric and its connection to the observables in the quantum mechanical setting discussed in [16, 24]. The adjoint action of $\eta_\pm$ maps the complex action in the equation (2) into the following real action

$$\begin{aligned}\mathfrak{s} &= \int d^4x\ \frac{1}{4}Tr\left(D\phi_1\right)^2 - \frac{1}{4}Tr\left(D\phi_2\right)^2 \\ &\quad + c_1\frac{m_1^2}{4}Tr(\phi_1^2) - c_2\frac{m_2^2}{4}Tr(\phi_2^2) \\ &\quad - c_3\frac{\mu^2}{2}Tr(\phi_1\phi_2) - \frac{g}{64}\left(Tr(\phi_1^2)\right)^2 - \frac{1}{8}Tr(F^2) \\ &\equiv \int d^4x\ \ \frac{1}{4}Tr\left(D\phi_1\right)^2 - \frac{1}{4}Tr\left(D\phi_2\right)^2 \\ &\quad - V - \frac{1}{8}Tr(F^2).\end{aligned} \tag{6}$$

The parameter c_3 indicates the different similarity transformations by taking the values ± 1 for $\eta_\pm$, respectively.

For convenience, let us rewrite the above real action in terms of each component of the fields ϕ_i^a as

$$\begin{aligned}\mathfrak{L}_2^{\rm ad} &= \frac{1}{2}(D_\mu\phi_i)^a\mathcal{I}_{ij}(D^\mu\phi_j)^a + \frac{1}{2}\phi_i^a H_{ij}\phi_j^a \\ &\quad - \frac{g}{16}\left(\phi_i^a E_{ij}\phi_j^a\right)^2 - \frac{1}{4}F^a_{\mu\nu}F^{a\mu\nu},\end{aligned} \tag{7}$$

where the matrices $H, \mathcal{I}$ and E are defined as

$$H := \begin{pmatrix} m_1^2 & -\mu^2 \\ -\mu^2 & -m_2^2 \end{pmatrix},\ \mathcal{I} := \begin{pmatrix} 1 & 0 \\ 0 & -1 \end{pmatrix}, \tag{8}$$
$$E := \begin{pmatrix} 1 & 0 \\ 0 & 0 \end{pmatrix}.$$

2.1. Higgs and gauge masses

Next, we define the trivial solution of the equations of motion by solving $\delta V = 0$ and $D_\mu\phi_i = 0$. Such vacuum is often referred to as Higgs vacuum. The first equation can be simplified by choosing an Ansatz $(\phi_i^0)^a(t,\vec{x}) = h_i^0\hat{r}^a(\vec{x})$ where $\hat{r} = (x,y,z)/\sqrt{x^2+y^2+z^2}$ and $\{h_i^0\}$ are some constants to be determined. Note that the vacuum solution has a rotational symmetry $SO(3)$ since $\hat{r}^a\hat{r}^a = 1$. Inserting this Ansatz into the equation (7), we find

$$V = -\frac{1}{2}h_i H_{ij} h_j + \frac{g}{16}h_1^4. \tag{9}$$

Then the vacuum equation $\delta V = 0$ is reduced to simple coupled third order algebraic equations

$$\begin{aligned}\frac{g}{4}(h_1^0)^3 - c_1m_1^2h_1^0 + c_3\mu^2h_2^0 &= 0, \\ c_2m_2^2h_2^0 + c_3\mu^2h_1^0 &= 0, \\ D_\mu\phi_\alpha &= 0.\end{aligned} \tag{10}$$

The resulting vacuum solutions are

$$\begin{aligned}h_2^0 = -\tfrac{c_2c_3\mu^2}{m_2^2}h_1^0,\ (h_1^0)^2 = 4\tfrac{c_2\mu^4+c_1m_1^2m_2^2}{gm_2^2} := R^2, \\ (A_i^0)^a = -\tfrac{1}{er}\epsilon^{iaj}\hat{r}^j + \hat{r}^a\mathcal{A}_i,\ (A_0^0)^a = 0.\end{aligned} \tag{11}$$

The $\mathcal{A}_i$ are arbitrary functions of space-time. The Higgs particle can be identified with the fundamental fields of the theory after spontaneous symmetry breaking of the continuous symmetry $SU(2)$ by Taylor expanding around the vacuum solution. Performing a Taylor expansion around the Higgs vacuum and keeping a focus on the second-order terms with only matter fields ϕ_i^a, the real Lagrangian (7) contains the following term

$$\mathfrak{s} = \int d^4x\ \frac{1}{2}\phi_i^a\left(-\partial_\mu\partial^\mu I_{ij}\delta^{ab} - \tilde{H}_{ij}^{ab}\right)\phi_j^b + \ldots,$$

where $\tilde{H}$ is a 6×6 block diagonal Hermitian matrix. After diagonalising the above term by redefining the fields with the eigenvectors of the non-Hermitian mass matrix $M_{ij}^{ab} := I_{ik}\delta^{ac}\tilde{H}_{kj}^{cb}$, we find that the masses of the fundamental fields after the symmetry breaking to be equal to the eigenvalues of M_{ij}^{ab} given as

$$m_0^2 = c_2\frac{\mu^4 - m_2^4}{m_2^2}\ ,\quad m_\pm^2 = K \pm \sqrt{K^2+2L}, \tag{12}$$

where $K = c_1m_1^2 - c_2\frac{m_2^2}{2} + \frac{3\mu^4}{2c_2m_2^2}$ and $L = \mu^4 + c_1c_2m_1^2m_2^2$. Notice that we only find three non-zero eigenvalues. The redefined fields with zero masses (eigenvalues) are called Goldstone fields, which can be absorbed into gauge fields A_μ^a by defining the new massive gauge fields. This process of giving mass to the previously massless fields is called the Higgs mechanism. The mass of the gauge fields can be found by expanding the kinetic term of ϕ around the Higgs vacuum $\phi_i^0 = h_i^0\hat{r}^a$. Without loss of generality, we can choose a particular direction of the vacuum by taking $\hat{r} = (0,0,1)^T$. This is possible due to the symmetry of the $SO(3)$ vacuum as discussed above. Keeping the term only quadratic in the gauge field, we find

$$\begin{aligned}&\frac{1}{2}(D_\mu\phi_i + D_\mu\phi_i^0)^a\mathcal{I}_{ij}(D_\mu\phi_i + D_\mu\phi_i^0)^a \\ &= \frac{1}{2}\left(eA_\mu\times\phi_i^0\right)^a\mathcal{I}_{ij}\left(eA_\mu\times\phi_j^0\right)^a + \ldots \\ &= \frac{1}{2}e^2h_i^0\mathcal{I}_{ij}h_j^0\left(A_\mu^1A^{1\mu} + A_\mu^2A^{2\mu}\right) + \ldots \\ &= \frac{1}{2}m_g^2\left(A_\mu^1A^{1\mu} + A_\mu^2A^{2\mu}\right) + \ldots,\end{aligned} \tag{13}$$

where the mass of the gauge field is identified to be $m_g := \sqrt{h_i^0\mathcal{I}_{ij}h_j^0} = e\frac{R\sqrt{m_2^4-\mu^4}}{m_2^2}$.

2.2. t'Hooft-Polyakov monopole

To find the monopole solutions, let us consider the following Ansatz

$$\begin{aligned}(\phi_i^{cl})^a(\vec{x}) = h_i(r)\hat{r}^a\ ,\ (A_i^{cl})^a = \epsilon^{iaj}\hat{r}^jA(r)\ , \\ (A_0^{cl})^a = 0,\end{aligned} \tag{14}$$

where the subscript cl denotes the classical solutions to the equations of motion (4). The difference between this Ansatz (14) and the Higgs vacuum (11)

is that the quantity h_i now depends on the spatial radius $h_i = h_i(r)$. Here we are only considering the static Ansatz to simplify our calculation, but one may, of course, also consider the time-dependent solution by utilising the Lorentz symmetry of the model and performing a Lorentz boost. According to Derrick's scaling argument [25], for the monopole solution to have finite energy, we require the two matter fields of the equation (14) to approach the vacuum solutions in the equation (11) at spatial infinity

$$\lim_{r\to\infty} h_1(r) = h_1^{0\pm} = \pm R \ , \qquad (15)$$
$$\lim_{r\to\infty} h_2(r) = h_2^{0\pm} = \mp\frac{c_2 c_3 \mu^2}{m_2^2} R.$$

Also, notice that at some fixed value of the radius r, the vacuum solutions ϕ_α^0 and monopole solutions ϕ_α^{cl} both belongs to the 2-sphere in the field configuration space. For example, ϕ_1^0 belongs to the 2-sphere with radius R because $(\phi_1^0)^2 = R^2$. Therefore, solutions ϕ_i^{cl} can be seen as a mapping between 2-sphere in space-time (where the radius is given by the profile function h_i) to 2-sphere in field configuration space. Such mapping has a topological number called the winding number $n \in \mathbb{Z}$, which can be explicitly realised by redefining the unit vector $\hat{r}^a$ as

$$\hat{r}_n^a = \begin{pmatrix} \sin(\theta)\cos(n\varphi) \\ \sin(\theta)\sin(n\varphi) \\ \cos(\theta) \end{pmatrix}. \qquad (16)$$

Therefore different n represent topologically inequivalent solutions.

Since we require the monopole and vacuum solutions to smoothly deformed into each other at spacial infinity, both solutions need to share the same winding number. It is important to note that winding numbers of ϕ_1 and ϕ_2 need to be equal to satisfy $D\phi_1 = D\phi_2 = 0$, and therefore we will denote the winding numbers of ϕ_1 and ϕ_2 as n collectively. If they are not equal, we would have $D\phi_1 = 0$ but $D\phi_2 \neq 0$. Next, let us insert our Ansatz equation (14) into the equations of motion equation (4). We will also redefine the Ansatz for the gauge fields to be $A_i^a = \epsilon^{aib}\hat{r}^b\left(\frac{1-u(r)}{er}\right)$, $A_0^a = 0$, which are more in line with the original Ansatz given in [26, 27], compared to equation (14). Inserting these expressions into the equations of motion equation (4), we find

$$u''(r) + \frac{u(r)\left[1-u^2(r)\right]}{r^2} \qquad (17)$$
$$+\frac{e^2 u(r)}{2}\left\{h_2^2(r) - h_1^2(r)\right\} = 0,$$

$$h_1''(r) + \tfrac{2h_1'(r)}{r} - \tfrac{2h_1(r)u^2(r)}{r^2} \qquad (18)$$
$$+g\left\{-c_1\tfrac{m_1^2}{g}h_1(r) + c_3\tfrac{\mu^2}{g}h_2(r) + \tfrac{1}{4}h_1^3(r)\right\} = 0,$$

$$h_2''(r) + \frac{2h_2'(r)}{r} - \frac{2h_2(r)u^2(r)}{r^2} \qquad (19)$$
$$+c_2 m_2^2\left\{h_2(r) + c_3\frac{\mu^2}{m_2^2}h_1(r)\right\} = 0.$$

Notice that these differential equations are similar to the ones discussed in [26, 27], but with the extra field h_2 and extra differential equation (19). In the Hermitian model, the exact solutions to the differential equations were found by taking the parameter limit called the BPS limit [26, 27], where parameters in the Hermitian model are taken to zero while keeping the vacuum solution finite. Here we will follow the same procedure and take the parameter limit where quantities in the curly brackets of equations (18) and (19) vanish but keep the vacuum solutions equation (11) finite. We will see in section 2.4 that we also find the approximate solutions in this limit.

2.3. The energy bound

Surprisingly, by utilising Derrick's scaling argument, one can find the lower bound of the monopole energy without the explicit form of the solution.

The energy of the monopole can be found by inserting the monopole solution into the corresponding Hamiltonian of equation (6).

$$\begin{aligned} \mathfrak{h} &= \int d^3x \ \ Tr\left(E^2\right) + Tr\left(B^2\right) \qquad (20)\\ &\quad +Tr\left\{(D_0\phi_1)^2\right\} + Tr\left\{(D_i\phi_1)^2\right\} \\ &\quad -Tr\left\{(D_0\phi_2)^2\right\} - Tr\left\{(D_i\phi_2)^2\right\} + V, \end{aligned}$$

where E, B are $E^i{}_a = F_a{}^{0i}$, $B^i{}_a = -\frac{1}{2}\epsilon^{ijk}F_a^{jk}$, $i,j,k \in \{1,2,3\}$. The gauge is fixed to be the radiation gauge (i.e $A_a{}^0 = 0, \partial_i A_a{}^i = 0$). Notice that our monopole Ansatz equation (10) is static with no electric charge $E_i^a = 0$ and therefore, the above Hamiltonian reduces to

$$\begin{aligned} E &= \int d^3x \ \ Tr\left(B^2\right) + Tr\left\{(D_i\phi_1)^2\right\} \qquad (21)\\ &\quad -Tr\left\{(D_i\phi_2)^2\right\} + V \\ &= 2\int d^3x \ \ B_i{}^a B_i{}^a + (D_i\phi_1)^a(D_i\phi_1)^a \\ &\quad -(D_i\phi_2)^a(D_i\phi_2)^a + \frac{1}{2}V. \end{aligned}$$

Here, we simplified our expression by dropping the superscripts $A_i^{cl} \to A_i$, $\phi_\alpha^{cl} \to \phi_\alpha$. We also keep in mind that these fields depend on the winding numbers $n \in \mathbb{Z}$. In the Hermitian model (i.e. when $\phi_2 = 0$), one can rewrite the kinetic term as $B^2 + D\phi^2 = (B - D\phi)^2 + 2BD\phi$ and find the lower bound to be $\int 2BD\phi$. Here we will follow a similar procedure but introduce some arbitrary constant $\alpha, \beta \in \mathbb{R}$ such that $B^2 = \alpha^2 B - \beta^2 B$ where $\alpha^2 - \beta^2 = 1$. This will allow

us to rewrite the above energy as

$$\begin{aligned} E &= 2\int d^3x\ \alpha^2\left\{B_i{}^a+\frac{1}{\alpha}(D_i\phi_1)^a\right\}^2 \\ &\quad -\beta^2\left\{B_i{}^a+\frac{1}{\beta}(D_i\phi_2)^a\right\}^2 \\ &\quad +2\left\{-\alpha B_i{}^a(D_i\phi_1)^a+\beta B_i{}^a(D_i\phi_2)^a\right\}+\frac{1}{2}V. \end{aligned} \tag{22}$$

To proceed from here, we need to assume extra constraints on α and β such that the following inequalities are true

$$\begin{aligned} \int d^3x\ \alpha^2\left\{B_i{}^a+\frac{1}{\alpha}(D_i\phi_1)^a\right\}^2 & \\ -\beta^2\left\{B_i{}^a+\frac{1}{\beta}(D_i\phi_2)^a\right\}^2 &\geq 0, \\ \int d^3xV &\geq 0. \end{aligned} \tag{23}$$

With these constraints we can now write down the lower bound of the monopole as

$$\begin{aligned} E &\geq 2\int d^3x\ \left\{-\alpha B_i{}^a(D_i\phi_1)^a+\beta B_i{}^a(D_i\phi_2)^a\right\} \\ &= 2\int d^3x\ -\alpha\left\{B_i{}^a\partial_i\phi_1^a+eB_i{}^a\epsilon^{abc}A_i{}^b\phi_1^c\right\} \\ &\quad +\beta\left\{B_i{}^a\partial_i\phi_2^a+eB_i{}^a\epsilon^{abc}A_i{}^b\phi_2^c\right\} \\ &= 2\int d^3x\ -\alpha\left\{B_i{}^a\partial_i\phi_1^a+\left(-e\epsilon^{abc}A_i{}^bB_i{}^c\right)\phi_1^a\right\} \\ &\quad +\beta\left\{B_i{}^a\partial_i\phi_2^a+\left(-e\epsilon^{abc}A_i{}^bB_i{}^c\right)\phi_1^a\phi_2^c\right\} \\ &= 2\int d^3x\ -\alpha\left\{B_i{}^a\partial_i\phi_1^a+\partial_iB_i{}^a\phi_1^a\right\} \\ &\quad +\beta\left\{B_i{}^a\partial_i\phi_2^a+\partial_iB_i{}^a\phi_1^a\right\} \\ &= 2\int d^3x\ -\alpha\partial_i\left(B_i{}^a\phi_1{}^a\right)+\beta\partial_i\left(B_i{}^a\phi_2{}^a\right) \\ &= \lim_{r\to\infty}\left(-2\alpha\int_{S_r}dS_iB_i{}^a\phi_1{}^a+2\beta\int_{S_r}dS_iB_i{}^a\phi_2{}^a\right), \end{aligned} \tag{24}$$

where in the fourth line, we used $D_iB_i^a=0$, which can be shown from the Bianchi identity $D_\mu\epsilon^{\mu\nu\rho\sigma}F^a_{\rho\sigma}=0$. The last line is obtained by using the Gauss theorem at some fixed value of the radius r. Since the ϕ_i^a in the integrand is only defined over the 2-sphere with a large radius, we can use the asymptotic conditions (15) and replace the monopole solutions $\{\phi_\alpha^a, B_i^a\}$ with the Higgs vacuum $\{(\phi_\alpha^0)^a, (B_i^0)^a\}$

$$\begin{aligned} E &\geq \left(-2\alpha\phi_1^{0a}+2\beta\phi_2^{0a}\right)\lim_{r\to\infty}\int_{S_r}dS_i(B_i^0)^a \\ &= \left(\mp 2\alpha R\hat{r}_n^a\mp 2\beta\frac{c_2c_3\mu^2}{m_2^2}R\hat{r}_n^a\right)\lim_{r\to\infty}\int_{S_r}dS_i(B_i^0)^a, \end{aligned} \tag{25}$$

where the upper and lower signs of the above energy correspond to the upper and lower signs of the vacuum solutions in equation (11). The explicit value of B_{0i}^a can be obtained by inserting the Higgs vacuum (11) into the definition of the magnetic field

$$B_i^a=-\frac{1}{2}\epsilon_i{}^{jk}\left(\partial_jA_k-\partial_kA_j+eA_j\times A_k\right)^a. \tag{26}$$

After a lengthy calculation, this expression can be simplified to $B_{0i}^a=\hat{\phi^0}^a b_i=\hat{r}_n^a b_i$, where $\hat{\phi^0}^a$ is a normalised solution $\sum_a\hat{\phi^0}^a\hat{\phi^0}^a=1$. The b_i is defined as

$$b_i\equiv-\frac{1}{2}\epsilon_{ijk}\left\{\partial^j\mathcal{A}^k-\partial^k\mathcal{A}^j+\frac{1}{e}\hat{r}_n\cdot\left(\partial^j\hat{r}_n\times\partial^k\hat{r}_n\right)\right\}. \tag{27}$$

Where $\mathcal{A}$ was defined in equation (11). Notice that integrating the first term over the 2-sphere gives zero by Stoke's theorem $\int_S\partial\times\mathcal{A}=\int_{\partial S}\mathcal{A}=0$, where one can show that Stoke's theorem on the closed surface gives zero by dividing the sphere into two open surfaces. The second term is a topological term which can be evaluated as

$$\int dS_iB_i=-\frac{4\pi n}{e}. \tag{28}$$

The explicit calculation is in [28]. This is the magnetic charge of the monopole solutions. Therefore integer n, which corresponds to the winding number of the solution, comes from the Ansatz $B_i^a=\hat{\phi^0}^a b_i$. In our case, there is an ambiguity of whether to choose $B_i^a=\hat{\phi_1^0}^a b_i$ or $B_i^a=\hat{\phi_2^0}^a b_i$. Now we see explicitly the reason why we choose to keep the same integer values for solutions ϕ_1^0 and ϕ_2^0. If the integer values of $\hat{r}_n^a$ in solutions ϕ_1^0, ϕ_2^0 are different, then the integration $\int_{S_r}dS_i(B_i^0)^a$ will be different, leading to inconsistent energy.

Finally, we find our lower bound of the monopole energy

$$\begin{aligned} E &\geq \mp 2R\left(\alpha+\beta\frac{c_2c_3\mu^2}{m_2^2}\right)\hat{r}_n^a\hat{r}_n^a\left(\frac{-4\pi n}{e}\right) \\ &= \frac{\pm 8\pi nR}{e}\left(\alpha+\beta\frac{c_2c_3\mu^2}{m_2^2}\right). \end{aligned} \tag{29}$$

Notice that we have some freedom to choose $\alpha,\beta\in\mathbb{R}$ as long as our initial assumptions (23) are satisfied. We will see in the next section that we can take a parameter limit of our model, which saturates the above inequality and gives exact values to α and β.

2.4. The fourfold BPS scaling limit

Our main goal is now to solve the coupled differential equations (17)-(19). Prasad, Sommerfield, and Bogomolny [26, 27] managed to find the exact solution by taking the parameter limit, which simplifies the differential equations. The multiple scaling limit is taken so that all the parameters of the model tend to zero with some combinations of the parameter remaining finite. The combinations are taken so that the vacuum solutions stay finite in this limit. Inspired by this, we will take here a fourfold scaling limit

$$g,m_1,m_2,\mu\to 0\,,\quad \frac{m_1^2}{g}<\infty\,,\quad \frac{\mu^2}{g}<\infty\,,\quad \frac{\mu^2}{m_2^2}<\infty. \tag{30}$$

This will ensure that the vacuum solutions equation (11) stays finite, but crucially the curly bracket parts

in equations (18) and (19) vanish. There is a physical motivation for this limit in which the mass ratio of the Higgs and gauge mass are taken to be zero (i.e. $m_{\text{Higgs}} << m_g$) as described in [29]. We will see in the next section that the same type of behaviour is present in our model, hence justifying equation (30). The resulting set of differential equations, after taking the BPS limit, is similar to the ones considered in [26, 27] with the slightly different quadratic term in equation (17). It is natural to consider a similar Ansatz as given in [26, 27]

$$u(r) = \frac{evr}{\sinh(evr)}, \tag{31}$$
$$h_1(r) = -\alpha f(r), \tag{32}$$
$$h_2(r) = -\beta f(r), \tag{33}$$

where $\alpha, \beta \in \mathbb{R}$ were introduced in section 2.3 and $f(r) \equiv \left\{v\coth(evr) - \frac{1}{er}\right\}$. One can check that this Ansatz indeed satisfies differential equations equation (17)-(19) in the BPS limit. We have decided to put a prefactor α and β in front of equations (32) and (33) to satisfy the differential equation (17). Note that if we take $\alpha = 1$, we get exactly the same as given in [26, 27], which is known to satisfy the first-order differential equation called the Bogomolny equation $B_i - D_i\phi = 0$. The Ansatz (31)-(33) only differs from the ones given in [26, 27] by the prefactors α and β, and therefore our Ansatz should satisfy the Bogomolny equation with the appropriate scaling to cancel the prefactor in equations (32) and (33)

$$B_i^b + \frac{1}{\alpha}(D_i\phi_1)^b = 0, \tag{34}$$
$$B_i^b + \frac{1}{\beta}(D_i\phi_2)^b = 0, \tag{35}$$

where $\phi_\alpha \equiv h_\alpha(r)\hat{r}_n$. If we compare these equations to the terms appearing in the energy of the monopole equation (22), then we can saturate the inequality in equation (29) by

$$E[\phi_1, \phi_2] = \frac{\pm 8\pi nR}{e}\left(\alpha + \beta\frac{c_2c_3\mu^2}{m_2^2}\right), \tag{36}$$

where upper and lower signs correspond to the vacuum solutions equation (11), when taking the square root. We can calculate the explicit forms of α and β by comparing the asymptotic conditions in equation (15)

$$\lim_{r\to\infty} h_1^\pm = h_1^{0\pm} = \pm R, \tag{37}$$
$$\lim_{r\to\infty} h_2^\pm = h_2^{0\pm} = \mp\frac{c_2c_3\mu^2}{m_2^2}R,$$

with the asymptotic values of equations (31)-(33)

$$\lim_{r\to\infty} u(r) = 0\ ,\ \lim_{r\to\infty} h_1^\pm(r) = -\alpha v, \tag{38}$$
$$\lim_{r\to\infty} h_2^\pm(r) = -\beta v.$$

By Derrick's scaling argument, the two asymptotic values (37) and (38) should match, resulting in algebraic equations for α and β. Using $\alpha^2 - \beta^2 = 1$ and assuming $m_2^4 \geq \mu^4$, we find the four set of real solutions

$$\alpha = \mp(\pm)\frac{m_2^2}{l}\ ,\quad v = (\pm)\frac{Rl}{m_2^2}\ ,\quad \beta = \pm(\pm)\frac{c_2c_3\mu^2}{l}, \tag{39}$$

where $l = \sqrt{m_2^4 - \mu^4}$. The plus-minus signs in the brackets correspond to the two possible solutions to the algebraic equation $\alpha^2 - \beta^2 = 1$. These need to be distinguished from the upper and lower signs of α and β, which correspond to the vacuums solutions (11). Inserting the explicit values of α and β to the energy equation (36) we find

$$E[\phi_1, \phi_2] \equiv (\pm)\frac{8\pi nR}{em_2^2}\left(\frac{-m_2^4 + \mu^4}{l}\right) = (\pm)\frac{-8\pi nR}{em_2^2}l, \tag{40}$$

with corresponding solutions

$$h_1^\pm(r) = \pm(\pm)\frac{m_2^2}{l}\left[\frac{Rl}{m_2^2}\coth\left(\frac{eRl}{m_2^2}r\right) - \frac{1}{er}\right], \tag{41}$$
$$h_2^\pm(r) = \mp(\pm)\frac{c_2c_3\mu^2}{l}\left[\frac{Rl}{m_2^2}\coth\left(\frac{eRl}{m_2^2}r\right) - \frac{1}{er}\right].$$

It is crucial to note that although it seems like there are two monopole solutions $\{h_1^\pm, h_2^\pm\}$, the two solutions are related non-trivially in their asymptotic limit by the constraint $\lim_{r\to\infty} h_2^\pm = (-c_2c_3\mu^2/m_2^2)\lim_{r\to\infty} h_1^\pm$ given in equation (10). For example, one can not choose $\{h_1^+, h_2^-\}$ as a solution as this will break the asymptotic constraint.

The solution (41) can be constrained further by imposing that the energy (40) is real and positive.

$$E[\phi_1, \phi_2] > 0 \implies -(\pm)\frac{8\pi nR}{em_2^2}l \implies -(\pm)n > 0. \tag{42}$$

Therefore we can ensure positive energy if $(\pm) = \text{sign}(n)$. The final form of the monopole solution with positive energy are

$$h_1^\pm(r) = \pm\text{sign}(n)\frac{m_2^2}{l}\left[\frac{Rl}{m_2^2}\coth\left(\frac{eRl}{m_2^2}r\right) - \frac{1}{er}\right], \tag{43}$$
$$h_2^\pm(r) = \mp\text{sign}(n)\frac{c_2c_3\mu^2}{l}\left[\frac{Rl}{m_2^2}\coth\left(\frac{eRl}{m_2^2}r\right) - \frac{1}{er}\right].$$

with energy $E = 8|n|\pi lR/em_2^2$. We conclude this subsection by observing that the above solution depends on the parameter c_3, which takes value $\{-1, 1\}$ depending on the choice of the similarity transformation. Choosing a different values of c_3 also result in a different asymptotic values (37), meaning solutions for $c_3 = 1$ and $c_3 = -1$ are topologically different. Since the energy is independent of c_3, two distinct solutions share the same energy. Respecting one of the main features of similarity transformation, which is to preserve the energy of the transformed Hamiltonian.

In the next section, we will investigate in detail how the solution changes and a new $\mathcal{CPT}$ symmetry emerges by changing the parameter values.

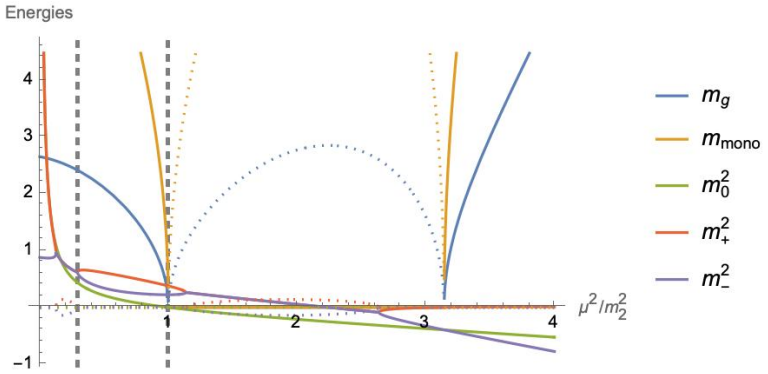

FIGURE 1. Monopole, gauge and Higgs masses plotted for $m_1^2/g = -0.44, \mu/g = -0.14, e = 2, c_1 = -c_2 = -1$. The solid line represents the real part, and the dotted line represents the imaginary part of the masses. The dotted vertical lines indicate the boundaries of the physical regions where all the masses acquire real positive values.

3. Results and discussion

This section will investigate the behaviour of solution (43) in different regimes of the parameter spaces. We will compare the physical regions of gauge particles, Higgs particles and monopoles found in the previous section. We will see that the two regions coincide, but the solutions in different regions possess different $\mathcal{CPT}$ symmetries. Different symmetries of solutions in different regions are not coincident, but the consequence of the three reality conditions stated in the introduction. In fact, it is deeply related to the real value of energy, which will be discussed extensively in [30].

3.1. Higgs mass and exceptional points

Let us recall the masses of the particles and monopole

$$m_0^2 = c_2\tfrac{\mu^4-m_2^4}{m_2^2}\ ,\ m_\pm^2 = K \pm \sqrt{K^2+2L}, \quad (44)$$
$$m_g = e\tfrac{Rl}{m_2^2}, M_{\text{mono}} = \tfrac{8|n|\pi lR}{em_2^2}.$$

where $K = c_1m_1^2 - c_2\frac{m_2^2}{2} + \frac{3\mu^4}{2c_2m_2^2}$ and $L = \mu^4 + c_1c_2m_1^2m_2^2$. Notice that the masses do not depend on c_3, meaning they do not depend on the similarity transformation as expected. We also comment that in the BPS limit, we have $m_0 = m_\pm = 0$, but m_g and $M_\pm$ stays finite, such that the ratios m_{Higgs}/m_g vanish in the BPS limit. This is in line with the Hermitian case [29], providing the physical interpretation with $m_{Higgs} << m_g$ for the BPS limit.

One may notice that when $c_2 = 1$, requiring positive mass $m_0^2 > 0$, implies that $\mu^4 - m_2^4 > 0$. This means the quantity $l = \sqrt{m_2^4 - \mu^4}$ is purely imaginary. One may then discard this region as unphysical. However, we will see in the next section that there is a disconnected region beyond $\mu^4 - m_2^4 > 0$, which admit real energy because R also becomes purely complex. This is not coincident, and in fact, we will see an emerging new $\mathcal{CPT}$ symmetry for the monopoles.

In the rest of the section, we will exclusively focus on the monopole and gauge masses. The main message of this section is the emerging symmetry responsible for the real value of the monopole masses. The requirement to make the whole theory physical demands also to consider the intersection of the physical regions between monopole masses and Higgs masses. As an example, we plot all the masses of the theory in Figure 1.

As one can see, intersection points of the physical regions of Higgs masses and monopole/gauge masses are non-trivial. In fact, they are bounded by two types of exceptional points. The first type is when two masses of Higgs particles coincide and form a complex conjugate pair. Such a point is known as an exceptional point where the mass matrix is non-diagonalisable, and the corresponding eigenvectors coincide. The second type is when the gauge and the monopole masses vanishes. Interestingly, this is where one of the Higgs masses also vanish. Since the mass matrix already has a zero eigenvalue, as the result of the spontaneous symmetry breaking, it seems the number of massless fields is increased. However, at this point, the mass matrix is also non-diagonalisable. Therefore one can not diagonalise the Hamiltonian to identify the field which corresponds to the extra massless fundamental field. Therefore this point is also an exceptional point. However, the eigenvalues do not become complex conjugate pairs beyond this point, and as one can see from Figure 1 that one of the mass square m_0^2 become negative, and gauge and monopole masses become complex but with no conjugate pair. We dub such a point as zero exceptional point to distinguish from the standard exceptional point.

3.2. Change in $\mathcal{CPT}$ symmetry and complex monopole solution

We begin by introducing the useful quantities $m_1^2/g \equiv X, \mu^2/g \equiv Y, \mu^2/m_2^2 \equiv Z$. The gauge mass, monopole mass and monopole solutions can be rewritten in terms of these quantities

$$m_g = eR\sqrt{1-Z^2},\ m_{\text{mono}} = \frac{8|n|\pi R}{e}\sqrt{1-Z^2}, \quad (45)$$

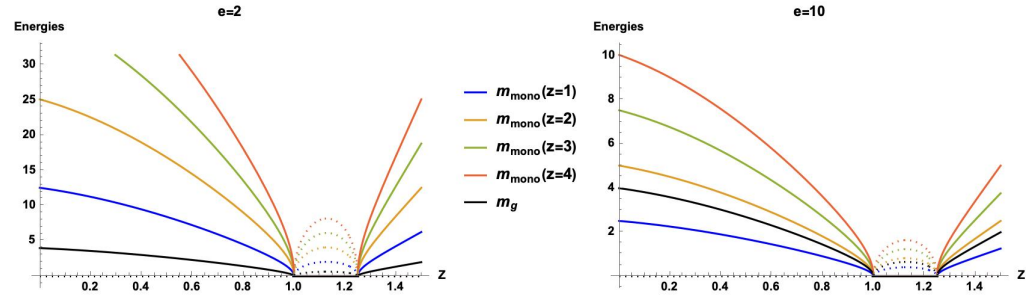

FIGURE 2. Monopole and gauge masses plotted for $X = 1, Y = 0.8, e = 2, c_1 = -c_2 = 1$. The solid line represents the real part, and the dotted line represents the imaginary part of the masses.

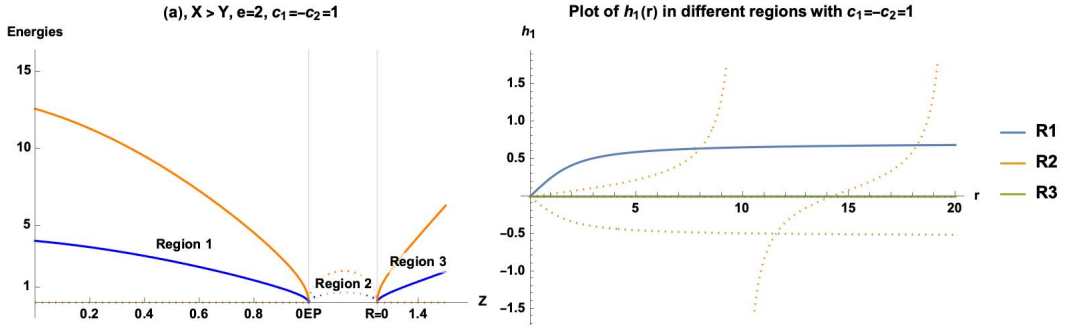

FIGURE 3. Both panels are plotted for $X = 1, Y = 0.8, n = 1, e = 2$. The solid line represents the real part, and the dotted line represents the imaginary part of the masses. Panel (a) shows the monopole and gauge masses against $Z \geq 0$, with vertical lines indicating the location of the boundaries of three regions. Panel (b) shows three profile function $h_1(r)$ defined on each region indicated in panel (a).

$$h_1^{\pm}(r) = \pm\frac{\text{sign}(n)}{\sqrt{1-Z^2}}\left[R\sqrt{1-Z^2}\coth(\hat{r}) - \frac{1}{er}\right], \tag{46}$$

$$h_2^{\pm}(r) = \mp\frac{\text{sign}(n)c_2c_3Z}{\sqrt{1-Z^2}}\left[R\sqrt{1-Z^2}\coth(\hat{r}) - \frac{1}{er}\right], \tag{47}$$

where $R^2 = 4(c_2ZY + c_1X)$ and $\hat{r} = eR\sqrt{1-Z^2}r$. The monopole masses are plotted against the gauge mass for fixed parameters with $n \in \{1, 2, 3, 4\}$ in Figure 2 with weak and strong couplings $e = 2, e = 10$. Notice that the gauge mass is smaller than any of the monopole masses for weak coupling, but when e is large enough, some of the monopole masses can become smaller than the gauge mass. This is clear by inspecting the monopole, and gauge mass in equation (45) and two masses coincide when $e = \sqrt{8|n|\pi}$. Note that $n = 0$ is not a monopole mass as it corresponds to the solution with zero winding number, which is topologically equivalent to the trivial solution.

From Figure 2, we also observe disconnected regions where both monopole and gauge masses become real to purely complex. A more detailed plot of this is shown in Figure 3. Region 2 is bounded by two points with lower bound $\mu^2/m_2^2 = 1$ corresponding to the zero exceptional point where the vacuum manifolds stay finite (i.e. spontaneous symmetry breaking occur). However, the Higgs mechanism fails because the Hamiltonian is non-diagonalisable, as discussed in the previous section. The upper bounds correspond to the point where the vacuum manifold vanishes. Therefore, the spontaneous symmetry breaking does not occur, implying that the gauge fields do not acquire a mass through the Higgs mechanism, resulting in a massless gauge field. Most crucially, an interesting region (denoted by region 3 in Figure 4) reappears as one increases the value of Z. The profile function in region 3 is purely complex, which signals that this may lead to complex energies. However, as one can see from Figure 3, the energy is real. The reason for the real energy is that the conditions stated in the introduction hold. We will specify below the $\mathcal{CPT}$ symmetry responsible for the real value of the energy. Note that the profile function h_2 only differ from h_1 by some factor in front. Therefore we omitted it from the plot.

Another physical region is when $c_1 = -c_2 = -1$. The monopole and gauge masses for this case is plotted in Figure 4. We observe almost an identical plot from the Figure 3 but with real and imaginary parts swapped. The profile functions also respect these changes as regions 1 and 3 no longer have a definite asymptotic value. The boundaries are unchanged, as one can see from the Figure 4.

Finally, there is an interesting parameter point $X = Y$ where region 2 vanishes (see Figure 5). The two boundaries $Z^2 = 1$ and $c_2ZY + c_1X = 0$ coincide when $X = Y$ and the zero exceptional point no longer exists because the spontaneous symmetry breaking does not occur in this case.

Next, let us explain the real value of the energies in different regions. First, to realise the conditions 1-3, stated in the introduction, we require the following

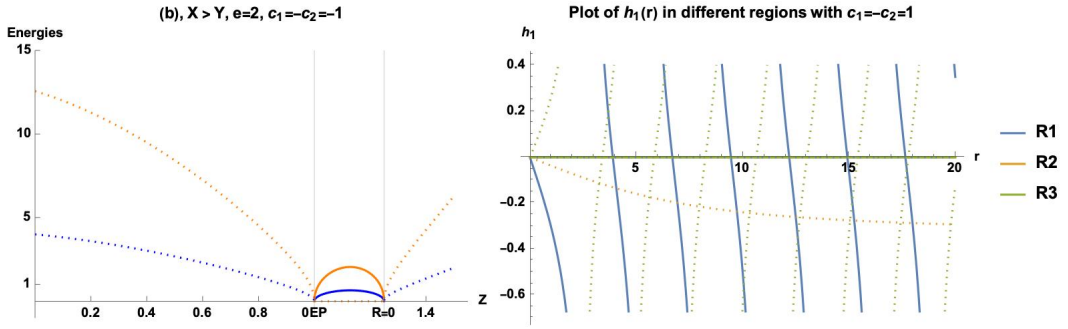

FIGURE 4. Both panels are plotted for $X = 1, Y = 1, n = 1, e = 2$. The solid line represents the real part, and the dotted line represents the imaginary part of the masses.

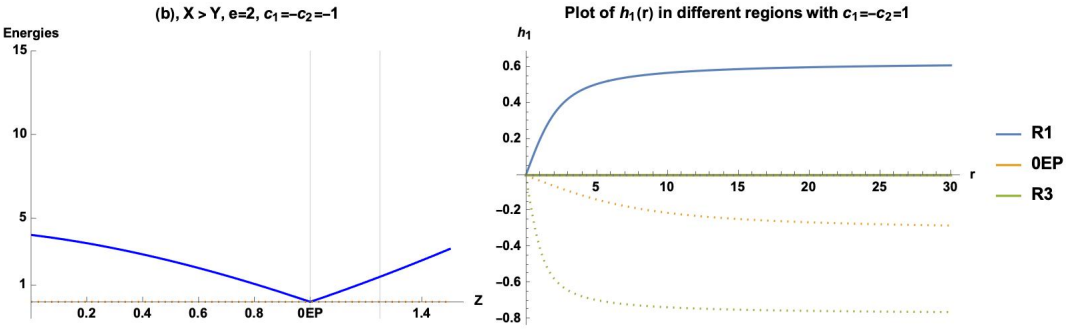

FIGURE 5. Both panels are plotted for $X = 1, Y = 1, n = 1, e = 2$. The solid line represents the real part, and the dotted line represents the imaginary part of the masses.

transformations

$$\begin{array}{cc} h_2^{\pm}(r) \to -h_2^{\pm}(r)\ , \quad h_1^{\pm}(r) \to h_1^{\pm}(r) & \text{in region 1} \\ \text{No symmetry} & \text{in region 2} \\ h_2^{\pm}(r) \to -\left(h_2^{\pm}(r)\right)^*\ , \quad h_1^{\pm}(r) \to \left(h_1^{\pm}(r)\right)^* & \text{in region 3} \end{array} .$$

By using the explicit forms of the solutions (46) and (47). We can show that the above transformations satisfy condition 2 stated in the introduction, in regions 1

$$h_2^{\pm}(r) \to -h_2^{\pm}(r) = h_2^{\mp}(r)\ , \quad h_1^{\pm}(r) \to h_1^{\pm}(r), \tag{48}$$

and in region 3

$$\begin{aligned} h_2^{\pm}(r) \to -\left(h_2^{\pm}(r)\right)^* = h_2^{\pm}\ , \\ h_1^{\pm}(r) \to \left(h_1^{\pm}(r)\right)^* = h_1^{\mp}. \end{aligned} \tag{49}$$

Notice that in regions 1 and 3, the $\mathcal{CPT}$ relates two distinct solutions in two different ways. For example, $h_2^{\pm}$ is mapped to $h_2^{\mp}$ in region 1, but it is mapped to itself in region 3.

Finally, the condition 3 stated in the introduction is satisfied because the energy does not depend on the $\pm$ signs of the solutions. This explains the real energies of complex monopoles in region 3 and complex energy in region 2. Indeed, we observe the predicted behaviour in Figure 3. Region 2 is a hard barrier between two $\mathcal{CPT}$ symmetric regions where solutions are either real or purely imaginary. The same analysis can be carried out in the other physical region $c_1 = -c_2 = -1$ where the symmetry is now

$$\begin{array}{cc} \text{No symmetry} & \text{in region 1} \\ \begin{array}{c} h_2^{\pm}(r) \to -\left(h_2^{\pm}(r)\right)^* \\ h_1^{\pm}(r) \to \left(h_1^{\pm}(r)\right)^* \end{array} & \text{in region 2} \\ \text{No symmetry} & \text{in region 3} \end{array} . \tag{50}$$

We have observed that one can find a well-defined monopole solution in two disconnected regions. However, in the full theory where we include the Higgs particles, it is only one of the regions which are considered physical. This is because the Higgs mass m_0^2 is either positive or negative depending on which side of $Z^2 = 1$ it is defined. Because two disconnected regions are defined on either side of the zero exceptional point $Z^2 = 1$, the full physical region restricts one from moving region 1 to region 3 by changing Z. This is most clearly seen in Figure 1 where the plot of m_0^2 (green line) becomes negative beyond the zero exceptional point. This may imply that the purely complex monopole solution we observed is not a possible solution of the theory. However, the purely complex solution can exist in the full physical region. An example of this is shown in the Figure 6 where we observe that the profile function h_1 (therefore h_2) is purely complex, and the Higgs masses, gauge mass are all real and positive.

4. CONCLUSIONS

We have found the t'Hooft-Polyakov monopole solution (43) in the non-Hermitian theory by drawing an

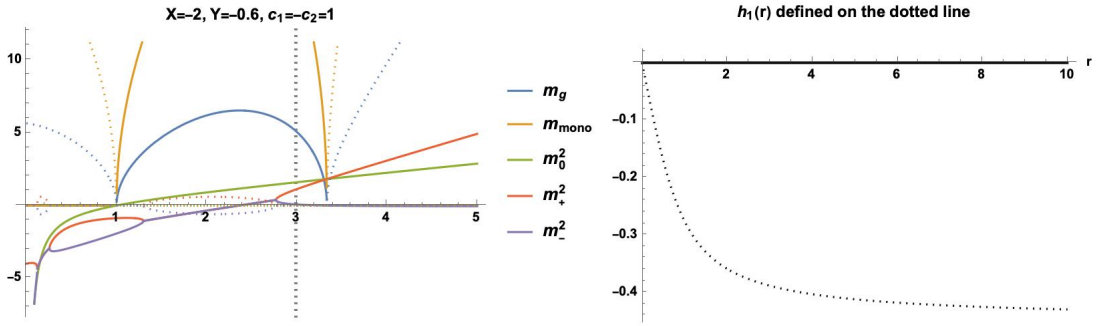

FIGURE 6. Both panels are plotted for $X = -2, Y = -0.6, c_1 = -c_2 = 1, n = 1, e = 2$. The solid line represents the real part, and the dotted line represents the imaginary part of the masses.

analogue from the standard procedure in the Hermitian theory. The monopole masses were plotted with the massive gauge and Higgs masses, where the physical region of the monopole masses coincided with that of the gauge mass. It was also observed that there are two distinct physical regions bounded by the zero exceptional point and the parameter limit where the vacuum manifold becomes trivial. The profile function (radial part of the monopole solution) is plotted in Figures 3, 4, 5, where it is real and purely complex in regions 1 and 3, respectively. Incidentally, the $\mathcal{CPT}$ symmetries of the solution are different in regions 1 and 3.

Acknowledgements

TT is supported by EPSRC grant EP/W522351/1.

References

[1] J. Alexandre, P. Millington, D. Seynaeve. Symmetries and conservation laws in non-Hermitian field theories. *Physical Review D* **96**(6):065027, 2017. https://doi.org/10.1103/PhysRevD.96.065027.

[2] J. Alexandre, J. Ellis, P. Millington, D. Seynaeve. Spontaneous symmetry breaking and the Goldstone theorem in non-Hermitian field theories. *Physical Review D* **98**(4):045001, 2018. https://doi.org/10.1103/PhysRevD.98.045001.

[3] P. D. Mannheim. Goldstone bosons and the Englert-Brout-Higgs mechanism in non-Hermitian theories. *Physical Review D* **99**(4):045006, 2019. https://doi.org/10.1103/PhysRevD.99.045006.

[4] P. Millington. Symmetry properties of non-Hermitian $\mathcal{PT}$-symmetric quantum field theories. *Journal of Physics: Conference Series* **1586**(1):012001, 2020. https://doi.org/10.1088/1742-6596/1586/1/012001.

[5] J. Alexandre, J. Ellis, P. Millington, D. Seynaeve. Spontaneously breaking non-Abelian gauge symmetry in non-Hermitian field theories. *Physical Review D* **101**(3):035008, 2019. https://doi.org/10.1103/PhysRevD.101.035008.

[6] J. Alexandre, J. Ellis, P. Millington, D. Seynaeve. Gauge invariance and the Englert-Brout-Higgs mechanism in non-Hermitian field theories. *Physical Review D* **99**(7):075024, 2019. https://doi.org/10.1103/PhysRevD.99.075024.

[7] J. Alexandre, J. Ellis, P. Millington. Discrete spacetime symmetries and particle mixing in non-Hermitian scalar quantum field theories. *Physical Review D* **102**(12):125030, 2020. https://doi.org/10.1103/PhysRevD.102.125030.

[8] A. Fring, T. Taira. Goldstone bosons in different $\mathcal{PT}$-regimes of non-Hermitian scalar quantum field theories. *Nuclear Physics B* **950**:114834, 2020. https://doi.org/10.1016/j.nuclphysb.2019.114834.

[9] A. Fring, T. Taira. Massive gauge particles versus Goldstone bosons in non-Hermitian non-abelian gauge theory, 2020. arXiv:2004.00723.

[10] A. Fring, T. Taira. Pseudo-Hermitian approach to Goldstone's theorem in non-Abelian non-Hermitian quantum field theories. *Physical Review D* **101**(4):045014, 2020. https://doi.org/10.1103/PhysRevD.101.045014.

[11] A. Fring, T. Taira. 't Hooft-Polyakov monopoles in non-Hermitian quantum field theory. *Physics Letters B* **807**:135583, 2020. https://doi.org/10.1016/j.physletb.2020.135583.

[12] J. Alexandre, J. Ellis, P. Millington. $\mathcal{PT}$-symmetric non-Hermitian quantum field theories with supersymmetry. *Physical Review D* **101**(8):085015, 2020. https://doi.org/10.1103/PhysRevD.101.085015.

[13] M. N. Chernodub, A. Cortijo, M. Ruggieri. Spontaneous non-hermiticity in the Nambu–Jona-Lasinio model. *Physical Review D* **104**(5):056023, 2021. https://doi.org/10.1103/PhysRevD.104.056023.

[14] M. N. Chernodub, P. Millington. IR/UV mixing from local similarity maps of scalar non-Hermitian field theories, 2021. arXiv:2110.05289.

[15] A. Fring. $\mathcal{PT}$-symmetric deformations of the Korteweg-de Vries equation. *Journal of Physics A: Mathematical and Theoretical* **40**(15):4215–4224, 2007. https://doi.org/10.1088/1751-8113/40/15/012.

[16] F. G. Scholtz, H. B. Geyer, F. J. W. Hahne. Quasi-Hermitian operators in quantum mechanics and the variational principle. *Annals of Physics* **213**(1):74–101, 1992. https://doi.org/10.1016/0003-4916(92)90284-S.

[17] J. Dieudonné. Quasi-Hermitian operators. *Proceedings of the International Symposium on Linear Spaces, Jerusalem 1960, Pergamon, Oxford* pp. 115–122, 1961.

[18] M. Froissart. Covariant formalism of a field with indefinite metric. *Il Nuovo Cimento* **14**:197–204, 1959. https://doi.org/10.1007/BF02724848.

[19] F. J. Dyson. Thermodynamic behavior of an ideal ferromagnet. *Physical Review* **102**(5):1230–1244, 1956. https://doi.org/10.1103/PhysRev.102.1230.

[20] T. Marumori, M. Yamamura, A. Tokunaga. On the "anharmonic effects" on the collective oscillations in spherical even nuclei. I. *Progress of Theoretical Physics* **31**(6):1009–1025, 1964. https://doi.org/10.1143/PTP.31.1009.

[21] S. T. Beliaev, V. G. Zelevinsky. Anharmonic effects of quadrupole oscillations of spherical nuclei. *Nuclear Physics* **39**:582–604, 1962. https://doi.org/10.1016/0029-5582(62)90416-9.

[22] D. Janssen, F. Dönau, S. Frauendorf, R. Jolos. Boson description of collective states. *Nuclear Physics A* **172**(1):145–165, 1971. https://doi.org/10.1016/0375-9474(71)90122-9.

[23] A. Fring, T. Taira. Non-Hermitian gauge field theories and BPS limits. *Journal of Physics: Conference Series* **2038**(1):012010, 2021. https://doi.org/10.1088/1742-6596/2038/1/012010.

[24] D. P. Musumbu, H. B. Geyer, W. D. Heiss. Choice of a metric for the non-Hermitian oscillator. *Journal of Physics A: Mathematical and Theoretical* **40**(2):F75–F80, 2007. https://doi.org/10.1088/1751-8113/40/2/F03.

[25] G. H. Derrick. Comments on nonlinear wave equations as models for elementary particles. *Journal of Mathematical Physics* **5**(9):1252–1254, 1964. https://doi.org/10.1063/1.1704233.

[26] M. K. Prasad, C. M. Sommerfield. Exact classical solution for the't Hooft monopole and the Julia-Zee dyon. *Physical Review Letters* **35**(12):760–762, 1975. https://doi.org/10.1103/PhysRevLett.35.760.

[27] E. B. Bogomolny. The stability of classical solutions. *Soviet Journal of Nuclear Physics (English Translation, United States)* **24**(4), 1976.

[28] J. Arafune, P. G. O. Freund, C. J. Goebel. Topology of Higgs fields. *Journal of Mathematical Physics* **16**(2):433–437, 1975. https://doi.org/10.1063/1.522518.

[29] T. W. Kirkman, C. K. Zachos. Asymptotic analysis of the monopole structure. *Physical Review D* **24**(4):999–1004, 1981. https://doi.org/10.1103/PhysRevD.24.999.

[30] F. Correa, A. Fring, T. Taira. Complex BPS Skyrmions with real energy. *Nuclear Physics B* **971**(2):115516, 2021. https://doi.org/10.1016/j.nuclphysb.2021.115516.

FROM QUARTIC ANHARMONIC OSCILLATOR TO DOUBLE WELL POTENTIAL

Alexander V. Turbiner*, Juan Carlos del Valle

Instituto de Ciencias Nucleares, Universidad Nacional Autónoma de México, Apartado Postal 70-543, 04510 México-City, Mexico

* corresponding author: turbiner@nucleares.unam.mx

Abstract. Quantum quartic single-well anharmonic oscillator $V_{ao}(x) = x^2 + g^2x^4$ and double-well anharmonic oscillator $V_{dw}(x) = x^2(1-gx)^2$ are essentially one-parametric, they depend on a combination $(g^2\hbar)$. Hence, these problems are reduced to study the potentials $V_{ao} = u^2 + u^4$ and $V_{dw} = u^2(1-u)^2$, respectively. It is shown that by taking uniformly-accurate approximation for anharmonic oscillator eigenfunction $\Psi_{ao}(u)$, obtained recently, see JPA 54 (2021) 295204 [1] and arXiv 2102.04623 [2], and then forming the function $\Psi_{dw}(u) = \Psi_{ao}(u) \pm \Psi_{ao}(u-1)$ allows to get the highly accurate approximation for both the eigenfunctions of the double-well potential and its eigenvalues.

Keywords: Anharmonic oscillator, double-well potential, perturbation theory, semiclassical expansion.

1. Introduction

It is already known that for the one-dimensional quantum quartic single-well anharmonic oscillator $V_{ao}(x) = x^2 + g^2x^4$ and double-well anharmonic oscillator with potential $V_{dw}(x) = x^2(1-gx)^2$ the (trans)series in g (which is the Perturbation Theory in powers of g (the Taylor expansion) in the former case $V_{ao}(x)$ supplemented by exponentially-small terms in g in the latter case $V_{dw}(x)$) and the semiclassical expansion in $\hbar$ (the Taylor expansion for $V_{ao}(x)$ supplemented by the exponentially small terms in $\hbar$ for $V_{dw}(x)$) for energies *coincide* [3]. This property plays crucially important role in our consideration.

Both the quartic anharmonic oscillator

$$V = x^2 + g^2x^4 , \tag{1}$$

with a single harmonic well at $x = 0$ and the double-well potential

$$V = x^2(1-gx)^2 , \tag{2}$$

with two symmetric harmonic wells at $x = 0$ and $x = 1/g$, respectively, are two particular cases of the quartic polynomial potential

$$V = x^2 + agx^3 + g^2x^4 , \tag{3}$$

where g is the coupling constant and a is a parameter. Interestingly, the potential (3) is symmetric for three particular values of the parameter a: $a = 0$ and $a = \pm 2$. All three potentials (1), (2), (3) belong to the family of potentials of the form

$$V = \frac{1}{g^2}\,\tilde{V}(gx) ,$$

for which there exists a remarkable property: the Schrödinger equation becomes one-parametric, both the Planck constant $\hbar$ and the coupling constant g appear in the combination $(\hbar g^2)$, see [2]. It can be immediately seen if instead of the coordinate x the so-called classical coordinate $u = (g\,x)$ is introduced. This property implies that the action S in the path integral formalism becomes g-independent and the factor $\frac{1}{\hbar}$ in the exponent becomes $\frac{1}{\hbar g^2}$ [4]. Formally, the potentials (1)-(2), which enter to the action, appear at $g = 1$, hence, in the form

$$V = u^2 + u^4 , \tag{4}$$

$$V = u^2(1-u)^2 , \tag{5}$$

respectively. Both potentials (4), (5) are symmetric with respect to $u = 0$ and $u = 1/2$, respectively.

Namely, this form of the potentials will be used in this short Note. This Note is the extended version of a part of presentation in AAMP-18 given by the first author [5].

2. Single-well potential

In [1] for the potential (4) matching the small distances $u \to 0$ expansion and the large distances $u \to \infty$ expansion (in the form of semiclassical expansion) for the phase ϕ in the representation

$$\Psi = P(u)\; e^{-\phi(u)} ,$$

of the wave function, where P is a polynomial, it was constructed the following function for the $(2n+p)$-excited state with quantum numbers (n,p), $n = 0,1,2,\ldots$, $p = 0,1$:

$$\Psi^{(n,p)}_{(approximation)} =$$

$$\frac{u^p P_{n,p}(u^2)}{(B^2 + u^2)^{\frac{1}{4}} \left(B + \sqrt{B^2 + u^2}\right)^{2n+p+\frac{1}{2}}}$$

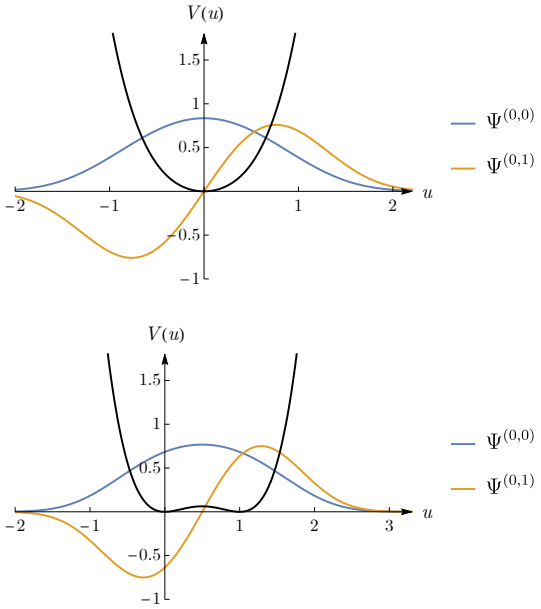

FIGURE 1. Two lowest, normalized to one eigenfunctions of positive/negative parity: for single-well potential (4), see (6) (top) and for double-well potential (5), see (9)(bottom). Potentials shown by black lines.

$$\times \exp\left(-\frac{A\ +\ (B^2+3)\,u^2/6\ +\ u^4/3}{\sqrt{B^2\ +\ u^2}}\ +\ \frac{A}{B}\right)\ , \tag{6}$$

where $P_{n,p}$ is some polynomial of degree n in u^2 with positive roots. Here $A = A_{n,p},\ B = B_{n,p}$ are two parameters of interpolation. These parameters $(-A),\ B$ are slow-growing with quantum number n at fixed p taking, in particular, the values

$$A_{0,0}\ =\ -0.6244\ , B_{0,0}\ =\ 2.3667\ , \tag{7}$$

$$A_{0,1}\ =\ -1.9289\ , B_{0,1}\ =\ 2.5598\ , \tag{8}$$

for the ground state and the first excited state, respectively. This remarkably simple function (6), see Figure 1 (top), provides 10-11 exact figures in energies for the first 100 eigenstates. Furthermore, the function (6) deviates uniformly for $u \in (-\infty, +\infty)$ from the exact function in $\sim 10^{-6}$.

3. Double-well potential: wavefunctions

Following the prescription, usually assigned in folklore to E. M. Lifschitz – one of the authors of the famous Course on Theoretical Physics by L. D. Landau and E. M. Lifschitz – when a wavefunction for single well potential with minimum at $u = 0$ is known, $\Psi(u)$, the wavefunction for double well potential with minima at $u = 0, 1$ can be written as $\Psi(u) \pm \Psi(u-1)$. This prescription was already checked successfully for the double-well potential (2) in [6] for somehow simplified version of (6), based on matching the small distances $u \to 0$ expansion and the large distances $u \to \infty$ expansion for the phase ϕ but ignoring subtleties emerging in semiclassical expansion. Taking the wavefunction (6) one can construct

$$\Psi^{(n,p)}_{(approximation)}\ = \frac{P_{n,p}(\tilde{u}^2)}{(B^2\ +\ \tilde{u}^2)^{\frac{1}{4}}\left(\alpha B\ +\ \sqrt{B^2\ +\ \tilde{u}^2}\right)^{2n+\frac{1}{2}}} \exp\left(-\frac{A\ +\ (B^2+3)\,\tilde{u}^2/6\ +\ \tilde{u}^4/3}{\sqrt{B^2\ +\ \tilde{u}^2}}\ +\ \frac{A}{B}\right) D^{(p)}\ , \tag{9}$$

where $p = 0, 1$ and

$$D^{(0)}\ =\ \cosh\left(\frac{a_0\tilde{u} + b_0\tilde{u}^3}{\sqrt{B^2+\tilde{u}^2}}\right)\ ,$$

$$D^{(1)}\ =\ \sinh\left(\frac{a_1\tilde{u} + b_1\tilde{u}^3}{\sqrt{B^2+\tilde{u}^2}}\right)\ .$$

Here

$$\tilde{u}\ =\ u\ -\ \frac{1}{2}\ , \tag{10}$$

$\alpha\ =\ 1$ and $A, B, a_{0,1}, b_{0,1}$ are variational parameters. If $\alpha\ =\ 0$ as well as $b_{0,1}\ =\ 0$ the function (9) is reduced to ones which were explored in [6], see Eqs.(10)-(11) therein. The polynomial $P_{n,p}$ is found unambiguously after imposing the orthogonality conditions of $\Psi^{(n,p)}_{(approximation)}$ to $\Psi^{(k,p)}_{(approximation)}$ at $k = 0, 1, 2, \ldots, (n-1)$, here it is assumed that the polynomials $P_{k,p}$ at $k = 0, 1, 2, \ldots, (n-1)$ are found beforehand.

4. Double-well potential: Results

In this section we present concrete results for energies of the ground state $(0,0)$ and of the first excited state $(0,1)$ obtained with the function (9) at $p = 0, 1$, respectively, see Figure 1 (bottom). The results are compared with the Lagrange-Mesh Method (LMM) [7].

4.1. Ground State (0,0)

The ground state energy for (5) obtained variationally using the function (9) at $p = 0$ and compared with LMM results [7], where all printed digits (in the second line) are correct,

$$E^{(0,0)}_{var}\ =\ 0.932\,517\,518\,401\ ,$$
$$E^{(0,0)}_{mesh}\ =\ 0.932\,517\,518\,372\ .$$

Note that ten decimal digits in $E^{(0,0)}_{var}$ coincide with ones in $E^{(0,0)}_{mesh}$ (after rounding). Variational parameters in (9) take values,

$$A\ =\ 2.3237\ ,$$
$$B\ =\ 3.2734\ ,$$
$$a_0\ =\ 2.3839\ ,$$
$$b_0\ =\ 0.0605\ ,$$

cf. (7). Note that b_0 takes a very small value.

4.2. First Excited State (0,1)

The first excited state energy for (5) obtained variationally using the function (9) at $p = 1$ and compared with LMM results [7], where all printed digits (in the second line) are correct,

$$E^{(0,1)}_{var} = 3.396\,279\,329\,936\ ,$$
$$E^{(0,1)}_{mesh} = 3.396\,279\,329\,887\ .$$

Note that ten decimal digits in $E^{(0,1)}_{var}$ coincide with ones in $E^{(0,1)}_{mesh}$. Variational parameters in (9) take values,

$$A = -2.2957\ ,$$
$$B = 3.6991\ ,$$
$$a_1 = 4.7096\ ,$$
$$b_1 = 0.0590\ ,$$

cf. (8). Note that b_1 takes a very small value similar to b_0.

5. Conclusions

It is presented the approximate expression (9) for the eigenfunctions in the double-well potential (5). In Non-Linearization procedure [8] it can be calculated the first correction (the first order deviation) to the function (9). It can be shown that for any $u \in (-\infty, +\infty)$ the functions (9) deviate uniformly from the exact eigenfunctions, beyond the sixth significant figure similarly to the function (6) for the single-well case. It increases the accuracy of the simplified function, proposed in [5] with $\alpha = 0$ and $b_{0,1} = 0$, in the domain under the barrier $u \in (0.25, 0.75)$ from 4 to 6 significant figures leaving the accuracy outside of this domain practically unchanged.

Acknowledgements

This work is partially supported by CONACyT grant A1-S-17364 and DGAPA grants IN113819, IN113022 (Mexico). AVT thanks the PASPA-UNAM program for support during his sabbatical leave.

References

[1] A. V. Turbiner, J. C. del Valle. Anharmonic oscillator: a solution. *Journal of Physics A: Mathematical and Theoretical* **54**(29):295204, 2021. https://doi.org/10.1088/1751-8121/ac0733.

[2] A. V. Turbiner, E. Shuryak. On connection between perturbation theory and semiclassical expansion in quantum mechanics, 2021. arXiv:2102.04623.

[3] E. Shuryak, A. V. Turbiner. Transseries for the ground state density and generalized Bloch equation: Double-well potential case. *Physical Review D* **98**:105007, 2018. https://doi.org/10.1103/PhysRevD.98.105007.

[4] M. A. Escobar-Ruiz, E. Shuryak, A. V. Turbiner. Quantum and thermal fluctuations in quantum mechanics and field theories from a new version of semiclassical theory. *Physical Review D* **93**:105039, 2016. https://doi.org/10.1103/PhysRevD.93.105039.

[5] A. V. Turbiner, J. C. del Valle. Anharmonic oscillator: almost analytic solution, 2021. Talk presented by AVT at AAMP-18 (Sept.1-3), Prague, Czech Republic (September 1, 2021).

[6] A. V. Turbiner. Double well potential: perturbation theory, tunneling, WKB (beyond instantons). *International Journal of Modern Physics A* **25**(02n03):647–658, 2010. https://doi.org/10.1142/S0217751X10048937.

[7] A. V. Turbiner, J. C. del Valle. Comment on: Uncommonly accurate energies for the general quartic oscillator. *International Journal of Quantum Chemistry* **121**(19):e26766, 2021. https://doi.org/10.1002/qua.26766.

[8] A. V. Turbiner. The eigenvalue spectrum in quantum mechanics and the nonlinearization procedure. *Soviet Physics Uspekhi* **27**(9):668–694, 1984. English Translation, https://doi.org/10.1070/PU1984v027n09ABEH004155.

TIME-DEPENDENT MASS OSCILLATORS: CONSTANTS OF MOTION AND SEMICLASICAL STATES

Kevin Zelaya

Czech Academy of Science, Nuclear Physics Institute, 250 68 Řež, Czech Republic
correspondence: kdzelaya@fis.cinvestav.mx

Abstract. This work reports the construction of constants of motion for a family of time-dependent mass oscillators, achieved by implementing the formalism of form-preserving point transformations. The latter allows obtaining a spectral problem for each constant of motion, one of which leads to a non-orthogonal set of eigensolutions that are, in turn, coherent states. That is, eigensolutions whose wavepacket follows a classical trajectory and saturate, in this case, the Schrödinger-Robertson uncertainty relationship. Results obtained in this form are relatively general, and some particular examples are considered to illustrate the results further. Notably, a regularized Caldirola-Kanai mass term is introduced in an attempt to amend some of the unusual features found in the conventional Caldirola-Kanai case.

Keywords: Time-dependent mass oscillators, Caldirola-Kanai oscillator, quantum invariants, coherent states, semiclassical dynamics.

1. Introduction

The search for exact solutions for time-dependent (nonstationary) quantum models is challenging task as compared to the stationary (time-independent) counterpart. In the stationary case, the dynamical law (Schrödinger equation) reduces to an eigenvalue equation associated with the energy observable, the Hamiltonian, for which several methods can be implemented to obtain exact solutions. Particularly, new exactly solvable models can be constructed from previously known ones through Darboux transformations [1] (also known as SUSY-QM). In the nonstationary case, it is still possible to recover an eigenvalue problem for the Hamiltonian if one restricts to the *adiabatic approximation* [2, 3]. However, in general, the latter is not feasible, and other workarounds should be implemented. Despite all these challenges, time-dependent phenomena find exciting applications in physical systems such as electromagnetic traps of charged particles and plasma physics [4–8].

The parametric oscillator is perhaps the most well-known exactly solvable nonstationary model in quantum mechanics. A straightforward method to solve such a problem was introduced by Lews and Riesenfeld [9] by noticing that the appropriate constant of motion (quantum invariant) admits a nonstationary eigenvalue equation with time-dependent solutions and constant eigenvalues. In this form, nonstationary models can be addressed similarly to their stationary counterparts. This paved the way to solve other time-dependent problems [10–14].

Recently, the Darboux transformation has been adapted into the quantum invariant scheme to construct new time-dependent Hamiltonians, together with the corresponding quantum invariant and the set of solutions [15–17]. Alternatively, other methods exist to build new time-dependent models, such as the modified Darboux transfomation introduced by Bagrov et al. [18], which relies on a differential operator that intertwines a known Schrödinger equation with an unknown one. This has led to new results in the nonstationary Hermitian regime [19–21]. A non-Hermitian PT-symmetric extension has been discussed in [22], and some further models were reported in [23, 24].

On the other hand, the point transformations formalism [25] has been proved useful to construct and solve time-dependent oscillators. This was achieved by implementing a geometrical deformation that transforms the stationary oscillator Schrödinger equation into one with time-dependent frequency and mass [26, 27]. This allows obtaining further information such as the constants of motion, which are preserved throughout the point transformation [25], leading to a straightforward way to get such constants of motion without imposing any ansatz. A further extension for non-Hermitian systems was introduced in [28], whereas a non-Hermitian extension of the generalized Caldirola-Kanai oscillator was discussed in [29].

In this work, the point transformation formalism is exploited to construct and study the dynamics of semiclassical states associated with time-dependent mass oscillators. This is achieved by using the aforementioned preservation of constants of motion and identifying their corresponding spectral problem. Notably, it is shown that one constant of motion leads to an orthogonal set of solutions, whereas a different one leads to nonorthogonal solutions that behave like semiclassical states. That is, Gaussian wavepackets whose maximum point follows the corresponding classical trajectory and minimize, in this case, the

Schrödinger-Robertson uncertainty principle. Two particular examples are considered to illustrate the usefulness of the approach further.

2. Materials and methods

Throughout this manuscript, the time-dependent mass $m(t)$ and frequency $\Omega^2(t)$ oscillator subjected to an external driving force $F(t)$ is considered. Such a model is characterized by the time-dependent Hamiltonian

$$\hat{H}_{\rm ck}(t) = \frac{\hat{p}^2}{2m(t)} + \frac{m(t)\Omega^2(t)}{2}\hat{x}^2 + F(t)\hat{x}, \quad (1)$$

with $\hat{x}$ and $\hat{p}_x$ the canonical position and momentum operators, respectively, with $[\hat{x}, \hat{p}_x] = i\hbar\mathbb{I}$. Henceforth, the identity operator $\mathbb{I}$ is omitted each time it multiplies a constant or a function. The corresponding Schrödinger equation

$$i\hbar\frac{\partial\psi}{\partial t} = -\frac{\hbar^2}{2m(t)}\frac{\partial^2\psi}{\partial x^2} + \frac{m(t)\Omega^2(t)x^2}{2}\psi + F(t)x\psi, \quad (2)$$

is recovered by using the coordinate representation $p_x \equiv -i\hbar\frac{\partial}{\partial x}$ and $\hat{x} \equiv x \in \mathbb{R}$.

The solutions of Eq. (2) have been discussed by several authors, see [27, 30–32]. Here, a brief summary of the point transformation approach discussed in [26, 27] is provided. This eases the discussion of semiclassical states and dynamics to be presented later in Section 3.

2.1. Point transformations

In general, the method of form-preserving point transformations relies on a geometrical deformation that maps an initial differential equation with variable coefficients into another one of the same form but with different coefficients. To illustrate this, be the stationary oscillator Hamiltonian

$$\hat{H}_{\rm osc} = \frac{\hat{p}_y^2}{2m_0} + \frac{m_0 w_0^2 \hat{y}^2}{2}, \quad [\hat{y}, \hat{p}_y] = i\hbar, \quad (3)$$

with $\hat{y}$ and $\hat{p}_y$ another couple of canonical position and momentum observables, respectively. The corresponding Schrödinger equation

$$i\hbar\frac{\partial\Psi}{\partial\tau} = -\frac{\hbar^2}{2m_0}\frac{\partial^2\Psi}{\partial y^2} + \frac{m_0 w_0^2 y^2}{2}\Psi, \quad (4)$$

admits the well-known solutions [2]

$$\Psi_n(y,\tau) = e^{-iw_0\left(n+\frac{1}{2}\right)\tau}\Phi_n(y), \quad (5)$$

where

$$\Phi_n(y) = \sqrt{\frac{1}{2^n n!}\sqrt{\frac{m_0 w_0}{\pi\hbar}}}e^{-\frac{m_0 w_0}{2\hbar}y^2}H_n\left(\sqrt{\frac{m_0 w_0}{\hbar}}y\right), \quad (6)$$

with $H_n(z)$ the Hermite polynomials [33], fulfills the stationary eigenvalue problem

$$H_{\rm osc}\Phi_n(y) = E_n^{(\rm osc)}\Phi_n(y), \quad E_n^{(\rm osc)} = \hbar w_0\left(n+\frac{1}{2}\right), \quad (7)$$

with $H_{\rm osc}$ the coordinate representation of $\hat{H}_{\rm osc}$, i.e., a second-order differential operator that admits a Sturm-Liouville problem.

To implement the point transformation, one imposes a set of relationships between the coordinates, time paramaters, and solutions of both systems in consideration [25]. In general one has

$$y(x,t), \quad \tau(x,t), \quad \Psi(y(x,t),\tau(x,t)) \equiv G(x,t;\psi), \quad (8)$$

where $G(x,t;\psi)$ is a reparametrization of Ψ as an explicit function of x, t, and ψ.

In the case under consideration, some further conditions are required to preserve the linearity and the Hermiticity of $\hat{H}_{\rm osc}$ and $\hat{H}_{\rm ck}(t)$. A detailed discussion on the matter can be found in [27]. Here, the final form of the point transformation is used, leading to

$$y(x,t) = \frac{\mu(t)x + \gamma(t)}{\sigma(t)}, \quad \tau(t) = \int^t \frac{dt'}{\sigma^2(t')}, \quad (9)$$

and

$$\Psi(y(x,t),\tau(t)) \equiv G(x,t;\psi) = A(x,t)\psi(x,t), \quad (10)$$

with $m(t) = \mu^2(t)$, together with $\sigma(t)$ and $\gamma(t)$ some real-valued functions to be determined.

By substituting (9) into the Schrödinger equation (4), and after some calculations, one arrives to a new partial differential equation for $\psi(x,t)$ that takes the exact form in (2). The latter allows obtaining

$$\begin{aligned} A(x,t) &= \sqrt{\frac{\sigma}{\mu}}\exp\mathcal{A}(x,t), \\ \mathcal{A}(x,t) &:= \left(i\frac{m_0 w_0}{\hbar}\frac{\mu}{\sigma}\left(\frac{W_\mu}{2}x^2 + W_\gamma x\right) + i\eta\right), \end{aligned} \quad (11)$$

where $\mathcal{A}(x,t)$ is a local time-dependent complex-phase and [27]

$$\begin{aligned} \eta(t) &:= \frac{m_0}{2\hbar}\frac{\gamma(t)W_\gamma(t)}{\sigma(t)} - \frac{1}{2\hbar}\int^t dt'\frac{F(t')}{\mu(t')}, \\ W_\mu(t) &= \sigma(t)\dot{\mu}(t) - \dot{\sigma}(t)\mu(t), \\ W_\gamma(t) &= \sigma(t)\dot{\gamma}(t) - \dot{\sigma}(t)\gamma(t), \end{aligned} \quad (12)$$

with $\dot{f}(t) \equiv \frac{df(t)}{dt}$ a short-hand notation for the time derivative. In the latter, $\sigma(t)$ and $\gamma(t)$ fulfill the nonlinear Ermakov equation

$$\ddot{\sigma}(t) + \left(\Omega^2(t) - \frac{\ddot{\mu}(t)}{\mu(t)}\right)\sigma(t) = \frac{w_0^2}{\sigma^3(t)}, \quad (13)$$

and non-homogeneous equation

$$\ddot{\gamma}(t) + \left(\Omega^2(t) - \frac{\ddot{\mu}(t)}{\mu(t)}\right)\gamma(t) = \frac{F(t)}{m_0\mu(t)}, \quad (14)$$

The solutions of the Ermakov equation are well-known [34–36] and computed from two linearly independent solutions of the associated linear equation

$$\ddot{q}_j(t) + \left(\Omega^2(t) - \frac{\ddot{\mu}(t)}{\mu(t)}\right)q_j(t) = 0, \quad j = 1,2, \quad (15)$$

through the nonlinear combination

$$\sigma(t) = \left[aq_1^2(t) + bq_1(t)q_2(t) + cq_2^2(t)\right]^{\frac{1}{2}}, \qquad (16)$$

with $b^2 - 4ac = -4\frac{w_0^2}{\mathcal{W}_0^2}$ and $\mathcal{W}_0 = Wr(q_1(t), q_2(t)) \neq 0$ the Wronskian of two linearly independent solutions of (15), which is in general a time-independent complex constant. The previous constraint on a, b, and c guarantees that $\sigma(t)$ is different from zero [26] for $t \in \mathbb{R}$.

In this form, one obtains a set of solutions $\{\psi_n(x,t)\}_{n=0}^{\infty}$ to the Schrödinger equation (2), where

$$\psi_n(x,t) = \sqrt{\frac{\mu(t)}{\sigma(t)}}[\mathcal{A}(x,t)]^{-1} e^{-iw_0\left(n+\frac{1}{2}\right)\tau(t)} \times e^{-\frac{m_0 w_0}{2\hbar}\left(\frac{\mu(t)x+\gamma(t)}{\sigma(t)}\right)^2} H_n\left(\sqrt{\frac{m_0 w_0}{\hbar}}\frac{\mu(t)x+\gamma(t)}{\sigma(t)}\right). \qquad (17)$$

From (10)-(11) it follows that

$$(\psi_m, \psi_n) := \int_{\mathbb{R}} dx\, \psi_m^*(x,t)\psi_n(x,t) = \int_{\mathbb{R}} dy \Psi_m^*(y,\tau)\Psi_n(y,\tau) = \delta_{n,m}, \qquad (18)$$

with z^* the complex conjugate of z. That is, the inner product is preserved and thus the set $\{\psi_n(x,t)\}_{n=0}^{\infty}$ is orthonormal in $L^2(\mathbb{R}, dx)$.

The expressions presented so far are general, and specific result may be obtained once the time-dependent mass and frequency terms are specified. This is discussed in the following sections.

Before concluding, an explicit expression for $\tau(t)$ can be determined in terms of the two linearly independent solutions $q_1(t)$ and $q_2(t)$ as well. One gets

$$\tau(t) = w_0^{-1} \arctan\left[\frac{\mathcal{W}_0}{2w_0}\left(b + 2c\frac{q_2(t)}{q_1(t)}\right)\right]. \qquad (19)$$

3. Results: Constants of motion and semiclassical states

Additional information can be extracted from the stationary oscillator into the time-dependent model. Particularly, point transformations preserve *first-integrals* of the initial equation [25]. In the context of the Schrödinger equation, such first-integrals correspond to constants of motion, also known as *quantum invariant*, associated with the physical models under consideration. From the stationary oscillator, it is straightforward to realize that the Hamiltonian $\hat{H}_{\rm osc}$ is a constant of motion that characterize the energy observable. In the time-dependent case, $\hat{H}_{\rm ck}(t)$ is no longer a constant of motion, as $\frac{d\hat{H}_{\rm ck}(t)}{dt} \neq 0$. This implies that an eigenvalue problem associated with $\hat{H}_{\rm ck}$ is not possible[1].

[1]One can still link an eigenvalue problem with $\hat{H}_{\rm ck}(t)$ under the adiabatic approximation [3]. This work focuses on exact solutions and such an approach will be disregarded.

On the other hand, an orthonormal set of solutions $\{\psi_n(x,t)\}_{n=0}^{\infty}$ has been already identified, and it is still unclear the eigenvalue problem that such a set solves. This problem was addressed by Lewis-Riesenfeld [9] while solving the dynamics of the *parametric oscillator*. They notice that even in the time-dependent regime, there may be a constant of motion $\hat{I}_0(t)$ that admits a spectral problem

$$\hat{I}_0(t)\phi(x,t) = \lambda\phi(x,t), \qquad (20)$$

where the eigenvalues λ are time-independent. The existence and uniqueness of such a quantum invariant is not necessarily ensured. Still, for the parametric oscillator, Lewis and Riesenfeld managed to find the quantum invariant and solve the related spectral problem.

Here, some quantum invariants associated with $\hat{H}_{\rm ck}$ can be found through point transformations. First, notice that the point transformation was implemented in the Schrödinger equation to get the time-dependent counterpart. The same transformation can be applied to a constant of motion of the harmonic oscillator to get the corresponding one on the time-dependent model. Particularly, by consider the eigenvalue problem (7), and after some calculations, one gets a first quantum invariant of the form

$$\hat{I}_1(t) := \frac{\sigma^2(t)}{2m_0\mu^2(t)}\hat{p}_x^2 + \frac{m_0}{2}\left(W_\mu^2(t) + w_0^2\frac{\mu^2(t)}{\sigma^2(t)}\right)\hat{x}^2 + \frac{\sigma W_\mu(t)}{2\mu(t)}(\hat{x}\hat{p}_x + \hat{p}_x\hat{x}) + \frac{\sigma W_\gamma(t)}{\mu(t)}\hat{p}_x + m_0\left(W_\gamma(t)W_\mu(t) + w_0^2\frac{\mu(t)\gamma(t)}{\sigma^2(t)}\right)\hat{x} + \left(\frac{m_0}{2}W_\gamma^2(t) + \frac{\gamma^2(t)}{\sigma^2(t)}\right). \qquad (21)$$

It is straightforward to show that $\hat{I}_1(t)$ is indeed a quantum invariant,

$$\frac{i}{\hbar}[\hat{H}_{\rm ck}, \hat{I}_1(t)] + \frac{\partial\hat{I}_1(t)}{\partial t} = 0. \qquad (22)$$

Moreover, $I_1(t)$, the coordinate representation of $\hat{I}_1(t)$, defines a Sturm-Liouville problem with time-dependent coefficients,

$$I_1(t)\psi_n(x,t) = \hbar w_0\left(n + \frac{1}{2}\right)\psi_n(x,t), \qquad (23)$$

which justifies the existence of the orthogonal set of solutions found in Section 2. Note that orthogonality has been alternatively proved in (18) using the preservation of the inner product.

Remarkably, there are still more quantum invariants to be exploited. To see this, let us consider the operators

$$\hat{a} = \sqrt{\frac{m_0 w_0}{2\hbar}}\hat{y} + i\frac{\hat{p}_y}{\sqrt{2m_0\hbar w_0}}, \qquad \hat{a}^\dagger = \sqrt{\frac{m_0 w_0}{2\hbar}}\hat{y} - i\frac{\hat{p}_y}{\sqrt{2m_0\hbar w_0}}, \qquad (24)$$

which factorize the stationary oscillator Hamiltonian as $\hat{H}_{\rm osc}=\hbar w_0(\hat{a}^\dagger\hat{a}+\frac{1}{2})$ and fulfill the commutation relationship $[\hat{a},\hat{a}^\dagger]=1$. Although $\hat{a}$ and $\hat{a}^\dagger$ are not constants of motion of $\hat{H}_{\rm osc}$, one can introduce a new pair of operators

$$\hat{\mathfrak{a}}:=e^{iw_0\tau}\hat{a},\quad \hat{\mathfrak{a}}^\dagger:=e^{-iw_0\tau}\hat{a}^\dagger, \tag{25}$$

where the straightforward calculations show that $\frac{i}{\hbar}[\hat{H}_{\rm osc},\hat{\mathfrak{a}}]+\frac{\partial\hat{\mathfrak{a}}}{\partial\tau}=0$, and similarly for $\hat{\mathfrak{a}}^\dagger$. That is, $\mathfrak{a}$ and $\mathfrak{a}^\dagger$ are quantum invariants of $\hat{H}_{\rm osc}$.

The latter can now be mapped into the time-dependent model, leading straightforwardly to new quantum invariants of $\hat{H}_{\rm ck}(t)$ of the form

$$\begin{aligned}\hat{I}_{\mathfrak{a}}(t)=e^{iw_0\tau(t)}\Bigg[&\frac{i}{\sqrt{2m_0\hbar w_0}}\frac{\sigma(t)}{\mu(t)}\hat{p}_x\\&+\left(\sqrt{\frac{m_0w_0}{2\hbar}}\frac{\mu(t)}{\sigma(t)}+i\sqrt{\frac{m_0}{2\hbar w_0}}W_\mu(t)\right)\hat{x}\\&+\left(\sqrt{\frac{m_0w_0}{2\hbar}}\frac{\gamma(t)}{\sigma(t)}+i\sqrt{\frac{m_0}{2\hbar w_0}}W_\gamma(t)\right)\Bigg],\end{aligned} \tag{26}$$

and its adjoint $\hat{I}^\dagger_{\mathfrak{a}}(t)$.

Before proceeding, it is worth to recalling that two arbitrary quantum invariants $\hat{I}(t)$ and $\hat{\tilde{I}}(t)$ of a given Hamiltonian $\hat{H}(t)$ can be used to construct further invariants. This follows from the fact that the linear combination $\ell\hat{I}(t)+\tilde{\ell}\hat{\tilde{I}}(t)$ and the product $\overline{\ell}\hat{I}(t)\hat{\tilde{I}}(t)$ of quantum invariants are also quantum invariants of the same Hamiltonian $\hat{H}(t)$, for ℓ, $\tilde{\ell}$, and $\overline{\ell}$ time-independent coefficients.

In this form, $\hat{I}_{\mathfrak{a}}(t)$ and $\hat{I}^\dagger_{\mathfrak{a}}(t)$ generate $\hat{I}_1(t)$ through

$$\hat{I}_1(t)=\hbar w_0\left(\hat{I}^\dagger_{\mathfrak{a}}(t)\hat{I}_{\mathfrak{a}}(t)+\frac{1}{2}\right), \tag{27}$$

which is analogous to the factorization of the stationary oscillator. Similarly, the commutation relationship $[\hat{a},\hat{a}^\dagger]=1$ of the stationary oscillator is preserved. One thus get $[\hat{I}_{\mathfrak{a}}(t),\hat{I}^\dagger_{\mathfrak{a}}(t)]=1$ together with

$$[\hat{I}_1(t),\hat{I}_{\mathfrak{a}}(t)]=-\hbar w_0\hat{I}_{\mathfrak{a}}(t),\ [\hat{I}_1(t),\hat{I}^\dagger_{\mathfrak{a}}(t)]=\hbar w_0\hat{I}^\dagger_{\mathfrak{a}}(t), \tag{28}$$

which means that $\hat{I}_{\mathfrak{a}}(t)$ and $\hat{I}^\dagger_{\mathfrak{a}}(t)$ are annihilation and creation operators, respectively, for the eigensolutions of $\hat{I}_1(t)$. The latter leads to

$$\begin{aligned}\hat{I}_{\mathfrak{a}}(t)\psi_{n+1}(x,t)&=\sqrt{\hbar w_0(n+1)}\psi_n(x,t),\\ \hat{I}^\dagger_{\mathfrak{a}}(t)\psi_n(x,t)&=\sqrt{\hbar w_0(n+1)}\psi_{n+1}(x,t),\end{aligned} \tag{29}$$

for $n=0,\ldots$.

On the other hand, the orthonormal set $\{\psi_n(x,t)\}_{n=0}^\infty$ can be used as a basis to expand any arbitrary solution $\psi(x,t)$ of (2) through

$$\psi(x,t)=\sum_{n=0}^\infty\mathcal{C}_n\psi_n(x,t),\quad \mathcal{C}_n:=(\psi_n(x,t),\psi(x,t)). \tag{30}$$

Now, from the above results, one may investigate the spectral problem related to the remaining quantum invariants $\hat{I}_{\mathfrak{a}}(t)$ and $\hat{I}^\dagger_{\mathfrak{a}}(t)$. By considering the annihilation operator $\hat{I}_{\mathfrak{a}}(t)$, one obtains the eigenvalue problem

$$\hat{I}_{\mathfrak{a}}(t)\xi_\alpha(x,t)=\alpha\xi_\alpha(x,t), \tag{31}$$

where the eigensolution $\xi_\alpha(x,t)$ can be expanded as the linear combination

$$\xi_\alpha(x,t)=\sum_{n=0}^\infty\widetilde{\mathcal{C}}_n(\alpha)\psi_n(x,t),\quad \alpha\in\mathbb{C}. \tag{32}$$

This corresponds to the construction of *coherent states* using the Barut-Girardelo approach [37]. The complex coefficients $\widetilde{\mathcal{C}}_n(\alpha)$ are determined by using the action of the ladder operators (29) and exploiting the orthonormality of the set $\{\psi_n(x,t)\}_{n=0}^\infty$. After substituting the linear combination $\xi_\alpha(x,t)$ into the corresponding eigenvalue problem in (31), one obtains the one-parameter normalized eigensolutions

$$\xi_\alpha(x,t)=\exp\left(-\frac{|\alpha|^2}{2\hbar w_0}\right)\sum_{n=0}^\infty\left(\frac{\alpha}{\sqrt{\hbar w_0}}\right)^n\frac{\psi_n(x,t)}{\sqrt{n!}}. \tag{33}$$

Henceforth, the latter are called *time-dependent coherent states* or semiclassical states interchangeably.

Similar to Glauber coherent states [38], the eigensolutions of the annihilation operator $\hat{I}_{\mathfrak{a}}$ are not orthogonal among themselves. This follows from the overlap between two solutions with different eigenvalues, let say α and β, leading to

$$|(\xi_\beta,\xi_\alpha)|^2=\exp\left(-\frac{|\alpha|^2+|\beta|^2-2\,\mathrm{Re}(\alpha^*\beta)}{\hbar w_0}\right), \tag{34}$$

which is different from zero for every $\alpha,\beta\in\mathbb{C}$, with the inner product defined in (18). Interestingly, the eigensolution $\xi_\alpha(x,t)$ can be brought into an alternative and handy expression by using the explicit form of $\psi_n(x,t)$ given in (17), together with the well-known summation rules for the Hermite polynomials. By doing so one gets

$$\begin{aligned}\xi_\alpha(x,t)\equiv&\sqrt{\frac{\mu(t)}{\sigma(t)}}\sqrt{\frac{m_0w_0}{\pi\hbar}}[\mathcal{A}(x,t)]^{-1}e^{-i\frac{w_0\tau(t)}{2}}\\&\times\exp\left[i\sqrt{\frac{2m_0w_0}{\hbar}}\left(\frac{\mu(t)x+\gamma(t)}{\sigma(t)}\right)\mathrm{Im}\,\widetilde{\alpha}(t)\right]\\\times\exp&\left[-\frac{m_0w_0}{2\hbar}\left(\frac{\mu(t)x+\gamma(t)}{\sigma(t)}-\sqrt{\frac{2\hbar}{m_0w_0}}\,\mathrm{Re}\,\widetilde{\alpha}(t)\right)^2\right],\end{aligned} \tag{35}$$

with $\widetilde{\alpha}(t)=\alpha e^{-iw_0\tau(t)}$. Thus, $\xi_\alpha(x,t)$ is a normalized Gaussian wavepacket with time-dependent width. The complex constants α plays the role of the initial conditions of the wavepacket at a given time t_0. See the discussion in the following section.

Despite the lack of orthogonality in the elements of the set $\{\xi_\alpha(x,t)\}_{\alpha\in\mathbb{C}}$, they can be still used as a non-orthogonal basis so that any arbitrary solution of (2) can be constructed through the appropriate linear superposition. That is, a given solution $\psi(x,t)$ of (2) expands as

$$\psi(x,t)=\int_{\mathbb{C}}\frac{d^2\alpha}{\pi\hbar}\mathfrak{C}(\alpha)\xi_\alpha(x,t), \tag{36}$$

where $\mathfrak{C}(\alpha) = (\xi_\alpha(x,t), \psi(x,t))$.

So far, the spectral problem related to the quantum invariants $\hat{I}_1(t)$ and $\hat{I}_\mathfrak{a}(t)$ has led to a discrete and a continuous representation, respectively, in which any solution of (2) can be expanded.

Although the eigenvalue problem related to the quantum invariant $\hat{I}^\dagger_\mathfrak{a}(t)$ can be established, it leads to non-finite norm solutions and is thus discarded.

3.1. Semiclassical dynamics

With the time-dependent coherent states already constructed, one can now study the evolution on time of such state and its relation with physical observables such as position and momentum $\hat{x}$ and $\hat{p}_x$, respectively. To this end, note that the quantum invariants obtained through point transformations preserve the commutation relation (28) of the corresponding operators of the stationary oscillator. That is, the set $\{\hat{I}_\mathfrak{a}(t), \hat{I}^\dagger_\mathfrak{a}(t), \hat{I}^\dagger_\mathfrak{a}(t)\hat{I}_\mathfrak{a}(t)\}$ fulfill the Weyl-Heisenberg algebra [39]. This allows the construction of a unitary displacement operator of the form [39]

$$\mathfrak{D}(\alpha;t) = e^{\alpha\hat{I}^\dagger_\mathfrak{a}(t) - \alpha^*\hat{I}_\mathfrak{a}(t)} = e^{-\frac{|\alpha|}{2}} e^{\alpha\hat{I}^\dagger_\mathfrak{a}} e^{-\alpha^*\hat{I}_\mathfrak{a}}, \quad \alpha \in \mathbb{C}, \tag{37}$$

so that

$$\begin{aligned} \mathfrak{D}^\dagger(\alpha,t)\hat{I}_\mathfrak{a}(t)\mathfrak{D}(\alpha,t) &= \hat{I}_\mathfrak{a}(t) + \alpha, \\ \mathfrak{D}^\dagger(\alpha;t)\hat{I}^\dagger_\mathfrak{a}(t)\mathfrak{D}(\alpha;t) &= \hat{I}^\dagger_\mathfrak{a}(t) + \alpha^*. \end{aligned} \tag{38}$$

It follows that the action of the first relationship acted on $\psi_0(x,t)$ leads to $\hat{I}_\mathfrak{a}(t)\mathfrak{D}(\alpha,t)\psi_0(x,t) = \alpha\mathfrak{D}(\alpha,t)\psi_0(x,t)$, from which one recovers the eigenvalue equation previously analyzed in (31) by identifying $\xi_\alpha(x,t) = \mathfrak{D}(\alpha,t)\psi_0(x,t)$. This corresponds to the coherent states construction of Perelomov [39].

So far, two different and equivalent ways to construct the solutions $\xi_\alpha(x,t)$ have been identified, a property akin to Glauber coherent states. To further explore the time-dependent coherent states, one can take the unitary transformations (38) and combine them with the relationship between the ladder operators and the physical position $\hat{x}$ and momentum $\hat{p}_x$ observables presented in (26). After some calculations one obtains

$$\langle\hat{x}\rangle_\alpha(t) = \sqrt{\frac{2\hbar}{m_0 w_0}}\frac{\sigma(t)}{\mu(t)} r\cos\left(w_0\tau(t) - \theta\right) - \frac{\gamma(t)}{\mu(t)}, \tag{39}$$

where $\alpha = re^{i\theta}$. By using (19) and some elementary trigonometric identities, one recovers an explicit expression in terms of $q_1(t)$ and $q_2(t)$ as

$$\begin{aligned} \langle\hat{x}\rangle_\alpha(t) = &-\frac{\gamma(t)}{\mu(t)} \\ &+ \sqrt{\frac{2\hbar w_0}{m_0 c}}\frac{r}{\mathcal{W}_0}\left[\left(\cos\theta + \frac{\mathcal{W}_0}{2w_0}c\sin\theta\right)\frac{q_1(t)}{\mu(t)}\right. \\ &\left. + \frac{\mathcal{W}_0}{w_0}c\sin\theta\frac{q_2(t)}{\mu(t)}\right]. \end{aligned} \tag{40}$$

Similarly, the calculations for the momentum observable leads to

$$\begin{aligned} \langle\hat{p}_x\rangle_\alpha(t) = &-m_0\frac{\mu(t)}{\sigma(t)}(W_\mu(t)\langle\hat{x}\rangle_\alpha(t) + W_\gamma(t)) \\ &- \sqrt{2m_0\hbar w_0}\,\frac{\mu(t)}{\sigma(t)} r\sin\left(w_0\tau(t) - \theta\right)). \end{aligned} \tag{41}$$

In the latter, $\langle\hat{\mathcal{O}}\rangle_\alpha(t) \equiv (\xi_\alpha(x,t), \hat{\mathcal{O}}\xi_\alpha(x,t))$ stands for the average value of the observable $\hat{\mathcal{O}}$ computed through the time-dependent coherent state $\xi_\alpha(x,t)$.

The expectation value of the momentum (41) can be further simplified so that it simply rewrites as

$$\langle\hat{p}_x\rangle_\alpha(t) = m(t)\frac{d}{dt}\langle\hat{x}\rangle_\alpha(t), \quad m(t) = m_0\mu^2(t), \tag{42}$$

which is an analogous relation to that obtained from the canonical equations of motion of the corresponding classical Hamiltonian. This is also consequence of the quadratic nature of the time-dependent Hamiltonian $\hat{H}_{\rm ck}(t)$ and the Ehrenfest theorem.

From the expectation values obtained in (39)-(42), a relationship between the complex parameter $\alpha = re^{i\theta}$ and the expectation values at a given initial time $t = t_0$ can be established. The straightforward calculations lead to

$$\begin{aligned} \begin{pmatrix} \mathrm{Re}\,\widetilde{\alpha}_{t_0} \\ \mathrm{Im}\,\widetilde{\alpha}_{t_0} \end{pmatrix} &= \begin{pmatrix} \sqrt{\frac{m_0 w_0}{2\hbar}}\frac{\gamma_{t_0}}{\sigma_{t_0}} \\ \sqrt{\frac{m_0}{2\hbar w_0}}W_{\gamma_{t_0}} \end{pmatrix} \\ &+ \begin{pmatrix} \sqrt{\frac{m_0 w_0}{2\hbar}}\frac{\mu_{t_0}}{\sigma_{t_0}} & 0 \\ \sqrt{\frac{m_0}{2\hbar w_0}}W_{\mu_{t_0}} & \frac{1}{\sqrt{2m_0\hbar w_0}}\frac{\sigma_{t_0}}{\mu_{t_0}} \end{pmatrix} \begin{pmatrix} \langle\hat{x}\rangle_{t_0} \\ \langle\hat{p}_x\rangle_{t_0} \end{pmatrix}, \end{aligned} \tag{43}$$

with $\widetilde{\alpha}_{t_0} = \alpha e^{-iw_0\tau_{t_0}} = re^{i(\theta - w_0\tau_{t_0})}$, $\tau_{t_0} = \tau(t_0)$, $\sigma_{t_0} = \sigma(t_0)$, $\gamma_{t_0} = \gamma(t_0)$, $W_{\gamma_{t_0}} = W_\gamma(t_0)$, $W_{\mu_{t_0}} = W_\mu(t_0)$, $\langle\hat{x}\rangle_{t_0} = \langle\hat{x}\rangle_\alpha(t_0)$, and $\langle\hat{p}_x\rangle_{t_0} = \langle\hat{p}_x\rangle_\alpha(t_0)$.

On the other hand, one can write the probability density associated with the time-dependent coherent state in terms of $\langle\hat{x}\rangle_\alpha(t)$ through

$$\begin{aligned} \mathcal{P}_\alpha(x,t) := |\xi_\alpha(x,t)|^2 = &\sqrt{\frac{m_0 w_0}{\pi\hbar}}\frac{\mu(t)}{\sigma(t)} \\ &\times \exp\left[-\frac{m_0 w_0}{2\hbar}\frac{\mu^2(t)}{\sigma^2(t)}\left(x - \langle\hat{x}\rangle_\alpha(t)\right)^2\right], \end{aligned} \tag{44}$$

which is a Gaussian wavepacket whose maximum follows the classical trajectory. That is, the time-dependent coherent state is considered as a *semiclassical state*.

Before concluding this section, it is worth exploring the corresponding uncertainty relations associated with the canonical observables, which can be computed by using (26), (31), and (38). After some calculations one gets

$$\begin{aligned} (\Delta\hat{x})^2_\alpha &= \frac{\hbar}{2m_0 w_0}\frac{\sigma^2(t)}{\mu^2(t)}, \\ (\Delta\hat{p}_x)^2_\alpha &= \frac{m_0\hbar w_0}{2}\frac{\mu^2(t)}{\sigma^2(t)}\left(1 + \frac{\sigma^2(t)W^2_\mu(t)}{w_0^2\mu^2(t)}\right), \end{aligned} \tag{45}$$

from which the uncertainty relation reduces to

$$(\Delta\hat{x})^2_\alpha\,(\Delta\hat{p}_x)^2_\alpha = \frac{\hbar^2}{4}\left(1+\frac{\sigma^2(t)W^2_\mu(t)}{w_0^2\mu^2(t)}\right), \qquad (46)$$

where it is clear that, in general, $\xi_\alpha(x,t)$ does not minimize the Heisenberg uncertainty relationship, except for those times t' at which $W_\mu(t')=0$. The latter follows from the fact that $\sigma\neq 0$ for $t\in\mathbb{R}$. Still, there are two special cases for which Eq. (46) minimizes at all times.

- For $\mu(t)=\mu_0$ and $\Omega(t)=w_1$, one can always find a constant solution $\sigma^4(t)=w_0^2/w_1^2$ so that $W_\mu=0$. The uncertainty relationship (46) is minimized, and the time-dependent Hamiltonian becomes

$$\hat{H}_{\rm ck}(t)=\frac{\hat{p}_x^2}{2m_0\mu_0^2}+\frac{m_0\mu_0^2w_1^2}{2}\hat{x}^2+F(t)\hat{x}, \qquad (47)$$

  which is nothing but a stationary oscillator with an external time-dependent driving force $F(t)$[2]. Thus, the uncertainty relation gets minimized in the stationary limit, as expected.
- For $\Omega^2(t)=w_0^2\mu^{-4}(t)$, there is a solution $\sigma(t)=\mu(t)$ for which $W_\mu=0$. This leads to a Hamiltonian of the form

$$\hat{H}_{\rm ck}(t)= \frac{1}{\mu^2(t)}\left(\frac{\hat{p}_x^2}{2m_0}+\frac{m_0w_0^2}{2}\hat{x}^2+\mu^2(t)F(t)\hat{x}\right). \qquad (48)$$

Although the solutions $\xi_\alpha(x,t)$ minimize the Heisenberg uncertainty relation only on some restricted cases, one can still explore the *Schrödinger-Robertson inequality* [40, 41]. This is defined for a pair of observables $\hat{A}$ and $\hat{B}$ through

$$\left(\Delta\hat{A}\right)^2\left(\Delta\hat{B}\right)^2\geq\frac{|\langle[\hat{A},\hat{B}]\rangle|^2}{4}+\sigma^2_{A,B}\,, \qquad (49)$$

where $\sigma_{A,B}:=\frac{1}{2}\langle\hat{A}\hat{B}+\hat{B}\hat{A}\rangle-\langle\hat{A}\rangle\langle\hat{B}\rangle$ stands for the correlation function.

For the canonical position $\hat{x}$ and momentum $\hat{p}_x$ observables one gets

$$\sigma^2_{x,p_x}=\frac{\hbar^2}{4w_0^2}\frac{\sigma^2(t)W^2_\mu(t)}{\mu^2(t)}\,, \qquad (50)$$

when computed through $\xi_\alpha(x,t)$. Thus, the semiclassical states $\xi_\alpha(x,t)$ minimize the Schrödinger-Robertson relationship for $t\in\mathbb{R}$.

4. Discussion: Conventional and regularized Caldirola-Kanai oscillators

So far, the most general setup has been addressed for a time-dependent mass oscillator. Two particular examples are considered in this section to further illustrate the usefulness and behavior of the so-constructed solutions and coherent states. Henceforth, all calculations are carried on by working in units of $\hbar=1$ to simplify the ongoing discussion. Throughout the rest of this manuscript, the following two time-dependent masses are considered:

$$\mu_{ck}(t)=e^{-\kappa t}, \qquad \kappa\geq 0, \qquad (51a)$$

$$\mu_{rck}(t)=e^{-\kappa t}+\mu_0, \qquad \kappa,\mu_0\geq 0. \qquad (51b)$$

The first one corresponds to the well-known Caldirola-Kanai oscillator [42, 43], which contains a mass-term that asymptotically approaches to zero. This is a rather unrealistic scenario in the context of the Schrödinger equation. Still, one can study the dynamics on a given time range, let say $t\in[0,T]$, where T denotes the time spent by the mass to reduce its initial value in a factor e^{-1}. In other words, $T=\kappa^{-1}$ is equivalent to the lifetime of a decaying system. One thus may disregard the dynamics for $t>T$. To amend such issue, the second mass term $\mu_{rck}(t)$ has been introduced, which transits from $\mu_{rck}(0)=1$ to $\mu_{ck}(t\to\infty)=\mu_0$. Thus, there is no need to introduce any artificial truncation on the time domain. The Hamiltonian associated with this mass-term will be called *regularized Caldirola-Kanai oscillator*. Despite the apparent advantages of the regularized system, analytic expressions for $\sigma(t)$ are significantly more complicated with respect to those obtained from $\mu_{ck}(t)$. Still, exact result can be obtained. The discussion is thus divided for each case separately.

4.1. Caldirola-Kanai case

The so-called Caldirola-Kanai system is another well-known nonstationary problem, characterized by time-dependent mass decaying exponentially on time. It was independently introduced by Caldirola [42] and Kanai [43] in an attempt to describe the quantum counterpart of a damped oscillator. This model has been addressed by different means, such using a Fourier transform to map the map it into a parametric oscillator [32], and using the *quantum Arnold transformation* [30].

For this particular case, a constant frequency $\omega^2(t)=w_1^2$ and a driven force $F(t)=\mathcal{A}_0\cos(\nu t)$, for $\nu,\mathcal{A}_0\in\mathbb{R}$, are considered. This leads to a forced Caldirola-Kanai oscillator Hamiltonian [10, 44] of the form

$$\hat{H}_{\rm ck}(t)=\frac{e^{2\kappa t}}{2m_0}\hat{p}_x^2+e^{-2\kappa t}\frac{m_0w_1^2}{2}\hat{x}^2+\mathcal{A}_0\cos(\nu t)\hat{x}. \qquad (52)$$

From the results obtained in previous sections, one gets the solutions to the Ermakov and nonhomogeneous equations as

$$\begin{aligned}\sigma(t)&=\left(aq_1^2(t)+bq_1(t)q_2(t)+cq_2^2(t)\right)^{\frac{1}{2}},\\ \gamma(t)&=\gamma_1q_1(t)+\gamma_2q_2(t)+\gamma_p(t),\end{aligned} \qquad (53)$$

[2] The Hamiltonian (47) is essentially stationary, for the term $F(t)$ can be absorbed through an appropriate reparametrization of the canonical coordinate.

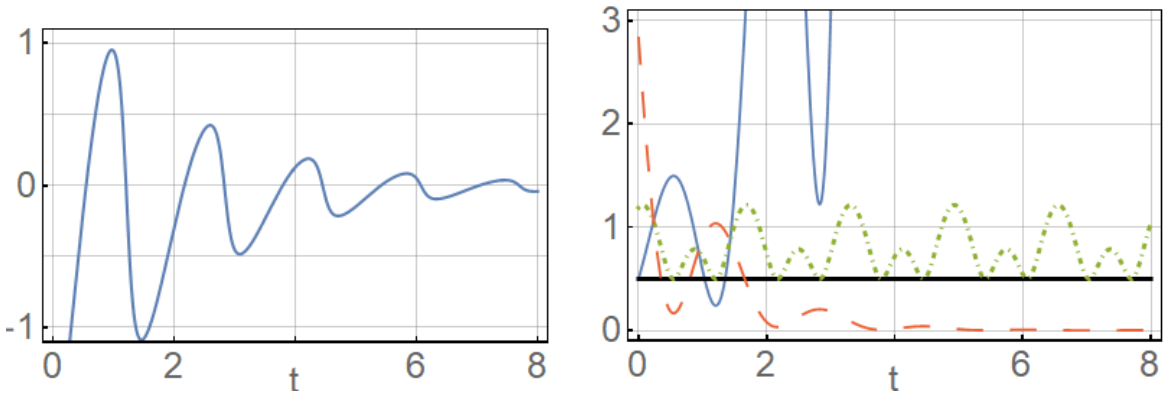

(A) . $W_\mu(t)$ (B).

FIGURE 1. (A) $W_\mu(t) = \sigma(t)\dot{\mu}(t) - \dot{\sigma}(t)\mu(t)$ for the Caldirola-Kanai mass term $\mu_{ck}(t)$. (B) Variances $(\Delta\hat{x})^2_\alpha$ (solid-blue), $(\Delta\hat{p}_x)^2_\alpha$ (dashed-red), the Schrödinger-Robertson uncertainty minimum (dotted-green), and the Heisenberg uncertainty minimum (thick-solid-black) associated with the coherent states $\xi_\alpha(x,t)$ and the mass term $\mu_{ck}(t)$. The parameters have been fixed as $a = c = w_0 = 1$, $w_1 = 2$, and $\kappa = 0.5$.

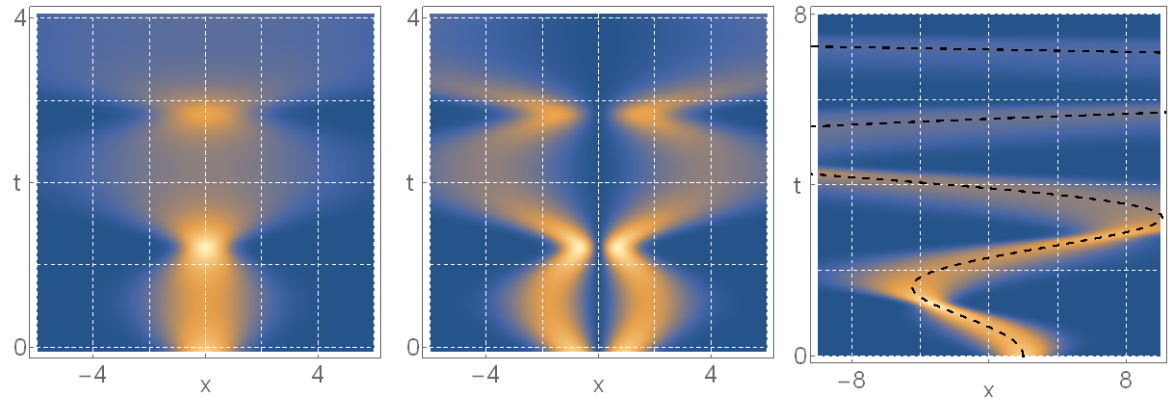

(A) . $n = 0$ (B) . $n = 1$ (C).

FIGURE 2. Probability density $\mathcal{P}_n = |\psi_n(x,t)|^2$ for $n = 0$ (A), $n = 1$ (B), and $\mathcal{P}_\alpha = |\psi_n(x,t)|^2$ (C) associated with the Caldirola-Kanai mass term $\mu_{ck}(t)$. For simplicity, the external force $F(t)$ and $\gamma(t)$ have been fixed to zero. The rest of parameters have been fixed as $w_0 = a = b = 1$, $w_1 = 2$, and $\kappa = 0.5$.

respectively, with γ_1 and γ_2 arbitrary real constants, $b^2 - 4ac = -16\frac{w_0^2}{w_1^2-\kappa^2}$, and

$$q_1(t) = \cos(\sqrt{w^2-\kappa^2}\,t), \quad q_2(t) = \sin(\sqrt{w^2-\kappa^2}\,t),$$
$$\gamma_p(t) = \mathcal{A}_0 e^{-kt}\frac{(w_1^2-\nu^2)\cos(\nu t) - 2\kappa\nu\sin(\nu t)}{(w_1^2+\nu^2)^2 - 4\nu^2(w_1^2-\kappa^2)}. \tag{54}$$

In the sequel, $\kappa = 0.5$ is consider so that the Caldirola-Kanai oscillator is constrained to the time interval $t \in [0,2]$. Further discussions concerning the dynamics will be restricted to such a time interval.

It is worth recalling that the zeros of $W_\mu(t)$ correspond to the times for which the Heisenberg uncertainty relationship saturates. Although the expression for $W_\mu(t)$ is rather simple in this case, determining the zeros consist of solving a transcendental equation. Thus, to get further insight, one may analyze Figure 1a, which depicts the behavior of such a function for $\mu_{ck}(t)$ (solid-blue). From the latter, one can see that zeroes do exist indeed, and thus one should expect points in time for which the Heisenberg inequality saturates. Despite the latter, the Schrödinger-Robertson inequality saturates at all times.

In Figure 1b, one can see the behavior of the variances, from which it is clear that the variance in the position blows up at time pass by, whereas the momentum variance squeezes indefinitely, approaching asymptotically to zero. This odd behavior results from a mass term that quickly decays, approaching zero but never converging to it. For those reasons, a truncation on the time interval was previously introduced in the form of a mean lifetime, which in this case becomes $T = \kappa^{-1} = 2$. In this form, one still has a realistic behavior for $t \in (0,2)$.

The previous results can be verified by looking at the probability density associated with the solutions $\psi_n(x,t)$ and the coherent state $\xi_\alpha(x,t)$, which is depicted in Figure 2. From those probability densities, one may see the increase on the position variance $(\Delta\hat{x})^2_\alpha$, for the wavepacket spreads rapidly on time,

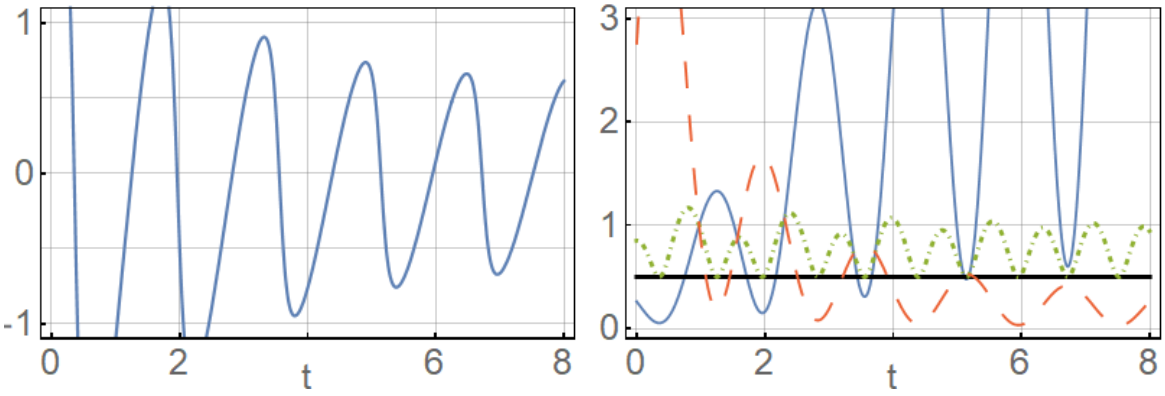

(A) . $W_\mu(t)$ (B).

FIGURE 3. (A) $W_\mu(t) = \sigma(t)\dot{\mu}(t) - \dot{\sigma}(t)\mu(t)$ for the regularized Caldirola-Kanai mass term $\mu_{rck}(t)$. (B) Variances $(\Delta\hat{x})^2_\alpha$ (solid-blue), $(\Delta\hat{p}_x)^2_\alpha$ (dashed-red), the Schrödinger-Robertson uncertainty minimum (dotted-green), and the Heisenberg uncertainty minimum (thick-solid-black) associated with the coherent states $\xi_\alpha(x,t)$ and the mass term $\mu_{rck}(t)$. The parameters have been fixed as $a = c = w_0 = 1$, $w_1 = 2$, $\mu_0 = 0.3$, and $\kappa = 0.5$.

to the point that, for times $t > 4$ is almost indistinguishable. For completeness, the classical trajectory is depicted as a dashed-black curve in Figure 2c, where the initial conditions $\langle\hat{x}\rangle_{t_0} = 2$ and $\langle\hat{p}_x\rangle_{t_0} = 0$ have been used.

4.2. Regularized Caldirola-Kanai

In this section, the *regularized Caldirola-Kanai oscillator* is introduced so that it amends the difficulties found in the Caldirola-Kanai for $t >> T$. This model is characterized by a constant frequency $\Omega^2(t) = w_1^2$ and a mass term $\mu_{rck}(t) = \mu_0 e^{-\kappa t} + \mu_1$, with $w_1, \mu_0, \mu_1, \kappa > 0$. The mass term will converge at a constant value (different from zero) and the anomalies found in the conventional Caldirola-Kanai case will be fixed. The main consequence of the mass regularization is that the classical equation of motion is not as trivial as in Section 4. In turn one has

$$\ddot{q}(t) + \left(w_1^2 - \frac{\kappa^2}{1+\mu_0 e^{\kappa t}}\right) q(t) = 0. \tag{55}$$

Two linearly independent solutions to the corresponding linear equation (15) can be found as

$$\overline{q}_1(t) = z(t)^{i\frac{w_1}{k}}\, {}_2F_1\left(\begin{matrix} A_1, A_2 \\ 1 - 2i\dfrac{w_1}{k}\end{matrix}\middle|\, \frac{-1}{z(t)}\right), \qquad \overline{q}_2(t) = \overline{q}_1^*(t), \tag{56}$$

where $z(t) = \mu_0 e^{\kappa t}$, $A_1 = -i\frac{w_1}{k} - i\sqrt{\frac{w_1^2}{k^2} - 1}$, and $A_2 = -i\frac{w_1}{k} + i\sqrt{\frac{w_1^2}{k^2} - 1}$. On the other hand, ${}_2F_1(a,b;c;Z)$ stands for the hypergeometric function [33], which converges in the complex unit-disk $|Z| < 1$. Given that $z(t) : \mathbb{R} \to (1,\infty)$, the solutions $\overline{q}_{1,2}(t)$ in (56) converge for $t \in \mathbb{R}$.

Since both solutions in (56) are complex-valued, with $\overline{q}_2 = \overline{q}_1^*$, one can construct a real-valued solution to the Ermakov equation by taking $q_1 = \mathrm{Re}(\overline{q}_1)$ and $q_2 = \mathrm{Im}(\overline{q}_1)$. To simplify the ongoing discussion, the external force is considered null, $F(t) = 0$. One thus obtains

$$\sigma^2(t) = a\ \mathrm{Re}[q_1(t)]^2 + b\ \mathrm{Re}[q_1(t)]\,\mathrm{Im}[q_1(t)] + c\ \mathrm{Im}[q_1(t)]^2, \tag{57}$$

$$\gamma(t) = \gamma_1\ \mathrm{Re}[q_1(t)] + \gamma_2\,\mathrm{Im}[q_1(t)], \tag{58}$$

where the Wronskian of the two linearly independent solutions $\mathrm{Re}\, q_1$ and $\mathrm{Im}\, q_1$ becomes $\mathcal{W}_0 = w_1$, leading to the constraint $b^2 - 4ac = -4\frac{w_0^2}{w_1^2}$.

Similarly to the Caldirola-Kanai case, the Heisenberg uncertainty relation saturates for times t_m such that $W_\mu(t_m) = 0$. In this case, an analytic expression for such points is fairly complicated. Instead, one may look at the behavior of $W_\mu(t)$ depicted in Figure 3a, from which it is clear that such points exist. On the other hand, Figure 3b reveals that, in contradistinction to the Caldirola-Kanai case, the position variance does not grow indefinitely in time. This is rather expected as, for asymptotic times $t >> 1$, the mass term converges to a finite value different from zero. That is, the Hamiltonian becomes stationary for asymptotic values.

Before conclude, the probability density for $\psi_n(x,t)$ and $\xi_\alpha(x,t)$ are shown in Figure 4. In the latter, it can be verified that the width of the wavepackets oscillates in a bounded way for times $t > 2$. Particularly, for the coherent state case of Figure 4c, the dynamics of the wavepacket can be identified clearly, where the maximum point follows the corresponding classical trajectory (dashed-black). Therefore, there is no need to introduce a truncation time T, for the mass converges to a constant value different from zero, remaining physically reasonable at all times.

5. Conclusions

In this work, the class of form-preserving point transformations has been used to construct the constants of

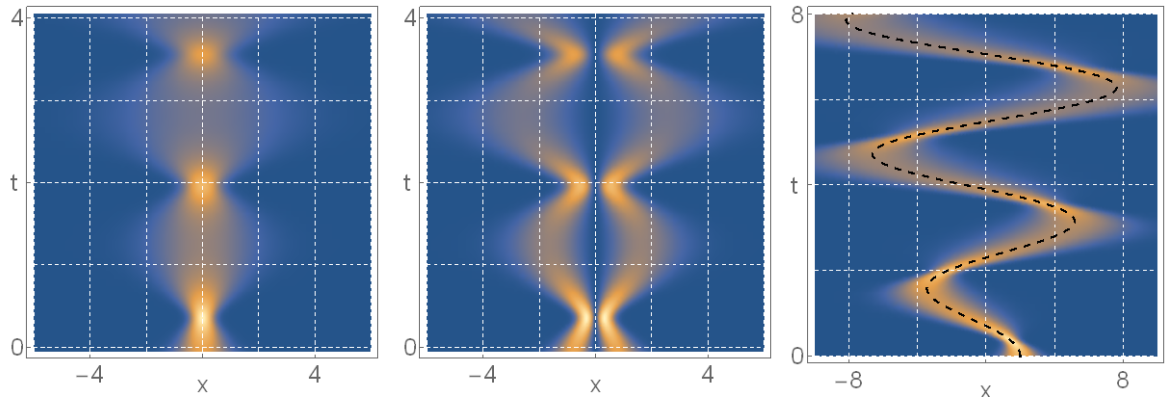

(A) . $n = 0$ (B) . $n = 1$ (C).

FIGURE 4. Probability density $\mathcal{P}_n = |\psi_n(x,t)|^2$ for $n = 0$ (A), $n = 1$ (B), and $\mathcal{P}_\alpha = |\psi_n(x,t)|^2$ (C) associated with the regularized Caldirola-Kanai mass term $\mu_{rck}(t)$. The rest of parameters have been fixed as $w_0 = a = b = 1$, $w_1 = 2$, $\mu_0 = 0.3$, and $\kappa = 0.5$.

motion for the family of time-dependent mass oscillators. This was achieved by exploiting the preservation of first-integrals on the initial stationary oscillator model. Since several constants of motion are already known for the initial system, the corresponding counterparts for the time-dependent model are straightforwardly constructed by implementing the appropriate mappings. Notably, three different constants of motion were identified, one that admits an orthogonal set of eigensolutions, another that permits non-orthogonal eigensolutions, and the third one that does not admit finite-norm solutions.

Interestingly, the non-orthogonal eigensolutions are actually coherent states, for they are constructed from the annihilation operator of the time-dependent oscillator. Furthermore, by exploiting the underlying Weyl-Heisenberg algebra fulfilled by the quantum invariants, it was possible to find exact expressions for the expectation values of the position and momentum observables. The latter revealed the coherent states are represented by Gaussian wavepacket whose maximum follows the corresponding classical trajectory.

Besides the latter properties, it was also found that, in general, the Schrödinger-Robertson uncertainty relation saturates for all times, whereas the Heisenberg one gets minimized only for some times. Still, two special time-dependent Hamiltonians exist so that the Heisenberg inequality saturates at all times, one of which is the stationary limit case, as expected.

Remarkably, the newly introduced regularized Caldirola-Kanai mass term admits exact solutions that regularize the unusual behavior observed in the conventional Caldirola-Kanai case. More precisely, the variances become bounded as well as the expectation values. This allows obtaining localization of particles, which is desired in physical implementations such as traps of charged particles.

ACKNOWLEDGEMENTS

The author acknowledges the support from the project "Physicist on the move II" (KINEÓ II), Czech Republic, Grant No. CZ.02.2.69/0.0/0.0/18_053/0017163. This research has been also funded by Consejo Nacional de Ciencia y Tecnología (CONACyT), Mexico, Grant No. A1-S-24569.

REFERENCES

[1] F. Cooper, A. Khare, U. Sukhatme. *Supersymmetry in Quantum Mechanics*. World Scientific, Singapore, 2001.

[2] F. Schwabl. *Quantum Mechanics*. Springer-Verlag, Berlin, 3rd edn., 2002.

[3] A. Bohm, A. Mostafazadeh, H. Koizumi, et al. *The Geometric Phase in Quantum Systems: Foundations, Mathematical Concepts, and Applications in Molecular and Condensed Matter Physics*. Springer-Verlag, Berlin, 2003.

[4] W. Paul. Electromagnetic traps for charged and neutral particles. *Reviews of Modern Physics* **62**(3):531–540, 1990. https://doi.org/10.1103/RevModPhys.62.531.

[5] M. Combescure. A quantum particle in a quadrupole radio-frequency trap. *Annales de l'IHP Physique théorique* **44**(3):293–314, 1986. http://www.numdam.org/item/AIHPA_1986__44_3_293_0/.

[6] D. E. Pritchard. Cooling neutral atoms in a magnetic trap for precision spectroscopy. *Physical Review Letters* **51**:1336–1339, 1983. https://doi.org/10.1103/PhysRevLett.51.1336.

[7] R. J. Glauber. *Quantum Theory of Optical Coherence*, chap. The Quantum Mechanics of Trapped Wavepackets, pp. 577–594. John Wiley & Sons, Ltd, 2006. https://doi.org/10.1002/9783527610075.ch15.

[8] B. M. Mihalcea, S. Lynch. Investigations on dynamical stability in 3D Quadrupole Ion Traps. *Applied Sciences* **11**(7):2938, 2021. https://doi.org/10.3390/app11072938.

[9] H. R. Lewis, W. B. Riesenfled. An exact quantum theory of the time-dependent harmonic oscillator and of a charged particle in a time-dependent electromagnetic

field. *Journal of Mathematical Physics* **10**(8):1458–1473, 1969. https://doi.org/10.1063/1.1664991.

[10] V. V. Dodonov, V. I. Man'ko. Coherent states and the resonance of a quantum damped oscillator. *Physical Review A* **20**:550–560, 1979. https://doi.org/10.1103/PhysRevA.20.550.

[11] V. V. Dodonov, O. V. Man'ko, V. I. Man'ko. Quantum nonstationary oscillator: Models and applications. *Journal of Russian Laser Research* **16**(1):1–56, 1995. https://doi.org/10.1007/BF02581075.

[12] I. Ramos-Prieto, A. R. Urzúa, M. Fernández-Guasti, H. M. Moya-Cessa. Ermakov-Lewis invariant for two coupled oscillators. *Journal of Physics: Conference Series* **1540**(1):012009, 2020. https://doi.org/10.1088/1742-6596/1540/1/012009.

[13] V. V. Dodonov. Invariant quantum states of quadratic Hamiltonians. *Entropy* **23**(5):634, 2021. https://doi.org/10.3390/e23050634.

[14] V. V. Dodonov, M. B. Horovits. Energy and magnetic moment of a quantum charged particle in time-dependent magnetic and electric fields of circular and plane solenoids. *Entropy* **23**(12):1579, 2021. https://doi.org/10.3390/e23121579.

[15] K. Zelaya, V. Hussin. Time-dependent rational extensions of the parametric oscillator: quantum invariants and the factorization method. *Journal of Physics A: Mathematical and Theoretical* **53**(16):165301, 2020. https://doi.org/10.1088/1751-8121/ab78d1.

[16] K. Zelaya. Nonstationary deformed singular oscillator: Quantum invariants and the factorization method. *Journal of Physics: Conference Series* **1540**:012017, 2020. https://doi.org/10.1088/1742-6596/1540/1/012017.

[17] K. Zelaya, I. Marquette, V. Hussin. Fourth Painlevé and Ermakov equations: quantum invariants and new exactly-solvable time-dependent Hamiltonians. *Journal of Physics A: Mathematical and Theoretical* **54**(1):015206, 2020. https://doi.org/10.1088/1751-8121/abcab8.

[18] V. G. Bagrov, B. F. Samsonov, L. A. Shekoyan. Darboux transformation for the nonsteady Schrödinger equation. *Russian Physics Journal* **38**(7):706–712, 1995. https://doi.org/10.1007/BF00560273.

[19] K. Zelaya, O. Rosas-Ortiz. Exactly solvable time-dependent oscillator-like potentials generated by Darboux transformations. *Journal of Physics: Conference Series* **839**:012018, 2017. https://doi.org/10.1088/1742-6596/839/1/012018.

[20] A. Contreras-Astorga. A time-dependent anharmonic oscillator. *Journal of Physics: Conference Series* **839**:012019, 2017. https://doi.org/10.1088/1742-6596/839/1/012019.

[21] R. Razo, S. Cruz y Cruz. New confining optical media generated by Darboux transformations. *Journal of Physics: Conference Series* **1194**:012091, 2019. https://doi.org/10.1088/1742-6596/1194/1/012091.

[22] J. Cen, A. Fring, T. Frith. Time-dependent Darboux (supersymmetric) transformations for non-Hermitian quantum systems. *Journal of Physics A: Mathematical and Theoretical* **52**(11):115302, 2019. https://doi.org/10.1088/1751-8121/ab0335.

[23] A. Contreras-Astorga, V. Jakubský. Photonic systems with two-dimensional landscapes of complex refractive index via time-dependent supersymmetry. *Physical Review A* **99**:053812, 2019. https://doi.org/10.1103/PhysRevA.99.053812.

[24] A. Contreras-Astorga, V. Jakubský. Multimode two-dimensional PT-symmetric waveguides. *Journal of Physics: Conference Series* **1540**:012018, 2020. https://doi.org/10.1088/1742-6596/1540/1/012018.

[25] W.-H. Steeb. *Invertible Point Transformations and Nonlinear Differential Equations*. World Scientific Publishing, Singapore, 1993. https://doi.org/10.1142/1987.

[26] K. Zelaya, O. Rosas-Ortiz. Quantum nonstationary oscillators: Invariants, dynamical algebras and coherent states via point transformations. *Physica Scripta* **95**(6):064004, 2020. https://doi.org/10.1088/1402-4896/ab5cbf.

[27] K. Zelaya, V. Hussin. Point transformations: Exact solutions of the quantum time-dependent mass nonstationary oscillator. In M. B. Paranjape, R. MacKenzie, Z. Thomova, et al. (eds.), *Quantum Theory and Symmetries*, pp. 295–303. Springer International Publishing, Cham, 2021. https://doi.org/10.1007/978-3-030-55777-5_28.

[28] A. Fring, R. Tenney. Exactly solvable time-dependent non-Hermitian quantum systems from point transformations. *Physics Letters A* **410**:127548, 2021. https://doi.org/10.1016/j.physleta.2021.127548.

[29] K. Zelaya, O. Rosas-Ortiz. Exact solutions for time-dependent non-Hermitian oscillators: Classical and quantum pictures. *Quantum Reports* **3**(3):458–472, 2021. https://doi.org/10.3390/quantum3030030.

[30] V. Aldaya, F. Cossío, J. Guerrero, F. F. López-Ruiz. The quantum Arnold transformation. *Journal of Physics A: Mathematical and Theoretical* **44**(6):065302, 2011. https://doi.org/10.1088/1751-8113/44/6/065302.

[31] N. Ünal. Quasi-coherent states for the Hermite oscillator. *Journal of Mathematical Physics* **59**(6):062104, 2018. https://doi.org/10.1063/1.5016897.

[32] I. Ramos-Prieto, M. Fernández-Guasti, H. M. Moya-Cessa. Quantum harmonic oscillator with time-dependent mass. *Modern Physics Letters B* **32**(20):1850235, 2018. https://doi.org/10.1142/S0217984918502354.

[33] F. Olver, D. Lozier, R. Boisvert, C. Clark. *NIST Handbook of Mathematical Functions*. Cambridge University Press, New York, 2010. ISBN 0521140633.

[34] V. P. Ermakov. Second-order differential equations: conditions of complete integrability. *Universita Izvestia Kiev Series III* **20**(9):1–25, 1880.

[35] A. O. Harin. "Second-order differential equations: conditions of complete integrability" (English translation). *Applicable Analysis and Discrete Mathematics* **2**:123–145, 2008.

[36] D. Schuch. *Quantum Theory from a Nonlinear Perspective: Riccati Equations in Fundamental Physics*. Spinger, Cham, 2018.

[37] A. O. Barut, L. Girardello. New "Coherent" States associated with non-compact groups. *Communications in Mathematical Physics* **21**(1):41–55, 1971. https://doi.org/10.1007/BF01646483.

[38] R. J. Glauber. Coherent and incoherent states of the radiation field. *Physical Review* **131**:2766–2788, 1963. https://doi.org/10.1103/PhysRev.131.2766.

[39] A. Perelomov. *Generalized coherent states and their applications*. Springer-Verlag, Berlin, 1986.

[40] H. P. Robertson. The uncertainty principle. *Physical Review* **34**:163–164, 1929. https://doi.org/10.1103/PhysRev.34.163.

[41] E. Schrödinger. Zum Heisenbergschen Unscharfeprinzip. *Proceedings of The Prussian Academy of Sciences* **19**:296–303, 1929.

[42] P. Caldirola. Forze non conservative nella meccanica quantistica. *Il Nuovo Cimento* **18**:393–400, 1941. https://doi.org/10.1007/BF02960144.

[43] E. Kanai. On the quantization of the dissipative systems. *Progress of Theoretical Physics* **3**(4):440–442, 1948. https://doi.org/10.1143/ptp/3.4.440.

[44] M. Dernek, N. Ünal. Quasi-coherent states for damped and forced harmonic oscillator. *Journal of Mathematical Physics* **54**(9):092102, 2013. https://doi.org/10.1063/1.4819261.

A NOTE ON ENTANGLEMENT CLASSIFICATION FOR TRIPARTITE MIXED STATES

Hui Zhao[a], Yu-Qiu Liu[a], Zhi-Xi Wang[b], Shao-Ming Fei[b,*]

[a] *Beijing University of Technology, Faculty of Science, Beijing 100124, China*

[b] *Capital Normal University, School of Mathematical Sciences, Beijing 100037, China*

[*] corresponding author: feishm@cnu.edu.cn

Abstract. We study the classification of entanglement in tripartite systems by using Bell-type inequalities and principal basis. By using Bell functions and the generalized three dimensional Pauli operators, we present a set of Bell inequalities which classifies the entanglement of triqutrit fully separable and bi-separable mixed states. By using the correlation tensors in the principal basis representation of density matrices, we obtain separability criteria for fully separable and bi-separable $2 \otimes 2 \otimes 3$ quantum mixed states. Detailed example is given to illustrate our criteria in classifying the tripartite entanglement.

Keywords: Bell inequalities, separability, principal basis.

1. Introduction

One of the most remarkable features that distinguishes quantum mechanics from classical mechanics is the quantum entanglement. Entanglement was first recognized by EPR [1], with significant progress made by Bell [2] toward the resolution of the EPR problem. Since Bell's work, derivation of new Bell-like inequalities has been one of the important and challenging subjects. CHSH generalized the original Bell inequalities to a more general case for two observers [3]. In [4] the authors proposed an estimation of quantum entanglement by measuring the maximum violation of the Bell inequality without information of the reduced density matrices. In [5] series of Bell inequalities for multipartite states have been presented with sufficient and necessary conditions to detect certain entanglement. There have been many important generalizations and interesting applications of Bell inequalities [6–8]. By calculating the measures of entanglement and the quantum violation of the Bell-type inequality, a relationship between the entanglement measure and the amount of quantum violation was derived in [9]. However, for high-dimensional multiple quantum systems the results for such relationships between the entanglement and the nonlocal violation are still far from being satisfied. In [10], an upper bound on fully entangled fraction for arbitrary dimensional states has been derived by using the principal basis representation of density matrices. Based on the norms of correlation vectors, the authors in [11] presented an approach to detect entanglement in arbitrary dimensional quantum systems. Separability criteria for both bipartite and multipartite quantum states was also derived in terms of the correlation matrices [12].

In this paper by using the Bell function and the generalized three dimensional Pauli operators, we derive a quantum upper bound for $3 \otimes 3 \otimes 3$ quantum systems. We present a classification of entanglement for triqutrit mixed states by a set of Bell inequalities. These inequalities can distinguish fully separable and bi-separable states. Moreover, we propose criteria to detect classification of entanglement for $2 \otimes 2 \otimes 3$ mixed states with correlation tensor matrices in the principal basis representation of density matrices.

2. Entanglement identification with Bell inequalities

We first consider relations between entanglement and non-locality for $3 \otimes 3 \otimes 3$ quantum systems. Consider three observers who may choose independently between two dichotomic observables denoted by A_i and B_i for the i-th observer, $i = 1, 2, 3$. Let $\widehat{V}_i$ denote the measurement operator associated with the variable $V_i \in \{A_i, B_i\}$ of i-th observer. We choose a complete set of orthonormal basis vectors $|k\rangle$ to describe an orthogonal measurement of a given variable V_i. The measurement outcomes are indicated by a set of eigenvalues $1, \lambda, \lambda^2$, where $\lambda = exp(\frac{i2\pi}{3})$ is a primitive third root of unity. Therefore the measurement operator can be represented by $\widehat{V}_i = \sum_{k=0}^{2} \lambda^k |k\rangle\langle k|$. Inspired by the Bell function (the expected value of Bell operator) constructed in [13], we introduce the following Bell operator,

$$\begin{aligned}\mathcal{B} = \sum_{j=1}^{2} \frac{1}{4} (&\widehat{A_1}^j \otimes \widehat{A_2}^j \otimes \widehat{A_3}^j + \lambda^j \widehat{A_1}^j \otimes \widehat{B_2}^j \otimes \widehat{B_3}^j \\ &+ \lambda^j \widehat{B_1}^j \otimes \widehat{A_2}^j \otimes \widehat{B_3}^j + \lambda^j \widehat{B_1}^j \otimes \widehat{B_2}^j \otimes \widehat{A_3}^j),\end{aligned} \tag{1}$$

where $\widehat{A_i}^j$ ($\widehat{B_i}^j$) denotes the j-th power of $\widehat{A_i}$ ($\widehat{B_i}$).

Next we construct three Bell operators in terms of Eq. (1). Consider three dimensional Pauli opera-

tors [14] $\widehat{X}$ and $\widehat{Z}$ which satisfy

$$\widehat{X}|k\rangle = |k+1\rangle,\ \widehat{Z}|k\rangle = \lambda^k|k\rangle,\ \widehat{X}^3 = I,\ \widehat{Z}^3 = I,$$

where I denotes the identity operator. Therefore, if we replace $\widehat{A}_i$ and $\widehat{B}_i$ with the following unitary operators, $\widehat{A}_1 = \widehat{Z}$, $\widehat{A}_2 = \lambda^2\widehat{X}\widehat{Z}$, $\widehat{A}_3 = \widehat{X}\widehat{Z}^2$, $\widehat{B}_1 = \widehat{Z}$, $\widehat{B}_2 = \widehat{X}\widehat{Z}^2$ and $\widehat{B}_3 = \lambda^2\widehat{X}\widehat{Z}$, we obtain

$$\begin{aligned}\mathcal{B}_1 =& \sum_{j=1}^{2}\frac{1}{4}[\widehat{Z}^j\otimes(\lambda^2\widehat{X}\widehat{Z})^j\otimes(\widehat{X}\widehat{Z}^2)^j + \lambda^j\widehat{Z}^j\otimes(\widehat{X}\widehat{Z}^2)^j \\ &\otimes(\lambda^2\widehat{X}\widehat{Z})^j + \lambda^j\widehat{Z}^j\otimes(\lambda^2\widehat{X}\widehat{Z})^j\otimes(\lambda^2\widehat{X}\widehat{Z})^j \\ &+ \lambda^j\widehat{Z}^j\otimes(\widehat{X}\widehat{Z}^2)^j\otimes(\widehat{X}\widehat{Z}^2)^j].\end{aligned} \tag{2}$$

If we choose unitary operators as follows, $\widehat{A}_1 = \lambda^2\widehat{X}\widehat{Z}$, $\widehat{A}_2 = \widehat{X}\widehat{Z}^2$, $\widehat{A}_3 = \widehat{Z}$, $\widehat{B}_1 = \widehat{X}\widehat{Z}^2$, $\widehat{B}_2 = \lambda^2\widehat{X}\widehat{Z}$ and $\widehat{B}_3 = \widehat{Z}$, we have

$$\begin{aligned}\mathcal{B}_2 =& \sum_{j=1}^{2}\frac{1}{4}[(\omega^2\widehat{X}\widehat{Z})^j\otimes(\widehat{X}\widehat{Z}^2)^j\otimes\widehat{Z}^j + \lambda^j(\lambda^2\widehat{X}\widehat{Z})^j \\ &\otimes(\lambda^2\widehat{X}\widehat{Z})^j\otimes\widehat{Z}^j) + \lambda^j(\widehat{X}\widehat{Z}^2)^j\otimes(\widehat{X}\widehat{Z}^2)^j \\ &\otimes(\widehat{Z})^j + \lambda^j(\widehat{X}\widehat{Z}^2)^j\otimes(\lambda^2\widehat{X}\widehat{Z})^j\otimes(\widehat{Z})^j].\end{aligned} \tag{3}$$

Taking $\widehat{A}_1 = \lambda^2\widehat{X}\widehat{Z}$, $\widehat{A}_2 = \widehat{Z}$, $\widehat{A}_3 = \widehat{X}\widehat{Z}^2$, $\widehat{B}_1 = \widehat{X}\widehat{Z}^2$, $\widehat{B}_2 = \widehat{Z}$ and $\widehat{B}_3 = \lambda^2\widehat{X}\widehat{Z}$, we have

$$\begin{aligned}\mathcal{B}_3 =& \sum_{j=1}^{2}\frac{1}{4}[(\lambda^2\widehat{X}\widehat{Z})^j\otimes\widehat{Z}^j\otimes(\widehat{X}\widehat{Z}^2)^j + \lambda^j(\lambda^2\widehat{X}\widehat{Z})^j \\ &\otimes(\widehat{Z})^j\otimes(\lambda^2\widehat{X}\widehat{Z})^j) + \lambda^j(\widehat{X}\widehat{Z}^2)^j\otimes\widehat{Z}^j \\ &\otimes(\lambda^2\widehat{X}\widehat{Z})^j + \lambda^j(\widehat{X}\widehat{Z}^2)^j\otimes\widehat{Z}^j\otimes(\widehat{X}\widehat{Z}^2)^j].\end{aligned} \tag{4}$$

Concerning the bounds on the mean values $|\langle\mathcal{B}_i\rangle|$ of the operators $\mathcal{B}_i$, $i = 1, 2, 3$, we have the following conclusions.

Theorem 1. For $3\otimes 3\otimes 3$ mixed states, we have the inequality, $|\langle\mathcal{B}_i\rangle| \le \frac{5}{4}$, $i = 1, 2, 3$.

Proof Due to the linear property of the average values, it is sufficient to consider pure states. Any triqutrit pure state can be written as,

$$\begin{aligned}|\psi\rangle =& c_1|000\rangle + c_2|011\rangle + c_3|012\rangle + c_4|021\rangle + c_5|022\rangle \\ &+ c_6|101\rangle + c_7|102\rangle + c_8|110\rangle + c_9|111\rangle \\ &+ c_{10}|120\rangle + c_{11}|122\rangle + c_{12}|201\rangle + c_{13}|202\rangle \\ &+ c_{14}|210\rangle + c_{15}|212\rangle + c_{16}|220\rangle + c_{17}|221\rangle \\ &+ c_{18}|222\rangle,\end{aligned} \tag{5}$$

where c_5, c_{11}, c_{13}, c_{15}, c_{16}, c_{17} and c_{18} are real and non-negative, $|c_1| \ge |c_i|$ for $i = 1, 2, \ldots, 18$, $|c_9| \ge |c_{18}|$ and $\sum_{i=1}^{18}|c_i|^2 = 1$. Therefore,

$$\begin{aligned}|\langle\mathcal{B}_1\rangle| =& |\frac{1}{4}(-c_1c_2 + 5c_1c_5 - c_2c_5 - c_6c_{10} + 2c_7c_8 \\ &+ 2c_9c_{11} + 2c_{12}c_{15} + 5c_{12}c_{16} - c_{13}c_{14} - c_{13}c_{17} \\ &- 4c_{14}c_{17} + 5c_{15}c_{16})| \\ \le& \frac{1}{8}\times 10\times\sum_{i=1}^{18}c_i^2 \\ =& \frac{5}{4}.\end{aligned} \tag{6}$$

Similarly one can prove that $|\langle\mathcal{B}_i\rangle| \le \frac{5}{4}$ for $i = 2, 3$. □

Theorem 2. If a triqutrit mixed state ρ is fully separable, then $|\langle\mathcal{B}_i\rangle| = 0$, $i = 1, 2, 3$.

The proof is straightforward. Due to the linear property of the average values, it is sufficient to consider pure states again. A fully separable pure state can be written as under suitable bases, $|\psi\rangle = |0\rangle\otimes|0\rangle\otimes|0\rangle\otimes|0\rangle$. Therefore $|\langle\mathcal{B}_i\rangle| = |tr(\rho\mathcal{B}_i)| = 0$.

Theorem 3. For bi-separable states $\rho_{i|jk}$ under bi-partition i and jk, $i \ne j \ne k \in \{1, 2, 3\}$, we have

$$\begin{aligned}&|\langle\mathcal{B}_1\rangle| \le \tfrac{3}{4},\quad |\langle\mathcal{B}_2\rangle| = 0,\quad |\langle\mathcal{B}_3\rangle| = 0,\\ &|\langle\mathcal{B}_1\rangle| = 0,\quad |\langle\mathcal{B}_2\rangle| \le \tfrac{3}{4},\quad |\langle\mathcal{B}_3\rangle| = 0,\\ &|\langle\mathcal{B}_1\rangle| = 0,\quad |\langle\mathcal{B}_2\rangle| = 0,\quad |\langle\mathcal{B}_3\rangle| \le \tfrac{3}{4},\end{aligned}$$

for $\rho_{1|23}$, $\rho_{3|12}$ and $\rho_{2|13}$, respectively.

Proof It is sufficient to consider pure states only. Every bi-separable pure state $\rho_{1|23}$ can be written as via a suitable choice of bases [15],

$$|\psi\rangle = |0\rangle\otimes(c_0|00\rangle + c_1|11\rangle + c_2|22\rangle),$$

where $|c_0| \ge |c_1| \ge |c_2|$ and $\sum_{i=0}^{2}|c_i|^2 = 1$. Therefore, we have by direct calculation,

$$\begin{aligned}|\langle\mathcal{B}_1\rangle| =& |\frac{1}{4}(5c_2c_0 - c_0c_1 - c_1c_2)| \\ \le& \frac{1}{8}(5\times(c_2^2 + c_0^2) + (c_0^2 + c_1^2)\times(c_1^2 + c_2^2)) \\ \le& \frac{3}{4}.\end{aligned}$$

It is straightforward to prove similarly, $|\langle\mathcal{B}_2\rangle| = 0$ and $|\langle\mathcal{B}_3\rangle| = 0$. For bi-separable states $\rho_{3|12}$ and $\rho_{2|13}$, the results can be proved in a similar way. □

The above relations given in Theorem 1-3 give rise to characterization of quantum entanglement based on the Bell-type violations. If we consider $|\langle\mathcal{B}_i\rangle|$, $i = 1, 2, 3$, to be three coordinates, then all the triqutrit states are confined in a cube with size $\frac{5}{4}\times\frac{5}{4}\times\frac{5}{4}$. The bi-separable states are confined in a cube with size $\frac{3}{4}\times\frac{3}{4}\times\frac{3}{4}$, see Figure 1.

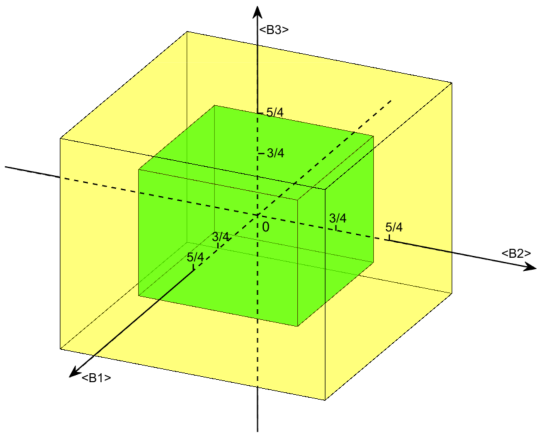

FIGURE 1. All states lie in the yellow cube, while in the green cube are bi-separable states.

3. ENTANGLEMENT CLASSIFICATION UNDER PRINCIPAL BASIS

Consider the principal basis on d-dimensional Hilbert space H with computational basis $|i\rangle$, $i = 1, 2, ..., d$. Let E_{ij} be the $d \times d$ unit matrix with the only nonzero entry 1 at the position (i, j). Let ω be a fixed d-th primitive root of unity, the principal basis is given by

$$A_{ij} = \sum_{m \in Z_d} \omega^{im} E_{m,m+j}, \tag{7}$$

where $\omega^d = 1$, $i, j \in Z_d$ and Z_d is Z modulo d. The set $\{A_{ij}\}$ spans the principal Cartan subalgebra of $gl(d)$. Under the stand inner product $(x|y) = tr(xy)$ of matrices x and y, the dual basis of the principal basis $\{A_{ij}\}$ is $\{(\omega^{ij}/d)A_{-i,-j}\}$, which follows also from the algebraic property of the principal matrices, $A_{ij}A_{kl} = \omega^{jk}A_{i+k,j+l}$. Namely, $A^\dagger_{i,j} = \omega^{ij}A_{-i,-j}$, and thus $tr(A_{ij}A^\dagger_{kl}) = \delta_{ik}\delta_{jl}d$ [10].

Next we consider the entanglement of $2 \otimes 2 \otimes 3$ systems. Let $\{A_{ij}\}$ and $\{B_{ij}\}$ be the principal bases of 2-dimensional and 3-dimensional Hilbert space, respectively. For any quantum state $\rho \in H^2_1 \otimes H^2_2 \otimes H^3_3$, ρ has the principal basis representation:

$$\begin{aligned}
\rho =& \frac{1}{12}(I_2 \otimes I_2 \otimes I_3 + \sum_{\substack{(i,j)\\ \neq(0,0)}} u_{ij}A_{ij} \otimes I_2 \otimes I_3 \\
&+ \sum_{\substack{(k,l)\\ \neq(0,0)}} v_{kl} I_2 \otimes A_{kl} \otimes I_3 + \sum_{(s,t)\neq(0,0)} w_{st} I_2 \otimes I_2 \otimes B_{st} \\
&+ \sum_{\substack{(i,j),(k,l)\\ \neq(0,0)}} x_{ij,kl}A_{ij} \otimes A_{kl} \otimes I_3 + \sum_{\substack{(i,j),(s,t)\\ \neq(0,0)}} y_{ij,st}A_{ij} \\
&\otimes I_2 \otimes B_{st} + \sum_{\substack{(k,l),(s,t)\\ \neq(0,0)}} z_{kl,st} I_2 \otimes A_{kl} \otimes B_{st} \\
&+ \sum_{\substack{(i,j),(k,l),(s,t)\\ \neq(0,0)}} r_{ij,kl,st}A_{ij} \otimes A_{kl} \otimes B_{st}),
\end{aligned} \tag{8}$$

where I_2 (I_3) denotes the two (three) dimensional identity matrix, $u_{ij} = tr(\rho A^\dagger_{ij} \otimes I_2 \otimes I_3)$, $v_{kl} = tr(\rho I_2 \otimes A^\dagger_{kl} \otimes I_3)$, $w_{st} = tr(\rho I_2 \otimes I_2 \otimes B^\dagger_{st})$, $x_{ij,kl} = tr(\rho A^\dagger_{ij} \otimes A^\dagger_{kl} \otimes I_3)$, $y_{ij,st} = tr(\rho A^\dagger_{ij} \otimes I_2 \otimes B^\dagger_{st})$, $z_{kl,st} = tr(\rho I_2 \otimes A^\dagger_{kl} \otimes B^\dagger_{st})$ and $r_{ij,kl,st} = tr(\rho A^\dagger_{ij} \otimes A^\dagger_{kl} \otimes B^\dagger_{st})$. Denote $T^{1|23}_1$, $T^{1|23}_2$, $T^{2|13}_1$, $T^{2|13}_2$, $T^{3|12}_1$ and $T^{3|12}_2$ the matrices with entries given by $r_{01,kl,st}$, $r_{11,kl,st}$, $r_{ij,01,st}$, $r_{ij,11,st}$, $r_{ij,kl,10}$ and $r_{ij,kl,20}$ $(i, j, k, l \in Z_2$, $s, t \in Z_3)$, respectively. Let $\|A\|_{tr} = \sum \sigma_i = tr\sqrt{AA^\dagger}$ be the trace norm of a matrix $A \in R^{m\times n}$, where σ_i are the singular values of the matrix A.

First we note that $\|T^{1|23}_1 - T^{1|23}_2\|_{tr}$ is invariant under local unitary transformations. Denote $UAU^\dagger$ by A^U. Suppose $\rho' = \rho^{(I\otimes U_2\otimes U_3)}$ with $U_2 \in U(2)$ and $U_3 \in U(3)$, $A^{U_2}_{ij} = \sum_{\substack{(i',j')\\ \neq(0,0)}} m_{ij,i'j'}A_{i'j'}$ and $B^{U_3}_{ij} = \sum_{\substack{(i',j')\\ \neq(0,0)}} n_{ij,i'j'}B_{i'j'}$ for some coefficients $m_{ij,i'j'}$ and $n_{ij,i'j'}$. The orthogonality of $\{A^{U_2}_{ij}\}$ and $\{B^{U_3}_{ij}\}$ requires that

$$\begin{aligned}
&tr(A^{U_2}_{ij}A^{U_2}_{kl}) = tr(U_2A_{ij}A^\dagger_{kl}U^\dagger_2) \\
=&tr(A_{ij}A^\dagger_{kl}) = 2\delta_{ik}\delta_{jl}; \\
&tr(B^{U_3}_{ij}B^{U_3}_{kl}) = tr(U_3B_{ij}B^\dagger_{kl}U^\dagger_3) \\
=&tr(B_{ij}B^\dagger_{kl}) = 3\delta_{ik}\delta_{jl}.
\end{aligned}$$

Hence, we have $M = (m_{ij,i'j'}) \in SU(3)$ and $N = (n_{ij,i'j'}) \in SU(8)$ since any two orthogonal bases are transformed by an unitary matrix. One sees that

$$\begin{aligned}
&\sum_{\substack{(i,j),(k,l),\\ (s,t)\neq(0,0)}} r_{ij,kl,st}A_{ij} \otimes A^{U_2}_{kl} \otimes B^{U_3}_{st} \\
=& \sum_{\substack{(i,j),(k,l),\\ (s,t)\neq(0,0)}} \sum_{\substack{(k',l'),(s',t')\\ \neq(0,0)}} r_{ij,kl,st}m_{kl,k'l'}n_{st,s't'}A_{ij} \otimes A_{k'l'} \\
&\otimes B_{s't'} \\
=& \sum_{\substack{(i,j),(k,l),\\ (s,t)\neq(0,0)}} (\sum_{\substack{(k',l'),(s',t')\\ \neq(0,0)}} m_{k'l',kl}r_{ij,k'l',s't'}n_{s't',st})A_{ij} \otimes A_{kl} \\
&\otimes B_{st}.
\end{aligned}$$

We have $T^{1|23}_1(\rho') = M^tT^{1|23}_1(\rho)N$ and $T^{1|23}_2(\rho') = M^tT^{1|23}_2(\rho)N$. Therefore,

$$\|T^{1|23}_1(\rho') - T^{1|23}_2(\rho')\|_{tr} = \|T^{1|23}_1(\rho) - T^{1|23}_2(\rho)\|_{tr}, \tag{9}$$

due to that the singular values of a matrix are the same as those of M^tTN when M and N are unitary matrices.

Theorem 4. If a mixed state ρ is fully separable, then $\|T^{1|23}_1 - T^{1|23}_2\|_{tr} \leq \sqrt{3}$.

Proof If $\rho = |\varphi\rangle\langle\varphi|$ is fully separable, we have $|\varphi_{1|2|3}\rangle = |\varphi_1\rangle \otimes |\varphi_{23}\rangle \in H^2_1 \otimes H^6_{23}$, where $|\varphi_{23}\rangle = |\varphi_2\rangle \otimes |\varphi_3\rangle \in H^2_2 \otimes H^3_3$. Then by Schmidt decomposition, $|\varphi_{1|2|3}\rangle = t_0|0\alpha\rangle + t_1|1\beta\rangle$, where $t^2_0 + t^2_1 = 1$. Taking into account the local unitary equivalence in $H^2_2 \otimes H^3_3$ and using (9), we only need to consider that $\{|\alpha\rangle, |\beta\rangle\} = \{|00\rangle, |01\rangle\}$. Then

$|\varphi_{1|2|3}\rangle = t_0|000\rangle + t_1|101\rangle$. $T_1^{1|23}$ and $T_2^{1|23}$ are given by

$$T_1^{1|23} = \begin{bmatrix} 0 & t_0t_1 & 0 \\ 0 & t_0t_1 & 0 \\ 0 & 0 & 0 \\ 0 & t_0t_1 & 0 \\ 0 & t_0t_1\omega^2 & 0 \\ 0 & 0 & 0 \\ 0 & t_0t_1 & 0 \\ 0 & t_0t_1\omega & 0 \end{bmatrix}^t, \tag{10}$$

$$T_2^{1|23} = \begin{bmatrix} 0 & t_0t_1 & 0 \\ 0 & -t_0t_1 & 0 \\ 0 & 0 & 0 \\ 0 & t_0t_1 & 0 \\ 0 & -t_0t_1\omega^2 & 0 \\ 0 & 0 & 0 \\ 0 & t_0t_1 & 0 \\ 0 & -t_0t_1\omega & 0 \end{bmatrix}^t. \tag{11}$$

with $\omega^3 = 1$. Therefore, we have

$$\begin{aligned} &\|T_1^{1|23} - T_2^{1|23}\|_{tr} \\ =&tr\sqrt{(T_1^{1|23} - T_2^{1|23})(T_1^{1|23} - T_2^{1|23})^\dagger} \\ =&\sqrt{12t_0^2t_1^2} \le \sqrt{3}. \end{aligned}$$

For a fully separable mixed state $\rho = \sum p_i|\varphi_i\rangle\langle\varphi_i|$, we get

$$\begin{aligned} &\|T_1^{1|23}(\rho) - T_2^{1|23}(\rho)\|_{tr} \\ =&\|T_1^{1|23}(\sum p_i|\varphi_i\rangle\langle\varphi_i|) - T_2^{1|23}(\sum p_i|\varphi_i\rangle\langle\varphi_i|)\|_{tr} \\ \le&\sum p_i\|T_1^{1|23}(|\varphi_i\rangle\langle\varphi_i|) - T_2^{1|23}(|\varphi_i\rangle\langle\varphi_i|)\|_{tr} \\ \le&\sqrt{3}, \end{aligned}$$

which proves the theorem. □

Theorem 5. For any mixed state $\rho = \sum p_i|\varphi_i\rangle\langle\varphi_i| \in H_1^2 \otimes H_2^2 \otimes H_3^3$, $\sum p_i = 1$, $0 < p_i \le 1$, we have:
(1) If ρ is $1|23$ separable, then $\|T_1^{1|23} - T_2^{1|23}\|_{tr} \le \sqrt{6}$;
(2) If ρ is $2|13$ separable, then $\|T_1^{2|13} - T_2^{2|13}\|_{tr} \le \sqrt{6}$;
(3) If ρ is $3|12$ separable, then $\|T_1^{3|12} - T_2^{3|12}\|_{tr} \le \sqrt{3}$.

Proof (1) If $\rho = |\varphi\rangle\langle\varphi|$ is $1|23$ separable, we have $|\varphi_{1|23}\rangle = |\varphi_1\rangle \otimes |\varphi_{23}\rangle \in H_1^2 \otimes H_{23}^6$, where $H_{23}^6 = H_2^2 \otimes H_3^3$. Then by Schmidt decomposition, one has $|\varphi_{1|23}\rangle = t_0|0\alpha\rangle + t_1|1\beta\rangle$, where $t_0^2 + t_1^2 = 1$. Taking into account the local unitary equivalence in $H_2^2 \otimes H_3^3$ and using (9), we only need to consider two cases (i) $\{|\alpha\rangle, |\beta\rangle\} = \{|00\rangle, |01\rangle\}$ and (ii) $\{|00\rangle, |11\rangle\}$.

For the first case we have $\|T_1^{1|23} - T_2^{1|23}\|_{tr} \le \sqrt{3}$ by Theorem 4. For the second case, we have $|\varphi_{1|23}\rangle = t_0|000\rangle + t_1|111\rangle$, where $T_1^{1|23}$ and $T_2^{1|23}$ are given by

$$T_1^{1|23} = \begin{bmatrix} t_0t_1 & 0 & t_0t_1 \\ t_0t_1 & 0 & -t_0t_1 \\ 0 & 0 & 0 \\ t_0t_1 & 0 & t_0t_1 \\ t_0t_1\omega^2 & 0 & -t_0t_1\omega^2 \\ 0 & 0 & 0 \\ t_0t_1 & 0 & t_0t_1 \\ t_0t_1\omega & 0 & -t_0t_1\omega \end{bmatrix}^t, \tag{12}$$

$$T_2^{1|23} = \begin{bmatrix} t_0t_1 & 0 & t_0t_1 \\ -t_0t_1 & 0 & t_0t_1 \\ 0 & 0 & 0 \\ t_0t_1 & 0 & t_0t_1 \\ -t_0t_1\omega^2 & 0 & t_0t_1\omega^2 \\ 0 & 0 & 0 \\ t_0t_1 & 0 & t_0t_1 \\ -t_0t_1\omega & 0 & t_0t_1\omega \end{bmatrix}^t. \tag{13}$$

Then we have

$$\begin{aligned} &\|T_1^{1|23} - T_2^{1|23}\|_{tr} \\ =&tr\sqrt{(T_1^{1|23} - T_2^{1|23})(T_1^{1|23} - T_2^{1|23})^\dagger} \\ =&\sqrt{24t_0^2t_1^2} \le \sqrt{6}. \end{aligned}$$

Now consider mixed state $\rho = \sum p_i|\varphi_i\rangle\langle\varphi_i|$. We obtain

$$\begin{aligned} &\|T_1^{1|23}(\rho) - T_2^{1|23}(\rho)\|_{tr} \\ =&\|T_1^{1|23}(\sum p_i|\varphi_i\rangle\langle\varphi_i|) - T_2^{1|23}(\sum p_i|\varphi_i\rangle\langle\varphi_i|)\|_{tr} \\ \le&\sum p_i\|T_1^{1|23}(|\varphi_i\rangle\langle\varphi_i|) - T_2^{1|23}(|\varphi_i\rangle\langle\varphi_i|)\|_{tr}, \end{aligned}$$

namely, $\|T_1^{1|23}(\rho) - T_2^{1|23}(\rho)\|_{tr} \le \sqrt{6}$.

(2) If $\rho = |\varphi\rangle\langle\varphi|$ is $2|13$ separable, we have $|\varphi_{2|13}\rangle = |\varphi_2\rangle \otimes |\varphi_{13}\rangle \in H_2^2 \otimes H_{13}^6$, where $H_{13}^6 = H_1^2 \otimes H_3^3$. Then by Schmidt decomposition, one has $|\varphi_{2|13}\rangle = t_0|0\alpha\rangle + t_1|1\beta\rangle$, where $t_0^2 + t_1^2 = 1$. Taking into account the local unitary equivalence in $H_1^2 \otimes H_3^3$, we obtain a similar equation of (9). Thus we only need to consider again the two cases (i) $\{|\alpha\rangle, |\beta\rangle\} = \{|00\rangle, |01\rangle\}$ and (ii) $\{|00\rangle, |11\rangle\}$.

In the first case, $|\varphi_{2|13}\rangle = t_0|000\rangle + t_1|101\rangle$, and $T_1^{2|13}$ and $T_2^{2|13}$ are zero matrices. In the second case, $|\varphi_{2|13}\rangle = t_0|000\rangle + t_1|111\rangle$, with $T_1^{2|13}$ and $T_2^{2|13}$ given by

$$T_1^{2|13} = \begin{bmatrix} t_0t_1 & 0 & t_0t_1 \\ t_0t_1 & 0 & -t_0t_1 \\ 0 & 0 & 0 \\ t_0t_1 & 0 & t_0t_1 \\ t_0t_1\omega^2 & 0 & -t_0t_1\omega^2 \\ 0 & 0 & 0 \\ t_0t_1 & 0 & t_0t_1 \\ t_0t_1\omega & 0 & -t_0t_1\omega \end{bmatrix}^t, \tag{14}$$

$$T_2^{2|13}=\begin{bmatrix} t_0t_1 & 0 & t_0t_1 \\ -t_0t_1 & 0 & t_0t_1 \\ 0 & 0 & 0 \\ t_0t_1 & 0 & t_0t_1 \\ -t_0t_1\omega^2 & 0 & t_0t_1\omega^2 \\ 0 & 0 & 0 \\ t_0t_1 & 0 & t_0t_1 \\ -t_0t_1\omega & 0 & t_0t_1\omega \end{bmatrix}^t. \quad (15)$$

Then we have

$$\begin{aligned} &\|T_1^{2|13}-T_2^{2|13}\|_{tr} \\ =&tr\sqrt{(T_1^{2|13}-T_2^{2|13})(T_1^{2|13}-T_2^{2|13})^\dagger} \\ =&\sqrt{24t_0^2t_1^2}\le\sqrt{6}. \end{aligned}$$

For the mixed state $\rho=\sum p_i|\varphi_i\rangle\langle\varphi_i|$, we have

$$\begin{aligned} &\|T_1^{2|13}(\rho)-T_2^{2|13}(\rho)\|_{tr} \\ =&\|T_1^{2|13}(\sum p_i|\varphi_i\rangle\langle\varphi_i|)-T_2^{2|13}(\sum p_i|\varphi_i\rangle\langle\varphi_i|)\|_{tr} \\ \le&\sum p_i\|T_1^{2|13}(|\varphi_i\rangle\langle\varphi_i|)-T_2^{2|13}(|\varphi_i\rangle\langle\varphi_i|)\|_{tr} \\ \le&\sqrt{6}. \end{aligned}$$

(3) If $\rho=|\varphi\rangle\langle\varphi|$ is $3|12$ separable, we have $|\varphi_{3|12}\rangle=|\varphi_3\rangle\otimes|\varphi_{12}\rangle\in H_3^3\otimes H_{12}^4$, where $H_{12}^4=H_1^2\otimes H_2^2$. Then by Schmidt decomposition, we have $|\varphi_{3|12}\rangle=t_0|0\alpha_0\rangle+t_1|1\alpha_1\rangle+t_2|2\alpha_2\rangle$, where $t_0^2+t_1^2+t_2^2=1$. Taking into account the local unitary equivalence in $H_1^2\otimes H_2^2$, we obtain similar equation of (9). We only need to consider the case $|\varphi_{3|12}\rangle=t_0|000\rangle+t_1|101\rangle+t_2|210\rangle$. We have

$$\begin{aligned} T_1^{3|12}&=\begin{bmatrix} 0 & 0 & 0 \\ 0 & t_0^2-\omega t_1^2+\omega^2t_2^2 & 0 \\ 0 & 0 & 0 \end{bmatrix}, \\ T_2^{3|12}&=\begin{bmatrix} 0 & 0 & 0 \\ 0 & t_0^2-\omega^2 t_1^2+\omega t_2^2 & 0 \\ 0 & 0 & 0 \end{bmatrix}. \end{aligned} \quad (16)$$

Using $1+\omega+\omega^2=0$, we have

$$\begin{aligned} &\|T_1^{3|12}-T_2^{3|12}\|_{tr} \\ =&tr\sqrt{(T_1^{3|12}-T_2^{3|12})(T_1^{3|12}-T_2^{3|12})^\dagger} \\ =&\sqrt{3(t_0^2+t_1^2)^2}\le\sqrt{3}. \end{aligned}$$

For the mixed state $\rho=\sum p_i|\varphi_i\rangle\langle\varphi_i|$, we get

$$\begin{aligned} &\|T_1^{3|12}(\rho)-T_2^{3|12}(\rho)\|_{tr} \\ =&\|T_1^{3|12}(\sum p_i|\varphi_i\rangle\langle\varphi_i|)-T_2^{3|12}(\sum p_i|\varphi_i\rangle\langle\varphi_i|)\|_{tr} \\ \le&\sum p_i\|T_1^{3|12}(|\varphi_i\rangle\langle\varphi_i|)-T_2^{3|12}(|\varphi_i\rangle\langle\varphi_i|)\|_{tr} \\ \le&\sqrt{3}. \end{aligned}$$

As an example, let us consider the $2\otimes2\otimes3$ state,

$$\rho=x|GHZ'\rangle\langle GHZ'|+(1-x)I_{12},\quad 0\le x\le1,$$

where $|GHZ'\rangle=\frac{1}{2}(|000\rangle+|101\rangle+|011\rangle+|112\rangle)$. By Theorem 4, we have that when $\|T_1^{1|23}-T_2^{1|23}\|=(2\sqrt{\frac{3}{2}}+1)x>\sqrt{3}$, i.e., $0.5021<x\le1$, ρ is not fully separable. By Theorem 5, when $\|T_1^{1|23}-T_2^{1|23}\|=\|T_1^{2|13}-T_2^{2|13}\|=(2\sqrt{\frac{3}{2}}+1)x>\sqrt{6}$, i.e., $0.7101<x\le1$, ρ is not separable under bipartition $1|23$ or $2|13$. When $\|T_1^{3|12}-T_2^{3|12}\|=\frac{7\sqrt{3}}{4}x>\sqrt{3}$, i.e., $0.5714<x\le1$, ρ is not separable under bipartition $3|12$.

4. Conclusions

We have presented quantum upper bounds for triqutrit mixed states by using the generalized Bell functions and the generalized three dimensional Pauli operators, from which the triqutrit entanglement has been identified. Our inequalities distinguish fully separable states and three types of bi-separable states for triqutrit states. Moreover, any triqutrits states are confined in a cube with size $\frac{5}{4}\times\frac{5}{4}\times\frac{5}{4}$ and the bi-separable states are in a cube with the size $\frac{3}{4}\times\frac{3}{4}\times\frac{3}{4}$. We have also studied the classification of quantum entanglement for $2\otimes2\otimes3$ systems by using the correlation tensors in the principal basis representation of density matrices. By considering the upper bounds on some the trace norms, we have obtained the criteria which detect fully separable and bi-separable $2\otimes2\otimes3$ quantum mixed states. Detailed example has been given to show the classification of tripartite entanglement by using our criteria.

Acknowledgements

This work is supported by the National Natural Science Foundation of China under grant Nos. 11101017, 11531004, 11726016, 12075159 and 12171044, Simons Foundation under grant No. 523868, Beijing Natural Science Foundation (Z190005), Academy for Multidisciplinary Studies, Capital Normal University, Shenzhen Institute for Quantum Science and Engineering, Southern University of Science and Technology (SIQSE202001), and the Academician Innovation Platform of Hainan Province.

References

[1] A. Einstein, B. Podolsky, N. Rosen. Can quantum-mechanical description of physical reality be considered complete? *Physical Review* **47**(10):777–780, 1935. https://doi.org/10.1103/PhysRev.47.777.

[2] J. S. Bell. On the Einstein Podolsky Rosen paradox. *Physics* **1**(3):195–200, 1964. https://doi.org/10.1103/PhysicsPhysiqueFizika.1.195.

[3] J. F. Clauser, M. A. Horne, A. Shimony, R. A. Holt. Proposed experiment to test local hidden-variable theories. *Physical Review Letters* **23**(15):880–884, 1969. https://doi.org/10.1103/PhysRevLett.23.880.

[4] P. Y. Chang, S. K. Chu, C. T. Ma. Bell's inequality and entanglement in qubits. *Journal of High Energy Physics volume* **2017**(9):100, 2017. https://doi.org/10.1007/JHEP09(2017)100.

[5] M. Li, S. M. Fei. Bell inequalities for multipartite qubit quantum systems and their maximal violation. *Physical Review A* **86**(5):052119, 2012. https://doi.org/10.1103/PhysRevA.86.052119.

[6] D. Collins, N. Gisin, S. Popescu, et al. Bell-type inequalities to detect true n-body nonseparability. *Physical Review Letters* **88**(17):170405, 2002. https://doi.org/10.1103/PhysRevLett.88.170405.

[7] S. W. Ji, J. Lee, J. Lim, et al. Multi-setting Bell inequality for qudits. *Physical Review A* **78**(5):052103, 2008. https://doi.org/10.1103/PhysRevA.78.052103.

[8] H. Zhao. Entanglement of Bell diagonal mixed states. *Physics Letters A* **373**(43):3924–3930, 2009. https://doi.org/10.1016/j.physleta.2009.08.048.

[9] D. Ding, Y. Q. He, F. L. Yan, T. Gao. Entanglement measure and quantum violation of Bell-type inequality. *International Journal of Theoretical Physics* **55**(10):4231–4237, 2016. https://doi.org/10.1007/s10773-016-3048-1.

[10] X. F. Huang, N. H. Jing, T. G. Zhang. An upper bound of fully entangled fraction of mixed states. *Communications in Theoretical Physics* **65**(6):701–704, 2016. https://doi.org/10.1088/0253-6102/65/6/701.

[11] J. I. de Vicente, M. Huber. Multipartite entanglement detection from correlation tensors. *Physical Review A* **84**(6):242–245, 2011. https://doi.org/10.1103/PhysRevA.84.062306.

[12] M. Li, J. Wang, S. M. Fei, X. Li-Jost. Quantum separability criteria for arbitrary dimensional multipartite states. *Physical Review A* **89**(2):767–771, 2014. https://doi.org/10.1103/PhysRevA.89.022325.

[13] W. Son, J. Lee, M. S. Kim. Generic Bell inequalities for multipartite arbitrary dimensional systems. *Physical Review Letters* **96**(6):060406, 2006. https://doi.org/10.1103/PhysRevLett.96.060406.

[14] D. Gottesman. Fault-tolerant quantum computation with higher-dimensional systems. *Chaos, Solitons & Fractals* **10**(10):1749–1758, 1999. https://doi.org/10.1016/S0960-0779(98)00218-5.

[15] H. A. Carteret, A. Higuchi, A. Sudbery. Multipartite generalisation of the Schmidt decomposition. *Journal of Mathematical Physics* **41**(12):7932–7939, 2000. https://doi.org/10.1063/1.1319516.